An investigation into the strength and thickness of biofouling deposits to optimise chemical, water and energy use in industrial process cleaning

Peck, Oliver

Award date:
2017

Awarding institution:
University of Bath

An investigation into the strength and thickness of biofouling deposits to optimise chemical, water and energy use in industrial process cleaning

Oliver Philip Wayland Peck

A thesis submitted for the degree of Doctor of Philosophy

University of Bath

Department of Chemical Engineering

March 2017

ABSTRACT

Biofouling is both a human health hazard and detrimental to process efficiency. Biofilm growth is inevitable on exposed surfaces, so an informed approach to cleaning and timely management are essential. Chemicals can readily kill cells, but the biofilm structure must be removed to prevent re-growth and maintain sterility. Chemical agents also pose health and environmental risks, but the typical alternative is to pump unsustainable volumes of cleaning solution through pipelines for mechanical cleaning. The aim of this research was to apply green cleaning principles to biofouling removal in industry, reducing the amount of chemicals, water and energy used in cleaning. Biofilms of *Escherichia coli* and *Burkholderia cepacia* were grown on polyethylene, glass and stainless steel 304, in single and mixed species cultures. Fluid dynamic gauging (FDG) utilises hydrodynamics to measure both the thickness and attached strength of the biofilms and therefore the optimum water usage for removal can be estimated, and is both relatively simple and inexpensive to operate. As well as using a static culture method, a drip flow reactor was built to develop biofilms under flow conditions. The use of FDG offers an original way of monitoring both the attachment strength and thickness of mixed species biofilms, and drip flow is an alternative to traditional biofilm growth methods for analysis of removal behaviours, with particular relevance to food production environments.

The adhesive and cohesive strengths of both single and mixed species biofilms increased up to 14 days' growth, and as previous studies suggest that this will be sustained over longer periods under flow conditions, cleaning prior to peak strength would be prudent – at later stages the risk of pathogens developing and contaminating the process would likely become too great, particularly if the biofilm is experiencing significant detachment which increasingly occurs with age. The development of greater, sustained thickness over time can also pose problems with heat transfer and enhanced pressure drop. Protein, a key component of the extracellular matrix, showed a strong correlation with the adhesive strength of mixed species biofilms. Biofilms grown on polyethylene attached more strongly in the early stages of growth than those on glass or steel, which may be due to the greater hydrophobicity of the surface. Chemicals can be used most effectively to weaken the outer layers, and sodium hypochlorite was also shown to be useful for weakening surface adhesion – the required shear stress for 95% removal was reduced by approximately 60% for 5 and 10-day old biofilms. There are more risks associated with chlorine-based disinfectants than the alternative, peracetic acid, although finding a suitable low concentration would be simple using this method.

There is no simple solution, complicated further by the unpredictability of the species present in industrial biofouling. The best way of minimising the risk of spoiling and contamination would be to clean surfaces with regularity, in the region of every 5 days rather than after a more prolonged period,

which would also serve to minimise the resources used by preventing biofilms from becoming too strongly attached or too thick. A chemical input would need to be determined by testing for the optimum concentration necessary for a suitable effect, thus eliminating excess use, and thereby reducing water and energy use in the process. Taking a multispecies sample from a process flow could offer a more realistic approximation of industrial biofilms. Surface coatings to prevent adhesion are the focus of much research, and could be an alternative to reactive methods.

Nomenclature

Symbol	Description	Units
a	Orbital radius of shaking table	m
A	Maximum cell number	[-]
A	Surface area	m^2
AB	Lewis acid-base polar interactions	
AFM	Atomic force microscopy	
ATP	Adenosine tri-phosphate	
BAC	Benzalkonium chloride	
BCA	Bicinchoninic acid	
BHI	Brain-heart infusion	
BR	Brownian movement forces	
BSA	Bovine serum albumin	
CBD	Calgary biofilm device	
CBR	CDC biofilm reactor	
C_d	Discharge coefficient	[-]
CDFF	Continuous depth fluid fermenter	
C_f	Fanning friction factor	[-]
CFD	Computational fluid dynamics	
CFU	Colony-forming units	[-]
c_i	Concentration of chemical species i in solution	
CIP	Cleaning-in-place	
CLSM	Confocal laser scanning microscopy	
COD	Chemical oxygen demand	
CSH	Cell surface hydrophobicity	
DAPI	4',6-diamidino-2-phenylindole	
DBNPA	2,2-dibromo-3-nitrilopropionamide	
DFR	Drip flow reactor	
d_h	Hydraulic diameter of duct	m
DLVO	Derjaguin-Landau-Varwey-Overbeek theory	
DNA	Deoxyribonucleic acid	
DO	Dissolved oxygen	
DSS	Dimethyldichlorosilane	
d_t	Diameter of gauging nozzle	m
d_{tube}	Diameter of gauging tube	m
EDTA	Ethylenediamenetetraacetic acid	
EL	Electrostatic surface charge interactions	
EPDM	Ethylene propylene diene monomer	
EPS	Extracellular polymeric substances	
f	Frequency of shaking table rotation	s^{-1}
FDG	Fluid dynamic gauging	
FISH	Fluorescent *in situ* hybridisation	
FTIR	Fourier transform infrared spectroscopy	
h	Interparticulate distance	m
h	Clearance distance between gauging nozzle and surface	m
H	Hydrostatic head	m
h_0	Clearance distance between nozzle and clean surface	m
HVAC	Heating, ventilation and air conditioning	
I	Ionic strength	Moles
LB-EPS	Loosely-bound EPS	
L_{eff}	Tube effective length	m
LW	Lifschitz-van der Waals interactions	

m	Mass flow rate	$kg.s^{-1}$
m_{actual}	Actual measured flow rate	$kg.s^{-1}$
m_{ideal}	Ideal calculated flow rate	$kg.s^{-1}$
MBC	Minimum bactericidal concentration	parts per million (ppm)
MDPE	Medium density polyethylene	
MIC	Microbially influenced corrosion	
M.I.C.	Minimum inhibitory concentration	parts per million (ppm)
MRD	Modified Robbins device	
n	Number of moles	Moles
n	Number of cell generations	[-]
N	Number of cells in a culture	[-]
N_0	Number of cells in previous generation	[-]
NMR	Nuclear magnetic resonance spectroscopy	
OCT	Optical coherence tomography	
OD	Optical density	
P	Hydrostatic pressure	$kg/(m.s^{-2})$
PBS	Phosphate-buffered saline	
PCA	Plate count agar	
PE	Polyethylene	
PEX	Cross-linked polyethylene	
PFA	Perfluoroalkoxy tatrafluoroethylene	
PMMA	Poly(methyl methacrylate)	
PVC	Poly(vinyl chloride)	
PVDF	Polyvinylidene fluoride	
r	Radial distance from nozzle centre	m
R_a	Average roughness	µm
R_f	Thermal resistance parameter	
R_{rms}	Root mean square roughness	µm
R_z	Average peak-to-valley height	µm
RDE	Rotating disk electrode	
Re	Reynolds number	[-]
RFC	Radial flow cell	
RM	Raman spectroscopy	
RNA	Ribonucleic acid	
RO	Reverse osmosis	
SEM	Scanning electron microscopy	
SEM-EDS	SEM with energy dispersion spectroscopy	
SEPS	Soluble extracellular polymeric substances	
SS	Stainless steel	
SWR	Standard working reagent	
TB-EPS	Tightly-bound extracellular polymeric substances	
TBT	Tributyltin	
TDR	Time-domain reflectometry	
TSB	Tryptic soy broth	
U_m	Mean pipe flow velocity	$m.s^{-1}$
uPVC	Unplasticised poly(vinyl chloride)	
UV	Ultraviolet	
v	Velocity	$m.s^{-1}$
VBNC	Viable but non-culturable cells	
w	Width of gauging nozzle rim	m
XDLVO	Extended DLVO theory	
z	Elevation head	m
z_i	Charge of chemical species i in solution	

zFDG	Zero-discharge fluid dynamic gauging	
α	Angle of gauging nozzle contraction at the tip	^{0}
γ_a	Surface free energy of surface a	
γ_{ab}	Interfacial tension between surfaces a and b	
δ	Fouling layer thickness	m
ΔG	Gibbs free energy	
ΔP_{12}	Pressure drop between points 1 and 2	Pa
θ	Contact angle	^{0}
λ	Cell culture lag period	s, min, hr
λ	Thickness of gauging nozzle rim	m
μ_f	Fluid dynamic viscosity	kg/(m.s)
μ_m	Increase in cell number over time (log gradient)	
µFD	Microfluidic device	
ρ_f	Fluid density	$kg.m^{-3}$
τ_{max}	Maximum applied shear stress	Pa
τ_o	Orbital shear stress on shaking table	Pa
τ_w	Wall shear stress	Pa

Contents

Figures

includes the rotating disc section at the centre, with 14 wells containing the biological samples. The scraper bar serves to exchange bacterial suspension and medium across the wells, and also to remove any surplus from the top.

Figure 14: A CFCC design used by Irving and Allen (2010) to study the formation and development of microalgal biofilms. The apparatus was modified from earlier designs to facilitate the substitution of substrate materials. The chamber was constructed using poly(methyl methacrylate) (PMMA) and attached to a multichannel peristaltic pump with silicone tubing.

Figure 15: A layered schematic of the radial flow cell (RFC), with a 2-dimensional depiction of the complete unit shown below. The fluid inlet is located beneath the cell with a glass disc as a base, and the structure (housing and lid) is built using Plexiglass, a trademarked PMMA formulation (Yung *et al.*, 1999).

Figure 16: A side view schematic of a drip flow reactor as used by Goeres *et al.,* (2009). The required angle of elevation is given by *x*, *a* is the length of the reactor base, *b* is the distance from the bottom of the influent end of the reactor to the laboratory surface, *c* is the distance from the effluent end to the laboratory surface, and *y* is the difference in elevation between *b* and *c*.

Figure 17: A schematic of the FDG nozzle in proximity to a test surface showing the flow stations and dimensions of the nozzle, where h_0 is the distance between the nozzle and the substrate, h is the clearance between the nozzle and the fouling surface, λ is the thickness of the nozzle rim, w is the width of the nozzle rim, d_t is the diameter of the nozzle, α is the angle of the nozzle contraction at the tip, d_{tube} is the diameter of the tube, and m is the mass flow rate of the fluid.

Figure 18: An example of a typical h/d_t vs. C_d plot, showing the two important zones.

Figure 19: A collection of images by Lewis *et al.,* (2012), showing: a) and b) the crater in a cake formed by the filtration of a yeast suspension through a membrane, after study with an FDG nozzle. Part c) is a schematic of the relationship between the nozzle and the crater.

Figure 20: A 96-well microtitre plate of type used for the biofilm viability assays in this section (https://www.edgebio.com/products/96-well-treated-microplates-u-bottom-50063)

Figure 21: Schematics of: a) the FDG apparatus in mass flow mode setup, in which the hydrostatic head, H, is identified as the key operational parameter which determines the pressure driving force controlling the siphon flow; and b) the FDG nozzle in proximity to a test surface, where h is the distance between the nozzle and the deposit surface, h_0 is the distance between the nozzle and the clean surface, w is the width of the nozzle rim, d_t is the nozzle diameter, d_{tube} is the diameter of the siphon tube, and m is the fluid mass flow rate. Points 1 to 4 denote the relevant areas with regards to pressure drop (ΔP).

Figure 22: A diagram showing the method used for making four separate strength measurements on each biofilm sample. Each line relates to a route traced by the FDG nozzle, at a clearance distance equal to the relevant h/d_t value.

Figure 23: An indication of how the thickness of the biofilm can be recorded as the nozzle approaches the surface. The profile of the fouled surface eventually reverts to the same curve as the clean, which represents complete removal of the deposit.

Figure 24: The mean absorbance values (OD600) for each biofilm species tested for the viability assay, with standard deviations added as error bars.

Figure 25: This graph shows the growth curve plotted from the optical density recordings for the *Escherichia coli* and *Burkholderia cepacia* suspended cultures.

Figure 26: C_D calibration curves for the FDG apparatus for the following hydrostatic head values: H = 20, 30, and 60 mm.

Figure 27: A 3D topographic AFM image showing the typical morphology of the polyethylene surface over an area of 25μm^2, along with a side profile of the surface.

Figure 28: A 3D topographic AFM image showing the typical morphology of the steel disc used for the static-grown biofilms over an area of 1μm^2, along with a side profile of the surface.

Figure 29: SEM images taken of the steel disc used in the static biofilm studies, with magnifications of the following resolutions; a) – x2000 and b) – x5500. Samples were gold sputter-coated prior to imaging.

Figure 30: SEM images taken of the steel plate used in the studies of biofilms grown under flow conditions, with magnifications of the following resolutions; a) x50, b) x2000, and c) x5000. Samples were gold sputter-coated prior to imaging.

Figure 31: Contact angle measurements on polyethylene in order to determine the critical surface energy. Image a) is taken using water as the fluid, and b) uses a 15% sodium chloride solution. The recorded angles are a) left = 79.4°, right = 79.6°, and b) left = 88.6°, right = 89.4°

Figure 32: Contact angle measurements on the glass petri dish in order to determine the critical surface energy. Image a) is taken using water as the fluid, and b) uses a 15% sodium chloride solution. The recorded angles are a) left = 8.4°, right = 8.4°, and b) left = 23.6°, right = 19.1°

Figure 33: The protein quantification standard curve taken using the absorbance data relative to BSA quantity shown in Table 5.

Figure 34: The polysaccharide quantification standard curve taken using the absorbance data relative to glucose quantity shown in Table 6.

Figure 35: Quantification of the protein found in isolated EPS samples taken from mixed species biofilms of *E. coli* and *B. cepacia*, and assessed using the cation exchange method and the standard curve in Figure 33. Errors were calculated from standard deviation values taken from the results for multiple biofilms grown for the same time period.

Figure 36: Quantification of the polysaccharide levels found in isolated EPS samples taken from mixed species biofilms of *E. coli* and *B. cepacia*, and assessed using the cation exchange method and the standard curve in Figure 34. Errors were calculated from standard deviation values taken from the results for multiple biofilms grown for the same time period.

Figure 37: Representative Nikon AZ100 optical microscope images of the polystyrene surface with *E. coli* biofilms incubated for five days: tested under FDG at: (a) $h/d_t = 0.3$, $\tau_{max} = 5 \pm 0.2$ Pa; (b) $h/d_t = 0.25$, $\tau_{max} = 8 \pm 0.4$ Pa; (c) $h/d_t = 0.2$, $\tau_{max} = 13 \pm 0.5$ Pa; (d) $h/d_t = 0.15$, $\tau_{max} = 18 \pm 0.6$ Pa. The percentages of biofilm removed at each stage (calculated using ImageJ) were: (a) 4%; (b) 41%; (c) 88%; (d) 99%.

Figure 38: Selected optical microscope images of the glass surface with *E. coli* biofilms incubated for five days: tested under FDG at (a) $h/d_t = 0.23$, $\tau_{max} = 5 \pm 0.2$ Pa; (b) $h/d_t = 0.19$, $\tau_{max} = 7 \pm 0.3$ Pa; (c) $h/d_t = 0.15$, $\tau_{max} = 10 \pm 0.3$ Pa; (d) $h/d_t = 0.11$, $\tau_{max} = 16 \pm 0.4$ Pa. The percentages of biofilm removed at each stage were: (a) 27%; (b) 72%; (c) 84%; (d) 97%.

Figure 39: Selected optical microscope images of *E. coli* biofilms on the stainless steel surface incubated for five days: tested under FDG at (a) $h/d_t = 0.24$, 5 ± 0.1 Pa (b) $h/d_t = 0.2$, 7 ± 0.3 Pa (c) $h/d_t = 0.15$, 13 ± 0.4 Pa (d) $h/d_t = 0.08$, 23 ± 0.5 Pa. The percentages of biofilm removed at each stage were: (a) 26%; (b) 43%; (c) 73%; (d) 100%.

Figure 40: The complete set of strength test results for *Escherichia coli* biofilms grown for a 5-day period on polyethylene, glass and stainless steel. A line to indicate the presence of two phases of removal has been added.

Figure 41: The complete set of strength test results for *Escherichia coli* biofilms grown for a 10 day period on polyethylene, glass and stainless steel.

Figure 42: The complete set of strength test results for *Escherichia coli* biofilms grown for a 14 day period on polyethylene, glass and stainless steel.

Figure 43: The complete set of strength test results for *Escherichia coli* biofilms grown for a 21 day period on polyethylene, glass and stainless steel.

Figure 44: The complete set of strength test results for *Escherichia coli* biofilms grown for a 28 day period on polyethylene, glass and stainless steel.

Figure 45: The overall strength test results for *Escherichia coli* biofilms grown on all three test surfaces shown, in terms of the shear stress required in order to remove 50% and 95% of the surface coverage. Values for the equivalent pipe flow velocity (using equation 23) are shown for selected data points (ms^{-1}).

Figure 46: Selected optical microscope images of *B. cepacia* biofilms grown on polyethylene for 5 days: tested under FDG at (a) h/d_t = 0.26, 4 ± 0.4 Pa (b) h/d_t = 0.21, 7 ± 0.1 Pa (c) h/d_t = 0.16, 11 ± 0.2 Pa (d) h/d_t = 0.11, 15 ± 0.1 Pa. The percentages of biofilm removed at each stage were: (a) 38%; (b) 60%; (c) 77%; (d) 99%.

Figure 47: Selected optical microscope images of *B. cepacia* biofilms grown on glass for 5 days: tested under FDG at (a) h/d_t = 0.26, 4 ± 0.4 Pa (b) h/d_t = 0.22, 6 ± 0.3 Pa (c) h/d_t = 0.17, 9 ± 0.4 Pa (d) h/d_t = 0.12, 14 ± 0.4 Pa. The percentages of biofilm removed at each stage were: (a) 25%; (b) 42%; (c) 74%; (d) 97%.

Figure 48: Selected optical microscope images of *B. cepacia* biofilms grown on stainless steel for 5 days: tested under FDG at (a) h/d_t = 0.25, 4 ± 0.2 Pa (b) h/d_t = 0.2, 7 ± 0.3 Pa (c) h/d_t = 0.15, 12 ± 0.3 Pa (d) h/d_t = 0.1, 16 ± 0.2 Pa. The percentages of biofilm removed at each stage were: (a) 14%; (b) 53%; (c) 91%; (d) 100%.

Figure 49: The complete set of strength test results for *Burkholderia cepacia* biofilms grown for 5 days on polyethylene, glass and stainless steel.

Figure 50: The complete set of strength test results for *Burkholderia cepacia* biofilms grown for 10 days on polyethylene, glass and stainless steel.

Figure 51: The complete set of strength test results for *Burkholderia cepacia* biofilms grown for 14 days on polyethylene, glass and stainless steel.

Figure 52: The complete set of strength test results for *Burkholderia cepacia* biofilms grown for 21 days on polyethylene, glass and stainless steel.

Figure 53: The complete set of strength test results for *Burkholderia cepacia* biofilms grown for 28 days on polyethylene, glass and stainless steel.

Figure 54: The overall strength test results for *Burkholderia cepacia* biofilms grown on all three test surfaces shown, in terms of the shear stress required in order to remove 50% and 95% of the surface coverage. Values for the equivalent pipe flow velocity are shown for selected data points (ms^{-1}).

Figure 55: Selected optical microscope images of mixed species biofilms grown on polyethylene for 5 days: tested under FDG at (a) h/d_t = 0.25, 4 ± 0.2 Pa (b) h/d_t = 0.20, 6 ± 0.1 Pa (c) h/d_t = 0.15, 12 ±

0.2 Pa (d) h/d_t = 0.10, 14 ± 0.4 Pa. The percentages of biofilm removed at each stage were: (a) 9%; (b) 45%; (c) 91%; (d) 100%.

Figure 56: Selected optical microscope images of mixed species biofilms grown on glass for 5 days: tested under FDG at (a) h/d_t = 0.25, 4 ± 0.5 Pa (b) h/d_t = 0.21, 5 ± 0.2 Pa (c) h/d_t = 0.15, 12 ± 0.2 Pa (d) h/d_t = 0.1, 14 ± 0.5 Pa. The percentages of biofilm removed at each stage were: (a) 17%; (b) 59%; (c) 94%; (d) 100%.

Figure 57: Selected optical microscope images of mixed species biofilms grown on stainless steel for 5 days: tested under FDG at (a) h/d_t = 0.25, 4 ± 0.5 Pa (b) h/d_t = 0.17, 10 ± 0.2 Pa (c) h/d_t = 0.1, 15 ± 0.2 Pa (d) h/d_t = 0.06, 19 ± 0.5 Pa. The percentages of biofilm removed at each stage were: (a) 23%; (b) 78%; (c) 95%; (d) 100%.

Figure 58: The complete set of strength test results for mixed species biofilms grown for 5 days on polyethylene, glass and stainless steel.

Figure 59: The complete set of strength test results for mixed species biofilms grown for 10 days on polyethylene, glass and stainless steel.

Figure 60: The complete set of strength test results for mixed species biofilms grown for 14 days on polyethylene, glass and stainless steel.

Figure 61: The complete set of strength test results for mixed species biofilms grown for 21 days on polyethylene, glass and stainless steel.

Figure 62: The complete set of strength test results for mixed species biofilms grown for 28 days on polyethylene, glass and stainless steel.

Figure 63: The overall strength test results for mixed species biofilms grown on all three test surfaces shown, in terms of the shear stress required in order to remove 50% and 95% of the surface coverage. Values for the equivalent pipe flow velocity are shown for selected data points (ms^{-1}).

Figure 64: A comparison of the estimated wall shear stress required to remove 95% (from surface coverage analysis using ImageJ) of *E. Coli*, *B. cepacia*, and mixed species biofilms grown on: (a) polyethylene, (b) glass and (c) stainless steel, after a range of incubation times. The error bars take into account the potential inaccuracy of the interpolation, and the scope for experimental errors.

Figure 65: A comparison of the estimated wall shear stress required to remove 95% of *B. cepacia* and mixed species biofilms from polyethylene, glass and stainless steel surfaces after a range of incubation times.

Figure 66: Comparisons between adhesive strength values and recorded amounts of a) protein and b) glucose in the equivalent biofilm samples. All data are taken from mixed species biofilms. The incubation periods (in days) are shown in the labels.

Figure 67: Graphs showing the average thickness of a) *E. coli*; b) *B. cepacia*; and c) mixed species biofilms as measured by FDG. The error bars show the minimum and maximum thicknesses measured for each incubation period.

Figure 68: Comparisons between biofilm thickness and recorded amounts of a) protein and b) glucose in the equivalent biofilm samples. All data are taken from mixed species biofilms. The incubation periods (in days) are shown in the labels.

Figure 69: The percentage of biofilm thickness reduction in terms of the estimated wall shear stress deduced from the mass flow rate at the respective nozzle clearance (h/d_t), for a biofilm of *E. coli* grown for 14 days on a polyethylene surface.

Figure 70: The percentage of biofilm thickness reduction in terms of the estimated wall shear stress deduced from the mass flow rate at the respective nozzle clearance (h/d_t), for a mixed species biofilm grown for 14 days on a glass surface.

Figure 71: A graph showing how the discharge coefficient (C_d) relative to the dimensionless nozzle clearance distance (h/d_t) differs compared to a calibration plot due to the presence of a *B. cepacia* biofilm grown for 10 days on stainless steel.

Figure 72: The estimated wall shear stress and selected equivalent mean pipe flow velocities in brackets (ms^{-1}) required to remove 50%, and 95% of *E. coli* biofilm thickness from glass, polyethylene and stainless steel, after a range of incubation periods. The error bars take into account the potential inaccuracy of the logarithmic interpolation and the scope for experimental errors.

Figure 73: The estimated wall shear stress and selected equivalent mean pipe flow velocities in brackets (ms^{-1}) required to remove 50%, and 95% of *B. cepacia* biofilm thickness from glass, polyethylene and stainless steel, after a range of incubation periods. The error bars take into account the potential inaccuracy of the logarithmic interpolation and the scope for experimental errors.

Figure 74: The estimated wall shear stress and selected equivalent mean pipe flow velocities in brackets (ms^{-1}) required to remove 50%, and 95% of mixed species biofilm thickness from glass, polyethylene and stainless steel, after a range of incubation periods. The error bars take into account the potential inaccuracy of the logarithmic interpolation and the scope for experimental errors.

Figure 75: Comparisons between cohesive strength values and recorded amounts of a) protein and b) glucose in the equivalent biofilm samples. All data are taken from mixed species biofilms. The incubation periods (in days) are shown in the labels.

Figure 76: CLSM images showing the extent of EPS coverage on *E. coli* biofilms grown on glass for (a) 14 days; and (b) 21 days.

Figure 77: CLSM images showing the presence of live and dead cells in *E. coli* biofilms grown on glass for (a) 14 days; and (b) 21 days. Live cells are stained green, dead cells are stained red.

Figure 78: Birds-eye and side view designs of the drip flow reactor chamber, with the upper and lower sections of the chamber shown separately in the side view. The dotted lines represent cavities and hollow regions in the chamber. The raised section of the lower chamber shows where the growth surface is located. All dimensions are in millimetres.

Figure 79: A side view of the drip flow reactor, situated on its accompanying stand tilted at a 10 degree angle. The dotted lines represent cavities and hollow regions in the chamber.

Figure 80: The spread of media flow rates recorded from the drip flow reactor with the preceding valve opened as minimally as possible. Volumes were recorded over 10 minute periods, of 30 instances.

Figure 81: The relationship between the set temperature of the water bath and the recorded temperature within the drip flow reactor.

Figure 82: a) Pressure drop recordings and b) C_D calibration curves for the pressure mode FDG apparatus for the following mass flow rates: m = 0.5, 1, and 2 g/s. The size of the symbols represents the potential for errors in the use of the stopwatch and balance.

Figure 83: A 3D topographic AFM image, a), showing the morphology of a glass coverslip used for biofilm growth under flow conditions, over an area of 4 μm^2, along with a side profile of the surface (b)).

Figure 84: A 3D topographic AFM image showing the typical morphology of the stainless steel 316 plate used for growing biofilms under flow conditions, over an area of 1μm^2, along with a side profile of the surface.

Figure 85: Optical microscope images of *E. coli* biofilms grown under flow on polyethylene for 5 days: tested under FDG at (a) $h/d_t = 0.25$, $\tau_w = 4 \pm 0.1$ Pa (b) $h/d_t = 0.18$, $\tau_w = 9 \pm 0.4$ Pa (c) $h/d_t = 0.11$, $\tau_w = 16 \pm 0.2$ Pa (d) $h/d_t = 0.08$, $\tau_w = 21 \pm 0.4$ Pa. The percentages of biofilm removed at each stage, measured using ImageJ, were: (a) 9%; (b) 46%; (c) 83%; (d) 96%.

Figure 86: Optical microscope images of the glass surface with *E. coli* biofilms incubated under flow for 5 days: tested under FDG at (a) $h/d_t = 0.23$, $\tau_w = 5 \pm 0.4$ Pa; (b) $h/d_t = 0.18$, $\tau_w = 10 \pm 0.5$ Pa; (c) $h/d_t = 0.12$, $\tau_w = 15 \pm 0.1$ Pa; (d) $h/d_t = 0.11$, $\tau_w = 18 \pm 0.2$ Pa. The percentages of biofilm removed at each stage were: (a) 21%; (b) 55%; (c) 88%; (d) 94%.

Figure 87: Optical microscope images of *E. coli* biofilms on the polished stainless steel plate under flow for 5 days: tested under FDG at (a) $h/d_t = 0.21$, $\tau_w = 8 \pm 0.2$ Pa (b) $h/d_t = 0.15$, $\tau_w = 14 \pm 0.1$ Pa (c) $h/d_t = 0.12$, $\tau_w = 19 \pm 0.1$ Pa (d) $h/d_t = 0.08$, $\tau_w = 25 \pm 0.2$ Pa. The percentages of biofilm removed at each stage were: (a) 39%; (b) 68%; (c) 86%; (d) 100%.

Figure 88: The complete set of strength test results for *Escherichia coli* biofilms grown for a 5-day period on polyethylene, glass and stainless steel, using the drip flow reactor.

Figure 89: The complete set of strength test results for *Escherichia coli* biofilms grown for a 10 day period on polyethylene, glass and stainless steel, using the drip flow reactor.

Figure 90: The complete set of strength test results for *Escherichia coli* biofilms grown for a 14 day period on polyethylene, glass and stainless steel, using the drip flow reactor.

Figure 91: The overall strength test results for *Escherichia coli* biofilms grown under drip flow on all three test surfaces shown, in terms of the shear stress required in order to remove 50% and 95% of the surface coverage. Values for the equivalent pipe flow velocity are shown for selected data points (ms^{-1}).

Figure 92: A comparison between the strength test results for *Escherichia coli* biofilms grown under drip flow and under static conditions, on all three test surfaces, shown in terms of the shear stress required in order to remove 95% of the surface coverage.

Figure 93: A comparison between the strength test results for *Escherichia coli* biofilms grown under drip flow and under static conditions, on all three test surfaces, shown in terms of the shear stress required to remove 50% of the surface coverage.

Figure 94: Optical microscope images of mixed species biofilms grown on polyethylene under flow for 5 days: tested under FDG at (a) $h/d_t = 0.24$, $\tau_w = 5 \pm 0.3$ Pa (b) $h/d_t = 0.17$, $\tau_w = 9 \pm 0.1$ Pa (c) $h/d_t = 0.14$, $\tau_w = 12 \pm 0.1$ Pa (d) $h/d_t = 0.1$, $\tau_w = 16 \pm 0.5$ Pa. The percentages of biofilm removed at each stage were: (a) 10%; (b) 49%; (c) 78%; (d) 94%.

Figure 95: Optical microscope images of mixed species biofilms grown on glass under flow for 5 days: tested under FDG at (a) $h/d_t = 0.24$, $\tau_w = 5 \pm 0.4$ Pa (b) $h/d_t = 0.17$, $\tau_w = 9 \pm 0.2$ Pa (c) $h/d_t = 0.14$, $\tau_w = 11 \pm 0.4$ Pa (d) $h/d_t = 0.11$, $\tau_w = 14 \pm 0.1$ Pa. The percentages of biofilm removed at each stage were: (a) 20%; (b) 53%; (c) 77%; (d) 99%.

Figure 96: Optical microscope images of mixed species biofilms grown under flow on stainless steel for 5 days: tested under FDG at (a) $h/d_t = 0.22$, $\tau_w = 6 \pm 0.3$ Pa (b) $h/d_t = 0.16$, $\tau_w = 10 \pm 0.4$ Pa (c) $h/d_t = 0.11$, $\tau_w = 16 \pm 0.4$ Pa (d) $h/d_t = 0.08$, $\tau_w = 20 \pm 0.3$ Pa. The percentages of biofilm removed at each stage were: (a) 18%; (b) 47%; (c) 86%; (d) 99%.

Figure 97: The complete set of strength test results for mixed species biofilms grown for 5 days on polyethylene, glass and stainless steel, using the drip flow reactor.

Figure 98: The complete set of strength test results for mixed species biofilms grown for 10 days on polyethylene, glass and stainless steel, using the drip flow reactor.

Figure 99: The complete set of strength test results for mixed species biofilms grown for 14 days on polyethylene, glass and stainless steel, using the drip flow reactor.

Figure 100: The overall strength test results for mixed species biofilms grown under drip flow on all three test surfaces shown, in terms of the shear stress required in order to remove 50% and 95% of the surface coverage. Values for the equivalent pipe flow velocity are shown for selected data points (ms^{-1}).

Figure 101: A comparison between the strength test results for mixed species biofilms grown under drip flow and under static conditions, on all three test surfaces, shown in terms of the shear stress required in order to remove 95% of the surface coverage.

Figure 102: A comparison between the strength test results for mixed species biofilms grown under drip flow and under static conditions, on all three test surfaces, shown in terms of the shear stress required in order to remove 50% of the surface coverage.

Figure 103: A comparison of the estimated wall shear stress required to remove 95% (from surface coverage analysis using ImageJ) of *E. Coli* and mixed species biofilms grown under drip flow conditions on: (a) polyethylene, (b) glass and (c) stainless steel, after a range of incubation times. The error bars take into account the potential inaccuracy of the interpolation, and the scope for experimental errors.

Figure 104: Comparisons between adhesive strength values and recorded amounts of a) protein and b) glucose in the equivalent biofilm samples grown under flow conditions. All data are taken from mixed species biofilms. The incubation periods (in days) are shown in the labels.

Figure 105: Graphs showing the average thickness of a) *E. coli*; and b) mixed species biofilms grown under flow conditions as measured by FDG. The error bars show the minimum and maximum thicknesses measured for each incubation period.

Figure 106: Graphs comparing the average thicknesses of a) *E. coli*; and b) mixed species biofilms grown under static and flow conditions as measured by FDG.

Figure 107: The percentage of biofilm thickness reduction in terms of the estimated wall shear stress deduced from the mass flow rate at the respective nozzle clearance (h/d_t), for a mixed species biofilm

grown for 10 days under drip flow on a polyethylene surface. The lines added indicate the two distinct phases of removal – rapid initial depletion and a slower removal of the surface layers.

Figure 108: The percentage of biofilm thickness reduction in terms of the estimated wall shear stress deduced from the mass flow rate at the respective nozzle clearance (h/d_t), for a biofilm of *E. coli* grown for 14 days under drip flow on a stainless steel surface, with the two phases indicated again.

Figure 109: The estimated wall shear stress and selected equivalent mean pipe flow velocities in brackets (ms^{-1}) required to remove 50%, and 95% of *E. coli* biofilm thickness from glass, polyethylene and stainless steel, after a range of incubation periods. The error bars take into account the potential inaccuracy of the logarithmic interpolation and the scope for experimental errors.

Figure 110: The estimated wall shear stress and selected equivalent mean pipe flow velocities in brackets (ms^{-1}) required to remove 50%, and 95% of mixed species biofilm thickness from glass, polyethylene and stainless steel, after a range of incubation periods. The error bars take into account the potential inaccuracy of the logarithmic interpolation and the scope for experimental errors.

Figure 111: A comparison between the thickness test results for *Escherichia coli* biofilms grown under drip flow and under static conditions, on all three test surfaces, shown in terms of the shear stress required in order to remove 95% of the surface coverage.

Figure 112: A comparison between the thickness test results for *Escherichia coli* biofilms grown under drip flow and under static conditions, on all three test surfaces, shown in terms of the shear stress required in order to remove 50% of the surface coverage.

Figure 113: A comparison between the thickness test results for mixed species biofilms grown under drip flow and under static conditions, on all three test surfaces, shown in terms of the shear stress required in order to remove 95% of the surface coverage.

Figure 114: A comparison between the thickness test results for mixed species biofilms grown under drip flow and under static conditions, on all three test surfaces, shown in terms of the shear stress required in order to remove 50% of the surface coverage.

Figure 115: A comparison of the estimated wall shear stress required to remove 95% thickness of *E. Coli* and mixed species biofilms grown under drip flow conditions on: (a) polyethylene, (b) glass and (c) stainless steel, after a range of incubation times. The error bars take into account the potential inaccuracy of the interpolation, and the scope for experimental errors.

Figure 116: Comparisons between cohesive strength values and recorded amounts of a) protein and b) glucose in the equivalent duct flow biofilm samples. All data are taken from mixed species biofilms. The incubation periods (in days) are shown in the labels.

Figure 117: Optical microscope images of mixed species biofilms grown under flow on stainless steel for 14 days and exposed to 100 mg/L sodium hypochlorite: tested under FDG at (a) $h/d_t = 0.25$, $\tau_w = 4 \pm 0.5$ Pa (b) $h/d_t = 0.21$, $\tau_w = 6 \pm 0.4$ Pa (c) $h/d_t = 0.15$, $\tau_w = 11 \pm 0.4$ Pa (d) $h/d_t = 0.1$, $\tau_w = 15 \pm 0.1$ Pa. The percentages of biofilm removed at each stage were: (a) 23%; (b) 52%; (c) 84%; (d) 97%.

Figure 118: The complete set of strength test results for mixed species biofilms grown on stainless steel using the drip flow reactor, after being exposed to a 100 mg/L sodium hypochlorite solution for 15 minutes and removed using FDG.

Figure 119: Optical microscope images of mixed species biofilms grown under flow on stainless steel for 14 days and exposed to 1000 mg/L sodium hypochlorite: tested under FDG at (a) $h/d_t = 0.25$, $\tau_w = 4 \pm 0.4$ Pa (b) $h/d_t = 0.20$, $\tau_w = 7 \pm 0.4$ Pa (c) $h/d_t = 0.16$, $\tau_w = 10 \pm 0.1$ Pa (d) $h/d_t = 0.12$, $\tau_w = 13 \pm 0.4$ Pa. The percentages of biofilm removed at each stage were: (a) 30%; (b) 53%; (c) 86%; (d) 100%.

Figure 120: The complete set of strength test results for mixed species biofilms grown on stainless steel using the drip flow reactor, after being exposed to a 1000 mg/L sodium hypochlorite solution for 15 minutes and removed using FDG.

Figure 121: The shear stress required to remove 95% surface coverage of mixed species biofilms grown under drip flow on stainless steel, comparing the effect of exposure to sodium hypochlorite on adhesive strength.

Figure 122: Optical microscope images of mixed species biofilms grown under flow on stainless steel for 14 days and exposed to 100 mg/L peracetic acid: tested under FDG at (a) $h/d_t = 0.25$, $\tau_w = 4 \pm 0.2$ Pa (b) $h/d_t = 0.18$, $\tau_w = 10 \pm 0.4$ Pa (c) $h/d_t = 0.11$, $\tau_w = 17 \pm 0.3$ Pa (d) $h/d_t = 0.06$, $\tau_w = 23 \pm 0.2$ Pa. The percentages of biofilm removed at each stage were: (a) 28%; (b) 73%; (c) 86%; (d) 94%.

Figure 123: The complete set of strength test results for mixed species biofilms grown on stainless steel using the drip flow reactor, after being exposed to a 100 mg/L peracetic acid solution for 15 minutes and removed using FDG.

Figure 124: Optical microscope images of mixed species biofilms grown under flow on stainless steel for 14 days and exposed to 1000 mg/L peracetic acid: tested under FDG at (a) $h/d_t = 0.25$, $\tau_w = 4 \pm 0.2$ Pa (b) $h/d_t = 0.18$, $\tau_w = 10 \pm 0.1$ Pa (c) $h/d_t = 0.12$, $\tau_w = 16 \pm 0.4$ Pa (d) $h/d_t = 0.06$, $\tau_w = 23 \pm 0.1$ Pa. The percentages of biofilm removed at each stage were: (a) 24%; (b) 63%; (c) 86%; (d) 99%.

Figure 125: The complete set of strength test results for mixed species biofilms grown on stainless steel using the drip flow reactor, after being exposed to a 1000 mg/L peracetic acid solution for 15 minutes and removed using FDG.

Figure 126: The shear stress required to remove 95% surface coverage of mixed species biofilms grown under drip flow on stainless steel, comparing the effect of exposure to peracetic acid on adhesive strength.

Figure 127: The percentage of biofilm thickness reduction in terms of the estimated wall shear stress deduced from the mass flow rate at the respective nozzle clearance (h/d_t), for a mixed species biofilm grown for 14 days under drip flow on a stainless steel surface. The biofilm was initially exposed to 1000 mg/L sodium hypochlorite for 15 minutes.

Figure 128: The shear stress required to remove 95% thickness of mixed species biofilms grown under drip flow on stainless steel, comparing the effect of exposure to sodium hypochlorite on cohesive strength.

Figure 129: The percentage of biofilm thickness reduction in terms of the estimated wall shear stress deduced from the mass flow rate at the respective nozzle clearance (h/d_t), for a mixed species biofilm grown for 14 days under drip flow on stainless steel. The biofilm was initially exposed to 1000 mg/L peracetic acid for 15 minutes.

Figure 130: The shear stress required to remove 95% thickness of mixed species biofilms grown under drip flow on stainless steel, comparing the effect of exposure to peracetic acid on cohesive strength.

Figure 131: An estimate of the total required contribution of water and sodium hydroxide to remove 95% surface coverage of mixed species biofilms from stainless steel, as the concentration of NaClO is increased from zero to 1000 mg/L. Equal weighting is given to the two components when producing the Total curve.

Figure 132: An estimate of the total required contribution of water and peracetic acid to remove 95% surface coverage of mixed species biofilms from stainless steel, as the concentration of PAA is increased from zero to 1000 mg/L. Equal weighting is given to the two components when producing the Total curve.

Figure 133: The result from the experiment undertaken to determine the effective length of the curved siphon tube. The mass flow rate is controlled via the hydrostatic head, and the pressure drop displayed is that for the unknown section of tubing. The equation of the trend line is included to show the gradient of the line.

Figure 134: The full set of contact angle measurements on polyethylene in order to determine the critical surface energy. From top to bottom: water, 5%, 10% and 15% sodium chloride

Figure 135: The full set of contact angle measurements on the stainless steel disc in order to determine the critical surface energy. From top to bottom: water, 5%, 10% and 15% sodium chloride

Figure 136: The full set of contact angle measurements on the stainless steel plate in order to determine the critical surface energy. From top to bottom: water, 5%, 10% and 15% sodium chloride

Figure 137: The full set of contact angle measurements on the glass petri dish in order to determine the critical surface energy. From top to bottom: water, 5%, 10% and 15% sodium chloride

Figure 138: The full set of contact angle measurements on the glass coverslip in order to determine the critical surface energy. From top to bottom: water, 5%, 10% and 15% sodium chloride

Figure 139: Zisman plots shown for the five surfaces examined for contact angles using water and 5, 10 and 15 % sodium chloride solutions: a) polyethylene; b) steel disc; c) steel plate; d) glass dish, and e) glass coverslip. The equations of the trendlines are shown as these indicate the means of calculating the critical surface areas.

Figure 140: A graph showing how the discharge coefficient (C_d) relative to the dimensionless nozzle clearance distance (h/d_t) differs compared to a calibration plot due to the presence of a biofilm. This particular biofilm was of *E. coli* grown for 14 days on a polyethylene surface.

Figure 141: A graph showing how the discharge coefficient (C_d) relative to the dimensionless nozzle clearance distance (h/d_t) differs compared to a calibration plot due to the presence of a mixed species biofilm grown for 14 days on a glass surface.

Tables

Table 1: Typical proportions of biofilm EPS constituents by mass (Sutherland 2001).

Table 2: The full set of absorbance value recorded for the biofilm viability assay. The mean and standard deviation results for each species are displayed in the bottom two rows, with the raw data and control values shown in Appendix 3.

Table 3: The R_a (average roughness), R_{ms} (root mean square roughness) and R_z (average peak-to-valley height) values for the polyethylene petri dish and the steel disc.

Table 4: The full set of contact angle results and air-liquid surface tensions, and the critical surface tensions in bold in the bottom row.

Table 5: The raw absorbance data relative to the quantity of BSA. The value for BSA = 0 (pure water) is subtracted from each value for the protein quantification standard curve.

Table 6: The raw absorbance data relative to the quantity of glucose. The value for glucose = 0 (pure water) is subtracted from each value for the polysaccharide quantification standard curve.

Table 7: The full set of average shear stress values required to remove 50% and 95% surface coverage of *E. coli*, *B. cepacia*, and mixed species biofilms grown under static conditions from polyethylene, glass and stainless steel.

Table 8: The full set of shear stress values required to remove 50% and 95% thickness of *E. coli*, *B. cepacia*, and mixed species biofilms grown under static conditions from polyethylene, glass and stainless steel.

Table 9: The R_a (average roughness), R_{ms} (root mean square roughness) and R_z (average peak-to-valley height) values for the polyethylene petri dish (shown in Section 5.4.1), the steel plate, and the glass coverslip. The data for the steel disc from Section 5.4.1 is also shown as a comparison.

Table 10: The full set of average shear stress values required to remove 50% and 95% surface coverage of *E. coli* and mixed species biofilms grown under drip flow conditions from polyethylene, glass and stainless steel.

Table 11: The full set of average shear stress values required to remove 50% and 95% thickness of *E. coli*, *B. cepacia*, and mixed species biofilms grown under drip flow conditions from polyethylene, glass and stainless steel.

Table 12: The components present in the M9 media used to grow biofilms throughout this research, and the ionic strengths of each component.

Table 13: The full set of absorbances taken from the biofilm assay conducted in order to compare the species *Escherichia coli* Nissle1917, *Pseudomonas aeruginosa* NCTC and *P. aeruginosa* PA01

1. INTRODUCTION

1.1 Context

Biofouling has been described as "the unwanted accumulation of biological material on man-made surfaces" (Flemming *et al.*, 2008). The biological materials can generally be classified into two groups; microorganisms (i.e. bacteria, fungi, algae), which form biofilms; and macro-organisms such as tubeworms and barnacles. In the context of fouling and cleaning, biofouling is the "accumulation of biological matter on a surface by growth and/or deposition to a level that causes operational problems including increased pressure drop across the system resulting in a reduction in the permeate production" (Ngene *et al.*, 2010).

Biofouling is observed in a vast selection of fields: food and pharmaceutical production, shipping, steel, petrochemicals, water desalination, and drinking water treatment and distribution (Henderson 2010). Taking the food industry as an example, biofilms can grow in a number of places including pipe bends, conveyor belts, floors and rubber seals, all surfaces which are exposed to local bacteria inhabitation (Blanchard *et al.*, 1998). Biofilm formation on conveyor belts has the potential to contaminate and impact upon food quality, such as colonies on an egg glaze or multi-layer biofilms on a baked bean line (Holah *et al.*, 1989, cited by Blanchard *et al.*, 1998). Spoiling and pathogenic bacteria can form biofilms on process surfaces, leading to product contamination, or at least deterioration in the colour, texture or taste of the food (Bott 1995). As well as the process equipment, cultures can also thrive on ceilings (as a result of condensation), gutters and drains of food processing facilities. Hygiene requirements in consumer industries (chiefly food, pharmaceuticals and water supplies) are stringent, and the ability of many micro-organisms to attach to existing layers can pose serious dangers for consumers (Chew *et al.*, 2004a) and can also harm the quality of the finished products. Instances of industrial biofouling are shown in Figure 1, inside a pipeline and a condenser tube.

Figure 1: a) Microbially-influenced corrosion inside an oil refinery pipeline (MERUS 2011). b) Biofouling inside a condenser tube (Daniels and Selby 2007)

By the nature of their existence, biofilms are particularly difficult to remove, and eliminating the risk of their persistence is virtually impossible. Typically, the atmospheric conditions found in processing plants are ideal for the proliferation of bacteria and the growth of biofilms, which makes the challenges regarding effective removal more difficult. The use of chemical disinfectants, most commonly chlorine-based, is still dominant in biofouling removal in industry, although the limitations of these methods (intrinsic resistance, chemical reactions with the biofilm matrix and corrosion products, the re-growth and persistence of cells, and contamination of sewage flows) are more widely observed (Lazarova *et al.*, 1999). Mechanical methods can often be a worthwhile alternative. Jets and lances can be used to apply water at force to a surface, although the water can energy demand can be large (Burfoot and Middleton 2009). 'Pigging' involves forcing a solid object through a fouled pipe and can be useful, albeit sometimes restricted by geometry and risking huge costs in the case of a blockage (O'Donoghue, 2003). Enzymes are able to structurally undermine biofilms to enable easier removal, although their specificity dictates that it can be difficult to use enzymes to target a diverse microbiological culture (Simões *et al.*, 2010).

The following research is concerned with the accumulation of biofilms formed on a selection of surfaces, and how efficiently they can be removed whilst maintaining a commitment to pursue Green Cleaning ideas and reduce chemical, water and energy use. In order to propose sustainable cleaning protocols for biofouling removal, biofilms were tested for their attachment and removal behaviour. The primary technique used was fluid dynamic gauging (FDG), a non-contact gauging method of conducting *in situ* characterisation of soft fouling layers with the additional advantage of requiring little in the way of prior knowledge of the deposit properties. Biofilms were grown on three different surfaces (polyethylene, glass and stainless steel) both on a shaking incubator and in a duct flow system. FDG-based testing was combined with other analytical methods, chiefly microscopic observation and surface and biofilm composition testing.

1.2 Structure of Report

In Chapter 2, a review of existing literature will be conducted to present an overview of biofilm attachment and growth processes, followed by the methods of cleaning and characterisation available. A description of the chosen analytical method will conclude the section. The aims and objectives of the research will then be outlined in Chapter 3.

The experimental section is divided into two sections. Firstly, the studies related to static-grown biofilms are described with the methods involved (Chapter 4) followed by a display of the results and related discussion points (Chapter 5). Similar sections follow concerning biofilms grown under duct flow conditions with the same sub-sections (Chapters 6 and 7). Finally, concluding remarks have been made with the ultimate aim of developing 'green cleaning' protocols for biofouling removal (Chapter 8).

2. LITERATURE REVIEW

2.1 Biofilms

Biofilms are the most successful form of biological life, measured by their success and omnipresence, and have the highest survival potential (Flemming 2011). The phenomenon of attachment was first observed by Zobell (1943) who noted a fall in the number of free-swimming bacteria in water when the water was transferred to a bottle, whilst the number of attached cells increased. The establishment of biofilms is a highly active process, and it has been established that the ratio of planktonic to biofilm-based cells in water distribution systems may be in the region of 1:1000 (Momba *et al.*, 2000). It is estimated that up to 97% of the single-celled organisms on Earth are associated with minerals rather than existing in the planktonic (free swimming) state (Nannipieri *et al.*, 2003).

The biofilm is therefore the standard mode of bacterial growth and proliferation in nature. The accumulation of biofilms on process surfaces requires a different set of explanations from those employed to tackle other fouling mechanisms such as phase transitions, scale formation, or corrosion (Characklis 1981). The dynamics of biofilm development carry with them a range of features which make negation of biofouling a wholly different challenge. Firstly, the intrinsic defence and re-growth mechanisms which biofilms benefit from ensure that their removal is markedly more difficult, and additionally the local conditions present in most industrial processes (e.g. temperature, humidity) provide an ideal environment for biofilm development.

2.2 Formation and Organisation of Biofilms

Within a system, bacteria are found as both floating cells (planktonic) or attached to a surface (biofilm), as shown on a basic level in Figure 2.

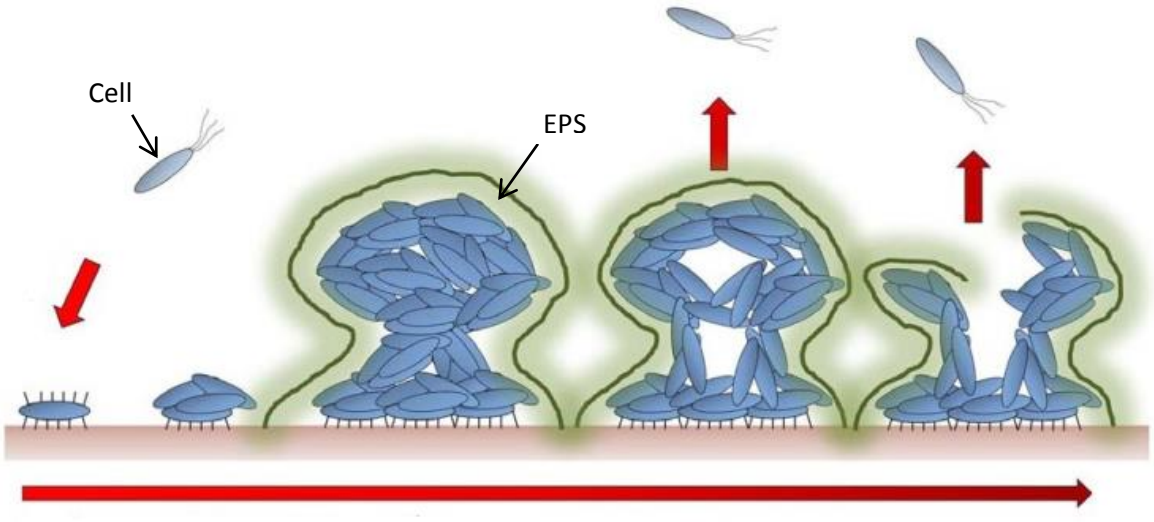

Figure 2: The cycle of biofilm attachment, maturity, detachment and eventual re-attachment (Garnett and Matthews 2012).

There are a number of ways in which biofilm organisms differ from their planktonic counterparts in terms of phenotype (characteristics). The function and activity of a biofilm is dependent on a much wider range of factors: individual bacteria reaction rates; the matrix structure; transportation into and within the biofilm; the composition of the matrix, and cell interactions (Chen and Chen 2000). A key factor in the complexity of the 3-D structure lies in the interaction of the biological, physical and chemical processes amongst the various spatial features (Costerton *et al.,* 1995). Essentially, biofilm cells live in an environment of metabolic cooperation and with a basic circulation system, and it is the reaction to their situation which defines the differences from planktonic cells (Kurzbaum *et al.,* 2010). Biofilms can develop advanced physical structures – aquatic cultures are regularly noted to assume a 'mushroom-like' appearance (Costerton *et al.,* 1994). To achieve this, cells accumulate in stalks normal to the substrate, accounting for the enhanced thickness, and this often occurs in conjunction with surrounding channels allowing for fluid (nutrient) flow (Stoodley *et al.,* 1994). This structure is noted to allow for effective cell to cell communication (Davies *et al.,* 1998). Ultimately, the morphology of a biofilm is dependent on a selection of the following conditions: nutrient availability, flow rate, temperature, and pH. They exhibit complex rheologies, usually dependent on the fluid shear during growth, and changes in the ionic envrionment (Stoodley *et al.,* 2002b). This may vary over time, dependent chiefly on the nutrients available and alterations in flow velocity (Melo and Bott 1997). In environments which lack a prevailing bulk fluid flow (soil, food etc.), biofilms tend to be denser and more uniform colonies (Auerbach *et al.,* 2000), and diffusion at the air-biofilm interface dominates mass transfer processes (Holden *et al.,* 1997). This enivronment-dependent variability is the most immediately apparent way in which biofilms pose more complex questions than planktonic cultures. The cells, combined with the extracellular matrix, behave in a manner similar to viscoelastic fluids, exhibiting irreversible viscous deformation and reversible elastic response, which serve to enhance the biofilm's mechanical stability (Stoodley *et al.,* 2002b).

Gene expression - the use of genetic code in the formation of functional products from DNA and RNA to proteins - can vary, and they can often interact with each other in very different ways, such as in a more co-ordinated matter as consortia, not unlike a mimic of the behaviour of multi-cellular organisms (Lindsay and von Holy 2006). A number of studies have indicated modified, distinct protein expressions on transition from the planktonic to the biofilm phase, resulting in physiological differences (Giaouris *et al.,* 2013). Furthermore, it has been shown that the production of the main extracellular matrix components in *Salmonella enterica* is also reliant upon the regulatory protein CsgD (Gerstel and Römling 2003). Hamilton *et al.,* (2009) discovered that *Salmonella typhimurium* showed detectable differential expression in 124 proteins, with 10% of the genome showing 2 or more alterations. These distinctions imply changes related to biofilm characteristics, such as low amino acid metabolism and resistance to stress.

Genetic analysis suggests that biofilm bacteria display a lower metabolic activity combined with upregulation (promotion) of genes supporting anaerobic growth. These behaviours are controlled by the cells' quorum sensing facilities, a network of signalling molecules (autoinducers), the proliferation and activity of which depends on the cell density of the local population (Lee *et al.,* 2011). These processes are part of the 'community' aspect of the biofilm environment, and as well as co-ordination, assist in providing the security necessary for survival and reproduction. When the concentration of autoinducers reaches a certain level, genetic expression of cells is regulated in order to control cell-to-cell behaviours (Nigaud *et al.,* 2010). Planktonic bacteria, conversely, are suited more to the colonisation of new substrata, with a greater risk to their own survival (Hernández-Jiménez *et al.,* 2013). This heightened stability is crucial in explaining the greater resistance of biofilm bacteria towards disinfection and the human immune system (Høiby *et al.,* 2011). Ironically, it is in the planktonic phase where bacteria pose the greatest danger to health – however the ability of biofilms to harbour pathogens (often in heterogeneous communities) and then release them in isolated outbreaks is regularly the root of the threat (Hernández-Jiménez *et al.,* 2013). The cells found in biofilms regularly display a greater resistance to antibiotics (O'Toole and Kolter 1998). Growth occurs at a notably slower rate than in the planktonic condition – this has in turn been linked to a slower take-up of biocides, a contibutory factor towards antibiotic resistance (Donlan and Costerton 2002). Other explanations for resistance include a higher number of persistant cells, quorum sensing, and efflux systems (Keren *et al.,* 2004).

Benefits of Biofilm Formation

The natural tendency of bacteria to form biofilms rather than to exist in the planktonic state offers certain advantages. The transition is recognised to be key to microbial growth, as a source of both nutrients and protection, and in accelerating gene transfer activity, as a result promoting evolutionary change (Jefferson 2004). The quorum sensing signalling processes promote a community-like effect, allowing biofilms to act in manners similar to multi-cellular organisms (Costerton *et al.,* 1999), allowing them to respond adeptly to changes in the environment, or be harnessed in industrial processes such as wastewater treatment or yeast aggregation in brewing. Nutrients are found in higher concentrations at surface interfaces than in the bulk fluid phase, therefore bacteria located at the surface benefit from superior growth, particularly important at times when nutrients are scarce. In nature, it is very rare for a consistent supply of nutrients to be available, and this requires biofilms to be highly resilient, typically more so than those grown under laboratory conditions (Kumar and Ting 2013). When subjected to starvation conditions, cells can become smaller and more resistant to environmental effects. Another option in these circumstances is to become viable but not culturable (VBNC) cells (Colwell 2009). Starvation survival state can arise either from a lack of nutrients or stress-related restrictions on growth or reproduction, and metabolic activity is reduced to a base minimum (Trevors 2011). This allows the biofilm to seek sanctuary from a wide range of stresses,

such as: extreme temperatures, pH fluctuations, UV irradiation, toxicity, water limitations, nutrient deficiencies and varying oxygen levels. The cells' DNA is usually protected in this scenario; instead the carbohydrates are metabolised first, followed by proteins and then some RNA (Trevors 2011). Organisms can take particular advantage of continuous boundary layer flow in order to both gain access to nutrients and readily expel wastes (Rittschof 2010). Aerobic species also take up oxygen by the aeration this flow provides (Melo and Bott 1997). Mixed biofilms can also benefit from a commensal relationship (sharing of food for the benefit of one species). Solid surfaces can offer a survival mechanism for bacteria, given that individual cells are frequently smaller than crevices in the roughness profile of the surface, and can gain protection from fluid shear removal (Fletcher 1992). Kinsella *et al.,* (2007) studied the attachment of *Salmonella typhimurium* to meat in comparison with the same cells suspended in meat juices, and showed that the surface-attached cells strongly reduced the incidence of cell death and injury due to hyperosmosis and low temperatures (in the region of 4 – 10 ºC).

Biofilms have the ability to survive under diverse environmental conditions, as they are more resistant to numerous external influences, including ultraviolet light, metal toxicity, acid exposure, dehydration and phagocytosis (consumption by other cells such as white blood cells or amoebas), as well as resistance to treatment with antimicrobial compounds (de la Fuente-Núñez *et al.,* (2013); Costerton *et al.,* (1999)). The mechanisms of this antimicrobial resistance are not understood, but there are the following theories:

- EPS may neutralise the agent by chemical reaction, or by the creation of a diffusion barrier. Diffusion can be delayed or prevented by charge interactions with the EPS, or exclusion due to the size of the antimicrobials and the viscosity of the EPS (Xue *et al.,* (2012); Lewis (2001)).
- Changes in membrane transport systems to adapt to the antimicrobial agents (Delcour 2009).
- Reduced metabolic activity and growth rates in biofilm-based bacteria (Lauchnor and Semprini 2013).
- Production of enzymes (Ciofu *et al.,* 2000).
- Presence of plasmids which may code for resistance (Russell 1997).

Furthermore, biofilms can act as protective niches for the growth of pathogens in natural setting, which coupled with the resistance to antimicrobial treatment, make pathogenesis a concern with respect to biofilms (Lindsay and von Holy 2006).

2.2.1 Organisms

A wide variety of organisms are known to exist and develop within biofilms. Bacteria are the most common and widely-studied micro-organisms in terms of surface colonisation and biofilm growth, although fungi, yeasts, algae, protozoa and viruses have all also been isolated in both industrial and

medical environments (Lindsay and von Holy 2006). Biofilm-forming ability varies not only between species, but also between strains of the same species (Srey *et al.*, 2013). A study by Patel and Sharma (2010), for example, indicated that the *Salmonella enterica* serovars (sub-species variations) Tennessee and Thompson were more adept at forming substantial biofilms on lettuce leaves than the other serovars Braenderup, Negev and Newport.

The proliferation of organisms on building external walls is slightly different, with various cyanobacteria, actinomycetes (anaerobic, gram-negative bacteria) and myxomycetes (fungi-like slime moulds) joining the usual array of bacteria, fungi and algae in biofilms (Crispim *et al.*, 2004). Other materials trapped by the matrix can include both organic and inorganic debris, due to the adsorption of sediments or the precipitation of inorganic salts and corrosion products (Momba *et al.*, 2000). The high number of negatively charged functional groups contained within the biofilm matrix often encourages metal ions dissolved in the water to effectively chelate and bind to the surface (Zaray *et al.*, 2005).

2.2.2 The Bacterial Growth Cycle

Microorganisms grow (in the presence of a sufficient supply of nutrients) by the basic principle of binary fission – i.e. one cell becoming two replications. For a simple rod-shaped species (such as *Escherichia coli*), the first phase is an elongation of up to twice the original cell length, at which point a partition (or septum) forms. The septum constricts the cell at the mid-point, until two daughter cells are formed.

The time which it takes for a bacterium to divide into two daughter cells is known as the generation time. The length of the generation time can vary hugely but tends to be between 30 minutes and 6 hours. The practical implication of exponential growth is that while the increase in numbers is initially quite slow, the rate of growth increases continuously until the numbers are increasing at an extremely rapid rate. Therefore if the existing culture is significant, cell numbers will also grow more rapidly, which is a particular issue when concerning food, and explains the need for refrigeration of fresh food and drink in order to keep numbers down (Madigan and Martinko 2006).

Exponential growth of microorganisms can be expressed mathematically as a geometric progression in the form of powers of two. Therefore the initial division of the first cell is expressed as $2^0 \rightarrow 2^1$, and the creation of four daughter cells is written $2^1 \rightarrow 2^2$. This relationship can then be summarised as:

$$N = N_0 2^n \tag{1}$$

where N is the final cell number, N_0 is the previous cell number, and n is the number of generations being taken into account. If t is taken as the time of growth, then the generation time, g, is equal to t/n.

However, exponential growth of a microbial culture cannot continue indefinitely. There are four different stages which make up the overall population growth curve:

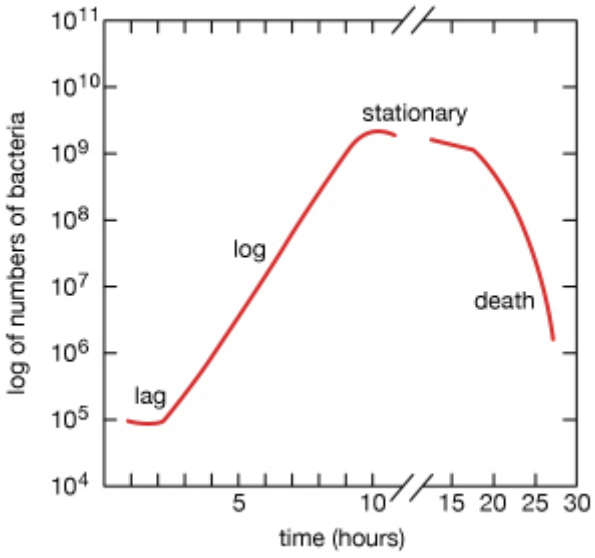

Figure 3: The standard growth for a planktonic bacterial culture, with the four main phases included (Rogers and Kadner 2007).

Predictive modelling of bacterial growth has many applications in anticipating the development of a culture and its implications. These include the judgement of a product's shelf life, the identification of critical stages in a process, and the optimisation of production chains (Zwietering *et al.*, 1990).

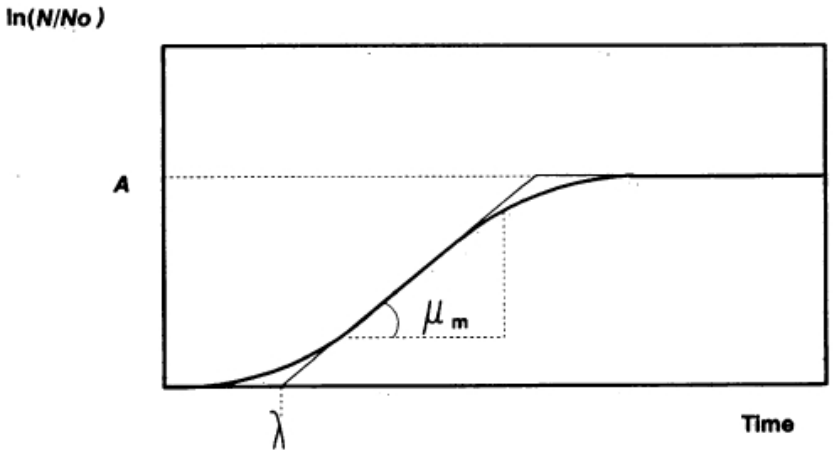

Figure 4: A graph showing the basic parameters for the creation of mathematical models for planktonic bacterial growth. The lag period is equal to λ, μ_m is the gradient of the line during exponential growth (estimated by deciding the section of the line which is approximately linear) and with A as the asymptotic value of maximum cell number established in the stationary phase. The logarithm of the relative population size is used due to the exponential mode of growth. Any decline due to the death phase is typically not included in models (Zwietering *et al.*, 1990).

The parameters included in Figure 4 are specifically biological, and this is advantageous compared to similar models in which mathematical parameters are used instead. If there is no biological meaning attached, it is difficult to assign start values to parameters. Additionally, separate calculations are necessary in order to interpret results using unrelated variables. Zwietering *et al.,* (1990) altered some classic mathematical models in order to express them as functions of biological parameters. An example of this is the Gompertz equation, which was originally written as:

$$y = a.\exp[-\exp(b - cx)] \quad (2)$$

The three parameters used here have a mathematical meaning only, and this paper re-evaluated it to meet the variables described in Figure 4 (for example, 'c' in the Gombertz equation is equivalent to μ_m.e/A). The equation was instead expressed as:

$$y = A.exp\left\{-exp\left[\frac{\mu_m.e}{A}(\lambda - t) + 1\right]\right\} \quad (3)$$

This equation was tested by developing *Lactobacillus plantarum* cultures and matching the experimental results to the curve predicted. Using a degree of accuracy of 95%, this model was deemed suitable for use.

Lag Phase

After inoculation (the supply of the source bacteria to the desired environment) has taken place, there is a lag period before any growth occurs, unless a culture in the growth phase is transferred to fresh medium under the same environmental conditions. An initial inoculation will result in a lag, and the same is true where a stationary phase culture is transferred into a new medium. A similar situation is likely to occur if a population is transferred from a rich medium into a poorer quality equivalent. Damage to cells by temperature, chemicals, or radiation will typically induce a lag, until which point as the conditions return to their previous state (Madigan *et al.,* 2010).

Exponential (Log) Phase

Once the culture has established itself into its surroundings, the bacteria begin to multiply with greater regularity. This is the start of the log phase, in which the size of the population follows the exponential pattern. This maximum growth rate will continue until limiting factors restrict, or even halt growth (Alden *et al.,* 2001). The culture will then enter the stationary phase.

Stationary Phase

Eventually the culture population will reach a steady state and begin to level off to a maximum limit. Growth is usually limited by either the exhaustion of the medium or a particular nutrient, or by the accumulation of a waste product in the medium. Throughout the stationary phase, there is no overall increase or decrease in the number of cells and the growth rate can be said to be zero (Heritage *et al.,* 1996). There may be some division of cells but this will be balanced out by the death of others. Other cell functions can typically still operate.

Death Phase

Cells will eventually die if incubation continues after they have reached the stationary phase, due to shortages of nutrients or oxygen, or as a result of the accumulation of toxic waste products (Madigan *et al.*, 2010). Changes in ion equilibrium, particularly the pH level, can also trigger a cessation of growth (Monod 1949). Programmed cell death is also recognised as a means of reduction in cell numbers, although the mechanisms relating to this are not particularly well understood. It is however believed to be vital in the regulation of growth in multicellular organisms and in protection against infections and cancer (Navarro *et al.*, 2008).

When cell death starts to dominate within the system, it is said to have entered the 'death phase', in which the total number of cells will begin to fall. However, it should be noted that individual living cells are in no way affected by this. The rate of death is also exponential, but is usually much slower than the rate of growth (typically there is no crash in population numbers).

2.2.3 Growth Conditions

Nutrients and Media

Microorganisms require nutrients for their metabolism – the collection of chemical reactions and organisation of molecules that constitute the basis for cell replication. The nutrients which are required are predominately comprised of just a few elements: nitrogen, oxygen, hydrogen, carbon, phosphorus and sulphur (Hayes 1985).

All cells make use of carbon, typically in the form of organic compounds. These include amino acids, fatty acids, acids, sugars and aromatic compounds. Bacterial cells contain around 13% nitrogen, as it is a crucial component of proteins and nucleic acids (Lodish *et al.*, 2000). Most prokaryotic bacteria use nitrogen in the form of NH_3, although some make use of NO_3^- and organic compounds such as amino acids. Phosphorus and sulphur are also essential – phosphorus is an important element in nucleic acids and phospholipids, and sulphur is present in some amino acids and vitamins (Black 2012). Certain metal ions (e.g. potassium and magnesium) are also required, albeit in smaller quantities.

Unlike animals, there is a significant variance in the requirement of oxygen for microorganisms. Those which can grow in atmospheric levels of oxygen are termed aerobes, and range from those which require it for growth to those whose function is merely boosted by its presence. It is often necessary to provide additional aeration, as the rate of oxygen consumption regularly exceeds the replacement diffusion from the air. This is provided by either agitation to the plate or tube by shaking, or by bubbling sterilised air in to the medium. Conversely, anaerobes cannot respire oxygen, and either grow in its presence without using it, or are harmed or killed by it (Koneman 2006).

A number of metals are also important for growth in still smaller amounts. Iron is the most important of these, largely due to its role in respiration and electron transport reactions (Blake II and Griff 2012). Other micronutrient metals include tungsten, cobalt and zinc.

The other important class of micronutrients are organic compounds called growth factors, including vitamin B and niacin, which are a group of proteins involved in the production of specific tissues. Most species are able to produce the components they need themselves, but others must obtain them from the local environment or nearby cells, so therefore they must be provided if grown in a laboratory (Strelkauskas *et al.*, 2010).

Culture Media Formulations

Culture media are prepared in order to provide the nutrients necessary for growth. The media must be selected and prepared with great care if the culture is to be grown successfully. Culture media fall into two main classifications. Firstly, there are defined media, which consist of precise measurements of chemicals in solution in distilled water. Most crucial is the type of carbon source present (often glucose) due to its importance for cell growth. If there is only one carbon source involved, the medium can be said to be 'simple' (Michels 2002). These are usually classed as 'minimal media', because they contain the minimum nutrients possible for growth. On the other hand, complex media are useful where the composition need not be precisely known, or where a naturally-acquired sample possesses a wide diversity of physiological states (Basu *et al.*, 2015). They contain impure substances which have high nutrient content, and originate from digests of microbial, animal or plant products. Examples include milk protein, beef extract, tryptic soy broth and yeast extract. Despite the disadvantage of an imprecise composition, a complex medium allows for some useful additions to be made. For example, an enriched medium contains a complex base with additional nutrients such as serum or blood (Madigan and Martinko 2006).

Temperature and pH

Of all the factors affecting the growth of bacteria, temperature is generally the most important. Too much variation will inhibit bacterial growth, and extreme temperatures will cause the cells to die. Generally speaking, the rate of growth rises with increasing temperature up to a point where protein denaturation reactions occur and all cell functions, including growth, cease. Most common bacteria in the natural world are mesophiles, which have minima around 10^0C, optimum temperatures at around 37^0C, and maxima at around 47^0C (Madigan and Martinko 2006).

Microorganisms also have an optimum pH range for growth, outside which smaller, stunted colonies are likely to form. If the media pH is vastly removed from the range, no growth will develop (Entis 2002). The pH level plays an important role in maintaining the required ion balance, and also in allowing cellular enzymes to function properly and facilitating the binding of hormones and growth factors to cell surface receptors. Undesirable alterations in pH can alter cell metabolism potentially

leading to cell death. Typically, growth media aim to provide a pH in the region of 7 – 7.4, although the desired level for a certain species can fall outside this range, in which case the media will need to be adapted accordingly. Regulation of pH is commonly achieved using bicarbonate-CO_2 systems or phosphate buffers (Mather and Roberts, 1998).

2.2.4 Mixed-Species Biofilms

The majority of biofilms consists of various different species in consortia with typically non-uniform arrangements, which can introduce additional concerns when tackling incidents of biofouling. Single, and often binary, systems can be considerable over-simplifications of the problem (Elvers *et al.*, 2002). Complex interactions, both intra- and interspecies, regular occur in such diverse communities, affecting formation, development and resistance, such as coaggreagtion (molecular cell-cell interaction between species) (Buswell *et al.*, 1997). This includes distinct variabilities within a certain biofilm, whereby the local composition at any particular region can influence the spatial organisation of cells and therefore the physical characteristics and integrity of the culture. Delayed growth (for example of 1-2 days) has been observed for mixed species biofilms (Lee *et al.*, 2014). Interactions between organisms in co-culture can be either competitive or synergistic, depending on the species in question and the external environment. For example, Zhang *et al.*, (2013) showed that a slow flow rate encouraged competition between *Pseudomonas aeruginosa* PA01 and *Flavobacterium sp.* CDC-65 strains as a result of nutritional limitations (irrespective of influent concentrations). Multi-species biofilms also often display a greater biomass than in cultures made from their individual components (Klayman *et al.*, 2009). Therefore, extrapolations from single species cultures to complex real-world biofilms are typically imprecise and misleading (Burmølle *et al.*, 2014).

There is regularly an order to the development of a mixed biofilm. Certain organisms, such as *Streptococcus oralis* are recognised to be 'first colonisers' in that they adept at initiating contact with surfaces. These species are then in a position to interact with further bacteria, which become second colonisers (Marsh 2006). A study by Cavalcanti *et al.*, (2014) indicated a link between the level of colonisation by a first coloniser with the extent to which a second coloniser can coaggregate. It has also been observed that the presence of the harmless *Streptococcus epidermidis* can facilitate the attachment and formation of the pathogenic *Listeria monocytogenes*, which has significant safety implications, especially in the food industry (Zameer *et al.*, 2010).

Collaboration

There are instances in which combinations of species can act in collaboration to form more biofilm. *Streptococcus pneumoniae* and *Haemophilus influenzae* are known to each produce more biofilm in co-culture. They share the same colonisation niche and are both closely associated with respiratory infections – their increase proliferation is believed to be due to an upregulation of growth-related genes when in contact with respiratory surfaces. A more in-depth investigation showed differing growth development for strain combinations across the two species, with only certain pairs showing

an increase in biofilm compared to single species communities, whereas some displayed less growth (Krishnamurthy and Kyd 2014). This suggests that patterns of co-culture communities are extremely difficult to predict, and depend on highly specific conditions and combinations. In the case of pathogens, such as the above pair of strains, the susceptibility of the individual to the species in question also impacts upon the ability to form effective biofilms (Krishnamurthy and Kyd 2014). A study by Cope *et al.*, (2011) supported the idea of synergistic interactions between *Streptococcus pneumoniae* and *Haemophilus influenzae*. The positive influence of *Burkholderia cenocepacia* on the biofilm development of *Pseudomonas aeruginosa* has also been recognised, with both species being able to present a viable infection risk (Bragonzi *et al.*, 2012).

In root canal infections, it is recognised that *Enterococcus faecalis* plays a major role, and studies tended to be based on single-species biofilms to reflect this (Ozok *et al.*, 2007). However, more recently, the presence of *Streptococcus mutans* has been recognised to instigate formation of a greater mass of biofilm, along with an increased resistance to antimicrobials (Darrag 2013). Furthermore, *S. mutans* is adept at penetrating the dentinal tract, a trait which continues in combination with other species (da Silva *et al.*, 2006).

A higher metabolic activity in mixed species biofilms has been noted, reputedly due to factors such as a greater porosity and enhanced growth kinetics and mass transfer efficiency, favouring nutrient consumption (Simões *et al.*, 2009). Metabolic and spatial interactions between multiple species form a key part of their organisational process, and are important in establishing a dynamic local environment. Hansen *et al.*, (2007) observed a collaborative relationship between *Acinetobacter* sp. C6 and *Pseudomonas putida* KT2440 when *P. putida* became able to adhere and grow biofilms close to *Acinetobacter* colonies and capture a key metabolite. Metabolic co-operation has also been shown to result in the liberation of additional nutrients which helps to maintain the characteristic diversity of natural biofilm cultures (Bradshaw and Marsh 1994).

Competitive and Inhibitory Behaviour

The competitive element of some mixed biofilms can complicate the growth behaviour. The study by Zhang *et al.*, (2013) (mentioned in the first paragraph of this section) into nutrient-limited interactions suggested that a *Pseudomonas* strain grew less biofilm in limited competition with *Flavobacterium* (also less than in a single-species culture). Additionally, the *Flavobacterium* exerted its superiority by occupying the relatively nutrient-rich outer layers, leaving the *Pseudomonas* cells mostly at the starved base. The reason given was that the room temperature conditions used resulted in a higher growth rate for *Flavobacterium*, although a faster flow offered greater growth for both species.

Another study compared the effects of 29 different strains (across several species) on the growth of *Listeria monocytogenes* in binary biofilms, and found that 16 of the strains restricted *L. monocytogenes* growth, and that only 4 had a positive impact on colony forming units (Carpentier and

Chassaing 2004). Coaggreagation was suggested as an explanation for the instances of greater proliferation, due to evidence of *L. monocytogenes* cells settling around microcolonies of the other species. Other combinations showed cells attaching as single cells, or as distinct microcolonies, depending on the secondary species. Related research by van der Veen and Abee (2011) considered the impact of media composition on formation and biocide resistance for single and mixed biofilms of *L. monocytogenes* and *Lactobacillus plantarum*. In brain heart infusion (BHI), *L. monocytogenes* strains dominated the mixed culture biofilm, yet the addition of manganese sulphate and/or glucose acted to reverse the trend in favour of *L. plantarum*. Resistance of the same biofilms to disinfection by benzalkonium chloride and peracetic acid was also investigated. In the majority of cases, the mixed species cultures offered greater resistance. Most interestingly, the use of peracetic acid on biofilms grown in BHI–Mn-G revealed a considerable difference between the resistance of *L. monocytogenes* cells in single and mixed cultures, yet *L. plantarum* was resistant in both cases, suggesting an as-yet-unexplained interaction between the species in co-culture biofilm.

Interestingly though, despite mixed cultures typically displaying greater resilience to biocides, some bacterial species can display antimicrobial properties in particular combinations. Dheilly *et al.*, (2010) used the supernatant fluid of a *Pseudoalteromonas* sp. liquid culture to inhibit the formation of *Paracoccus* sp. and *Vibrio* sp. single-species biofilms, and this also led to a higher percentage of non-viable cells in the biofilms formed. The fluid also impaired biofilm growth of the pathogens *E. coli*, *P. aeruginosa*, and *Salmonella enterica*. This property appears to be a characteristic of the *Pseudoalteromonas* genus, conferring benefits in the acquiring of nutrients and the colonisation of surfaces (Doiron *et al.*, 2012).

Removal of Mixed Biofilms

It is typical for a greater resistance to antimicrobial compounds to be noted in mixed-species biofilms than for corresponding single-species communities. Elvers *et al.*, (2002) grew biofilms of various combinations of 4 bacteria species and 3 types of fungus under flow in a modified Robbins device, and tested their suscepitibilty to an isothiazolone (a group of biocides used frequently in the water, fabric and paper industries) in comparison with monoculture biofilms. A notably greater resistance to the isothiazolone was observed for the bacteria in mixed cultures (the fungi displayed less resistance) – the single-species cultures were entirely eliminated in some cases. Other works have shown similar trends in enhanced resistance (Brown and Gilbert (1993); Costerton *et al.*, (1987)). It can be shown that a single species can offer an enhanced antimicrobial resistance to the entire biofilm rather than simply to its own cells, a community aspect which is not a feature for the same species combination in planktonic form (Lee *et al.*, 2014).

The enhanced metabolism noted in mixed biofilms is associated with a resulting increase in EPS productivity, and both factors are implicated in the ease of biofilm removal (Simões *et al.*, 2007), with the potential to provide an extra protective barrier to disinfectants.

Low-load compression testing conducted by Paramonova (2009) suggested that biofilms of coaggregating species were on average 4 times stronger than non-coaggregating combinations in the same mode of growth. Coaggreagation typically allows for tighter packing of cells conferring a higher density and therefore strength (Costerton *et al.*, 1999), with fewer voids in the structure. However, the same study did identify that *Streptococcus sanguis* was capable of forming strong, dense biofilms as a monoculture, which were then weakened by the presence of a non-coaggregating partner. This again highlights the risk of broad generalisations.

2.2.5 Extracellular Polymeric Substances

The organic compounds which contain the overall matrix are known by the collective title of extracellular polymeric substances (EPS). Geesey (1982) defined them as "extracellular polymeric substances of biological origin that participate in the formation of microbial aggregates". These substances are high molecular weight polymers both produced and excreted by the micro-organisms present, predominately comprising of polysaccharides, proteins and nucleic acids, with the additional presence of lipids and complexed metal ions (Zhang *et al.*, 2014b). Their chemical structure varies in accordance with the organisms which produce them, as well as being influenced by the environmental conditions (Momba *et al.*, 2000). Different organisms produce different amounts of EPS, although it is recognised that the amount of EPS increases with the age of the biofilm (Leriche *et al.*, 2000). However, Skillman *et al.*, (1998) also noted that in mixed-species biofilms, EPS proliferation was not linked to the relative proportions of the organisms present. The importance of EPS to the formation and survival of biofilms in evident in the considerable metabolic expense of its production (Karunakaran *et al.*, 2011).

EPS Functions

The EPS is a highly hydrated and chemically complex matrix which acts both as a storage facility for nutrients and a means of entrapping other microbes and further non-cellular materials (Lindsay and von Holy 2006). The matrix exhibits a 3D, gel-like structure in which the cells are virtually immobilised (Wingender *et al.*, 1999). The actual structure is formed from complex combinations of intermolecular interactions, including hydrogen bonding and multivalent cation bridging effect (Lin *et al.*, 2014). Glycosyl linkage between polysaccharides and lipids has been indicated to be one particular method, with a hydroxyl group removed from the polysaccharide to promote bonding with other molecules (Conrad *et al.*, 2003). An EPS matrix contains a vast array of functional groups, strongly influencing properties such as hydrophobicity, adhesion and flocculation (Lin *et al.*, 2014). The primary role of the polysaccharides is to provide structure to the biofilm matrix, determining its overall physical stability. This structural stability is partly dependent on the composition of the polysaccharides present (Branda *et al.*, 2006). It also mediates adherence to surfaces (subsequently also assisting accumulation), protecting the cells from detachment due to fluid/mechanical shear. Long *et al.*, (2009) demonstrated a decline in cell deposition in a flow-through system (with a

peristaltic pump) for four distinct species (*Escherichia coli* BL21, *Pseudomonas sp.* QG6, *Rhodococcus sp.* QL2 and *Bacillus subtilis*) after EPS removal via cation exchange resin. Chandraprabha *et al.,* (2010) also showed a similar decrease in adhesive forces after EPS was removed from *Acidithiobacillus ferrooxidans* biofilms using ethylenediaminetetraacetic acid (EDTA), following a centrifugation step after which the cells were resuspended in 100 mM EDTA solution and reincubated at 37^{O}C. EPS allows the culture to resist a range of stresses, ranging from shortages in water and nutrients to antimicrobial agents (Kives *et al.,* 2006). Also, it facilitates the accumulation of enzymes which digest macromolecules for nutrition (Miqueleto *et al.,* 2010). The strength of the structure is something which develops over time to reach a maximum level, and it is known that 'young' biofilms often show little more resistance to external factors than planktonic cells, whilst multilayer biofilms can pose considerable difficulties in disinfection (Sutherland 1999). Even if the cleaning process succeeds in killing all the cells present, failure to remove the matrix foundations will inevitably allow for the re-colonisation of the surface (Kives *et al.,* 2006). Biofilm colonies on sinters (hot spring deposits) with associated EPS in depicted below in Figure 5. The hot spring outflows displayed a range of recorded temperatures from 30 to 91 ^{0}C and had a pH of between 2.1 and 2.3. The sinters shown in Fig. 2 were isolated from areas close to vents, towards the top of the given temperature range, with relatively high water and gas discharge.

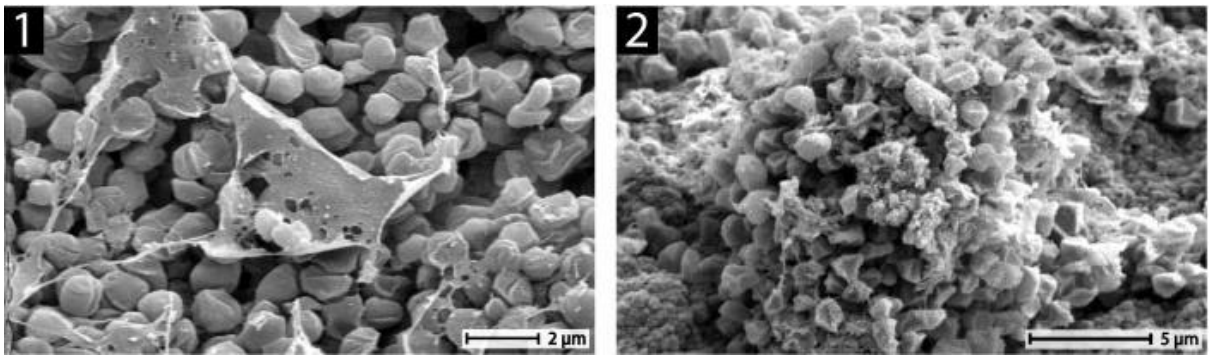

Figure 5: Image 1 - An electron micrograph image of biofilm colonisation on sinter retrieved from acid-sulphate-chloride springs, complete with associated EPS. Image 2 – An image of a conical microcolony from the same set of samples (Schinteie *et al.*, 2007).

Factors Influencing EPS Composition

Environmental conditions and nutrient availability can affect both the yield of EPS and the size and composition of the molecular components via cell signalling, and so can therefore exert huge control over the formation of biofilms. The bacteria are able to live in a relatively long-term community at high cell densities, and a major factor in this is communication and cooperation between the cells (Laspidou and Rittmann 2002).

The conditions required for growth depend on the organism in question – for example *Escherichia coli* O157:H7 bacteria can form biofilms under starvation conditions, whilst *Pseudomonas aeruginosa* is noted for its ability to grow and prosper under most nutrient and environmental conditions, including a remarkable adaptability to changing conditions and stresses (Lisle *et al.*, (1998); Breidenstein *et al.*, (2011)). The particular sources of carbon used as the polysaccharide base and nitrogen used by the microorganisms are known to impact upon the yield of EPS (Datta and Basu, 1999). EPS production is believed to be encouraged by a high carbon - nitrogen ratio, nitrogen limitation allowing for the exclusive use of excess sugars in the production of polysaccharides (Quelas *et al.*, 2006). In paper production for example, it is regarded that the inherently high carbon content and low nitrogen and phosphorus levels contribute significantly to biofilm growth (Väisänen *et al.*, 1994). Production also varies according to the growth phase which the culture is present in, and the peak for EPS occurs at different stages (usually either the exponential or stationary phases) according to the species involved.

Rates of polysaccharide production are also dependent on the pH of the growth media (which may differ from the optimum pH for biofilm growth) and the temperature of the surroundings, often favoured by a temperature below the optimum for bacterial growth (van den Berg *et al.*, 1995). Bayer *et al.*, (1990) reported the positive impact of high oxygen availability on polysaccharide levels. The cohesive energy of a biofilm was shown by Ahimou *et al.*, (2007a) to be correlated to the EPS polysaccharide content (and the depth of the layer). Higher fluid shear in growth may also promote a stronger EPS matrix, allowing for a closer alignment of polymer strands and therefore stronger electrostatic interactions (Stoodley *et al.*, 2002b). The protein content within the extracellular matrix provides low molecular weight nutrients for the cells by acting as enzymes in the digestion of exogenous molecules (Wingender *et al.*, 1999). The most abundant amino acids present in EPS are typically glutamic acid, aspartic acid, alanine acid and leucine acid (accounting for approximately 40% of total proteins) (Dignac *et al.*, 1998). Studies which have attempted to quantify or explain the relative content of polysaccharides and proteins in EPS have produced varying answers, which indicate the impact of species and conditions on EPS production and composition (Li *et al.*, 2008). Furthermore, the determined composition is known to depend on the method of extraction used, introducing further unpredictability to results (Park and Novak 2007). The following table summarises the typical composition of the overall matrix structure:

Table 1: Typical proportions of biofilm EPS constituents by mass (Sutherland 2001).

Component	**% of Matrix**
Water	up to 97%
Microbial cells	2-5%
Polysachharides	1-2%
Proteins	<1-2%
DNA and RNA	<1-2%
Ions	Variable

Studies have indicated that low nutrient concentrations are conducive to EPS accumulation, resulting in the use of minimal growth media (i.e. those with the minimum nutrients required for maintaining growth) for biofilm cultivation of some microorganisms, as opposed to nutrient-rich broths (Dewanti and Wong 1995). Ryu *et al.*, (2004) showed that *Escherichia coli* O157:H7 would form biofilms on steel in M9 minimal media, but not in lettuce juice or tryptic soy broth (TSB). The carbon source in the media is believed to be integral to EPS production, glucose being viewed as the most effective (Gauri *et al.*, 2009). However, accumulation using different carbon sources will ultimately be dependent on concentration and the bacteria strain (Jung *et al.*, 2013). Based on research in this area, it is possible that fouling mitigation could be attempted by the control of EPS formation. Adjustment of the feedwater and the environmental conditions would be key. Control of pH and the carbon-nitrogen ratio could have potential, as could the provision of sufficient dissolved oxygen (DO), given that a low DO has been shown to promote EPS production (Lin *et al.*, 2014). More clarity in the characterisation of EPS production and composition would be most likely be required, however.

The EPS can be classified as either soluble EPS (SEPS) or bound EPS, depending on the location of the culture. Bound EPS, with which the biofilm is attached to a surface, is sub-classified as tightly bound (TB-EPS) or loosely bound (LB-EPS), with TB-EPS comprising the inner layer and LB-EPS the outer regions. Su *et al.*, (2013) found that TB-EPS content was five times (by weight) the content of LB-EPS. The carbohydrate and protein content in LB-EPS is known to be most dependent on the influent carbon-to-nitrogen ratio, whilst there is no relationship between the two for TB-EPS (Ye *et al.*, 2011). Part of the variation in EPS composition within a biofilm is related to oxygen availability, as they tend to contain both aerobic and anaerobic zones due to oxygen mass transfer resistance (Sheng *et al.*, 2010).

EPS Analysis

Acquiring a sample of EPS from a biofilm has traditionally proved to be difficult (both in terms of gathering sufficient volumes and efficiently digesting samples), so therefore most of the accurate known information is qualitative and from EPS associated with planktonic bacteria (Kives *et al.*, 2006). The polysaccharide alginate is an exception in that it has been characterised in depth, having

been isolated from *Pseudomonas aeruginosa* infections in cystic fibrosis patients, although similar studies of other components are more difficult to conduct (Rehm and Valla 1997). There are long-established methods of evaluating protein and carbohydrate content, which will be discussed in Section 2.8.1, although these are somewhat generic in that they do little to isolate or characterise specific components.

An investigation by (Kives *et al.*, 2006) on *P. fluorescens* cultures suggested compositional differences between the polysaccharides in EPS found in planktonic and biofilm environments. Improved methods of extraction and digestion are key to further improvements in EPS characterisation. If the EPS can be extracted, there are many spectroscopic methods available for analysis: Fourier transform-infrared spectroscopy, X-ray photoelectron spectroscopy and Raman spectroscopy to name three (Zhang *et al.*, 2014a).

2.3 Attachment of Biofilms

The initial attachment, growth, maturity, and eventual dispersal of biofilms follow a standard general pattern. The series of phases of biofilm growth and development is shown in simple graphical form in Figure 6, and described in greater detail in the subsequent sections.

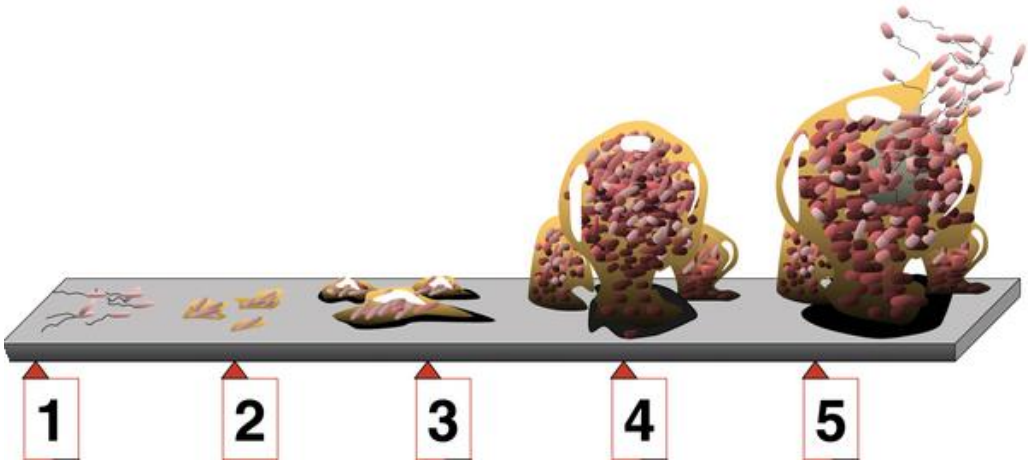

Figure 6: The five significant stages of biofilm development: 1) initial attachment; 2) irreversible attachment; 3) first stage of maturation; 4) second stage of maturation (exponential growth); 5) dispersion following the stationary phase (Monroe 2007).

2.3.1 Initial Attachment

The methods of attachment follow the same principles as for any molecular bonding – i.e. typically one or a combination of ionic, hydrogen, van der Waals and covalent bonding. Therefore, given that all surfaces are open to at least one form of bonding, any surface can experience biofilm formation (Rittschof 2010). It is common for complex biofouling processes to begin with the initial development of biofilms adjacent to the surface, forming a slime film which can provide the foundation for macro-

organisms (especially in marine environments) (Stanczak 2004), and can also facilitate the entrapment of colloidal and suspended particulates (Salinas Rodriguez 2011).

The potential for surface attachment is initially instigated by hydrodynamic pressures, resulting in the exposure of a surface to a fluid flow transporting micro-organisms (Altmann and Ripperger 1997). There then exists a boundary layer (the laminar sub-layer) adjacent to the surface in which shear forces are low and flow is laminar, into which molecules and organisms with at least one dimension of less than 500μm can actively enter or become trapped without the prospect of forced removal (Rittschof 2010). Essentially the attachment and development of a biofilm depends on the interactions between three components: the cells, the surface, and the surrounding medium (Van Houdt and Michiels 2005). For growth to initiate there must first be ample available nutrients in the local environment. Effectively the supply of nutrients acts to regulate the transition of the organisms from suspension to the substrate surface. Organic matter (i.e. the EPS) accumulates on the surface which allows for colonisation by a small number of cells. In order to initiate viable biofilms, bacteria must be sufficiently mature, i.e. preferably in the log phase, although the nutrient source may permit the use of cells in the stationary phase.

There three recognised methods of interaction for the establishment of a biofilm (Al Juboori and Yusaf 2012) – these are physico-chemical interactions with the surface (e.g. van der Waals forces), ligand-receptor interactions (such as via charged or OH groups on a conditioning film) (Flemming 2011), and adhesion between the EPS and cell appendages (Hori and Matsumoto 2010). Covalent bonds have been identified from adsorbed EPS using Fourier-transform infrared (FTIR) and X-ray adsorption fine structure spectroscopy (Omoike and Chorover 2004). Atomic force microscopy (AFM) has also been utilised to show evidence of hydrogen-bonding between phosphates in EPS and silica substrates (Kwon *et al.*, 2006).

This initial attachment is reversible, and can be explained by various transport phenomena, including electrostatic and physical interactions between the cells and substrate (Lindsay and von Holy 2006). This first step may initially be the rate limiting step of the entire process (Momba *et al.*, 2000). The physico-chemical interactions present are typically explained by a thermodynamic approach, the Derjaguin-Landau-Verwey-Overbeek (DLVO) theory, or the extended DLVO theory (Al Juboori and Yusaf 2012). DLVO theory is depicted graphically in Figure 7. The thermodynamic approach considers the surface free energies of the interacting surfaces, although this is difficult to apply to the initial attachment stage because the interface is yet to be formed (Hori and Matsumoto 2010). Theoretically at least, adsorption should commence if contact between the cell and surface reduces the total free energy of the system (Hadjiev *et al.*, 2007). Minimising the total free energy promotes a stable system:

$$\Delta G = \gamma_{12} - \gamma_{13} - \gamma_{23} \quad (4)$$

where ΔG is the Gibbs free energy of adhesion per unit area and γ is the interfacial tension between the stated surfaces where 1 is the cell, 2 is the surface and 3 is the bulk fluid (Mozes *et al.*, 1987).

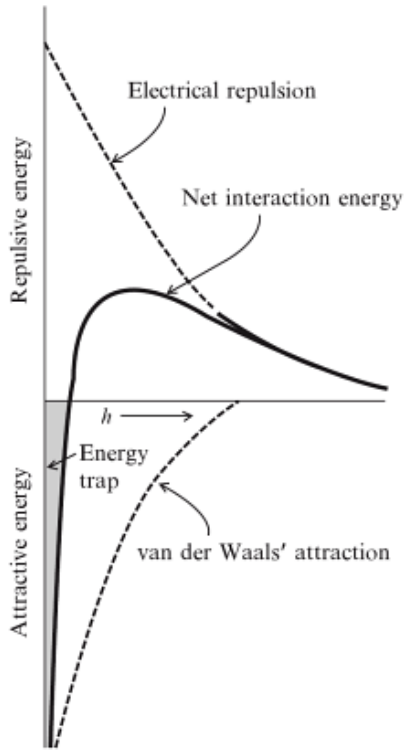

Figure 7: The net energy of interaction between two particles in accordance with DLVO theory, with *h* being the interparticulate distance (Nutan and Reddy 2009).

DLVO theory incorporates the principles of particle attraction and collision, which is more appropriate to biofilm establishment (as although DLVO theory concerns colloidal particles, bacteria are of comparable area-to-volume ratios) (Bos *et al.*, 1999). It states that the total interaction energy between a particle (or cell) and a submerged surface is the sum of four non-covalent interactions. These are the Lifshitz-van der Waals (LW) interactions, Lewis acid-base (AB) polar interactions, electrostatic (EL) surface charge interactions, and Brownian movement (BR) forces (van Oss 2006). Adhesion can take place if the total interaction energy is negative – with positive interaction energy, repulsion is favoured.

The significance of hydrophobicity and hydrophilicity was defined in the extended DLVO theory (XDLVO) by van Oss (1993). If the free energy of interaction between two identical submerged surfaces is negative, the surface is considered to be hydrophobic, and vice versa. The Baier curve (Fig. 5) shows a relationship between surface free energy and bacterial adhesion, indicating an optimum value for minimal growth of between approximately 20 and 30 mN/m. Surfaces possessing a high surface energy (which are typically hydrophilic and often negatively charged), such as stainless steel, are rarely free of bacterial colonisation (Hočevar *et al.*, 2014). Very low energy surfaces include

Teflon and other fluorocarbon compounds, and whilst there has been little investigation into bacterial adhesion in this region, it is suggested that there are polar interactions present with fluorocarbon surfaces which offer better potential for adhesion (Schrader 1982).

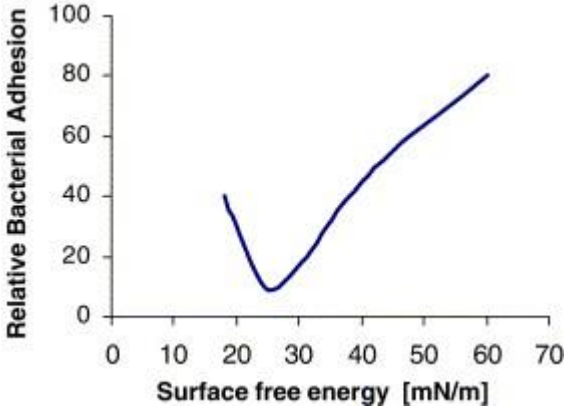

Figure 8: The Baier curve, showing bacterial adhesion relative to critical surface energy (Baier 1980).

Work conducted by Pereni *et al.*, (2006) concerning the attachment of *Pseudomonas aeruginosa* AK1 to a selection of surfaces displayed good support for the Baier curve (Figure 8):

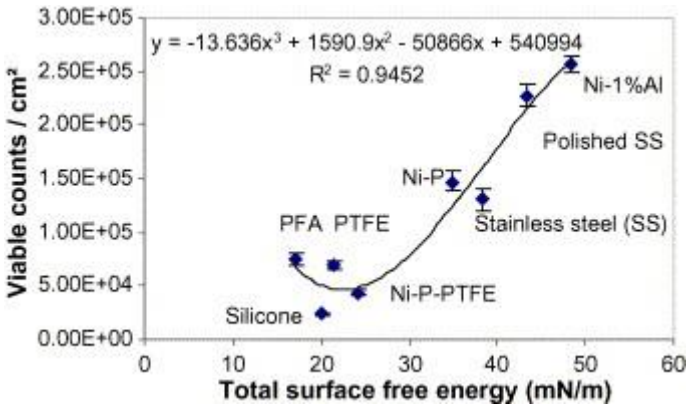

Figure 9: *Pseudomonas aeruginosa* AK1 adhesion, measured by viable cell counts, to a range of substrates. The results show a strong agreement with the Baier curve (Fig. 8) (Pereni *et al.*, 2006).

The apparent simplicity of the Baier curve can be misleading however, as adhesion concerns the interaction between the surface energies the bacteria and the surrounding medium as well as the substrate, and this can be shown to manifest itself as localised variations on the same surface (Fletcher and Pringle 1985). Other factors are also of importance, such as the contours of the surface (roughness) and the chemical interactions involving the cells and EPS.

EPS chains tend to contain both hydrophobic and hydrophilic groups and so therefore are able to bond effectively to both surfaces, a unique property which explains their high adhesive ability (Lin *et al.*, 2014). EPS-forming macromolecules (usually the result of the breakdown of living matter) adsorb in preference to bacteria, forming a 'conditioning' layer which is attractive to cells as a nutrient source.

Cell adsorption may be influenced by attractive and repulsive forces at very short distances from the surface (for example ≤1 nm or 5-10 nm) (Korber *et al.,* 1995). Most cells carry a negative surface charge which alone would favour repulsion from the surface; however cell surfaces tend to be hydrophobic and such interactions with the surface can overcome the repulsive forces

Where a sufficient attractive force is present, adhesion can proceed to an extent dependent on a few major factors. Mass transport can dictate the rate of microbial accumulation on the surface, and also affect the stability of the biofilm via shear forces (a high shear force can promote a thinner yet more stable biofilm) (Characklis 1990). The characteristics of the surface can be significant in determining the nature of attachment. Surface roughness is significant, as are hydrophobicity and hydrophilicity, and the impacts of these factors will be discussed in more depth later (Section 2.5). The concentration of microorganisms in the feed is directly linked to the aggregation rate of bacteria on the surface (Koop *et al.,* 1989). Finally, the electrostatic interactions which play a part in adhesion can be interfered with either by an alteration in the ionic strength of the solution ((Hori and Matsumoto 2010) showed that a decrease in ionic strength can lead to an increase in repulsive energy and therefore greater biofouling), as can the solution pH which can affect the charge on the surface (Brant and Childress 2002). Up until this stage, cells detach frequently from the surface and it may be the case that only a small proportion of the cells remain attached, although this is enough for the long-term development to proceed (Kumar and Ting 2013). Cells must first undergo the relevant morphological changes in transition to biofilm, and until these occur will always be prone to premature detachment (Stoodley *et al.,* 2002a).

2.3.2 Irreversible Attachment

The subsequent stage is irreversible attachment, which is initiated by the production of more EPS which acts to strengthen the bond with the surface (Yebra *et al.,* 2006). Once strengthened, the biofilm cannot be easily removed, instead requiring heat, increased shear forces, disinfectants or surfactants, or enzyme action to break the bonds within the EPS (Srey *et al.,* 2013). The transition from reversible to irreversible attachment can occur within seconds to minutes (Van Der Mei *et al.,* 2008). This is carried out by the stimulation of sensory proteins located in the cell membranes, creating cell-to-cell bridges which ultimately create a firm adhesion with the substrate (Lindsay and von Holy 2006). A genetic influence involved in irreversible attachment has been shown to be true for *Pseudomonas aeruginosa* by means of genetic modification (O'Toole and Kolter, 1998). Bacterial settlement allows genes such as *lasR* and *lasL* to produce chemical cues which encourage further cells to join the growing cluster. This is mediated by a variety of short-range intermolecular attractions, namely dipole-diploe, hydrogen, ionic and covalent bonds, and also hydrophobic interactions (Westgate *et al.,* 2011). Active cells will continue to consume nutrients in order to continue producing EPS and for further reproduction (Yebra *et al.,* 2006).

2.3.3 Exponential Phase and Maturity

Microscopic analysis suggests that structural maturity can require ten or more days to be reached (dependent on growth conditions) (Heydorn *et al.,* 2000). The extent to which the biofilm can develop, once established, is again influenced by a consortium of factors. The total thickness reached depends mostly upon the supply of nutrients – an increase in supply from 4 mgL^{-1} to 10 mgL^{-1} was shown to increase thickness by more than 40% (Bott and Miller 1983). Higher nutrient levels also favour a spacious structure, favouring the diffusion of nutrients to the bacteria from the bulk flow. This is also crucial for oxygen transfer for aerobic bacteria. A biofilm will also continue to develop on a contaminated surface in the absence of planktonic bacteria if there are sufficient nutirents available (Melo and Bott 1997). Thickness can also be dictated by fluid velocity. It is known that a relatively slow flow rate encourages thicker biofilm growth – a velocity of 0.54 ms^{-1} was shown to grow a biofilm ten times thicker over 15 days than a velocity of 2 ms^{-1} (Pinheiro *et al.,* 1988). Velocity increases are also believed to increase the density of biofouling layers (Melo and Bott 1997). This density also tends to come with greater strength and resilience (Radu *et al.,* 2012). Fluid flow is therefore key to the extent of biofilm maturity, either by mass transport or shear stress. Microbial activity is also highly sensitive to temperature, and small alterations in temperature as likely to trigger major changes in growth. Bott and Pinheiro (1977) showed that *E. coli* thickness could be increased by up to 80% by raising temperature from 30°C to 35°C. Thicker biofilms eventually become compliant to the effects of the fluid flow, becoming prone to deformation (McKee 1991).

2.3.4 Stationary Phase

However, a high rate of cell multiplication resulting in sporadic detachment can occur, balancing the levels of microorganisms within the biofilm and the suspension. This is a continuous parallel process, which means that the overall biofilm growth rate can be expressed as the relationship between the rates of attachment and detachment. There may also be 'streamer' cells loosely attached to the biofilm (Irving and Allen 2011). Furthermore, there is usually also a balance between cell reproduction within the biofilm and the death of certain cells which cease being active. Active cells will continue to consume nutrients in order to continue producing EPS and for further reproduction (Yebra *et al.,* 2006).

Eventually the development process will establish a steady state in which there is maximum cell adhesion and a stable growth rate (Ascon-Cabrera *et al.,* 1995), representing a total colonisation of the surface region, whereby various features can be established. Micro-colonies of bacteria can form where they are enclosed by the polymer matrix, whilst at the same time less dense pockets may be noticeable where water channels can flow, transporting nutrients and waste products. Other planktonic cells can also be trapped by the EPS to produce a more ecologically variable biofilm.

2.3.5 Detachment

After a certain period of time, however, cells can detach and either transfer to another surface or return to the planktonic state. This is a process which occurs continuously throughout a biofilm's development, typically to allow for proliferation onto new surfaces for survival (Kroukamp *et al.,* 2010). Nutrient starvation (often population density mediated) can trigger dispersion as a means of migration to a richer area in order to start a new cycle of biofilm formation (O'Toole *et al.,* 2000). Bulk detachment, however, is typically observed towards the end of the life span of the culture.

The release of detached cells may occur either individually or as aggregates (Walter *et al.,* 2013). Generally, there are three mechanisms implicated in detachment:

- sloughing: the sudden and apparently random loss of regions of biofilm;
- erosion: the regular loss of single cells or small clumps due to external forces or cell cycle factors;
- abrasion: removal due to the collision of particles with the biofilm surface (Derlon *et al.,* 2008).

The structure of the biofilm is known to be significant in determining the mode of detachment. Uniformly thick biofilms tend to lose cells mostly due to regular erosion of surface biomass, whereas sloughing is more commonly observed in heterogeneous cultures (Stoodley *et al.,* 1997). A smoother surface can suggest that a biofilm may be softer and of a lower strength as they possess weaker particle-particle interactions, allowing the structure to become more readily deformed and stretched in the direction of the flow and allowing for an easier detachment (Shen *et al.,* 2015). Biofilm strength appears to correlate directly with biofilm density, which is typically increased with a higher fluid shear stress and substrate loading rate (Wasche *et al.,* 2002).

The conditions under which the biofilms are grown have also been shown to have an impact on the removal characteristics. A study by Applegate and Bryers (1991) suggested that, in comparison to each other, biofilms grown under carbon limited conditions formed less EPS and considerably favoured erosion-based removal over sloughing, whilst oxygen limited conditions were shown favour repeated sloughing yet rarely detached. Rochex and Lebeault (2007) observed high erosion rates at both low and high glucose concentrations, and also noted that high nitrogen levels promoted sloughing tendencies. They suggested that nutrient limitation, especially nitrogen, was advisable in order to limit accumulation and the size of detaching clusters. It may, however, simply be that a critical thickness can be reached, at which point sloughing becomes an inevitable process (Melo and Bott 1997). Whilst sloughing can remove biomass down the surface, it is a distinctly unreliable method for the controlled, mass removal of an attached culture (Choi and Morgenroth 2003).

Detachment may be as a result of an increase in fluid shear (Stoodley *et al.*, 2002b). Steep changes in applied shear forces are noted to trigger an immediate response in detachment, although this is generally a temporary effect (Bakke 1986). Certain enzymes can also facilitate such movement, for example via the release of EPS (Kaplan *et al.*, 2004). Pili are often responsible for the movement as they exhibit gliding motility, an energy-intensive process which facilitates smooth movement over a surface (Lindsay and von Holy 2006). Tests of biofilms under flow conditions have driven the belief that shear forces have the greatest influence on detachment, although recently phenotypic mechanisms and enzymatic action have been given greater consideration (Walter *et al.*, 2013). Phenotypic responses are, however, believed to be influenced in turn by fluid shear (Hall-Stoodley and Stoodley 2005). Despite the range of potential influences on detachment, reproducible experiments have been shown to be possible where appropriate and consistent methods are used (Walter *et al.*, 2013).

The cycle may also come to an end if there is a lack of available nutrients (O'Toole and Kolter 1998). Deliberate glucose starvation was shown by Hunt *et al.*, (2004) to result in rapid detachment of *P. aeruginosa* biofilms. Detachment to different niches is another important survival method for a culture, as at a certain stage the colonisation of new surfaces will be essential for nutrient sources (Webb *et al.*, 2003a). It is an important step for consideration in the distribution of pathogens in both infection and the contamination of water systems (Fux *et al.*, 2004).

Controlled depletion of oxygen supply to *Shewanella oneidensis* has been shown to result in detachment within five minutes, due to a failure to adapt to the change quickly enough (Thormann *et al.*, 2005). Starvation influences age-related detachment due to the increased deposition of EPS triggering deepening nutrient and oxygen gradients between the enriched outer layers and the starved core cells, requiring the need for escape mechanisms for the submerged regions (Allison *et al.*, 1998). Decay in the surface-attached cells weakens the overall structure and encourages sloughing (Picioreanu *et al.*, 2001). The same effect can also occur due to stagnation in the flow (Davies 1999). However, Castegnier *et al.*, (2006) showed that long-term starvation is not necessarily fatal for a biofilm – a biofilm persisted for 129 days under unstable hydraulic conditions caused by starvation. Detachment via a constant shear stress is believed to be dominated by erosion, mostly of small particles which dominate number-based detachment distributions, yet despite this when analysed by mass sloughing is primarily responsible (Choi and Morgenroth 2003).

The role of cell death in the biofilm life cycle is one of the least understood areas (Fagerlind *et al.*, 2012). Webb *et al.*, (2003b) observed death and lysis (breakdown of cell integrity) within colonies of *P. aeruginosa* biofilms. Barraud *et al.*, (2006) noted the link between death and nitric oxide production in mature cells, including the lack of cell death in mutant strains which do not produce nitric oxide. Nutrient supply is known to be closely linked to both cell death and dispersal (Schleheck *et al.*, 2009), suggesting that the death of cells encourages the acceleration of dispersal.

2.4 The Impact of Biofouling

Biofouling is a vast, multi-faceted problem with practical implications on a global scale. Whilst biofilms are harnessed in a positive manner by industries as diverse as wastewater treatment and fuel cell production, the unwanted presence of surface-attached biological matter can present significant concern for engineers. The scale of risk is heightened by the potential of sessile (attached) cultures to detach and re-enter the prevailing flow – therefore the impact is seen both in the fouling of the surface itself, and in detachment and transit to new locations (a major reason for biofilm persistence in a system) (Matin *et al.,* 2011). All submerged surfaces will eventually experience fouling for a range of biological and hydrodynamic reasons, which will be discussed later (Murthy and Venkatesan 2009). The costs can be severe – for example the aquaculture industry (the farming of aquatic organisms) is estimated to spend between 5 and 10% of industry value on dealing with biofouling (Fitridge *et al.,* 2012). There are certain surfaces, such as silicones (Nejadnik *et al.,* 2008), which are generally attached to less strongly, but forms of microorganism will always settle on any surface regardless of surface energy or surface chemistry, as they are advantageous environments compared with the bulk liquid (Petrova and Sauer 2012).

Contamination can occur at all stages of production – for example den Aantrekker *et al.,* (2003) described how pasteurised milk can be exposed to bacteria associated with raw milk via the presence of biofilms in the production plants, which detach and migrate into aerosol systems. Biofilms can act as reservoirs for continuous contamination, often before or after heat treatment (sterilisation, pasteurisation, curing etc.) (Kives *et al.,* 2006). Detachment is also responsible for cross-contamination, when food passes over fouled surfaces (Kusumaningrum *et al.,* 2003). The potential for pathogens and reduced shelf-lives reduce the profitability of the venture so are therefore highly undesirable (Lindsay and von Holy 2006). In power plants, the problems can be sorted into a few broad groups: blockage of cooling water resulting in damage to pumps; the clogging of condenser tubes; reduction in heat transfer efficiency; and the acceleration of corrosion. Several incidences of total plant shutdowns have occurred (Rajagopal and Jenner 2012).

In industrial processing, it is typically an inadequately-cleaned surface which promotes the build-up of soils which act as a base for biofilm development (Giaouris *et al.,* 2013). The sheer amount of biomass which can attach is indicated by one example of the accumulation in the intake tunnel of a coastal power plant which was estimated at 578 tonnes (predominately mussels by mass) (Rajagopal and Jenner 2012). The scale of the problem has resulted in the establishment of a billion dollar global industry, encompassing biocide production, cleaning, consultancy and the development of preventative measures. Furthermore, this is exacerbated by the low efficacy and wastefulness of many antifouling measures which leads to repeated disinfection (Flemming 2011).

Biofilms have also been implicated in a range of diseases and infections, including in the lung tissue of cystic fibrosis patients and in serious wounds. The ability of biofilms to detach and re-colonise other surfaces allows infections to spread across multiple organs in the human body (Hernández-Jiménez *et al.,* 2013). The pathogenic nature of some biofilms also presents a major risk for patients with permanent medical devices attached, such as intravascular catheters and implants. Occurrence of infection for such patients has been noted for many hundreds of years, and in addition the functionality of the devices can be deteriorated resulting in the need for regular replacements (Lindsay and von Holy 2006). Management of biofilm-related infection is especially difficult given the heightened resistance to biocides and environmental stresses (Davies 2003), giving serious conditions a greater opportunity to persist (Costerton *et al.,* 2003). In general, biofilms are believed to be responsible for between 65 and 80% of all infections, so the challenge of overcoming biocide resistance is a crucial one (Costerton *et al.,* 1999). The tendency for surface bacteria to form biofilms is also considered to be the most significant barrier to wound healing (James *et al.,* 2008). Skin is the primary defence to bacterial adhesion and colonisation and so therefore this defence is compromised where a wound is present (Niyonsaba *et al.,* 2006). Additionally, biofilm bacteria frequently do not initiate the same level of inflammation as planktonic bacteria, and so can therefore be overlooked by traditional sampling techniques (Costerton *et al.,* 1999). Dental plaques are another way in which biofilms can impact upon human health. Accumulation is greatest at stagnant sites i.e. those which are protected from removal (either natural or via manual cleaning) (Marsh 2004). Development of plaques has been shown to proceed even on clean surfaces over time, and irrespective of age, diets and nationalities (Percival *et al.,* (1991); Nyvad (1993)).

Contamination

Due to the ability of microorganisms to colonise any surfaces with water present, pipelines and networks for water distribution are hugely prone to contamination. If the intention is to provide drinking water, then the challenge is to ensure that water can be supplied in the necessary volume and pressure with the safety that is expected. Growth in these systems is usually found on the inside of pipes, in fact it is estimated that this applies to around 95% of the total bacteria in the pipe (Declerck *et al.,* 2009). The impact occurs when bacteria dissociate from the surface into the bulk fluid (Momba and Makala 2004). The potential of biofilms to acts as host environments for pathogenic species is of great concern, as they provide a safe setting for survival, growth and eventual release into the water system. The metabolic activities of the bacteria are also capable of producing harmful compounds such as endotoxins, hydrogen sulphide, and nitrites, which are then released into the bulk fluid (Wingender and Flemming 2011).

Mechanical Damage

Mechanical failures can result from one or more of the following occurrences; breakages requiring the replacement of pipe sections, open reservoirs or backward siphoning as a result of a reduction in the

pressure of the flow. The cost of mechanical repairs and replacements is also calculated to include the resulting loss of production (Müller-Steinhagen 2000). A form of damage peculiar to biological fouling is the process of microbially-influenced corrosion (MIC), a severe process resulting in 'pitting', the production of cavities in the surface (Vargas *et al.*, 2014). MIC has impacted upon copper piping in buildings across the world, notably the comprehensive collapse of the pipe network in a hospital in Scotland, in which the repair cost was estimated at £100 million (Keevil 2004). MIC is also an example of industrial pressure being a driver of research into fouling mitigation (Vargas *et al.*, 2014), and subsequently investigations were undertaken by the turn of the 21st century which suggested that biofilms act as mediators for interactions between the metal and the surrounding environment with the potential to alter pH, oxygen levels, and the presence and variety of ions. This alteration of substrate behaviour can as a result be monitored and manipulated to inhibit microbial corrosion in an environmentally-friendly manner (Videla and Herrera 2005). Models of metal-microbe interactions have also been developed as a result of this (Vargas *et al.*, 2014). Despite these advancements however, MIC is still believed to be responsible for 20-30% of total corrosion-related costs, resulting in financial losses of $30-50 billion per year in the US alone (Trivedi *et al.*, (2014); Al-Darbi *et al.*, (2002)) - an indication of the complexity and severity of biofouling events.

Hydraulics and Heat Transfer

The hydraulic properties of the process equipment may be damaged by the presence of fouling, particularly if it's key functions concern heat or mass transfer (Tuladhar *et al.*, 2000). Foulants reduce heat transfer between process fluids by reducing heat recovery and narrowing the flow area in heat exchangers, thus restricting fluid flow (Kays and London 1964). For fluid-based systems (aqueous or otherwise), if the temperature of the heat exchanger is similar to that of the environment, biofilm attachment is the inevitable result (Frota *et al.*, 2014). Deposits generally exhibit a relatively low thermal conductivity, acting as an insulating layer which increases heat transfer resistance and therefore damages thermal operating efficiency. This is primarily because biofilms can contain up to 99% water, and thus their conductivity is similar to that of stationary water and much lower than metals used as pipe construction materials (Characklis and Cooksey 1983). The thermal performance is proportionally affected by heat transfer resistance, and the fluid dynamics are altered due to frictional resistance and limitations in the flow cross-sectional area (Tian *et al.*, 2010). Even very thin films can strongly affect heat transfer performance (Zhao *et al.*, 2005).

HVAC (heating, ventilation and air conditioning) applications are prone to air-side fouling which can both adversely affect its cooling capacity and increase the air-side pressure drop. Research into air dust deposition in HVAC systems greatly outweighs that conducted into biofouling, however. Pu *et al.*, (2009) conducted investigations on biofouled finned tube heat exchangers, suggesting that the heat transfer coefficient decreases gradually when the fouled area advanced beyond 10%. A 60% coverage showed a coefficient reduction of 16% for a flow of $2ms^{-1}$. The same study showed an even

greater impact upon the air-side pressure drop: for a flow of 0.5ms^{-1}, an increase in biofouling of 60% enhances the pressure drop by approximately 41%. The pumping and utility costs would therefore need to be heightened considerably in order to overcome this. Damage to heat exchanger performance can be highly severe in cooling systems in hydroelectric power plants for example, and the heat exchangers often require total shutdown of the plant in order to be dismantled.

These issues are by no means unique to biological fouling, indeed they are prevalent for all fouled surfaces (Melo and Bott 1997), but biological deposits carry certain extra features. Besides, fouling methods regularly combine forces, and metabolic activity can trigger corrosion due to pH changes. Similarly, the sticky nature of many biofilms often attracts other particulates (Melo and Bott 1997). Without off-line cleaning, the active foulant is typically very resistant to attack and difficult to remove. The addition of chemical biocides can be helpful but often at a considerable environmental cost (Frota *et al.*, 2014).

Pressure Drop

There are often issues with heightened pressure drop related to fouling, especially where there is significant accumulation to cause a limitation in the flow cross-sectional area (Chew *et al.*, 2004b). Biofilms often also increase the roughness of the surface, which also contributes to the problem by creating additional disturbances and increasing friction. A further problem related to this is that many fouling models assume a uniform surface, which leads to low predictions of fouling effects (Müller-Steinhagen 2000). Chenoweth (1987) suggested that excessive pressure drop contributes to heat exchanger replacement requirements more than actual heat transfer issues. Maldistribution (uneven distribution of flow) is a concern for heat exchangers, often a result of fouling blockages (Thulukkanam 2013). Flow losses can also be a result of drag forces introduced by the viscoelastic properties of many biofouling deposits (Singh 2006).

Financial Implications

The costs attributed to biofouling are the result of impacts such as interference with the process, deterioration of the product (quantity or quality), damage to materials and hardware, and the need for component replacements as a result of cleaning (Flemming 2011). Cleaning of equipment may result in a decline in productivity as sections of the facility may require temporary shutdown.

The costs which arise tend to be attributable to the following:

- Higher operational (energy) costs - reduced thermal efficiency and greater pressure drop;
- Greater capital investment on hardware replacements and repairs;
- Higher maintenance costs;
- The cost of additives and chemicals for cleaning (Nguyen *et al.*, 2012);

- Excess heat transfer area to compensate (average of approximately 30% (Thackery 1980). This leads to increased transport costs due to size and weight, extra space required, installation expense, as well as extra costs for cleaning and fuel (Müller-Steinhagen 2000).

The costs have generally proved difficult to quantify due to the sheer range of factors involved. Certain estimates exist, and although they tend to be focussed on a particular industry, nevertheless indicate the undesirable contribution attributable to biofilms. For example, Abdul Azis *et al.,* (2001) suggested that the costs of biofouling to the desalination industry alone is approximately $15 billion worldwide each year. An alternative approach is to quantify the costs in terms of the disinfection duty or fouling-related energy losses – for example thousands of tons of chlorine are used per day worldwide in the disinfection of power plants (Cloete 2003). In terms of energy duty, a biofilm of 25um thickness on a ship hull has been shown to increase drag by 8%, and thicker, rougher biofilms can show increases of up to 22% (Characklis 1990).

Domestic Biofouling

The tendency for biofilms to form in household settings should also not be neglected. The sources of offending microorganisms include contaminated food, contaminated water, human contact, air, insects or pets (Teixeira *et al.,* 2007). Cross-contamination (the transfer of bacteria between foods or from humans to food) is a major cause of biofilm establishment in domestic kitchens. Additionally, food can be at risk due to incorrect storage temperatures, inadequate cooking or contact of cooked or raw foods with hands or utensils (Teixeira *et al.,* 2007). *Salmonella* spp. are pathogens responsible for a common foodborne infection, believed to be mostly due to cross-contamination and inadequate cooking of food containing raw eggs (Gillespie *et al.,* 2005). Multidrug-resistant *Salmonella typhymurium* has become more prevalent, presenting an increasing health problem which emphasises the need for surveillance programs (Altekruse *et al.,* 1997). Food preparation can lead to the bacterial colonisation of surfaces including chopping boards, taps, kettles and refrigerators (Haysom and Sharp 2003). This contrast with *Listeria monocytogenes*, which is more typically the result of post-processing contamination of foods, and can be isolated from the production plant in question (Jacquet *et al.,* 1993).

The inner surfaces of domestic plumbing pipes can also experience extensive biofouling. Water distribution systems are very closely monitored so that pathogenic bacteria do not tend to proliferate in this scenario, yet taste and odour can be adversely affected. The elderly and small children may still be at risk, however (Percival and Walker 2001).

Bathrooms are another section of the home which experiences regular biofilm accumulation. A focus of research in this area has been growth on shower heads, as bacteria present in the water supply can attached to the exposed outer plates of the head, and also to pre-attached cells (Vornhagen *et al.,* 2013). Various pathogenic species can be enriched via showerhead biofilms, including members of

the genera *Staphylococcus*, *Methylobacterium* and *Escherichia* (Feazel *et al.*, 2009). In addition to these health risks, the biofilms can also be unsightly and can contribute to microbial-influenced corrosion (MIC) which can damage the head (Bloetscher *et al.*, 2010).

2.5 Factors Influencing Biofouling

All materials used for the construction of pipes are known to facilitate the attachment of micro-organisms (Momba and Makala 2004). Despite this, however, the extent to which bacteria can grow on various surfaces is known to vary. The initial adhesion of cells is mediated either through direct attachment to the surface, or through binding to molecules adsorbed onto the surface, so therefore the specific properties of the substrate will play a role (Xu and Siedlecki 2012). There are various suggested factors as to how this occurs.

2.5.1 Roughness

Although hydrophobicity, surface free energy and surface charges are known to influence bacterial adhesion, the influence of surface roughness is considered to be the most significant (Quirynen and Bollen (1995); Quirynen *et al.*, (1990)). Whilst surface energy can also play an important role, a sufficiently textured surface can mask its effects (Quirynen and Bollen 1995). A higher roughness offers both a greater surface area for colonisation and extra niches for growth to occur, and it also minimises the effect of fluid shear forces, providing shelter for newly-attached bacteria in the reversible development phase (Rimondini *et al.*, 1997). In some cases, surface features can create turbulence, and the suggestion is that turbulent flow can enhance adhesion by impinging planktonic cells on the surface (Donlan and Costerton 2002). Both the number and extent of attached cells have been shown to increase with roughness (Characklis *et al.*, (1990); Oh *et al.*, (2009)). This reported impact upon ultimate extent of growth is contested - Momba and Makala (2004) found that while rougher surfaces can experience a more immediate spurt of growth, ultimately the proliferation on smooth and rough surfaces was practically the same. Al-Ahmad *et al.*, (2013) also observed negligible influence of roughness on biofilm composition despite the major role it plays in initial colonisation. There is however a minimal point at which it ceases to be a factor - roughness levels of less than 0.2µm do not impact either the amount or characteristics of the resulting biofilm (Bollen *et al.*, 1996). In general it is accepted that surface features with a similar size to the cells will experience the greatest microbial retention (Medilanski *et al.*, (2002); Whitehead and Verran (2006); Wu *et al.*, (2011)) – they offer suitably-sized niches for protection during attachment and growth.

Microscopic studies of early-stage dental plaques have indicated that initial colonisation occurs mostly in cracks and pits in the enamel, implying the favouring of a rougher surface (Nyvad and Fejerskov 1987). Carlén *et al.*, (2001) showed that an unpolished glass ionomer surface was rougher than an unpolished composite resin, and that it subsequently bound more protein and bacteria. Polishing the composite resin increased the roughness and greater adhesion was observed, whereas

the same process had little effect on the roughness of the glass resulting in no observed difference in binding levels.

Additionally, it may not simply be the extent of biofilm formation which is affected by roughness. Chaturongkasumrit *et al.*, (2011) noted not only a greater adhesion of *Listeria monocytogenes* on a rougher conveyor belt surface, but also a heightened resistance to cleaning agents. Mei *et al.*, (2011) used AFM to show that the impact of surface roughness continues to affect adhesive strength after the 'bond-strengthening' phase (the development of irreversible attachment). This may be due to increased contact times encouraging stronger adhesion – and it is known that the transition from reversible to irreversible bonds occurs within seconds to minutes on smooth surfaces (Van Der Mei *et al.*, 2008).

Although observing the overall roughness and applying it to biofilm growth is a useful tool of analysis, the actual topography of the surface can influence the adhesion and proliferation of cells. For example, the presence of parallel grooves on the surface results in cell growth along the direction of the grooves (Walboomers *et al.*, 1999). Turner *et al.*, (2000) also demonstrated how cells may prefer to grow on the pillars of a specifically-fabricated silicon structure than in the corresponding wells (it is also noted that the cells still favoured the wells over a comparison smooth surface). Ultimately cells appear to prefer irregular surfaces for adhesion, with particular emphasis on anti-symmetric surfaces, i.e. 'cliffs' with adjacent convex and concave profiles (Curtis *et al.*, 2001). The relative porosity of wood has been shown to encourage biofilm growth by trapping bacteria and nutrients (Adetunji and Isola 2011).

2.5.2 Surface Energy

Contact angle measurements are the typical and simplest way of determining the surface energy of a sample, in that a high energy surface will experience more complete 'wetting' with the same liquid, and therefore a lower contact angle. However it should be remembered that this test is only ideal for surfaces with a roughness on a sub-micrometer level (Adamson and Gast 1997) – results for rougher surfaces must be treated with some caution. A low surface energy makes a surface more hydrophobic, resulting in decreases aqueous wetting (Santiago *et al.*, 2006). The surface free energy of a solid is defined as the change in total surface energy per surface area, assuming constant temperature, pressure and moles:

$$\gamma_s = \left(\frac{\delta G}{\delta A}\right)_{T,P,n} \tag{5}$$

where G is the total surface energy, A is the surface area, and n is the number of moles. Young's Equation governs the relationship between the interfacial surface tensions when a liquid makes contact with an exposed solid surface:

$$\gamma_{SV} = \gamma_{SL} + \gamma_{LV} cos\theta \tag{6}$$

in which γ refers to the free energy at the interface between the species in subscript (solid, vapour, liquid), and θ is the measured contact angle.

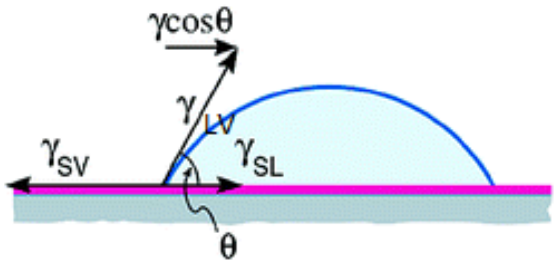

Figure 10: The contact angle, θ, of a liquid droplet on a substrate. The surface tensions (γ) are also shown at each of the three interfaces (Tadmor 2004).

Once the contact angle of the droplet is determined, there are various ways of translating this to find the surface free energy. Using Young's equation, the energy for the water-air interface is a standard value ($\gamma_{LV} = 0.072 Nm^{-1}$), although the solid-vapour surface energy is variable due to factors such as roughness variations, manufacturing process, or defects (Buckley 1981), which effectively results in two unknown variables. The Zisman Theory determines a critical surface energy belonging to a theoretical liquid which would completely wet the surface in question (ie θ = 0). This is achieved by testing the contact angle of a range of liquids with a known γ_{LV} component on the surface (Zisman 1964). A more hydrophilic surface will have a higher critical surface energy (equating to a higher difference between γ_{SV} and γ_{SL} – using this method, these values do not need to be found) . This value is determined graphically by use of a 'Zisman plot' of cos θ and the γ_{LV} values to find γ at cos θ = 1.

There are four more complex way of determining surface energy from contact angle measurements, which typically require computational algorithm software to solve. The Owens-Wendt geometric mean approach uses the following equation:

$$\gamma_L(1 + cos\theta) = 2\sqrt{\gamma_S^d \gamma_L^d} + 2\sqrt{\gamma_S^p \gamma_L^p} \quad (7)$$

It is derived from the work required for adhesion, which is equal to the geometric mean of the cohesive work of solid-solid and liquid-liquid particles (Owens and Wendt 1969). The superscripts d and p refer to the dispersive and polar attractions respectively, the sum of which comprises the total free energy of a surface (Yao *et al.*, 2017). Liquids with known dispersive and polar components are therefore required for this method to work. The Wu harmonic mean method works on the same basis, but substitutes the geometric mean for the harmonic mean, resulting in the following (Wu 1971):

$$\gamma_L(1 + cos\theta) = \frac{4\gamma_S^d \gamma_L^d}{\gamma_S^d + \gamma_L^d} + \frac{4\gamma_S^p \gamma_L^p}{\gamma_S^p + \gamma_L^p} \quad (8)$$

Alternatively, the van Oss acid-base approach comprises of the sum of the Lifschitz-van der Waals (LW) and Lewis acid-base (AB) components of interaction (with the polar components of each surface considered separately) (van Oss *et al.*, 1988):

$$\gamma_L(1 + cos\theta) = 2(\sqrt{\gamma_S^{LW}\gamma_L^{LW}} + \sqrt{\gamma_S^{+}\gamma_L^{-}} + \sqrt{\gamma_S^{-}\gamma_L^{+}}) \quad (9)$$

The use of equations of state is the final common method, of which there are a few variations. They take a purely thermodynamic approach, avoiding the potential for inaccuracies in contact angle measuements. They state that the interfacial free energy is determined by the liquid surface tension and solid surface free energy only (Chibowski and Perea-Carpio 2002). All four of these methods are considerably more complex than the Zisman plot which, whilst it lacks a genuine theoretic background and doesn't provide the actual surface energy value, remains very useful for the comparison of a selection of surfaces, producing a hierarchy of surface energy (Perrozzi *et al.*, 2014).

Effect of Surface Energy on Bacterial Adhesion

The hydrophobic/hydrophilic nature of the surface is known to have an effect on microbial adhesion in aquatic environments (Momba *et al.,* 2000), as this will alter the contact angle between the flow and the substrate surface. Hydrophobic surfaces promote low wetting, promoting cell adhesion in conjunction with membrane fusion and protein folding and aggregation (Alsteens *et al.,* 2007). Such surfaces encourage greater accumulation of proteins which then act as specific binding sites for bacteria (Lindh 2002). The general consensus is that hydrophobic cells display stronger adhesion to a surface, and that hydrophobic surfaces are favoured by all bacteria (Geoghegan *et al.,* 2008). Interactions between two hydrophobic materials are known to be notably strong (Desrousseaux *et al.,* 2013). Conversely, artificial hydrophilisation of a resin composite surface was shown by Okada *et al.,* (2008) to inhibit the amount of retained bacteria in correlation with increased concentration of coating. Cell surfaces with a high nitrogen:carbon ratio (due to proteins) are more hydrophobic, whereas high oxygen:carbon surfaces promote hydrophilicity (Reid *et al.,* 1999). The hydrophobicity or hydrophilicity of the cells depends mostly on the strain, but cell age and the environment are also important factors (Bos *et al.,* 1999).

Hydrophobic attractions between non-polar molecules (or between one non-polar and one polar molecule in water) are suggested to be a consequence of the hydrogen-bonding energy of nearby water molecules (van Oss 1995). Oliveira *et al.,* (2001) studied adhesion on four polymer surfaces and showed an increase in attached *Staphylococcus epidermidis* cells in accordance with increasing hydrophobicity. Sheng *et al.,* (2008) studied bacterial colonisation of metals and deduced that reduced hydrophobicity weakened the forces of adhesion. This weaker binding at the surface should allow for easier removal (Zhao *et al.,* 2005). Hydrophobic attractions have long been recognised as an important factor in the initial adhesion of bacteria (Fattom and Shilo 1984).

Bos *et al.*, (2000) investigated biofilm formation on glass with sections coated in the hydrophobic dimethyldichlorosilane (DSS), and suggested that substrate hydrophobicity is most significant in biofilm retention, whilst it plays little part in the adhesion process. Perhaps more interestingly, the same study implied that a relatively large number of bacteria were retained in regions where there was a hydrophobic/hydrophilic interface. In support to this, previous evidence suggests that proteins bind most effectively in heterogeneous regions of wetting tendency (Ruardy *et al.*, 1997). Raut *et al.*, (2010) showed no correlation between cell surface hydrophobicity (CSH) and adhesion of *Candida albicans* yeast to polystyrene, suggesting the relative unimportance of surface hydrophobicity in adhesion to surfaces.

A high surface free energy has been shown to collect more attached bacteria in the case of dental plaques (Quirynen and Bollen 1995). Klotz (1994) showed that CSH played an important role in the adhesion of *Candida albicans* yeast cells to substrates by promoting hydrophobic interactions between the cells and the surface. There is no simple answer regarding the relationship between surface energy and adhesion, with conflicting findings reported. Where there is an increase in surface free energy, there becomes a greater intermolecular force between the cells and the solid surface, which has the potential to enhance the extent of adhesion (Yabune *et al.*, 2005). The surface energy of the cells themselves will also have an impact. Usually, a hydrophilic cell will attach preferably to a hydrophilic surface. Hydrophobic low energy surfaces are typically preferred in industrial and marine biofouling control due to their lower interactions with living cells (Vladkova 2007). The aforementioned Baier curve (Figure 8) indicates how cell adhesion can increase for both notably hydrophobic and hydrophilic surfaces. Research by McGuire and Swartzel (1987) supported this idea of a region of minimal adhesion at 30-35 nM/m.

Fluorinated resin coatings have been demonstrated to reduce the adhesion of organic matter to surfaces via a reduction in surface free energy – Tsibouklis *et al.*, (1999) reported a reduction in cell count for a mixed-strain *Pseudomonas* biofilm from 200000 to 51200 per view field area with the application of a poly(perfluoroacrylate) film. Berry *et al.*, (2000) also showed that *Pseudomonas aeruginosa* and *Staphylococcus aureus* were both failed to form biofilms on a phosphorylcxholine-coated fluoroplastic compared with the same surface either untreated or impregnated with silver oxide. These results suggest the impact which surface energy-reducing treatments can have on biofilm formation, in the late case even more so than the antimicrobial silver oxide.

2.5.3 Surface Charge

The presence of favourable surface charges may also alter the tendency of bacteria to gather on the surface (Lindsay and von Holy 2006). The study by Carlén *et al.*, (2001) on plaque formation showed an increase in biofilm in accordance with increased inorganic, positively charged elements on the studied surfaces after polishing (also the cause of greater surface roughness). Greater exposure of silicon, aluminium and barium were observed, and it is recognised that most bacteria-binding

constituents are acidic and negatively-charged under standard neutral pH conditions (Johnsson *et al.,* 1993).

The EPS typically carries ionisable functional groups, chiefly carboxyl, phosphoric and hydroxyl groups. These can be readily dissociated, thus rendering EPS negatively charged at a neutral pH. Cell walls also typically have a negative charge. The greatest dissociation occurs at higher pH levels, and so therefore the surface charge of the EPS tends to increase with pH (Wu *et al.,* 2010). The zeta potential in sludge flocs was shown to increase linearly with the total EPS content (Meng *et al.,* 2006). The cohesiveness of EPS is partly due to electrostatic interactions, resulting from multivalent crosslinking cations which bridge negatively charged sites (Chen and Stewart 2002).

2.5.4 Substrate Materials

A study by Waines *et al.,* (2011) compared biofilm formation on a selection of plumbing materials over 84 days, revealing that plastic-based cross-linked polyethylene (PEX) and ethylene propylene diene monomer (EPDM) supported greater levels of biofilm than both copper and stainless steel. However, on the other hand a similar investigation carried out by Kerr *et al.,* (1998) showed that cast iron piping founded less biofilm than plastic-based medium density polyethylene (MDPE) and unplasticised polyvinyl chloride (uPVC). This is a familiar contradiction which highlights the complexity of surface effects with respect to biofilm adhesion.

A study by Hyde *et al.,* (1997) studied the ease of removal of *Klebsiella pneumonia, Escherichia coli,* and *Salmonella choleraisuis* using sodium hypochlorite under mild agitation, and suggested the following hierarchy of materials for the propensity of strong biofilm development: stainless steel > polypropylene > glass > machined perfluoroalkoxy tatrafluoroethylene (PFA), rotationally-molded PFA, silicone-coated glass > polyvinylidene fluoride (PVDF), injection-molded PFA.

Mott and Bott (1991) studied the adhesion of *Pseudomonas fluorescens* on electropolished and unpolished stainless steel 316, glass and fluorinated ethylene polypropylene and noted that the steel used ‘as received’ (i.e. not electropolished) displayed a greater mass of biofilm than the polished steel and the other two surfaces (Fig. 8). The explanation for the greater accumulation may concern a change in roughness or surface charge, or a combination of the two, but it is a clear illustration of the variation which can be observed between different surfaces.

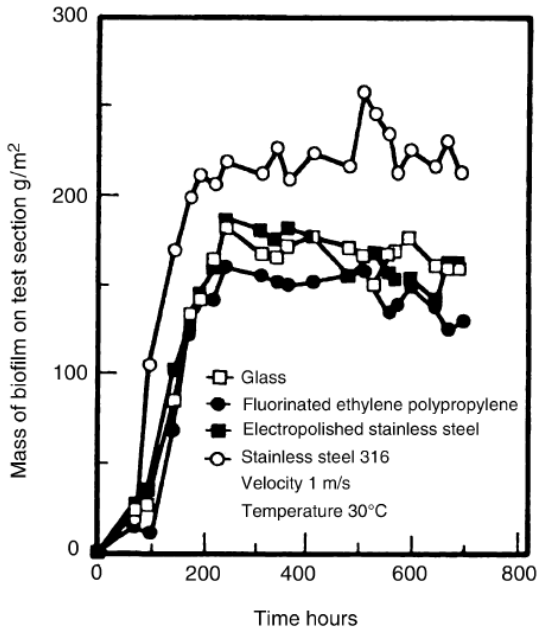

Figure 11: A comparison of the mass of biofilm accumulated on various surfaces from a study by Mott and Bott (1991)

The material may be able to supply greater nutrients for bacterial growth which will encourage biofilm formation; in water transportation it is recognised that the material used for the construction of pipes has an impact upon the quality of water delivered. Corrosive materials, such as cast iron, tend to encourage biofilm accumulation, as opposed to more inert materials (glass, stainless steel etc.). Cast iron surfaces are also noted to encourage the decay of disinfectant residuals when chlorine or chloramines are used (Baribeau *et al.*, 2005).

2.5.5 Summary

Ultimately, all of the above factors are recognised to have a potential impact upon biofilm adhesion, although the ways in which they can combine in relation to a given surface mean that it is difficult to define precisely the importance of each. They are, however, all able to affect both the rate of colonisation and the structure and strength of the biofilm (Busscher *et al.*, 1995). Attachment is therefore a complex process, and one in which the nature of the surface, whilst important, does not necessarily have the deciding say in how biofilms form. The conditions of the local environment are usually as crucial as any surface factor, as described by Gubner and Beech (2000), who found that the concentration and chemistry of the EPS are more important than either surface roughness or hydrophobicity. Additionally, research by Lorite *et al.*, (2011) supported this, suggesting that the presence of phosphate groups on the surface contained within a conditioning film was of primary significance. Any alterations in surface chemistry would in turn have the ability to alter the roughness, energy or charge of the surface, underlining the complexity of such analyses.

2.6 Removal of Biofouling

Biofilms have developed many different defence mechanisms against disinfection over millions of years, to the extent that biofouling is a problem which can effectively never be eliminated. Antifouling measures are therefore time-dependent rather than permanent (Flemming *et al.*, 2011). Ironically, it can be noted that industrial plants tend to provide optimum conditions (temperature, moisture) for the establishment of biofilms.

In laboratories, cells have traditionally been studied in the planktonic (free-swimming) phase, although bacteria are predominantly found in biofilms throughout most natural, clinical and industrial settings (O'Toole and Kolter 1998). It is recognised that bacteria in biofilms are more resistant to cleaning materials than those in planktonic suspension, and that the same methods of characterisation and removal cannot effectively be applied to both cases (Parker *et al.*, 2014). For some disinfectants, the concentration must be increased by between 10 and 100 times in order to achieve the same level of deactivation of biofilm-based bacteria compared with those free in suspension (Blanchard *et al.*, 1998). This is naturally mostly due to the extracellular polymeric substances, which are important for attachment and resistance to natural shear forces. The EPS can also act as a physical barrier to disinfectants, with the matrix providing a shield-like effect through which chemicals and enzymes must penetrate and diffuse (Buckingham-Meyer *et al.*, 2007). This process has been occasionally shown to chemically 'exhaust' biocides – especially chlorine, which can react with organic constituents faster than it diffuses (Chen and Stewart 1996). Effective cleaning methods should therefore seek to break up the matrix, in order to allow better access for disinfectants to attack (Mathieu *et al.*, 2014).

Other reasons for resistance include the altered environment in which biofilm bacteria reside. The physiological adaptations which cells must undergo to exist within biofilm conditions (sessile growth, slow development under nutrient stresses, continuous contact with low levels of disinfectant) result in further opposition to cleaning (Bridier *et al.*, 2011a). Disinfectants are typically less effective in dealing with slow growing/stationary cells or those with a slow metabolism (a feature of biofilm cultures) (Borriello *et al.*, 2004). There is often a gradient of growth rates within a biofilm, with the faster growing top layer cells being generally more susceptible to killing (Lewis 2001). The concept of 'persister' cells is one which has more recently been applied to those on the surface-attached layer, referring to those which are more resistant to removal and trigger re-growth of the culture (Davies 2003). Effectively, they act as protective guardians for the biofilm, lying dormant under the presence of a biocide and triggering multiplication when the biocide is removed (Cogan 2013). The exact phenotypic explanation for the formation of persisters is unclear, but the severe nutrient starvation at the base is likely to be a major factor (Shafahi and Vafai 2010). The proximity of the surface also results in boundary layer effects, especially in laminar regimes where the boundary layer is substantial enough to restrict the movement and mixing of cells (Donlan 2002). The stratified nature of biofilms

lends them a certain level of cohesive integrity (Zhang and Bishop 1994a), which has been shown to offer greater tensile strength in correlation with the age of the biofilm (Ohashi *et al.*, 1999).

The threat of biofouling cannot be entirely eliminated – antifouling measures are only temporary, time-dependent restrictions of growth, and regular disinfection is required in order to prevent their continuous development (Flemming 2011). In essence, killing the cells alone does not necessarily equate to cleaning. Furthermore, given the resistance mechanisms and inherent resilience of biofilms and the accordingly high levels of biocides required, the push for technologies focussed on detachment and dispersal rather than killing are desired (Jones *et al.*, 2011).

2.6.1 Chemical Cleaning

Disinfection is defined by the Codex Alimentarus (the international standards in food safety) as "the reduction of the number of micro-organisms in the environment, to a level that does not compromise food safety or suitability" (CAC 2003). It is crucial in distribution systems, particularly when concerned with the spread of water-borne diseases. The industrialised world has largely eliminated such illnesses by removing pathogens from drinking water supplies and production processes. Bacteria will often survive the standard treatment process (especially biofilms) so the final disinfection step is necessary to destroy them (Momba *et al.*, 2000). Biocides differ from antibiotics in that they are applied to suspensions and surfaces to kill or inhibit microorganisms, whereas antibiotics are synthesised by living organisms themselves (White and McDermott 2001). Biocides are usually applied at much greater concentrations than antibiotics, as they do not have to take into account issues of toxicity and bioavailability. The non-specific nature of biocide activity (coagulation, membrane damage) further encourages a non-targeted approach in which vast quantities are used, compared with antibiotic use, where targeted antibodies can be used at low concentrations due to their specificity (White and McDermott 2001). Chemical addition usually follows one of three methods: a continuous dose at a level by which control can be maintained; intermittently high 'shock' doses designed to remove biofilms accumulated in the intervening period; or a more regular intermittent dose in short periods in order to minimise colonisation (Bott 1998). Higher velocities are known to improve biocide effectiveness due to improved mass transfer and shear rates (Bott and Taylor 1997), although doubling the fluid velocity tends to result in a quadrupling of the energy required (Bott 1998). The minimum amount of cleaning chemical required can be expressed as either minimum inhibitory concentration (M.I.C.) or minimum bactericidal concentration (MBC), depending on whether the priority is to inhibit further growth, or to kill the resident cells. M.I.C. is defined as the lowest concentration of an antmicrobial required to inhibit visible growth of a microorganism after overnight incubation, and MBC is the lowest concentration which will prevent growth after subculture on to antibiotic-free media (Andrews 2002).

Chlorine, Chlorine-Derivatives and Other Halogens

Chlorine and chlorine-derivatives have long been commonly used as a disinfectant in water-based systems. Sodium hypochlorite (bleach) is a standard example. The explanations for chlorine-controlled inactivation are disputed, but it is suggested that reactions with amino acids in cell membranes or cytoplasm result in cell death (Dychdala 2001). The chlorine demand of a biofilm (high demand occurs in areas of high biomass) is dependent on the purity of the water in the system (Lu *et al.*, 1999).

There are some simple alternatives which have been shown to produce promising results. Chloramine (NH_2Cl) has shown itself to be less reactive than pure chlorine, and so therefore has a greater presence in the system for a longer period of time. It has also been suggested that chloramine displays better penetration into biofilms than free chlorine (Samrakandi *et al.*, 1997). This feature acts to limit the survival and potential regrowth of bacteria which is prevalent in chlorine-disinfected systems (LeChevallier *et al.*, 1987). Comparisons of apparatus disinfected with a combination of chlorine and chloramine compared with those disinfected with just chlorine show stronger and more significant negative correlations between residual concentration of disinfectant and numbers of bacteria present (Momba and Makala 2004). It is, however, notable that even continuous residuals of chlorine disinfectants can never be truly relied upon to eliminate the presence of bacteria, as communities are capable of adapting in response to disinfection methods (Williams *et al.*, 2005).

Bromine has had a more limited range of use compared to chlorine, with applications centred around swimming pool and potable water disinfection. In such environments, it has been shown to be less effective against *Legionella pneumophila* than chlorine, although populations can be controlled with a maintained bromine residual (Thomas *et al.*, 1999). Iodine has been used for similar purposes, although its efficacy is less well known (Kim *et al.*, 2002).

Halogen-releasing compounds are another related group of biocides, which release halogens upon contact with water. They include BCDMH (2,4- dibromo-5,5-dimethylhydantoin), which is slightly soluble in water, releasing the disinfectants hypobromous acid and hypochlorous acid on contact. Effectively, this means that their impact is equivalent to the addition of free chlorine or bromine, and little difference has been noted in their efficacy (McCoy and Wireman 1989).

Alcohols

Alcohol-based disinfectants tend to be effective against a good range of organisms, and are usually robust in the presence of other organic materials. They act to both damage cell membranes and denature proteins. In testing, 70% ethanol has been shown to reduce vegetative *Salmonella* populations completely (i.e. to below 5 $\log_{10}$ CFU), with concentrations as low as 15% having been shown to be equally effective under low-pH (e.g. 3) conditions (Wong *et al.*, (2010); Møretrø and Daeschel (2004)). Unfortunately, when used in high volume, alcohol use can become uneconomical

and present health and fire risks, and so therefore practical use tends to be limited mostly to hand disinfectants (Møretrø *et al.*, 2012).

Aldehydes

Aldehydes (usually in the form of glutaraldehyde) are recognised to be highly effective in the inactivation of bacteria. Its efficacy in combating *Legionella* has been utilised in treating biofilm formation in cooling towers and water systems, in which Pope and Dziewulski (1992) showed that a dosage of 100mgL^{-1} could treat four towers. Similarly, McCall *et al.*, (1999) noted a 3-log reduction in *Legionella* cells in under an hour in a model plumbing system. However, these same studies noted that continuous high doses of glutaraldehyde were required for longer-lasting control. Another use of aldehydes has traditionally been the disinfection of heat-sensitive medical devices, against fungi, spores and viruses as well as bacteria (Loukili *et al.*, 2004). Recently, however, there has been concern about reduced susceptibility of targeted strains to aldehydes, with decreasing biocidal activity reported (Van Klingeren and Pullen 1993).

Quaternary Ammonium Compounds

Quaternary ammonium compounds (QACs) are cationic surfactants which also act as disinfectants (Huang *et al.*, 2009). Benzalkonium chloride (BAC) is a particularly popular example, using in food processing and environmental and medical applications. They chiefly act to disrupt the membrane and therefore release the contents of the cell (Jahn *et al.*, 1999). They offer good matrix penetration in combination with low toxicity and propensity for corrosion (Ko *et al.*, 2007). Huang *et al.*, (2009) showed that BAC was more effective than the halogen-releaser 2,2-dibromo-3-nitrilopropionamide (DBNPA) and the organic isothiazolone at killing sessile cultures of *Pseudomonas aeruginosa* collected from a paper machine, due to its ability to trigger cell lysis and the release of cellular components (Russell and Chopra 1996). As with other chemical biocides, however, there are issues regarding acquired resistance. The poor biodegradability of QACs results in them having longer contact times with target bacteria, and prolonged exposure of weak residual concentrations encourages resistance to develop via changes in cell morphology (Tezel and Pavlostathis (2011); Dynes *et al.*, (2009)).

Peracetic Acid

Peracetic acid is an oxidising agent which has the advantage of decomposing into safe waste products (van der Veen and Abee 2011). In addition to this, it is minimally toxic and non-corrosive at typical required concentrations (Kovaleva *et al.*, 2010). It is most commonly used in food and medical environments (Bridier *et al.*, 2011b). Its high oxidative potential is believed to be a major factor in its antimicrobial ability; other proposed reasons include a non-specific mode of attack, high reactivity against cellular proteins and DNA, and a small size assisting in diffusion through the biofilm matrix (Vázquez-Sánchez *et al.*, 2014). Non-specificity combined with high oxidative potential give peracetic acid similar levels of efficacy against many different species, where other biocides often

show greater variability with respect to species (Bridier *et al.*, 2011b). Tests by Vázquez-Sánchez *et al.*, (2014) showed that peracetic acid was more effective against *Staphylococcus aureus* than benzalkonium chloride and sodium hypochlorite in both the biofilm and planktonic cases. However, higher tolerance to peracetic acid (and other oxidising agents) was observed for biofilms with a high EPS content, suggesting a protective deactivating layer (Martin *et al.*, 2008). There are also concerns that, whilst it is effective as a biocide, it can 'fix' blood and proteins to surfaces, increasing the risk of re-growth (Kampf *et al.*, 2004).

Sodium Hydroxide

Sodium hydroxide (NaOH) is a regular active component in cleaning-in-place (CIP) regimes and dishwashing and cleaning products. It is a very strong base which is able to break most chemical bonds in cells and therefore dissolve tissues (Elexson *et al.*, 2014). Long-term treatments with NaOH have been very promising in trials on cooling system pipes (Calazans *et al.*, 2012), and TenEyck (2009) showed its significant efficacy in reducing the numbers of a range of organisms. Another study showed that dilute NaOH can weaken the mechanical strength of biofilm clusters, resulting in deformation under flow (Xavier *et al.*, 2005). Its ability to remove organic fouling layers (proteins and fats) has led to its wide use for cleaning in the food industry (Brugnoni *et al.*, 2012).

Cleaning-in-Place

CIP remains the most widely-used cleaning practise in the manufacturing industry. A definition provided by Romney (1990) describes CIP as "cleaning of complete items of plant or pipeline circuits without dismantling or opening of the equipment", with "little or no manual involvement", under "conditions of increased turbulence and velocity". Most CIP systems rely on circulating cleaning fluids through the process in order to rinse away any loose material and to alter the physical characteristics of the fouling so that it can be more easily removed by erosion or dissolution (Saikhwan *et al.*, 2007). This combination of chemical and hydraulic actions is effective in removing a considerable range of deposits, which is why it remains a popular procedure, although the nature of the flow and the fluids used must be tailored to meet the foulant in question (Chew *et al.*, 2004b). Remedies used in one particular situation are often not directly applicable to another. The factors which can limit the effectiveness of CIP are extensive, and include the age of the fouling layer, disinfectant temperature and the turbulence of the solution, along with the typical parameters affecting chemical cleaning (Bremer *et al.*, 2006).

Food production plants make extensive use of clean-in-place ideas. The dairy industry is a prominent example, with sequential caustic (alkali) and acid wash steps being used. The caustic step, normally using sodium hydroxide, is carried out to remove proteins and carbohydrates (Chisti 1999).The acid step (e.g. nitric acid) is crucial in removing any mineral scale deposited by the caustic wash, and also removes any alkaline products from process surfaces (Bremer *et al.*, 2006). The use of strong acids and alkalis offers the most efficient cleaning, yet results in labour and care-intensive storage and

handling issues. On the other hand, more moderate-strength solutions often simply do not remove sufficient amounts of biofilm (Furukawa *et al.,* 2010). Testing of procedures can also be difficult due to the multi-phase nature of most CIP programmes, making process optimisation both time-consuming and difficult to specify (Kumari and Sarkar 2014).

2.6.2 Limitations of Chemical Disinfection

Removal Failure

A recurring problem with chemical-dominated approaches to biofilm removal is the way in which biofilms are treated as a 'technical disease', and are thus tackled in a way analogous to medical procedures (Flemming 2011). This ignores the evidence that biofilm growth is dependent upon the matrix structure being able to support growth, meaning that focussing merely on killing cells does little to negate the problem. A chemical-based approach alone is therefore limited if the biofilm structure remains intact (Flemming *et al.,* 1996). It favours killing rather than cleaning, which are wholly different principles when applied to biofilms. Rapid cell growth kinetics ensure that regrowth will typically commence shortly after treatment, regardless of the cleaning methods (Stewart *et al.,* 1996), and so therefore the key action appears to be the detachment of the surface-attached layer. Merely adding a free chlorine residual to a fluid bulk has very little effect on the numbers of bacteria present in biofilms, as survival and multiplication of micro-organisms can often still be observed even after a regular, consistent supply. Chemical agents can only control the symptoms of the infection - the biofilms remain and will support rapid regrowth as long as the organic material is present (Lund and Ormerod 1995).

The extent to which dead cells can be ignored when analysing biocide efficacy was demonstrated by (Schulte *et al.,* 2004). When cell presence was quantified using a colony count method (cultivation), the number of viable cells fell from 10^7 per cm^2 to less than 10^1 per cm^2. However, with a total cell count method, the number of cells present was shown to be in the region of 10^5 or 10^6 per cm^2, implying the failure to remove the biofilm structure, making re-growth inevitible.

Toxicity and Contamination

By definition, all biocides are naturally toxic, and most are also corrosive (Sondossi *et al.,* 1986). Chlorine and bromine – based chemicals are popular disinfectants due to their oxidising potential, which attack the structure of cell membranes, leading to cell lysis and death. However, they also present the risk of forming high levels of hazardous by-products (Torres *et al.,* 2011). Both the disinfectants themselves and the related by-products have the potential to endanger operators' health (dependent on concentration), as well as contributing to plant damage and environmental issues (Pechaud *et al.,* 2012). Regulations require consideration and quantification of the following factors when approving biocides: acute and repeat-dose toxicity, irritation and corrosivity, sensitization, mutagenicity, carcinogenicity, toxicity for reproduction and physicochemical properties (Cloete and Flemming 2012).

Chlorine is noted as the largest single cause of major toxic incidents (Das and Blanc 1993). Chlorine and hydrogen chloride are corrosive to metals and vegetation, and chloro-hydrocarbons are linked to ozone destruction (Das and Blanc 1993). Widespread use of biocides in domestic cleaning products has seen many regarded as potential contaminants (Daughton and Ternes 1999), and their impact upon the environment when used in industrial applications is beginning to be grasped. Acidic and alkaline solutions, such as those used in clean-in-place strategies can lead to wastewaters with low or high pH levels. Wastewaters can also be produced with high chemical oxygen demands (COD) due to cleaning chemicals and removed deposits (Nishijima *et al.,* 2014). Excessive use and the related emissions can contaminate surface water environments and pose threats to plant life and other organisms, even after 72-93% removal via wastewater treatment (Ying and Kookana 2007). For example, triclosan is recognised to be toxic to algae at a level of 0.2 ugL^{-1} (Yang *et al.,* 2008). European Community regulations insist on the reduction of damaging biocides, or the proposal of sustainable alternative strategies (Xavier *et al.,* 2005). The Biocidal Products Directive (active from May 2000) demands the risk assessment of biocides to humans, animals and the environment, taking into account acceptable exposure levels and the absorption rate for the relevant routes of uptake (van Hemmen 1999). A vast array of data is now required including end-use formulation, residue chemistry, environmental fate and ecotoxicity. This is in contrast to early biocide use, where the requirements considered were effective antimicrobial activity, broad efficacy, stability and persistence, and economic feasibility (Sondossi *et al.,* 1986).

Environmental contamination is by no means limited to added biocides either – tributyltin (TBT) based antifouling paints have been banned for use on ship hulls after being the industry standard since the 1970s (Mukherjee *et al.,* 2009). TBT is poisonous to many organisms (in particular being implicated in the masculisation of female species) and may also enter the human food chain (Straw and Rittschof (2004); Heidrich *et al.,* (2001). This shows how widely-used biocides can later be revealed to have harmful effects upon exposure to the wider environment, and in the case of TBT, the long term effects of its replacements are yet to be fully determined (Mukherjee *et al.,* 2009).

The toxicity of many biocides ensures that there are also issues concerning their handling and disposal. Depending on the class of biocide, there are different disposal routes to be applied: organics may be burned, halogens can be reacted to form inactive solid residues, and acids and alkalis can be neutralised (Müller-Steinhagen 2000).

Reactivity

Another problem associated with disinfection is the potential for the production of organic substances which can then be used as an energy source to promote further bacterial growth. This will result in regrowth after the initial reduction upon addition of the disinfectant. In order to negate this, less reactive and more persistent compounds are required to maintain a consistently high level of disinfectant which can infiltrate the biofilm more effectively (Momba *et al.,* 2000). The problem of

resistance is one which is immensely difficult to avoid, given that selection of resistant populations (whatever the mechanism of development) is the inevitable end result of biocide use, once the susceptible strains have been eliminated (Sondossi *et al.*, 1986). Many commercial polymer-based membranes have shown sensitivity to the oxidative power of chlorine, with resultant harmful compounds having been found in water supplies, although chlorine-tolerant membranes are now in production. Chlorine dioxide is an alternative which produces less harmful by-products, but it is costly and presents handling issues as it cannot be produced on site (Saad 1992). Chlorines are a less reactive alternative, although they are still able to react to form carcinogenic compounds which can permeate membranes (Nguyen *et al.*, 2012). Chlorine also reacts readily with various substances which may be found in water channels, including iron, ammonia, and a number of organic compounds, such as those found in the EPS. It also frequently interacts with pipe corrosion and deposits which may be present.

Acquired Resistance

The emergence and development of bacteria which are resistant or insusceptible to biocidal action is another concern. Overuse of biocides can also create niches where mutations providing antimicrobial resistance prevail (Albrich *et al.*, 2004). Resistance to antibiotics has been observed for many years, due to over-use in medical treatments and their inclusion in animal feed, and there is now belief that the same traits can offer resistance to disinfecting biocides (termed cross-tolerance). Antibiotic-resistant bacteria have also been found in food processing environments, suggesting that this transfer may be mutual (Poole 2005). Such resistance is sometimes due to an innate insusceptibility to a certain antimicrobial species, whilst in other cases an acquired resistance is needed, either via a genetic mutation or transfer from a foreign body (Davies 1997). The mechanism of resistance can vary – ranging from inactivation of the biocide, to the development of efflux systems, to simply persisting in growth despite the biocide's presence (Sondossi *et al.*, 1986). Some biocides can be immune from this effect, in so far as they may exhibit non-specific disinfection mechanisms, usually by attacking the physical integrity of the cells, rather than negating the growth of a particular species (Jones 1999). The effect of biocide resistance on human health is contested, given that the concentrations used are typically high enough to counter multiple bacterial processes, although the lingering presence of residues may provoke multiple resistances, and there is the issue of hazardous by-products to consider as well (White and McDermott 2001).

Non-Specificity

Disinfectants tend to be comprised of multiple antimicrobial chemicals at substantial concentrations in order to be effective against a range of species, as opposed to being formulated to attack a certain target (Gilbert and McBain 2003). This approach, whilst being designed for maximum efficacy, self-evidently leads to an overuse of biocides. In addition, disinfection is not expected to remove or

deactivate all the living cells in a system as per sterilisation (Cerf *et al.*, 2010), which will inevitably lead to re-growth of biofilms.

To put it simply, the solution to the negative environmental and health impacts of disinfectants lies in either using environmentally-friendly biocides which break down to harmless products after use (i.e. peracetic acid or hydrogen peroxide), or to find methods of adapting the treatment process to reduce the amount of chemical input required (Bott 1998). A combination of the two approaches is likely to be the ideal approach for the most effective reduction in environmental impact.

2.6.3 Mechanical Cleaning

Hydrodynamic forces are an alternative tool for the removal of biofilms. Such methods are particularly useful where a reduction in chemical use is desired, or simply where the action of chemical disinfectants is simply not working to a satisfactory standard. Flow conditions can be manipulated to promote shear stresses close to the biofouling surface in order to prevent attachment and growth, which is where knowledge of the shear properties of the deposit proves useful. The age of the layer can also have an impact, as the strength of the deposit often increases with time, due to reactions between organic components, reduction of layer voidage or the production of adhesive extracellular materials (Chew *et al.*, 2004b). Early investigations observed increasing detachment at greater Reynolds numbers, which translates to a greater flow velocity and therefore also a greater applied shear stress (Choi and Morgenroth 2003). The use of hydraulic cleaning methods, such as flushing and backwashing, are especially widely-used in reducing fouling in cross-flow membrane filtration processes, which is important given the problems with reactions and penetration in the chemical mitigation of membrane biofouling (Nguyen *et al.*, (2012); Lin *et al.*(2010)).

Effects on fouling behaviour via shear forces are normally affected by two different factors: drag force which instigates the removal of particles, and lift force which can reduce the risk of the initial adhesion taking place (Perry and Kandlikar 2007). Lift force is created where there is fluid flowing past a particle in association with a permanent surface, caused by the relatively high velocity (and therefore lower pressure) in the bulk flow. The pressure difference drives the lift force. Biofilms, however, display more complex rheological behaviour. Stoodley *et al.*, (1999) indicated that biofilms behave as elastic or viscoelastic solids under a shear stress of below 5 Pa, and as viscoelastic fluids at higher stresses. The authors suggested that these behaviours may contribute to the large pressure drops often noted in biologically fouled pipes. Nevertheless, there is a relationship between increasing shear stress and increases in both the size of removed clumps and the number of detachment events (Walter *et al.*, 2013).

Mechanisms

Incremental step change in local shear stress is recognised to be the main driver in hydrodynamic biofilm detachment. Pechaud *et al.*, (2012) showed that an increment of 2.5 Pa produced a mean

removal of 65% biomass and 28% in reduction of coverage. This treatment gave better results for both criteria than disinfection with sodium hypochlorite at a concentration of 150 mgL^{-1}, although combined treatments out-performed both (to be discussed more later). A compression effect was noted at higher stress increments, which could hamper subsequent chemical cleaning by restricting penetration. Mathieu *et al., (*2014) also observed that a shear stress increase of 0.2 Pa up to 10 Pa resulted in the erosion of more than half of attached cells. Erosion is believed to be the dominant process of removal – increased shear stresses were shown by Walter *et al.*, (2013) to have no impact on the number of sloughing events observed (suggesting no notable structural alterations). However, sloughing can be an important process in removal, as greater biofilm heterogeneity encourages the development of localised stress peaks which in turn trigger greater detachment (Telgmann *et al.*, 2004).

Stoodley *et al.*, (2002b) showed that *P. aeruginosa* biofilms grown under a low shear are less dense and easier to detach by mechanical forces (i.e. at lower shear). Such biofilms (also those grown under static conditions) tend to have clumps of cells dislodged more easily when there is an increase in flow rate (Stoodley *et al.*, 1998). Likewise, biofilms grown under high shear will detach at higher shear forces. The growth conditions give the matrix an inherent internal tension in equilibrium with the shear stress applied, which means that the removal stress must overcome these forces (Stoodley *et al.*, 1999). Experiments by Stoodley *et al.*, (2002b) suggested that removal onset occurred at a shear stress of roughly two or three times that of the fluid shear for growth. Differences in the efficacies of cleaning are particularly marked when comparing those grown under laminar and turbulent flow (Simões *et al.*, 2005a).

Mechanical Methods

Mechanical fouling removal methods work in ways which are similar to hydraulic protocols, in that physical force is favoured over chemical disinfection. Steam-blasting and hydro-blasting are common examples of mechanical treatment. There is no guarantee of superior removal efficiency, however, and they are both time and labour intensive (Müller-Steinhagen 2000). Care must be taken to prevent damage, particularly with delicate systems such as heat exchangers, and this can contribute substantially to the labour and time requirements.

Spray balls are a simple and cheap method of cleaning the walls of tanks and other reactors. They are a generally effective way of distributing cleaning liquids onto the inner surfaces of a tank. Small jets of fluid are ejected from holes in the spray balls and hit the tank walls, and this delivery method means that the holes can be configured in a way specifically designed to meet the tank geometry or application (Collins and Huey 2015). A problem with this method is that by the time the cleaning liquid has reached the walls, the jets can be dispersed to an undesirable degree: therefore, in order to clean effectively, there is often a need for high volumes or concentrations of detergents, high temperatures, or an extended cleaning time. Their widest use is in tanks used for products of low

viscosity (Packman *et al.*, 2008). The use of sponge balls is an option for the cleaning of straight tubes in heat exchangers and tubular membranes, although they are more frequently a fouling prevention measure (Al-Bakeri and El Hares 1993). They are adept at removing soft scales from heat transfer surfaces. Similarly, drills can be fitted with drill bits or brushes (or both) for particularly clogged tubes. Plugs and scrapers can also be fired through a pipe using air or hydrodynamic force – scrapers remove most deposits when fired at 3 to 6 ms^{-1} (Müller-Steinhagen 2000). With such methods, unfortunately, there is the recurring risk of removing protective oxide layers along with the fouling deposit, running the risk of encouraging corrosion (Müller-Steinhagen 2000). Regular cleaning should typically prevent this from occurring, but this will in turn only exacerbate the lengthy shut-down times.

Plug methods, or "pigging" as such techniques are collectively known, are similarly effective ways of removing deposits, but the design of the system in question has a major influence on their potential success. The presence of bends and branches, for example, can present insurmountable difficulties, so systems often have to be designed specifically with pigging in mind (Flemming 2011). Pigs can only access very simple geometries, so uniform pipes with constant diameters are a necessity (Cordell 1991). Such situations are rare, given that most systems involve branches, valves or instrumentation. Their use has therefore been mostly restricted to product recovery in the hydrocarbon industries, with forays into food and pharmaceuticals (Quarini 2002). Quarini (2002) suggested the use of 'ice pigs' as an improved pigging method, combining the abrasive force of traditional pigs with smarter characteristics, such as the ability to flow in a fluid-like fashion and never get stuck in a pipe. Tests showed that the ice pig follows a plug flow regime whenever possible, yet is also able to access other pipe geometries. They are also very environmentally friendly.

2.6.4 Other Methods

Ultrasound and Microbubbles

Studies have shown that ultrasonic devices operating at 40Hz are adept at removing biofilms from food processing equipment. This is achieved by the generation of cavitational bubble activity and has been proven to work for removing biofilm from a variety of surfaces. Associated acoustic streaming effects (acoustic energy-induced turbulence) are also effective in transporting detached deposits away from the surface (Lamminen *et al.*, 2004). Microbubbles (10-50 µm diameter) are formed on a cyclic basis whereby they grow and collapse over short periods of time, releasing focused energy in the process and creating fluid shear effects in the local environment (Kirzhner *et al.*, (2009); Baker *et al.*, (2001)). High acoustic intensity is responsible for collapse, in which the bubble radius is substantially reduced (Erriu *et al.*, 2014).The contraction of the bubble wall results outgoing pressure wave and rising internal gas temperatures (up to in the region of 5000 K), which are able to produce free radicals from water and other molecules (Bigelow *et al.*, 2009). The antimicrobial result of this effect is due partly to the free radicals attacking EPS and cellular components, with other causes being

surface resonance due to pressure gradients at the cell wall, shear forces due to microstreaming, and the formation of hydrogen peroxide following the degradation of water (Joyce *et al.*, 2003).

Bacterial detachment depends upon the following: ultrasonic intensity, exposure time, and the distance and position of the transducer relative to the fouled surface. It has also been suggested that the application of acoustic energy (either continuous or intermittent) before biofilm formation has taken place may impede the attachment (Ridgway and Flemming 1996). Unfortunately, however, such devices can only be used on open surfaces, so therefore it is not applicable to pipes, which is a serious limitation for the assessment of fouling in many practical simulations (Oulahal-Lagsir *et al.*, 2003). Damage to membranes has also been reported (Kyllönen *et al.*, 2005).

The stable existence of nanobubbles at water-solid interfaces is a relatively recent discovery. Their ability to inhibit protein adsorption and remove adsorbed proteins is one which could be of great worth against biofouling (Wu *et al.*, 2005). Their use in fouling removal in based on more established techniques of air-water cleaning such as sparging or flushing. Efficient air distribution is considered to be an important obstacle in these methods, and air entrapment in the system after cleaning should be avoided (Cornelissen *et al.*, 2007).

UV Irradiation

Ultraviolet irradiation is a physical process which can be used to inactivate and destroy bacteria and viruses (Parrotta and Bekdash 1998). It is used in water disinfection, and functions by producing hydroxyl radicals which reduce organic carbon availability thus inhibiting growth, and also by degrading larger macromolecules into smaller fragments (Lehtola *et al.*, 2003). However, the performance of UV disinfection is restricted by the nature of both the species and the solution (in varying susceptibility to UV effects), and also the spatial distribution of the fouling. It is also relatively expensive, and therefore its use has been primarily limited to small, fully-automated systems (Nguyen *et al.*, 2012).

Enzymes

Enzymes are widely considered to be a viable tool for biofilm removal, given that they are capable of undermining the matrix's structural cohesion without presenting any recognised environmental risks (Pechaud *et al.*, 2012). Soluble antimicrobial enzymes are usually classified as either proteinases or polysaccharide-degrading (Orgaz *et al.*2007). In a manner similar to chemical disinfection, the efficiency of enzymatic biofilm treatment depends primarily on the selection to meet the biofilm composition, and the capacity of the enzyme to penetrate the matrix (Marcato-Romain *et al.*, (2012); Xavier *et al.*, (2005)). Mass transfer both in the boundary layer and into the matrix must therefore be considered (Stewart 1998), and therefore, overall, there are a number of factors affecting the scope of enzyme action in a given situation. Boundary layer transfer depends on hydrodynamic conditions and biofilm roughness, and internal mass transfer on biofilm structural properties including porosity and

density (Eberl *et al.*, (2000); Zhang and Bishop (1994b)). Tests by Pechaud *et al.*, (2012) suggested that enzyme action, combined with hydrodynamic effects, can be equally effective at removing base layer cells as at eroding the outer layers (90% mass removal and 88% coverage reduction were recorded). Opinion is divided as to whether these methods are superior to non-enzymatic biocide use, with Fang *et al.*, (2010) and Bloss and Kampf (2004) reporting inferior results for enzymes. This suggests that enzymes can be a desirable replacement for chemical disinfectant, but ultimately that success of either method depends on various factors specific to a case.

2.6.5 Establishing Effective Cleaning Protocols

In an investigation into the cohesive properties of mature biofilms, Derlon *et al.*, (2008) subjected deposits to both controlled erosion and abrasion mechanisms, indicating firstly that biofilms showed more basal cohesion with increasing depth, and significantly that the base 20% of biomass exhibited considerable strength and resisted erosive stress of 13 Pa. This, coupled with evidence of prevailing active microorganisms, implies that a purely mechanical approach may not be sufficient for a comprehensive removal of deposits. The same stable base effect was shown by Möhle *et al.*, (2007).

Methods of biofilm removal which combine a hydrodynamic (or other mechanical) approach with chemical disinfectants tend to be more effective. Simões *et al.*, (2005b) assessed the relative removal efficiencies of mechanical and combined methods. They found that the hydraulic treatment left 76% of the biofilm on the surface, and when chemical treatments were applied prior to fluid agitation, the remaining biofilm ranged from 3% to 62% (seven different surfactants were used). These results highlight the potential efficacy of combined methods, whilst also underlining the importance of biocide selection. The aforementioned study by Pechaud *et al.*, (2012) also compared synergistic removal methods with single hydrodynamic or chemical cleaning. When a disinfection step was followed by a stress increment, an 80% removal of biomass was observed (compared with 63% and 35% loss for hydrodynamic and chemical methods respectively). A large improvement was observed for surface coverage reduction, with 70% removal compared to 28% and 9% for the single method treatments. However, they did also find that substituting the NaClO with the commercial enzyme Savinase® gave the best results of all, which indicates that it may be possible to reach the most efficient cleaning results without chemical input at all. Applying the hydrodynamic treatment prior to the enzyme would assist in penetration, although this would double the water duties coupled with the final post-enzyme hydrodynamic input. A explanation for the benefits of this sequence was offered by Mathieu *et al.*, (2014), who observed that ‘shock’ chlorination led to a loss of biofilm cohesion and therefore easier shear detachment, whereas the application of mechanical stresses resulted in a condensed collapse of the structure and a more cohesive biofilm. Coufort *et al.*, (2007) described a layer structure in mechanical removal which appears to support this idea – their study showed a top layer (comprising approximately 60% of the total biomass) which could be removed at a low shear,

followed by an intermediate 20% section with a higher detachment shear, and a base layer of the remaining 20% which was much more difficult to remove.

Investigations into removal patterns relative to flow velocities and wall shear stresses are of huge importance in reducing chemical consumption, with recognition that to double velocity quadruples the required pumping power (Lens *et al.*, 2003). It is therefore essential that a better idea of the optimum requirement for sufficient removal is known, by gaining a better understanding of the nature and dynamics of the deposits. It should be noted that, similar to biofilm growth analysis, comparisons between removal techniques can show inaccuracies due to varying controls on substrata, media, flow conditions etc.

2.7 Biofilm Reactors

2.7.1 Standard Culture Procedure

In order to develop biofilms in a laboratory, the culture inoculum must first be grown. This follows a number of similar basic procedures starting with an original sample, frozen in glycerol to prevent the formation of ice crystals which would kill the bacteria. The chosen sample will then be transferred by loop into a tube, or streaked onto an agar plate, containing a growth medium (Pommerville 2010). The media can vary in composition, but they invariably contain yeast extract, meat extract, tryptone or other proteins, and often salts (such as NaCl). Together the media components should contain all the nutrients necessary for growth (i.e. carbon, oxygen, nitrogen and phosphorus). The tubes/plates are then incubated, with constant shaking if necessary.

Commonly, once the culture has been incubated (usually overnight), it is subsequently diluted in fresh medium and inoculated into microtitre plates to carry out a static assay. This process requires plates with numerous wells (normally 96, although plates with fewer, larger wells may be more appropriate in some cases) for the biofilms to be established within (Barua *et al.*, 2008). This is particularly important for basic biofilm viability assays, typically using a crystal violet stain for a photometer absorbance test (Christensen *et al.*, 1985). The microtitre plates are usually plastic, typically polystyrene or PVC. As well as the viability of the species to form biofilms, the susceptibility of cells to antimicrobial agents has also been measured in this fashion, making it a simple yet informative mode of growth (Das *et al.*, 1998).

2.7.2 Flow-Based Applications

However, particularly in engineering applications, it is often desirable to grow biofilms in a flow-based system, in order to simulate the effects of fluid dynamics (e.g. pipe flow) by establishing a culture in situ in a distribution system. In flow-based systems, the forces of attraction with the surfaces must develop in order to be greater than the shear force of the flow, promoting more-strongly attached biofilms (Schmidt *et al.*, 2004). There are various different apparatuses which can be utilised for this purpose. The most accurate designs related to process industries, especially food, are ones

which apply a consistent shear force to the growing cells whilst supplying a constant source of low-nutrient media (Luppens *et al.*, 2002). The range of methods available can present its own problems, often rendering comparison between research groups invalid, due to structural and physiological differences inherent between growth modes (Garrett *et al.*, 2008).

A basic method of simulating flow is to use a shaking table, typically with the biofilms being grown on microtitre plates as for 'static' cultures. This mode of growth is specifically relevant to urinary catheters and sections of the circulatory system, yet the establishment of a consistent shear force has a wider application, so long as the shaking frequency and orbital diameter are set correctly (Moreira *et al.*, 2015). The presence of a shearing force sets the shaking method above entirely static conditions for practical simulation due to bacterial attachment being more readily achievable where there is a consistent shear.

2.7.3 Robbins Device and Modifications

A commonly-used flow system is the Robbins device, first designed by McCoy and Costerton (1982). It consists of a plastic or metal tube section into which test materials can be inserted to form part of the tube wall, yet removed when desired. The device can be connected up to a nutrient reservoir, a heater and a peristaltic pump which allow the continuous system to develop. The Robbins device is useful as it can be inserted directly into a pipe due to its cylindrical geometry, including incorporation into an existing network in parallel for *in situ* assessment of fouling removal methods (Brown and Gilbert 1995). Long-term monitoring of fouling can be conducted given the scope for a large number of sampling points. It is cheap, easy to use, and very reliable, although the biofilms grown can be variable given that the hydraulic conditions can be difficult to control or define (Lens *et al.*, 2003). A gradient can often develop from one side to the other, making for inconsistent samples (Verran and Jones 2000). Nevertheless, it was an important tool in the earlier studies of biofilm resistance to antibiotics and the control of bacterial corrosion (Ruseska *et al.*, 1982). The cleaning fluid can be pumped through the system using a centrifugal pump, with the biofilms resident on the metal studs within the flow. An important function of this method is to test the efficacy of the cleaning process at various experimental parameters, including ranges of temperatures, concentrations and flow rates (Blanchard *et al.*, 1998).

Certain adaptations have been made to the Robbins device. The initial modified Robbins device (MRD) was described by Nickel *et al.*, (1985), in which a multiport sampling catheter was attached. An annonated diagram of the MRD is shown in Figure 12. A further example is the Chemostat-coupled modified Robbins device, offering a greater number of sample surfaces for the growth and monitoring of biofilms over extended lengths of time, and the ability to control the growth rates of adhering planktonic cells (Jass *et al.*, 1995). There is also the Pedersen device, commonly used for bacteria quantification purposes, consisting of microscope slides arranged parallel to the flow, and

slotted into acrylic holders. Its creation was mainly inspired by an interest into flow in electrochemical concentration cells (Pedersen 1982).

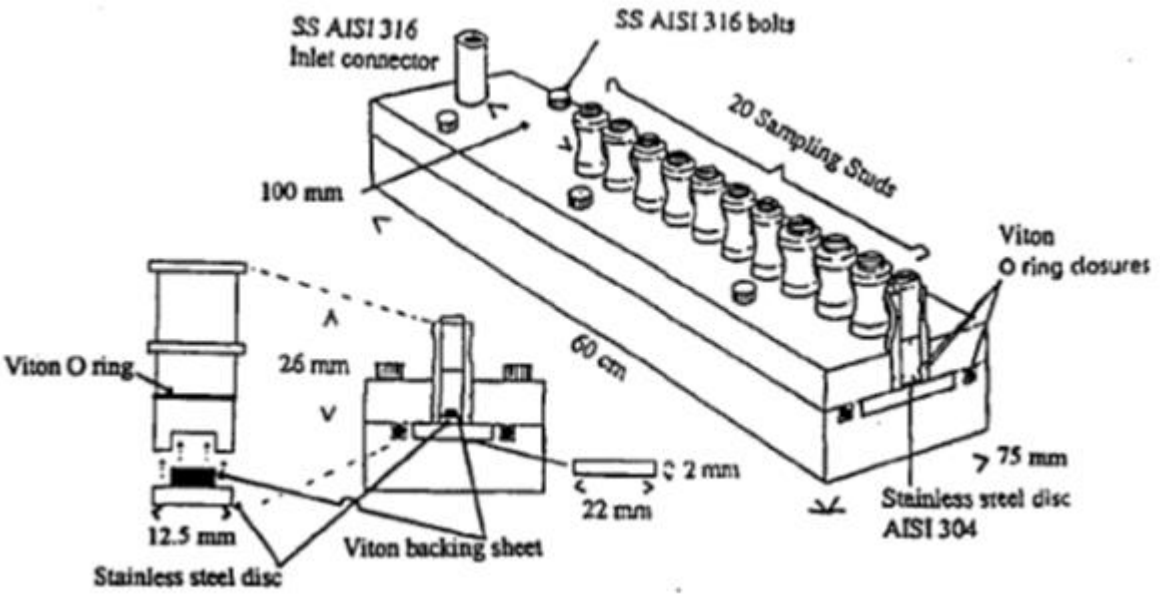

Figure 12: A diagram of the modified Robbins device, including (Blanchard *et al.*, 1998)

The Calgary biofilm device (CBD) was designed as an adaptation to the MRD, with the aim of achieving a better model for rapid testing of antibiotic susceptibility (Ceri *et al.*, 1999). The CBD consists of a top section acting as a lid with 96 pegs, including a sealed top which allows the pegs to be removed without opening the reactor and risking contamination. The bottom compartment serves as a 96-well plate, with the pegs sitting in the channels. The flow is channelled in order to achieve a consistent shear forces across all pegs, resulting in equivalent biofilms in all sites (validation by Ceri *et al.*, (1999) showed a standard deviation of 0.383 log CFU per peg after 24 hours). It has the additional benefit of not requiring pumps or tubing, a typical source of contamination. A cheaper alternative to Robbins device-style apparatuses was trialled by Luppens *et al.*, (2002), in which 13mm coupons were held vertically in a culture container connected to a pump.

2.7.4 CDFF and CFCC

The ability to grow steady state biofilms (i.e. those whose total cell volume is kept consistent by balancing growth and detachment) is frequently desired, due to the potential for measuring the effects of changes to the system. The constant depth film fermenter (CDFF) is a classic example of such a device, first developed by Coombe *et al.*, (1984). It consists of a flat plate, over which there is a flow of medium and a wiper blade which is passed over the surface at certain intervals in order to remove excess growth. The major practical issue with the CDFF is that some cultures will form biofilms which do not reach the height of the scraper and therefore will not be of the same thickness. Logically this makes the biofilm less reproducible, yet they will reach a more ‘natural’ steady state under the

effects of shear (Dibdin and Wimpenny 1999). With a comparable appearance, Donlan (2000) developed the CDC biofilm reactor (CBR) to study the disinfection of *Legionella pneumophila* biofilms in potable water systems. A polyethylene top was fitted with eight polypropylene rods which descend vertically into the reactor, each supporting three removable stainless steel coupons for biofilm growth. The baffled stirrer in the centre provides constant mixing and a consistent shear to the surface of the coupons. It operates as a continuous stirred tank reactor, with an inlet and an overflow 'arm' on the side.

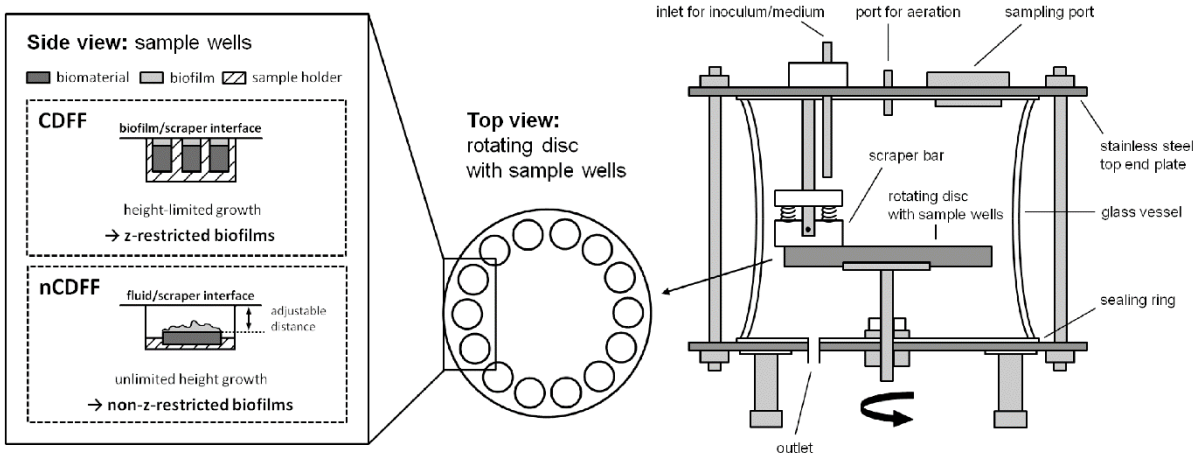

Figure 13: A schematic of the constant depth film fermenter (CDFF), along with a variant – the non-constant depth film fermenter (nCDFF) - as described by Lüdecke *et al.*, (2014). The fermenter includes the rotating disc section at the centre, with 14 wells containing the biological samples. The scraper bar serves to exchange bacterial suspension and medium across the wells, and also to remove any surplus from the top.

Gilbert and Keasling (2004) designed and ran a continuous flow culture chamber (CFCC) with the aim of facilitating non-destructive imaging of biofilms (negating the risk of handling damage due to shear forces at the gas-liquid interface). This apparatus consisted of a polymer frame into which two channels were cut, with holes drilled for stainless steel tubing to be passed through to provide entry and exit for the fluid. A peristaltic pump with an appropriate head is selected to deliver the required flow rate, firstly for the bacteria to circulate the system to seed the cell, and then for nutrients to feed the established biofilm (Gilbert and Keasling 2004). Donlan (2000) reported a very good reproducibility of biofilms using the CFCC, with standard deviations of biofilm densities ranging from 0.06 to 0.18 log CFU per coupon. However, tests conducted by Goeres *et al.*, (2005) suggested that the baffle rotation speed has the potential to introduce significant unpredictability if it is not carefully controlled.

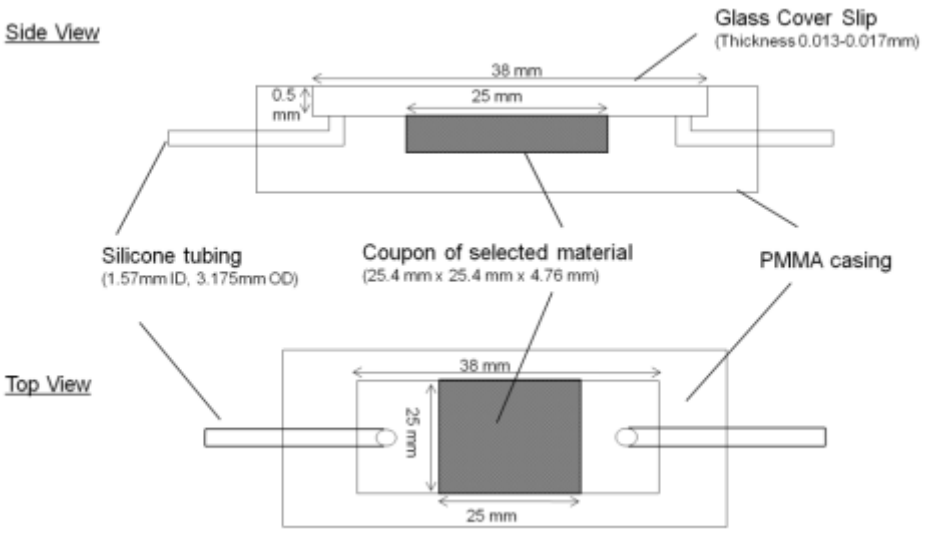

Figure 14: A CFCC design used by Irving and Allen (2010) to study the formation and development of microalgal biofilms. The apparatus was modified from earlier designs to facilitate the substitution of substrate materials. The chamber was constructed using poly(methyl methacrylate) (PMMA) and attached to a multichannel peristaltic pump with silicone tubing.

2.7.5 Radial Flow Cells

Another area for investigation has been the effect of velocity and shear on growth patterns. The identification of shear stress patterns on biofilm growth was first studied by Fowler and McKay (1980) with their radial flow cell (RFC) model, in which media was delivered between two horizontal parallel discs. More growth was observed towards the fringes of the discs, away from the inlet, and could be used to display the minimum velocity required to prevent adhesion. The main drawback with the RFC is the unpredictability in interpreting the relationship between shear stress and detachment – the flow regime near to the inlet is difficult to model accurately (Fryer *et al.,* 1985), and the hydrodynamics of the system can be harder to relate to practical situations (Bryers and Characklis 1992). Fryer and Slater (1987) used a 'tapered tube' model in an attempt to remedy these issues, where the diameter of the tube was reduced on a gradual basis, thus increasing the velocity of the fluid flow as it passes downstream. The tests were designed to determine the shear stress required to maintain a clean surface. It was also shown that a reduction in surface temperature reduced the necessary minimum shear. The primary issue with the use of a regular tapering is that the increase in shear stress over distance is not linear (Bott 1995).

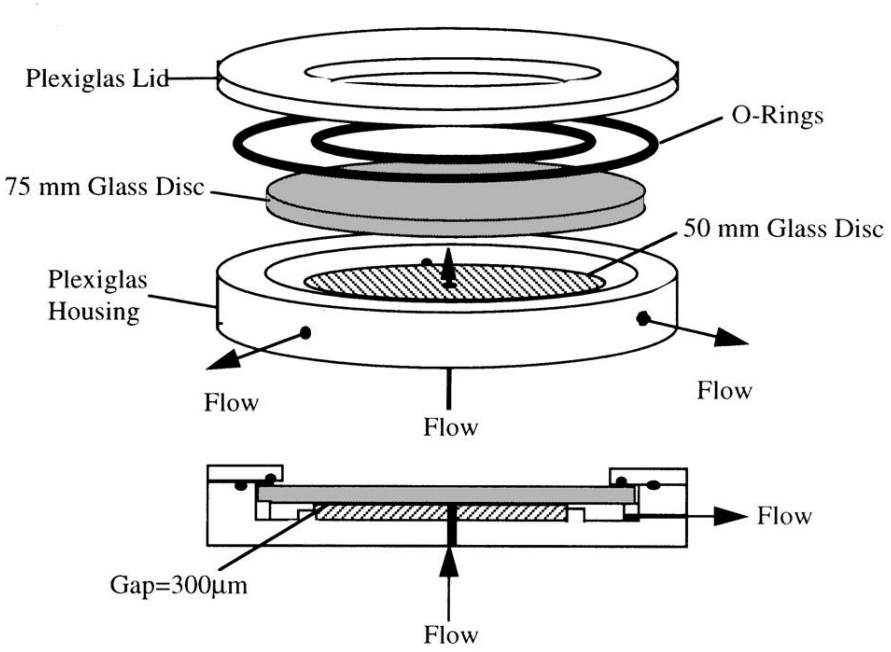

Figure 15: A layered schematic of the radial flow cell (RFC), with a 2-dimensional depiction of the complete unit shown below. The fluid inlet is located beneath the cell with a glass disc as a base, and the structure (housing and lid) is built using Plexiglass, a trademarked PMMA formulation (Yung *et al.*, 1999).

2.7.6 Drip Flow Reactor

The drip flow reactor (DFR) was developed by Stewart *et al.*, (2001) in order to provide a low shear, high gas transfer environment for growth. In engineering terms, the DFR is classified as a plug flow reactor, resulting in variable nutrient composition and therefore differing cell densities along the length of the surface. The mild shear effects result in a relatively smooth, sheet-like biofilm surface which has particular relevance in simulating food conveyor belts, catheters and lungs (Goeres *et al.*, 2009). The smooth surface is also beneficial for microscopic analysis, given that they bear fewer architectural features. Biofilms grown using this method benefit from forming close to the air-liquid interface, which allows for more efficient oxygen transfer and consumption (Lauchnor and Semprini (2013); Wijman *et al.*, (2007)).

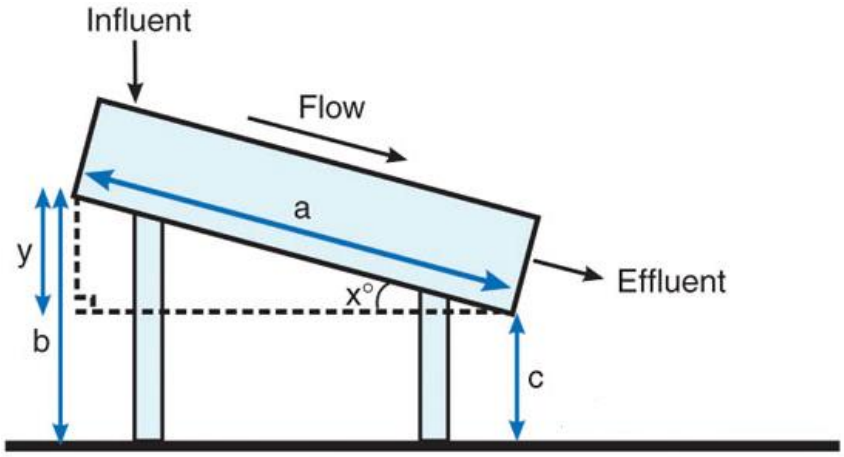

Figure 16: A side view schematic of a drip flow reactor as used by Goeres *et al.*, (2009). The required angle of elevation is given by *x*, *a* is the length of the reactor base, *b* is the distance from the bottom of the influent end of the reactor to the laboratory surface, *c* is the distance from the effluent end to the laboratory surface, and *y* is the difference in elevation between *b* and *c*.

2.8 The Study of Biofilms

There are various analytical techniques which can be utilised in order to better understand the nature of a biofilm, and the processes which led to its establishment. There are relatively simple methods aimed at estimating the numbers of colony forming units (CFUs) present and establishing the amount of biomass present, as well as more complex imaging techniques designed to give a greater understanding about the structures of the biofilms. Similarly, there has been much research into the nature of fouling, biological or otherwise, in order to better understand how the adverse effects of unwanted deposits can be mitigated. An important aim is to develop *in situ* methods of characterisation, given the often-volatile nature of biological deposits when removed from their origins.

2.8.1 Biofilm Characterisation

Enumeration

A simple way to estimate the number of bacteria grown is to use agar plate counts. Plate count agar (PCA) is one form of agar growth medium containing traces of peptone, yeast extract, glucose and agar. The biofilm is swabbed and diluted in Ringer's solution (a solution of several salts in water) in a dilution series, and appropriate dilutions are then spread onto PCA and incubated. Individual colonies can then be counted to give a good approximation of the numbers of bacteria present (Blanchard *et al.*, 1998). Alternatively, the swab samples can simply be diluted in distilled water. In all cases, care must be taken that the cells are not damaged during the process and thus rendered non-culturable.

Attached bacteria can also be counted using the membrane filtration procedure. Filter membrane with set pore size and diameter are placed on agar plates to be incubated. The attached viable count

(CFU/cm^2) is defined as the average number of colonies multiplied by the dilution factor, divided by the slide surface area (Momba and Makala 2004).

Viability can also be assessed by measuring adenosine tri-phosphate (ATP) quantities. ATP is an activated energy carrier in all viable cells and is therefore recognised as an indicator for biofilm viability (Karl 1980). Siebel *et al.*, (2008) observed strong correlations between ATP quantification and a plate counting method, also finding it to be a less labour and time intensive protocol, yet a relative lack of knowledge of ATP concentrations in naturally-occurring bacteria is a limitation at present.

Absorbance

The optical density can be used to determine the cell mass/cell number, assuming the existence of a standard curve. Absorbance (reduction in light intensity) is proportional to concentration of bacteria for a specified cell type. Standard curves of mass v. absorbance can be generated for each combination of population, reactor, wavelength etc. Optical density is measured by transmitting light, normal to the biofilm interface, through the biofilm, and the measured optical density is that of the surface, biofilm, bulk fluid and suspended microorganisms combined (Bakke *et al.*, 2001). This method does not distinguish between living and dead bacteria, or between different species, although the latter problem can be disregarded if the culture is tested for purity prior to inoculation and if all apparatus is kept sterile.

The most common variation of protocol used to quantify biofilm formation via absorbance is the microtitre plate assay, described by Christensen *et al.*, (1985). Following the desired incubation period, and after wash sequences with a saline to remove any planktonic cells, the attached culture is subjected to a stain (e.g. crystal violet). Optical density is then measured using a plate reader, which quantifies the level of adherence to the surface. The tube method operates under a similar staining principle, although in this case the culture is decanted into a tube which is inverted after being stained. The amount of biofilm formed is inferred from the existence of stain lining the inner surface of the tube (Christensen *et al.*, 1982).

EPS Analysis

The composition and volume of EPS produced is of relevance to biofilm analysis, and in order to conduct tests the extracellular polymers must be isolated from the overall biofilm produced. There are many minor variations in how this is carried out, but the procedures are fundamentally similar. Separation is generally carried out using centrifugation after suspension in a saline buffer, although the finer details of the process depend on the method of analysis. A simple procedure is to dry the dissolved polymers in a vacuum and compare their dry weight to that of the combined weight of the cells and EPS (Dhanasekaran *et al.*, 2014).

Alternatively, a colorimetric method is often favoured. In a review of EPS isolation methods, Denkhaus *et al.*, (2007) concluded that cation exchange was favourable, a method which releases EPS by destabilising the cross-linked matrix structure using ion substitution reactions with calcium ions in the biofilm. The solution is dyed according to a selected protocol, and the absorbance reading is related to the protein or polysaccharides present. A protocol for polysaccharide content was explained by DuBois *et al.*, (1956), which involves adding 95.5 wt% sulphuric acid and 80 wt% phenol to the isolated EPS mixture. This method is still favoured, with only minor alterations relating to mixing methods and concentrations of reagents suggested. The original protocol for protein quantification originates from the same era (Lowry *et al.*, 1951). The Lowry protocol relies on the reactivity of copper ions with peptide nitrogen and is still widely used, although important limitations are now recognised. Bradford (1976) took into account the potential interferences with the Lowry procedure (including carbohydrates and other metal ions such as potassium or magnesium), and suggested the use of the Coomassie Brilliant Blue G-250 dye instead. Similarly, Smith *et al.*, (1985) was concerned with the pH sensitivity of the Lowry method, as well as its cumbersome procedural nature. They suggested the use of bicinchoninic acid (BCA) in the sodium salt form due to its stability and specific reactivity with copper ions. Both the Bradford and Smith methods have become popular since their publications.

2.8.2 Imaging Techniques

Confocal Laser Scanning Microscopy

The thickness of the biofilm and the nature of its association with the substrate can be analysed by confocal laser scanning microscopy (CLSM). It is a three-dimensional method using laser beams and fluorescent molecular probes, and the digital imaging can build up reconstructions of the local environment (Lindsay and von Holy 2006). The samples are excited using the laser beams, and the resulting fluorescence is observed with a pass filter and a magnification lens (Irving and Allen 2011). This technique can only recognise excitation at specific wavelengths, but a set of images at different wavelengths can be compiled and enhanced using a computer.

CLSM is a particularly versatile method of imaging, and has the advantage of being able to conduct non-destructive (in situ or ex situ) examinations of potentially very thick biofilms. Destructive testing has traditionally been favoured for most biofilm analysis, although the potential for alteration of the structure makes it difficult to obtain reliable information about biofilm composition (Wang *et al.*, 2013). The non-destructive nature of CLSM has made it particular popular for studying the biofilm architecture and spatial arrangements down to a single cell scale, and also the nature of the EPS matrix (Bridier *et al.*, 2013). The use of fluorescence makes it notably useful for studying the distribution of cells due to the coloured light emissions from the attached fluorescent dyes (Wilkinson and Schut 1998). Such dyes are becoming increasingly diverse, with growing ability to specifically target cells or other matrix constituents, providing better insights into the traits which guide biofilm

development (Bridier *et al.*, 2013). Live/dead staining is an option available with CLSM, where two stains can be used in conjunction to clearly depict areas of viable and non-viable cells. Propidium iodide is favoured as a 'dead' stain, as it is unable to permeate the membranes of living cells, so when combined with a stain which penetrates all cells, leaves two fluorescing colours (Hope and Wilson 2003).

Fluorescent imaging is particularly useful for depicting growth on steel surfaces, which is a focus for this project. Optical microscopy on steel surfaces can be problematic given that the opaque nature of the substrate will not let beams of light pass though. This issue can be negated if an inverted microscope is available, as they are more ideally suited to observing living cultures on metal surfaces. CLSM allows the attached cells to be stained beforehand, resulting in the background textures of the steel being negated. Epifluorescence microscopy can alternatively be used with similar results (Mattila *et al.*, 1997). Information gleaned from CLSM is typically limited to the distribution and amounts of cells and EPS, although Wagner *et al.*, (2009) combined the technique with Raman spectroscopy to detect changes in chemical diversity. Confocal microscopy and scanning electron microscopy (SEM) have the potential to observe the dynamics and settlement relationships of mixed species biofilms at different times of growth, offering possibilities to learn about inter-species cell interaction (Doiron *et al.*, 2012).

Scanning Electron Microscopy

The physical thickness of the biofilm can be calculated if the refractive index is known (Bakke *et al.*, 2001). Scanning electron microscopy (SEM) is a surface imaging technique which may be used for this purpose. SEM is a high vacuum technique, so the samples must first be dried and fixed (Jhass *et al.*, (2014). Wang *et al.*, (2013) grew *Salmonella* biofilms (of six different strains) on stainless steel plates for up to 7 days and, once the plates were rinsed with saline, the samples were air dried and fixed in 2% (v/v) glutaraldehyde in sodium cacodylate buffer. Samples are then typically coated with gold in order to improve the thermal conductivity, although there are occasions in which this can be problematic, including the study of soft fouling layers in which the original structure can be compromised (Blankemeier *et al.*, 2010). It can observe the morphology of the biofilms, and has been used in a number of fields in which they are prevalent, particularly medicine (Lindsay and von Holy 2006). The study by Jhass *et al.*, (2014) examined biofilm growth on craniofacial plates, focusing on accumulation around screws, holes and other protrusions. Wang *et al.*, (2013) used SEM to indicate the development of a mature biofilm over a seven day period, and also presented evidence of injured cells using the technique. Kavita *et al.*, (2013) showed how SEM can be used to compare the surfaces of *Vibrio* species, indicating that one was smooth and compact, and the other loose and irregular in shape. The porosity and pore size distribution of the related EPS was also studied. When combined with energy dispersion spectroscopy (SEM-EDS), the chemical composition of a surface can also be studied (Huang *et al.*, 2014).

A significant disadvantage of using SEM for biofilm analysis is that the drying procedures can be damaging to a previously well-hydrated biofilm, carrying the risk of slumping due to the collapse of extracellular polymers. This distorts the sample, given that the EPS is typically 95% water, and makes the polymers appear more like fibres than an extensive matrix structure (Characklis and Marshall 1990). Sample preparation times can also be lengthy (Little *et al.,* 1991).

Atomic Force Microscopy

Atomic force microscopy (AFM) is a high-resolution form of scanning probe microscopy which does not require staining or coating, so therefore can be observed in situ. Fluctuations in biofilm thickness can be analysed, and surface roughness can be depicted and quantified. The additional benefit of this is that the EPS can be examined in conjunction with the biofilm with minimal risk of damage or disruption (Lindsay and von Holy 2006). Also, samples need not be imaged under vacuum, an advantage over electron microscopy (Núñez *et al.,* 2005). Bacteria can be studied in both liquid and air environments. The formation of biofilms at interfaces makes them ideal for study using AFM (Beech *et al.,* 2002). Air interfaces tend to provide better images, although a liquid environment keeps the cells hydrated and allows for elasticity and adhesion measurements to be made. Adhesion between the cell surface and the tip is measured as the tip is removed, which causes a reduction in the force exerted on the tip and an abrupt change in deflection (Volle *et al.,* 2008).

AFM is operated in one of three modes. Firstly, there is non-contact mode in which a small, sharp tip is used to scan the surface of an object. As the tip is moved over the surface, attractive van der Waals forces between the two cause the probe to deflect when in close proximity, allowing an image of the contours of the surface to be generated. The tip-sample distance must be maintained and contact must be prevented. If accidental contact is made, the tip can stick to the surface and stop vibrating due to the meniscus force on the liquid layer. This can occur regularly if the feedback control system is not sufficiently highly performing. A solution to this issue is ‘tapping’ mode, whereby the tip is deliberately brought into contact with the surface. In this instance the image is drawn from both the van der Waals forces and the force of the contacts with the surface (McCarty and Mahmoodi 2015). Tapping mode offers higher resolutions with minimum damage being caused to the sample. A greater oscillation amplitude is used in order to prevent trapping by the meniscus forces (Geisse 2009). The other option, contact mode, involves permanent contact which scrapes the surface. This offers the greatest image resolution, but risks damaging the surface layer and can experience sticking action and slip motion during scanning (Thormann *et al.,* 2010). Beech *et al.,* (1996) used AFM for the estimation of bacterial cell dimensions. Núñez *et al.,* (2005) displayed the power of AFM in biological imaging by showing the motility mechanisms of predator cells attacking a biofilm. Compared with light microscopy, the resolution of AFM is far superior, allowing structures to be observed to the order of tens or hundreds of nanometres (Dufrêne 2002). Sub-nanometre resolution is also possible (Beech *et al.,* 2002).

Epifluorescence Microscopy

Epifluorescence microscopy can be used as an alternative method for counting cells. In order to do this, biofilm samples are rinsed thoroughly with distilled water and stained with a 0.1% acridine orange solution. The samples are then covered with a glass slip and examined under the microscope (at 1000x magnification. Pictures are then taken at various locations across the sample using a digital microscope camera, and the number of cells is counted manually and average to obtain a cell density per unit square (Irving and Allen 2011). For example, acridine orange acts as a fluorescent dye which is excited in the ultraviolet range (Lindsay and von Holy 2006). Another compound which is regularly used is 4', 6-diamidino-2-phenylindole (DAPI) to be used as the dye, as it is reported to have a more stable fluorescence. However, there are two disadvantages to direct microscopic techniques such as this. Firstly, they are not particularly sensitive (densities of 10^3 microorganisms per millilitre are usually required for suitable detection), and also the type of bacteria cannot be readily determined. For bacteria determination, fluorescent in situ hybridisation (FISH) can be used, where fluorescent-labelled probes can identify specific species (Kornreich *et al.*, 2012).

Other Imaging Methods

The development of the biofilm can also be monitored non-destructively in situ. For example, Fourier transformation infrared spectroscopy (FTIR) can detect bacterial biofilms as they form, as the stretching of the proteins and carbohydrates is clear when bacteria attach to substrates (Momba *et al.*, 2000).

2.8.3 Biofilm Thickness Measurements

In the case of biofouling, it is important that an idea of the thickness of the biofilm is known, as well as counting viable cells or identifying EPS composition. In industrial settings, thicker biofilms carry greater ability to increase pressure drop in pipes, restrict throughflow, and further insulate against effective heat transfer. Furthermore, a substantially thick biofilm suggests that a certain level of maturity has been reached, hinting at a greater propensity to detach and transfer implicated cells. Thickness is important with respect to cleaning as it determines the distance through which nutrients must diffuse in order to penetrate the biofilm, and also for biocides to have an impact on the surface-attached cells (Peyton 1996). Other information can also be estimated from thickness, such as volume, wet weight and the number of species present (Boulêtreau *et al.*, 2011).

Optical Microscopy

Optical microscopy is perhaps the simplest method of acquiring an estimate of the thickness of a biofilm. The vertical displacement required to focus from the clean surface to the biofilm-fluid interface is proportional to the biofilm thickness (Bakke and Olsson 1986). This approach is hampered mostly by its low sensitivity and highly approximated results. Furthermore, multiple recordings are required to give an average thickness, although these figures can offer estimates of the roughness of the biofilm surface (the same is true of electrical conductance methods) (Peyton 1996).

CLSM

CLSM is also frequently used to study the 3-D nature of biofilms, usually with an interest in their architectural features (Wood *et al.*, 2000). Hope *et al.*, (2002) used protrusions (or stacks) from confocal imaging to indicate the greater presence of viable bacteria in the outer layers and mostly non-viable bacteria in the internal regions. This combines the use of the 'stack' facility to indicate the thickness of the biofilm, in conjunction with live/dead fluorescent staining, to give a detailed projection of the structure (including voids and channels). However, the use of fluorescent dyes has the potential to affect biofilm formation, and CLSM use is ultimately limited by the penetration depth (Dreszer *et al.*, 2014).

Other Imaging Methods

Nuclear magnetic resonance imaging (NMR) has been used as a non-invasive biofilm monitoring technique. Research by Graf von der Schulenberg *et al.*, (2008) established protocols for the use of NMR in determining the spatial distribution of biofilm and the evolution of the velocity field with the development of biofouling. Subsequent applications have focussed primarily on velocity distributions rather than the physical profiling of biofilms, however (Vrouwenvelder *et al.*2009).

Optical coherence tomography (OCT) can give high-resolution images for the characterisation of growth, thickness and structural features. Haisch and Niessner (2007) demonstrated its use in three-dimensional monitoring of transient biofilm processes including spatial resolution, although they noted its limitations in studying thick biofilms due to penetration issues. Dreszer *et al.*, (2014) then showed its use in *in situ* measurement of biofilm thickness in a cross-flow membrane system, showing an increase in thickness over time.

Staal *et al.*, (2011) used planar optodes (O_2 sensitive dye immobilised in a polymer layer on a transparent carrier) to map oxygen distribution in order to assess the landscape of biofilms. Whilst this is simpler than similar imaging techniques from a technical point of view, there are many variables affecting oxygen concentration which cannot be explained solely by biofilm distribution (e.g. fluid flow rate and regional variations).

Fourier-transform infrared spectroscopy (FTIR) can be useful for determining the functional group structure of a biofilm. Hu *et al.*, (2013) identified the presence of the major EPS constituent groups using FTIR (polysaccharides, proteins and lipids). Similarly, Raman spectroscopy (RM) can offer additional information about chemical components, along with gathering additional knowledge of the EPS structure (Wagner *et al.*, 2009). Whilst FTIR records vibrations of polar groups (e.g. N-H and O-H), Raman scattering signifies changes in non-polar groups (e.g. C-C), which means that they can be used to complement one another (Wang *et al.*, 2013). Distinct peaks from both sets of results can therefore be combined to offer a clear picture of the molecular components of the biofilm.

Volumetric Displacement

This method involves simply comparing the difference in volumetric displacement in a system between the fouled surface and the clean surface, after the biofilm has been scraped away (Peyton 1996). Zelver (1979) used a tubular reactor system into which sample tubes were inserted. After the desired period of time, the fouled sample cell was placed in a surfactant solution in another cell, after which the change in fluid height due to the sample was recorded.

Picologlou *et al.,* (1980) found that biofilm accumulation caused an increase in frictional resistance, and that the resistance was dependent on the biofilm's thickness. The major limitation here is that only an average thickness over the measured area can be determined (Peyton 1996). Biomass measurements can be used as a more simplistic alternative estimation method (Dodds *et al.*, 1999).

Electrical Methods

Measurement via electrical conductance, however, does allow for localised readings to be taken. It uses a micrometer and electrode to determine when a circuit is completed with a metal surface (Hoehn and Ray (1973). The needle records a small current on reaching the biofilm surface, which then increases significantly when it touches the metal (Peyton 1996).

Rotating disk electrodes (RDEs) have been used to measure the thicknesses of thin biofilms *in situ*, for specific applications such as on river beds (Herbert-Guillou *et al.,* 1999). The diffusion rate through the biofilm is recorded by measuring variations in the limiting current versus the rotation speed. The diffusion rate is equal to the diffusion coefficient of the electroactive species divided by the thickness (Herbert *et al.*, 1997). Boulêtreau *et al.*, (2011) used an RDE to study thicker biofilms (up to 500µm) in comparison with thicknesses obtained from microscopic analysis, and whilst a good correlation was shown, the RDE gave estimates which were 1.8 times lower than those taken microscopically.

Thermal Sensors

Reyes-Romero *et al.,* (2014) presented a sensor using AC thermal excitation as a method of observing biofilm development. A heater and temperature probe were set up to act as the sensor. Current applied to the heater produces a power signal and the resulting temperature oscillations are recorded by the probe. The amplitude and phase shift are related to the thickness and composition of the biofilm. Results of the study showed that it was effective for continuous monitoring of biofilm development. The method described required the biofilm to be grown on the surface of the sensor, which may not be suitable for a range of studies. Also, thick biofilms were shown to result in the reflected wave vanishing before reaching the thermistor.

2.8.4 Biofilm Strength Measurements

The simplest way of getting an idea of the attachment strength of a biofilm is to apply a wash to the surface and recording the percentage of cells which remain attached, known as the attachment

strength (S_R) (Dickson and Koohmaraie 1989). Methods such as this, whilst being very simple to conduct and useful in direct comparison of species, offer little in the way of real attachment strength data and cannot realistically be related to cleaning protocols. Quantification of the shear stress required to remove a substantial proportion of biofilm has direct relevance to industrial cleaning processes and can be used to suggest fine tunings of removal methods.

Radial Flow Cell

The radial flow cell (RFC), as described in Section 2.7.5, was used by Perni *et al.*, (2007) to study the resistance of *Listeria monocytogenes* biofilms to detachment. Shear stresses in an RFC are known to vary according to the radial position of the flow, and this study was able to identify a radius beyond which cells were unaffected by shear, suggesting a critical stress for removal (i.e. an attachment strength).

Rotating Disc Reactor

Abe *et al.*, (2012) described the use of a rotating disc reactor for growing drinking water biofilm samples on coupons, mounted on the reactor and rotated in a submerged position at differential shear stresses, similar to the RFC. This was applied to study the effects of hydrodynamic and chemical cleaning methods by Mathieu *et al.*, (2014). AFM was used to quantify volumetric removal on a before and after basis, allowing biofilm cohesive strength to be quantified.

Another example of a rotating reactor was utilised by Azeredo and Oliveira (2000). Glass cylinders were inserted into a stirred reactor to act as growth sites. After the formation of the biofilms, the cylinders were transferred to separate glass containers and subjected to varying shear stresses (in the form of rotations per minute). A speed of 500 rpm was sufficient to remove 47% of biofilm thickness, consisting of the layers of low density. The top speed of 2000 rpm was able to reduce the biofilm to a remaining 7.2% of the original thickness.

Microfluidic Funnel Device

The microfluidic device (µFD) consists of one or more microchannels, and has been applied to various applications in the study of bacteria, including social behaviours and quorum sensing (Shumi *et al.*, 2013). Galajda *et al.*, (2007) showed how an adaptation with funnel-shaped openings (microfluidic funnel device - µFFD) concentrated the swimming bacteria towards the funnel walls. In the method conducted by Shumi *et al.*, (2013), inoculation was conducted via gravitational force through the inlet channel, and saliva was pumped through the channel. The size of the remaining aggregates was calculated using an inverted microscope, and the fraction of remaining adhering cells quantified.

Rectangular Duct System

Hamanaka *et al.*, (2012) used a rectangular vessel for biofilm removal tests. Coupons were incubated in 24-well microtitre plates before being placed onto the base of the duct. Water was pumped through

the vessel at a fixed velocity of 15 $Lmin^{-1}$, and agar plate counts and CLSM imaging were conducted in order to assess removal. Distinctions in strength were observed between nutrient-rich and starvation growth conditions, although information about removal effectiveness relative to biofilm structure was inconclusive. Lackner *et al.*, (2009) used a similar setup to test the impacts of various growth surface modifications on bacterial attachment.

AFM

Atomic force microscopy can also be used to assess biofilm cohesion by actively removing layers, in the form of cohesive energy per unit volume of biomass. Measurements of the height of the sample in nanometres and the friction force are collected as the AFM tip scans across the surface, allowing the mass of biofilm displaced to be related to the applied force (Ahimou *et al.*, 2007b). The ability to measure the cohesive strength of biofilms is notably less –explored than adhesive strength measurements, and some previous examples of strength recordings are unclear as to which (adhesive or cohesive) the results refer to, complicating comparison attempts (Ahimou *et al.*, 2007b). Abe *et al.*, (2012) used AFM in this fashion to show the removal of biofilm in the form of layers using increasing shear stresses and consecutive imaging. The number (and cost) of tips required may be an issue, however, with Mathieu *et al.*, (2014) reporting a change of tip after every three imaging series.

Micromanipulation and Millimanipulation

The technique of micromanipulation (initially developed to study the properties of cells) was modified by Liu *et al.*, (2002) to study both the adhesive and cohesive forces present in fouling layers. A steel probe was designed to draw fouling material away from a surface via a controlled deformation method, with the strength values obtained from the work required to trigger removal. Tomato paste was used as a test material, and the cohesive strength was shown to exceed the adhesive strength, a significant property for cleaning protocols. Studies have shown how rheology and interfacial properties play a role in both attachment strength and removal behavior (Liu *et al.*, 2006). Ali *et al.*, (2015) adapted this to develop a millimanipulation device in order to tackle the problem of measuring the stronger cohesive forces found in food soils, with the added benefit of being able to gauge deeper layers. This is a promising method of studying deformation behavior and strengths (both cohesive and adhesive) of soft layers, although it is a very recent development so the full breadth of its use is yet to be fully explored.

2.8.5 Fouling Detection Methods

Various methods have been trialled for their efficacy in studying fouling and its removal, with some success. Different foulants require different modes of removal, so therefore a good diagnosis of the type and extent of fouling are important (Melián-Martel *et al.*, 2012). Autopsy methods have been used for the characterisation, prediction, prevention and control of fouling, which encompass the range of imaging techniques discussed previously as well principles as diverse as zeta potential, traction force and solute rejection (Pontié *et al.*, 2005). Whilst autopsies serve a useful purpose in

identifying the foulants present, they are less informative with regards to the accumulation and development processes of fouling, and signify little about the hydrodynamic impacts upon the process in question.

Heat transfer performance can be a useful method for monitoring deposits, and unsurprisingly this is especially true for fouling in heat exchangers. Reduction in thermal efficiency can be expressed using a thermal resistance parameter (R_f) which is proportionally related to deposit mass per unit area. An investigation by Delplace and Leuliet (1995) into plate heat exchanger fouling used the overall heat transfer performance to assess conductivity, which serves to average out the effects of deposit structure variation and changes to flow patterns, resulting in a potentially geometry-specific and/or crude measurement. Alternatively, heat flux sensors offer an *in situ* method of thermal conductivity estimation (Davies *et al.,* 1997). The sensor allows the thermal resistance to be measured at a selection of different points on removable tubes, with the tube then cut into sections in order to measure the mass gravimetrically. This method has some promise for measuring fouling masses, although further information, such as thickness, would require further assumptions and it does not reveal much about the removal behaviour.

Electrical resistance or conductivity can also be used in similar fashions, where there is electric heating or electrodes present. Chen *et al.,* (2004) pioneered a method in which electrical and thermal resistance were measured simultaneously. They obtained consistent, positive relationships between the two resistances for both the fouling accumulation and cleaning stages, and therefore suggested that electrical resistance measurements could be useful in tracking fouling development. Alterations in electrical conductivity can also be interpreted to signify changes in deposit structure and relate to the fouling growth rate (Guérin *et al.,* 2007). On the downside, electrodes are invasive, and electric heating is not widespread enough to be a widely used method (Wallhäußer *et al.*, 2012).

On-line fouling detection can be carried out using a variety of sensory methods based on acoustic, optical and ultrasonic principles. The sensor must not interfere with the fouling process to produce unnatural physical features, and additionally, non-invasive methods are favourable. Deciding on the precise location of the sensor is also important, as portable devices are generally unfeasible without access to the pipes during the process. Sensors must also be robust in the face of chemical, physical and thermal attacks from the process environment (Withers 1996).

Ultrasonic devices have proved useful for measuring the presence and extent of deposits where traditional physical probes are unsuitable, such as fouling on pipe walls or coatings on food products (Passos and Ribeiro 2010). Mairal *et al.,* (1999) indicated how ultrasonic time-domain reflectometry (TDR) could be used for the real-time monitoring of membrane fouling (specifically of calcium sulphate fouling in RO desalination). Their results showed a good correlation between signal amplitude decline and fouling development, including detecting the initiation and removal phases.

This has been supported by further studies (Sanderson *et al.*, 2002). The ultrasound method works by measuring the reduction in velocity between two sensors which results after encountering an unwanted deposit. The *in situ* nature of ultrasonic techniques have made it promising for studying biofilm development, along with the ability to detect early developments. Kujundzic *et al.*, (2007) and Wallhäußer *et al.*, (2012) successfully detected biofilm growth on three different surfaces. Statistical significance, however, appeared to rely on a certain amount of EPS per unit area being present, despite this not necessarily being correlated to the amount of biofilm. Unfortunately it is highly sensitive to fluctuations in temperature and is also only valid where the surface is flat (Tuladhar *et al.*, 2000).

Acoustic monitoring is a similar alternative. A small transducer can be bonded to the inside of a plate heat exchanger in order that it will be affected by the build-up of a fouling layer. The presence of fouling on the sensor dampens the amplitude of the vibrations and shifts the natural frequency (Prakash *et al.*, 2005). However, sensors can be problematic in that they do not always experience the same fouling as the surrounding area, due to both surface effects and the protrusion which they present. They must also be regularly and efficiently cleaned (Withers 1996).

Alternatively, fouling within a pipe system can be estimated by conducting analysis of the resulting flow. The extent of fouling is found by calculating the pressure drop along the pipe and comparing the results to a clean system (Bott 1988). Fouling in a pipe results in a reduction in the mean square area of the flow channel, leading to a pressure drop. The required equipment for this analysis tends to already be present for standard pressure monitoring (Wallhäußer *et al.*, 2012). However, these methods fail to take into account the variations in depth and composition which inevitably occur in natural systems, instead yielding average measurements and assuming uniform fouling thickness (Tuladhar *et al.*, 2000). A further issue with pressure drop analysis is that the flow can be subject to pipe geometry – for example, if a biofilm does not protrude beyond the viscous sublayer, the friction factor of the colonies will not affect the pressure drop (Janknecht and Melo 2003).

2.8.6 Summary - Requirements for Biofouling Studies

The issues which hinder the above methods are of particular concern when considering soft deposits, such as biofilms. In particular, deposits found in process equipment the food and biotechnology industries often contain prominent liquid fractions, and so therefore traditional or conventional gauging methods are unsuitable due to their need for contact via a probe or similar device. This would lead to inaccurate measurements as the fragile deposit layer would be readily deformed upon contact, and furthermore may be prone to contamination by a probe (Bridge *et al.*, 2001). Also, deposits which contain a biological component invariably shrink or slump outside of their natural environment (Tuladhar *et al.*, 2000). Biofilms are rarely homogeneous, so there is a tendency for fouling levels to vary in concentration considerably at various points. The physical nature of biofilms makes them easily compressible which indicates that they must therefore be studied *in situ*.

Some methods of analysis contain necessary preparation steps which can change or distort the physical properties. For example, the SEM process includes vacuum desiccation and sputter coating with gold or silver, both of which can sink or flatten the biofilm so that less information can be acquired from analysis, especially regarding thickness and spatial structure (Alhede *et al.*, 2012). This also means that the biofilm cannot be effectively studied both before and after a removal (strength test) phase, as integral physical properties of the deposit may be compromised. Similarly, CLSM has drawbacks in that the staining step is reliant upon penetration of the matrix which can be unreliable for thicker biofilms, and additionally certain species can produce fluorescent signals with an irregular distribution (Tomás *et al.*, 2010). Substrates must also be transparent to be tested using CLSM, which limits its use to certain materials only. These methods are also extremely expensive for a large number of samples.

These parameters dictate that the gauging method must not involve physical contact with the deposit surface, be operable in situ, and be adaptable to conduct 'local' measurements to account for variability in concentration. Measurements based on process effects (pressure drop, heat transfer etc.) can produce results which are not significant enough to impact on decision-making when deposits are localised or small in stature. Another important consideration is the requirement of prior knowledge of the physical properties of the deposit. This is undesirable given that the layer may be prone to change or be variable by location, making measurements tricky. It is, however, necessary to analyse the shear strength of the fouling layer in order to more easily design appropriate flow conditions for cleaning (Chew *et al.*, 2004b).

Approaches to monitoring the behaviour of fouling deposits tend to be either integrated or localised (Wilson 2005). Integrated methods (e.g. pressure drop, thermal conductivity) collect data over a wider area and are delivered as an average, and thus are susceptible to inaccuracies concerning geometric uniformity of the deposit. Localised approaches target a certain point and assume it to be representative of the sample. With such methods, obtaining information which is truly representative is a challenge, as is finding a method which does not involve a probe or other physical contact. Combining the best aspects of both the integrated and localised approaches – acquiring representative data of an entire sample, taking into account local variations whilst not disturbing the surface - would offer the potential of achieving the best possible information. An optimum cleaning protocol would be developed using knowledge of the thickness and strength of the layer, obtained *in situ* and under conditions similar to those of the process environment (Wilson 2005). An issue regarding this testing is that the scaling-down of realistic process conditions for testing can be both costly and time-consuming.

Developing a Solution

Tuladhar *et al.*, (2000) considered a range of gauging techniques with potential for measuring the thickness of soft deposits. These were hugely varied and included ultrasound methods, silicon sensors

and the use of electrical conductivity. Unfortunately the bulk of these methods fail to meet all three crucial criteria; non-contact, analysis *in situ*, and no requirement of prior knowledge of the physical properties of the deposit. A vast selection of online monitoring techniques were also reviewed by Janknecht and Melo (2003). These included electrical capacitance, differential turbidity (intensity of light), pressure drop and heat transfer coefficient. These methods tend to lack the ability to take localised measurements, and so therefore the deposit removal at a given point would be related to a standardised thickness measurement for the entire system. Fouling thickness can be measured relatively simply with a micrometer, but this approach requires a needle to make contact with the deposit and the surface, which is inappropriate for biofouling. Pre-determination of the nature of the fouling is another major hurdle to overcome, and the majority of the techniques considered require a calibration step (especially those using online sensors). Microscopy (e.g. CLSM) would meet most of the requirements, but as previously described (sections 2.8.3 and 2.8.4) the cost is prohibitive and the preparatory methods run a high risk of damaging the samples. A wide range of microscopic and spectrometric methods were reviewed in depth by Denkhaus *et al.*, (2007), and whilst they praised the sensitivity and clarity of most techniques, the risk of damage was flagged as a recurring issue.

The only method which met all the criteria set out by Tuladhar *et al.*, (2000) was pneumatic gauging, in which a jet of pressurised air is forced towards the desired surface, and certain parameters such as shape or relative position can be determined from the resulting flow or pressure (Liu *et al.*, 2012). The technique of fluid dynamic gauging was therefore suggested as a solution, differing from pneumatic proximity gauging in two important respects; the fluid from the process is used in gauging rather than air, and this is drawn through the nozzle rather than forced outwards onto the surface.

2.9 Fluid Dynamic Gauging

Fluid dynamic gauging (FDG) has displayed great promise as a potential solution to the difficulties inherent in soft fouling layer characterisation (Tuladhar *et al.*, (2000); Chew *et al.*, (2004a); Chew *et al.*, (2004b)). It simply utilises the principles of fluid dynamics to determine the position of a surface relative to the gauge nozzle. The main requirement for the technique to be applicable is that the sample must remain stiff throughout the gauging process (Ali *et al.*, 2013). In certain situations this can be a constraint as layer swelling is sometimes observed prior to removal (Gordon *et al.*, 2014). Aside from that, FDG is an ideal measurement tool for the characterisation of soft deposits.

As well as benefitting from being a non-contact method, FDG has the additional advantage of not requiring much in the way of prior knowledge of the physical properties of the deposit, which can be complex and time consuming. The technique works in the liquid environment using the flow rate and pressure drop to measure the thickness of the layer, and the suction force of the fluid is able to test the adhesive and cohesive strengths. The flow conditions can also be controlled in a relatively simple manner, and the closed system prevents the invasion of any foreign matter. The ability to measure

thickness *in situ* and in real time is of particular interest for studying biological fouling layers, as it eliminates the risk of altering or damaging the nature of the sample in transit. Being able to quantify biofilm thickness is an indicator of the extent of fouling. The volume and mass are important properties with respect to the thermodynamic impact of the deposit (Characklis 1981). Thickness monitoring offers a means of early warning to commence cleaning before the problem can develop beyond a certain point. Thicker biofilms also tend to restrict oxygen and nutrient penetration to the deeper layers, encouraging weakening of the matrix and a higher rate of natural detachment, increasing the contamination risk (Characklis 1981). A thickness accuracy resolution of ±2 μm is currently attainable using FDG (Gordon *et al.*, 2012). Finally, it has the advantage of being both simple and inexpensive to operate.

Tuladhar *et al.*, (2000) demonstrated the functionality by using a simple, stagnant bath of fluid. This method has been labelled 'quasi-static FDG', given that there is a small flow through the nozzle yet the bulk fluid remains predominately stagnant. This basic setup was the foundation of all subsequent developments in FDG, as it demonstrates the principles of the technique in its simplest form.

2.9.1 Basic Principles

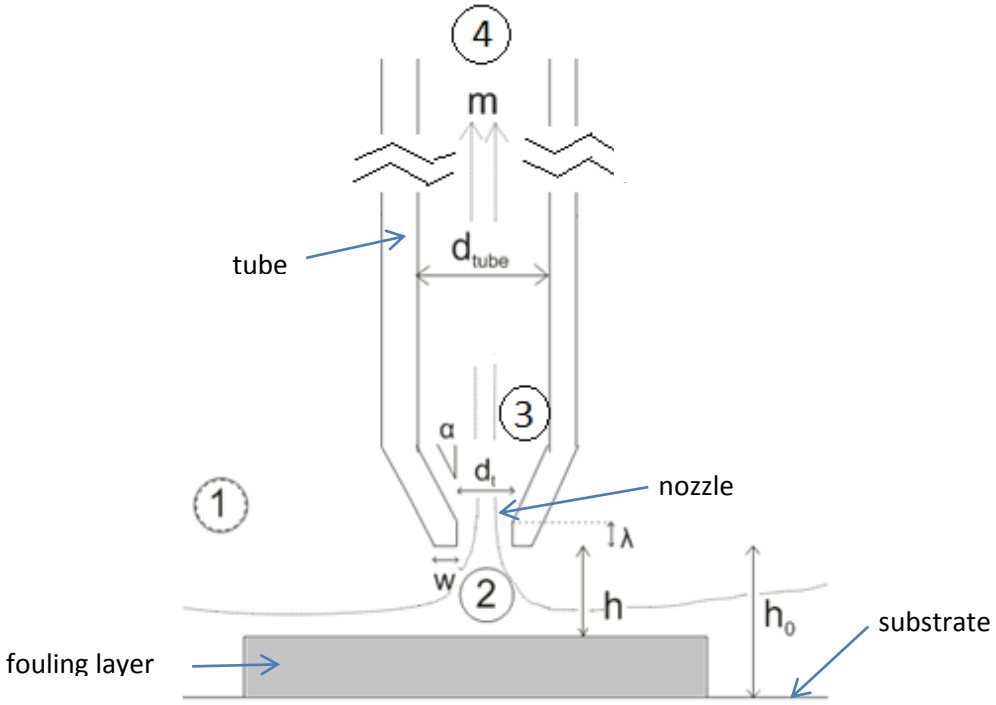

Figure 17: A schematic of the FDG nozzle in proximity to a test surface showing the flow stations and dimensions of the nozzle, where h_0 is the distance between the nozzle and the substrate, h is the clearance between the nozzle and the fouling surface, λ is the thickness of the nozzle rim, w is the width of the nozzle rim, d_t is the diameter of the nozzle, α is the angle of the nozzle contraction at the tip, d_{tube} is the diameter of the tube, and m is the mass flow rate of the fluid.

The four points of relevance within the FDG setup are as follows: 1) the bulk fluid surrounding the gauge; 2) the area under the focus of the nozzle; 3) the connection between the nozzle and the tube; and 4) the outlet of the siphon tube.

The controlled variable during the gauging process is the distance between the nozzle and the substrate, h_0, given that this impacts upon the pressure drop, ΔP, and the mass flow rate, m. The relationship between the clearance distance (h) and the mass flow rate can be established. However, these variables can be converted to dimensionless forms, which makes them applicable to a wider range of experimental conditions. For a given geometry, suction flow into the nozzle is dependent upon eight variables:

$$m = f\{\rho_f, \mu_f, h, d_t, \Delta P_{13}, w, \lambda\} \tag{10}$$

where μ_f and ρ_f are the dynamic viscosity and density of the fluid respectively. Buckingham's theorem (Buckingham 1914) states that n variables which share r primary quantities can be expressed using $(n-r)$ dimensionless groups. Therefore, Equation 10 can be expressed in five dimensionless terms:

$$\frac{m}{\frac{\pi}{4}d_t^2\sqrt{2\rho_f \Delta P_{13}}} = f\left\{\frac{h}{d_t}, Re, \frac{w}{d_t}, \frac{\lambda}{d_t}\right\} \tag{11)}$$

where h/d_t is the dimensionless separation distance, and the Reynolds number, Re, is expressed as:

$$Re \sim \frac{m}{\mu_f d_t} \tag{12}$$

or for the FDG system:

$$Re_t = \frac{4m}{\pi \mu_f d_t} \tag{13}$$

The terms w/d_t and λ/d_t are constant for a specific nozzle configuration, so can be removed from the above expression.

The left hand side of Equation 11 is derived from Bernoulli's equation. The Bernoulli equation explains the conservation of energy within a flowing fluid, with the total energy from the pressure, kinetic and potential energy components remaining equal between two points in a system (such as a pipe or the FDG nozzle). If points 1 and 3 (from Figure 17) are considered, the following equation holds true:

$$\frac{P_1}{\rho_1 g} + \frac{v_1}{2g} + z_1 = \frac{P_3}{\rho_3 g} + \frac{v_3}{2g} + z_3 \tag{14}$$

Equation 14 above is shown in terms of pressure, velocity and potential heads (all have the dimension of metres). P, v, and z are the hydrostatic pressure, velocity and elevation head values at points 1 and

3 in the diagram. There is no difference in elevation due to the nozzle being submerged in the tank, and there is no bulk flow within the tank, so the equation can be simplified thus:

$$\frac{P_1}{\rho_1 g} = \frac{P_3}{\rho_3 g} + \frac{v_3}{2g} \tag{15}$$

The velocity within the tube at point 3 is therefore:

$$v_3 = \sqrt{\frac{2\Delta P_{13}}{\rho}} \tag{16}$$

And, given that the ideal mass flow rate is equal to the product of the velocity and density of the fluid, and the cross-sectional area, it can be said that:

$$m_{ideal} = \sqrt{\frac{2\Delta P_{13}}{\rho}} . \rho . \frac{\pi}{4} d_t^2 \tag{17}$$

Or:

$$m_{ideal} = \frac{\pi}{4} . d_t^2 . \sqrt{2\rho_f \Delta P_{13}} \tag{18}$$

This means that for ideal flow, this term would be equal to 1 (the mass flow rate divided by itself). However, the geometry of the FDG nozzle introduces energy losses to the flow, and instead the following equation can be used to describe the relationship between the measured flow rate and the theoretical flow rate as calculated using Bernoulli's equation:

$$C_d = \frac{m_{actual}}{\frac{\pi}{4} d_t^2 \sqrt{2\rho_f \Delta P_{13}}} 19))$$

in which the new symbol, C_d, is termed the discharge coefficient, and becomes a key property of the FDG system. Tuladhar, et al., (2000) showed that C_d is closely dependent on h/d_t, and varies negligibly with the Reynolds number, however C_d is shown to be influenced by Re at low Re values. Figure 18 shows a plot of C_d against h/d_t.

The remaining unknown in Equation 19 is of ΔP_{13}, the pressure drop around the nozzle region. However, the following relationship is known:

$$\Delta P_{13} + \Delta P_{34} = \Delta P_{14} \tag{20}$$

ΔP_{14} is the overall driving force for the gauging flow induced by the pressure difference. ΔP_{34} can be determined experimentally by operating the gauge having removed the nozzle, which has the effect of eliminating the losses around the nozzle ($\Delta P_{13} = 0$) . The siphon flow is operated within the laminar regime, so the Hagen-Poiseuille equation can be used:

$$\Delta P_{34} = \frac{128\mu_f . m . L_{eff}}{\rho_f \pi d_{tube}^4} \tag{21}$$

All the terms in the above equation are known, with the exception of L_{eff}, or the effective length of the tube. This value takes into account the effect of pipe bends on the flow regime to give the equivalent length of straight tubing required in order to produce the same situation. Unfortunately it is not a factor which can be easily deduced – instead a set of experiments need to be run, where the nozzle is removed (to make ΔP_{13} insignificant), the clearance (h) is set and the hydrostatic head (H) is varied to isolate the effective length as the remaining unknown variable impacting upon the flow rate. Once L_{eff} is known, ΔP_{34} can be easily found and subtracted from ΔP_{14} (ρgH) to give ΔP_{13} and therefore the ideal mass flow rate.

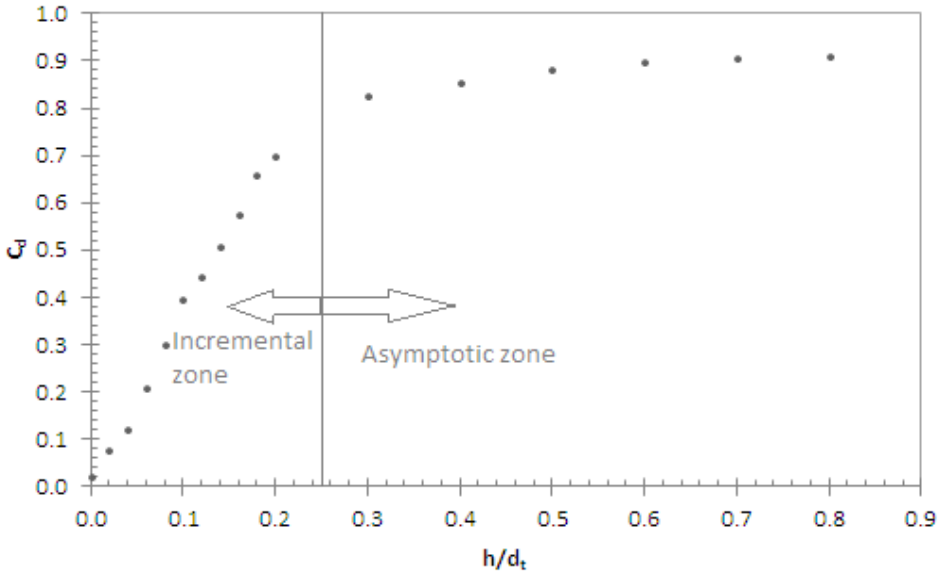

Figure 18: An example of a typical h/d_t vs. C_d plot, showing the two important zones.

A typical FDG calibration plot shows two distinct zones – firstly the incremental zone, where h/d_t is less than a certain value (usually approximately 0.25), in which C_d increases consistently showing a high sensitivity to the value of h/d_t, and the asymptotic zone at higher separations where C_d begins to level off. In the asymptotic zone, the height clearance has a negligible impact on the C_d value.

A plot of C_d versus h/d_t using a clean surface can be used as a calibration curve in order to measure the height difference caused by a fouling layer. The plot drawn using the fouling layer can be adjusted until it matches the 'clean' curve, and the necessary change in h/d_t required can be converted to give the change in h dictated by the height of the deposit. The extent of fouling (i.e. the layer thickness) is termed δ, which is equal to $h_0 - h$, where h_0 is the original clearance distance without a deposit.

Mass Flow Mode

The original method of operation for FDG is 'mass flow mode' (Chew *et al.*, 2004b). The nozzle is held normal to the surface, and the pressure profile altered as a result of a change in proximity to the surface. The fluid is siphoned into the nozzle using a fixed negative pressure drop between the surface of the deposit and the discharge point after it has been drawn through the gauge. The resultant flow rate can then be measured. This is done by using an electronic balance, recording the change in mass between two defined time intervals. Mass flow mode is chiefly suited to applications where the pressure is at an approximately ambient level, as it becomes both cheap and simple to supply a pressure driving force using a hydrostatic head (Ali *et al.*, 2013).

However, there are certain scenarios in which this approach can be undesirable. Manipulating pressure differences over small scales can be a challenge, especially at higher pressures. Additionally, significant variations in flow rate can present a risk if there are hazardous liquids present (Ali *et al.*, 2013). Tuladhar *et al.*, (2003) showed that if the gauging flow rate is a significant fraction of the bulk flow, the gauging and bulk flow rates could become interdependent, resulting in changes in the bulk flow. In this instance differing and conflicting calibration results would be recorded for the same gauging parameters.

Pressure Mode

Alternatively, FDG can be operated in 'pressure mode', in which the flow rate is instead maintained at a constant level, and the pressure drop around the nozzle is recorded. This is particularly useful for high pressure systems or where a consistent gauging flow is preferred (Gu *et al.*, 2011). Membrane cross flow-based applications benefit from a stable duct flow rate, and additionally the act of imposing a fixed pressure difference would require a pressure-controlled discharge reservoir (Lister *et al.*, 2011).

This scenario means that instead of setting a fixed pressure drop and measuring the flow rate, the flow is maintained at a steady level and the pressure difference between points 1 and 3 is measured using a pressure transducer. A consistent flow rate is useful when studying membrane or biological fouling, as the flow has the potential to impact physically upon the fouling layer, which is increasingly desired as a controlled variable in itself for the measurement of surface stresses. The technique is heavily dependent on the use of reliable and sensitive pressure differential equipment in order to be sufficiently accurate (Lister *et al.*, 2011). Ali *et al.*, (2013) demonstrated how pressure mode FDG could measure fouling layers in an annular flow cell at high temperature and pressure. This study benefitted from the fixed flow rate and the insensitivity to operating pressure offered by this configuration.

2.9.2 Strength Measurements

FDG was developed with the aim of measuring the thickness of deposits, although the stresses applied also allow the adhesive and cohesive strengths of samples to be quantified. The strength of the layer is

essentially a measure of its response to a shear stress being imposed by the cleaning fluid in question (Chew *et al.*, 2004b). It has traditionally been a difficult parameter to quantify, partly for physical reasons but also because it has the tendency to vary over time as the deposit ages (Müller-Steinhagen 2000). The ageing affect is viewed as being a result of extended reactions between organic components, as well as reduction in voidage usually due to generation of additional extracellular material (such as EPS in the case of biofouling (Chew *et al.*, 2004b). Various methods developed to tackle this are outlined in Section 2.8.4. Another method is the use of impinging jets, used by Deshpande and Vaishnav (1982) to analyse tissue deformation. As previously explained, Tuladhar *et al.*, (2000) developed FDG as an adaptation of the impinging jet method with regards to conducting thickness measurements, although it was later observed that the stress induced by the gauging flow could trigger disturbance or deformation of the deposit surface (Tuladhar *et al.*, 2002). In standard gauging experiments, such deformation would be a drawback, although the resulting ability to use the technique to study deposit strength and removal offers an extra dimension to FDG. Furthermore, moving the nozzle closer to the surface in gradual stages allows a series of thickness measurements to be recorded, so essentially a single test has the potential to reveal both the original thickness of the layer followed by a series of additional thickness measurements as sections of the deposit are sucked away by the gauging flow. Chew *et al.*, (2004b) recorded the adhesive strengths of layers in terms of a yield point of the deposit, and showed the fluid velocities to be of the same order (albeit higher) than those utilised in cleaning-in-place applications. This is a significant feature of FDG in comparison to other techniques, as combined with its relative simplicity, it means that a wealth of important information about the nature of the deposit can be readily acquired. Understanding the mechanisms of removal is vital for developing effective cleaning protocols, and FDG allows the gradual disturbance of layers or sections of the deposit to be observed (Gu *et al.*, 2009a). Figure 19 indicates how deposit removal due to FDG can be shown.

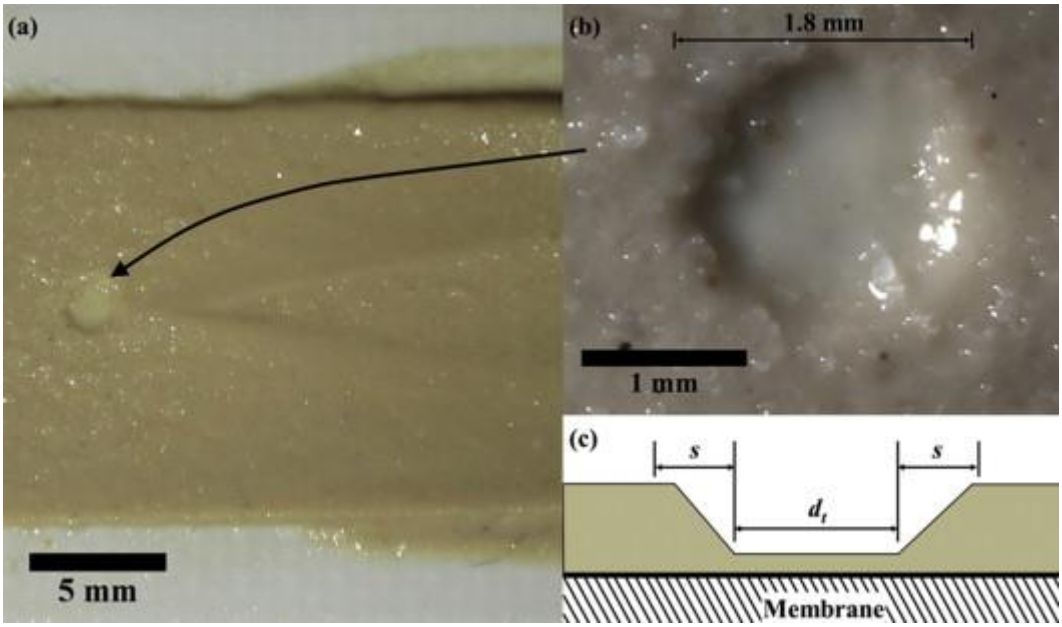

Figure 19: A collection of images by Lewis *et al.*, (2012), showing: a) and b) the crater in a cake formed by the filtration of a yeast suspension through a membrane, after study with an FDG nozzle. Part c) is a schematic of the relationship between the nozzle and the crater.

The shear stress acting on the surface can be determined with the use of computational fluid dynamics (CFD), although an appropriate analytical approximation is the equation which represents the radial flow between two parallel discs:

$$\tau_{w,max} = \mu \frac{3m}{\rho \pi h^2} \frac{1}{r} \tag{22}$$

where τ_w is the wall shear stress, μ is the dynamic viscosity of the fluid, ρ is the density of the fluid, and r is the radial distance from the central axis of the nozzle. Chew *et al.*, (2004b) verified the use of Equation 22, showing a consistent agreement with CFD simulations for the calculated shear stress values, especially for the critical region underneath the nozzle (shown in Section 2.9.1).

Shear stresses can then be converted to the equivalent mean pipe flow velocity using Equation 23:

$$U_m = \sqrt{\frac{2\tau_w}{\rho C_f}} \tag{23}$$

where C_f is the fanning friction factor and U_m is the mean pipe flow velocity. For turbulent flow regimes, C_f is typically equal to 0.005.

Thus far, Möhle *et al.*, (2007) have demonstrated the ability of FDG to measure the adhesive strength of biofilms (inoculated from activated sludge) grown on sandblasted polycarbonate discs by quantifying the applied shear stress using the model of laminar flow between parallel discs. Furthermore, the cohesive strength of biofilms and EPS was analysed using FDG by Otto (2008) by

way of monitoring the thickness of *Streptococcus mutans* biofilms at different stages in the removal process. Salley *et al.*, (2012) showed how FDG operated using liquid expulsion can monitor the removal of *Synechococcus* sp. biofilms on polyethylene and stainless steel surfaces, and suggested the existence of a two-tier structure - a compact layer adjacent to the surface and a loose upper layer.

2.9.3 Configurations

The original experiments in fluid dynamic gauging were carried out using a static rig (quasi-static FDG), which is effectively a tank in which a stationary bulk fluid is siphoned through the nozzle. While this is still a useful technique for studying fouling and cleaning effects and for the comparison of materials, it is not a common practical situation. To this end, duct flow FDG was pioneered with the aim of simulating pipe flow to test the validity of the method. It was demonstrated that FDG could reliably be used to study the behaviour of fouling layers where the liquid is subject to a bulk flow (Tuladhar *et al.*, 2003). With the nozzle fully submerged in the liquid, the hydrostatic head imposed by the gauging flow acts alongside the pressure head resulting from the flow through the duct. Otherwise, operation is similar to the static mode. The exception to this is where the gauging flow becomes a sufficiently large fraction of the bulk flow that it triggers different flow regimes (Tuladhar *et al.*, 2003). Typically this is a situation to be avoided as the results become substantially more complicated to analyse.

Gu *et al.*, (2009b) made the transition to a flow cell with an annular geometry. The flow patterns in annular systems were previously well-understood in the context of fouling and cleaning analysis, and this study showed that FDG was applicable for quasi-static conditions, as well as laminar, transitional and turbulent flow regimes.

Given that a key advantage of FDG is the ability to study a fouling layer at multiple locations. With this aim in mind, Gordon *et al.*, (2010) introduced the idea of the scanning fluid dynamic gauge (sFDG). The mobile, automated nozzle can make local measurements of soil thickness and strength over a larger and more representative surface area. This study also suggested the use of sFDG as analogous to atomic force microscopy on a large (mm) scale, revealing the contours of the deposit over the entire area, provided that there is no removal.

For applications in pressure mode, it is often desired for the system to be under aseptic conditions or for the volumes of hazardous or valuable liquids to be minimised. Having established that the FDG principle worked equally well when the fluid is ejected from the nozzle, Salley *et al.*, (2012) incorporated a syringe pump to deliver a controlled flow rate over an extended period of time whilst maintaining a closed experimental system. This method is termed zero discharge fluid dynamic gauging, or zFDG. This has particular value in the study of biofilms, given that biological deposits are typically sensitive to contamination or disturbances. Yang *et al.*, (2014) demonstrated comparable C_d calibration plots for the sucking and ejection regimes, concluding that zFDG was capable of

determining layer thickness. It was observed, however, that the ejection regime displayed a higher discharge coefficient, which (using computational fluid dynamics) was shown to be due to altered flow patterns around the nozzle. Successful comparison was also made by between the shear stresses recorded in cohesive breakdown tests and the yield stresses recorded in rheological tests, showing that zFDG could be applied to make deposit strength measurements.

An alternative tool for analysis of the impact of gauging on the sample is to combine the FDG process with real-time imaging, such as confocal laser scanning microscopy (CLSM) or optical microscopy. This is used to monitor measurements of the mechanical, chemical and structural properties of the deposits on a more local level, which helps with the development of imaging techniques as well as with understanding the dynamics which occur (Sahoo *et al.*, 2008).

3. AIMS & OBJECTIVES

3.1 Aim

Green cleaning is a facet of the pursuit of sustainability – the moderated use of resources to preserve them for future generations. In summary, the focus is to suggest and implement ways in which the amount of chemicals, water and energy used in cleaning can be reduced without making sacrifices in terms of efficacy or provide guidelines for cleaning propocols i.e. when to clean. Chemical cleaning agents without potential health or environmental impacts are very few and far between. However, the shearing force of water can be used for cleaning, dependent upon the resistance of the deposit to shear effects (Durkee 2006). Currently, methods are developed by using trial and error.

With that in mind, the aim of this research is to apply green cleaning principles to the removal of biofouling in industrial applications. Fluid dynamic gauging is a technology which utilises hydrodynamic phenomena to measure the thickness and strength of deposits and by doing so the optimum water usage can be estimated. FDG has not previously been applied to study mixed species biofouling under static and flow conditions. This allows for the development of effective green cleaning protocols, which minimise energy usage and environmental impacts. This new method of obtaining experimental data for biofouling removal can be used to directly make suggestions for cleaning protocols. Currently, methods are developed by using trial and error.

3.2 Objectives

3.2.1 Testing Biofilms on Different Surfaces

Three surfaces will be used as biofilm growth substrates – polyethylene, glass and stainless steel 304. The intention here is that they will be representative of the range of surfaces regularly used for domestic and industrial processes. Given that factors such as roughness and surface energy are widely recognised to play a role in bacterial attachment, the differing surface properties of each material may prove significant in explaining the adhesive strength results reported.

3.2.2 Testing Different Species of Biofilm

It is widely observed and recognised that, in the vast majority of situations, bacterial biofilms consist of multiple species acting as a community. For this reason, using a mixed species culture for testing is crucial. The research will also use the constituent strains as single-species biofilms, which will allow any developmental differences caused by mixed cultures to be observed, and also to judge the effects of ageing and surface material independently of any added complications due to community interactions. It is also a strong possibility that the results will show the variety of thicknesses and strengths between species, and if that is the case then any directives for future cleaning processes would need to bear this in mind.

3.2.3 Methods Used

Fluid dynamic gauging (FDG) has been pioneered as an effective and versatile way of studying soft fouling layers. It requires little knowledge of the deposit prior to testing and is both relatively simple and inexpensive to operate. It has particular use in the study of biological fouling layers because it allows them to be analysed *in situ* and without the need for physical contact, minimising the risk of disturbance which biofilms are prone to. The ability to measure both the thickness of the deposits and quantify their adhesive and cohesive strengths offers FDG a versatility which gives it a clear advantage over other methods investigated for this purpose.

Alongside fluid dynamic gauging, supplementary characterisation tests will also be carried out in order to seek explanations for any trends or features discovered. Firstly, these will involve analysis of the substrates used as growth sites. The roughness and surface energy of the materials will be quantified and compared with relevance to the strength of attachment observed. Additionally, the extracellular polymeric substances will be analysed for changes in coverage or composition with reference to deposit layer strength, and the prevalence of dead cells in biofilms will also be considered as a potential variable concerning the aging process.

Biofilms will be grown under both static and duct flow conditions. The duct flow regime is a simulation of pipe flow scenarios in industrial processes, allowing the biofilms to develop in a way similar to that in which they would grow in the food or pharmaceutical industries. A duct flow rig will be designed and built during the course of the investigation, and in the meantime biofilms will be grown in static conditions with the aim of providing extra insight into the mechanisms of biofilm development and how the impact of flow influences them.

4. METHODS – Static-Grown Biofilms

This chapter explains the procedures undertaken in the study of the adhesion and removal behaviour of *Escherichia coli* and *Burkholderia cepacia* biofilms grown under static conditions, using fluid dynamic gauging (FDG) and a selection of characterisation techniques. The objective here is to assess the development of biofilms over a 28-day period, seeking explanations for any patterns observed using microscopy and surface and biofilm analysis methods, and working towards efficient green cleaning methods.

4.1 Materials

4.1.1 Bacteria Strains

Three strains of bacteria were tested for their ability to form biofilms under static conditions, wherein there is no bulk flow (the only fluid movement being orbital due to a shaker). These were as follows: *Escherichia coli* Nissle1917; and two variants of *Pseudomonas aeruginosa* (PA01 and NCTC 6750). Both *E. coli* and *P. aeruginosa* are well-studied organisms with regards to biofilm studies, and their common presence in aquatic systems makes them ideal and relevant test materials for industrial biofouling simulation (Vanysacker *et al.*, (2014); Timmis (2002)). Protocols for *E. coli* biofilm growth are well-established, and as a species it has been extensively characterised (Fletcher (1977); Pratt and Kolter (1998)). Both species are recognised to form biofilms on a number of different surfaces, which is essential for the studying and comparison of fouling mechanisms with an industrial focus (O'Toole and Kolter 1998). *P. aeruginosa* biofilms have also been widely characterised, including studies into their thickness (Stewart *et al.*, 1993) to porosity (Zhang and Bishop 1994). With the growth mechanisms and physical development of these species well-understood, it is therefore possible to grow reliable and repeatable cultures for fouling testing.

Burkholderia cepacia was then selected as an additional species to use as both a comparison and for mixed species biofilm development. Interest in its occurrence in industrial scenarios is emerging, due to its ability to survive prolonged exposure to high concentrations of many common industrial biocides, including benzalkonium chloride and triclosan (Rose *et al.*, 2009). This trademark of resistance to commercial biocides makes it a favourable test species for green cleaning methodology, and it is particularly prevalent in the pharmaceutical industry, as well as petroleum and others (Thomas 2011) ensures that it fits within the scope of this research. Furthermore, it has been shown to colonise a range of surfaces, including glass and metals (Walker 2005).

All species were kept in deep frozen storage (at -80 ^{O}C), with 1.5 mL of prepared culture supplemented with 300 µL glycerol in order to prevent the formation of ice crystals.

4.1.2 Culture Media

Cultures were grown in M9 minimal medium (De Kievit *et al.*, 2001), containing 47.7 mM $Na_2HPO_4.7H_2O$, 21.7 mM KH_2PO_4, 8.6 mM NaCl, 18.7 mM NH_4Cl, 0.5% (wt/vol) casein

hydrolysate, 1 mM $MgSO_4$ and 11.1mM glucose (all chemicals were sourced from SigmaAldrich). As is customary for minimal media formulations, this recipe provides a methodically concocted source of minimum nutrients for growth, along with one carbon source (glucose).

Ionic Strength

The ionic strength of the M9 media was calculated in the testing processes. Correlations between ionic strength and bacterial adhesion have regularly been studied (Gordon and Millero (1984); Gross and Logan (1995)), whilst alterations in ionic charges present have been shown to alter the strength of bacterial bonding and thus influence detachment (Olsson *et al.*, 2012). The ionic strength, *I*, is calculated via the following equation:

$$I = \frac{1}{2}\sum_i c_i z_i^2 \tag{24}$$

where *i* is each chemical species in series, and *c* and *z* are the concentration and charge of the species respectively. With the formulation reported previously, the ionic strength of the media is calculated to be 0.194 M (full working is shown in Appendix 1). With de-ionised reverse osmosis (RO) water used for the FDG tests, an equivalent ion concentration must be added. This equates to 11.34 gL^{-1} of a monovalent salt – in this case sodium chloride (NaCl) was used.

4.1.3 Test Surfaces

Three different substrates were selected for static biofilm analysis and comparison: (i) polyethylene (PE) petri dishes with a diameter of 55 mm; (ii) glass petri dishes of 50 mm diameter; and (iii) stainless steel 304 (SS) discs of 50 mm diameter. The properties of each surfaces were characterised using atomic force microscopy, scanning electron microscopy and contact angle analysis. Prior to each growth incidence, the steel and glass surfaces were washed with an isopropanol solution.

4.2 Biofilm Assays

Biofilm viability assays were conducted based on the standard protocol described by Christensen *et al.*, (1985). The three test strains (section 4.1.1) were cultured overnight at 37 ^oC, and then diluted in fresh media to an optical density (OD600) of 0.06. The diluted cultures were added to a 96-well polyethylene microtitre plate, with a row of four plates dedicated to each strain plus another row of pure medium for control purposes. The plate was then incubated at 37 ^oC on an incubator (Stuart Mini Gyro-Rocker SSM3) rotating at a speed of 40 rpm. Cells attached to the bottom of the wells and formed biofilms. After 24 h the supernatant fluid was pipetted out and replaced with another 200µL of fresh medium. Incubation was resumed for another 24 h period.

Figure 20: A 96-well microtitre plate of type used for the biofilm viability assays in this section (https://www.edgebio.com/products/96-well-treated-microplates-u-bottom-50063)

In order for the biofilm growth to be quantified, the wells were washed with 0.9 % saline and stained with crystal violet (Boleij *et al.*, 2011). The absorbance of the content of each well (including the control wells) were measured and recorded using an automatic plate reader (VERSAmaxTunable Plate Reader BN 02877) at a wavelength of 595 nm, as wavelengths in the region of 600 nm are a good option for most bacterial cultures, with the advantage that the media components contribute less to the overall absorbance than at lower frequencies (Burton and Kaguni 1997).

4.2.1 Biofilm Growth Protocol

The protocol of incubation for all the subsequent biofilm testing scenarios in Section 4 followed the same method for growth as detailed for the assay, with the biofilms instead being established on the surfaces detailed above (section 4.1.3). The maximum orbital shear stress applied by the incubator ($\tau_{0,\ max}$) is the important parameter in the static growth system, and can be defined as:

$$\tau_{O\ max} = a\sqrt{\mu\rho(2\pi f)^3} \tag{25}$$

with a being the orbital radius of the shaker, f the frequency of rotation (rotation/sec), and μ and ρ the dynamic viscosity and density of the media respectively (Wang *et al.*, 2014). With an orbital radius of 1 cm and operated at a rotational speed of 40 rpm, the maximum orbital shear stress is calculated to be 0.086 Pa.

A range of incubation periods set at 5, 10, 14, 21 and 28 days was chosen as a good spread of ages for means of realistic assessment the stages of growth and development. Separate samples on all three test surfaces were grown for each of the time periods.

4.2.2 Growth Curves

A series of tests were conducted in order to display growth curves for the relevant species, in both liquid culture form and as biofilms, with the aim of showing their development over time in accordance with the theory behind bacterial growth as explained in Section 2.2.2. This allows for the

phases of growth to be identified (lag, exponential, stationary, death) and for the generation time (required for the population to double in number) to be calculated.

An *Escherichia coli* Nissle1917 culture was cultivated in M9 media in a 10 mm Universal container, being shaken in an incubator maintained at 37 ^{0}C. After each hour, samples were taken from the culture and analysed for their optical density (OD600). This process was continued up to the point at which the turbidity of the culture ceased to increase.

4.3 FDG Apparatus

Fluid dynamic gauging was employed throughout this research in order to study the removal behaviour of all biofilms grown under the aforementioned conditions. The strength and thickness tests for the static biofilms were conducted under mass flow mode (Section 2.9.1).

Figure 21 shows the apparatus used in this study in mass flow mode, complete with the exhaust siphon tube delivering the gauged fluid into a beaker placed on a balance (beaker and balance not shown). The nozzle (shown in proximity to a fouled surface in Figure 17 in Section 2.9.1) has a diameter of 5 mm, allowing a shear stress range of approximately 2 – 60 Pa to be applied.

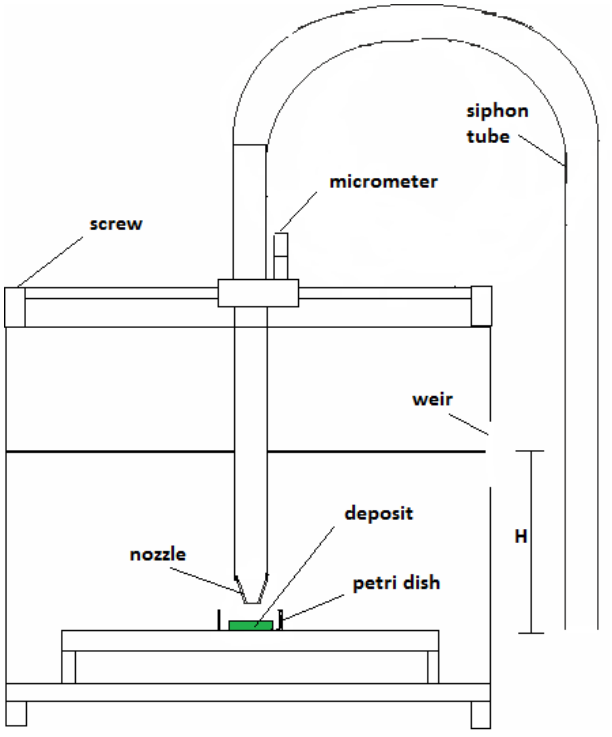

Figure 21: A schematic of the FDG apparatus in mass flow mode setup, in which the hydrostatic head, H, is identified as the key operational parameter which determines the pressure driving force controlling the siphon flow.

The clearance distance of the nozzle (h) is controlled by the micrometer. The fluid inlet tube is connected to a tank situated on a high shelf (pre-filled prior to experiments), and the fluid outlet tube

is drained into a sink. The siphon tube draws fluid out through the gauge and into a beaker situated on an electronic balance (Sartorius TE4101).

4.3.1 FDG Calibration

Having determined $L_{eff,}$ the remaining experimental parameter (shown in Appendix 2), the next preparatory stage was to conduct test runs of the FDG apparatus in order to produce calibration plots of mass flow rate against nozzle clearance in their dimensionless forms (C_d and h/d_t). The resulting curve should resemble the one shown in section 2.9.1 (Figure 18). This procedure also allows for enhanced familiarity with the apparatus. Calibration curves were carried out at H = 20 mm, 30 mm and 60 mm in order to test the operability at varying hydrostatic heads. This can be a useful method of inflicting a greater range of shear stresses on the deposit surface. The calibration plot is shown in Section 5.3.

4.4 Surface Characterisation

As detailed in the literature review (Section 2.5), surface roughness and surface energy are widely believed to be major factors in biofilm adhesion (Xu and Siedlecki 2012). With this in mind, analyses were carried out as a means of comparing the profiles of the surface, and their surface energies in order to help explain and support the biofilm removal results. The stainless steel plate and the glass coverslips used in the flow experiments (Section 6) were characterised in addition to the steel discs and the polyethylene and glass petri dishes used for growing biofilms in this section.

4.4.1 Surface Roughness

Atomic Force Microscopy

The polyethylene petri dishes, glass coverslips and both steel surfaces were examined using atomic force microscopy (AFM) in order to visualise the morphological profiles of the growth surfaces in a high resolution three-dimensional manner. The proliferation, size and shape of surface imperfections are known to be a factor in the process of cell adhesion and therefore also in biofilm establishment. A Digital Instruments Nanoscope IIIA (with a tip length of 225µm) was operated in ‘tapping mode’ (Section 2.8.2) and the material sample sizes used were 5 mm x 5 mm. Samples were washed prior to imaging with RO water.

Scanning Electron Microscopy

The steel surfaces were also analysed using a JEOL SEM6480LV scanning electron microscope (SEM), offering birds-eye views of the surface at a range of magnifications – x50, x2000, and x5000. The main value of this investigation is to display crevices and similar surface features, and therefore to assess whether or not these features are likely to encourage bacterial attachment. The surfaces were sputter-coated with gold prior to imaging – this conductive coating has the effect of preventing the surface from being charged by the electron beams.

4.4.2 Surface Energy

Along with the roughness of the surfaces, the surface energy (and therefore wetting potential) is also widely recognised to play a role in the propensity of biofilms to attach to various surfaces (Finlay *et al.*, (2002); Lewandowski and Beyenal (2014)). A set of critical surface energy tests were therefore conducted with the aim of establishing which of the surfaces used were more hydrophobic or hydrophilic. It has been shown that strength of cell adhesion is generally proportional to surface energy (Hallab *et al.*, 2001). The Zisman plot method was chosen due being relative quick and simple to conduct, whilst being recognised to be accurate where the surface energies of the liquids used are well known. For this case, measurements were compiled using water and 5, 10, and 15% sodium chloride solutions. Contact angle measurements were carried out using a Dataphysics Contact Angle System OCA, which lowers a fluid droplet onto the surface to be measured. Three measurements were taken for each NaCl concentration on each surface in order to attain repeatability. The results are shown in Section 5.4.2.

4.5 Biofilm Characterisation – Cation Exchange

The nature of the EPS composition of biofilms can be investigated, and in doing so trends may be revealed which relate to changes in strength of attachment. The protein and polysaccharide levels can be sampled using the cation exchange method.

The first step is to isolate the EPS from planktonic cells and any other unwanted materials present. The biofilm is removed from the surface with a cell scraper and suspended in phosphate-buffered saline (PBS) with a composition of 8 gL^{-1} NaCl, 0.2 gL^{-1} KCl, 1.15 gL^{-1} $Na_2HPO_4.7H_2O$ and 0.2 gL^{-1} KH_2PO_4 and shaken for 30 minutes. The sample is then placed in an ultrasonic bath for 2 minutes followed by homogenisation with an ultrasonic probe in pulsating mode for 10 pulses at 45 W. This treatment has been shown to be effective for cell removal (Dreszer *et al.*, 2013), ensuring that the EPS can be analysed in isolation.

Finally, the EPS must be dissolved into the liquid. This is achieved via the addition of a cation exchange resin in the sodium form (Na^+) at a rate of 0.2 g per 1 mL sample. The mixture is shaken for 2 hours at room temperature. The Na^+ in the resin is exchanged for the Ca^{2+} in the sample, allowing for the dissolution of the EPS. The suspension was then centrifuged at 9000 g (g being the Earth's gravitational force) for 20 minutes at 4°C to separate the cells from the EPS for effective content analysis. This method is known to produce a good yield of EPS without causing unnecessary damage to cells (e.g. lysis) should they be required for any further reason (Frølund *et al.*, 1996).

4.5.1 Standard Curves and Quantification

The protein and polysaccharides in the resulting solution was then quantified. First of all, standard curves were derived from stock solutions. This was carried out by making up ranges of concentrations

of glucose (for polysaccharides) and bovine serum albumin (BSA) (for proteins) solutions, and applying the procedures detailed below.

4.5.2 Protein

The procedure for protein quantification using bicinchoninic acid (BCA) was described by Smith *et al.*, (1985). The standard BCA reagent consists of two components. Reagent A is a solution containing 1% BCA-Na_2, 2% $Na_2CO_3.H_2O$, 0.16% Na_2 tartrate, 0.4% NaOH and 0.95% $NaHCO_3$. Reagent B is 4% $CuSO_4.5H_2O$ in deionised water. The standard working reagent (SWR) is formed by mixing reagents A and B to the ratio of 50:1.

The quantification procedure begins by mixing 100 µL of sample (standard or test) with 2 mL of SWR in a test tube. Immediately, a colour change is observed. The absorbance of the samples is then measured at 562 nm and compared to a reagent 'blank'. This allows a standard curve to be plotted, or for a test sample to be compared to a previously compiled standard. In this instance, bovine serum albumin (BSA) was used as the protein standard for comparison.

4.5.3 Polysaccharides

A similar method for polysaccharide composition was described by DuBois *et al.*, (1956). The two reagents required in this case are 95.5% sulphuric acid and an 80 vol% phenol solution. 2 mL of the standard (glucose) or test solution is pipetted into a test tube, followed by 0.05 mL of the phenol solution. Subsequently, 5 mL of sulphuric acid is added rapidly. They were then left to stand for 10 minutes, and then heated in a water bath at 25 - 30°C for a further 10-20 minutes. It was found that all of the solutions became opaque using this method (and therefore unsuitable for the absorbance step). Alternative formulations were used by Masuko *et al.*, (2005), in which lower inputs of sulphuric acid were trialled and the high sensitivity of colour response was noted. Therefore, in this case the sulphuric acid input was reduced to 3mL per sample, and colour graduation was visible. Absorbance was measured at 490 nm.

Mixed species biofilms were used for both cases, due to the greater proliferation of such cultures in nature and industry compared to single-species biofilms. They were grown on all three surfaces for periods of 5, 10, 14, 21 and 28 days, as used for the strength and thickness tests.

4.6 FDG TESTS

4.6.1 Strength Tests

Biofilm strength tests were conducted by using the gauge to apply a certain shear stress to the surface and remove sections of the deposit, then using microscopic methods to quantify the proportion of bacteria remaining. Biofilms were grown on each of the polyethylene, stainless steel and glass surfaces for periods of 5, 10, 14, 21 and 28 days. This was done using the protocol outlined in Section 4.2.1.

Before FDG testing, imaging was performed using a Nikon Eclipse E400 optical microscope in order to provide images of the fouled surface prior to removal. The samples were then placed under the gauge at different nozzle clearance heights (h/d_t) to impose a range of shear stresses in order to test the yield shear strength of the biofilm deposits. The 5 mm diameter focus of the nozzle allows for multiple shear stresses to be applied to each sample, which enables local variations to be taken into account. As detailed in section 4.1.2, 14.08 gL^{-1} of sodium chloride was added to the water in order to maintain the ionic strength levels found in the growth media. Four tests were carried out on each sample, each tested at a different h/d_t value. This method is shown in a simple schematic below:

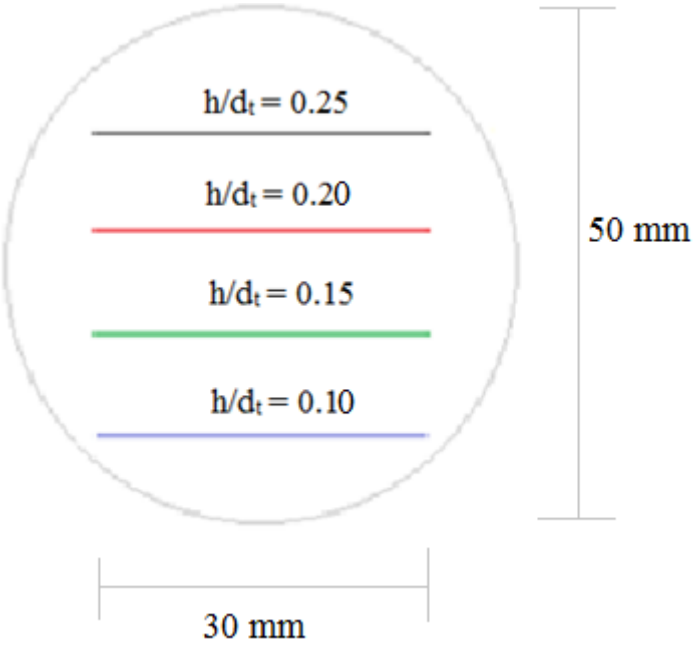

Figure 22: A diagram showing the method used for making four separate strength measurements on each biofilm sample. Each line relates to a route traced by the FDG nozzle, at a clearance distance equal to the relevant h/d_t value.

Tests were conducted on each surface to ensure that three repeats of each h/d_t value were completed. After shear stresses were applied to the samples, the surfaces were again analysed under the microscope at each gauged line, and the percentage reduction in surface coverage resulting from the FDG process was measured. This was done so using ImageJ (developed for the public domain by the US National Institutes of Health), by making surface area calculations of the coverage of biofilm in the sample size of the image taken by the microscope. A selection of examples of the images used for this analysis (from all three surfaces) are shown in Section 5.6, along with numerical analysis of the results and the related discussions.

4.6.2 Thickness Tests

As discussed in Section 2.9.2, fluid dynamic gauging is adept as measuring both the strength and thickness of fouling deposits. Thickness measurements are taken with a resolution of ±5 µm, whilst

strength measurement resolution is dependent on the mass flow rate and nozzle proximity to the surface. The alteration made to the fluid flow rate due to the presence of the fouling layer can be used to deduce the thickness of the layer, with average values taken from several points for each sample, as per intention of the original FDG experiments. It is also possible to take multiple thickness readings in this manner from each sample, recording the thickness as the nozzle is moved progressively closer to the surface. In the previous section (4.6.1) the ability of the gauge to remove the biofilm is used to measure the shear stress required to entirely clean the surface – in this case the intention is to assess the nature of biofilm removal in terms of live changes in thickness as layers are removed. Due to the resolution of the measurements being ±5 µm, and the cells being approximately 2 µm in length and 0.5 µm in width, the accuracy of the readings will be partly dependent on the thickness itself – greater accuracy would be expected at greater biofilm thicknesses.

In the same manner as the strength tests, biofilms were grown on all three surfaces for periods of 5, 10, 14, 21 and 28 days for thickness analysis. The method of FDG operation followed the same steps as for the calibration stage, in that at above a certain point on the biofilm surface, the nozzle was moved gradually closer to the substrate surface with the mass flow being recorded at each step. Measurements of biofilm thickness can be taken using the flow data from the FDG experiments in comparison with the calibration data taken relating to the clean surfaces. A plot of C_d versus h/d_t using a clean surface can be used as a calibration curve in order to measure the height difference caused by a fouling layer, and how it changes as the nozzle is moved gradually closer. The extent of fouling (δ) can be measured at each step.

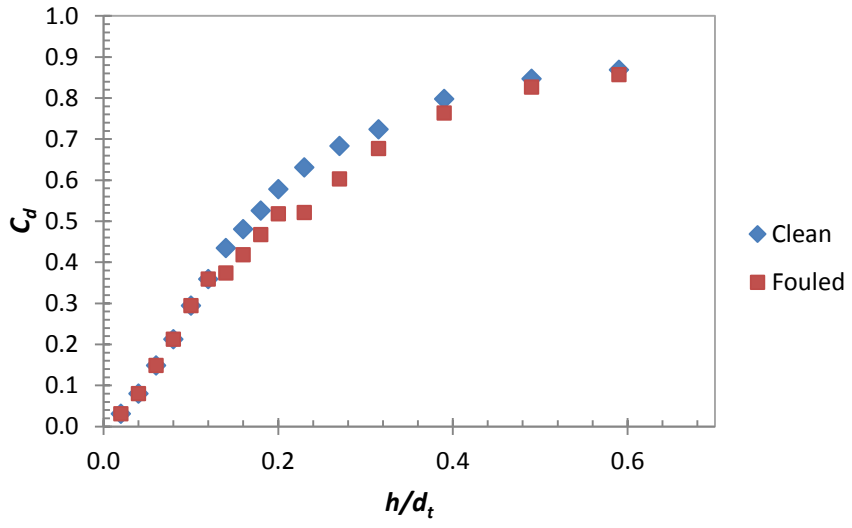

Figure 23: An indication of how the thickness of the biofilm can be recorded as the nozzle approaches the surface. The profile of the fouled surface eventually reverts to the same curve as the clean, which represents complete removal of the deposit.

The thickness values are of some importance to the understanding of biofilm development, although more significantly, the tendency of fouling material to be removed as the stress applied reaches a certain level allows the cohesive strength of the deposit to be quantified. Alongside the adhesive strength taken from the surface coverage tests in the previous section, these results will give a detailed picture of the removal mechanisms and deformation behaviour under stress. In clean-in-place (CIP) systems, it is generally believed that 1.5 ms^{-1} (which equates to 5.6 Pa – equation 23) is suitable for cleaning pipelines effectively, although disinfectants along with acids and alkalis also form part of standard CIP cleaning procedures (Goode 2012). Although this value of 1.5ms^{-1} is largely anecdotal rather than empirically derived, it is recognised in industry as a benchmark (Davy 2010). Where surfaces are exposed to higher velocities than this, they become easier to clean, although the use of chemicals and increased temperatures is still standard – in most cases the introduction of different geometries (dead-ends, crevies etc.) is the most likely problem factor which flow rates, chemicals and temperatures have little impact on the ease of cleaning (Jensen and Friis 2005). The range of growth time periods involved will ideally be a useful measure of the evolving maturity of the EPS matrix over time, and offer suggestions as to how this relates to the removal behaviour. This test of cohesive strength does not however give an indication of the biofilm topography.

4.7 Biofilm Characterisation – Confocal Microscopy

4.7.1 EPS Coverage

The EPS plays an essential role in the structural integrity of biofilms, and so therefore loss or degradation of extracellular organic matter may be an observable explanation for age-related weakening or strengthening of biofilms. Removal of EPS is known to be closely related to the inactivation of bacteria (Tachikawa *et al.,* 2009). Images of biofilms grown on glass coverslips for periods of 14 and 21 days were taken using a confocal microscope (Zeiss CLSM 510META). The coverslips were removed from the wells, blotted carefully on tissue paper and washed in a 0.9% NaCl solution in small petri dishes on a horizontal shaker for one minute. This process is repeated a second time. The washed coverslips can then be stained by placing in empty petri dishes and adding approximately 800µL (enough to submerge the coverslip) of a calcofluor white stain (containing 1% Calcofluor White M2R and 0.5% Evans blue) along with one drop of 10% KOH solution. Excess stain is removed by further washes in sodium chloride solution, firstly by adding some to the petri dishes used for staining and leaving them for one minute on the horizontal shaker, and then by repeating the earlier washing step in new dishes. The coverslips are finally blotted and placed on microscope slides face down, and sealed in place by applying nail varnish around the edges of the slips.

4.7.2 Live/Dead Staining

Subsequently, a second set of CLSM images were taken with stains to identify the presence of living and dead cells in 14 and 21-days old biofilms grown on glass coverslips. The tendency of cells to die

or lyse at a particular stage of their life span has been linked to biofilm dispersal (Schleheck *et al.*, 2009), and dual staining can be conducted in order to clearly depict regions of dead cells. Acridine orange binds to nucleic acids, which allows it to produce a green fluorescence from all cells present. Propidium iodide, on the other hand, enters cells with compromised membranes, staining dead cells red. A quenching effect ensures that cells with both stains fluoresce red, so therefore live cells show as green and dead cells as red. The same process as described for biofilm growth on the glass coverslips for the EPS coverage imaging was repeated with the following exceptions for staining. A combined stock solution of 1mM acridine orange and 1mM propidium iodide in PBS was made for combined staining (Mascotti *et al.*, 2000). The dishes must then be covered with foil when left to stain, as acridine orange is vulnerable to degradation due to direct sunlight.

5. RESULTS AND DISCUSSIONS: Static-Grown Biofilms

5.1 Biofilm Assay: Strain Comparison

The absorbance of each well in question (four of each strain plus the four control wells) were measured and recorded using the plate reader. The mean absorbance of the control samples was subtracted from the values for the biofilm wells, and mean and standard deviation results for each strain were calculated and displayed in the table below.

Table 2: The full set of absorbance value recorded for the biofilm viability assay. The mean and standard deviation results for each species are displayed in the bottom two rows, with the raw data and control values shown in Appendix 3.

	E. coli	PA NCTC	PA01
	0.3289	0.0873	0.0303
	0.4008	0.0781	0.0385
	0.4044	0.0538	0.0648
	0.4447	0.1022	0.0548
Mean	**0.395**	**0.080**	**0.047**
S.D.	**0.048**	**0.020**	**0.016**

The mean absorbance values for each strain are summarised in Figure 24, with standard deviations included as error bars.

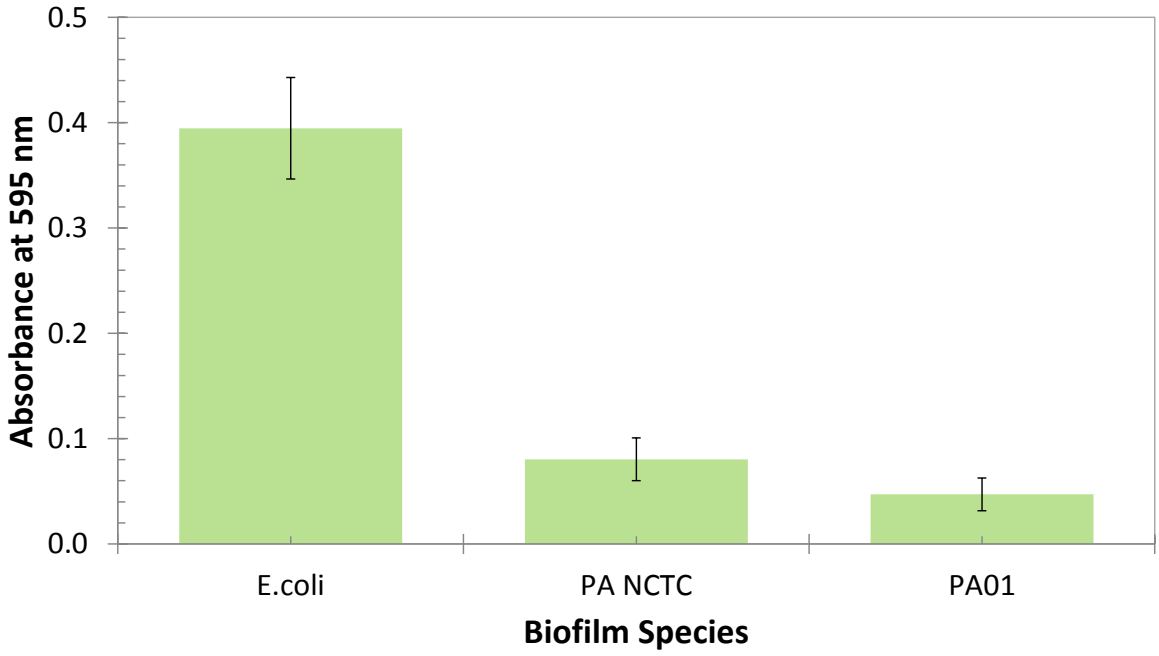

Figure 24: The mean absorbance values, taken at a wavelength of 595nm, for each biofilm species tested for the viability assay, with standard deviations added as error bars.

As Figure 24 shows, the *E. coli* Nissle1971 sample produced considerably more developed and better-attached biofilms than both *P. aeruginosa* strains. Consequently, in the remaining experiments using biofilms, the *E.coli* strains will be grown as the primary species, with the previously chosen *Burkholderia cepacia* as an additional species.

5.2 Growth Curves

Both the *Escherichia coli* and *Burkholderia cepacia* strains were grown in liquid culture in M9 media, with the optical density (OD600) being recorded after each hour. This was continued up to the point at which there ceased to be an increase in density and a stationary phase was reached. It should be noted that dead cells are not differentiated by this analysis, so no meaningful decrease would ever be recorded. The results for both species are shown in Figure 25:

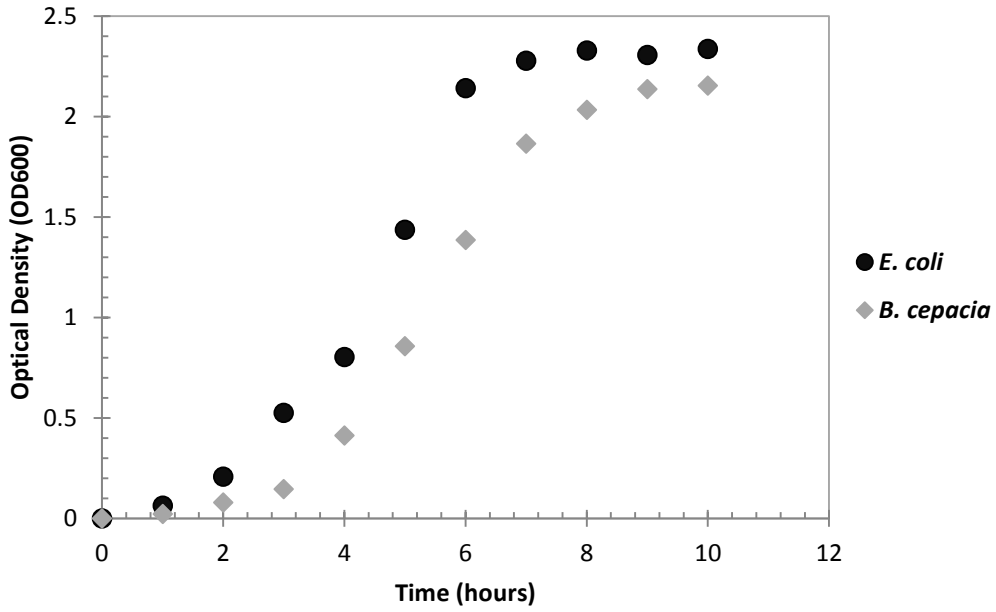

Figure 25: This graph shows the growth curve plotted from the optical density recordings for the *Escherichia coli* and *Burkholderia cepacia* suspended cultures.

The curve for *E. coli* clearly shows the initial lag phase in which there is a delayed growth in numbers, followed by the exponential growth phase between 2 hours and 6 hours where multiplication of cells accelerates rapidly. There is then evidence that the culture is beginning to enter its stationary phase after about 6 hours, where restrictions in nutrient availability and physical space begin to limit the potential for growth. It is not possible to observe any death of mature cells using this particular method.

The growth curve for *Burkholderia cepacia* displays the same core characteristics as *E. coli*. The initial lag period, followed by the phase of exponential growth and finally the stationary phase are all distinctly noticeable. However, it can be seen that the lag phase is more prolonged, taking at least 3

hours before growth begins to escalate. A stable maximum level is only reached after 9 hours, which is a considerable delay in comparison with the *E. coli* growth curve.

These results suggest that the cultures can be used to cultivate a new biofilm after 5 hours, as at this point in time there will be sufficient numbers of viable cells to both attach to the surface and continue to grow.

5.3 FDG Calibration

The aim of conducting calibration runs of the FDG apparatus was to test its functionality under the conditions described, with the particular desire to operate the system under a range of hydrostatic heads. A combined graph of all 3 calibrations (H = 20, 30 and 60 mm; ρgH = 196, 294 and 589 Pa) is shown below in Figure 26.

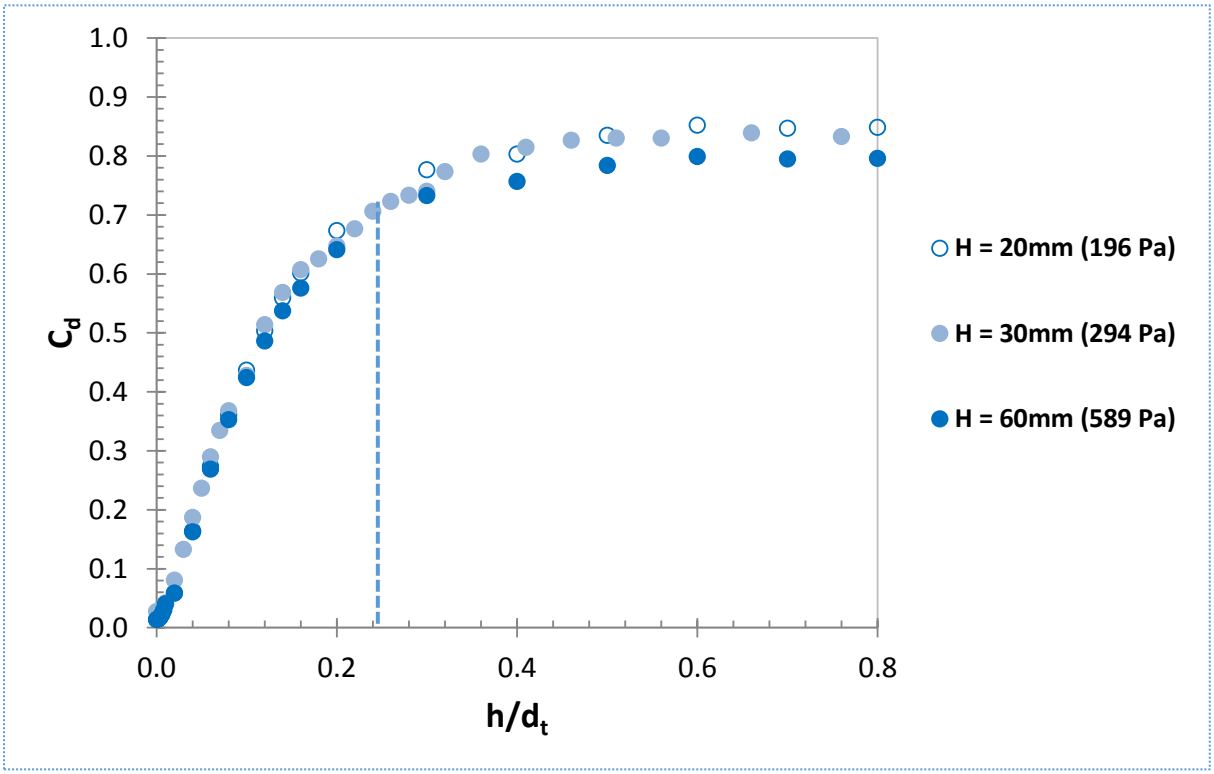

Figure 26: C_d calibration curves for the FDG apparatus for the following hydrostatic head values: H = 20, 30, and 60 mm. C_d is calculated using Equation 19. The dotted line shows where $h/d_t = 0.25$, at the transition between the incremental and asymptotic zones.

The curves all show the typical stages for an FDG C_d versus h/d_t plot: the incremental zone where $0 < h/d_t <$ approx. 0.25 (mark it on the plot), in which C_d steadily increases, and the asymptotic zone where C_d becomes virtually constant (at an approximate value between 0.8 and 0.85). Various cases were compared by Gu *et al.*, (2009) for duct flow experiments (and CFD simulations) and the values taken for C_d upon reaching the asymptotic zone fell between 0.78 and 0.9 This confirms that the gauge will be operable at these conditions and can therefore be used for this research. The size of the

symbols represents the potential for errors inherent in the use of the stopwatch and balance. The similarities between the results in the incremental zone indicate that the errors are largely insignificant.

5.4 Surface Characterisation

5.4.1 Surface Roughness

AFM

The tapping mode AFM profiles for the polyethylene and steel disc are shown first. They are displayed in three-dimensional topographic form, starting with polyethylene.

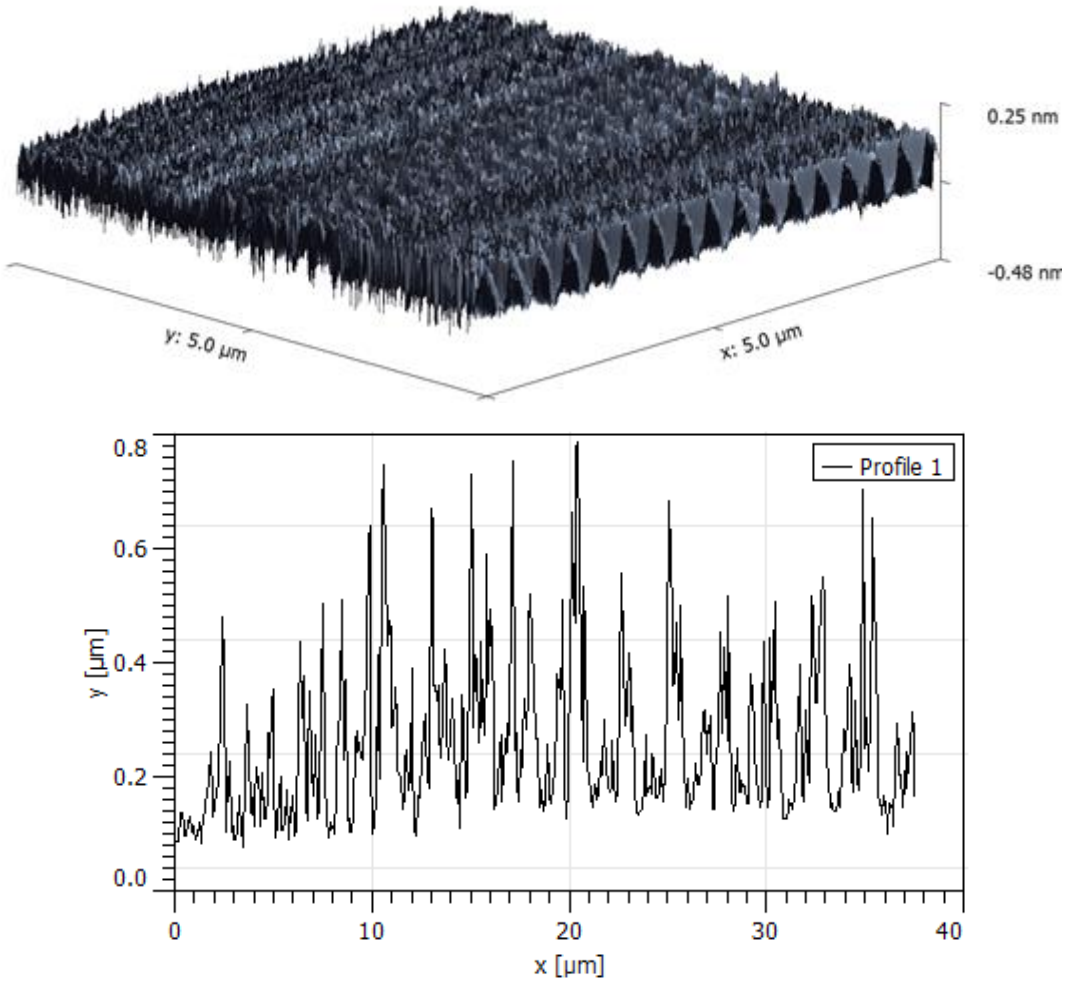

Figure 27: A 3D topographic AFM image showing the typical morphology of the polyethylene surface over an area of 25µm^2, along with a side profile of the surface.

The polyethylene petri dish surface appears to very smooth, with features which do not exceed 0.5nm in height. These imperfections are therefore irrelevant in comparison to the size of the cells (both species are typically approximately 2µm in length) and would offer nothing in the way of shelter or enhance surface area for colonisation. Looking at image b), there are typical peak-to-trough heights of 0.24 to 0.7 µm, with some troughs with widths of approximately 2 µm which could allow cells to

settle. Mostly, however, the surface features are not significant large to confer benefits to biofilm formation. Surface energy and surface charges may be able to exert a greater impact on attachment here.

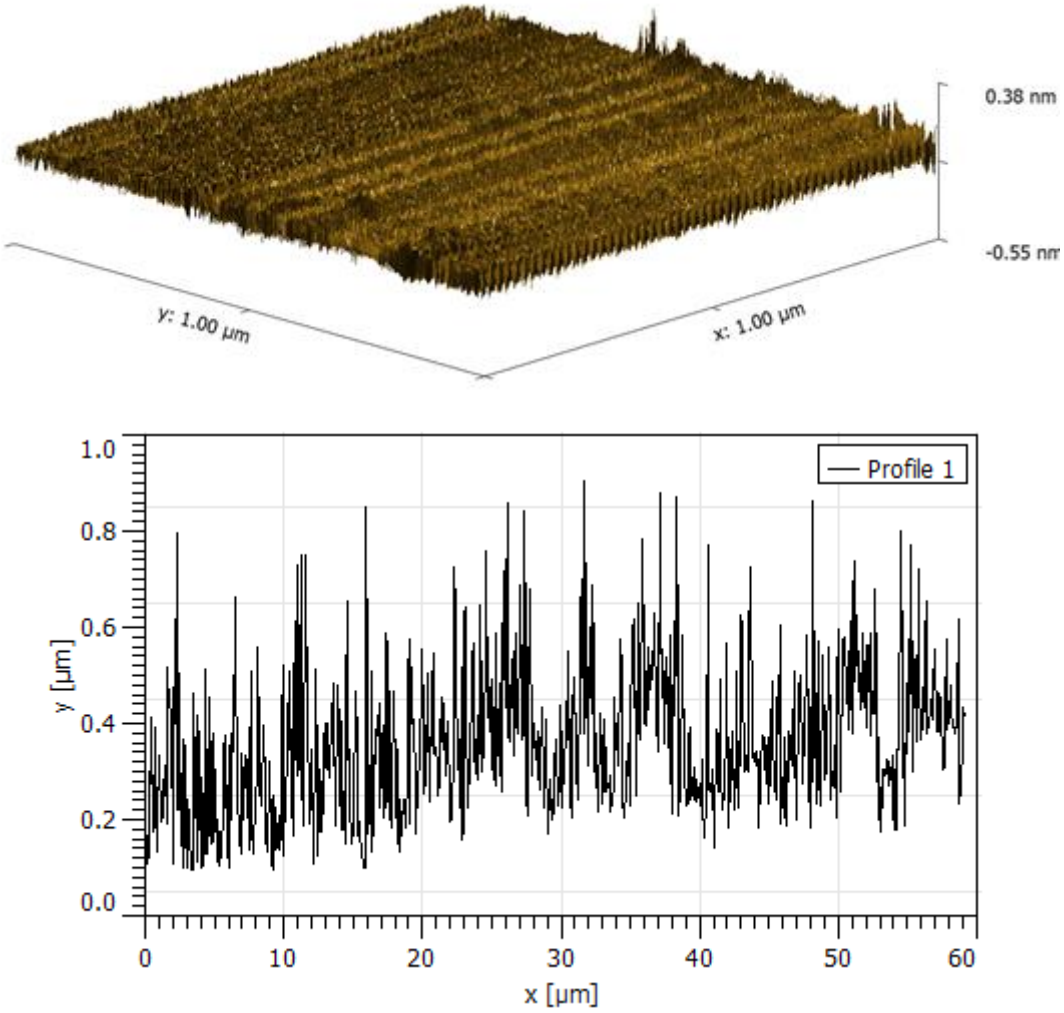

Figure 28: A 3D topographic AFM image showing the typical morphology of the steel disc used for the static-grown biofilms over an area of 1µm^2, along with a side profile of the surface.

The steel disc shows a similar surface profile to the polyethylene petri dish, in that the surface features do not exceed 0.55nm in height. Likewise, these features should not be expected to have a noticeable impact on the propensity of cells to attach. Image b) suggests a rather jagged, rough surface, but when it comes to assessing their size it can be seen that few are wide enough to allow cells to attach within. Peak-to-trough heights are in a similar region to the polyethylene surface shown above. It seems unlikely that surface roughness will play an important role in any distinctions between the surfaces. The quantified roughness values for the above surfaces are now shown in Table 3.

Table 3: The R_a (average roughness), R_{ms} (root mean square roughness) and R_z (average peak-to-valley height) values for the polyethylene petri dish and the steel disc.

	Surface Material		
	Polyethylene	**Steel Disc**	**Glass ()**
R_a	0.256µm	0.210µm	
R_{rms}	0.315µm	0.272µm	
R_z	0.823µm	0.740µm	

Although roughness is often considered to be the most significant surface factor in biofilm attachment and development (Quirynen and Bollen 1995), this is considered to be dependent on the size of the surface features, concerning whether or not they are large enough to either provide shelter for bacteria or disturb the external fluid flow patterns. Neither surface analysed above exhibit enough of a prominent profile to have an impact on bacterial attachment and biofilm development in comparison to each other. Alternatively, surface energy may be more significant for attempting to explain the differences in attachment strength and thickness.

SEM

The scanning electron microscopy images of the steel surfaces are now shown, beginning with the steel disc used in the static-grown biofilm strength and thickness tests.

a)

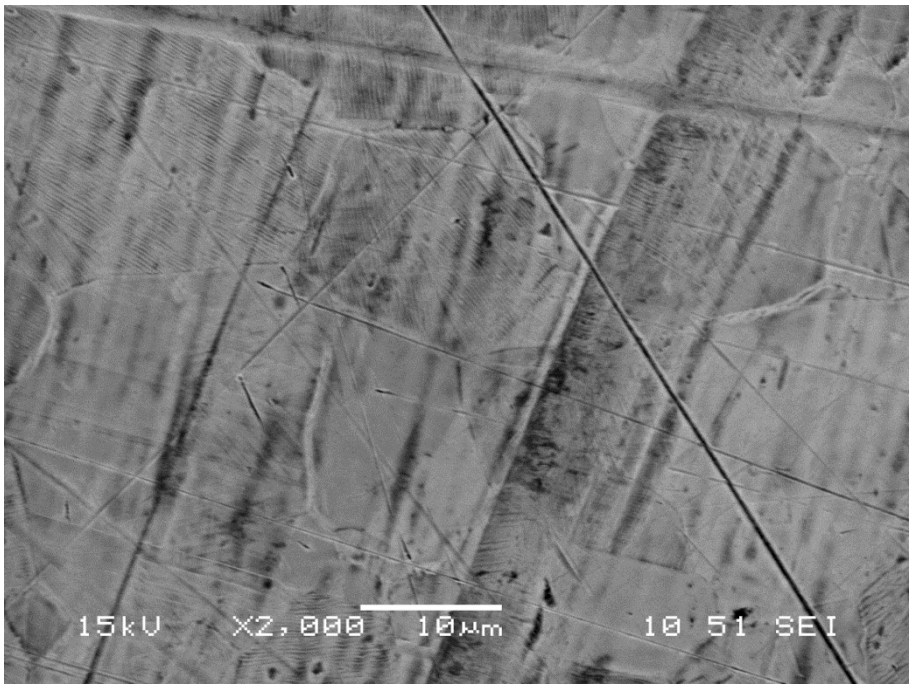

b)

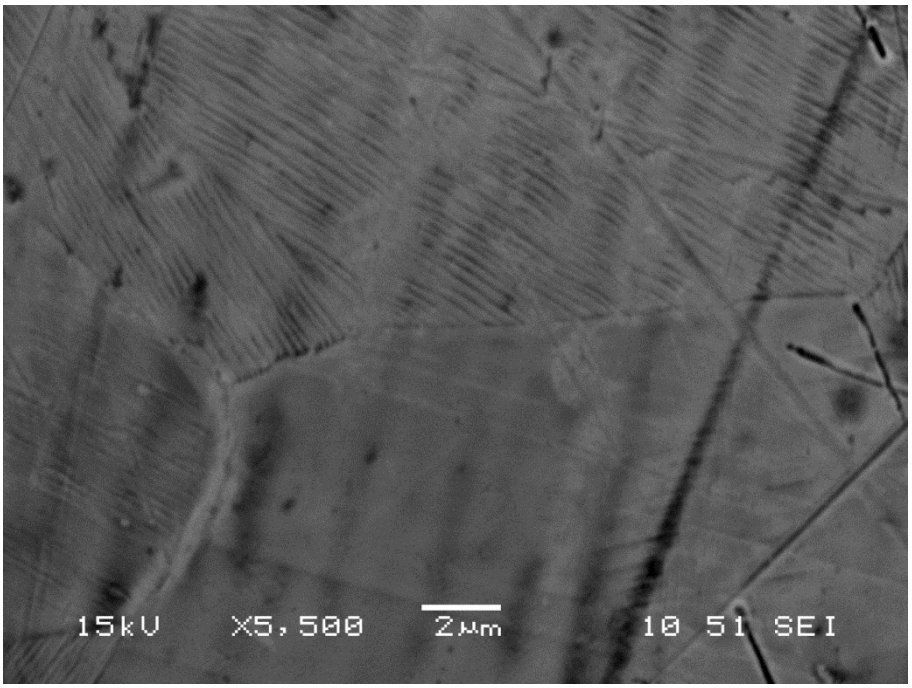

Figure 29: SEM images taken of the steel disc used in the static biofilm studies, with magnifications of the following resolutions; a) – x2000 and b) – x5500. Samples were gold sputter-coated prior to imaging.

The AFM images of the steel discs (Figure 28) suggested that there was little potential for enhancement of biofilm attachment and development as a result of surface roughness, and the SEM

images appear to support this. Any crevices in the surface appear as faint lines in the top image (x50) and no amount of further magnification makes these imperfections appear any more significant. The bottom image (x5500) clearly shows that there are no available crevices for the cells to attach to. Each of the species used is typically 2µm in length and 0.5µm in width, and the 2µm scale on this image is therefore useful for imagining the presence of a cell on the surface. The largest crevices may be able to accommodate a cell long-ways but there is little suggestion that this is viable for a widespread influence on cell attachment.

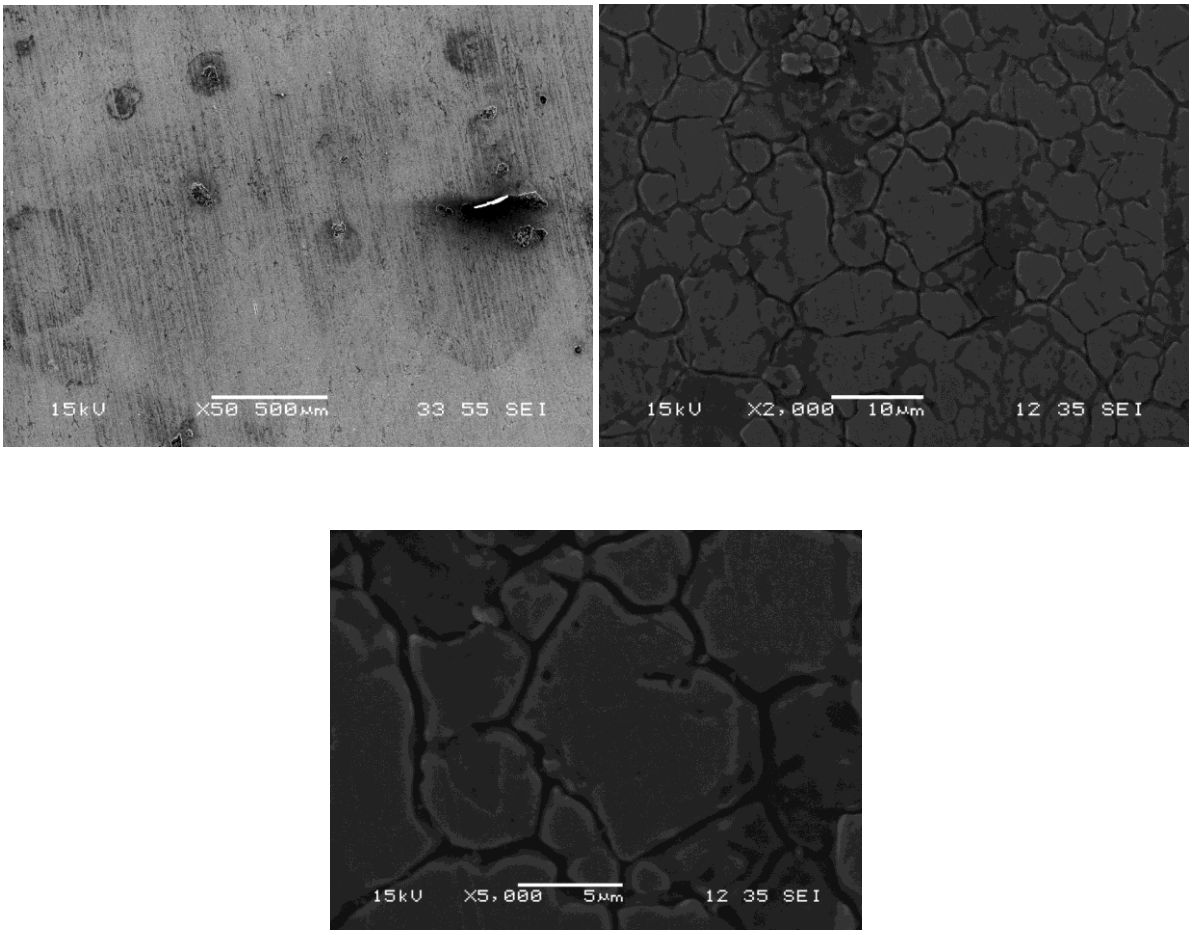

Figure 30: SEM images taken of the steel plate used in the studies of biofilms grown under flow conditions, with magnifications of the following resolutions; top left) x50, top right) x2000, and bottom) x5000. Samples were gold sputter-coated prior to imaging.

In comparison with the steel disc, it is clear that the surface appearance of the steel plate may be more able to influence the attachment of cells for the development of biofilms. Even the top image in this case shows the presence of scar-like features on the surface, which is reasonable to suspect may be due to small craters, the largest of which may be between 50-100 µm based on the scale included. Areas such as these should therefore be able to harbour colonies of cells, and help to propagate their multiplication across the surface in general. The middle and bottom images suggest that the areas which appear smooth in the top image are riddled with crevices themselves. These cracks are only

slightly larger than those witnessed on the disc, but they are considerably more plentiful and may be able to encourage the collaboration of nearby cells to form biofilms. However, the AFM image (Figure 84) suggests that the cracks may not be especially deep (in the order of nanometres) so their efficacy may be highly limited – the 'crater' regions may be a better indicator of any enhanced biofilm development.

5.4.2 Surface Energy

Below are the results for the surface energy analysis using the Zisman plot method to determine critical surface energy. To begin with are a selection of results indicating the difference between the contact angles using water and a sodium chloride solution.

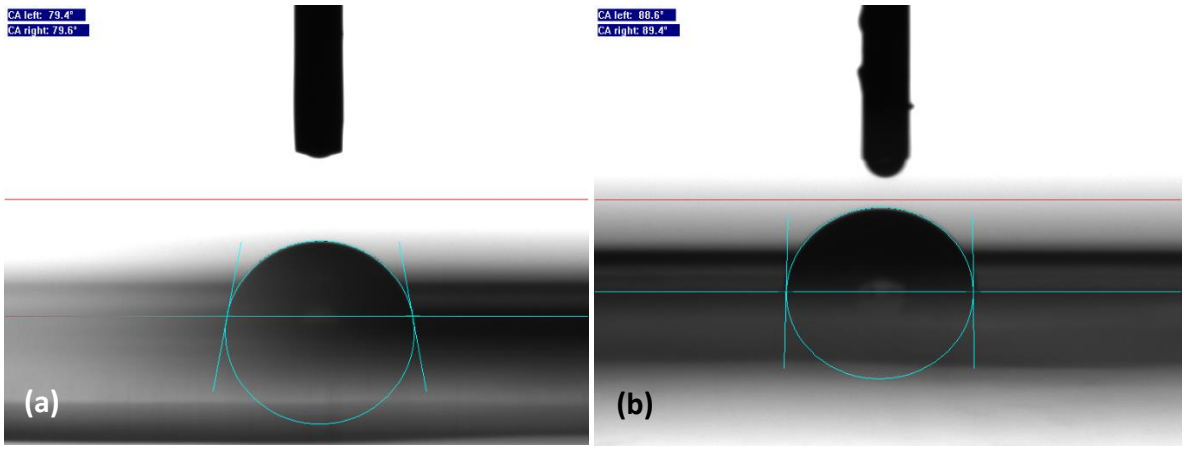

Figure 31: Contact angle measurements on polyethylene in order to determine the critical surface energy. Image a) is taken using water as the fluid, and b) uses a 15% sodium chloride solution. The recorded angles are a) left = 79.4°, right = 79.6°, and b) left = 88.6°, right = 89.4°

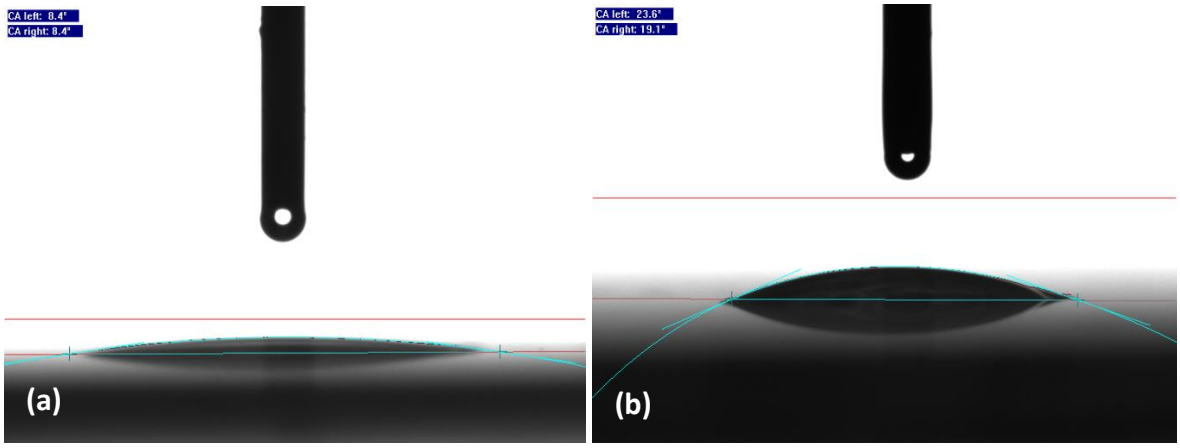

Figure 32: Contact angle measurements on the glass petri dish in order to determine the critical surface energy. Image a) is taken using water as the fluid, and b) uses a 15% sodium chloride solution. The recorded angles are a) left = 8.4°, right = 8.4°, and b) left = 23.6°, right = 19.1°

The transition from water to the ionic NaCl solution has a clear impact on the recorded contact angle in both cases above. This can therefore be used in order to determine to the air-liquid tension (γ_{LV}) of

fluid necessary to completely wet the surface ($\cos\theta = 1$). Zisman plots were plotted from the full set of results taken from each of the five surfaces tested and are shown in Appendix 4. The critical surface areas of each surfaces were then calculated from the above graphs, and are summarised in the table below.

Table 4: The full set of contact angle results and air-liquid surface tensions, and the critical surface energy (CSE) in bold in the bottom row.

		cosθ (θ = mean contact angle)				
Test Liquid	**γ_{LV}**	**Polyethylene**	**Steel Disc**	**Steel Plate**	**Glass Dish**	**Glass Coverslip**
Water	0.0727	0.18 ± 0.026	0.78 ± 0.034	0.75 ± 0.021	0.99 ± 0.030	0.83 ± 0.019
5% NaCl	0.0744	0.12 ± 0.015	0.70 ± 0.025	0.71 ± 0.031	0.98 ± 0.010	0.80 ± 0.019
10% NaCl	0.0762	0.07 ± 0.012	0.68 ± 0.022	0.66 ± 0.018	0.96 ± 0.022	0.67 ± 0.014
15% NaCl	0.0779	0.02 ± 0.020	0.59 ± 0.019	0.62 ± 0.030	0.93 ± 0.017	0.52 ± 0.023
CSE	**-**	**0.047 ± 0.003**	**0.066 ± 0.004**	**0.063 ± 0.009**	**0.072 ± 0.007**	**0.071 ± 0.014**

From Table 4 above, it can be taken that the glass petri dish is the most hydrophilic, whereas the polyethylene petri dish is the most hydrophobic. The full hierarchy is thus, in order of hydrophilicity:

Glass Dish > Glass Coverslip (treated with HMDS) > Steel Disc > Steel Plate > Polyethylene Dish.

From this, is can be seen that the glass surfaces are the most hydrophilic, and therefore should experience the most wetting with the same liquid, followed by steel, with polyethylene being more hydrophobic. In Section 2.5.2, it was mentioned that hydrophobic surfaces are generally believed to encourage greater protein accumulation and promote cell adhesion, and that they are favoured by all bacteria. Other research has suggested that hydrophobicity plays a greater role in biofilm retention than in the additional adhesion. In general, though, hydrophobic surfaces are believed to show more adhesion, although there has been conflicting research on this. The surface energy of the cells themselves play a role (hydrophilic cells generally preferring hydrophilic surfaces), and this will depend partly on their growth environment.

5.5 Biofilm Characterisation – Cation Exchange

5.5.1 Standard Curves

Initially, the standard curves were drawn from the absorbance data produced. The absorbance recorded for the pure water sample is subtracted from each value to show the change due to the addition of the quantity of BSA, and to produce a relationship with the line passing through the origin.

Table 5: The raw absorbance data relative to the quantity of BSA. The value for BSA = 0 (pure water) is subtracted from each value for the protein quantification standard curve.

BSA [mg/mL]	Absorbance [OD600] (raw)	Absorbance [OD600] (net)
0	0.178	0
0.095	0.184	0.006
0.182	0.191	0.013
0.298	0.202	0.024
0.367	0.223	0.045
0.462	0.246	0.068

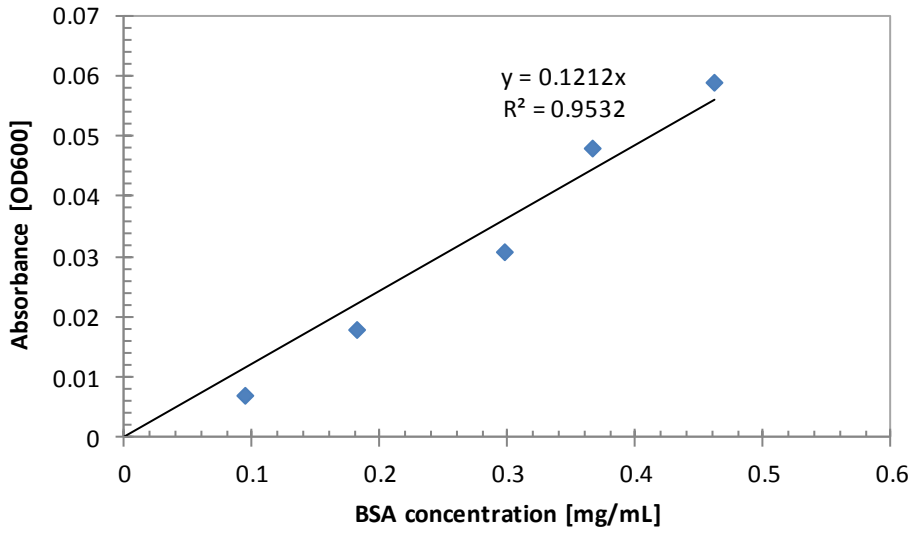

Figure 33: The protein quantification standard curve taken using the absorbance data relative to BSA quantity shown in Table 5.

Table 6: The raw absorbance data relative to the quantity of glucose. The value for glucose = 0 (pure water) is subtracted from each value for the polysaccharide quantification standard curve.

Glucose [mg/mL]	Absorbance [OD600] (raw)	Absorbance [OD600] (net)
0	0.130	0
2	0.426	0.296
5	0.550	0.42
7	0.676	0.546
11	0.875	0.745
16	1.553	1.423

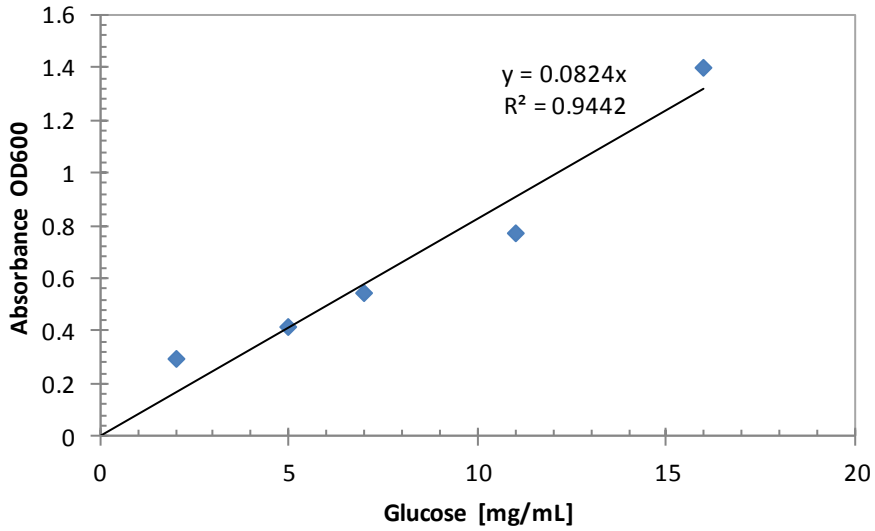

Figure 34: The polysaccharide quantification standard curve taken using the absorbance data relative to glucose quantity shown in Table 6.

The graphs in Figures 33 and 34 both show suitable correlations between absorbance and the quantities of BSA and glucose used, and are therefore suitable for studying the levels of protein and polysaccharides in the EPS as the biofilms age.

5.5.2 Quantification

Below in Figure 35 is the amount of protein found in the EPS of mixed species biofilms grown for 5, 10, 14, 21 and 28 days.

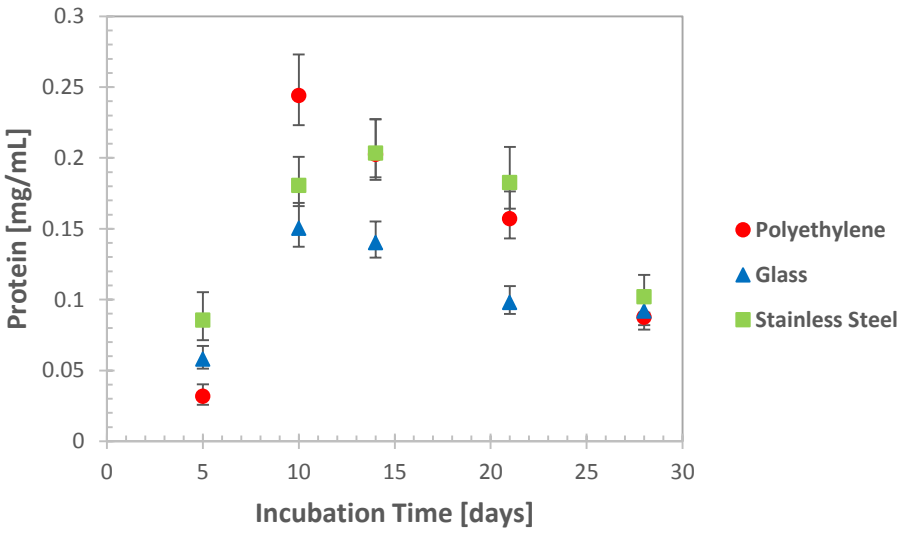

Figure 35: Quantification of the protein found in isolated EPS samples taken from mixed species biofilms of *E. coli* and *B. cepacia*, and assessed using the cation exchange method and the standard curve in Figure 33. Errors were calculated from standard deviation values taken from the results for multiple biofilms grown for the same time period.

Figure 35 shows that the amounts of protein found in the mixed species biofilms reach peaks around 10-14 days, having increased considerably from the quantities in the 5-day biofilms. A steady decline ensues after the peak region, although for all surfaces, the amount of protein found is greater than after 5 days. This decline could signify either a decrease in biofilm density or a degradation of EPS even as the cells continue to reproduce. Ahimou *et al.*, (2007) conducted similar tests, and observed strong peaks in both proteins and polysaccharides after 8 days before much lower values were observed after 12 days – the peak is similar here although there is not the same marked decline, but there were some differences in EPS isolation method. Additionally, they used *Pseudomonas aeruginosa* as their test species.

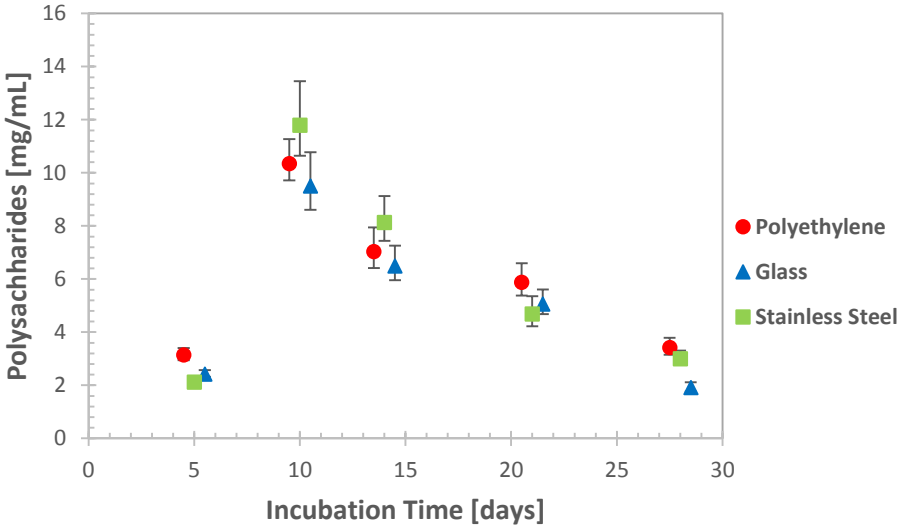

Figure 36: Quantification of the polysaccharide levels found in isolated EPS samples taken from mixed species biofilms of *E. coli* and *B. cepacia*, and assessed using the cation exchange method and the standard curve in Figure 34. Errors were calculated from standard deviation values taken from the results for multiple biofilms grown for the same time period.

The quantity of polysaccharides recorded in Figure 36 shows a much more defined, consistent pattern than the proteins. The trend is broadly similar, in that a peak in polysaccharides is seen after 10 days before the level declines as the biofilms continue to age. The rate of decline is much greater, as the quantities at 5 and 28 days are comparable. The trend in this case bears a closer resemblance to the results presented by Ahimou *et al.*, (2007), although their studies did not extend beyond 12 days. The decrease in concentration of both key components could have the potential to affect strength of attachment and biofilm cohesion if it signifies the breakdown of EPS structure.

5.6 Strength Tests

5.6.1 *Escherichia coli* Biofilms

E. coli - 5 Days

Figure 37 shows an example of optical microscopic images for strength test results obtained from biofilms grown for 5 days on polyethylene. All four images in the figure were taken from biofilm grown on an individual petri dish, moving the FDG nozzle along the surface in separate lines, with the nozzle being moved slightly closer to the surface each time. The values for both the dimensionless clearance distance and the shear stress applied as a result are included in the description below.

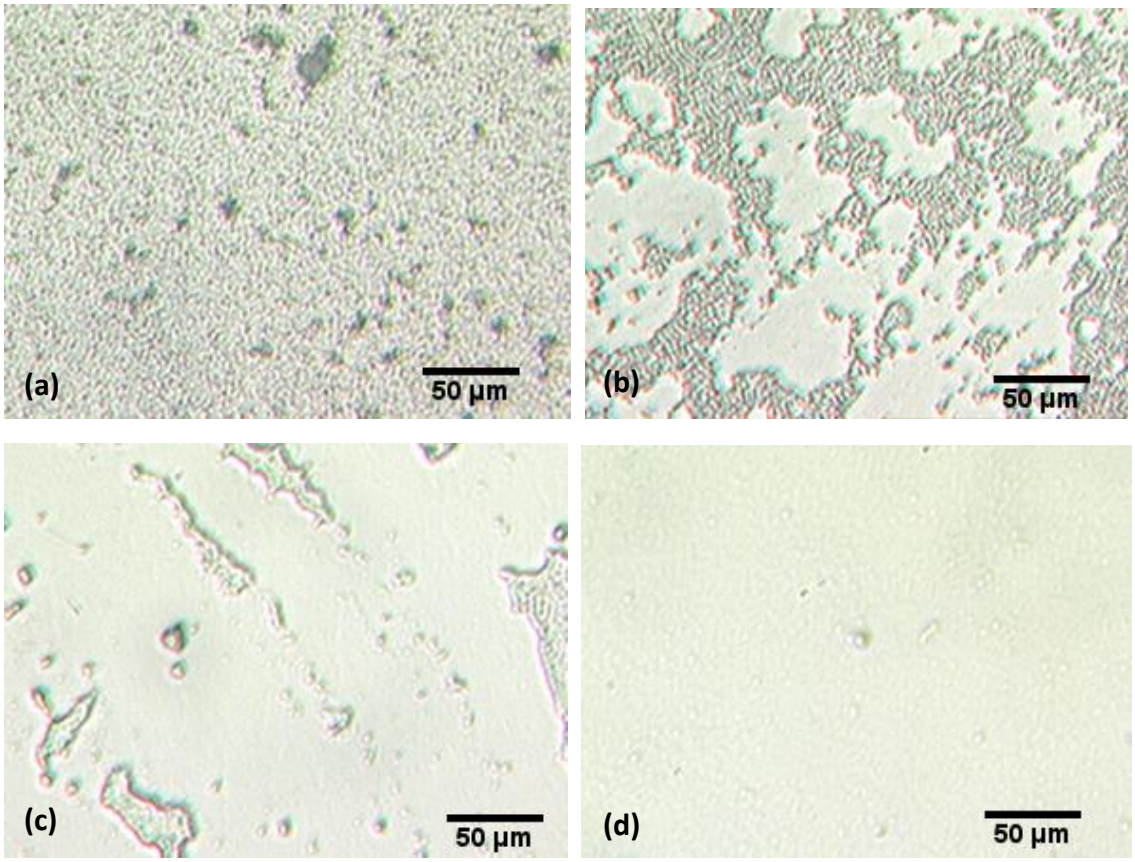

Figure 37: Representative Nikon AZ100 optical microscope images of the polystyrene surface with *E. coli* biofilms incubated for five days: tested under FDG at: (a) $h/d_t = 0.3$, $\tau_{max} = 5 \pm 0.2$ Pa; (b) $h/d_t = 0.25$, $\tau_{max} = 8 \pm 0.4$ Pa; (c) $h/d_t = 0.2$, $\tau_{max} = 13 \pm 0.5$ Pa; (d) $h/d_t = 0.15$, $\tau_{max} = 18 \pm 0.6$ Pa. The percentages of biofilm removed at each stage (calculated using ImageJ) were: (a) 4%; (b) 41%; (c) 88%; (d) 99%.

The set of images above give a clear picture of what is able to be understood via the FDG tests in this section. For this sample, as the figure from part (a) to part (d) and the shear stress applied is increased, it can be clearly seen that the removal of biofilm from the substrate has accelerated accordingly. The application of 5 ± 0.2 Pa does not appear to disturb the proliferation of the biofilm at all. However, following a relatively small step increase to 8 ± 0.4 Pa, approximately half of the surface is clean, suggesting that the culture is being removed in clumps rather than as a more gradual process. Regions

of biofilm are left in place in part (c) after the stress is raised to 13 ± 0.5 Pa, whilst most of the surface has been laid bare. The final image, in which the surface is clean, suggests that a shear stress of between 13 and 18 ± 0.6 Pa is necessary to eliminate the biofilm from polyethylene.

Figure 38 shows an equivalent strength test on a glass surface, taken with a different light setting. The same process was used as for polyethylene, and the biofilms were again grown for 5 days.

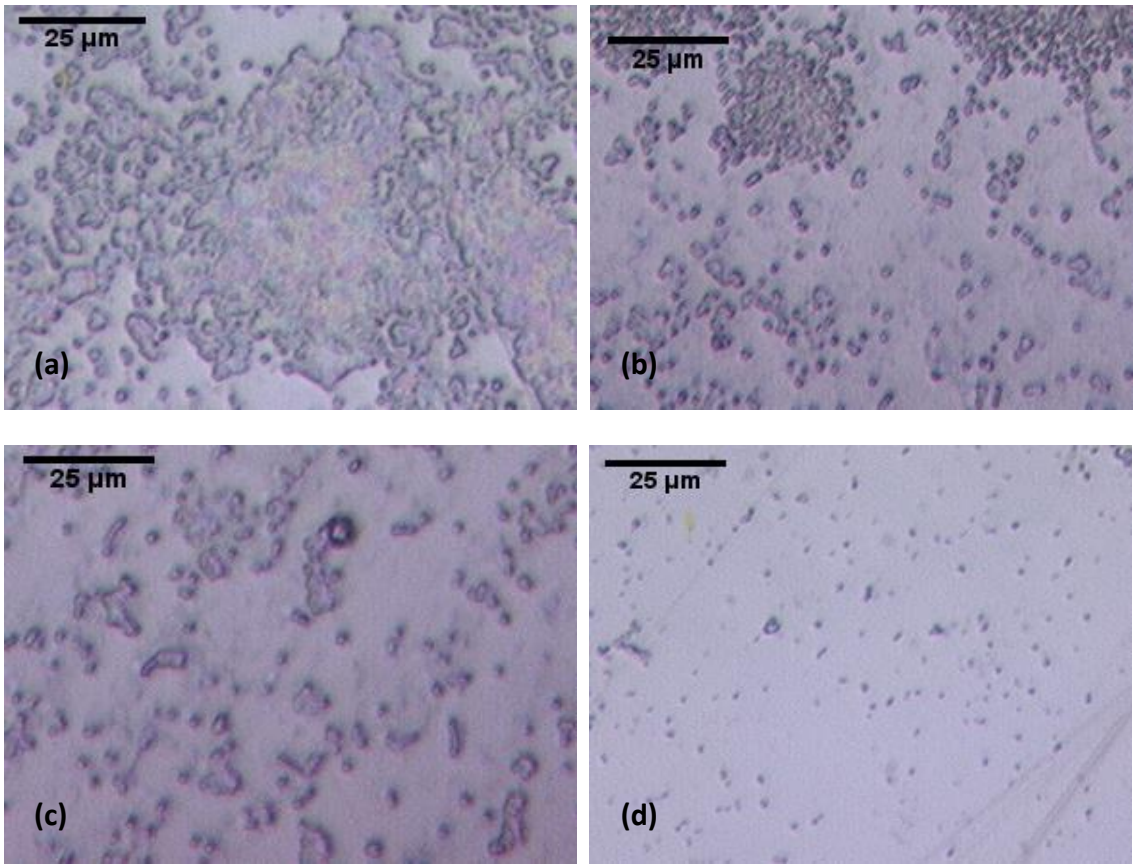

Figure 38: Selected optical microscope images of the glass surface with *E. coli* biofilms incubated for five days: tested under FDG at (a) $h/d_t = 0.23$, $\tau_{max} = 5 \pm 0.2$ Pa; (b) $h/d_t = 0.19$, $\tau_{max} = 7 \pm 0.3$ Pa; (c) $h/d_t = 0.15$, $\tau_{max} = 10 \pm 0.3$ Pa; (d) $h/d_t = 0.11$, $\tau_{max} = 16 \pm 0.4$ Pa. The percentages of biofilm removed at each stage were: (a) 27%; (b) 72%; (c) 84%; (d) 97%.

A similar pattern of removal can be seen for biofilms formed on glass. The most significant difference from the equivalent result for polyethylene in Figure 37 is the readiness with which the biofilm is sheared off. A shear stress of 5 Pa was able to instigate a 27% reduction in surface coverage, a level which had virtually no impact on the polyethylene-based culture. Approximately 72% of the glass surface is cleaned after the application of 7 Pa (Image (b)), whereas for the polyethylene surfaces, approximately twice as much stress is required to remove the same amount. This is a substantial reduction in biofilm present for what is quite a small step increase in stress. Much of the biofilm which remains at this point is able to survive the increase to 10 Pa, suggesting that cells are able to form strong bonds with the glass substrate. After the 16 Pa test, all but a few cells have been removed.

Finally, the set of 5 day *E. coli* biofilms is completed with those grown on stainless steel, shown below in Figure 39.

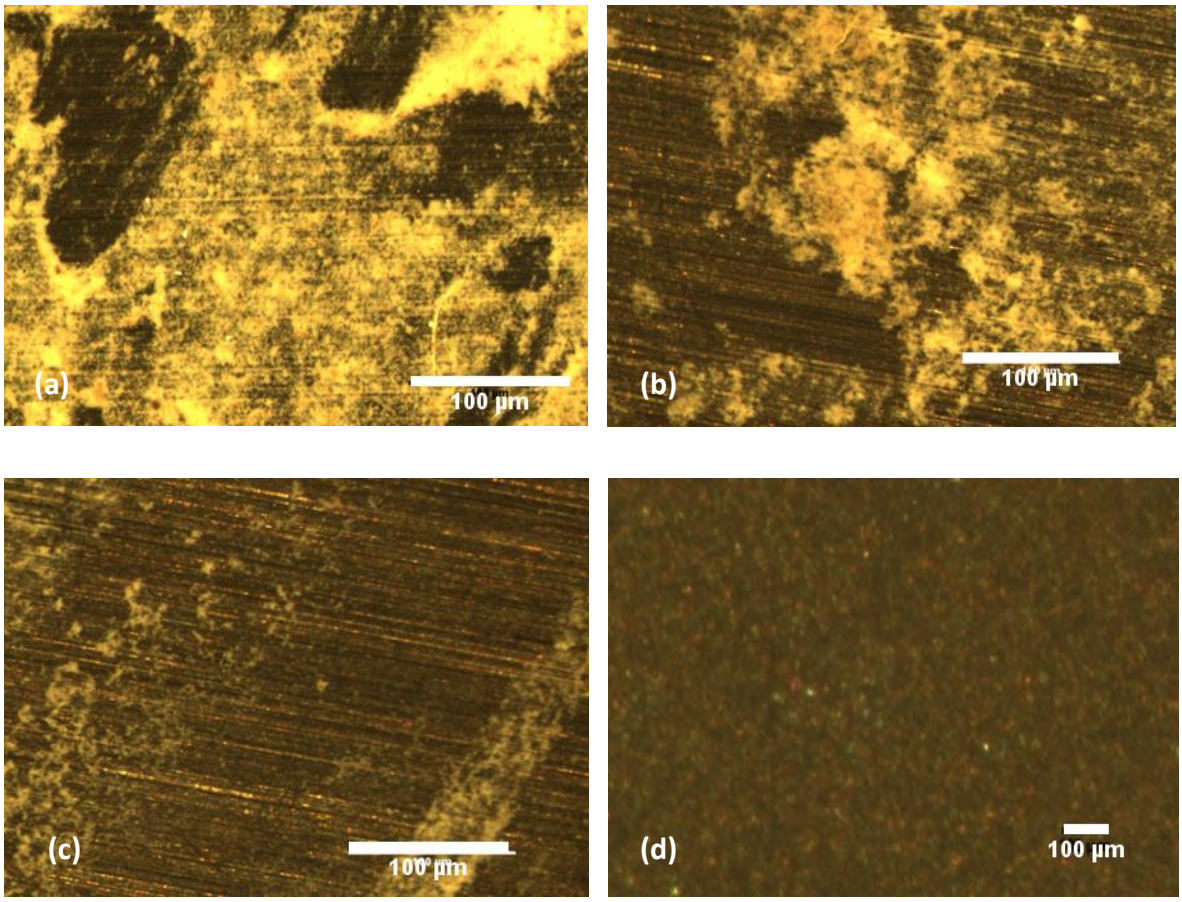

Figure 39: Selected optical microscope images of *E. coli* biofilms on the stainless steel surface incubated for five days: tested under FDG at (a) h/d_t = 0.24, 5 ± 0.1 Pa (b) h/d_t = 0.2, 7 ± 0.3 Pa (c) h/d_t = 0.15, 13 ± 0.4 Pa (d) h/d_t = 0.08, 23 ± 0.5 Pa. The percentages of biofilm removed at each stage were: (a) 26%; (b) 43%; (c) 73%; (d) 100%.

In part (a) of Figure 39, we can see that the extent of removal in this example is 26%, quite similar to the amount of biofilm displaced from the glass surface for the same shear stress (5 ± 0.1 Pa). After an increase to 7 ± 0.3 Pa, there has been a more widespread reduction in surface coverage, although less than from glass for the same stress. The application of 13 ± 0.4 Pa in part c) has removed three quarters of the cells, although there is evidence that regions of biofilm have remained in place. This is comparable to the same stage in the polyethylene-based test in Figure 37, which is suggests a resilience not noticeable on glass, despite the presence of clean regions in part a) which was not evident for polyethylene. This is a timely reminder of the importance of localised measurements when testing for the attachment strength of biofilms, a key feature of fluid dynamic gauging. In part d), the large increase in shear stress has cleaned the surface entirely.

Figure 40 below compiles the removal data for all the strength tests carried out, for each surface, on the *E. coli* biofilms grown for 5 days. Error bars have been added to a selection of the data points in order to account for potential inaccuracies in shear stress and coverage measurements, based on the error ranges inherent in FDG measurements and the biofilm coverage estimation in the ImageJ program.

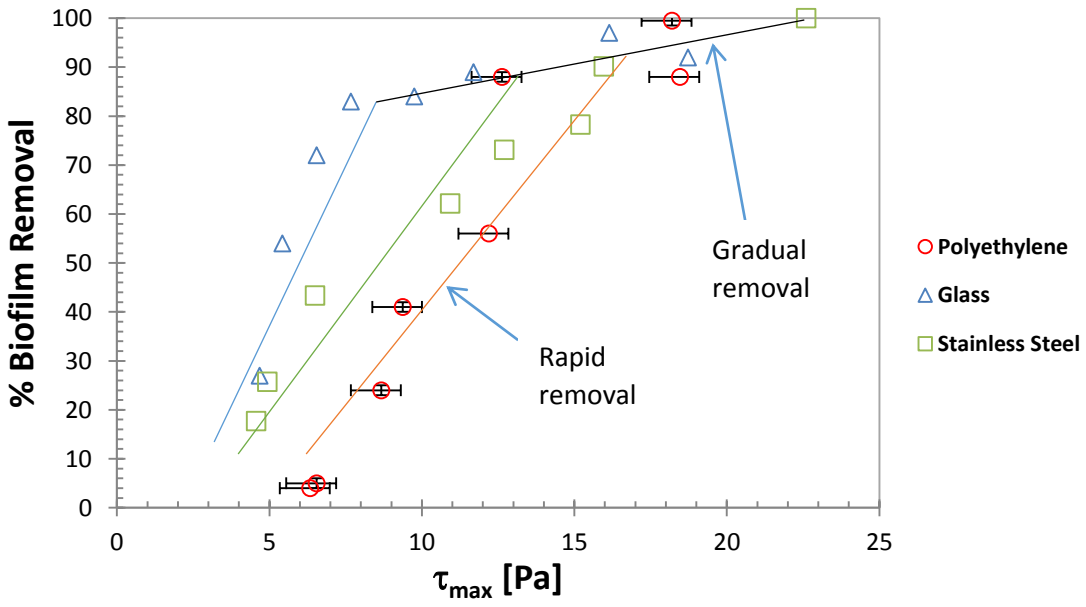

Figure 40: The complete set of strength test results for *Escherichia coli* biofilms grown for a 5-day period on polyethylene, glass and stainless steel. Lines have been added to indicate the presence of two stages of removal, and the distinction between the surfaces in the first stage.

Some trends in removal are clearly observed in Figure 40. There is the tendency of all cases to remove biofilm in a similar pattern. Following the initiation of removal (at a yield point), there tends to be a rapid reduction in surface coverage with an increase of 2 to 3 Pa. The later stages (i.e. the removal of the remaining 20%) are notably slower, and despite the shear stress being already at a high level, large increases in stress can be induced with diminishing removal results. This shows that surface attachment of biofilms can occur in highly variable strengths, with some colonies remaining suggesting two tiers of removal (something which was observed in Figures 37-39 above). Two-stage lines have been added to the graph to show this effect, with the first stage split according to the strength differences between the three surfaces. As is shown, for the first 80% removal there is a strength hierarchy (glass the weakest, polyethylene the strongest), yet this effect is less pronounced when concerning the most strongly attached 20% (the black line). This must be taken into account when designing cleaning protocols.

In comparing the strength of attachment on different surfaces for the 5 day growth period, the clearest result to spot is that the biofilms grown on glass were the weakest. That said, there are still instances

of resistance up to 16 and 19 Pa which indicates that whilst most of the cells attached less strongly to glass, there is still the potential to form well-adhered regions of biofilm. It appears, albeit less clearly, that the polyethylene-based biofilms are stronger after 5 days than those grown on stainless steel. Again, this loses its significance when it comes to the removal of the remaining 20% of cells. So whilst there looks to be variations in adhesive strength according to the substrate material, *E. coli* appears able to form areas of strong attachment to all the surfaces.

E. coli - 10 Days

Subsequently, *E. coli* biofilms were grown for 10 days on the same set of surfaces with the aim of assessing the impact of the extended incubation period on biofilm adhesive strength. Below in Figure 41 the complete strength test data is shown.

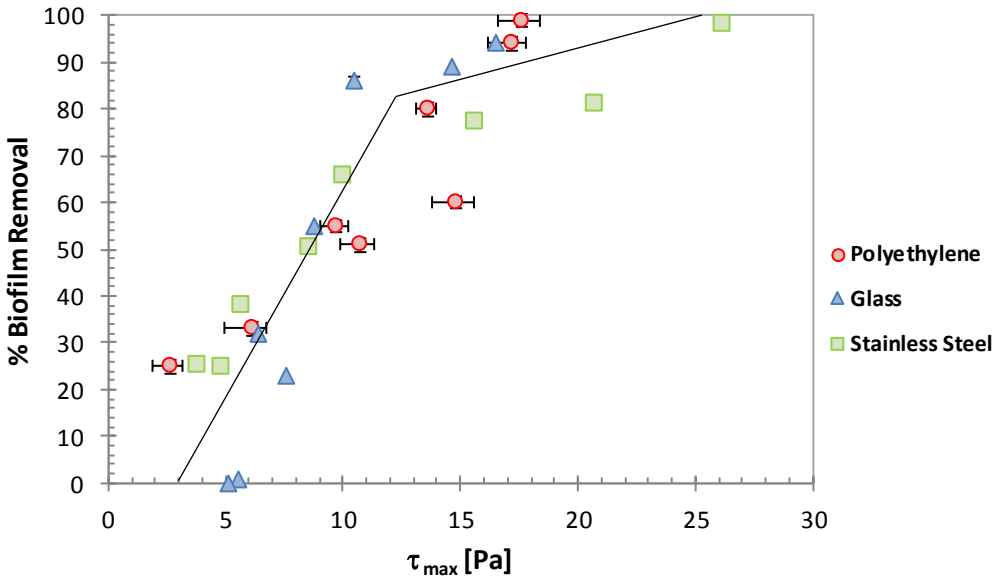

Figure 41: The complete set of strength test results for *Escherichia coli* biofilms grown for a 10 day period on polyethylene, glass and stainless steel.

In Figure 41, it can be seen that at the 10 day stage, there is relatively little difference between the surface attachment strengths of each surface, in contrast to the three coloured trend lines for 5 days in Figure 40. It appears to be most difficult to remove the first sections of biofilm from glass where surfaces remain fully fouled at 5-6 Pa, yet as the shear stress is increased further (to approximately 10 Pa) this distinction is no longer noticeable. If anything, the biofilms grown on polyethylene now appear to be the strongest. Compared with the graph for 5 day biofilms (Figure 40), there is a considerably more gradual removal taking place here – the removal of 50% of surface coverage typically occurs between 3 and 10 Pa as opposed to between 4 and 8 Pa in the previous section. This could be evidence of the biofilms becoming thicker, as this would require the removal of more cells to expose the bare surface.

E. coli - 14 Days

E. coli biofilms were then grown for 14 days on the same set of surfaces in order to assess the impact of the additional four days on biofilm adhesive strength. Below in Figure 42 the complete strength test data is shown.

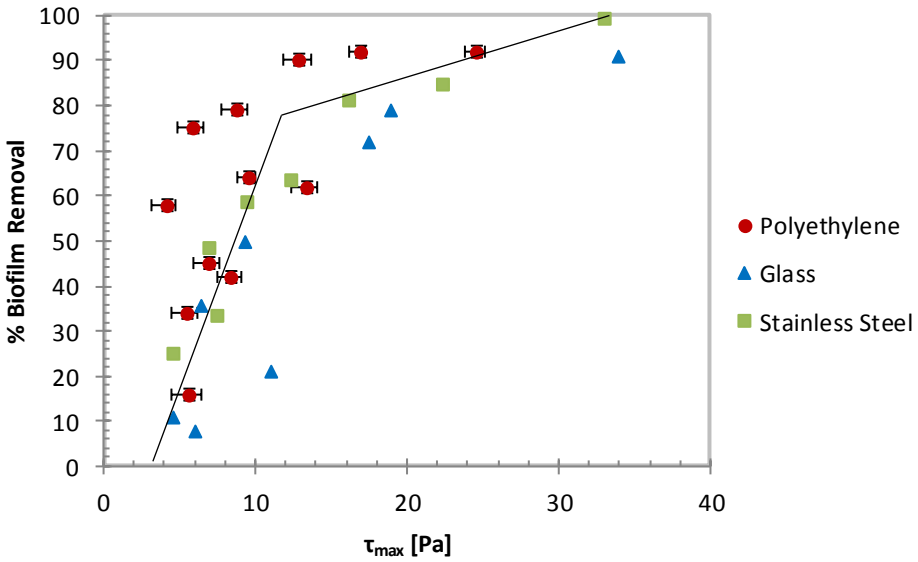

Figure 42: The complete set of strength test results for *Escherichia coli* biofilms grown for a 14 day period on polyethylene, glass and stainless steel.

The compiled results for 14 days in Figure 42 indicate the relative weakness of the attachment to polyethylene of these biofilms. Approximately 75% removal can be seen in the region of 8-12 Pa, yet on the surfaces shear stresses of 16 Pa appear to be necessary. The stage at which removal is initiated does not appear to have altered much, and the same seems to be true for the rate of removal as the stress increases. There is however evidence that biofilms are capable of remaining attached to all three surfaces at stresses greater than 25 Pa, and this persistence of smaller regions of biofilm accounts for the greater stresses required in order to completely clean the surface.

E. coli - 21 Days

Subsequently, *E. coli* biofilms were grown for 21 days on the same set of surfaces with the aim of checking whether or not the adhesive strength continues to increase.

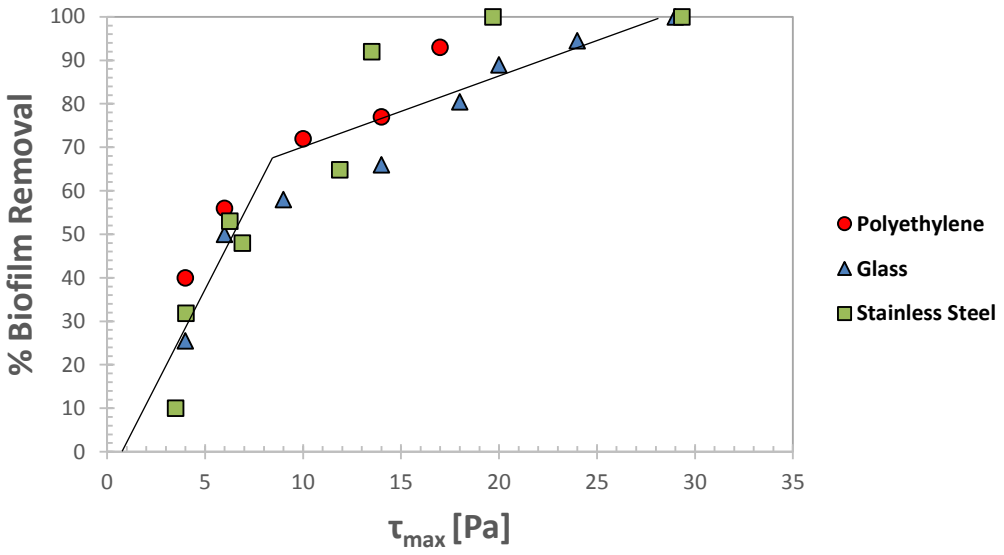

Figure 43: The complete set of strength test results for *Escherichia coli* biofilms grown for a 21 day period on polyethylene, glass and stainless steel.

The above graph suggest that *E. coli* biofilms attach most strongly to glass after 21 days of incubation. A tenth of the biofilm grown on glass is able to survive over 20 Pa of shear stress, whereas those grown on the other surfaces are all but eliminated by this stage. The removal of the first 40% of cells can be seen to occur in a short space of time irrespective of the surface material, before a more gradual, almost linear reduction in coverage until the surface is clean. The steel and polyethylene are clean after a 20 Pa shear stress, and the glass by 29 Pa, which are all lower than the equivalent values for the 14-day biofilms. This appears to be conclusive evidence that they have passed beyond a point where the attachment is becoming weaker.

E. coli - 28 Days

Finally, *E. coli* biofilms were grown for 28 days on the same set of surfaces with the aim of assessing whether there would be any further impact from extending the incubation period further.

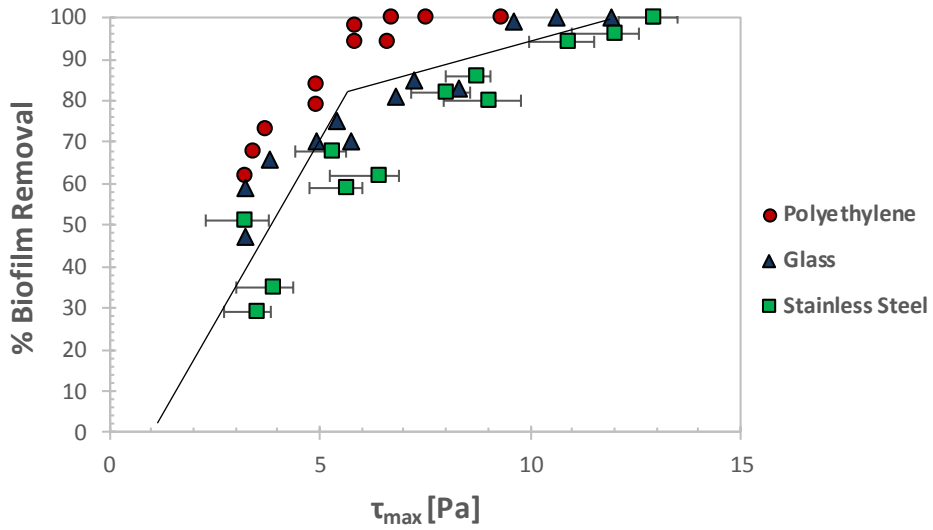

Figure 44: The complete set of strength test results for *Escherichia coli* biofilms grown for a 28 day period on polyethylene, glass and stainless steel.

There is a substantial weakening of attachment as incubation is extended up to 28 days. After 21 days, at least 20 Pa was necessary to clean any of the surfaces, but after 28 days the strongest remaining biofilms were those grown on stainless steel which required 13 Pa to remove. On polyethylene, the weakest of the three, as little as 6-7 Pa was sufficient, a contrast to the earlier stages where a relatively strong adhesion was observed and 50% removal was harder than for the other surfaces – those regions of biofilm which attached readily may have reached a natural detachment phase sooner. There is a clear hierarchy of strength at this point, with results for the three surfaces quite distinct from one another. What is also notable is how little evidence of extensive strong attachment there is – even on stainless steel, as much as 50% of the surface was cleaned using a stress of just over 3 Pa. After 21 days, however, the weakest (polyethylene) only saw a 40% reduction in coverage at this stage. This graph suggests that a point in ageing has been reached where a coverage of strongly-attached biofilm is simply no longer possible.

Summary

Having collected results for the full set of strength tests for *E. coli* biofilms, it is beneficial to look at a compiled display of results in order to achieve the best overall method of studying trends according to the effects of both the incubation periods and the substrate material. Figure 45 is an interpolation showing the estimated shear stress and mean pipe flow velocity (calculated using Eq. (2)) required to remove 50 % and 95% of the biofilm surface coverage plotted against the incubation times. The interpolation is based on the use of logarithmic trendlines to fit the curves from the graphs in Figures 40 to 44. In all cases, logarithmic curves provided the most accurate fit to the data points. The error bars included here are representative of the accuracy of the trend line fit for each case, calculating the standard error in shear stress required for 50% or 95% removal.

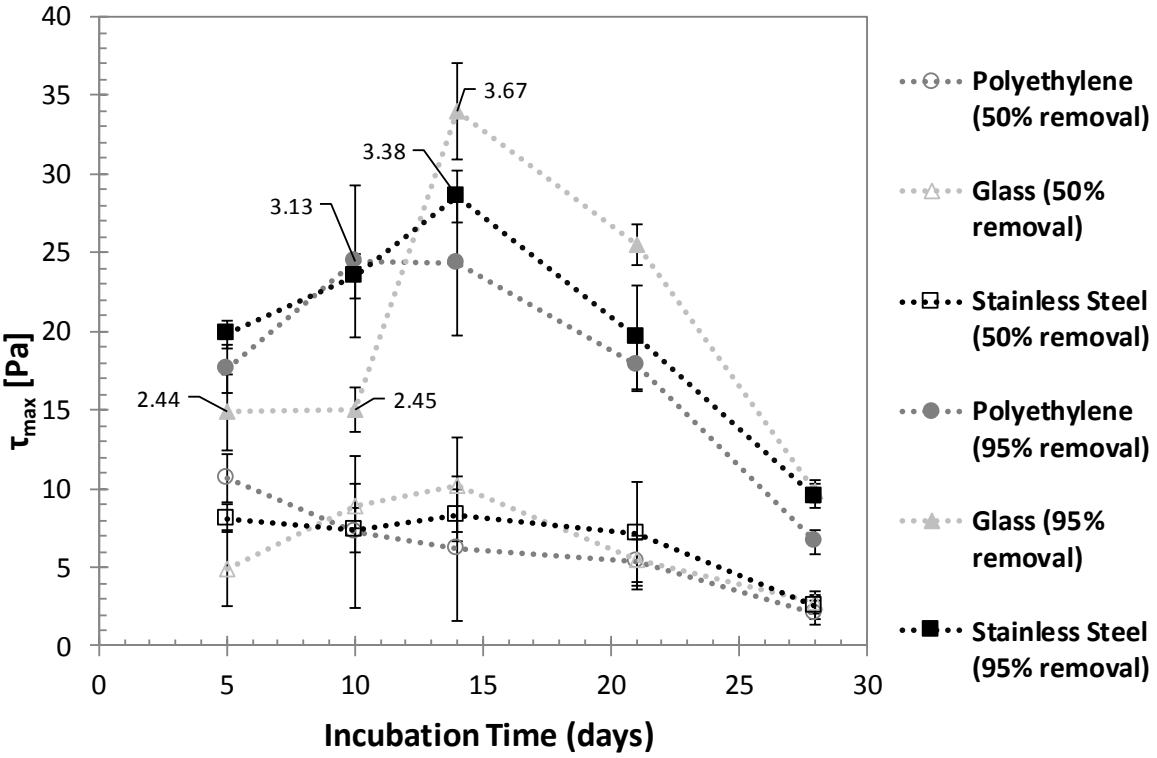

Figure 45: The overall strength test results for *Escherichia coli* biofilms grown on all three test surfaces shown, in terms of the shear stress required in order to remove 50% and 95% of the surface coverage. Values for the equivalent pipe flow velocity (using equation 23) are shown for selected data points (ms^{-1}).

Looking at the points for 50% removal, there appears to be little difference between most of the values for the three surfaces. The values are relatively wide apart after 5 days, although taking into account how they appear to switch places after 10 and 14 days, this is likely to be due to wider fluctuation in values rather than a removal trend. The only general pattern to be observed is a decrease in strength which can be seen for all three surfaces, suggesting that large coverage proportions of older biofilms can be removed with relative ease.

Based on the figures for 95% surface removal, after 10 days' incubation the biofilms grown on polyethylene and stainless steel were stronger than those grown on glass (24 Pa shear stress required to eliminate polyethylene based biofilms, 14 Pa to remove from glass). This stage proved to be the peak strength for the polyethylene biofilms, unlike on the other surfaces where the strength continued to increase up to 14 days. After having previously been the weakest, the attachment to the glass dishes became considerably stronger by this stage (33 Pa required), whilst the polyethylene samples are more readily removed with a stress of 22 Pa. This would imply a stronger, or more consistent, initial attachment of *E. coli* biofilms to polyethylene and an earlier maturation. It is possible that, once initiated, the glass-based biofilms become more firmly established despite experiencing difficulties in

the early stages. A decline in adhesive strength was noticeable on all three surfaces after growth periods of 21 and 28 days despite the daily provision of fresh medium, suggesting the weakening of EPS structures (due to degradation of components). Additionally, the variations between the surfaces decreased as the biofilms aged, which is logical given that the surface-attached layer is already in place and continued development is dependent on cell multiplication rather than surface adhesion. These results suggest that cleaning *E. coli* biofilms from glass surfaces should be relatively more straight-forward, provided it is carried out regularly before the biofilms become established.

For steel and polyethylene surfaces, however, initial attachment is more rapid and therefore more energy would be required to clean them where sterility is an important factor. The strong early attachment of bacteria to polyethylene is followed by an earlier maturation and hence a more rapid weakening of bonds, and dispersion. Waiting for the biofilms to reach their weakest point at 28 days is unlikely to ever be an advisable course of action due to the risk of contamination and potential further infiltration of pathogens. Ideally there should be a balance between cleaning regularly enough to avoid health risks, and avoiding excessive cleaning with an eye on reducing water and energy usage.

5.6.2 *Burkholderia cepacia* Biofilms

The same procedure was then conducted in order to test the strength of attachment of *Burkholderia cepacia* biofilms to the same three surfaces, after 5, 10, 14, 21 and 28 days of incubation.

B. cepacia – 5 Days

As before, the first set of biofilms were incubated for 5 days. The results are shown below, with the first set taken for the polyethylene substrate.

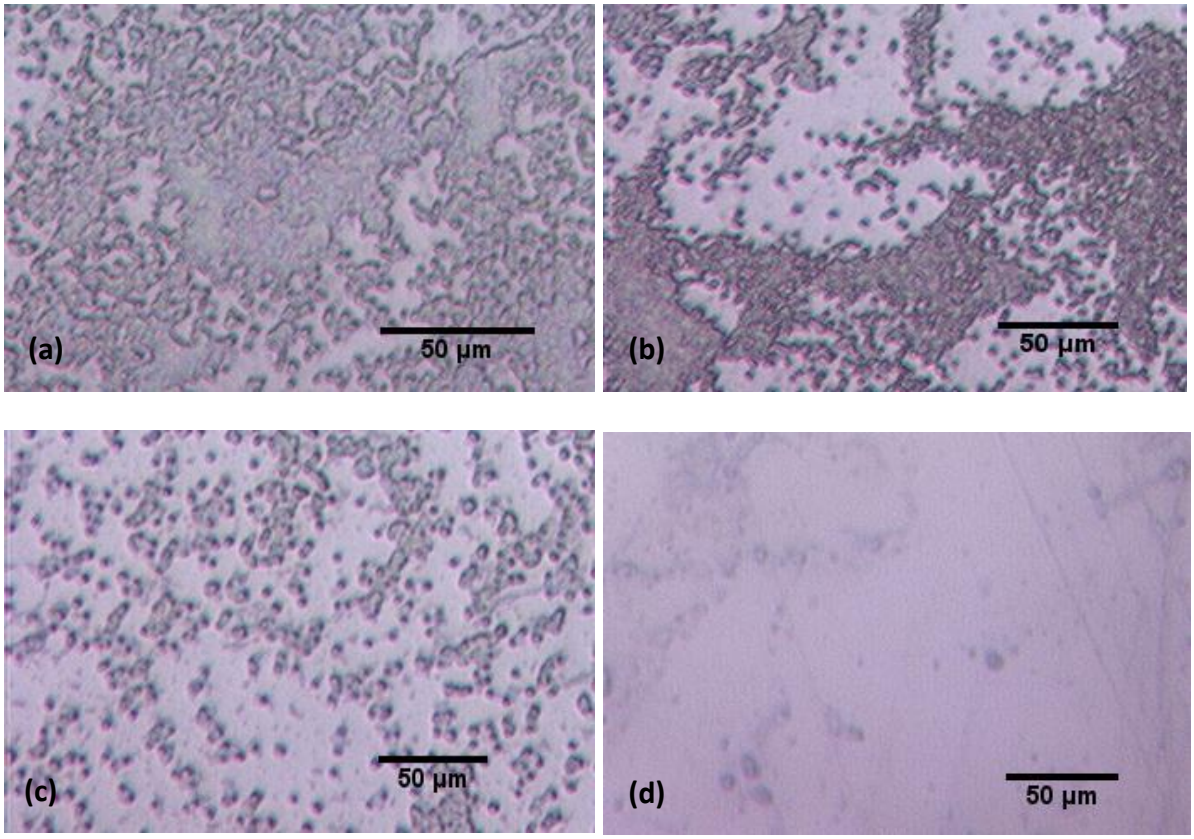

Figure 46: Selected optical microscope images of *B. cepacia* biofilms grown on polyethylene for 5 days: tested under FDG at (a) h/d_t = 0.26, 4 ± 0.4 Pa (b) h/d_t = 0.21, 7 ± 0.1 Pa (c) h/d_t = 0.16, 11 ± 0.2 Pa (d) h/d_t = 0.11, 15 ± 0.1 Pa. The percentages of biofilm removed at each stage were: (a) 38%; (b) 60%; (c) 77%; (d) 99%.

The removal pattern shown in Figure 46 is similar to that observed for the *E. coli* biofilms. In image b) the removal of regions can be observed, after which the remaining regions are depleted to leave isolated clusters of cells before the surface is entirely clean. In comparison to the *E. coli* biofilms grown for 5 days on polyethylene, these results suggest that the attachment is weaker in this case. The surface has been cleaned by a shear stress of 15 ± 0.1 Pa, compared to 18 ± 0.6 Pa for *E. coli*. This is even more noticeable in the early stages – 8 ± 0.4 Pa was required to remove 41% of the *E. coli* surface coverage, whereas 38% of *B. cepacia* could be removed using only 4 ± 0.4 Pa.

Now, in Figure 47 the results for glass are shown.

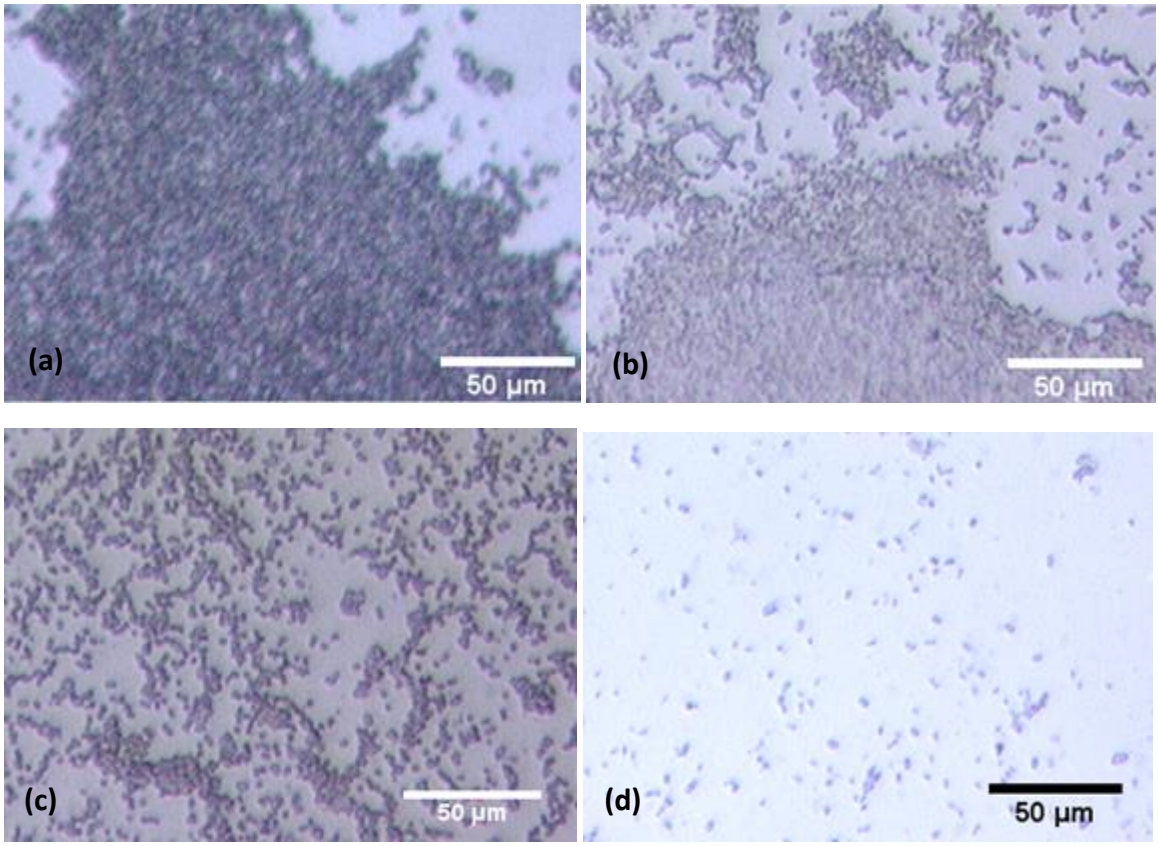

Figure 47: Selected optical microscope images of *B. cepacia* biofilms grown on glass for 5 days: tested under FDG at (a) h/d_t = 0.26, 4 ± 0.4 Pa (b) h/d_t = 0.22, 6 ± 0.3 Pa (c) h/d_t = 0.17, 9 ± 0.4 Pa (d) h/d_t = 0.12, 14 ± 0.4 Pa. The percentages of biofilm removed at each stage were: (a) 25%; (b) 42%; (c) 74%; (d) 97%.

The results for glass-based biofilms show similarities to those for polyethylene. The stages of removal are the same, and the stress required to clean the surface (up to 97% in this case) is similar. The only noticeable distinction is the relative resistance to removal in the first stage – 25% of cells removed rather than 38% under a stress of 4 ± 0.4 Pa. The same is true when comparing the results to those for *E. coli* grown on glass. In that case, 7 ± 0.3 Pa was able to remove up to 72% of the biofilm, compared with only 42% removal using 6 Pa shear stress here. There are however closer similarities for image d) – 14 ± 0.4 Pa (*B. cepacia*) and 16 ± 0.4 Pa (*E. coli*) required to remove 97% of coverage.

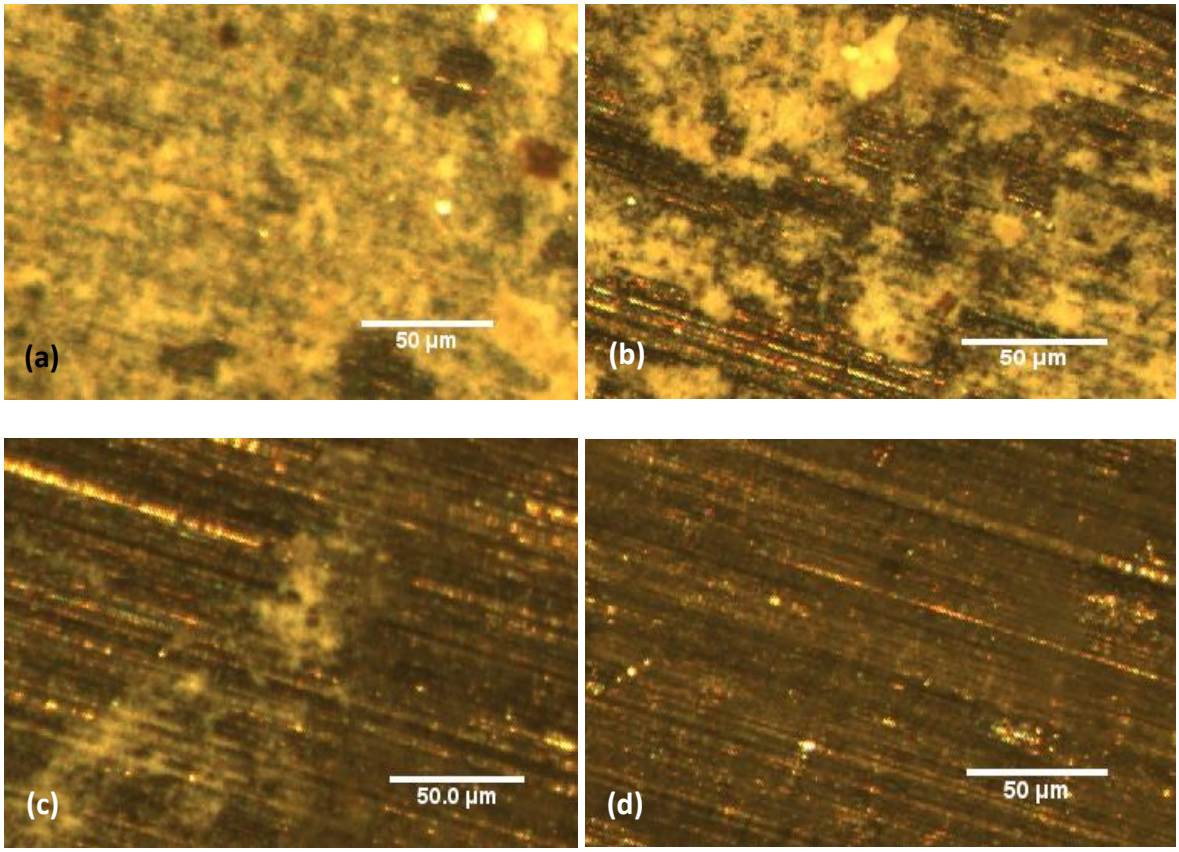

Figure 48: Selected optical microscope images of *B. cepacia* biofilms grown on stainless steel for 5 days: tested under FDG at (a) h/d_t = 0.25, 4 ± 0.2 Pa (b) h/d_t = 0.2, 7 ± 0.3 Pa (c) h/d_t = 0.15, 12 ± 0.3 Pa (d) h/d_t = 0.1, 16 ± 0.2 Pa. The percentages of biofilm removed at each stage were: (a) 14%; (b) 53%; (c) 91%; (d) 100%.

The stress required to eliminate the biofilm from the stainless steel surface is again similar to those for polyethylene and glass. This range of 14 to 16 Pa for complete removal contrasts with the greater variance seen for the *E. coli* strength tests. As for the removal images in the figure and the associated percentage removals, there is similarly little difference in strength between steel and the other two surfaces.

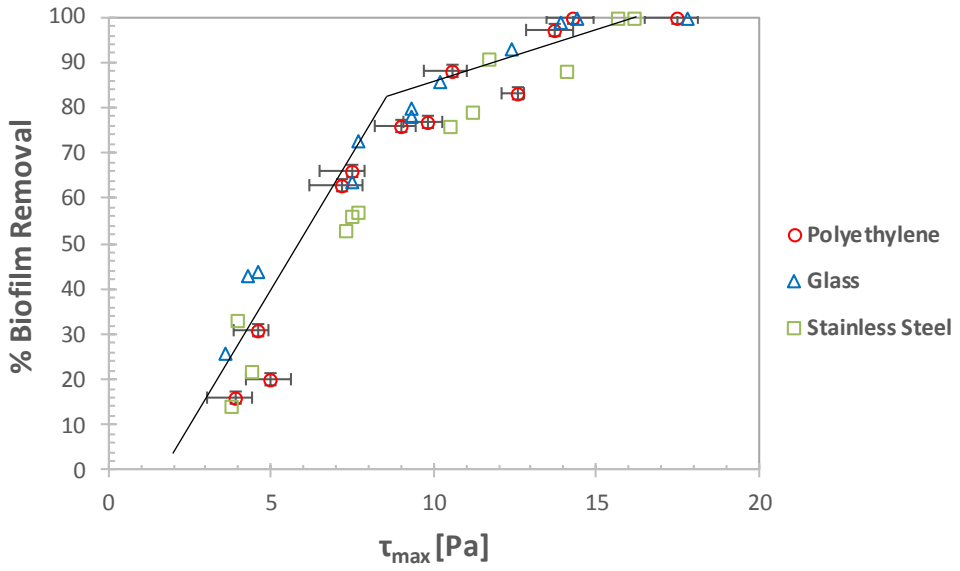

Figure 49: The complete set of strength test results for *Burkholderia cepacia* biofilms grown for 5 days on polyethylene, glass and stainless steel.

Figure 49 shows again how the removal behaviour of *B. cepacia* biofilms was very similar across all the surfaces after 5 days' incubation. The results for polyethylene and glass are in particular very close together, with the suggestion that attachment may have been slightly stronger to stainless steel, noticeably in the range between 10 and 15 Pa, during which approximately 75-85% of coverage was removed from steel compared to 85-95% from polyethylene and glass. The biofilms do appear to be weaker than their *E. coli* counterparts. This can be seen in the initial point of removal at 3-4 Pa as opposed to 5 Pa in Figure 40, and also in the region in which the surface is cleaned (14-16 Pa rather than 18 Pa and beyond).

B. cepacia – 10 Days

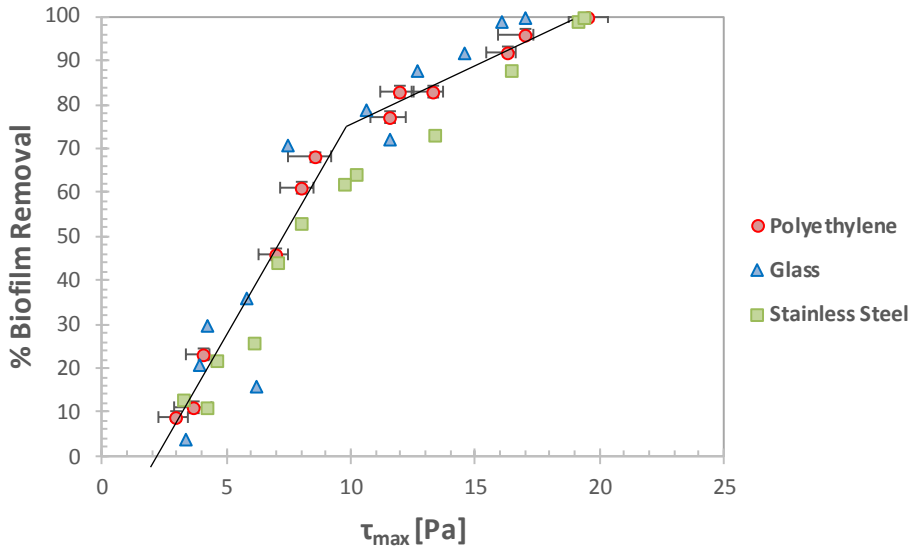

Figure 50: The complete set of strength test results for *Burkholderia cepacia* biofilms grown for 10 days on polyethylene, glass and stainless steel.

Figure 50 shows that the removal behaviour for all three surfaces is again very similar after 10 days' incubation, as was the case for 5 days. It does however indicate, as suggested earlier, that the biofilms on stainless steel were more strongly attached. This distinction becomes noticeable in the range above 50% removal – up to this point there is little difference between the results for the three surfaces. In order to reduce the surface coverage by 75%, a shear stress of 10-12 Pa is sufficient for polyethylene and glass surfaces whereas 14 Pa is required for stainless steel. If approximately half of the attached cells display greater resilience on steel, then this should be sufficient to suggest that the potential for stronger attachment is greater – the weakest-attached regions are equally easy to remove regardless of the surface. A general increase in strength from the results for 5 days is noticeable – complete removal now requires 16-20 Pa as opposed to 14-16 Pa.

B. cepacia – 14 Days

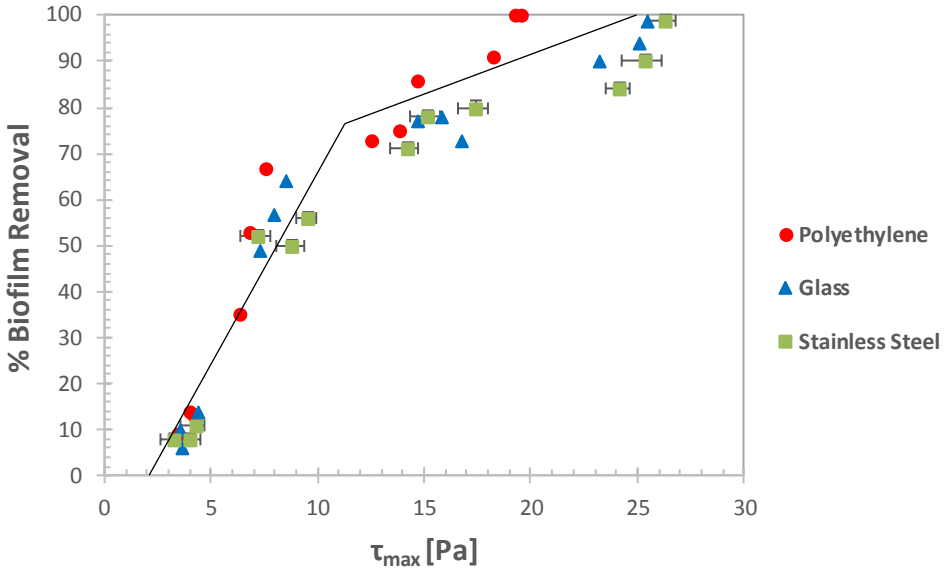

Figure 51: The complete set of strength test results for *Burkholderia cepacia* biofilms grown for 14 days on polyethylene, glass and stainless steel.

The main distinction in the graph in Figure 51 from the respective results from the 5 and 10 day experiments is the greater dispersion of data points. The polyethylene results are noticeably weaker than the others, with the data curve following a similar pattern to the previous incubation periods. For glass and stainless steel, however, the rate of removal slows considerably once the first 70-75% has been eliminated. This is the first major sign of an increase in adhesive strength, and interestingly it has occurred at the same stage as it had for *E. coli*. If this is to be the peak biofilm age for strength, as it was for *E. coli*, then it can be said that the attachment of *B. cepacia* is weaker, as all the surfaces can be cleaned with a shear stress of 27 Pa whereas 34 Pa was required for the same result for *E coli*.

B. cepacia – 21 Days

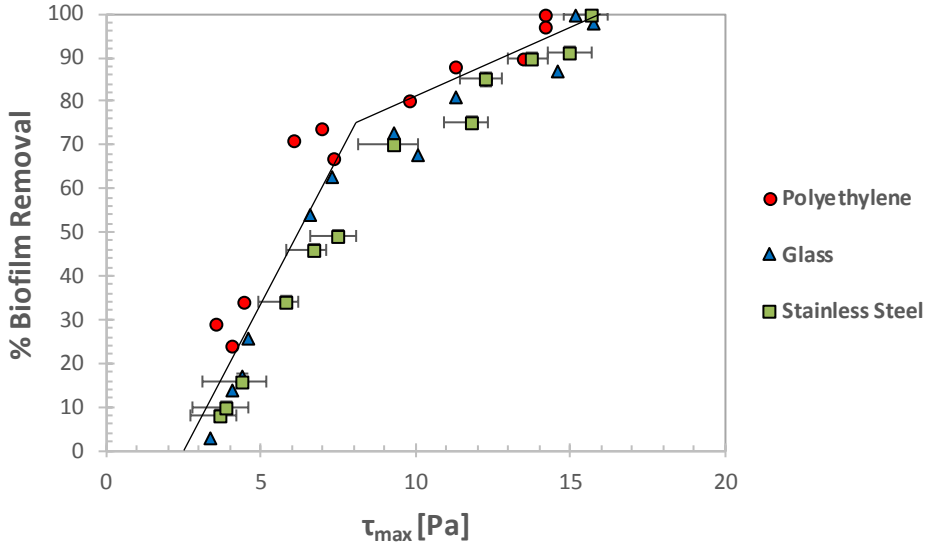

Figure 52: The complete set of strength test results for *Burkholderia cepacia* biofilms grown for 21 days on polyethylene, glass and stainless steel.

After the more dispersed spread of data points in the previous section for 14-day biofilms, the results here have returned to the more uniform curves seen in the earlier stages. The graph suggests that the biofilms on polyethylene are slightly easier to remove than those grown on the other surfaces. A shear stress of 7 Pa was able to remove over 70% of cells from polyethylene, compared with approximately 50% from steel. The total yield strengths of 14-16 Pa are considerably lower than the 19-26 Pa range for those grown for 14 days. The extent of the loss in adhesive strength is steep, as they are also weaker than the 10-day old biofilms. Again, they are weaker than the equivalent *E. coli* biofilms, which has consistently been the case for all the *B. cepacia* results so far.

B. cepacia – 28 Days

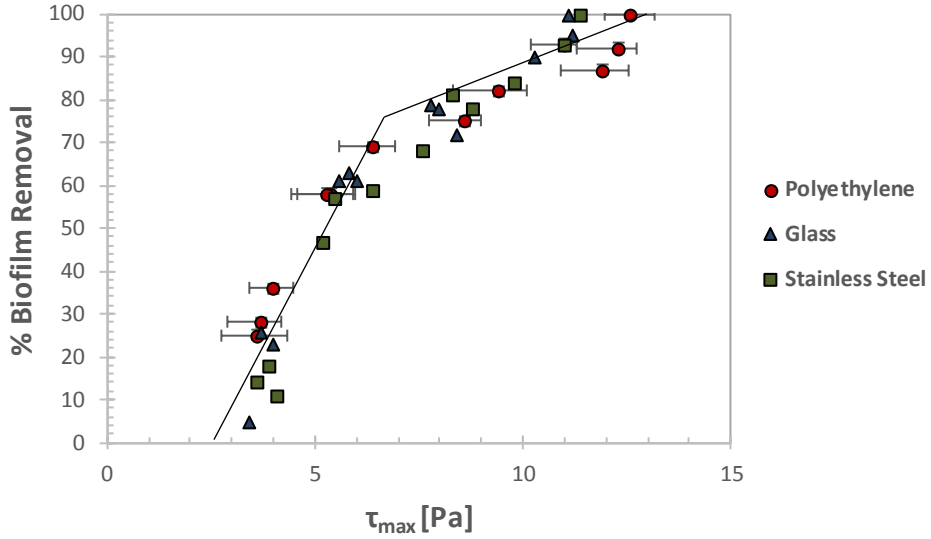

Figure 53: The complete set of strength test results for *Burkholderia cepacia* biofilms grown for 28 days on polyethylene, glass and stainless steel.

In the summary graph for 28 days (Figure 53), there is little difference between the three surfaces in terms of removal behaviour. The one exception to this is the relative difficulty in removing the final 20% of the biofilms on polyethylene, which is intriguing in itself as this is the first time in which the polyethylene-based cells have been the most difficult to remove. These biofilms are the weakest of the section, requiring no more than 12 Pa to clean all the surfaces, and approximately 5 Pa to reduce the surface coverage by 50%. This has the effect of continuing the downward trend in strength started by the 21-day biofilms and echoes that seen for *E. coli*.

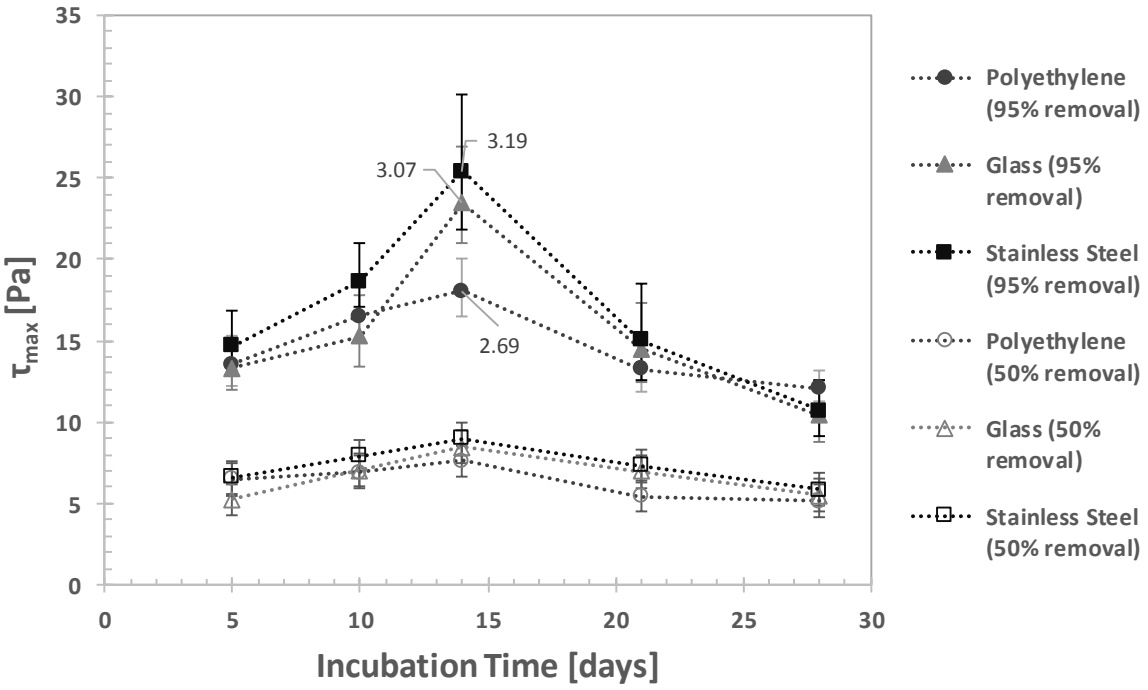

Figure 54: The overall strength test results for *Burkholderia cepacia* biofilms grown on all three test surfaces shown, in terms of the shear stress required in order to remove 50% and 95% of the surface coverage. Values for the equivalent pipe flow velocity are shown for selected data points (ms^{-1}).

Now, as shown in Figure 54, we can compare the effects of varying incubation times on the adhesive strength of *B. cepacia* biofilms across the three chosen surfaces. The peak in strength at the 14-day point seen in the *E. coli* results in recognisable again here, this time for all surfaces (polyethylene peaked after 10 days previously). With the exception of a fairly modest peak point for polyethylene, the three 95% removal curves follow very similar patterns, showing little difference in *B. cepacia* adhesion across the different surfaces. There is a notable increase in strength on glass and stainless steel after 14 days, implying that the suggestion that the greatest resistance to hydraulic removal occurs after 14 days provided by the *E. coli* tests may be a typical feature for bacteria such as these. What is also similar is the stress required to remove 50% of the surface coverage. All values are in the range of 5 to 9 Pa, and the variation between surfaces and incubation periods is quite minimal. Up until 21 days, the *E. coli* biofilms proved more difficult to remove than *B. cepacia* from all surfaces. After 28 days, approximately 10 Pa appears to be sufficient regardless of species or surface material.

In terms of the efficient, safe removal of the biofilms, the same guidelines would apply. Removal with minimum water or energy would take place after 28 days, although this would be inadvisable in the majority of cases due to the risk of contamination. One would expect the optimum point of cleaning to be early on in the biofilm development process i.e. regular cleaning.

5.6.3 Mixed Species Biofilms

Mixed Species – 5 Days

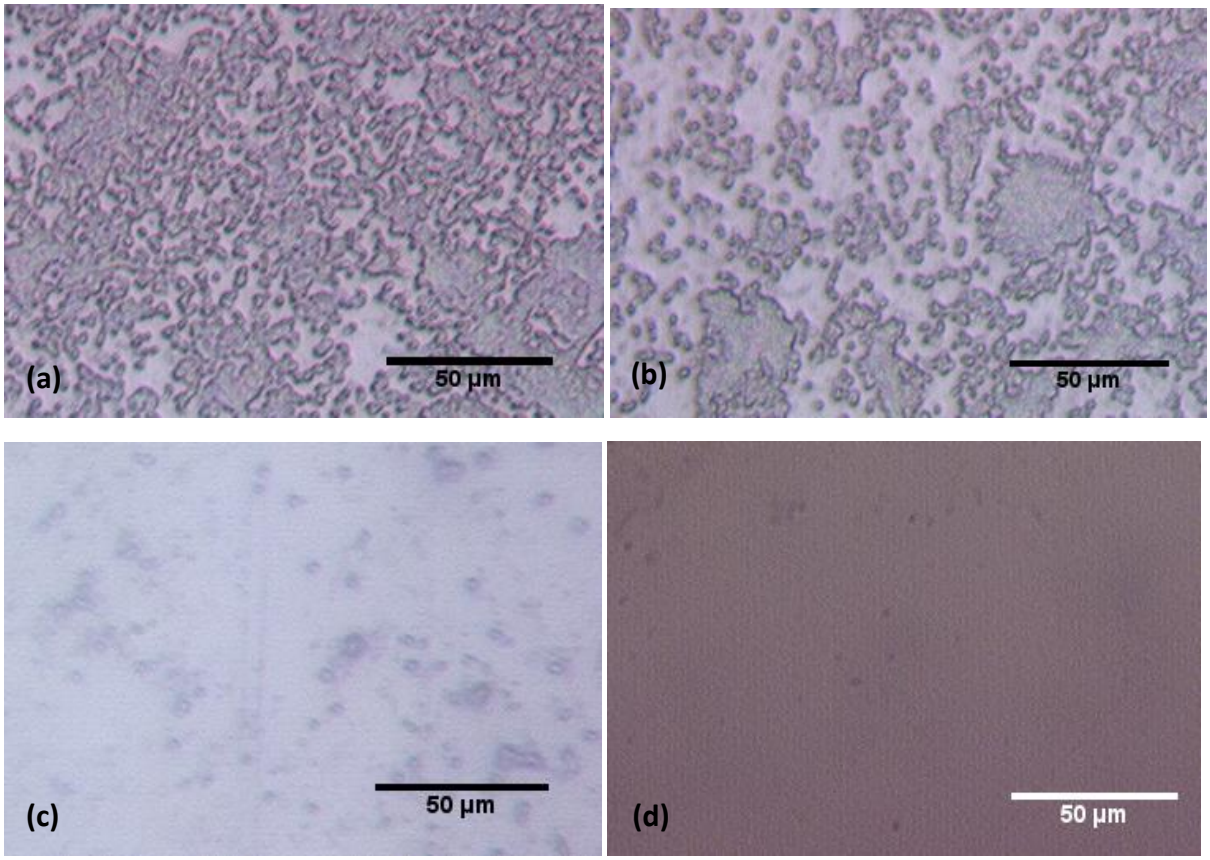

Figure 55: Selected optical microscope images of mixed species biofilms grown on polyethylene for 5 days: tested under FDG at (a) h/d_t = 0.25, 4 ± 0.2 Pa (b) h/d_t = 0.20, 6 ± 0.1 Pa (c) h/d_t = 0.15, 12 ± 0.2 Pa (d) h/d_t = 0.10, 14 ± 0.4 Pa. The percentages of biofilm removed at each stage were: (a) 9%; (b) 45%; (c) 91%; (d) 100%.

The removal of the mixed species biofilms from polyethylene in Figure 55 suggests a similar yield strength to the *B. cepacia* biofilms in the previous section. The point of complete removal occurs after a shear stress of 14 ± 0.4 Pa, whereas 15 ± 0.1 Pa produced the same effect for *B. cepacia*. Biofilm of *E. coli* showed a greater resilience in general. On the other hand, only 9% of coverage was removed with 4 ± 0.2 Pa, which resulted in as much as 38% of *B. cepacia* cells being removed at the same stage.

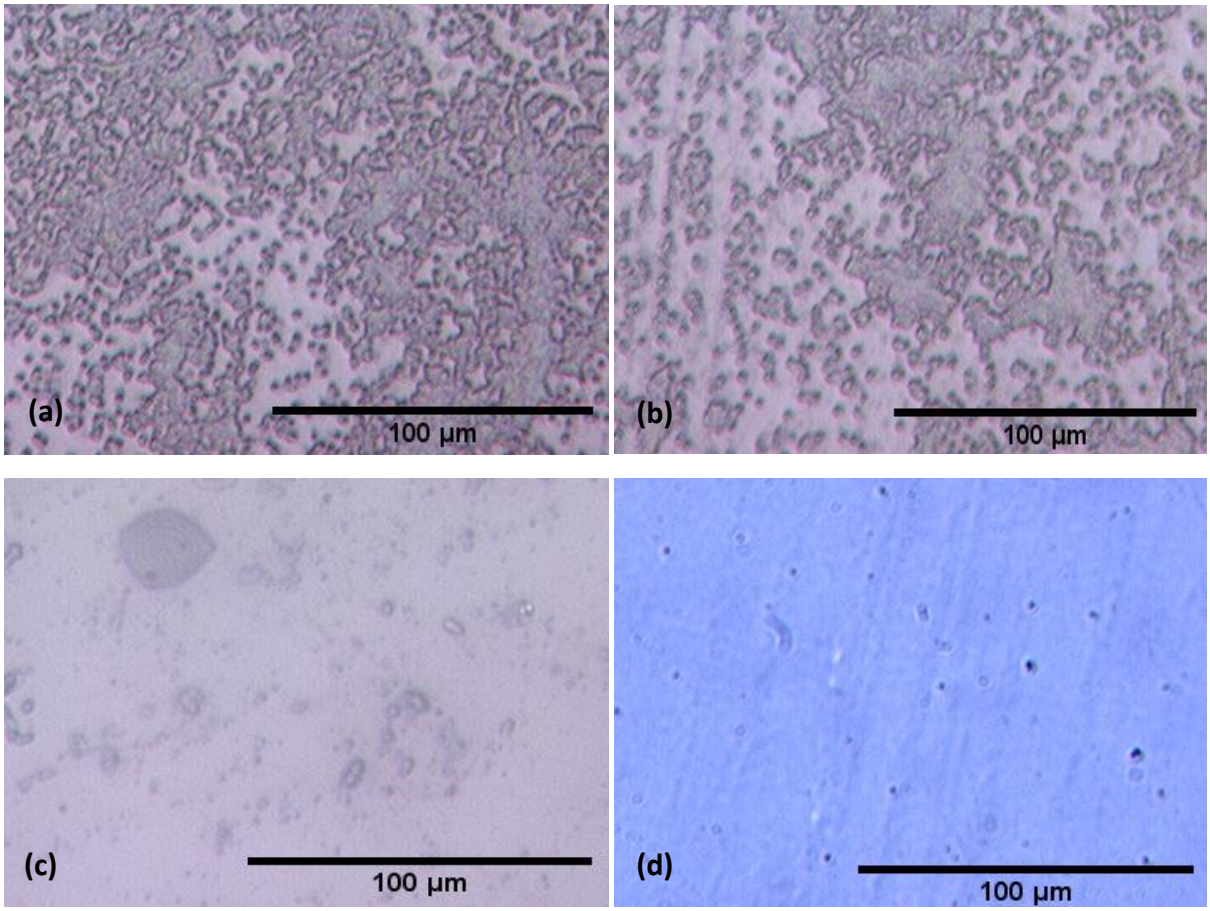

Figure 56: Selected optical microscope images of mixed species biofilms grown on glass for 5 days: tested under FDG at (a) h/d_t = 0.25, 4 ± 0.5 Pa (b) h/d_t = 0.21, 5 ± 0.2 Pa (c) h/d_t = 0.15, 12 ± 0.2 Pa (d) h/d_t = 0.1, 14 ± 0.5 Pa. The percentages of biofilm removed at each stage were: (a) 17%; (b) 59%; (c) 94%; (d) 100%.

The point of removal from glass similarly echoes that of 5-day old *B. cepacia* biofilms, with the surfaces being cleaned with a stress of 14 ± 0.5 Pa, in contrast with the greater strength of *E. coli* cultures. A lower shear stress (4 ± 0.5 Pa) again has less removal effect, reducing coverage by 17%, with the same stresses removing approximately 25% from the monocultures. The strength of these biofilms has a close resemblance to those grown on polyethylene in Figure 55.

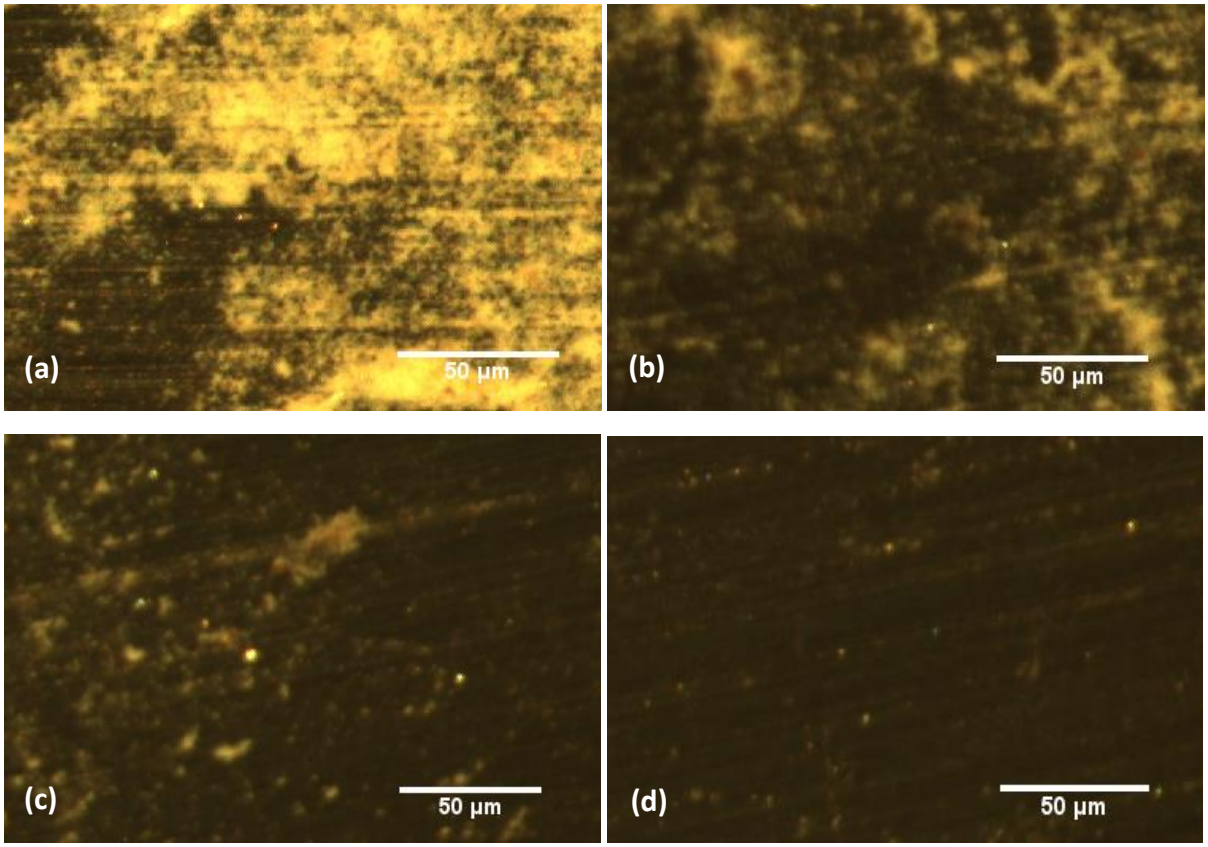

Figure 57: Selected optical microscope images of mixed species biofilms grown on stainless steel for 5 days: tested under FDG at (a) h/d_t = 0.25, 4 ± 0.5 Pa (b) h/d_t = 0.17, 10 ± 0.2 Pa (c) h/d_t = 0.1, 15 ± 0.2 Pa (d) h/d_t = 0.06, 19 ± 0.5 Pa. The percentages of biofilm removed at each stage were: (a) 23%; (b) 78%; (c) 95%; (d) 100%.

Again, the resilience of these mixed biofilms is closer to that of *B. cepacia* to *E. coli*. The most stark signifier of this is that 10 ± 0.2 Pa is able to remove 78% of the biofilm, yet for *E. coli*, 13 ± 0.4 Pa is able to remove only 73%. There is an increase in yield strength compared to the polyethylene and glass-based biofilms, although more of the surface was cleaned with a stress of 4 Pa.

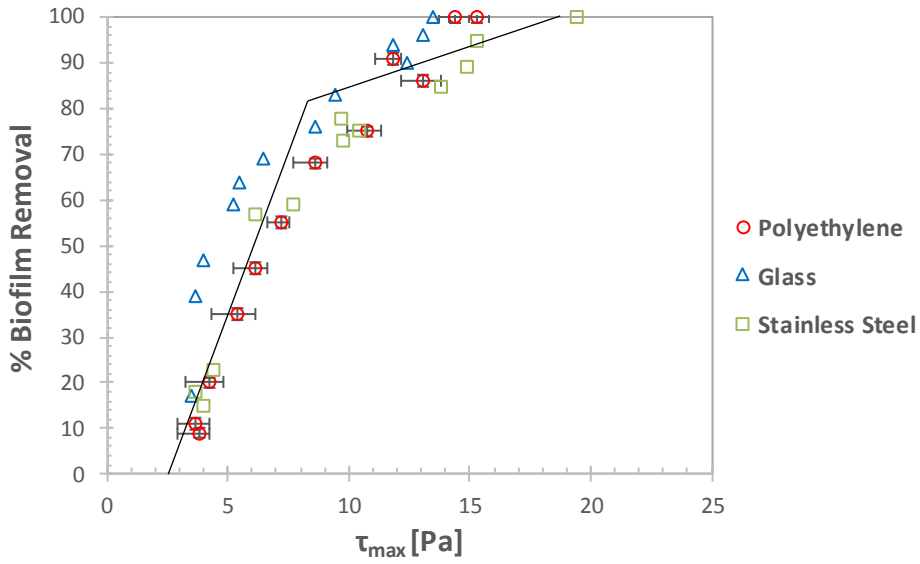

Figure 58: The complete set of strength test results for mixed species biofilms grown for 5 days on polyethylene, glass and stainless steel.

There are two main points which can be made from the evidence in Figure 58; firstly that the biofilms grown on glass appear to be the weakest. This is especially clear in the earlier stages, where shear stresses in the region of 4-5 Pa have removed up to 50% of the cell coverage. On the other surfaces, as little as 25% is removed by the same stress. This would suggest that the mixed biofilms have experienced considerable difficulty in establishing extensive networks on glass after 5 days, although some smaller clusters of cells are clearly able to form. Secondly, the biofilms grown on stainless steel are the most resilient to removal. This becomes apparent once approximately 80% of the biofilm has been removed – prior to this point there is little difference in strength. Those remaining cells then require typically 2-3 Pa extra shear stress in order to achieve the same effect.

The stage at which complete removal is achieved is very close to that for *B. cepacia* (in the region of 15-18 Pa) and considerably lower than for *E. coli*. Depending on the results for the following sections, this could be informative about the nature of how the two species interact within the biofilm.

Mixed Species – *10 Days*

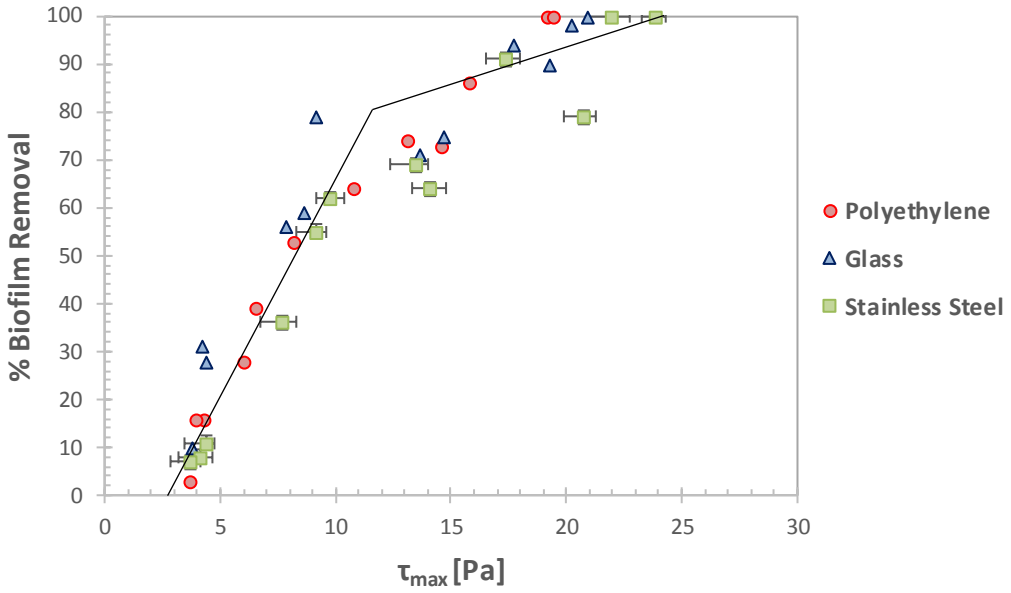

Figure 59: The complete set of strength test results for mixed species biofilms grown for 10 days on polyethylene, glass and stainless steel.

Differences between the adhesive strengths of mixed species biofilms on the three surfaces are much harder to determine than they were for the 5-day incubation. With the exception of a couple of outliers, the data points for each surface display a very close similarity. The primary difference from the graph after 5 days (Figure 58) is the more gradual removal of the first sections of biofilm. In this instance, the progression from initial removal to 50% cleaning occurs between 3-9 Pa, whereas after 5 days the same change in coverage took place in the 3-7 Pa region. This suggests that the biofilms are beginning to develop a more widespread adhesion at this stage, with cells being removed much more gradually rather than with large sections being displaced at once.

Mixed Species – *14 Days*

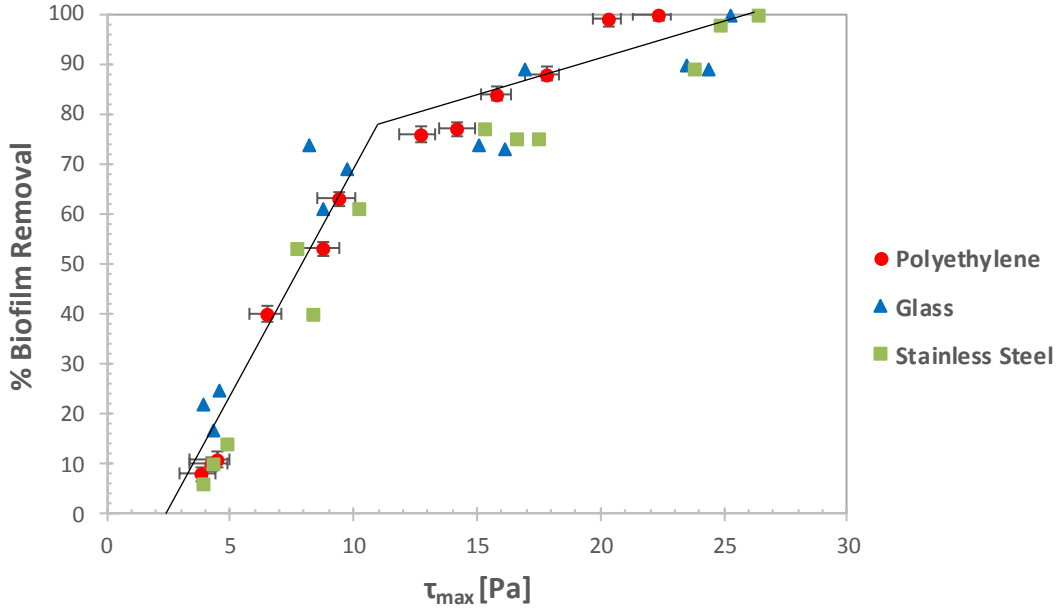

Figure 60: The complete set of strength test results for mixed species biofilms grown for 14 days on polyethylene, glass and stainless steel.

There appears to be two distinct phases in the removal of mixed species biofilms after 14 days. The first 70% of surface coverage can be removed between a change in shear stress of 3 to 10 Pa, a gradual but consistent reduction in biofilm proliferation similar to that observed for the 10-day growth. Following this stage, however, increases in shear stress have a much more negligible effect, and removal of the remaining 25% requires increases in stress of up to 25 Pa. A similar pattern was noted for *B. cepacia*, and to an extent for *E. coli*, although in the case of the latter a greater dispersion of data points led to a less clear trend. In contrast, here there is relatively little distinction between the results for the different surfaces, with the arguable exception of a lesser resilience of polyethylene-based biofilms towards the removal of the final 10% of cells. This would appear to account for the levelling out of total yield strength on polyethylene between 10 and 14 days, in comparison to the continuing increase in strength on the other surfaces. Yet again it can be noted that it is in the removal of the final regions of biofilm which dictates the differences in cleaning difficulty between surfaces, and to an extent between incubation periods.

Mixed Species – *21 Days*

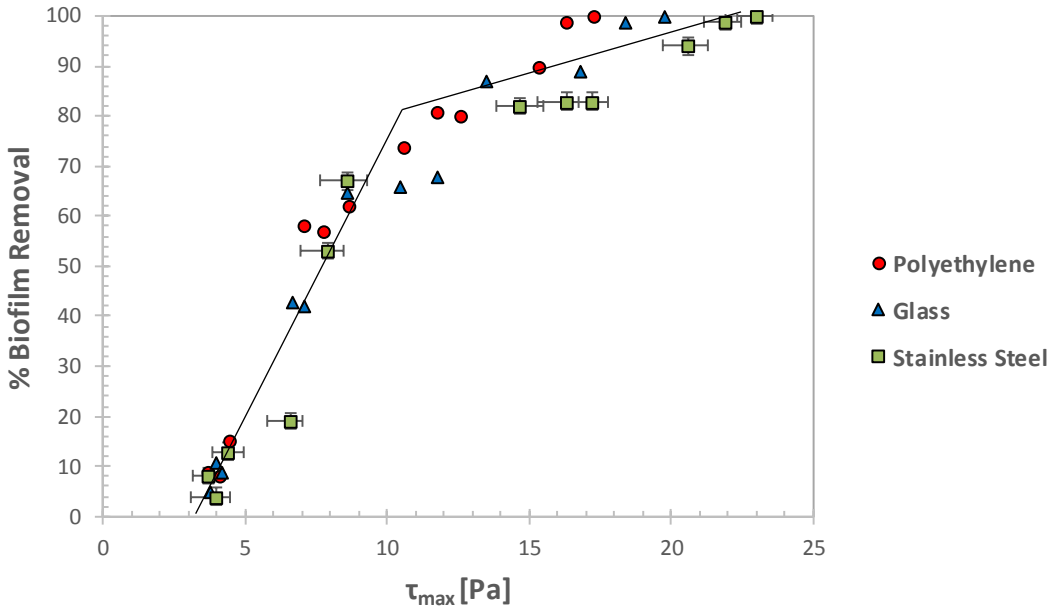

Figure 61: The complete set of strength test results for mixed species biofilms grown for 21 days on polyethylene, glass and stainless steel.

The clearest and most important difference between Figure 61 and the respective graph for 14 days is that all of the data show an overall reduction in strength compared with those results. Dependent on the surface, complete cleaning of the surface now requires between 18 and 23 Pa, compared to between 22 and 27 Pa previously. However, the pattern of removal of the first 70-75% of surface coverage is extremely similar, with a less abrupt flattening-out of the curve beyond this point accounting for the relative ease of removal. The exception to this is the stainless steel-based biofilms, which still exhibit a level of resilience when reduced to the remaining 25% of surface-attached cells, suggesting that the biofilms are able to establish a more enduring attachment to steel than the other surfaces.

Mixed Species – *28 Days*

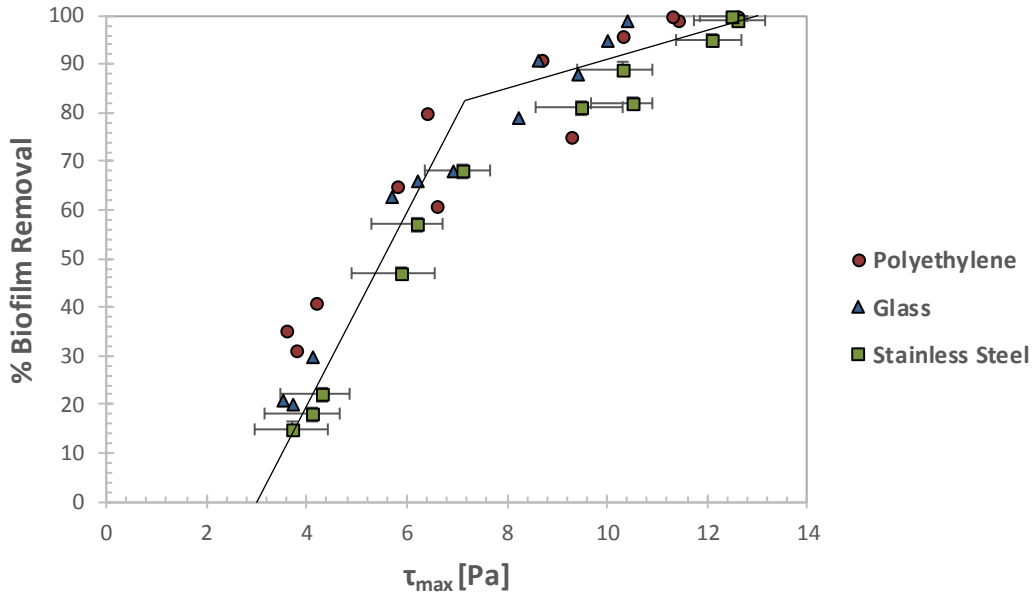

Figure 62: The complete set of strength test results for mixed species biofilms grown for 28 days on polyethylene, glass and stainless steel.

As was the case for both monocultures, the mixed biofilms are easiest to remove at the 28 day stage. Shear stresses in the region of 10-13 Pa are capable of cleaning all of the biofilm from the surface, a considerable fall from 17-23 Pa after 21 days' growth. The other important observation from Figure 62 is that the data points follow a much more linear path of removal relative to increasing shear stress, compared to the previously observed result of the increased difficulty in removing the last 25% of surface coverage. This suggests that resilient attachment to the surface is effectively non-existent after 28 days of incubation, and it could be inferred that the cultures have reached their dispersion phase. This makes the cells easier to remove, but dispersion of bacteria has the potential to present contamination issues.

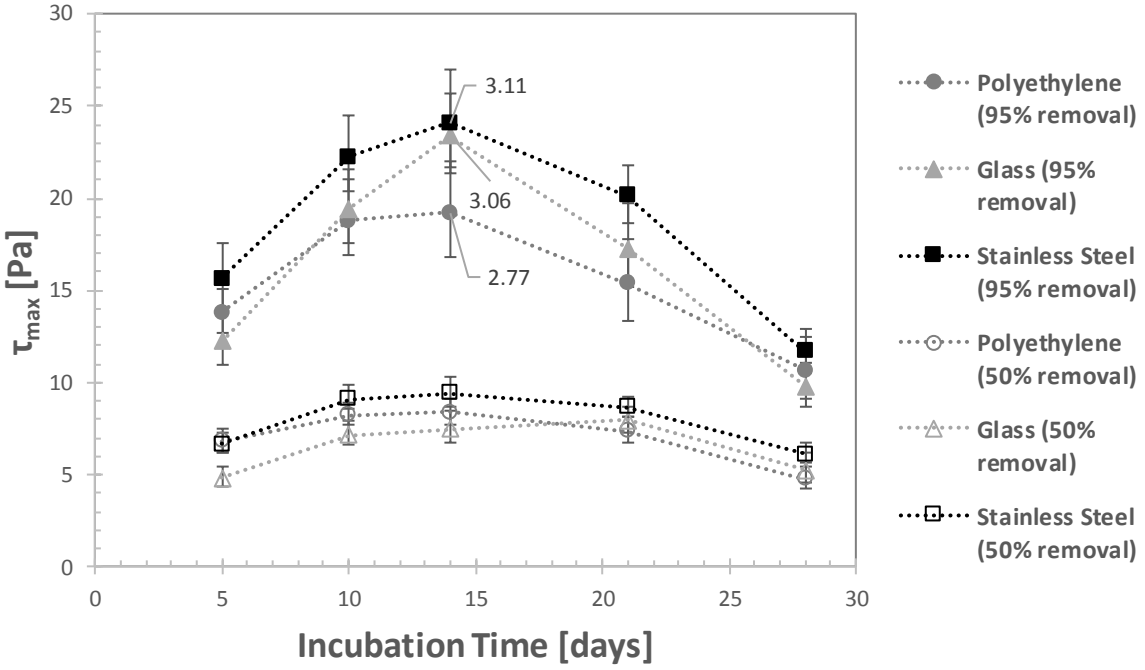

Figure 63: The overall strength test results for mixed species biofilms grown on all three test surfaces shown, in terms of the shear stress required in order to remove 50% and 95% of the surface coverage. Values for the equivalent pipe flow velocity are shown for selected data points (ms^{-1}).

Figure 63 shows the combined adhesive strength test results for mixed species biofilms across all three surfaces. As was the case for the *E. coli* and *B. cepacia* biofilms, the strength of attachment increases up to the 14-day point and then decreases thereafter. Similarly, polyethylene does not experience any particular peak increase, instead showing a close similarity in attachment strength between 10 and 14 days. A large increase in strength on glass is again observed after 14 days. The presence of the peaks in strength being at the same stage as for the monocultures is not especially surprising, given that the same species are used here. The stress required to remove 95% of the surface coverage bears a much closer resemblance to the results for *B. cepacia*, which may be the result of competition between the species for nutrients and surface area if *B. cepacia* was able to establish a competitive advantage. Likewise, the curves for 50% removal are very similar for *B. cepacia* and the mixed species biofilms. Also, as was observed in the previous sections, approximately 10 Pa is able to remove most of the cells when grown for 28 days, which may support the idea that the detachment phase has commenced as neither the species nor the surface appears to have much of an impact on ease of removal.

There is little new to report with regards to efficient cleaning methods. Once again a suitable balance between regular cleaning (and therefore amount of water used), and management of contamination risk over time would need to be established.

5.6.4 Strength Tests Discussion

The majority of the trends of attachment strength relative to incubation time from the rest of this section hold true for each variation in terms of species and surface. The following three graphs in Figure 64 separate the results by surface, in order to gain a clearer picture of how the biofilms interact with each surface and to compare the relationships between the removal behaviour of the strains independent of the variations due to the surface.

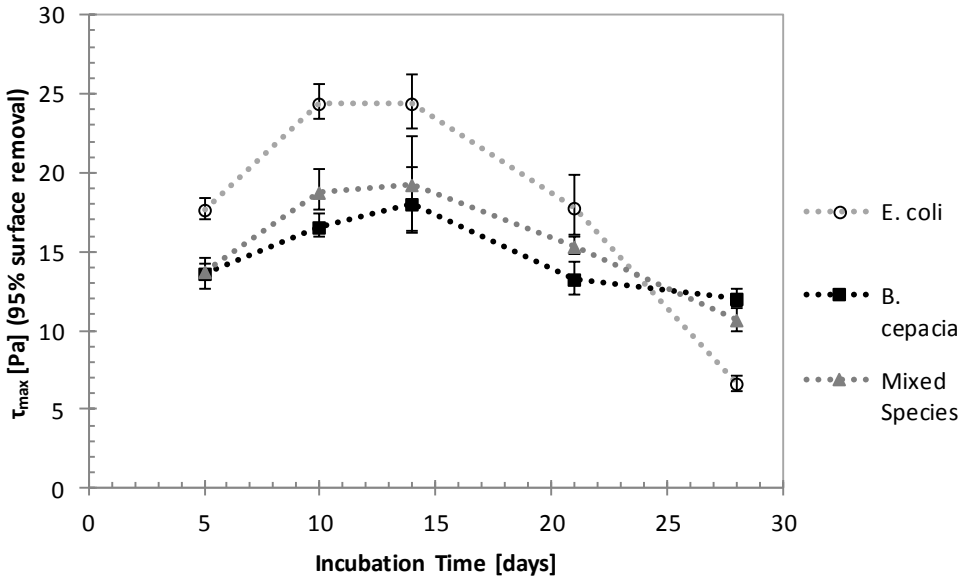

a)

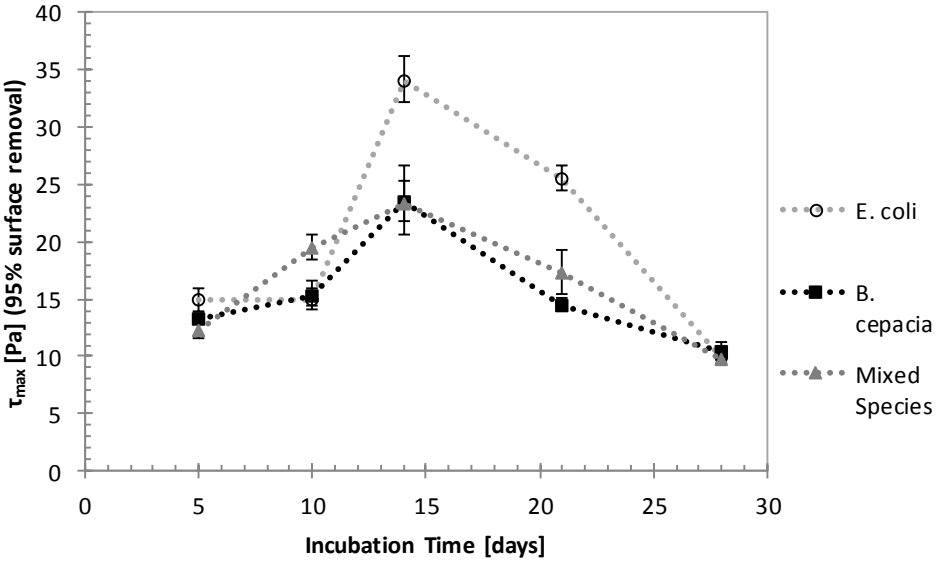

b)

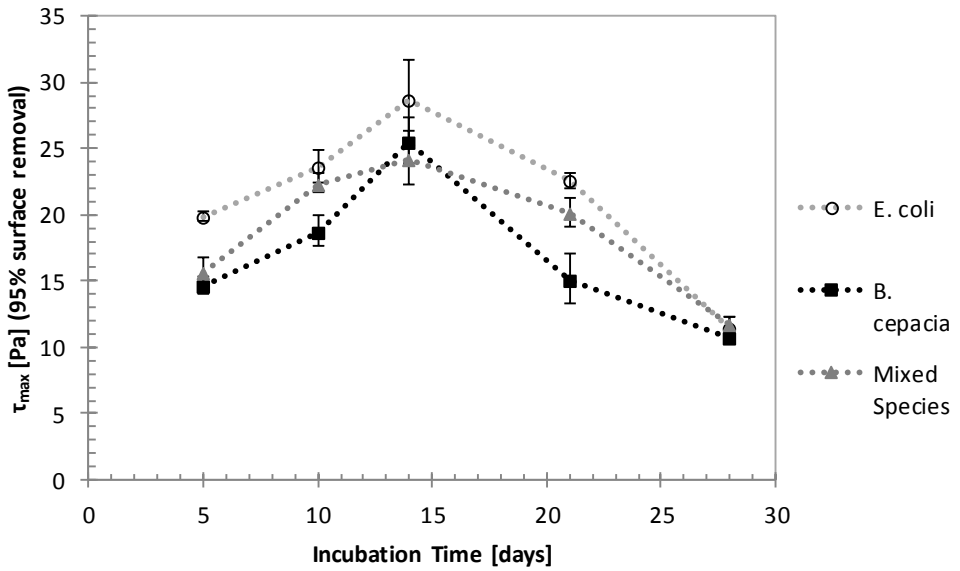

c)

Figure 64: A comparison of the estimated wall shear stress required to remove 95% (from surface coverage analysis using ImageJ) of *E. Coli*, *B. cepacia*, and mixed species biofilms grown on: (a) polyethylene, (b) glass and (c) stainless steel, after a range of incubation times. The error bars take into account the potential inaccuracy of the interpolation, and the scope for experimental errors.

As shown in Figure 64, the general trend of strength relative to incubation time does not change with respect to surface material or species. Every permutation starts relatively weak after 5 days before increasing in strength through 10 and 14 days, and eventually weakening in attachment resulting in the easiest removal occurring after 28 days. Biofilms grown on polyethylene show more gradual change both in the increase and decline in strength, whist those attached to glass and stainless steel exhibit sharper reses and fall, and are generally very similar with the exception of the *E. coli* biofilms on glass which proved to be unusually strong at the 14-day peak. An interesting exception is the delay in strength increase between 5 and 10 days on glass, which could be advantageous in terms of cleaning. The biofilms grown on polyethylene showed the weakest retention of cells, which, regarding the surface energy results, would contradict the literature unless the cells themselves were hydrophilic. The polyethylene-based biofilms did tend to reach their peak strength more rapidly than the others, however, which could be explained by an enhanced adhesive potential allowing the cells to establish biofilms more efficiently. The thickness reduction tests support this idea, with polyethylene-based biofilms all showing an earlier peak in strength. Combining these results with the critical surface energy values would suggest that whilst initial adhesion may be enhanced by a hydrophobic surface, once biofilms become established the surface energy has little impact.

This means that all of the biofilms are easier to remove after being allowed to grow for 28 days or longer, which presents the immediately obvious risk of pathogens and other contaminants being able to prosper, which is even more of a problem if cells are already naturally detaching as was hinted at

by the removal patterns in the results for 28 days. On the other hand, to clean every 5 days (or more frequently) would be much more costly, and if chemical disinfectants were used, issues regarding toxicity and reactivity etc. would be enhanced and the potential for the biofilms to acquire resistance to the chemical used would be much heightened.

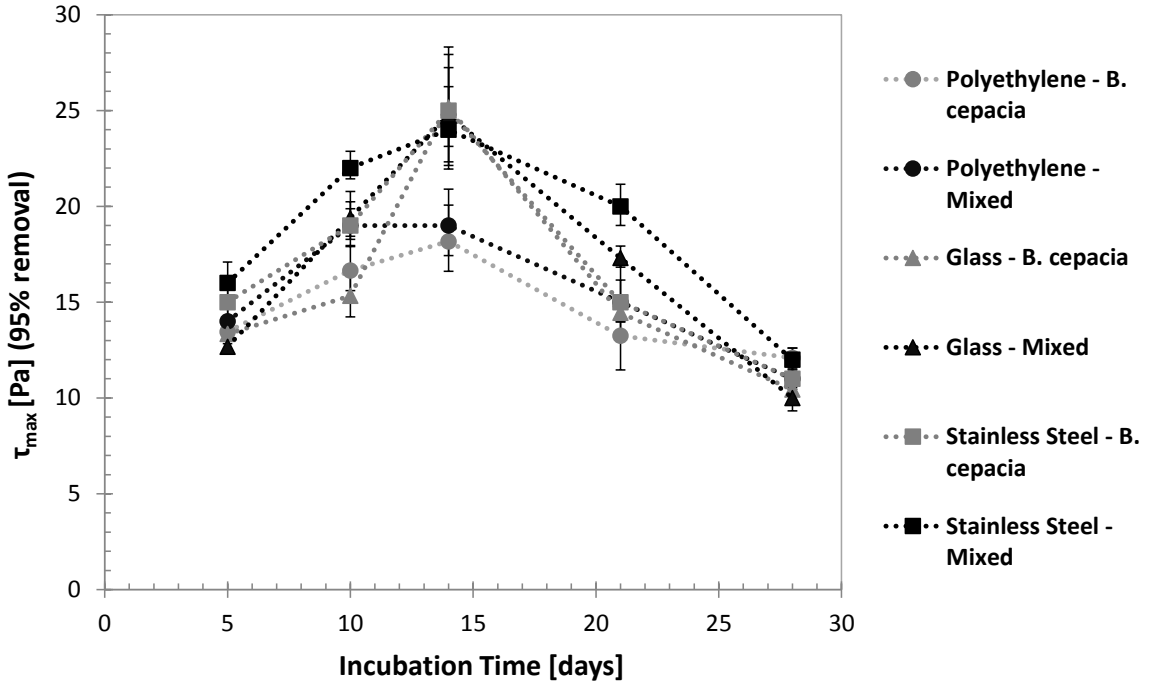

Figure 65: A comparison of the estimated wall shear stress required to remove 95% of *B. cepacia* and mixed species biofilms from polyethylene, glass and stainless steel surfaces after a range of incubation times.

The data in Figure 65 indicates the relative similarity between the removal behaviour of *Burkholderia cepaic* and mixed biofilms, as was observed on multiple occasions in the step-by-step results earlier in this section. This was also noticeable in Figure 64, where the curves for *E. coli* tend to differ from the other two on each surface. In Figure 65, it is clear that the curves all follow similar courses, and are particularly close at the 5 and 28-day points as well as the pairs for each surface showing similar adhesive strength after 14 days. The tendency of mixed species attachment to closely resemble that of *B. cepacia* suggests that competitive behaviour is taking place between the two species, with *E. coli* struggling to form adhesive bonds with the surface. Possible reasons for this are discussed in Section 2.2.4: competition for nutrients or media formulations being the more simplistic, although it is also possible that *E. coli* occupies the more nutrient-rich outer layers, leaving *B. cepacia* at the surface layer which would therefore govern the resistance to removal.

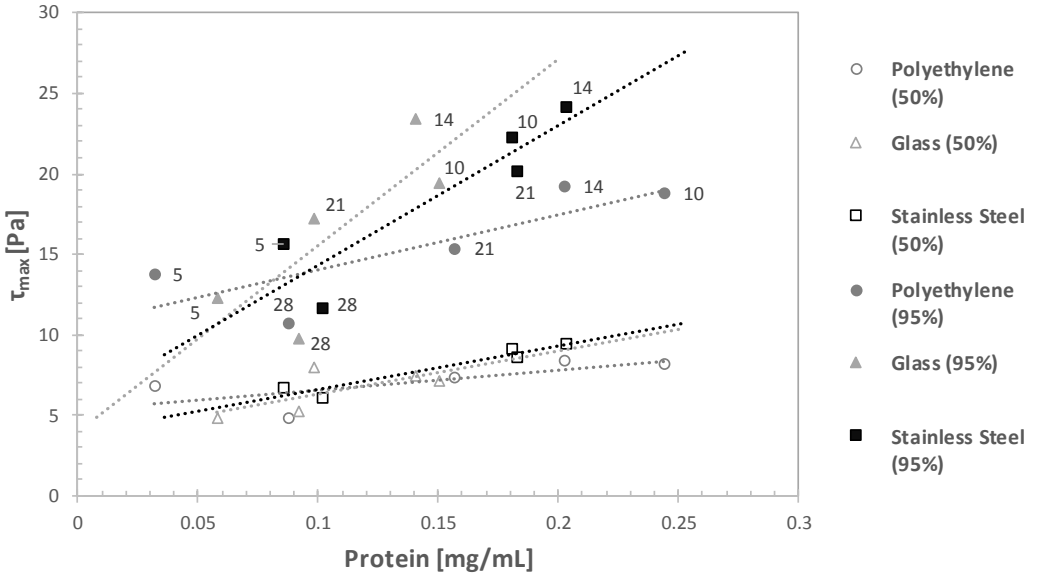

a)

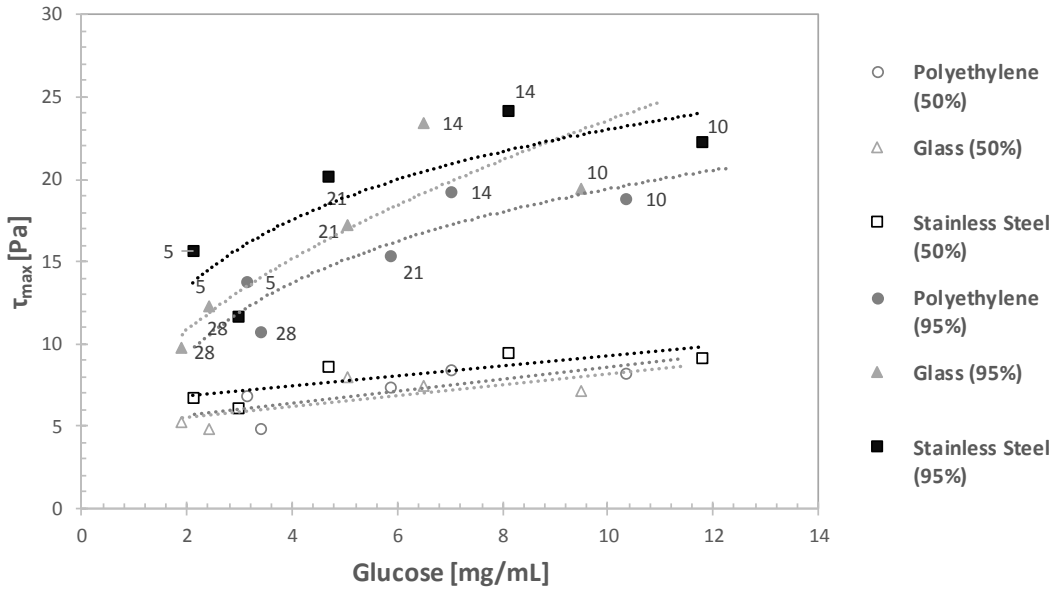

b)

Figure 66: Comparisons between adhesive strength values and recorded amounts of a) protein and b) glucose in the equivalent biofilm samples. All data are taken from mixed species biofilms. The incubation periods (in days) are shown in the labels.

Figure 66 is an attempt to show the relationship between the amount of proteins and polysaccharides measured and the results of the strength section for mixed biofilms on the three surfaces. Linear trends were observed in graph a), indicating a direct relationship between protein concentration and adhesive strength, and this could therefore play a significant role in the surface adhesion of a biofilm. The steepest gradient in seen on glass, where greater increases in strength can be seen for an increase in protein concentration. There are two key differences: the protein peak occurs just before the peaks in

adhesive and cohesive strength (both 14 days for all surfaces), and a less pronounced decline after 28 days. The most likely explanation for the first point is that the impact of the first stage of EPS degradation takes a short period to have an effect on removal behaviour – in fact the adhesive strength of biofilms on both polyethylene and stainless steel increased little between 10 and 14 days, suggesting that the reversal of the trend had already begun. There is also a positive trend between adhesive strength and polysaccharide levels, although the points fit to a logarithmic curve, suggesting a limitation to the impact of sugar concentration on adhesion as it continues to increase. Similar to the observation for the strengths compared to incubation time, the ease of removal of the first 50% is seemingly unrelated to protein or polysaccharide levels, supporting the idea of the formation of stronger regions of biofilm. It can also be seen how the peak in polysaccharide quantity precedes the peak in adhesive strength by a few days, occurring at 10 days whereas the strength continues to increase up to 14 days.

Table 7: The full set of average shear stress values required to remove 50% and 95% surface coverage of *E. coli*, *B. cepacia*, and mixed species biofilms grown under static conditions from polyethylene, glass and stainless steel.

	Removal from Polyethylene [τ_{max}] [Pa]					
	E. coli		***B. cepacia***		**Mixed Species**	
Days	**50%**	**95%**	**50%**	**95%**	**50%**	**95%**
5	10.6	17.6	6.5	13.6	6.8	13.8
10	7.2	24.4	6.9	16.5	8.2	18.8
14	6.2	24.4	7.6	18.1	8.4	19.2
21	5.3	17.8	5.5	13.3	7.4	15.4
28	2.1	6.6	5.1	12.1	4.8	10.7

	Removal from Glass [τ_{max}] [Pa]					
	E. coli		***B. cepacia***		**Mixed Species**	
Days	50%	95%	50%	95%	50%	95%
5	4.9	14.9	5.2	13.3	4.8	12.3
10	8.9	15.0	7.0	15.3	7.2	19.4
14	10.2	34.0	8.5	23.5	7.5	23.4
21	5.4	25.5	7.0	14.5	7.9	17.3
28	2.8	9.9	5.5	10.4	5.3	9.8

	Removal from Stainless Steel [τ_{max}] [Pa]					
	E. coli		***B. cepacia***		**Mixed Species**	
Days	**50%**	**95%**	**50%**	**95%**	**50%**	**95%**
5	8.1	19.8	6.6	14.7	6.7	15.7
10	7.3	23.5	8.0	18.7	9.1	22.3
14	8.3	28.6	9.0	25.4	9.4	24.1
21	7.1	19.6	7.4	15.1	8.6	20.1
28	2.5	9.5	5.9	10.7	6.1	11.7

5.7 Thickness Tests

The average values for the thickness of biofilms grown on all three surfaces are displayed in Figure 67 below:

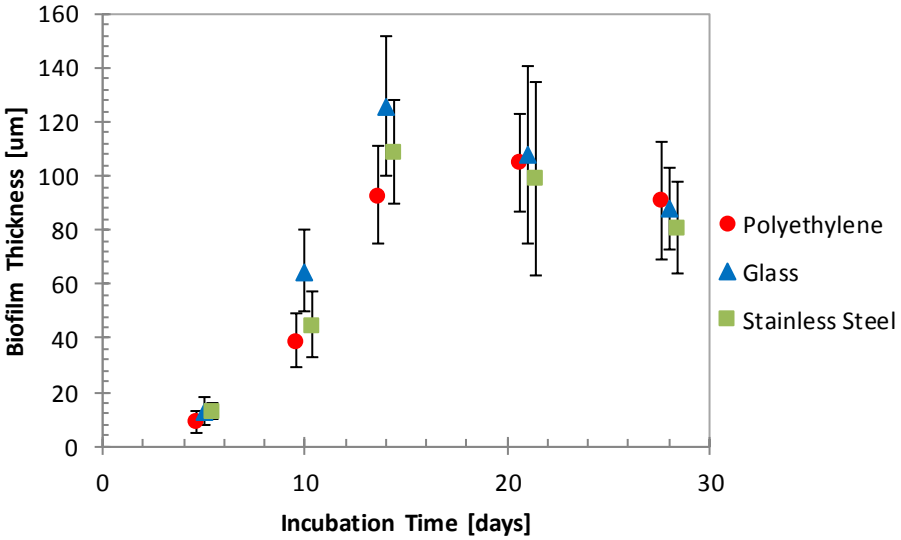

a)

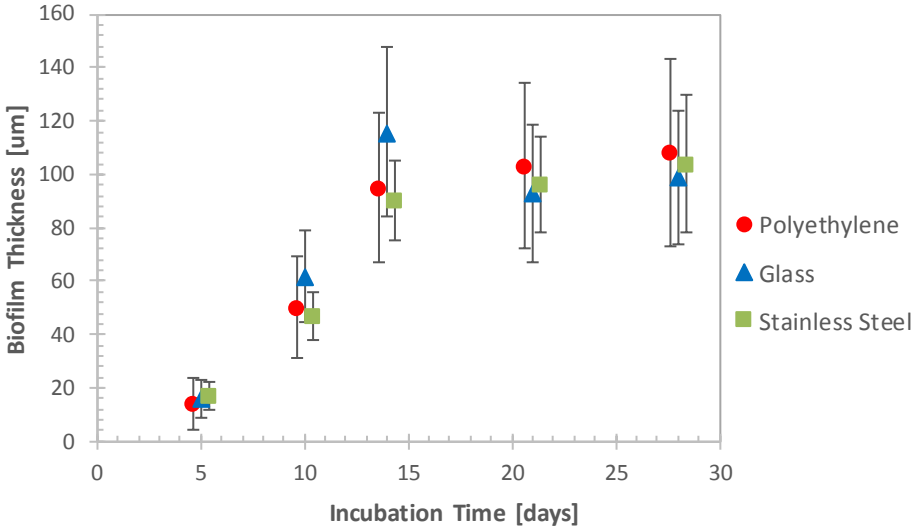

b)

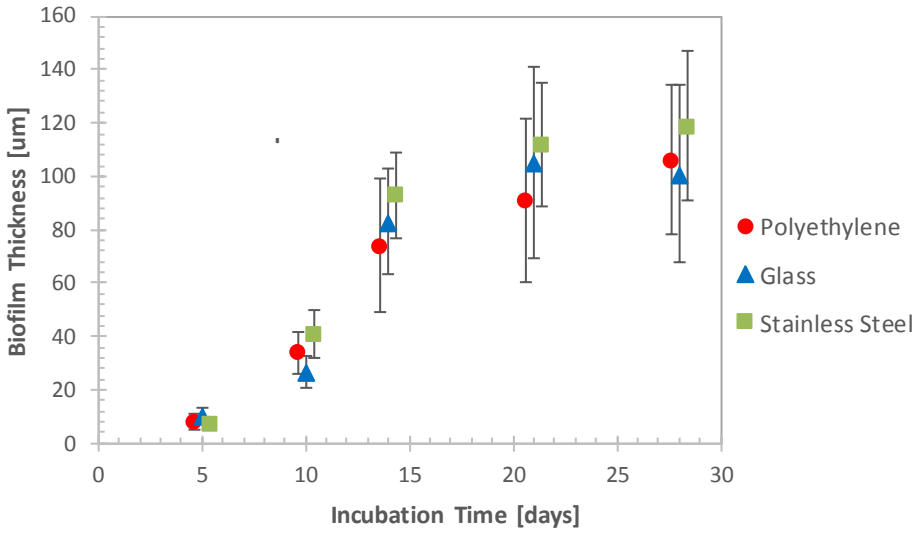

c)

Figure 67: Graphs showing the average thickness of a) *E. coli*; b) *B. cepacia*; and c) mixed species biofilms as measured by FDG. The error bars show the minimum and maximum thicknesses measured for each incubation period.

These results suggest a consistent, rapid increase in thickness up to the 14-day growth point, followed by the beginnings of a slow natural reduction once the biofilms have fully matured. The results after 5 days should be treated with some caution given the gauge's thickness resolution of ±5 µm, although even allowing for that the trend of consistent increase holds true. In general, the table shows strong similarities between the thicknesses experienced across the surfaces and the bacteria involved, suggesting that whilst the substrate may impact upon the ability of biofilms to attach, it has little effect on the potential thickness of the deposits. The mixed species biofilms appear to continue to become thicker all the way up until 28 days albeit more slowly, whilst the monocultures have either completely levelled off or begun to show signs of a slight decline in thickness. How much longer this would continue for is impossible to say from these results, but it does suggest a delay in the development of more complex, thicker structures, which may support the idea of inter-species competition having an impact upon the growth of the biofilms. However, it may be risky to draw too many conclusions from this given the variation between the minimum and maximum recorded values for each data point. What can be confirmed, though, is that the biofilms clearly do not decline in thickness in the same way in which they lose adhesive strength. This is in keeping with phases of growth detailed in Section 2.3, in which ageing biofilms begin to experience detachment at a rate similar to their growth, so although cells are more readily removed the thickness of the biofilms does not radically change.

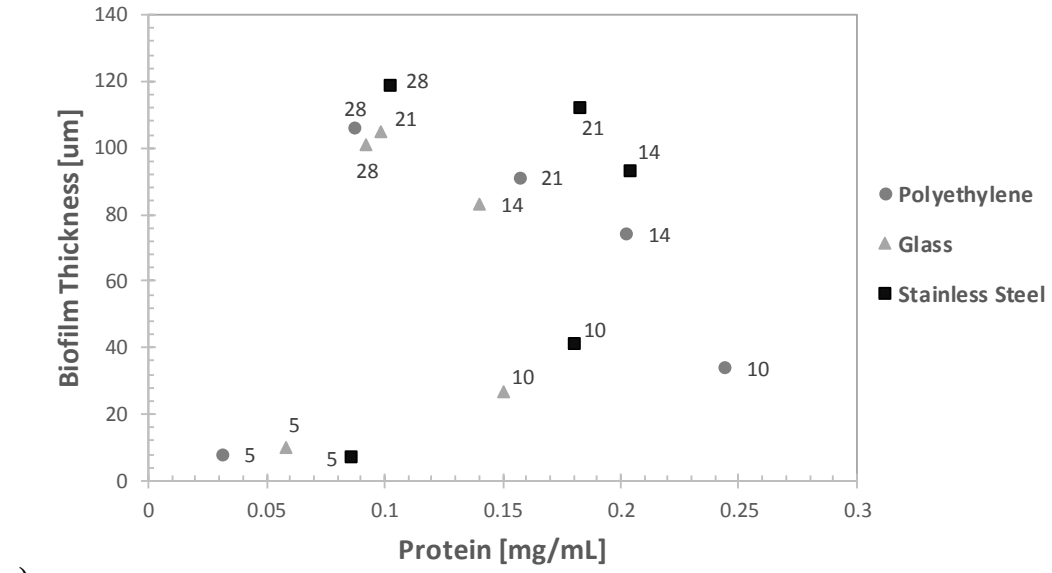

a)

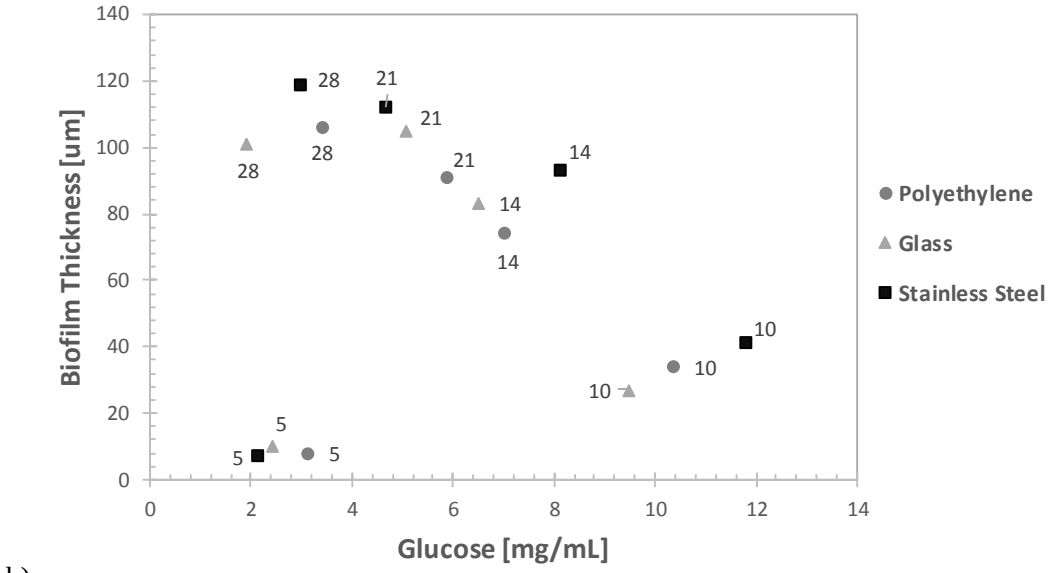

b)

Figure 68: Comparisons between biofilm thickness and recorded amounts of a) protein and b) glucose in the equivalent biofilm samples. All data are taken from mixed species biofilms. The incubation periods (in days) are shown in the labels.

Figure 68 suggests that the concentrations of protein and polysaccharides in a biofilm do not increase in line with the thickness of the biofilm. Both graphs show that the thickness of the biofilms continue to increase whilst the protein and glucose levels peak in around 10-14 days, showing again the greater correlation with biofilm strength. The key difference is that the thickness does not experience a decline as the incubation period is extended towards the later ages. This could signify either a decrease in biofilm density or a degradation of EPS even as the cells continue to reproduce. It may coincide with the phase of dispersal, where it is considered easier for the outer layers to slough off with low resistance.

5.7.1 Thickness Reduction

Is this section it can be seen how the shear stress inflicted by the nozzle can remove layers of the biofilm, ideally giving an idea of the cohesive strength of the biofilms and how they can be removed. Firstly, below is a selection of examples of these tests, in order to indicate how the gradual removal of the deposit proceeds as the shear stress applied is increased.

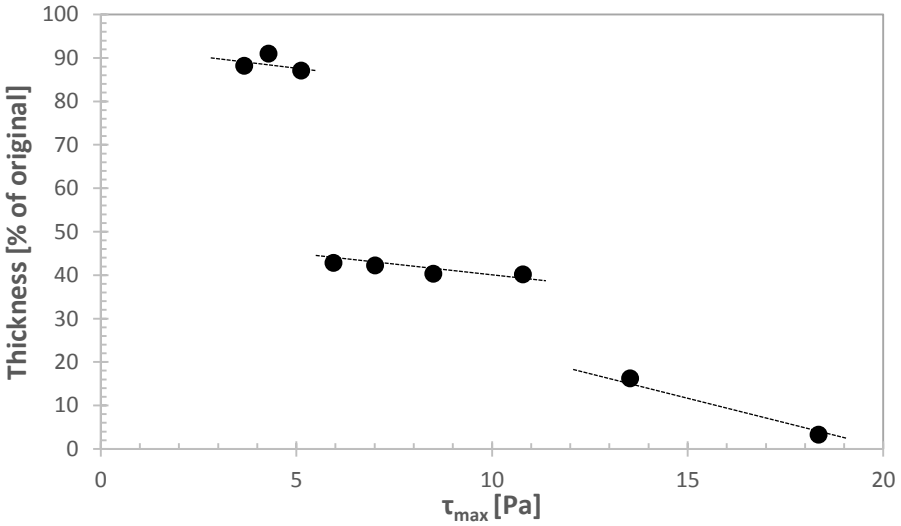

Figure 69: The percentage of biofilm thickness reduction in terms of the estimated wall shear stress deduced from the mass flow rate at the respective nozzle clearance (h/d_t), for a biofilm of *E. coli* grown for 14 days on a polyethylene surface.

The example shown in Figure 69 displays how the step-by-step reduction in biofilm thickness proceeds. The plot of C_d versus h/d_t is shown in Appendix 5, showing the displacement in the x-axis for a certain discharge coefficient, as the difference in h/d_t values is equal to $h-h_0$, or δ as it is otherwise known. The reduction in thickness due to increasing shear stress can be expressed as a remaining percentage of this value. This reduction is shown in Figure 69, where the loss of biofilm is shown relative to shear stress. Sections of biofilm appear to have been removed rather than it being a gradual process – in this example there are four distinct stages: a small layer is removed with approximately 3-4 Pa: this is followed by the removal of a large section at 6 Pa; there are then two roughly similar reductions in thickness before the biofilm has effectively been eliminated using a stress of 18 Pa. As a comparison, it was shown in the previous section that 27 Pa was able to remove the surface coverage for an equivalent biofilm, which indicates that the increase from 18 to 27 Pa is focussed on removing surface-attached cells from specific regions. Indeed the same strength test showed that just 14 Pa was able to remove 89% of the surface coverage, so this suggests that only certain regions exhibit this extra attachment strength.

Next we can look at a different set of results, this time for a mixed species biofilm grown on glass.

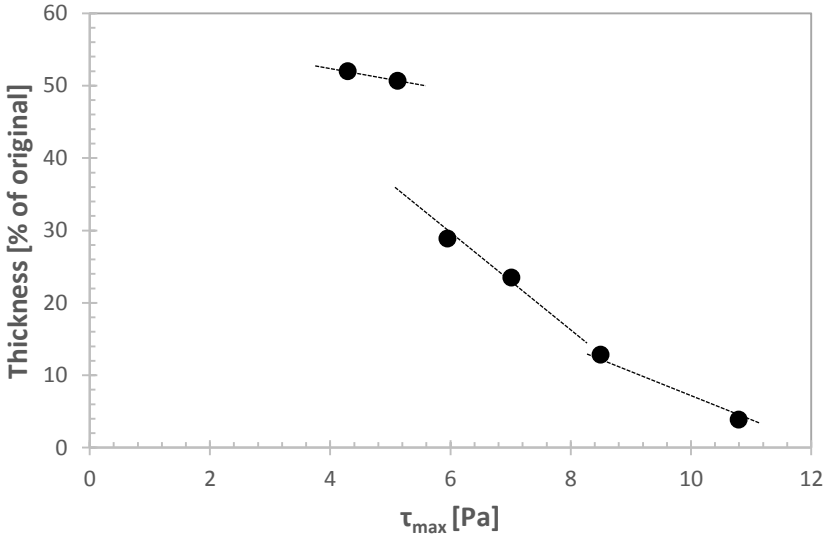

Figure 70: The percentage of biofilm thickness reduction in terms of the estimated wall shear stress deduced from the mass flow rate at the respective nozzle clearance (h/d_t), for a mixed species biofilm grown for 14 days on a glass surface.

There is less difference between the test and calibration curves (shown in Appendix 5) this time around, partly because the biofilm began with a thickness of 79.9 Pa rather than the 92.6 Pa of the previous example. Figure 70 indicates that there is a similar dynamic of removal, with layers being sucked away from the outer surface of the biofilm. The first bulk removal has taken away the outer 50% of the biofilm, which is notably greater than the 10% removed at the same stage in the previous example. The remaining biofilm was removed more gradually than the previous case, where there was a second bulk loss followed by a static period. Overall removal was much easier in this instance, with the biofilm reduced to what would appear to be a surface layer by a shear stress of approximately 11 Pa, compared to 18 Pa for the *E. coli* biofilm, suggesting a markedly lower cohesive strength. This despite reaching a similar thickness after incubation, suggesting little correlation between complex development and strength. Whether the tests for *B. cepacia* show similarity of the *E. coli* monoculture in this regard, or echo the similarity with the mixed species biofilms observed in the adhesive strength tests remains to be seen.

The following example is for a biofilm grown on stainless steel.

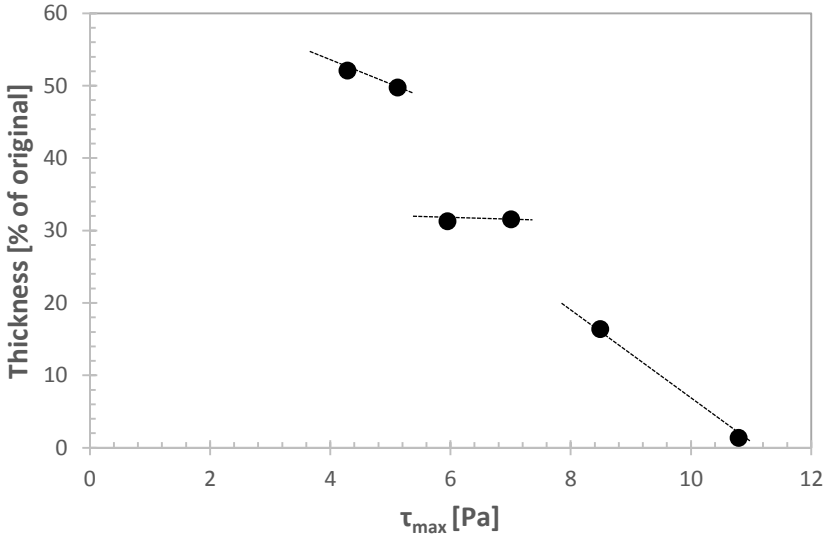

Figure 71: A graph showing how the discharge coefficient (C_d) relative to the dimensionless nozzle clearance distance (h/d_t) differs compared to a calibration plot due to the presence of a *B. cepacia* biofilm grown for 10 days on stainless steel.

The biofilm in the above example reached a thickness of 43.5 Pa, which means that the plot of C_d vs. h/d_t offers little clue as to the removal profile, similar to the mixed species biofilm examined previously. Figure 71 suggests a closer resemblance in profile to the *E. coli* biofilm in Figure 69, as there are two major bulk removals of biofilm at 4 Pa and 6 Pa. In terms of strength however, there is a strong similarity to the mixed species biofilm, as the initial reduction in thickness removes the full top half of the layer and the surface layer is exposed at approximately 11 Pa. On this basis, the cohesive strength of the *B. cepacia* and mixed species biofilms show a similarity much like the adhesive strength, and although this is for 10 days' growth rather than 14, the suggestion is that the *E. coli* biofilm has a generally much greater resistance to removal than the others. In order to draw better conclusions, the complete set of thickness reduction tests need to now be examined.

Results

Having conducted a full set of thickness and removal tests on all three surfaces with each culture and mixed-species biofilms, the results can be analysed for trends in how the bulk of a biofilm is removed, and how easily this can be done. Whilst image analysis is helpful in quantifying the surface coverage (i.e. the adhesive strength of biofilms); the cohesive strength between layers is also of importance and can be quantified using thickness reduction tests.

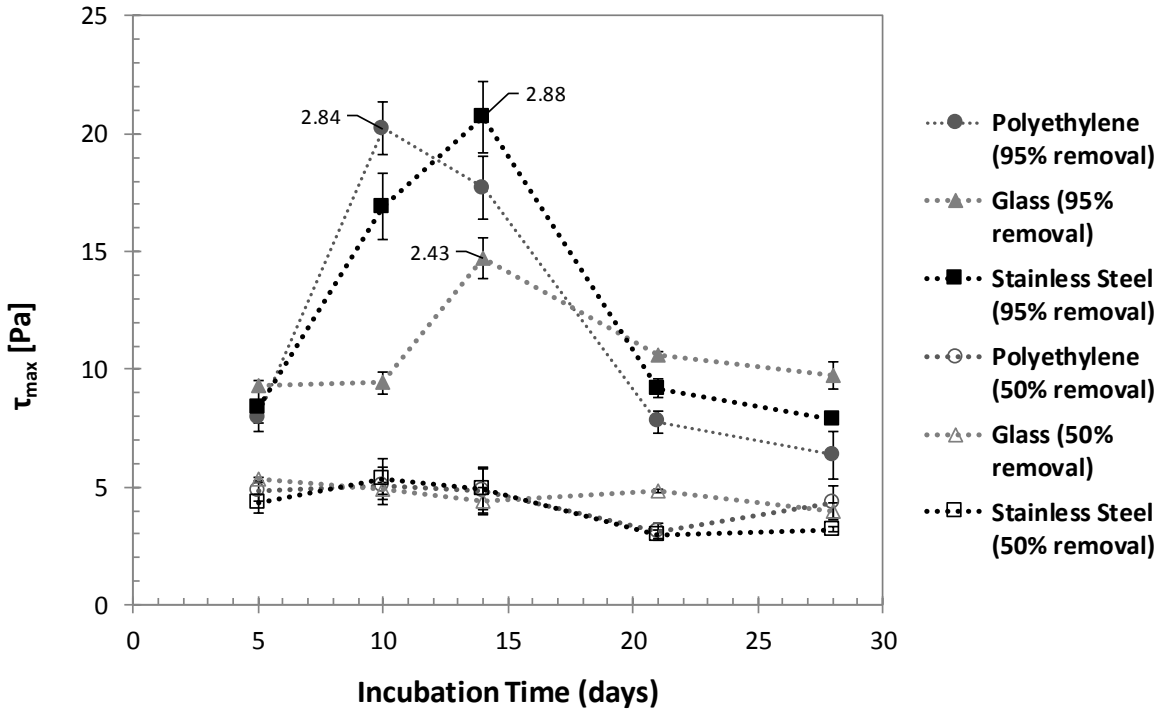

Figure 72: The estimated wall shear stress and selected equivalent mean pipe flow velocities in brackets (ms^{-1}) required to remove 50%, and 95% of *E. coli* biofilm thickness from glass, polyethylene and stainless steel, after a range of incubation periods. The error bars take into account the potential inaccuracy of the logarithmic interpolation and the scope for experimental errors.

Generally, the relationship between thickness reduction and velocity in this section echo the results from the strength tests. The biofilms grown for 5 and 21-28 days were the easiest to remove, whilst those grown for 10 and 14 days proved to be more resilient. The trend was less clear for the glass-based biofilms, in which removal rates were similar with the exception of the notable cohesive strength of the 14-day biofilms. Figure 72 assimilates these results to show the patterns, with the same method as with Figure 45 from the previous section.

Figure 72 shows that the strength peak for polyethylene occurs after 10 days (approximately 20 Pa), and for glass the strength of 5-day and 10-day biofilms is comparable (9-10 Pa), the point for 14 days appearing to be the beginning of its peak – a value of approximately 15 Pa, which is also incidentally the lowest peak of the three substrates. The results in Figure 72 also supports the concept of the attachment, maturation and dispersion stages of biofilm development, and bears a resemblance to the graph for the *E. coli* strength tests in Figure 45. The first phase (initial and irreversible attachment) is analogous with the fragile attachment seen after the 5-day incubation. Maturation seem to occur at approximately the 10-14 day period with peaks as high as 20-21 Pa (or 2.8-2.9 m/s) for polyethylene and steel. By the time biofilms had spent 21 – 28 days in incubation, growth on all three substrates would appear to have reached the dispersion phase, accounting for the relative ease of removal at

lower shear stress. Older biofilms are also at risk from sloughing, which is the tendency of large portions of biofilm to detach suddenly under shear. Interestingly, the stress required to remove the top 50% of biofilm does not appear to be dependent on the surface or the incubation period.

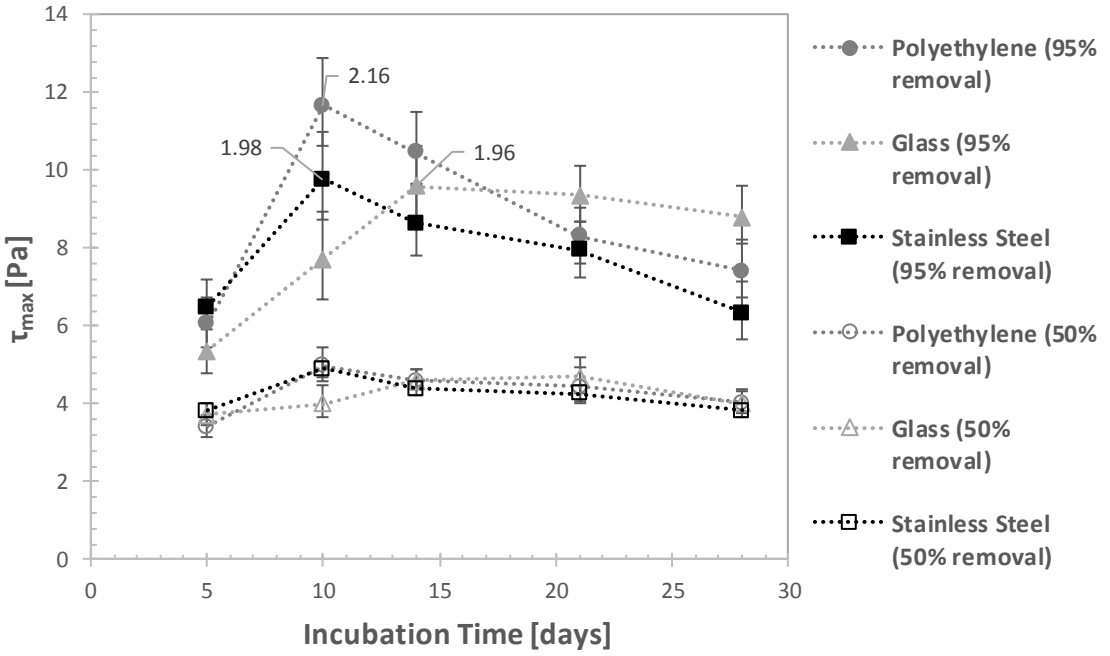

Figure 73: The estimated wall shear stress and selected equivalent mean pipe flow velocities in brackets (ms^{-1}) required to remove 50%, and 95% of *B. cepacia* biofilm thickness from glass, polyethylene and stainless steel, after a range of incubation periods. The error bars take into account the potential inaccuracy of the logarithmic interpolation and the scope for experimental errors.

The most notable difference between the graph in Figure 73 and the same results for *E. coli* biofilms is that these biofilms exhibit a far lower cohesive strength. The hardest to remove according to Figure 73 are the 10-day old biofilms grown on polyethylene requiring 12 Pa to reduce thickness by 95% - the greatest strength observed for *E. coli* was as high as 21 Pa. This is similar to the results for adhesive strength in the previous section, but the difference between the two strains is much greater (almost double at peak points). A similarity between the two graphs is that glass-based biofilms appear to differ in terms of removal patterns over time from the other two surfaces. It is difficult to say with any certainty why this should be the case, given that this is not concerning the biofilm surface layer, but the extent of difference along with exhibiting the lowest peak strength in both cases suggests that it may not be coincidence. The shear stress required for 50% removal again differs little across surfaces and incubation periods, and is similar to that for *E. coli*, but this is again unsurprising given what it represents.

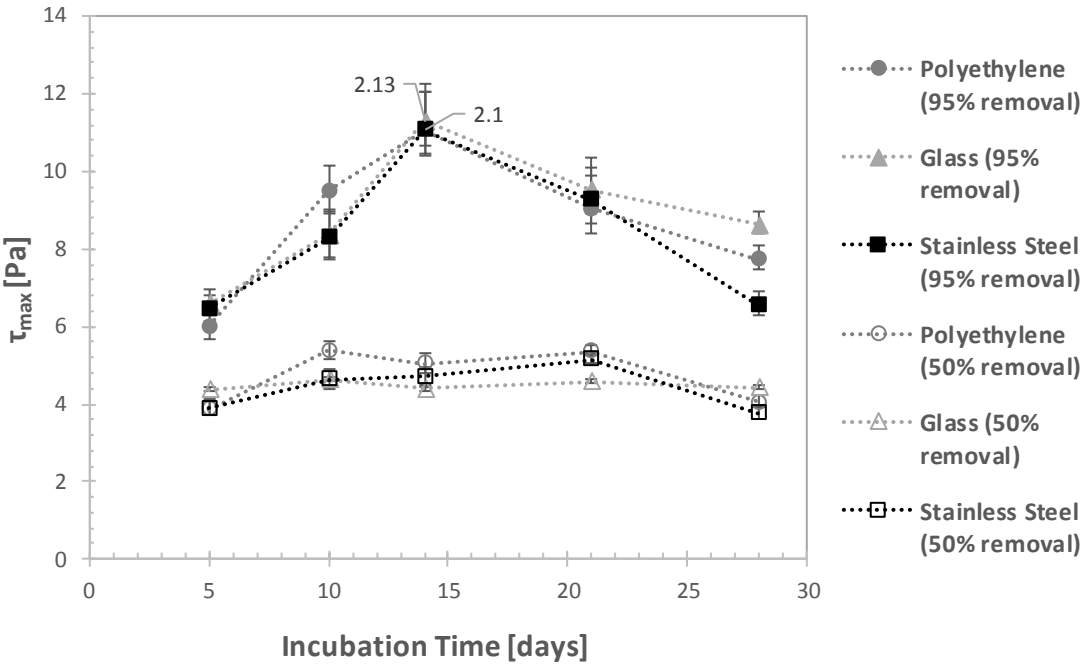

Figure 74: The estimated wall shear stress and selected equivalent mean pipe flow velocities in brackets (ms^{-1}) required to remove 50%, and 95% of mixed species biofilm thickness from glass, polyethylene and stainless steel, after a range of incubation periods. The error bars take into account the potential inaccuracy of the logarithmic interpolation and the scope for experimental errors.

As was observed for the adhesive strength tests, the removal of mixed species biofilms bears a closer resemblance to *B. cepacia* removal. However this is only in terms of the shear stresses required, ranging from 6 to 11 Pa for 95% removal – the trends regarding removal dependent on the surfaces and incubation times are quite different. For the *B. cepacia* biofilms there was much more variation in strength depending on those other variables, but the mixed biofilms there is a more uniform set of results where the surfaces appear to have little impact on bulk removal requirements. The 14-day peaks are almost identical for all three surfaces. Again, 50% removal shear stresses do not appear to alter with any significance.

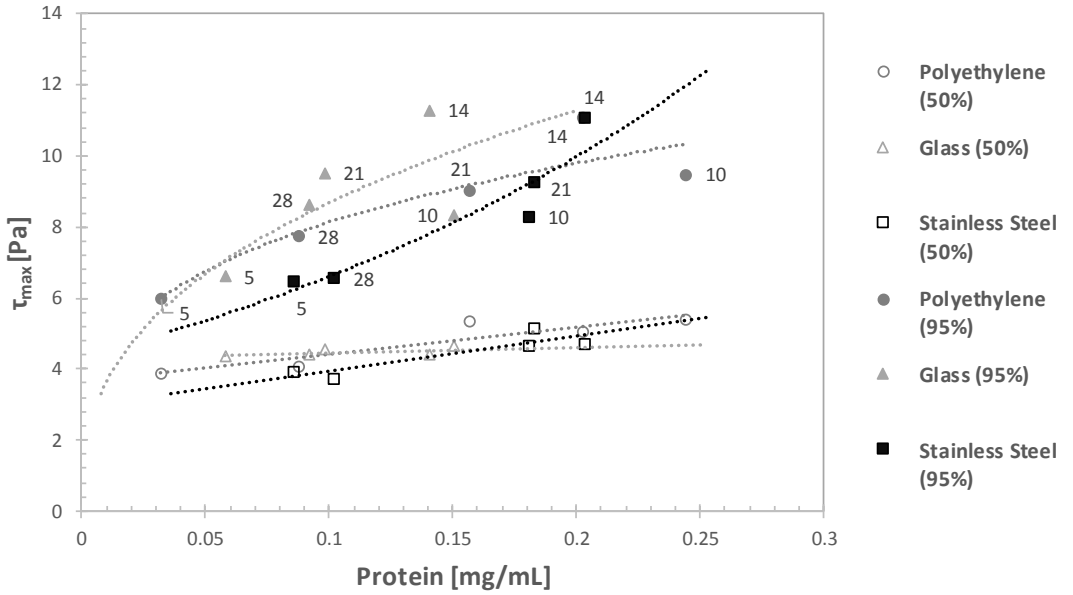

a)

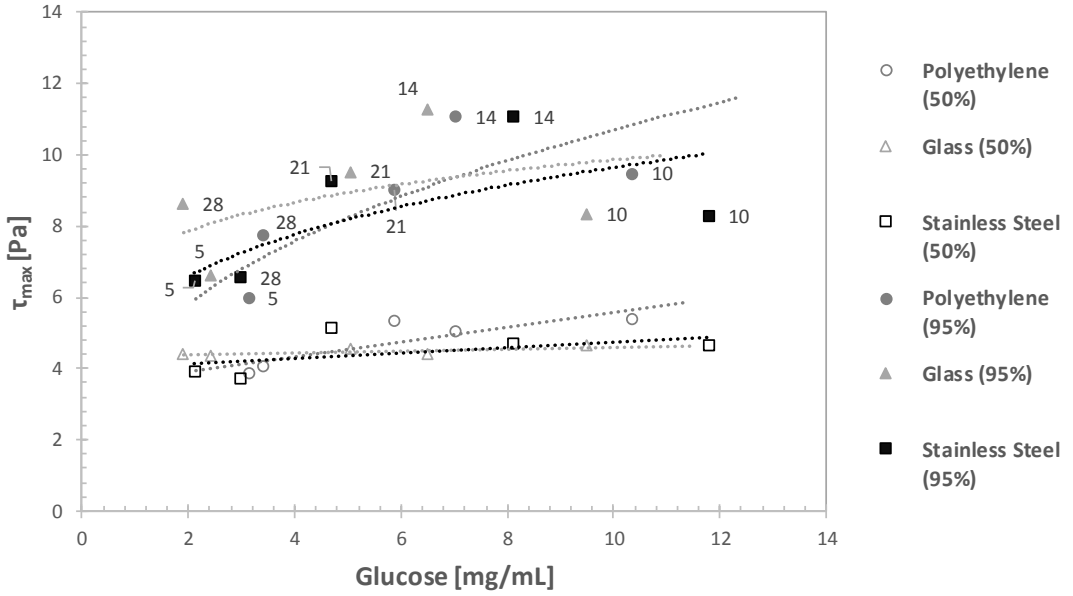

b)

Figure 75: Comparisons between cohesive strength values and recorded amounts of a) protein and b) glucose in the equivalent biofilm samples. All data are taken from mixed species biofilms. The incubation periods (in days) are shown in the labels.

Similarly, there appears to be a correlation between protein concentration and cohesive strength, although the relationship is less clear. The linear trendlines are no longer suitable as they were for adhesive strength, the results here being more suited to the logarithmic curves seen for glucose in Figure 66. The implication here is that there is more of a limit to the effect of protein levels on the adhesive strength, with the gradients starting to reduce as the protein continues to increase. The exception to this rule is the biofilms grown on stainless steel, where the strength can be seen to be consistently dependent on protein concentration, with the rate of increase growing exponentially (at

least within the limits of this data). As for graph b), the correlation between polysaccharides and cohesive strength was notably weaker. The figures tend to suggest that the levels of protein in the biofilm are more of a factor in biofilm strength than polysaccharides, particularly in establishing strong bonds with the surface. In comparison with Figure 68, protein and polysaccharide concentrations are much more closely linked to cohesive strength than the thickness of the biofilm. This could indicate the degradation of EPS and/or the death of cells, as despite there being no loss of thickness as the biofilms continue to age, there is a reduction in both components and a greater ease of removal of non-surface layers.

Summary

To conclude this section, the surface material has a negligible impact upon the thicknesses which biofilms can reach. There is also little difference with regards to the species involved. In general terms they grow in an exponential fashion up to 14 days, and then remain at that particular thickness (80-120 Pa) at least until 28 days have passed. However, although total biofilm thickness becomes stationary after 14 days of growth, removal via hydrodynamic processes starts to become easier as the biofilms age. This was also witnessed in the adhesive strength section, whereby the biofilms were typically more strongly-attached after 14 days before becoming easier to remove thereafter. This is where the dynamics of the growth cycle become more relevant.

In accordance with the theory of biofilm development (section 2.3), this is a hallmark of the stationary phase in which detachment processes begin to occur alongside continuing cell reproduction. Sloughing, for example, is viewed as being inevitable for biofilms once they reach a certain thickness as the connection between the outer layers and the surface becomes more distant. The increased deposition of EPS due to age can result in deepening nutrient and oxygen gradients between the cells at the surface, which are frequently starved, and those at the outer layers who are able to access greater resources. This makes structural weakness a regular reality of older, thicker biofilms, which will logically have a significant effect on cohesive strength. Cell death is another possibility, although as discussed in section 2.3, it is a poorly understood factor in the biofilm life cycle. It is possible to observe the presence of dead cells using microscopic methods, however, even if the mechanisms responsible are not determinable.

Regarding the species themselves, it can be said using results from both strength and thickness test results, that *E. coli* is able to form considerably stronger biofilms than either *B. cepacia* or the mixed biofilms containing both species. After the strength tests, this was presumed to be the case following results where removal from the surface required maximum shear stresses of 25-35 Pa for *E. coli* but only 15-25 Pa for *B. cepacia* and mixed species. Having tested the cohesive strength via thickness reduction in this section, the difference has been shown to be even more pronounced. That a strong surface attachment should appear to lead to a stronger cohesion sounds unsurprising at first, although in terms of cell reproduction is not necessarily a given. More likely is that *E. coli* is able to produce a

stronger extracellular matrix, which is the common feature of adhesive strength and cohesion. The similarity observed between the strength of *B. cepacia* and mixed species biofilms in both cases suggests that, rather than developing a collaboration, the two species are acting on competition with one another. This process can take various forms, such as one occupying the nutrient-rich outer layers, or the restriction of growth to microcolonies. Whatever the explanation, this shows that despite the general observation that mixed species biofilms exhibit greater resistance to biocides, this is not automatically the case for resistance to hydrodynamic stresses.

With regards to cleaning, carrying it out after either 5 or 21-28 days would result in the easiest removal. If the decision was made to clean after 21 days or more of growth, this would carry a greater risk of contamination due to the opportunity for the dispersal of pathogenic cultures. The relative ease of removal at this stage implies that sections of biofilm can readily detach from the bulk deposit, and it is logical due to the findings of these experiments to suggest that this may regularly occur under normal process flow conditions. On the other hand, the greater regularity of cleaning after every 5 days would incur greater energy and water requirements. A cleaning protocol would therefore be dependent on the industry in question (for example, food production may demand the regular cleaning option due to the enhanced dangers of biological contamination).

Table 8: The full set of shear stress values required to remove 50% and 95% thickness of *E. coli*, *B. cepacia*, and mixed species biofilms grown under static conditions from polyethylene, glass and stainless steel.

	Removal from Polyethylene [τ_{max}]					
	E. coli		***B. cepacia***		**Mixed Species**	
Days	**50%**	**95%**	**50%**	**95%**	**50%**	**95%**
5	4.9	8.0	3.4	6.1	3.9	6.0
10	5.0	20.2	5.0	11.7	5.4	9.5
14	4.8	17.7	4.6	10.5	5.0	11.1
21	3.1	7.8	4.4	8.3	5.4	9.0
28	4.3	6.4	4.0	7.4	4.1	7.7

	Removal from Glass [τ_{max}]					
	E. coli		***B. cepacia***		**Mixed Species**	
Days	50%	95%	50%	95%	50%	95%
5	5.3	9.3	3.7	5.4	4.4	6.6
10	4.9	9.4	4.0	7.7	4.6	8.4
14	4.4	14.7	4.6	9.6	4.4	11.3
21	4.8	10.6	4.7	9.4	4.6	9.5
28	4.0	9.7	4.0	8.8	4.4	8.6

	Removal from Stainless Steel [τ_{max}]					
	E. coli		***B. cepacia***		**Mixed Species**	
Days	**50%**	**95%**	**50%**	**95%**	**50%**	**95%**
5	4.3	8.4	3.8	6.5	3.9	6.4
10	5.3	16.9	4.9	9.8	4.6	8.3
14	4.9	20.7	4.4	8.6	4.7	11.1
21	3.0	9.2	4.3	8.0	5.2	9.3
28	3.2	7.9	3.8	6.3	3.7	6.5

5.8 Biofilm Characterisation – Confocal Microscopy

5.8.1 EPS Coverage

Here was can assess whether or not there is a significant difference in the proliferation of EPS between 14 and 21 days' incubation, the period in which the weakening of the biofilms appears to commence.

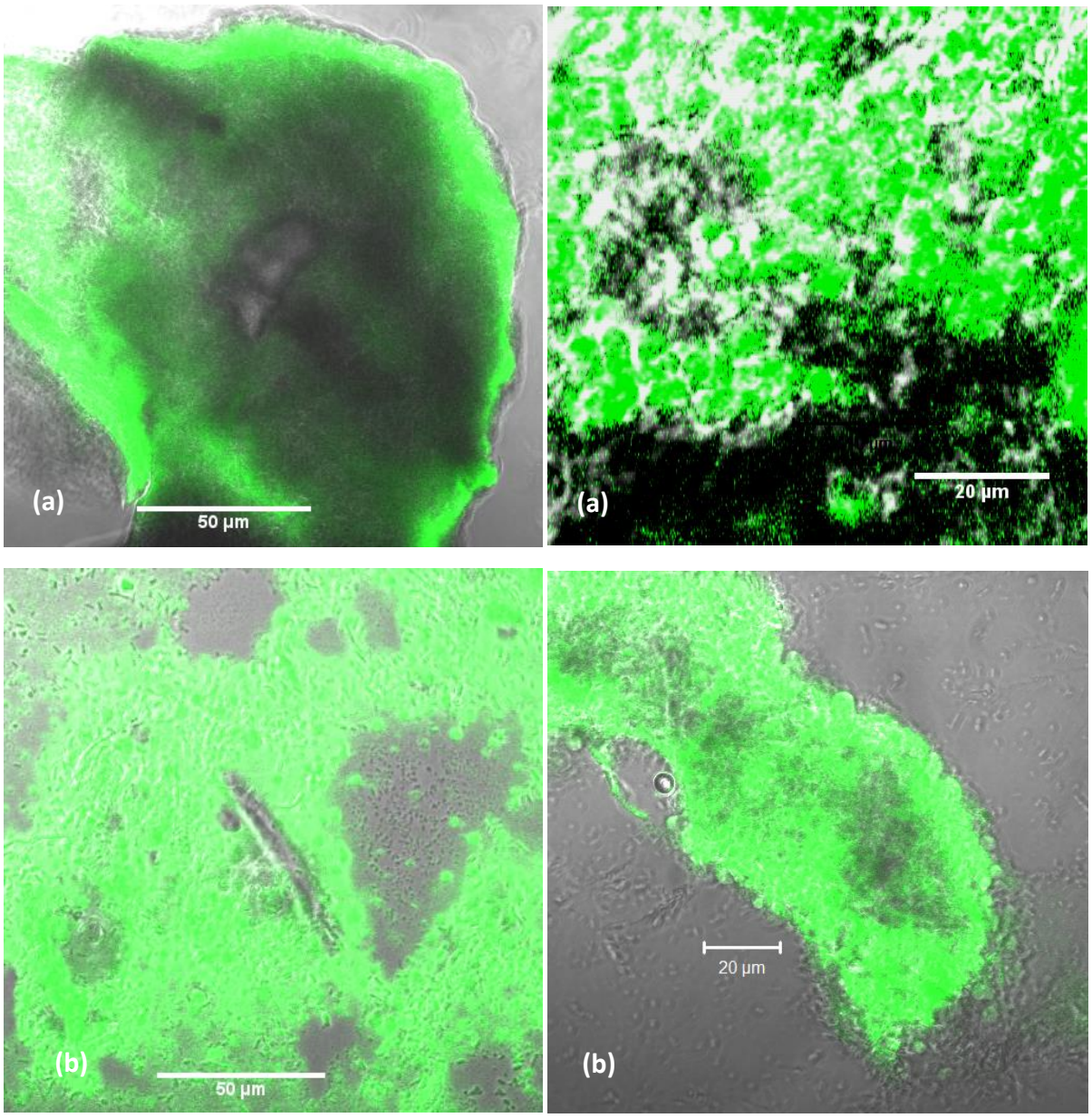

Figure 76: CLSM images showing the extent of EPS coverage on *E. coli* biofilms grown on glass for (a) 14 days; and (b) 21 days.

The images in Figure 76 do not suggest a particularly close relationship between the extent of EPS coverage and strength of attachment. Both 14-day images show a substantial coverage, but the bottom-left image has a similarly extensive amount of EPS. There is also little difference in the density of biofilm-containing regions. From this evidence there appears to be little to suggest that it is

a reduction in EPS coverage which leads to easier removal of biofilms. This contrasts with a reduction in protein and polysaccharide content over this time period, which was shown in the previous section to have a relevant correlation with a loss of biofilm strength. It is possible that some of the proteins and polysaccharides have suffered degradation and formed simpler hydrocarbons (aldehydes, ketones etc.), or that there has been losses of EPS which have not impacted upon the ratio of coverage.

5.8.2 Live/Dead Staining

The widespread death of component cells is also recognised as a source of reduction of stability and biofilm loss. Differential staining of cells and CLSM imaging has been employed in order to assess whether or not this could be a possible reason for the loss of strength between 14 and 21 days instead.

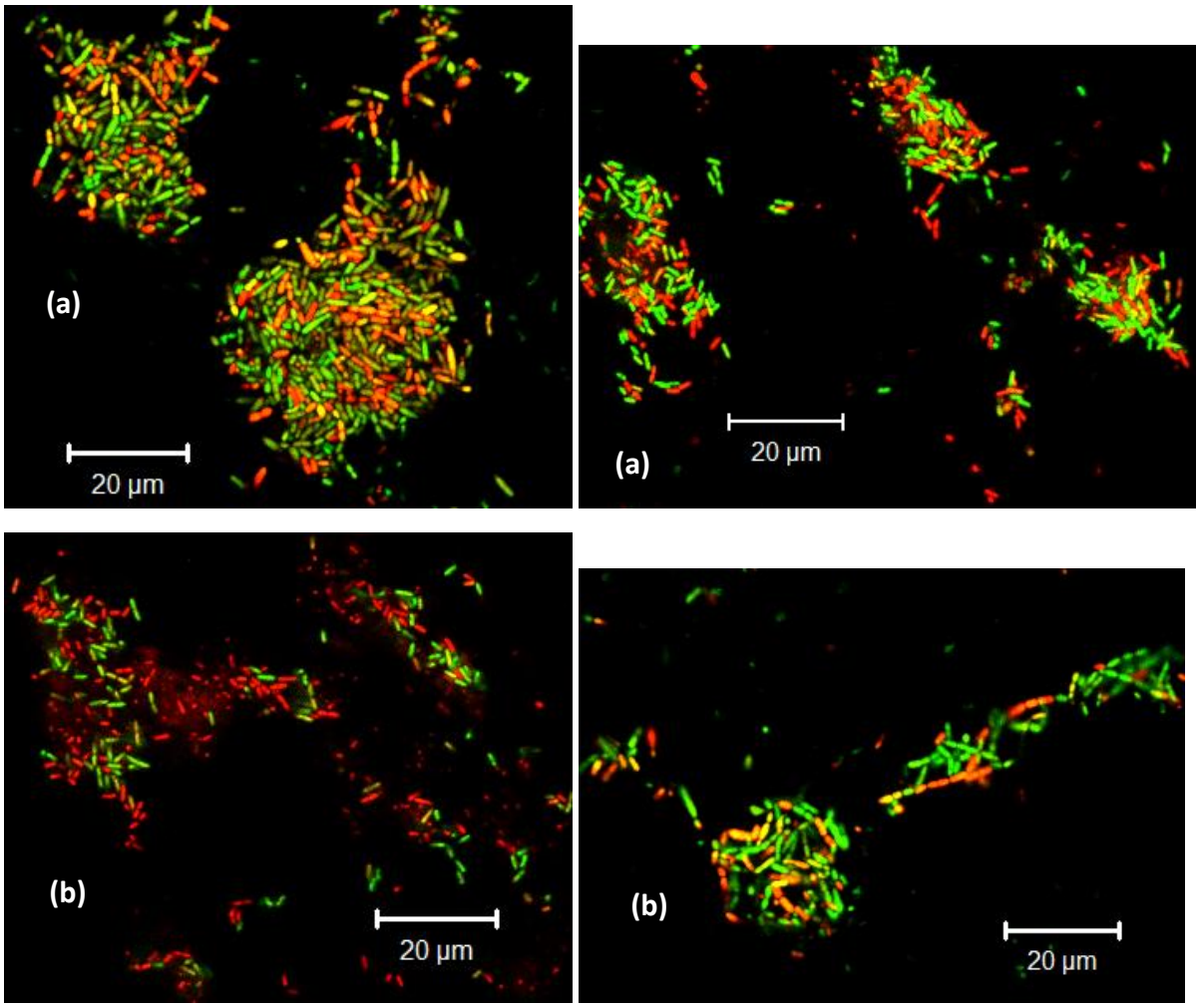

Figure 77: CLSM images showing the presence of live and dead cells in *E. coli* biofilms grown on glass for (a) 14 days; and (b) 21 days. Live cells are stained green, dead cells are stained red.

As with the EPS coverage staining tests above, there is not much conclusive evidence in Figure 77 to suggest that a significant increase in dying cells is a major cause of ease of biofilm removal. Even after 14 days, it can be seen that there is a reasonable presence of dead cells in amongst the regions of biofilm, the point at which they have been recognised as being at their strongest. The 21-day image on

the left has a dinstinct presence of dead cells (they also appear to be reduced in number) , yet the respective mage on the right shows mostly live cells. The long-term development of biofilms consists of a continuous process of cell death and reproduction, so therefore trends regarding live/dead cell proportions can be relatively difficult to spot. The images do suggest, however, that the biofilms are still producing new, living cells and this can be taken as evidence that cell death is unlikely to be a significant factor in the first stage of biofim structural weakening.

6. METHODS – Biofilms Grown Under Flow Conditions

This chapter explains the procedures undertaken in the study of the adhesion and removal behaviour of *Escherichia coli* and *Burkholderia cepacia* biofilms grown under duct flow conditions using fluid dynamic gauging (FDG). The objective here is to assess the development of biofilms up to and including 14 days of growth, observing how the strength of attachment and thickness of the cultures) effects of fluid dynamics on the establishment of a culture. The use of chemical biocides is also studied in this section, in order to assess how much impact they have on biofilm removal compared to purely hydrodynamic methods, and therefore balance the amounts of water and chemicals used in cleaning in keeping with green cleaning principles.

6.1 Materials

6.1.1 Bacteria Strains

As for Chapter 4, biofilms were grown using *Escherichia coli* Nissle1917, and mixed-species biofilms of *E. coli* and *Burkholderia cepacia*. Monoculture biofilms of *B. cepacia* were not grown this time around due to the similarities to the mixed species biofilms in the previous section and the limitation of being able to run only one incubation at a time due to the nature of the reactor.

6.1.2 Culture Media

All biofilms were grown using M9 minimal media, as detailed in Section 4.1.2.

6.1.3 Test Surfaces

Some alterations were required for the growth surfaces in this section due to the features and geometries of the duct flow apparatus. The polyethylene petri dishes were used again, but the bases were sliced into 25 x 25 mm^2 pieces. This approach was not possible with the glass petri dishes, so glass coverslips (24 x 24 mm^2) were used instead. The glass used for the coverslips had been pre-treated with hexamethyldisilazane (HMDS), which makes the surface more hydrophobic (as demonstrated in Section 5.4.2) to assist coverage for coating purposes. Finally, a stainless steel 316 plate of dimensions 160 x 25 mm^2 was prepared in order to fit the dimensions of the duct (Section 6.2.1).

6.2 Duct Flow Apparatus

There are various different flow apparatuses which can be utilised for this purpose. The most appropriate designs to simulate process industries are ones which apply a consistent fluid shear force to the cells whilst supplying a constant media source.

Various methods for growing biofilms under flow conditions were discussed in section 2.7. A drawback for many, however, is that they do not easily relate to practical situations which is an important pre-requisite for the study of industrial cleaning processes. The radial flow cell is a prime example of this issue – whilst useful for studying the effects of velocity or shear on biofilm growth, the conditions involved to not compare easily to real world situations (the flow regime near to the

inlet is particularly difficult to model). The constant depth film fermenter, with its scraper attachment to maintain a maximum biofilm height, also bears little resemblance to reality. The Robbins device employs a more relevant flow regime, but is aimed mostly at *in situ* testing, and removing and replacing samples for characterisation is problematic.

Linear flow systems are preferable for simulating industrial flow conditions. The continuous flow culture chamber is such a system, with a coupon placed in a trough through which growth media is pumped. The drip flow reactor (DFR) is, however, the chosen system for biofilm growth in this section, as it is the most relatable to pipe geometry operating as it does as a linear duct with the media pumped from one end to the other. It has particular relevance to areas concerning the food and pharmaceutical industries, producing an effect similar to that of a conveyor belt, and produces biofilms with fewer architectural features for ease of microscopic analysis (Goeres *et al.*, 2009). They are also relatively simple to design and build.

6.2.1 Drip Flow Reactor Design

The reactor is a simple concept in terms of design – it is the connections to pumps and feed tanks which provide the majority of the complications. The criteria for the design can be summarised as follows:

- The geometry of the reactor must be suitable for the test surfaces to be contained. The steel plate of dimensions 160 x 25mm must be able to be placed in the flow chamber, separating the chamber into lower and upper sections with some extra space provided for the chamber to be covered and sealed securely. Lower and upper sections of the reactor must therefore be completely separable for easy removal of samples with minimal disturbance.
- The upper section must allow the media to flow freely along the growth surface and then smoothly through the outlet.
- The lower section is necessary for a heat exchange system to be included, supplied with a water bath and a peristaltic pump.
- A stand which allows for the angle of the flow chamber relative to the table to be altered according to flow requirements (0, 5 and 10 degrees).
- Inlet and outlet fittings with diameters equal to 5 mm to allow tubing to be connected, for media to be pumped into the chamber and effluent to be drained out.

Shown below are the design sketches for the drip flow reactor. Firstly, there are the side-view sketches of the upper and lower sections of the flow chamber.

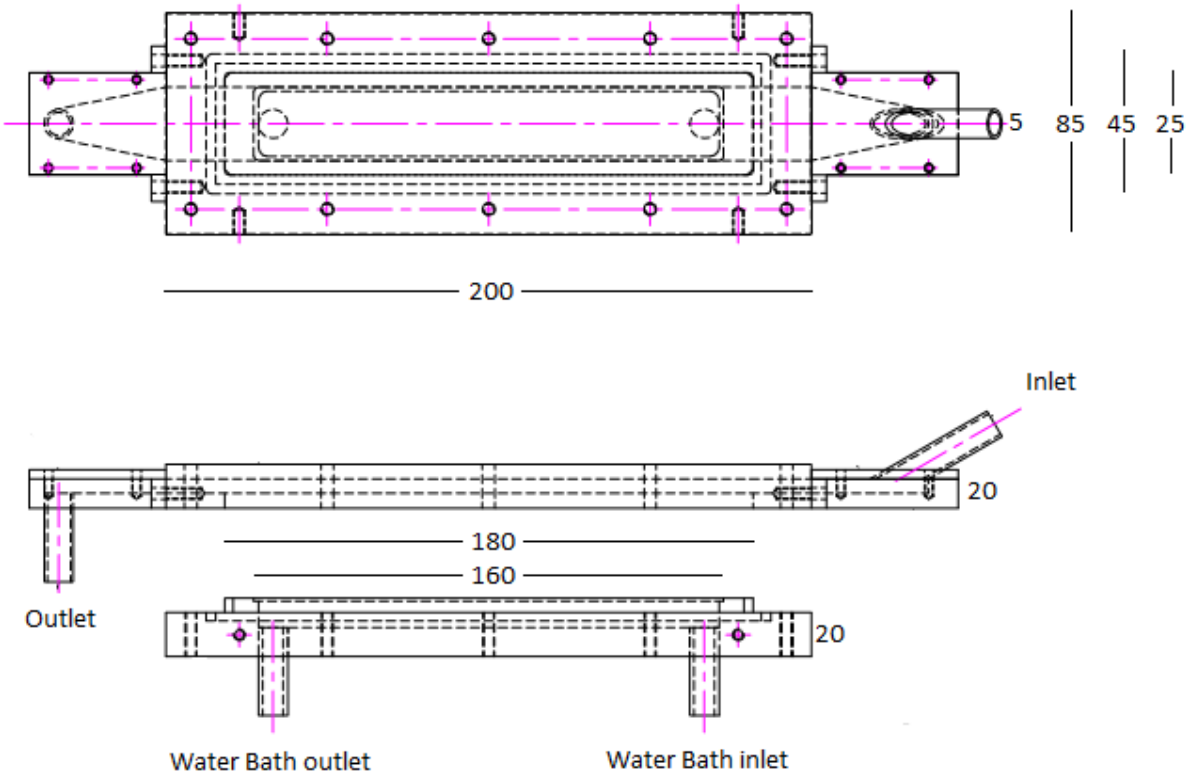

Figure 78: Birds-eye and side view designs of the drip flow reactor chamber, with the upper and lower sections of the chamber shown separately in the side view. The dotted lines represent cavities and hollow regions in the chamber. The raised section of the lower chamber shows where the growth surface is located. All dimensions are in millimetres.

The primary function of this view is to show how the reactor is sealed together in order to function properly. The protruding section of the lower half takes the space of the 20x180 mm dotted region of the top half, leaving the 10 mm high chamber within for the biofilms to grow on the 'dashed' growth surface. The inlet and outlet are shown on the upper section in the form of 5 mm diameter extensions on each side. Similarly, the heating section of the lower chamber is represented by 10 mm diameter tubes at the bottom, flowing through to an open section directly underneath the biofilm growth surface.

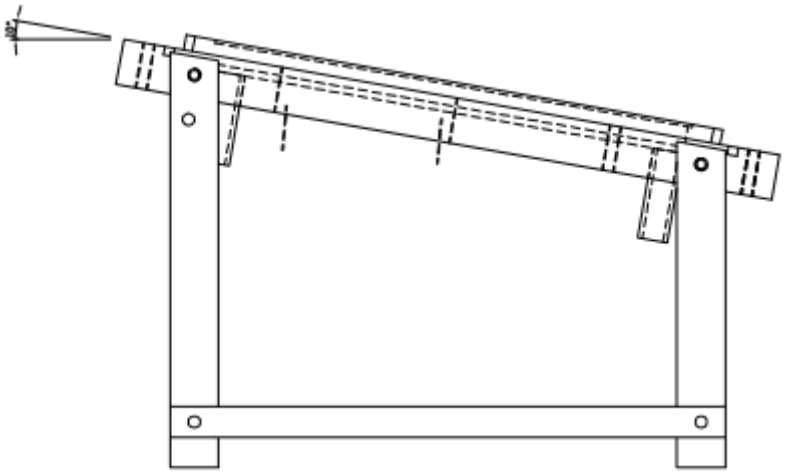

Figure 79: A side view of the drip flow reactor, situated on its accompanying stand tilted at a 10 degree angle. The dotted lines represent cavities and hollow regions in the chamber.

The view in Figure 79 shows the overall setup of the system, with the reactor chamber fitted to its stand. The angle of the chamber to the work surface can be set at 5 or 10 degrees, and can be operated as a downward or upward slant as desired, to use different flow regimes in order to alter the physical characteristics of the biofilms.

6.2.2 Drip Flow Reactor Operation

The media required for biofilm growth was supplied to the reactor using a feed tank of a volume of 30 litres with the flow controlled using a valve opened as minimally as possible to permit a trickle flow. The tank was situated on an elevated shelf to negate the requirement of a pump. The flow rate was estimated by collecting media in a measuring cylinder for ten minutes at a time, and the graph is shown in Figure 80 in Section 7.1. The general range of flow rates was between 40 and 80 mL per 10 minute interval.

The heating for the reactor was provided using a water bath, connected to the lower section of the reactor with a peristaltic pump. The water passed through one tube (the inlet) through the chamber and through the other outlet tube from which it was returned to the water bath to be recycled. This ensured that the water need not be replaced or topped up at any point in the growth process, regardless of the length of incubation period. The desired temperature of the water bath was determined by trial and error, recording the temperature of the air by the reactor outlet once it had reached a stable level, at different water bath temperatures (with the pump running at maximum power). The chamber is short enough for differences in temperature along it to be neglected. The relationship between water bath temperature and reactor temperature are shown in Section 7.1.

The outlet of the reactor was fixed to a tube which transferred the used media to a waste bucket which was disinfected and emptied on a regular basis.

6.3 FDG Tests

To ensure that the investigation was free from contamination, the apparatus needed to be kept sterile and therefore enclosed. The method chosen to implicate this was a reciprocating gauge complete with a syringe pump which would act to recycle the flow. This requires the gauge to operate under pressure mode (section 2.9.1) with a constant mass flow rate set with the syringe pump. A new set of calibration runs were undertaken in order to test the functionality of the gauge under pressure mode, and are shown in Figure 82 in Section 7.2.

6.3.1 Strength Tests

Biofilm strength tests were, as for Section 4.6, conducted by using FDG to apply a controlled shear stress to the surface and then using microscopic methods to quantify the percentage of bacteria remaining. Biofilms were grown on the stainless steel plate (160 x 25 mm), polyethylene and glass coverslips (both 25 x 25 mm) for periods of 5, 10 and 14 days. This was done using the protocol outlined in Section 4.2.1.

Imaging was performed using a Nikon Eclipse E400 optical microscope in order to provide images of the fouled surface prior to removal. FDG testing was conducted in the same manner as in Section 4.6, albeit operating under pressure mode. Tests were conducted on each surface to ensure that three repeats of each h/d_t value were completed. Following the gauging process, the surfaces were again analysed under the microscope, and the percentage reduction in surface coverage measured. A selection of examples of the images used for this analysis (from all three surfaces) are shown in Section 7.4, along with numerical analysis of the results and the related discussions.

6.3.2 Thickness Tests

Thickness measurements were taken with a resolution of ± 5 µm. The pressure drop recorded due to the presence of the fouling layer can be used to deduce the thickness of the layer, with average values taken from several points for each sample, as per intention of the original FDG experiments, by comparing the data plots with the calibration data from a clean surface. Biofilms were grown on all three surfaces for periods of 5, 10 and 14 days for thickness analysis. Multiple pressure drop readings were taken from each sample as the nozzle is moved gradually closer to the surface, as was done in Section 4.6.2, in order to quantify the cohesive strength of the biofilm.

Alongside the adhesive strength taken from the strength tests Section 6.3.1, these results will give an overall picture of the removal mechanisms and layer cohesion behaviour under stress. The results can then be compared to those shown in Chapter 5 for the static case, along with input from the surface and biofilm characterisation steps.

6.4 Impact of Chemical Biocides

With consideration for the water and energy duties required for mechanical cleaning, it is also prudent to test the efficacy of a combined chemical-mechanical approach. If an input of disinfectant can

substantially reduce water usage, this would be beneficial overall in the pursuit of a green cleaning protocol.

Sodium hypochlorite (NaClO) was chosen as the first chemical to be tested, due to its popularity (among other chlorine derivatives) in the food industry (Fukuzaki 2006). Secondly, peracetic acid (CH_3CO_3H) was used as an alternative, due to increasing interest in its potential as a disinfectant and a substantial amount of recent research in that direction. Mixed-species biofilms were grown under drip flow conditions on the stainless steel plate for 5, 10 and 14 days. Prior to removal, the FDG tank was filled with solutions of the respective chemical and left for 15 minutes, followed by commencement of the gauging process. Each chemical was used at concentrations of 100 and 1000 mg/L due to biofilm weakening and removal being observed at similar levels in previous research (Almatroudi *et al.*, (2016); Vázquez-Sánchez *et al.,* (2014)). This is in accordance with the so-called 'shock chlorination' method, in which relatively high concentrations are applied for short periods of time, as opposed to the method of adding low level residuals (typically up to 10mg/L) over prolonged periods (Seiler (2006); Xue *et al.*, (2017)). Results were taken for both adhesive strength and thickness reduction (cohesive strength) and are presented in the next section.

7. RESULTS AND DISCUSSIONS: Biofilms Grown Under Flow Conditions

7.1 Drip Flow Reactor Setup

The mean flow rate of media through the reactor chamber was observed and the spread of values is shown below in Figure 80.

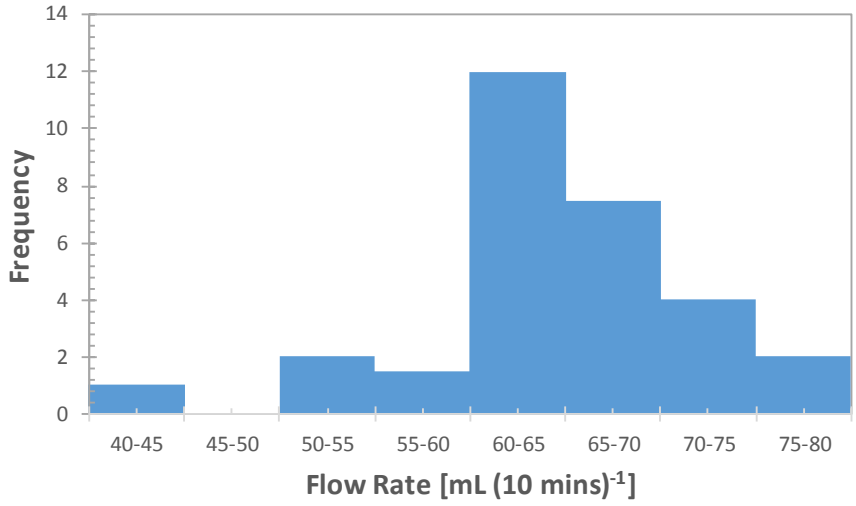

Figure 80: The spread of media flow rates recorded from the drip flow reactor with the preceding valve opened as minimally as possible. Volumes were recorded over 10 minute periods, of 30 instances.

A mean flow rate of 64.7 mL per 10 minutes (with a standard deviation of 7.22) was recorded, which equates to 9.3 $Lday^{-1}$. This ensures that the feed tank must be refilled every three days for the duration of all biofilm growth. The Reynolds number indicates whether the flow through the duct is laminar or turbulent:

$$Re = \frac{\rho U d_h}{\mu} \tag{25}$$

where U is the velocity [m/s], and d_h is the hydraulic diameter [m] which is equal to 0.022 m. At mean flow rate, the flow operates with a Reynolds number of 4.8, so therefore well within the laminar regime.

The result for the reactor temperature in relation to the water bath temperature is shown in Figure 81.

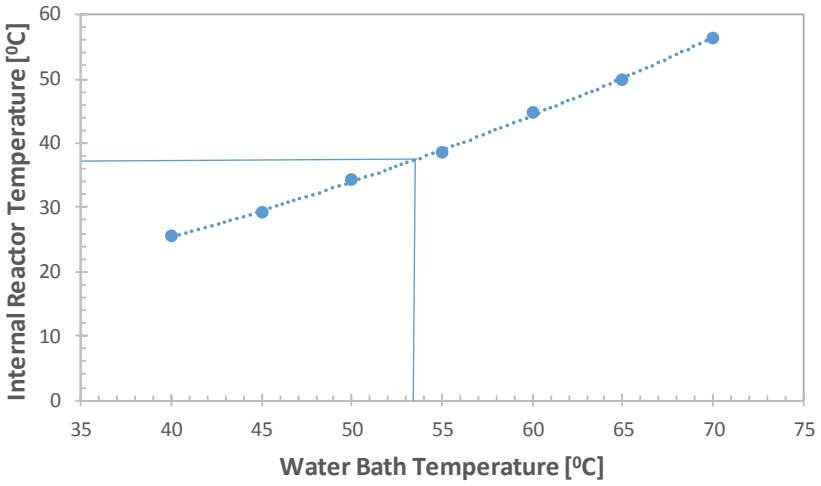

Figure 81: The relationship between the set temperature of the water bath and the recorded temperature within the drip flow reactor.

Figure 81 suggests that a water bath temperature of approximately 53^0C will be sufficient to set the temperature of the reactor chamber at the desired 37^0C for optimum biofilm growth.

7.2 FDG Calibration

The calibration step from Section 5.3 required a re-run, given the switch to pressure mode and the introduction of the syringe pump, under a range of mass flow rates. A combined graph of 3 calibrations (m = 0.5, 1 and 2 g/s) is shown below in Figure 82, firstly in terms of the pressure drop recorded, and then converted into discharge coefficient.

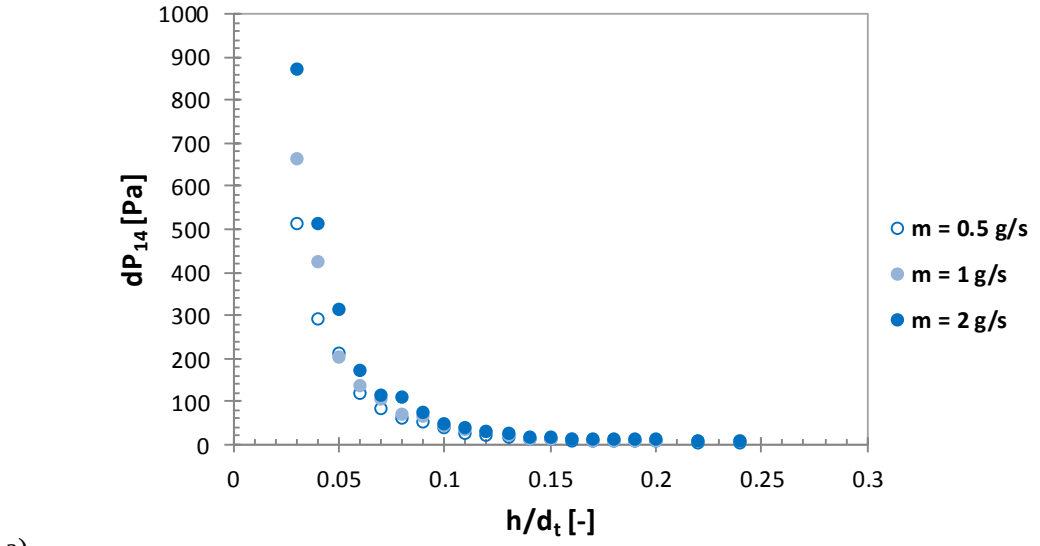

a)

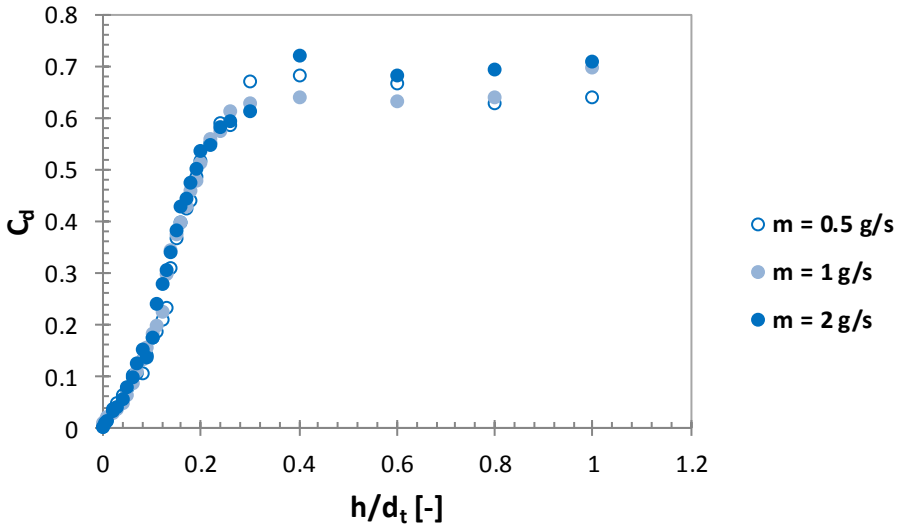

b)

Figure 82: a) Pressure drop recordings and b) C_D calibration curves for the pressure mode FDG apparatus for the following mass flow rates: m = 0.5, 1, and 2 g/s. The size of the symbols represents the potential for errors in the use of the stopwatch and balance.

The results in the incremental zone show a good level of consistency and strong correlation with h/d_t in that region, and confirms that the gauge will be operable under these conditions and can therefore be used effectively for the tests in this section.

7.3 Surface Characterisation

This section contains the atomic force microscopy results for the surfaces relevant to this section, in accordance with the methodology detailed in Section 4.4.1. Firstly, Figure 83 shows the topographic image and side profile of a glass coverslip used in the flow experiments.

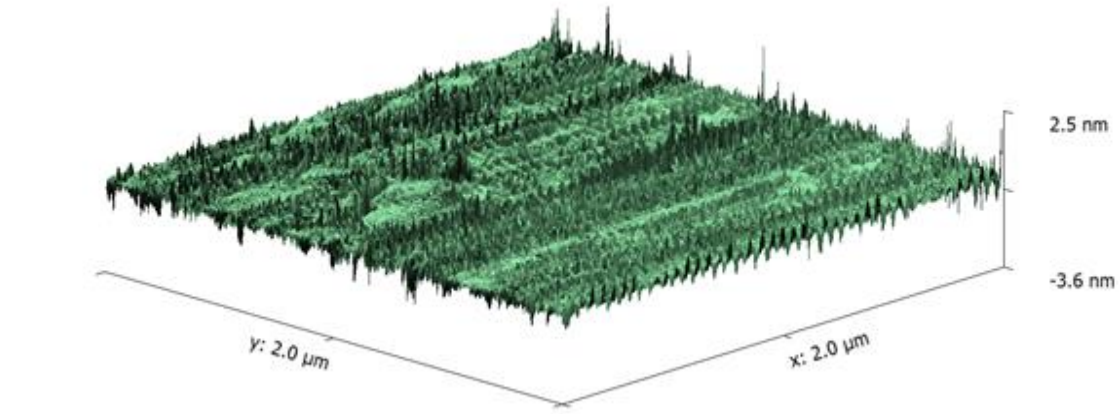

a)

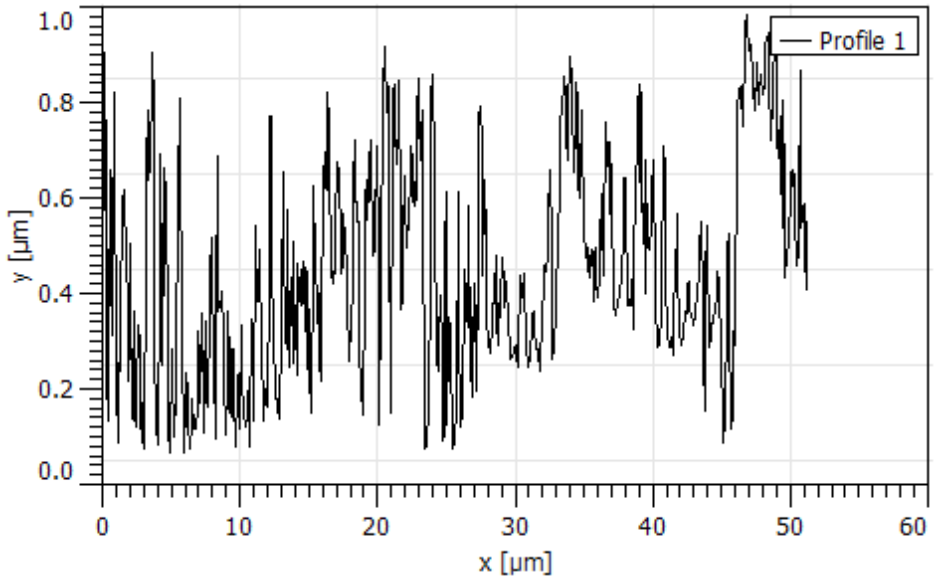

b)

Figure 83: A 3D topographic AFM image, a), showing the morphology of a glass coverslip used for biofilm growth under flow conditions, over an area of 4 µm^2, along with a side profile of the surface (b)).

In Figure 83a, the topographic image shown displays surface imperfections of sizes of approximately 3 nm. There are features which are believed to be conducive to biofilm formation, such as regions of variation between protrusions and flatter areas, but as was mentioned in the literature review (section 2.5.1) these are likely to be too small to have much of an effect. Features of a size similar to that of the cells are believed to be ideal for cell retention, yet the imperfections are mostly smaller than the cells themselves. As the side profile in Figure 83b shows, the surface has many peaks and troughs across the surface, but the troughs tend to be smaller than the cells used in any of the experiments (with a couple of exceptions).

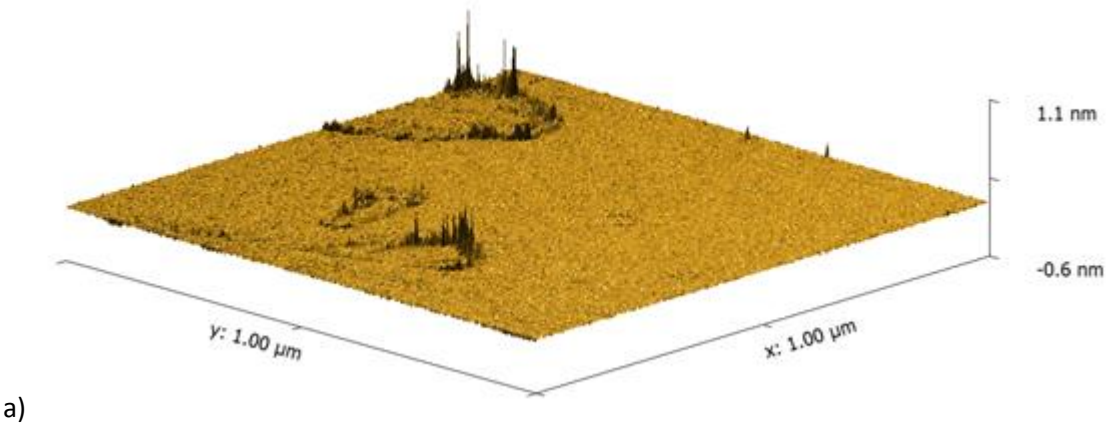

a)

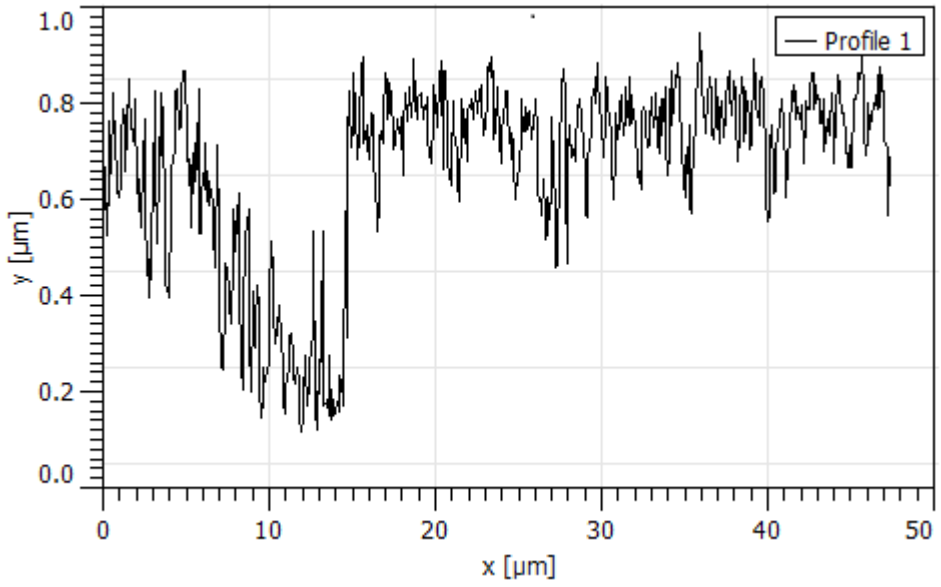

b)

Figure 84: A 3D topographic AFM image showing the typical morphology of the stainless steel 316 plate used for growing biofilms under flow conditions, over an area of 1µm^2, along with a side profile of the surface.

Figure 84a shows that there are instances of greater imperfections on the steel plate than on the disc, but these are still relatively insignificant in height (at approximately 1nm) compared to the size of the cells. Additionally, aside from these isolated peaks, the surface is extremely smooth elsewhere and is likely to introduce little or no turbulence to the flow. The side profile in Figure 84b is a good indicator of this – the presence of a notable trough stands alongside an otherwise relatively uniform surface. Given the dimensions of the cells and the crevices, the smoother surfaces may well be preferable as the rougher surfaces may provide more of a chellenge for adhesion. The width of the trough shown (about 10µm) could allow cells to lodge themselves inside, although it is a very shallow crater so the impact of is likely to be minimal. As Table 9 indicates, the plate was much less rough than the steel disc used for the static case in Section 5.

Table 9: The R_a (average roughness), R_{ms} (root mean square roughness) and R_z (average peak-to-valley height) values for the polyethylene petri dish (shown in Section 5.4.1), the steel plate, and the glass coverslip. The data for the steel disc from Section 5.4.1 is also shown as a comparison.

	Surface Material			
	Polyethylene	**Glass Coverslip**	**Steel 316 Plate**	**Steel Disc 304 (Static)**
R_a	0.256µm	0.175µm	0.089µm	0.210µm
R_{rms}	0.315µm	0.242µm	0.137µm	0.272µm
R_z	0.823µm	0.828µm	0.487µm	0.740µm

7.4 Strength Tests

7.4.1 *Escherichia coli* Biofilms

The *E. coli* biofilms grown under drip flow conditions were tested for adhesive strength using fluid dynamic gauging operating under pressure mode. Biofilms grown for 5 days are discussed first.

E. coli – 5 days

The strength test results for biofilms grown on polyethylene slips (25x25 mm^2) are shown in Figure 85:

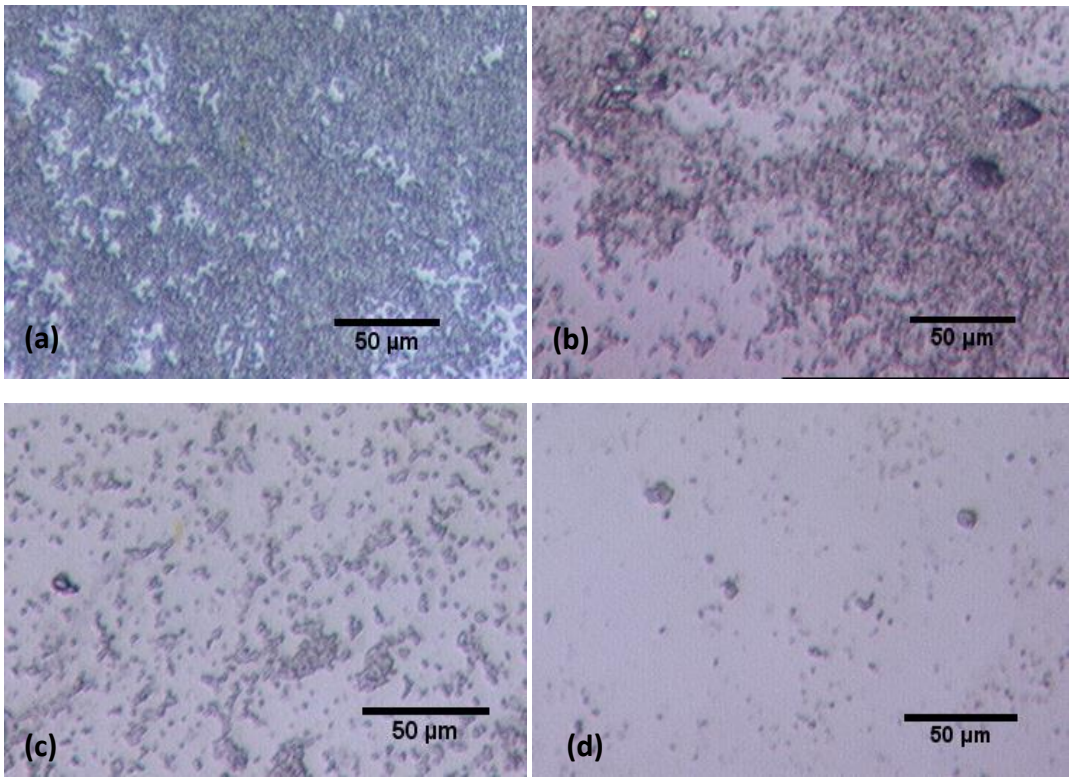

Figure 85: Optical microscope images of *E. coli* biofilms grown under flow on polyethylene for 5 days: tested under FDG at (a) h/d_t = 0.25, τ_w = 4 ± 0.1 Pa (b) h/d_t = 0.18, τ_w = 9 ± 0.4 Pa (c) h/d_t = 0.11, τ_w = 16 ± 0.2 Pa (d) h/d_t = 0.08, τ_w = 21 ± 0.4 Pa. The percentages of biofilm removed at each stage, measured using ImageJ, were: (a) 9%; (b) 46%; (c) 83%; (d) 96%.

From Figure 85, the patterns of removal of biofilms grown under drip flow would appear to be similar to those grown under static conditions (Figures 37 to 57). Within the space of the four images, the surface coverage has altered gradually from a covered surface to having only isolated cells remaining. Parts a) and b) bear a close resemblance to their counterparts from the static section (5.6.1), with 46% being removed with 9 Pa, compared to 41% removal after a shear stress of 8 Pa. There is evidence that the more resilient regions of biofilm are harder to remove in this case, however, with a scattered presence of cells remaining after 21 Pa – only 1% remained under 18 Pa shear stress for the static-grown biofilms. This may be as a result of the consistent supply of fresh media in the duct, allowing stronger bonds with the surface to be formed.

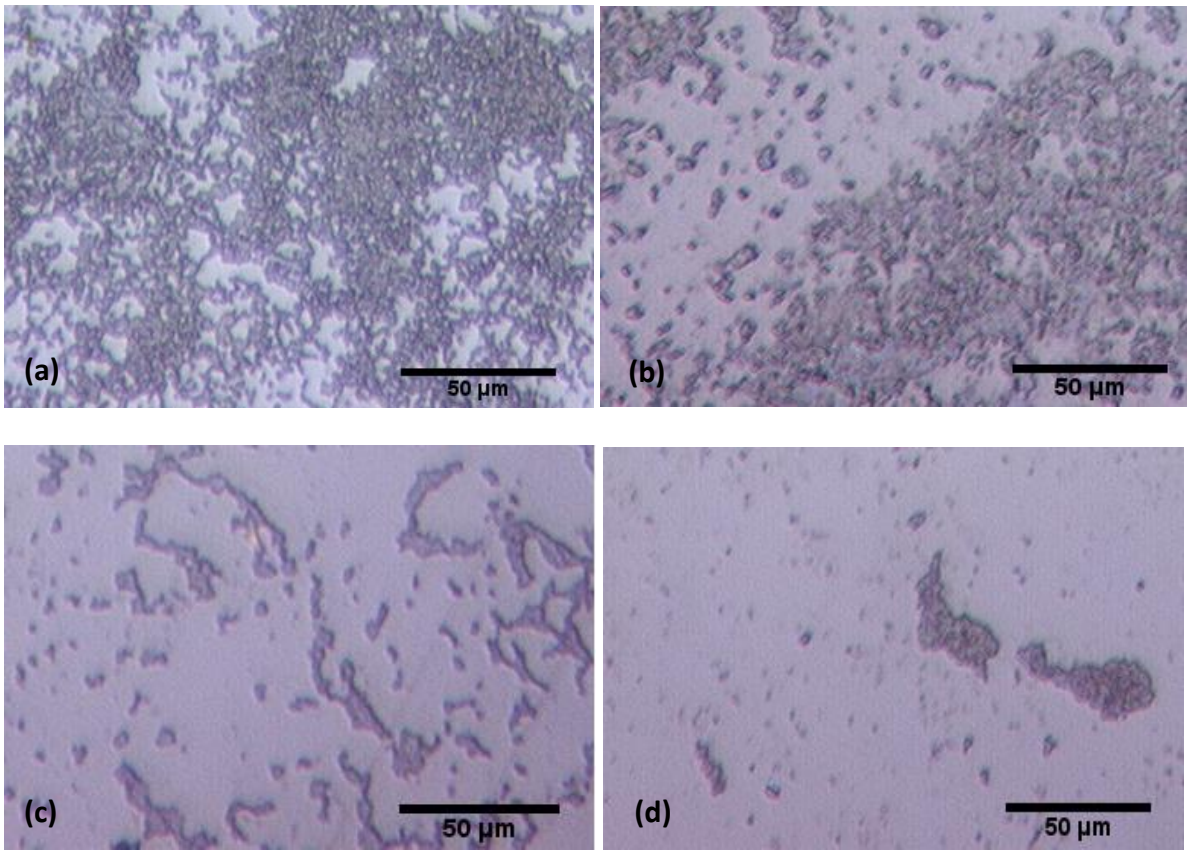

Figure 86: Optical microscope images of the glass surface with *E. coli* biofilms incubated under flow for 5 days: tested under FDG at (a) $h/d_t = 0.23$, $\tau_w = 5 \pm 0.4$ Pa; (b) $h/d_t = 0.18$, $\tau_w = 10 \pm 0.5$ Pa; (c) $h/d_t = 0.12$, $\tau_w = 15 \pm 0.1$ Pa; (d) $h/d_t = 0.11$, $\tau_w = 18 \pm 0.2$ Pa. The percentages of biofilm removed at each stage were: (a) 21%; (b) 55%; (c) 88%; (d) 94%.

The first point of note in Figure 86 is the ease at which 21% of biofilm can be removed from glass, compared to image a) from the polyethylene-based sample. This is similar to the equivalent case for the static biofilms, where there was no widespread strong attachment to glass after 5 days (although they eventually had the highest peak after 14 days). There is, however, signs of small clusters remaining attached in image d), which is more reminiscent of the polyethylene sample for this section

than previous glass-based biofilms. Removal of the strongest-attached biofilms appears so far to be notably more difficult when grown under drip flow.

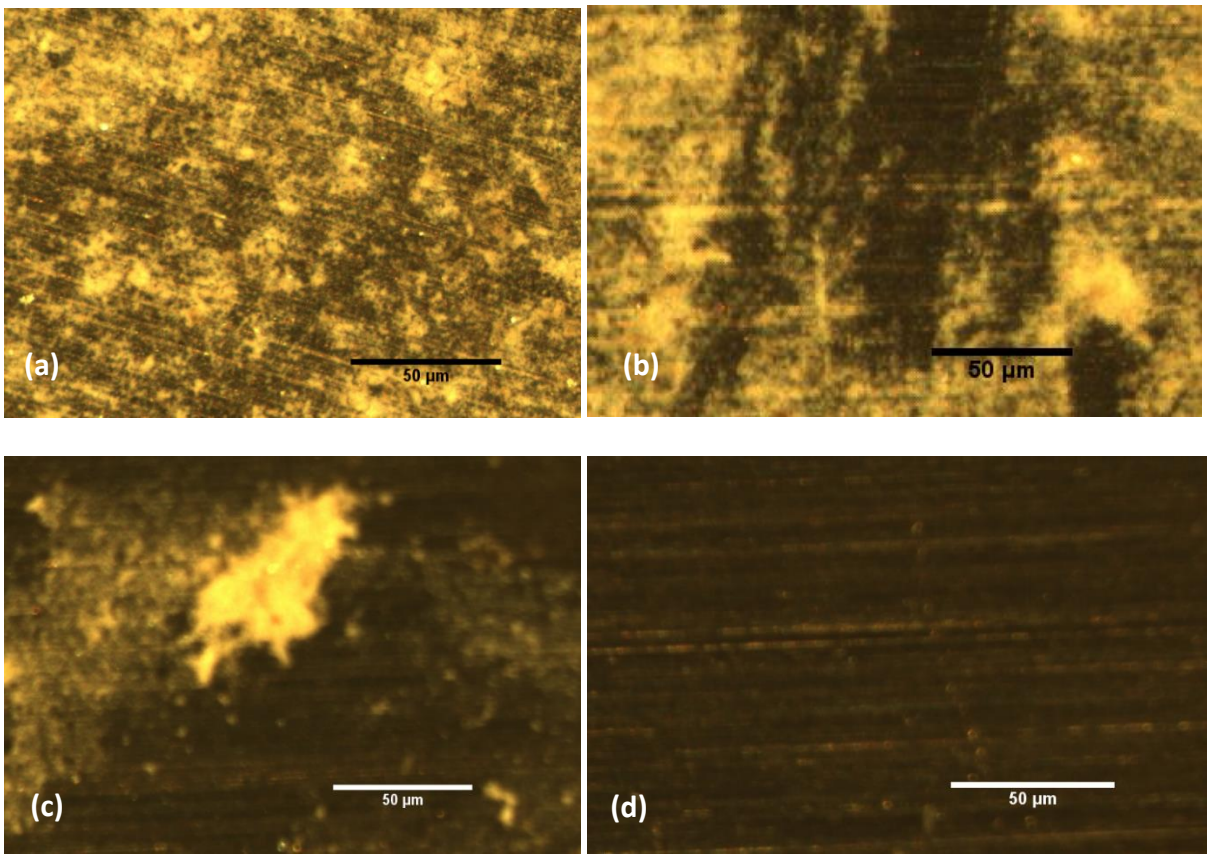

Figure 87: Optical microscope images of *E. coli* biofilms on the polished stainless steel plate under flow for 5 days: tested under FDG at (a) h/d_t = 0.21, τ_w = 8 ± 0.2 Pa (b) h/d_t = 0.15, τ_w = 14 ± 0.1 Pa (c) h/d_t = 0.12, τ_w = 19 ± 0.1 Pa (d) h/d_t = 0.08, τ_w = 25 ± 0.2 Pa. The percentages of biofilm removed at each stage were: (a) 39%; (b) 68%; (c) 86%; (d) 100%.

The effect of drip flow conditions on attachment to stainless steel over 5 days is similar again to polyethylene and glass. There is little effect on the removal of the more weakly-attached areas of biofilm, yet the stress required to remove the last remaining regions of cells is again higher than for the biofilm grown under static conditions. The 25 Pa required to clean this surface is the highest yet observed for removal of 95% or more of surface coverage, suggesting that the introduction of flow has had an impact on adhesive strength, albeit a rather modest impact at the 5-day stage.

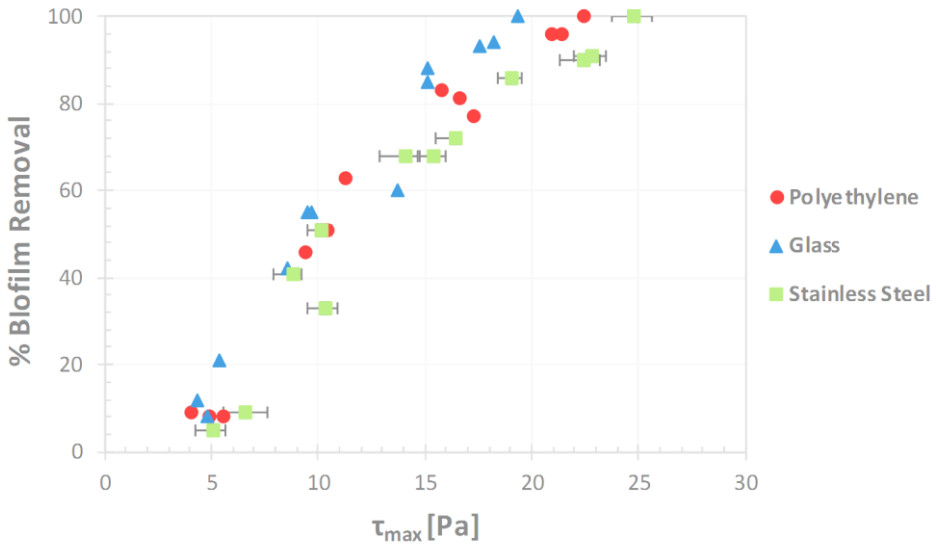

Figure 88: The complete set of strength test results for *Escherichia coli* biofilms grown for a 5-day period on polyethylene, glass and stainless steel, using the drip flow reactor.

The relative uniformity of adhesive strengths across all three surfaces is the most striking feature of this graph. This has rarely been the case in previous instances, particularly after 5 days where distinctions between surface attachments tend to be more pronounced. The spread of data points for the equivalent case for static-grown biofilms (Figure 40) was especially wide – a shear stress of 9 Pa, for example, was able to remove between 25% and 80% of biofilm depending on the surface. Here however, the extent of removal shows a strong correlation with shear stress regardless of substrate. The removal of the final 20% of biofilm hints at a dependence on surface, with biofilms on glass being easiest to remove and those on stainless steel being most difficult, but it would be unwise to draw major conclusions from this. That said, the hierarchy is the same as was recorded for the static case, so it may be a worthwhile observation.

E. coli – 10 days

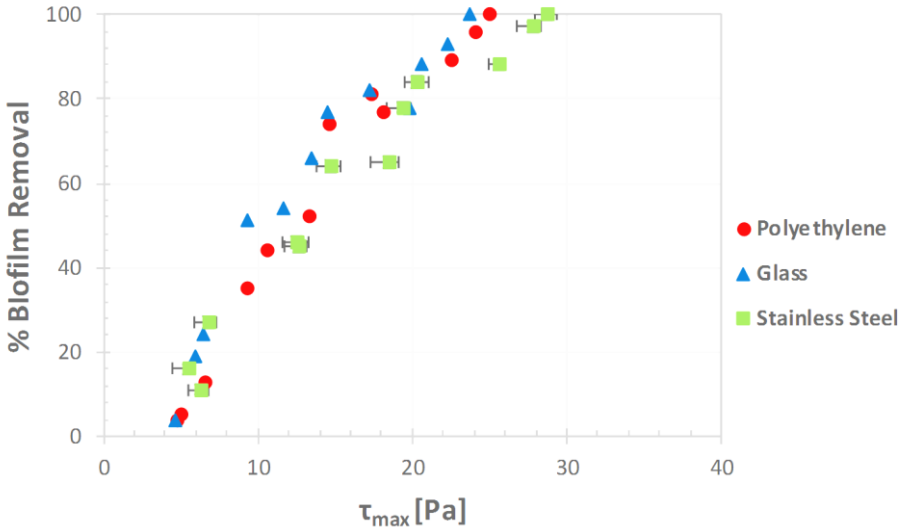

Figure 89: The complete set of strength test results for *Escherichia coli* biofilms grown for a 10 day period on polyethylene, glass and stainless steel, using the drip flow reactor.

The relative similarity between the removal behaviour from all three surfaces continues through to 10 days. Recalling the graph for static-grown *E. coli* biofilms after 10 days (Figure 41), there was a widely scattered distribution of data points. The shear stresses required for complete removal adhere to the same hierarchy as well, albeit one weak and difficult to ascertain. The increase in adhesive strength from 5 to 10 days is noticeable, although small. The removal of 50% of surface coverage required approximately 10-14 Pa, compared to 9-12 Pa after 5 days which, taking into account the potential for errors can barely be considered an increase. Complete removal does see an increase in difficulty, with at least 23 Pa required (18 Pa after 5 days). As was customary for the static case, there is a hurdle to overcome in order to remove the final 15%, particularly from stainless steel. Growing biofilms under drip flow conditions appears to make little difference to the trend for certain regions of biofilm to be more strongly attached than the rest.

E. coli – 14 days

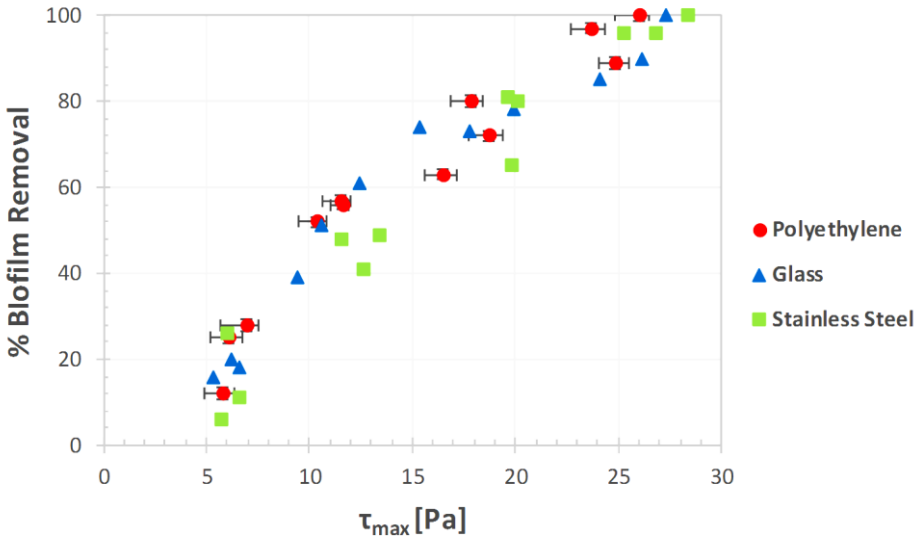

Figure 90: The complete set of strength test results for *Escherichia coli* biofilms grown for a 14 day period on polyethylene, glass and stainless steel, using the drip flow reactor.

The adhesive strength results shown in Figure 90 are a continuation of what has been observed from the previous two graphs. There is a high level of consistency to the results which crosses the variation in surface materials. Although there has been another small increase in strength of attachment, there remains little in the way of distinction in adhesion to different surfaces. From Figure 90 alone, it is inconclusive as to whether there is a surface to which biofilms adhere to most strongly under drip flow. Similarly, there is not much difference in shear stress required for total removal from the equivalent static-grown biofilms. It is, however, a different story when considering partial removal. For the static biofilms, removal of 50% or more was observed for all surfaces using 10 Pa – when grown under flow there is a more gradual loss of coverage as shear stress is increased, suggesting a greater resistance of more biofilm regions to cleaning.

Summary

Figure 91 shows the strength data for *E. coli* grown under flow conditions across the three time periods, followed by the same display for mixed species biofilms.

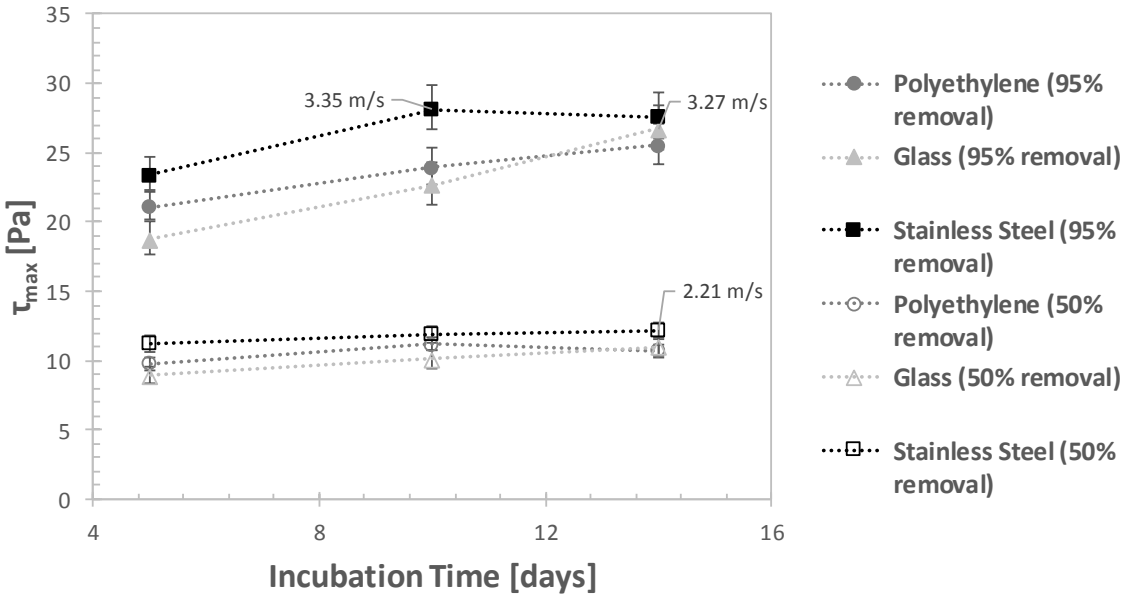

Figure 91: The overall strength test results for *Escherichia coli* biofilms grown under drip flow on all three test surfaces shown, in terms of the shear stress required in order to remove 50% and 95% of the surface coverage. Values for the equivalent pipe flow velocity are shown for selected data points (ms^{-1}).

Variations in adhesive strength as the incubation time increases are gradual for all surfaces tested. As was true for the static case, biofilms grown on glass take longer to become established, although this is nowhere near as pronounced this time around. The slight decline in strength of biofilms on stainless steel and the increase in removal requirement for polyethylene of just 1 Pa suggests that there is unlikely to be a further increase in strength beyond this point. The results for 50% removal underline the consistency of the results observed in this section – distinctions between surfaces and biofilm age are minimal throughout. Comparisons to the results for the static case are now shown.

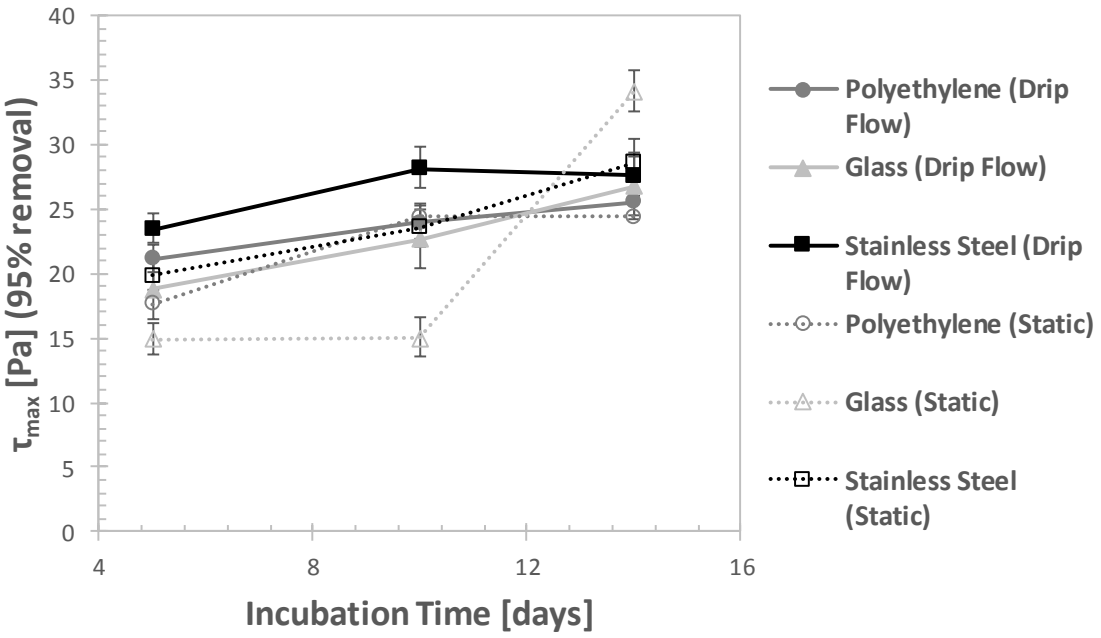

Figure 92: A comparison between the strength test results for *Escherichia coli* biofilms grown under drip flow and under static conditions, on all three test surfaces, shown in terms of the shear stress required in order to remove 95% of the surface coverage.

The above graph in Figure 92 indicates the minimal difference between 95% removal of biofilms grown under static and drip flow conditions. There is again the exception of static biofilms grown on glass, in which the shear stress required rose to an unprecedented 33 Pa (despite the attachment to glass being the weakest up to this point), than although this distinction was previously discussed in the static section 5.6.1. This graph suggests that, whatever else may vary as a result of the introduction of a prevailing flow to the growth process, ease of removal of the full surface coverage of biofilm is largely unaffected. It is interesting that the biofilms grown on stainless steel are the strongest (in terms of both 50% and 95% removal), when the steel plate was shown to be the smoothest surface in Section 7.3, although as discussed there the imperfections on all surfaces were relatively small in height and so the relevance of this is difficult to say, if any.

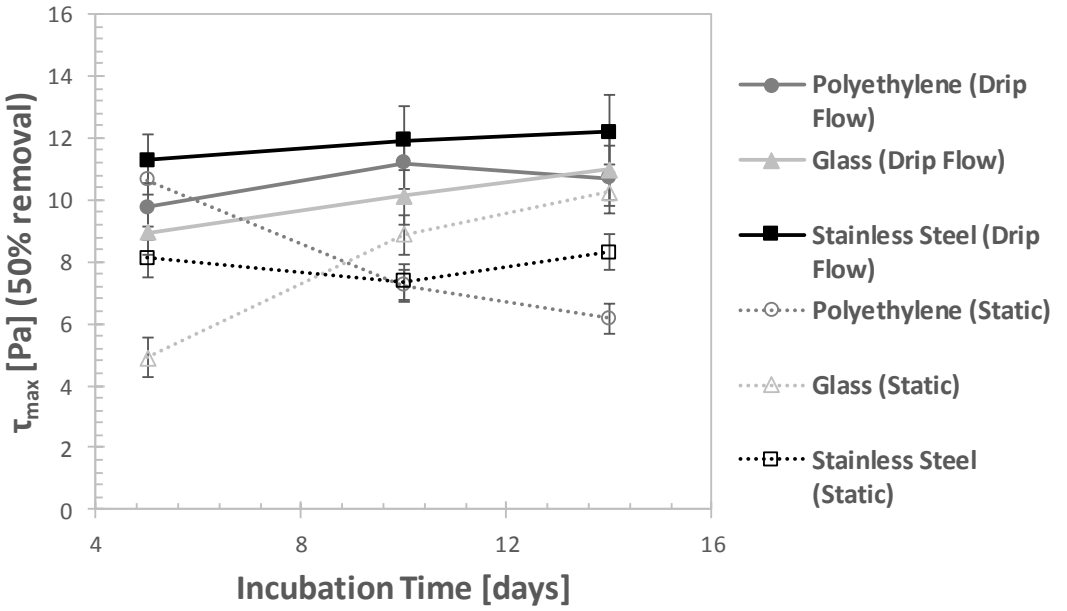

Figure 93: A comparison between the strength test results for *Escherichia coli* biofilms grown under drip flow and under static conditions, on all three test surfaces, shown in terms of the shear stress required to remove 50% of the surface coverage.

There is a more noticeable difference in the shear stress required to remove 50% of surface coverage, however. The values taken for the static biofilms fluctuate considerably, but the values for drip flow are consistently higher. The major indication here is that whilst removing 95% of the biofilm does not become more difficult under flow conditions, there is a more widespread presence of strongly inter-connected biofilms. As mentioned in the discussion for the polyethylene-based biofilms, this is most likely due to the consistent supply of growth media to the surface, promoting a stronger attachment.

With regards to cleaning, it largely depends on the problem at hand whether there should be a different strategy or not. As removal of the entire biofilm is typically essential (e.g. to alleviate a contamination risk) then there is no difference to be recommended. However, if the main issue is concerning the physical presence of biofilm (e.g. pressure drop, heat transfer), then a greater hydrodynamic force could be necessary for regular removal of bulk. This needs to confirmed in the thickness reduction section, however.

7.4.2 Mixed Species Biofilms

Mixed Species – 5 days

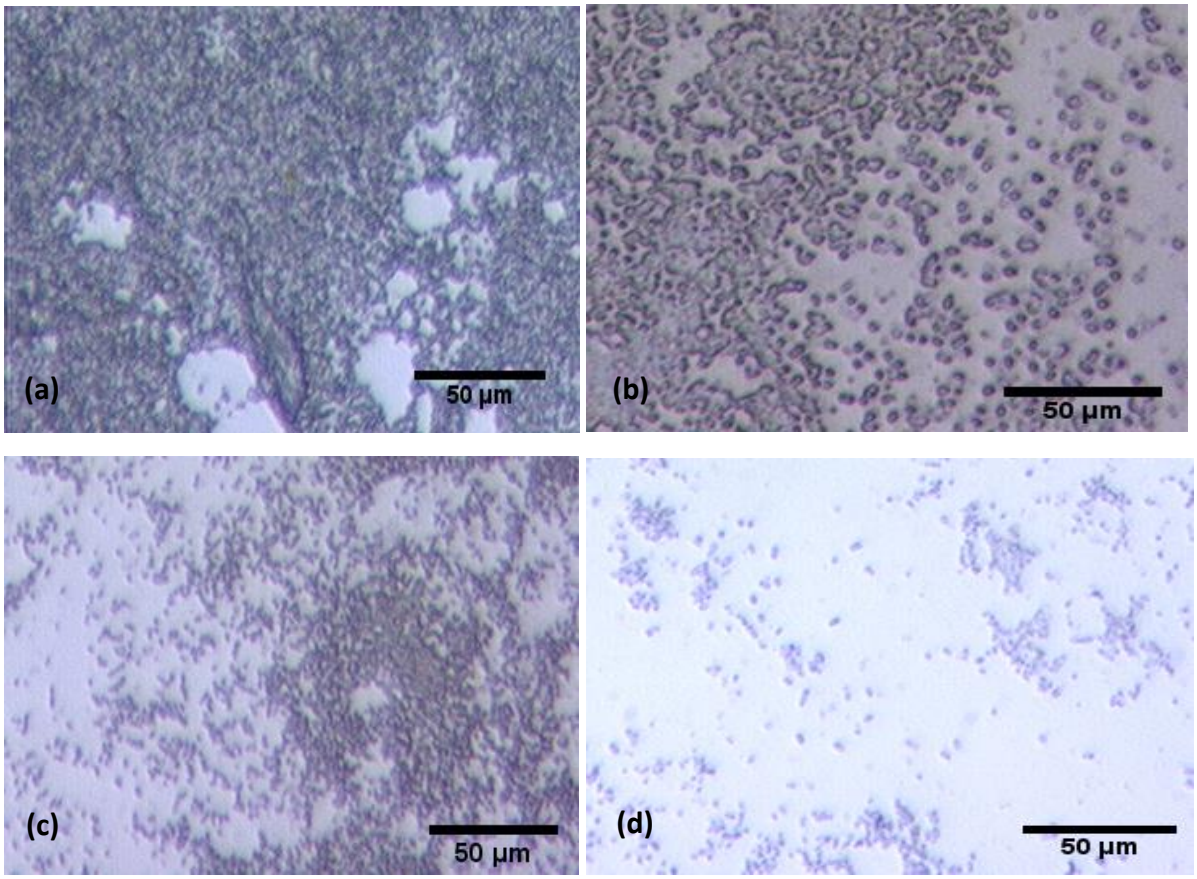

Figure 94: Optical microscope images of mixed species biofilms grown on polyethylene under flow for 5 days: tested under FDG at (a) h/d_t = 0.24, τ_w = 5 ± 0.3 Pa (b) h/d_t = 0.17, τ_w = 9 ± 0.1 Pa (c) h/d_t = 0.14, τ_w = 12 ± 0.1 Pa (d) h/d_t = 0.1, τ_w = 16 ± 0.5 Pa. The percentages of biofilm removed at each stage were: (a) 10%; (b) 49%; (c) 78%; (d) 94%.

The mixed species biofilms grown under drip flow conditions in Figure 94 display a greater adhesive strength than the 5-day old static biofilms (Figure 55). In the static case, the surface was cleaned using a shear stress of 14 Pa, whereas the drip flow sample had retained some biofilm under a stress of 16 Pa. Similarly, the static-grown biofilm was reduced in coverage by 45% with a shear stress of just 6 Pa, and the drip flow biofilm experienced a loss of 49% under 9 Pa. As was the case for the static biofilms, though, the mixed species samples were notably weaker than the *E. coli* biofilms. A shear stress of 21 Pa was unable to entirely remove the *E. coli* biofilm from the surface in the previous section.

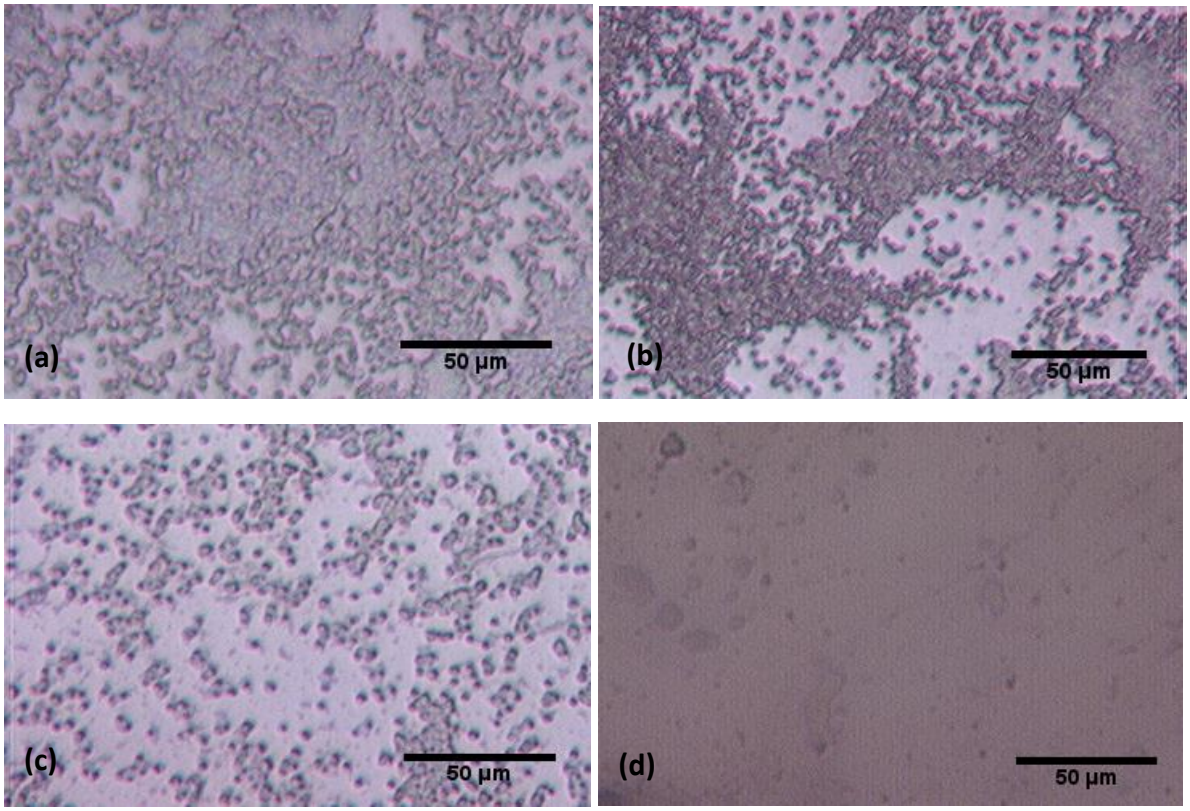

Figure 95: Optical microscope images of mixed species biofilms grown on glass under flow for 5 days: tested under FDG at (a) $h/d_t = 0.24$, $\tau_w = 5 \pm 0.4$ Pa (b) $h/d_t = 0.17$, $\tau_w = 9 \pm 0.2$ Pa (c) $h/d_t = 0.14$, $\tau_w = 11 \pm 0.4$ Pa (d) $h/d_t = 0.11$, $\tau_w = 14 \pm 0.1$ Pa. The percentages of biofilm removed at each stage were: (a) 20%; (b) 53%; (c) 77%; (d) 99%.

For the glass surface, complete removal of the mixed biofilm does not appear to be any more difficult than it was for the static biofilms grown for the same duration. Recalling the pattern observed for *E. coli* in the previous section, removing 50% of the surface coverage proved to require a greater shear stress however. In this regard, the increase from 5 to 9 Pa in order to induce this effect is substantial. This biofilm is still easier to remove than the *E. coli* equivalent which was able to remain, in depleted form, after the application of 18 Pa.

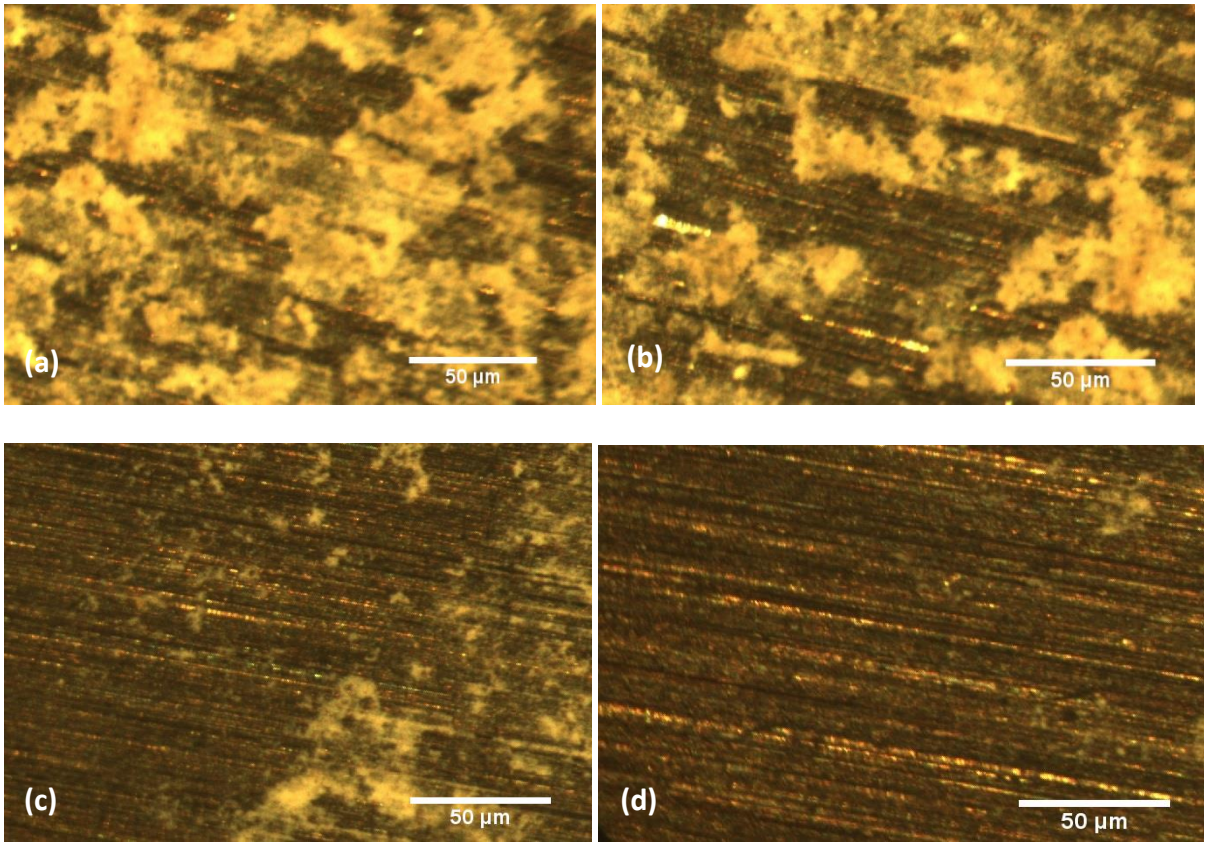

Figure 96: Optical microscope images of mixed species biofilms grown under flow on stainless steel for 5 days: tested under FDG at (a) h/d_t = 0.22, τ_w = 6 ± 0.3 Pa (b) h/d_t = 0.16, τ_w = 10 ± 0.4 Pa (c) h/d_t = 0.11, τ_w = 16 ± 0.4 Pa (d) h/d_t = 0.08, τ_w = 20 ± 0.3 Pa. The percentages of biofilm removed at each stage were: (a) 18%; (b) 47%; (c) 86%; (d) 99%.

The effect of the use of drip flow conditions for the growth of mixed species biofilms on stainless steel is very similar to that seen for glass. The application of 10 Pa shear stress is able to remove 47% of the surface coverage, compared to 78% for the static case, but 19 or 20 Pa was required to completely remove both biofilms from the surface. Again, the adhesive strength was exceeded by the *E. coli* biofilms, where 25 Pa was required to eliminate the cells from the surface.

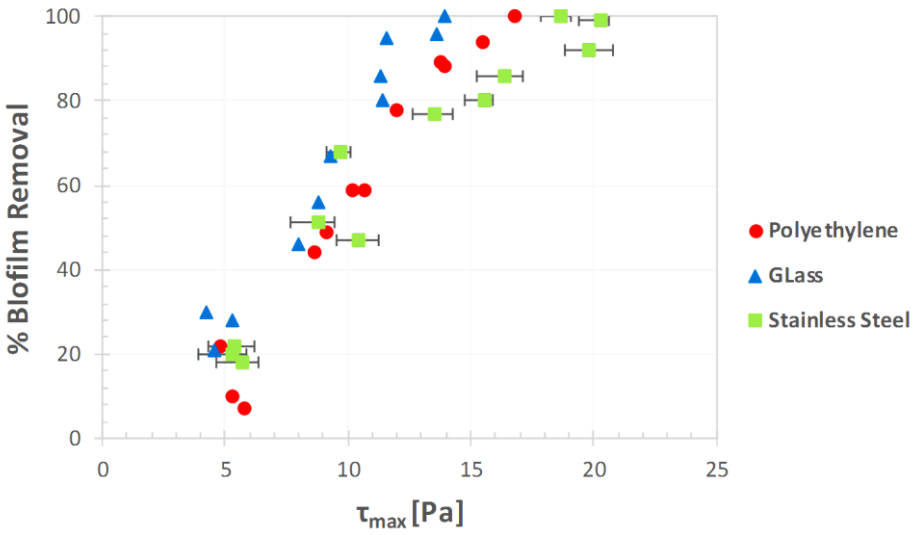

Figure 97: The complete set of strength test results for mixed species biofilms grown for 5 days on polyethylene, glass and stainless steel, using the drip flow reactor.

As was recognised in the analysis of each surface individually, there is little difference in the shear stress required to remove 95% of mixed species biofilms grown under drip flow compared to those grown under static conditions. For the static case (Figure 58), 95% removal was achieved using between 13 and 20 Pa (the 20 Pa being a relative outlier from a stainless steel sample), and the same range of total removal stresses can be seen here. The important difference is to be found in the dynamics of removal in the stages between the original biofilm and the clean surface. The transition here is more gradual, as stresses in the region of 10 Pa are required to remove 50% coverage for example – for the static case, 5 to 7 Pa was capable of achieving the same impact. This is significant because the presence of widespread biofilm can present its own issues to a system, independent from the inherent risk of any pathogenic species being present. The same trend was observed at the same stage for the *E. coli* biofilms in the previous section, particularly for the first 50% of removal. After this point, the rate of removal slows down slightly, resulting in the higher total removal strengths of 18-25 Pa. The point remains, however, that the primary impact of flow appears to a more widespread resistance to hydrodynamic forces, an effect which must be taken into account in cleaning protocols.

Mixed Species – 10 days

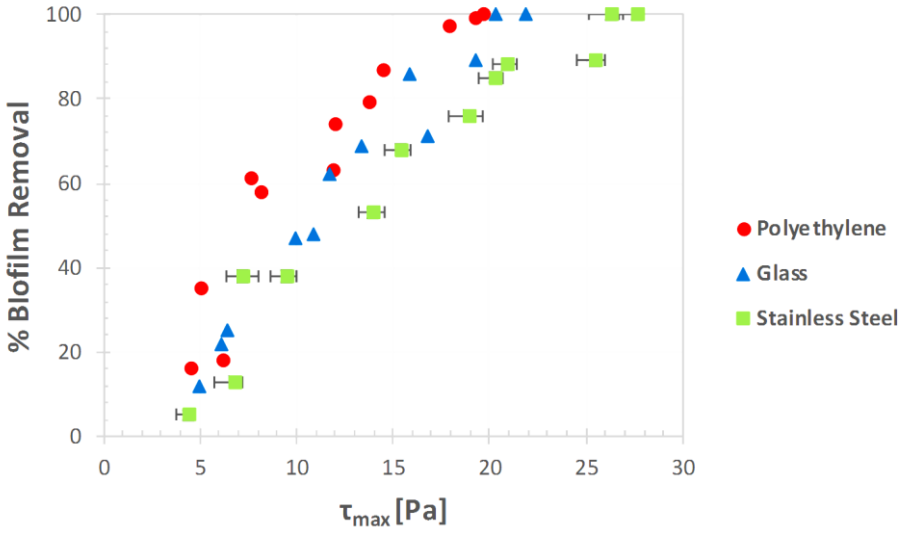

Figure 98: The complete set of strength test results for mixed species biofilms grown for 10 days on polyethylene, glass and stainless steel, using the drip flow reactor.

This graph shows the widest spread of data so far, with the suggestion that the biofilms grown on polyethylene are the weakest of the three. It can also be seen, particularly in the removal of the final 30%, that those grown on stainless steel are considerably stronger. Whilst the shear stresses required for complete removal from glass and stainless steel have each increased by approximately 5 Pa, the increase for polyethylene is closer to 2 Pa. A similar premature slowdown was observed for the *E. coli* biofilms, and for some of the static cases. It can be seen again that the increase in strength is accounted for by the most resistant 20-30% - removal of the first 50% is no more difficult than it was after 5 days' growth, in fact over 60% could be removed from polyethylene using the same shear stress.

Mixed Species – 14 days

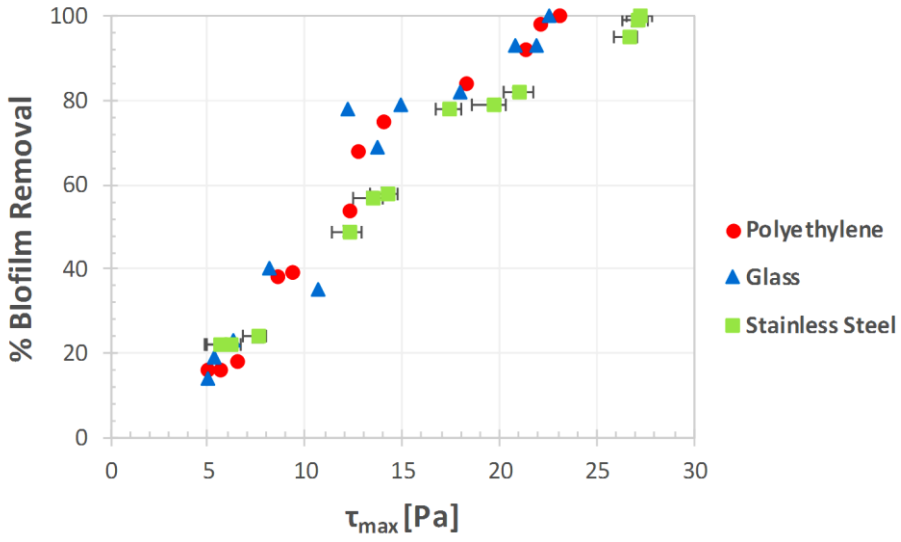

Figure 99: The complete set of strength test results for mixed species biofilms grown for 14 days on polyethylene, glass and stainless steel, using the drip flow reactor.

The transition to the 14 day incubation sees a further, small increase in shear stress required to clean the surface (between 1 and 4 Pa depending on the material). The more gradual nature of the removal process is a more noticeable and significant result, however, which suggests a more developed and mature biofilm. The consistency of the results has also returned to its previous level, with there being little between the three surfaces in terms of strength and few outliers. The biofilms grown on stainless steel are again the strongest, with the difference from the other surfaces noticeable when removing the final 20% of the surface coverage.

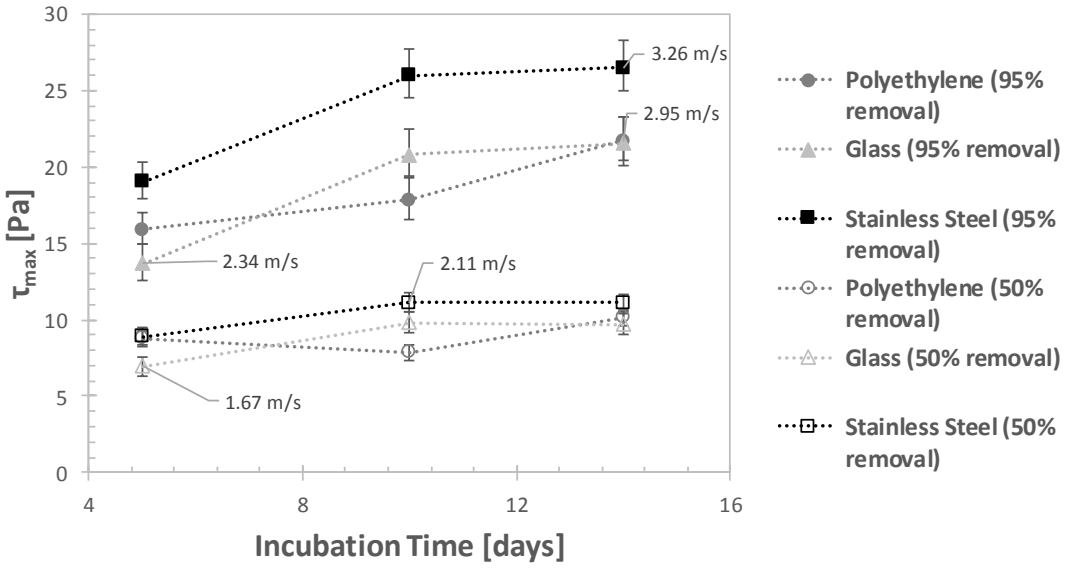

Figure 100: The overall strength test results for mixed species biofilms grown under drip flow on all three test surfaces shown, in terms of the shear stress required in order to remove 50% and 95% of the surface coverage. Values for the equivalent pipe flow velocity are shown for selected data points (ms^{-1}).

The increases in shear stress required to remove 95% of the surface coverage are similar to those observed for *E. coli*, between 4 and 7 Pa over the course of the transition from 5 to 14 days. The strength of the steel and glass-based biofilms increased only marginally between 10 and 14 days, and based on previous results it is likely that they are peak values for both surfaces. One difference in this section is the relatively high strength of the biofilms grown on stainless steel, where the results are distinct from the other surfaces at all stages. Fluctuations between shear stress values for 50% removal are greater than observed for *E. coli*, although again there are no overall trends regarding the effect of ageing. Removal of 50% from stainless steel is more difficult, although the difference is not a great one.

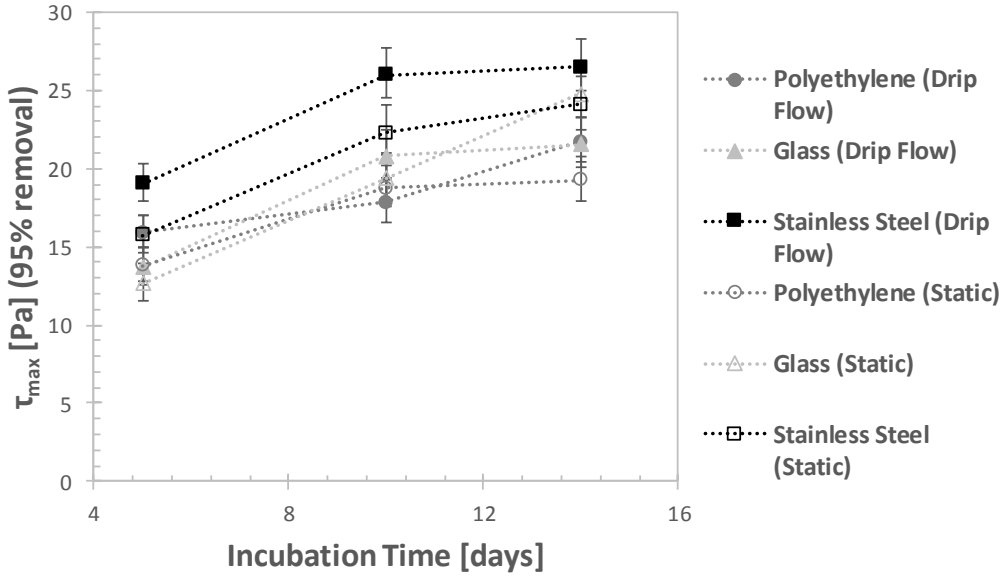

Figure 101: A comparison between the strength test results for mixed species biofilms grown under drip flow and under static conditions, on all three test surfaces, shown in terms of the shear stress required in order to remove 95% of the surface coverage.

As was observed for the *E. coli* biofilms, there is not much in the way of a clear distinction between the difficulty of removing 95% of surface coverage in the static and drip flow cases. The exception to this is the drip flow biofilms grown on stainless steel, which are the strongest for each incubation period. Otherwise, the patterns of strength increases are similar for the two cases, and any effects relating to the surface material appear to be inconclusive.

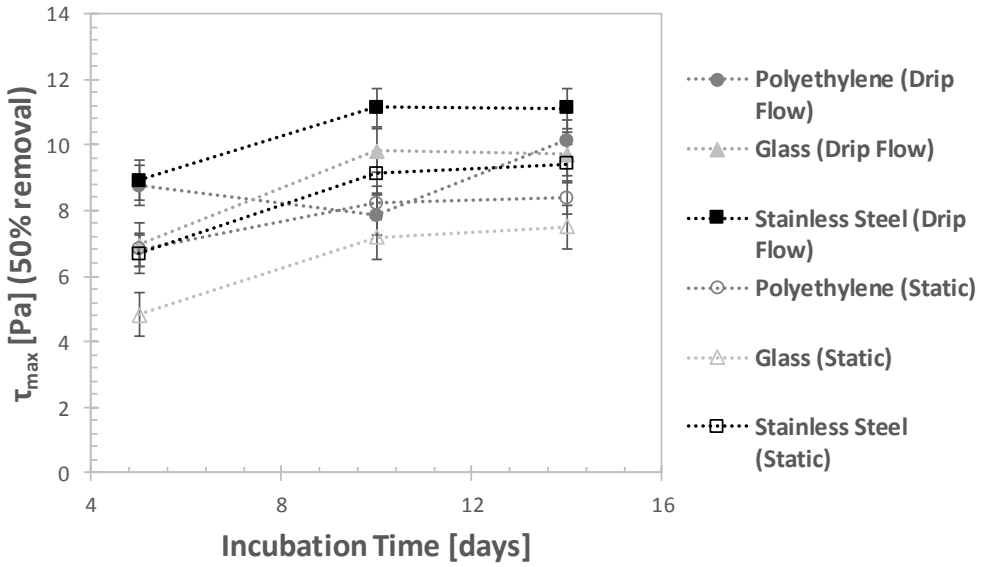

Figure 102: A comparison between the strength test results for mixed species biofilms grown under drip flow and under static conditions, on all three test surfaces, shown in terms of the shear stress required in order to remove 50% of the surface coverage.

Again, the key difference in strength between the static and drip flow cases lies in the difficulty in removing the first 50% of the biofilm i.e. the extent to which the cultures are able to develop under the two regimes. With the exception of the 10-day old biofilms on polyethylene, the rest of the data points all show an increase of approximately 2 Pa in the stress required to reduce coverage by 50%. This accounts for substantial percentage increases in strength given the low values involved. It appears to be consistent that the addition of flow has the effect of producing a wider resistance to hydrodynamic removal across a biofilm.

7.4.3 Strength Tests Discussion

In almost all cases (except for *E. coli* grown on stainless steel), the biofilms in this section showed a gradual increase in adhesive strength as they aged. Figure 103 compares the *E. coli* and mixed species biofilms in terms of their attachment to each surface independently.

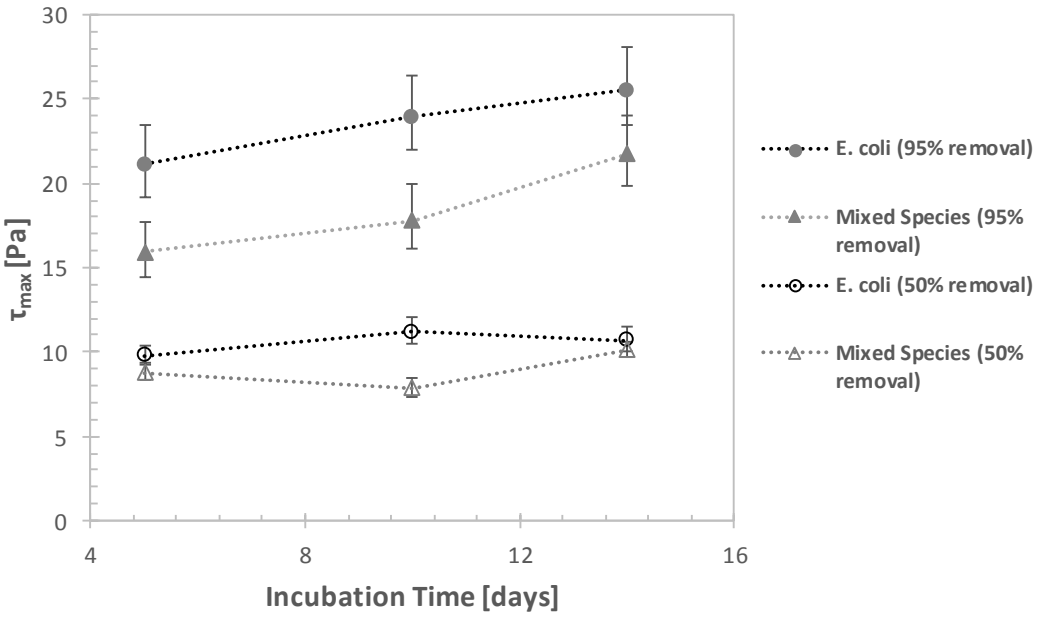

a)

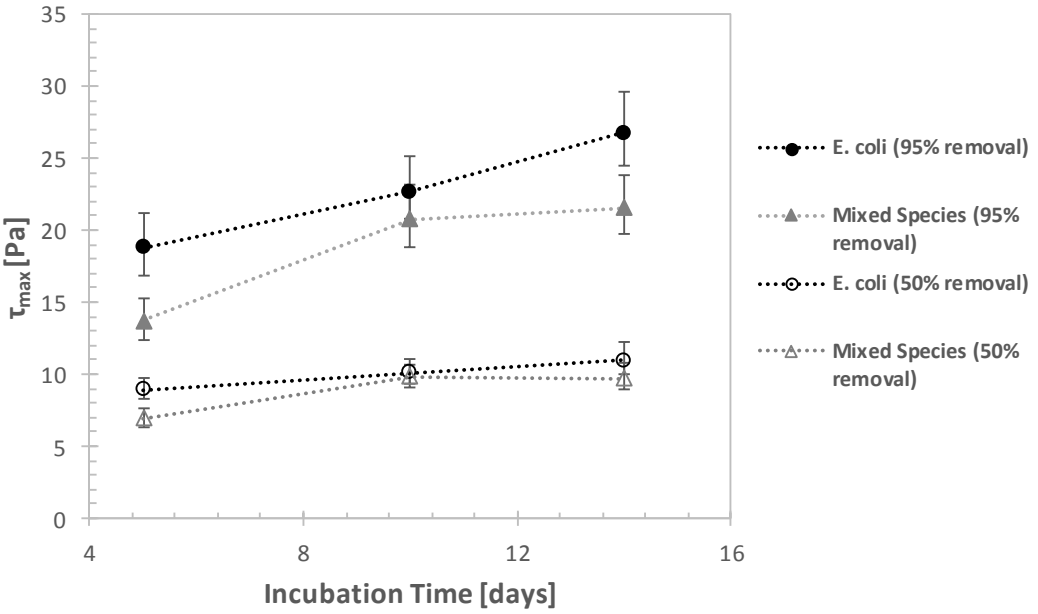

b)

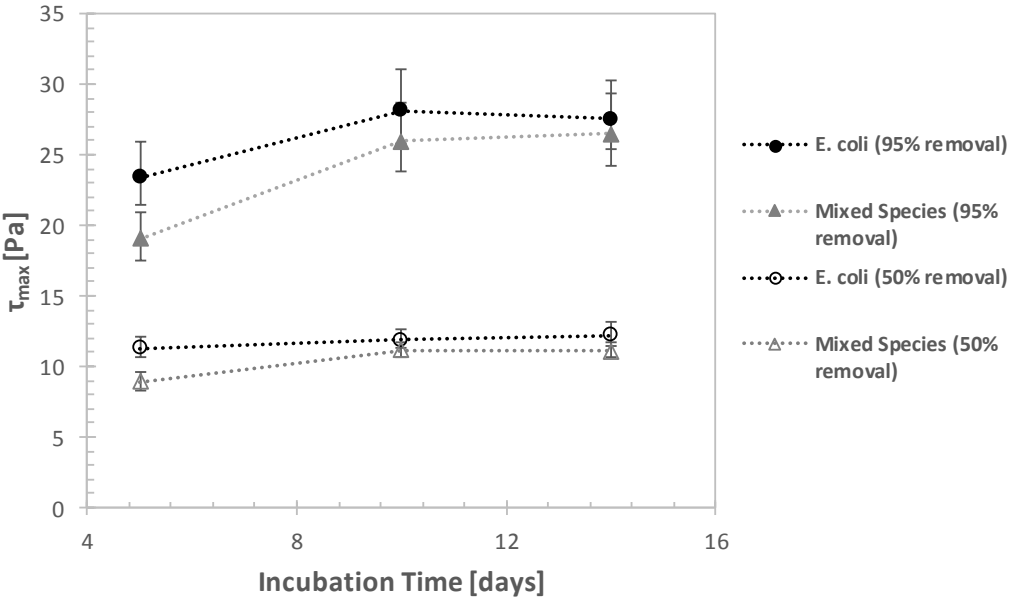

c)

Figure 103: A comparison of the estimated wall shear stress required to remove 95% (from surface coverage analysis using ImageJ) of *E. Coli* and mixed species biofilms grown under drip flow conditions on: (a) polyethylene, (b) glass and (c) stainless steel, after a range of incubation times. The error bars take into account the potential inaccuracy of the interpolation, and the scope for experimental errors.

It can be seen from the graph in Figure 103 that the steady increase in adhesive strength with biofilm age is consistent across all three surfaces, for both the monoculture and the mixed species biofilms. The increase on glass is more rapid, after starting from a position of relative weakness at 5 days, whilst biofilms grown on stainless steel reach a peak at 10 days and remain at approximately the same strength through to 14 days. Whilst the polyethylene and glass-based biofilms do not experience the same lack of strength increase, it seems logical to make the assumption that they will start to do so when the incubation period is extended further, based on the results for the static case and the similarities between the strength patterns on different surfaces in general. There seems to be little difference between the ageing process for any of the biofilms grown under flow compared to the static case, so any subsequent decline is likely to also be similar.

As has already been recognised in the individual parts of this section, the requirement for total biofilm removal does not appear to be significantly affected by the presence of flow, but a difference is more recognisable for the 50% removal. The shear stress requirement for this does not appear to be affected much by the surface material or the age of the biofilm, so this suggests that the biofilms are able to establish themselves very quickly under drip flow conditions, presenting additional issues for cleaning. The water and energy costs related to more regular cleaning would be a concern if more regular cleaning was carried out due to this feature, and it is possible that this would make the avoidance of chemical disinfectants effectively impossible without incurring greater cost and wastage.

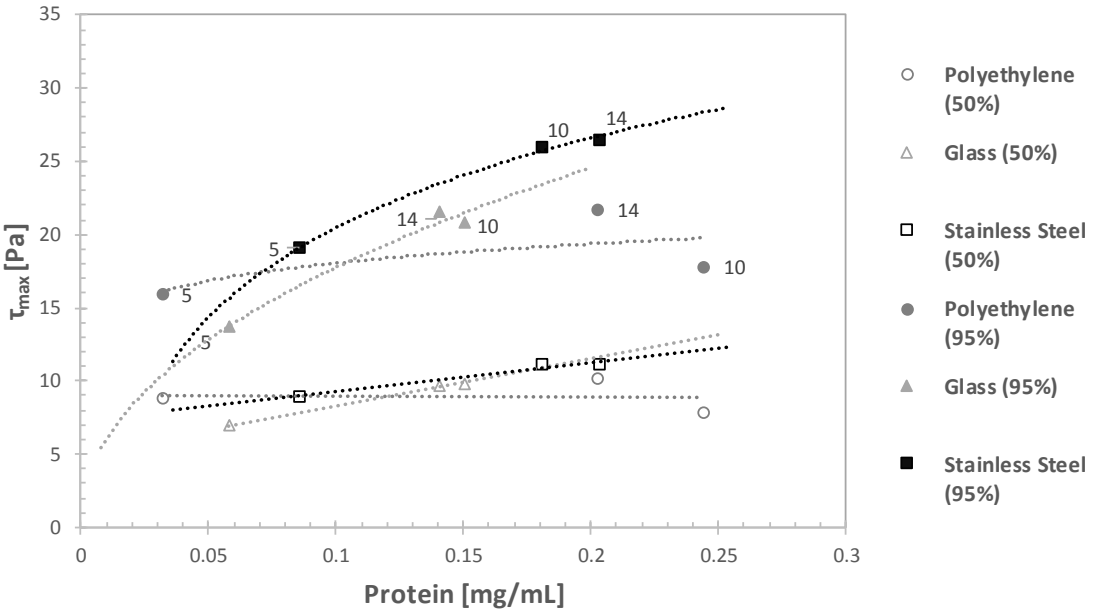

a)

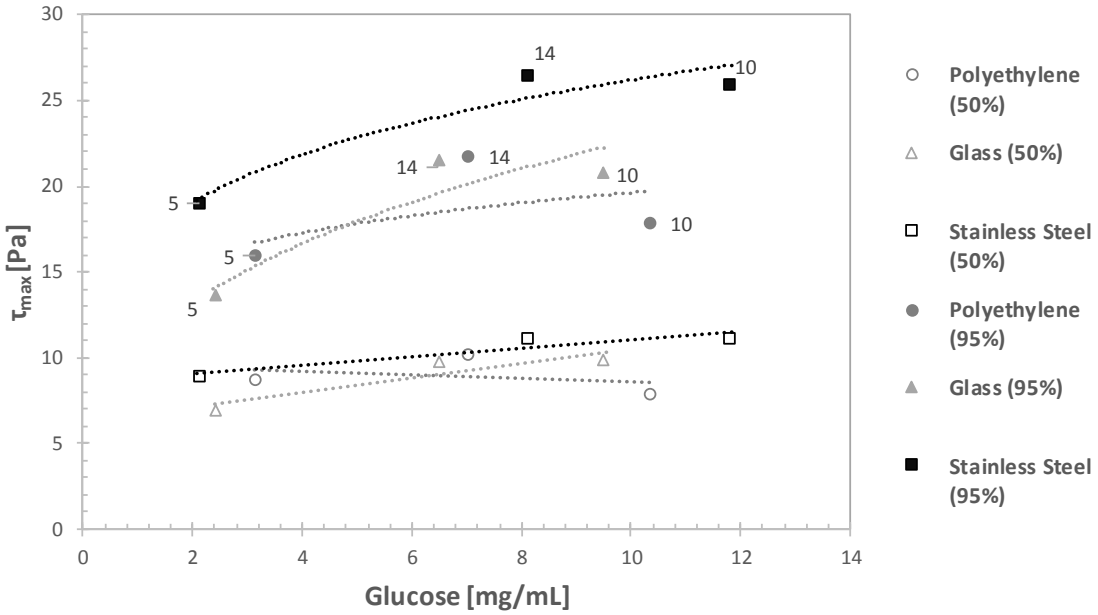

b)

Figure 104: Comparisons between adhesive strength values and recorded amounts of a) protein and b) glucose in the equivalent biofilm samples grown under flow conditions. All data are taken from mixed species biofilms. The incubation periods (in days) are shown in the labels.

The relationship shown in Figure 104 between adhesive strength and protein concentration suggests, similar to that shown for the static case (Figure 66), that protein may have an impact on the adhesive quality of a biofilm. Again, the correlation for polyethylene is the weakest and implies little relation between protein and strength. The other surfaces, however, have both a direct relationship and a strong correlation between the two values. In the static case, there appeared as though there may also

be a link between glucose and adhesive strength, although for the flow case there is little to suggest that. There was also no correlation between polysaccharides and cohesive strength in the previous section, and this result lends weight to the idea that the amount of protein present has more impact on the strength of a biofilm than the amount of polysaccharides.

Table 10: The full set of average shear stress values required to remove 50% and 95% surface coverage of *E. coli* and mixed species biofilms grown under drip flow conditions from polyethylene, glass and stainless steel.

	95% Removal [τ_{max}] – *E. coli* [Pa]					
	Polyethylene		**Glass**		**Stainless Steel**	
Days	**50%**	**95%**	**50%**	**95%**	**50%**	**95%**
5	9.8	21.1	9.0	18.8	11.3	23.4
10	11.2	23.9	10.1	22.7	11.9	28.1
14	10.7	25.5	11.0	26.8	12.2	27.6

	95% Removal [τ_{max}] – Mixed Species [Pa]					
	Polyethylene		**Glass**		**Stainless Steel**	
Days	**50%**	**95%**	**50%**	**95%**	**50%**	**95%**
5	8.8	15.9	7.0	13.7	8.9	19.1
10	7.9	17.8	9.8	20.8	11.1	26.0
14	10.1	21.7	9.7	21.5	11.1	26.5

7.5 Thickness Tests

The average values for the thickness of biofilms grown under dip flow conditions on all three surfaces are displayed in Figure 105 below. The thickness of a biofilm can negatively impact upon the pressure drop and heat transfer along a pipe, and thicker biofilms are also prone to shed clusters of cells into the flow, so it is of significant importance.

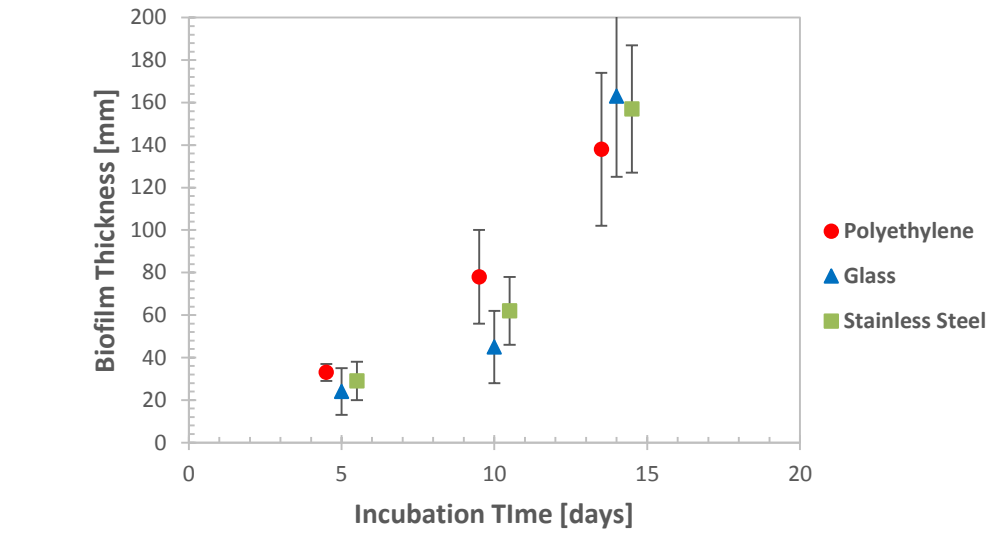

a)

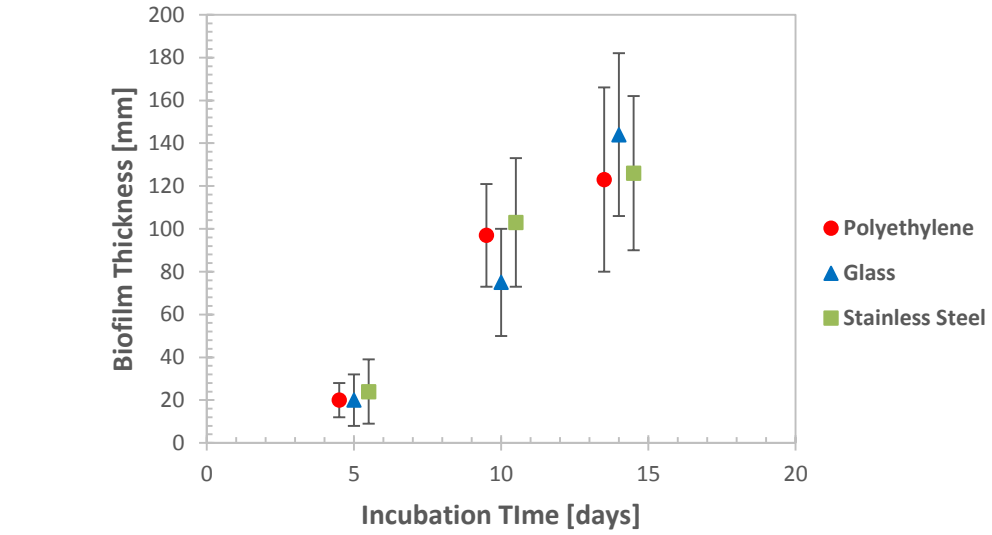

b)

Figure 105: Graphs showing the average thickness of a) *E. coli*; and b) mixed species biofilms grown under flow conditions as measured by FDG. The error bars show the minimum and maximum thicknesses measured for each incubation period.

From Figure 105, it can be seen that the thickness of both the *E. coli* and mixed species biofilms increases at a consistently high rate from 5 days through to 14. The nozzle resolution (±5 µm) may invalidate the accuracy of the 5-day results to an extent, although the increase in thickness between 5 and 10 days is still substantial. An interesting distinction is that the mixed species biofilms show a much greater increase in thickness at 10 days, but *E. coli* catches up by the time we reach 14 days. It is certainly possible that they would continue to grow beyond this point, although we have seen from the static case that the point at which removal becomes easier occurs independently of this, and that thickness can continue to increase despite the biofilms becoming structurally weaker.

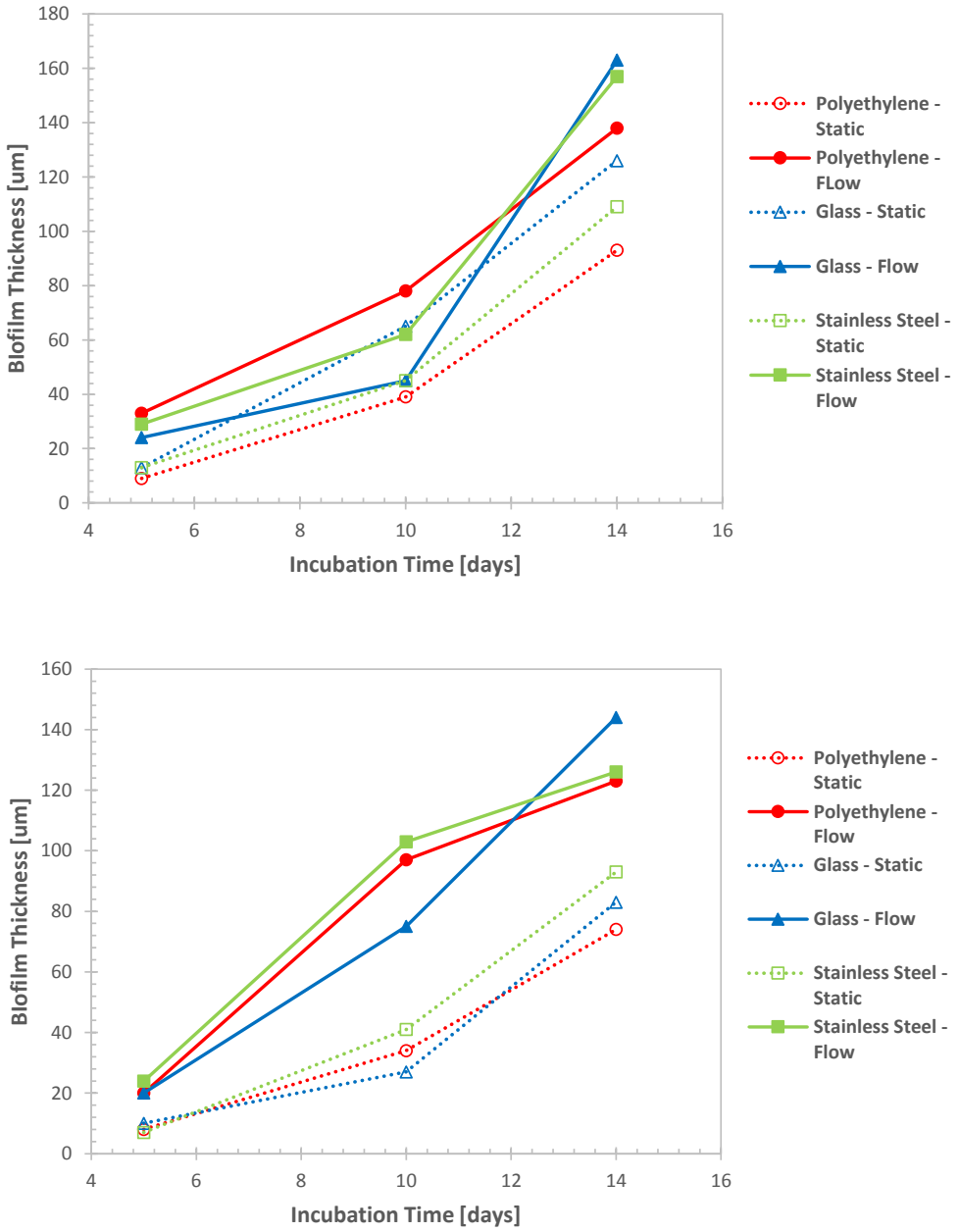

Figure 106: Graphs comparing the average thicknesses of a) *E. coli*; and b) mixed species biofilms grown under static and flow conditions as measured by FDG. Error bars are shown on the individual plots in Figures 67 and 105 – they are not included here for visual clarity.

According to Figure 106, the drip flow method is conducive to growing thicker biofilms than the static conditions used. Biofilms take longer to establish on glass for both *E. coli* and the mixed species culture, with the exception of the *E. coli* static case. The ability of all biofilms tested to reach thicknesses of 20-35 µm after just 5 days is a considerable increase from the sub-10 µm thicknesses of the static biofilms at the same stage. Then, interestingly, the mixed species biofilms become thicker than their *E. coli* counterparts at 10 days (70-100 µm compared to 40-80 µm), despite the opposite being true for the static case. However, this trend is reversed by 14 days where the *E. coli* biofilms are

thicker, reaching as much as 160 µm. With the range of values recorded being so high (shown by the error bars in Figure 105), it could be argued that the thicknesses at 14 days are too similar to draw conclusions, and that there may be a maximum at which the outer regions of cells are unable to remain attached regardless of the flow regime (or lack thereof). That the drip flow maximum thicknesses are all greater than the static cases shows that the presence of a prevailing flow does allow for thicker biofilms to be grown – whether or not this will impact on the layer removal dynamics will hopefully be answered in the following section.

7.5.1 Thickness Reduction

As with section 5.7.1, the FDG process can be used to analyse how the shear stress inflicted by the gauging flows can remove layers of the biofilm, estimating the cohesive strength of the biofilms in the process. Two graphical examples are shown below.

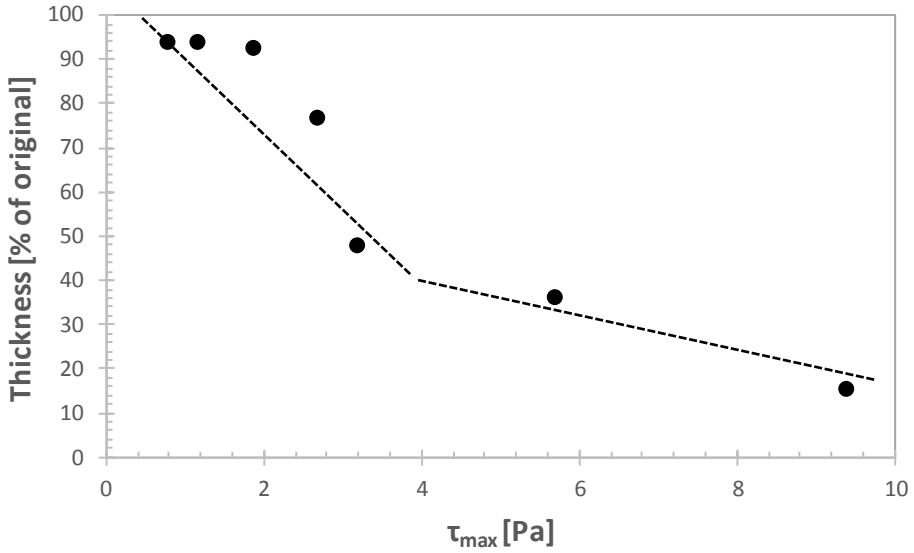

Figure 107: The percentage of biofilm thickness reduction in terms of the estimated wall shear stress deduced from the mass flow rate at the respective nozzle clearance (h/d_t), for a mixed species biofilm grown for 10 days under drip flow on a polyethylene surface. The lines added indicate the two distinct phases of removal – rapid initial depletion and a slower removal of the surface layers.

Figure 107 indicates a familiar pattern of removal, with the suggestion of one significant point of biofilm loss at between 2 and 3 Pa. This phase removed the outer 50% of the biofilm, and occurred much earlier than in the examples shown for the static case in Section 5.7.1. The remaining biofilm was removed gradually, with small losses leaving little more than 10% thickness remaining with a shear stress of 10 Pa. This has some similarity with Figure 71, in which a similar extent of removal was observed at that stage for a 10-day old biofilm grown on stainless steel. Following this is a result for a 14 day *E. coli* biofilm grown on stainless steel.

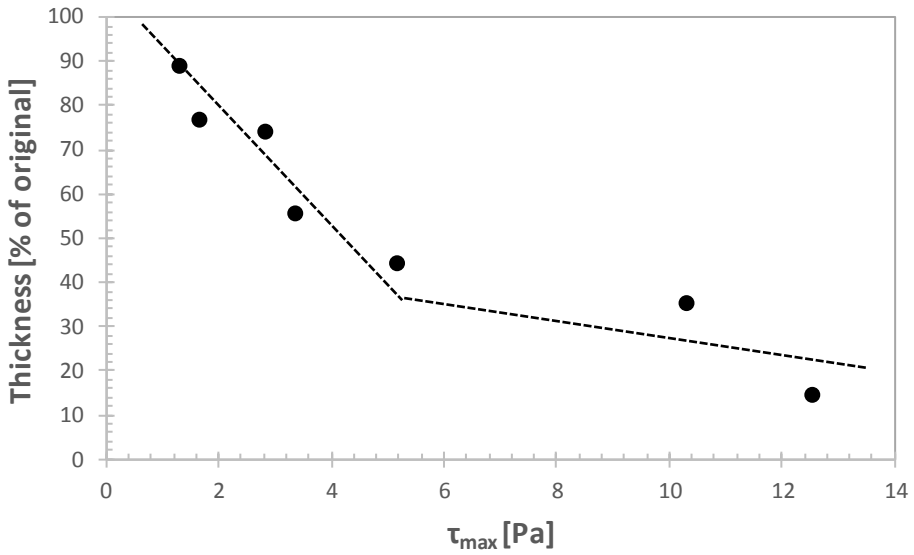

Figure 108: The percentage of biofilm thickness reduction in terms of the estimated wall shear stress deduced from the mass flow rate at the respective nozzle clearance (h/d_t), for a biofilm of *E. coli* grown for 14 days under drip flow on a stainless steel surface, with the two phases indicated again.

The above test lacks the phase of a bulk removal, which was typical for previous examples. Instead, there is a smoother loss of biofilm as the shear stress is increased. This biofilm also appears to be stronger than the previous one, with 50% removal experienced using 4 Pa and total removal at approximately 14-15 Pa. In Section 5, an *E. coli* biofilm grown for 14 days on polyethylene required 18 Pa to reduce it to the surface level only, and 5 Pa to reduce the thickness by 50%. It appears to require less stress to reach both stages in this case, and may indicate that biofilms grown under drip flow exhibit a poorer cohesion than the static ones, although the surface is different.

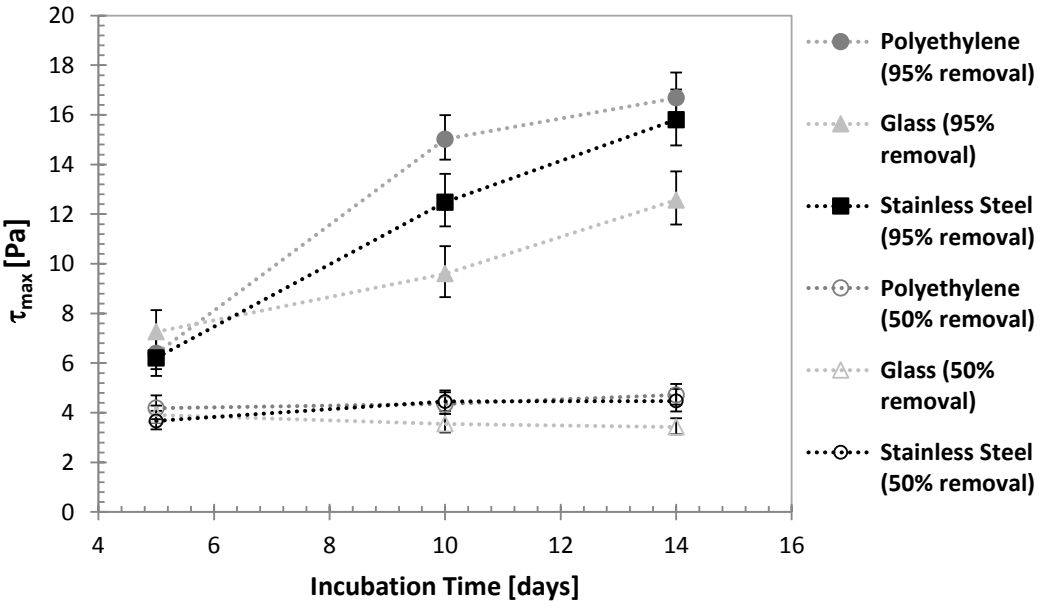

Figure 109: The estimated wall shear stress and selected equivalent mean pipe flow velocities in brackets (ms^{-1}) required to remove 50%, and 95% of *E. coli* biofilm thickness from glass, polyethylene and stainless steel, after a range of incubation periods. The error bars take into account the potential inaccuracy of the logarithmic interpolation and the scope for experimental errors.

Removal of *E. coli* biofilms grown under drip flow conditions show a consistent increase in cohesive strength over longer periods of time, at least up to 14 days. The surface material has little impact in the earlier stages, with biofilms grown on all three surfaces having a very similar strength. However after growing for 10 days, there becomes a clear difference between the surfaces with those grown on polyethylene being the strongest and those grown on glass being the weakest. This hierarchy continues up to 14 days although the difference in strength does not become more pronounced. Ease of removal of the top 50% is virtually the same for all surfaces and growth periods, as was the case for the static biofilms.

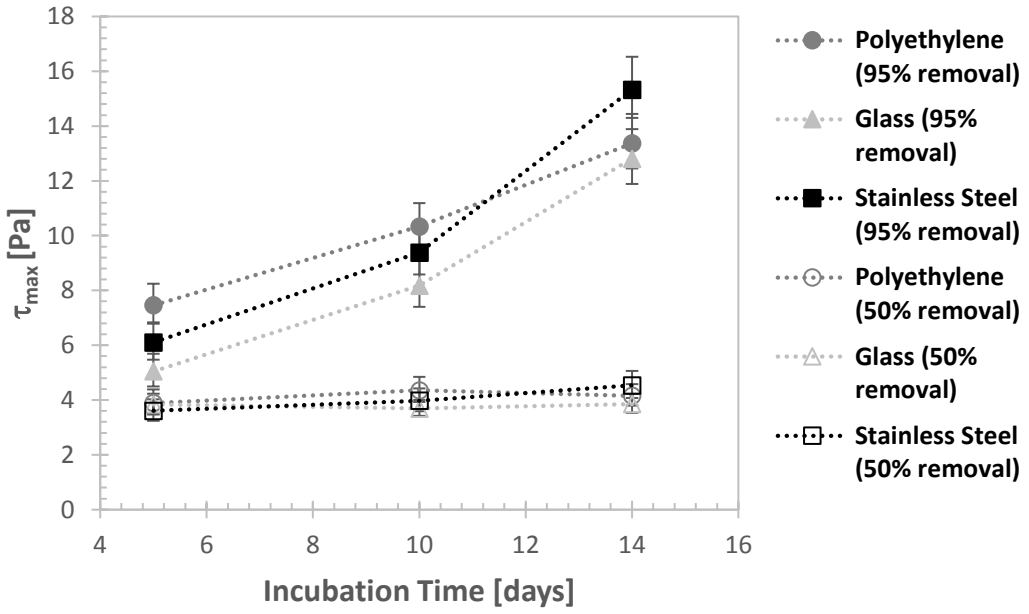

Figure 110: The estimated wall shear stress and selected equivalent mean pipe flow velocities in brackets (ms^{-1}) required to remove 50%, and 95% of mixed species biofilm thickness from glass, polyethylene and stainless steel, after a range of incubation periods. The error bars take into account the potential inaccuracy of the logarithmic interpolation and the scope for experimental errors.

The mixed species biofilms show a similar pattern to the *E. coli* biofilms. There is an increase in cohesive strength as the biofilms age, especially those grown on stainless steel where the rate of change of strength was seen to increase between 10 and 14 days. Apart from that exception, there are close similarities with *E. coli*, with polyethylene-based biofilms being the strongest and those grown on glass being the weakest. There is similarly little variation among the 50% removal data. The strength values are also very similar, increasing from 5-7 Pa after 5 days to 12-16 Pa after 14 days.

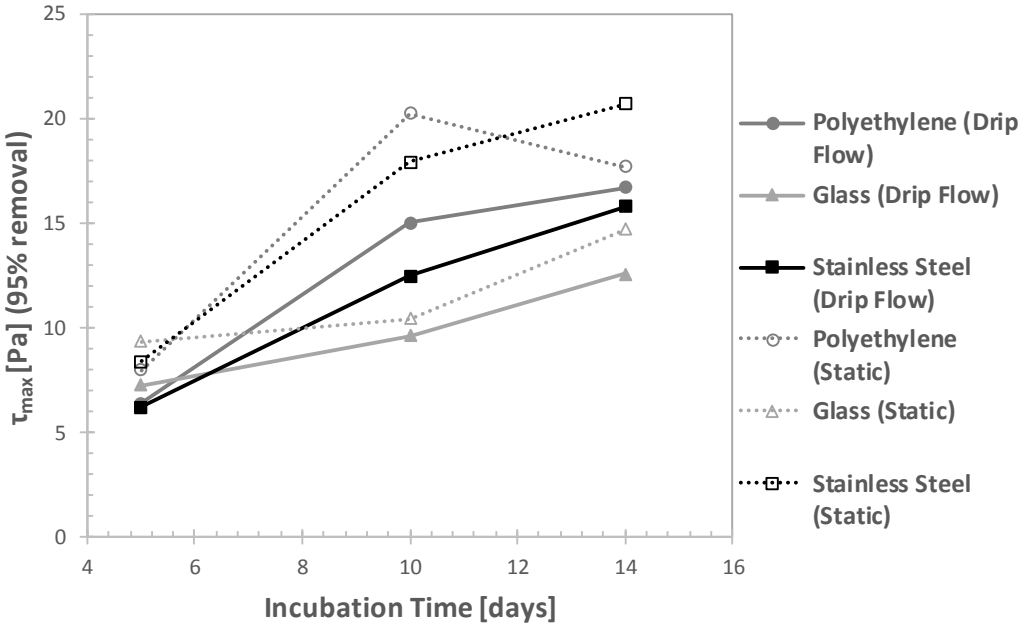

Figure 111: A comparison between the thickness test results for *Escherichia coli* biofilms grown under drip flow and under static conditions, on all three test surfaces, shown in terms of the shear stress required in order to remove 95% of the surface coverage. Error bars are shown on the individual plots in Figures 72 and 109 – they are not included here for visual clarity.

For all three surfaces, the biofilms grown under drip flow showed a lower cohesive strength than the static biofilms. This is true at every single point in Figure 111. The only area of uncertainty is the effect of increasing the age of the drip flow biofilms beyond 14 days, which was not possible within the confines of this research. The only reference point to take is the fact that the static-grown biofilms on polyethylene had already begun to weaken after 10 days, yet the equivalent drip flow biofilms continued to become stronger. It has been observed that biofilms grown under a low shear force tend to be more porous and prone to sloughing (van Loosdrecht *et al.*, 2002), so this may be the cause of the relative cohesive weakness compared to the static biofilms.

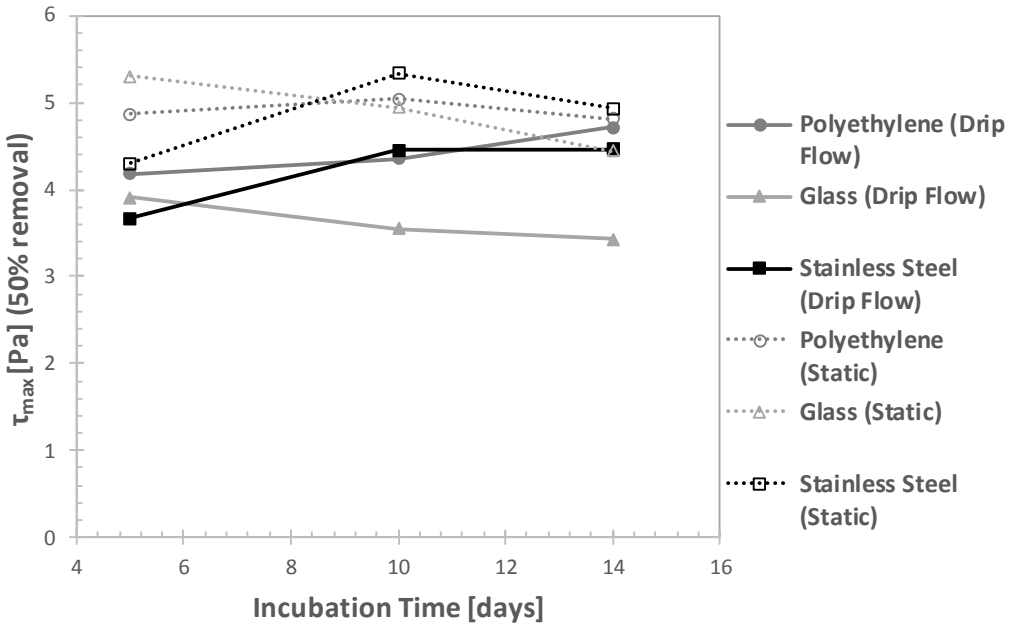

Figure 112: A comparison between the thickness test results for *Escherichia coli* biofilms grown under drip flow and under static conditions, on all three test surfaces, shown in terms of the shear stress required in order to remove 50% of the surface coverage.

As with Figure 111, removal of the top 50% of the *E. coli* biofilms proved to be easier than for the equivalent static biofilms. This suggests that the relative cohesive weakness hinted at in the previous figure is a comprehensive one, within all layers of the biofilms. It strongly indicates that growing the cultures under drip flow conditions results in structurally weaker biofilms, even though in the majority of cases the surface attachment was stronger than the static case (section 7.4.1).

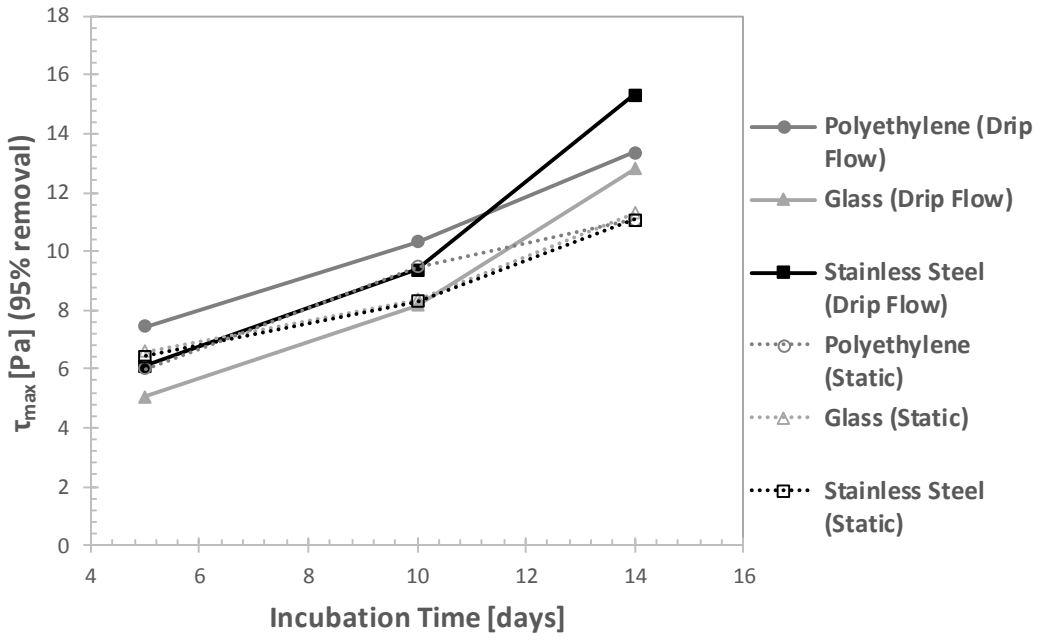

Figure 113: A comparison between the thickness test results for mixed species biofilms grown under drip flow and under static conditions, on all three test surfaces, shown in terms of the shear stress required in order to remove 95% of the surface coverage.

In contrast to the *E. coli* results shown previously, Figure 113 suggests that mixed species biofilms do develop a greater cohesive strength when grown under drip flow conditions compared to static conditions. Furthermore, the rate of increase continues to rise between 10 and 14 days, and it is possible that this may continue over a longer period. In particular, the biofilms grown on stainless steel see a large increase in strength over this stage, from 9 to 15 Pa.

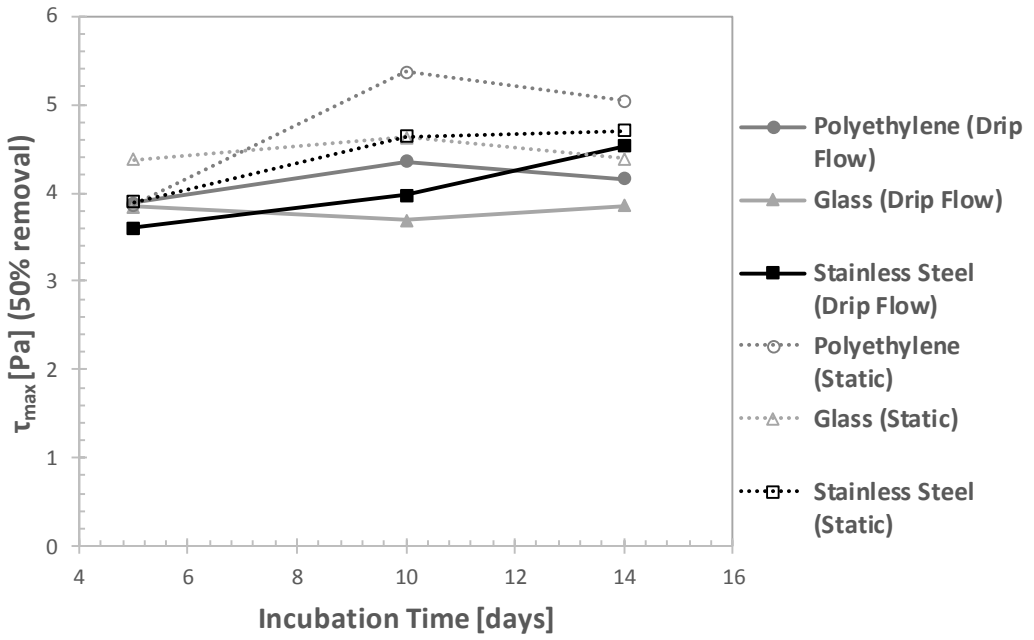

Figure 114: A comparison between the thickness test results for mixed species biofilms grown under drip flow and under static conditions, on all three test surfaces, shown in terms of the shear stress required in order to remove 50% of the surface coverage.

For 50% removal, the picture is similar to that seen for *E. coli*. Whereas the graph for 95% removal suggested a greater cohesive strength for mixed species biofilms grown under flow, 50% removal still appears to occur more readily than for the static biofilms. A similar strength increase is observed for stainless steel, but is still lower than the equivalent static biofilm. Studied in combination, these graphs suggest that mixed species biofilms are able to build a stronger lower core region in the drip flow case, which was not observed for *E. coli*.

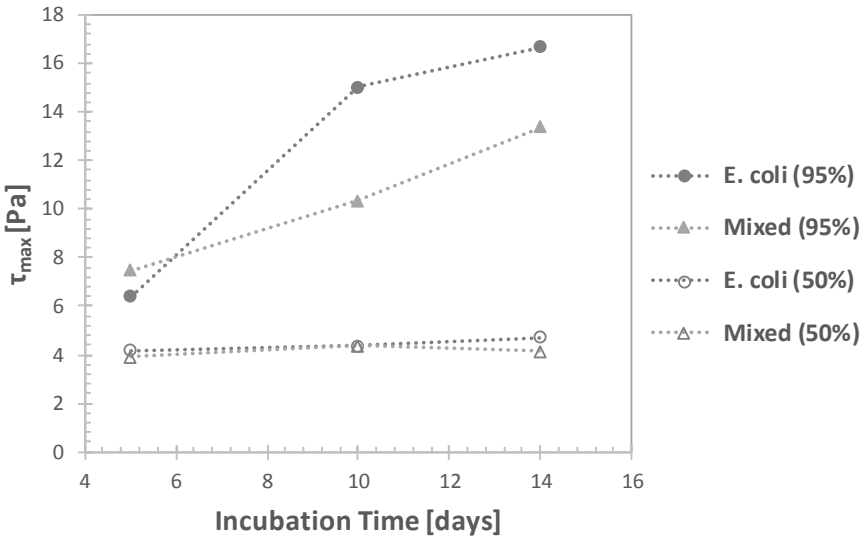

a)

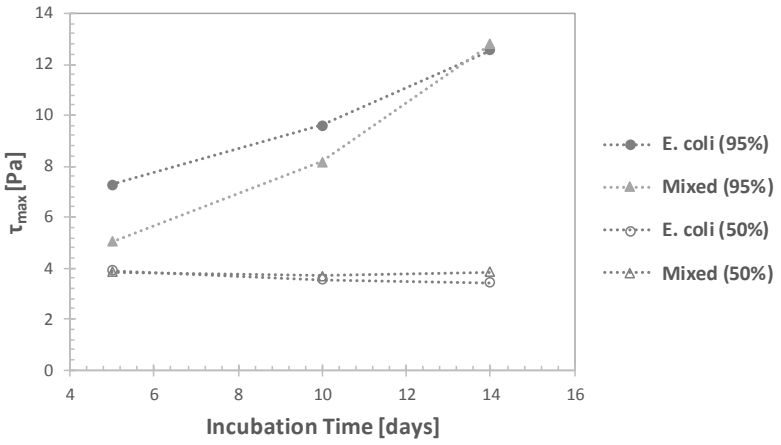

b)

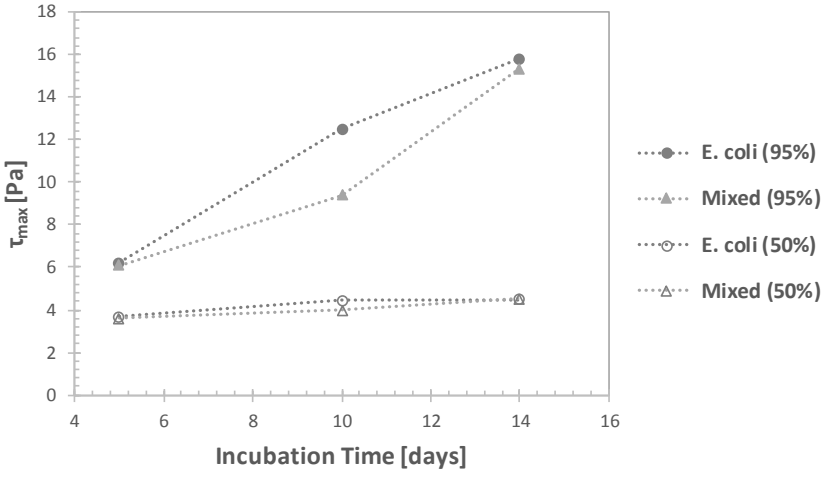

c)

Figure 115: A comparison of the estimated wall shear stress required to remove 95% thickness of *E. Coli* and mixed species biofilms grown under drip flow conditions on: (a) polyethylene, (b) glass and (c) stainless steel, after a range of incubation times. The error bars take into account the potential inaccuracy of the interpolation, and the scope for experimental errors.

The most obvious point to take from the above figure is that the *E. coli* biofilms have a greater cohesive strength than their mixed species counterparts, as was also observed for the static case. However, it can also be seen that the strength of the mixed species biofilms is increasing at a greater rate between 10 and 14 days, as well as the indication in Figures 113 and 114 that the mixed species biofilms also showed greater cohesion when grown under flow conditions than under static conditions.

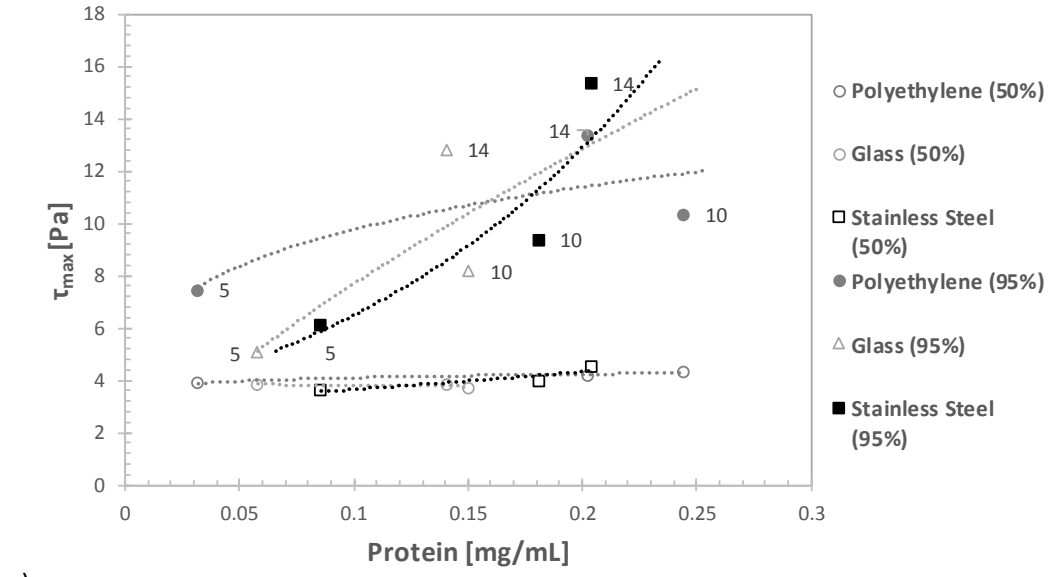

a)

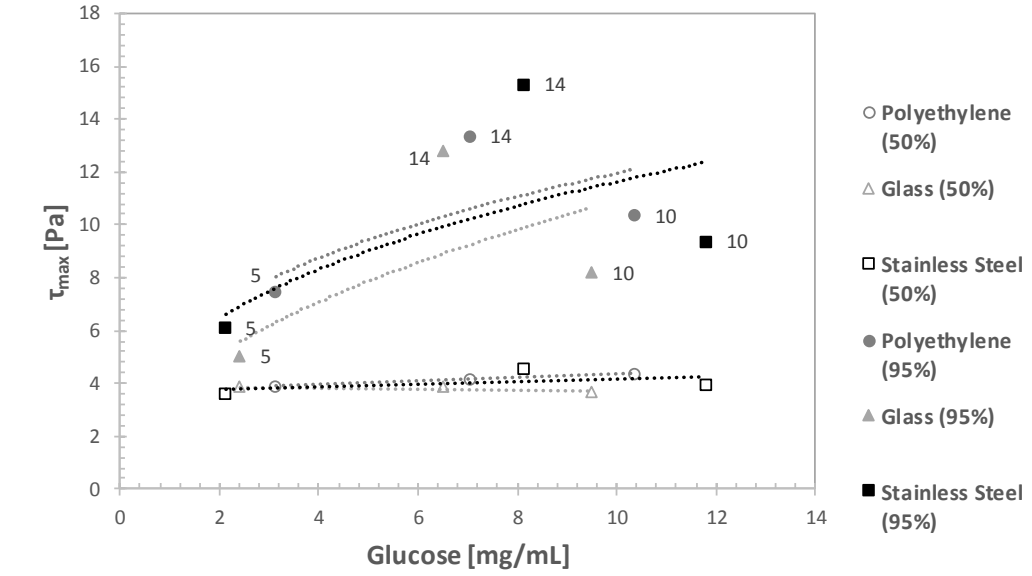

b)

Figure 116: Comparisons between cohesive strength values and recorded amounts of a) protein and b) glucose in the equivalent duct flow biofilm samples. All data are taken from mixed species biofilms. The incubation periods (in days) are shown in the labels.

Figure 116a indicates a reasonable link between the amount of protein present in mixed species biofilms and their cohesive strength. The relationship is particularly strong for those grown on stainless steel. The result is similar to that seen for the static case (Figure 75). From all sections it appears that protein has more of an impact on adhesive strength than cohesion. As for Figure 116b, there is again a weak correlation between glucose levels and biofilm strength, and the peak in glucose after 10 days is at odds with the peak in strength after 14 days. Removal of 50% thickness is shown to be unrelated to either protein or polysaccharide concentration, and would support the idea than any impact due to either component is largely confined to the resilience of the surface layer.

Summary

The surface materials used had no bearing on the eventual thickness of the biofilms grown, as had been the case for the biofilms grown under static conditions. The *E. coli* biofilms typically reached greater thicknesses after 14 days, although not to a substantial degree, and there is no suggestion that this difference had an impact upon removal behaviour. The weakening effect as biofilm age progresses beyond 14 days was a key point in the discussion of Section 5, yet it can only be speculated on here. However, it is again the case that both the adhesive and cohesive strengths of the biofilms increases over the course of the period from 5 to 14 days.

A major difference from the static case is that the shear stresses required for removal are similar for *E. coli* and mixed species biofilms, compared to the relative strength of *E. coli* static biofilms (which were stronger on all surfaces compared to those grown under drip flow). The mixed species biofilms, on the other hand, required a higher shear stress for 95% removal on all surfaces than they had under static conditions.

The need to clean surfaces operating under flow conditions with regularity is shown again by the results in this section. It could be predicted that older biofilms will begin to weaken in accordance with both the static results and detachment theory, but whether or not this is true the same dangers relating to an untreated contaminated surface apply. Biofilms are believed to be more prone to sloughing when grown under a low shear, and this would exacerbate the risk of pathogens being released into the flow. The balance would again be with the amount of water and pumping power required, but regular cleaning would typically be the best option.

Table 11: The full set of average shear stress values required to remove 50% and 95% thickness of *E. coli*, *B. cepacia*, and mixed species biofilms grown under drip flow conditions from polyethylene, glass and stainless steel.

	Removal from Polyethylene [τ_{max}]			
	E. coli		**Mixed Species**	
Days	**50%**	**95%**	**50%**	**95%**
5	4.2	6.4	3.9	7.5
10	4.4	15.0	4.4	10.3
14	4.7	16.7	4.2	13.4

	Removal from Glass [τ_{max}]			
	E. coli		**Mixed Species**	
Days	**50%**	**95%**	**50%**	**95%**
5	3.9	7.3	3.8	5.0
10	3.6	9.6	3.7	8.2
14	3.4	12.6	3.9	12.8

	Removal from Stainless Steel [τ_{max}]			
	E. coli		**Mixed Species**	
Days	**50%**	**95%**	**50%**	**95%**
5	3.7	6.2	3.6	6.1
10	4.5	12.5	4.0	9.4
14	4.5	15.8	4.5	15.3

7.6 Impact of Chemical Biocides

7.6.1 Strength Tests

The mixed species biofilms grown on stainless steel under drip flow conditions were tested for adhesive strength, after having been exposed to solutions of sodium hypochlorite and peracetic acid, using fluid dynamic gauging operating under pressure mode. Biofilms grown for 14 days are displayed in the same fashion as in previous sections, beginning with those treated with sodium hypochlorite.

Sodium Hypochlorite

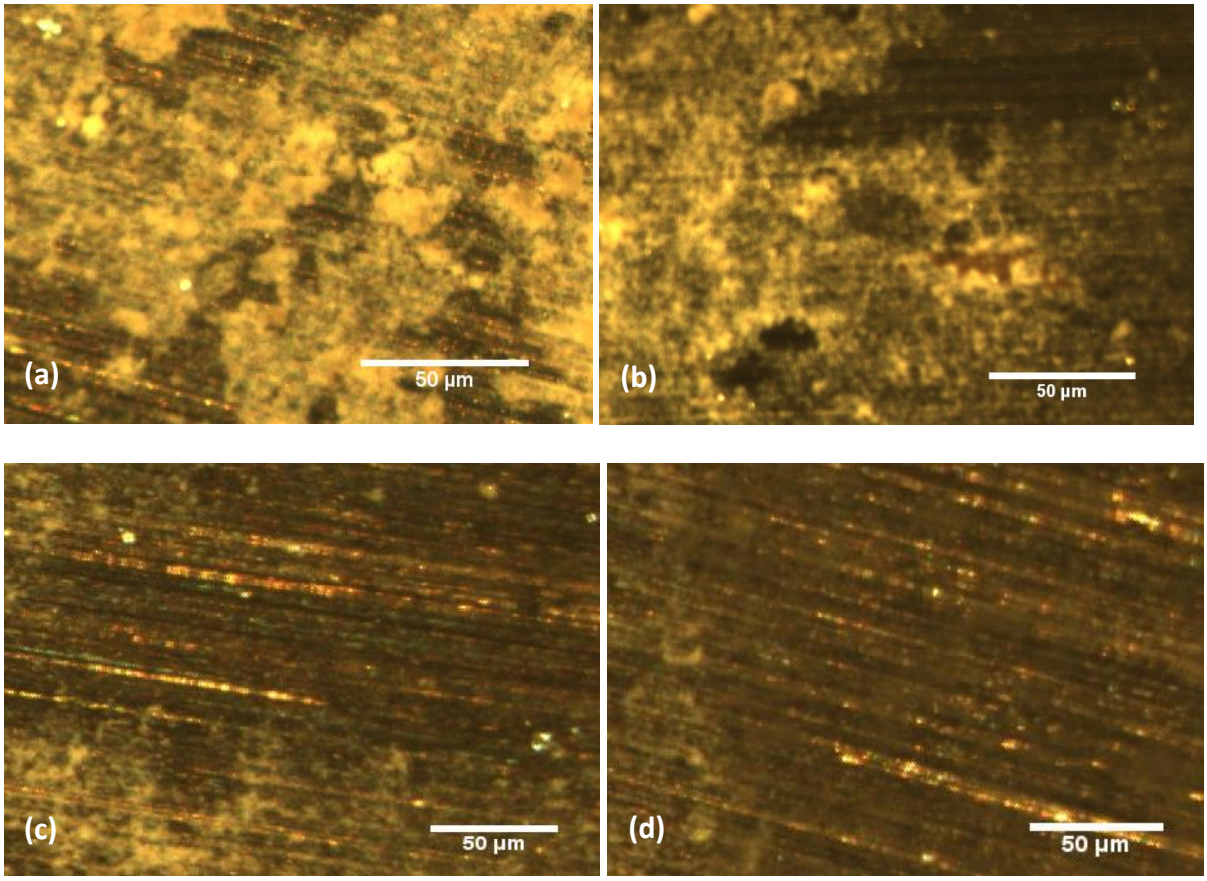

Figure 117: Optical microscope images of mixed species biofilms grown under flow on stainless steel for 14 days and exposed to 100 mg/L sodium hypochlorite: tested under FDG at (a) h/d_t = 0.25, τ_w = 4 ± 0.5 Pa (b) h/d_t = 0.21, τ_w = 6 ± 0.4 Pa (c) h/d_t = 0.15, τ_w = 11 ± 0.4 Pa (d) h/d_t = 0.1, τ_w = 15 ± 0.1 Pa. The percentages of biofilm removed at each stage were: (a) 23%; (b) 52%; (c) 84%; (d) 97%.

The effect of exposing the biofilms to 100 mg/L sodium hypochlorite can be clearly seen in the relative ease with which biofilm can be removed from the surface. In section 7.4.2, 14-day old mixed species biofilms grown under flow on stainless steel were removed using only hydrodynamic forces, and 27 Pa was required to remove 95% of biofilms from the surface. In the figure above, 15 Pa was able to remove 97% of the biofilm, a substantial weakening of the surface adhesion. The same effect can also be seen at the earlier stages: image b) shows a 52% reduction with 6 Pa, yet the same removal without the chemical input required 12 Pa of shear stress. Figure 118 now shows the removal behaviour for biofilms grown for 5, 10 and 14 days.

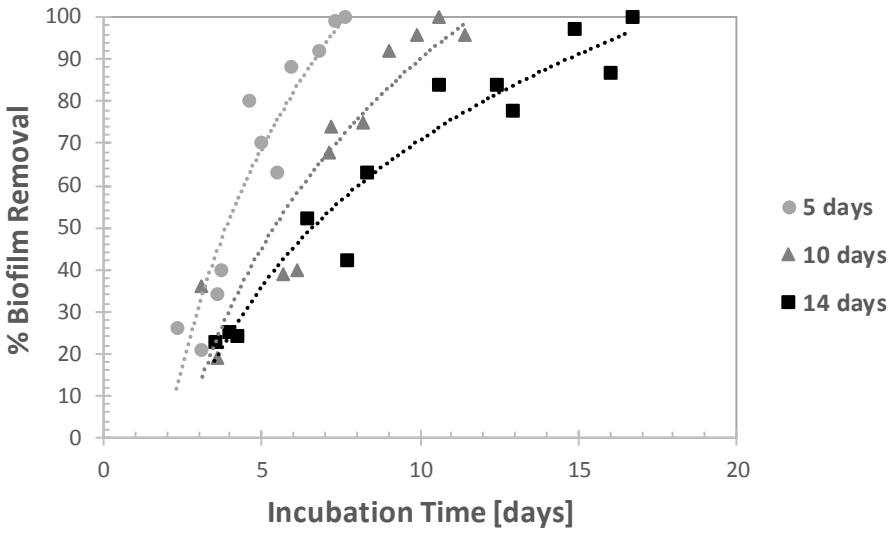

Figure 118: The complete set of strength test results for mixed species biofilms grown on stainless steel using the drip flow reactor, after being exposed to a 100 mg/L sodium hypochlorite solution for 15 minutes and removed using FDG.

Figure 118 shows that the aging effect observed in previous sections remains intact after the incorporation of sodium hypochlorite disinfectant. At both the 50% and 95% removal stages, each age shows a clear reduction in shear stress required compared to the hydrodynamic method. This applied to removal of 95% surface coverage in particular, where less than half the shear stress is necessary for 5 and 10 day-old biofilms after the chemical exposure.

Now, the effect of increasing the NaClO concentration to 1000 mg/L is analysed.

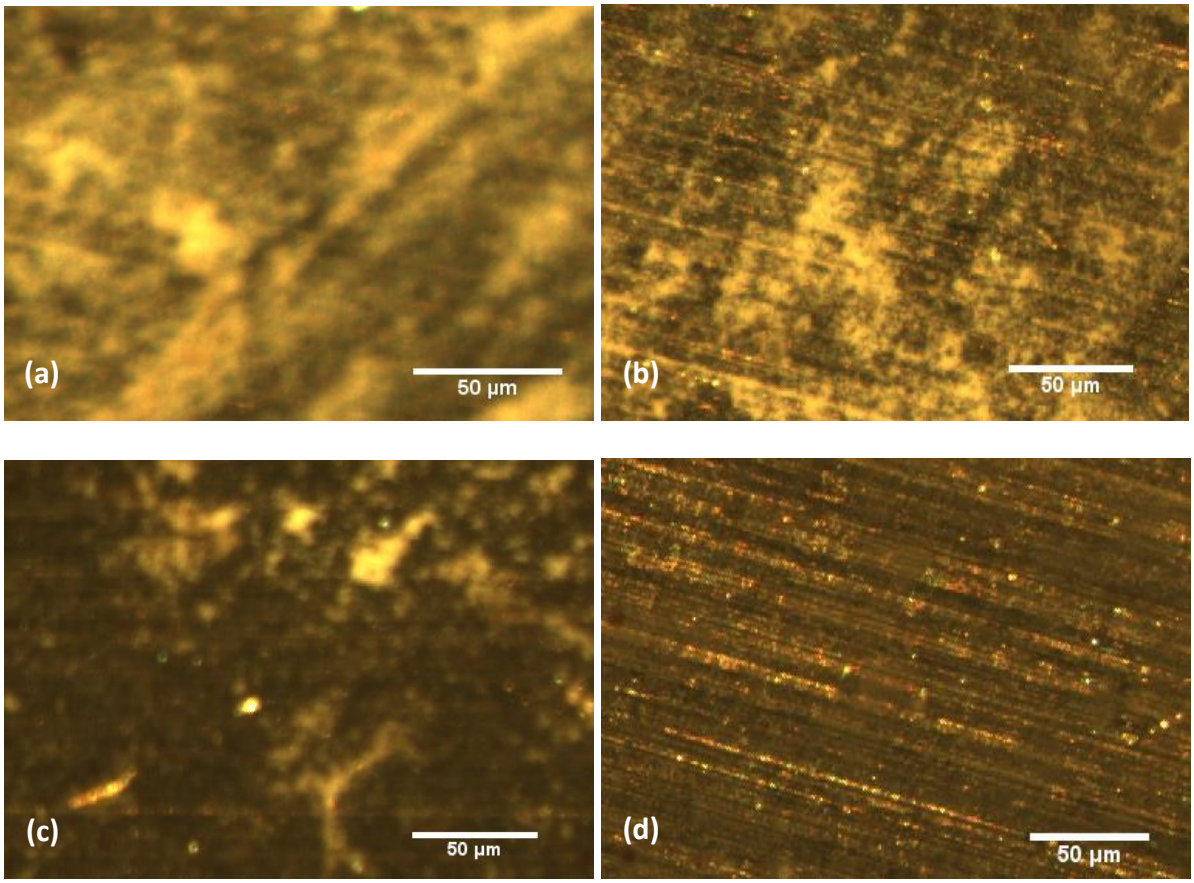

Figure 119: Optical microscope images of mixed species biofilms grown under flow on stainless steel for 14 days and exposed to 1000 mg/L sodium hypochlorite: tested under FDG at (a) $h/d_t = 0.25$, $\tau_w = 4 \pm 0.4$ Pa (b) $h/d_t = 0.20$, $\tau_w = 7 \pm 0.4$ Pa (c) $h/d_t = 0.16$, $\tau_w = 10 \pm 0.1$ Pa (d) $h/d_t = 0.12$, $\tau_w = 13 \pm 0.4$ Pa. The percentages of biofilm removed at each stage were: (a) 30%; (b) 53%; (c) 86%; (d) 100%.

There is a further decrease in biofilm adhesive strength due to the step change in NaClO concentration. In Figure 119, 13 Pa was required to clean the surface, compared to 15 Pa in the previous section. Little or no change can be observed for the earlier stages – 30% and 50% removal do not appear to become any easier.

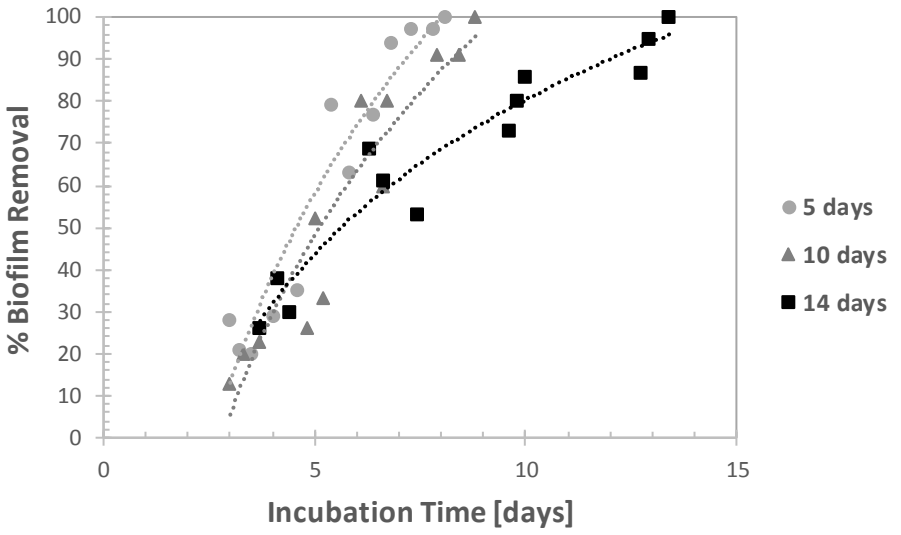

Figure 120: The complete set of strength test results for mixed species biofilms grown on stainless steel using the drip flow reactor, after being exposed to a 1000 mg/L sodium hypochlorite solution for 15 minutes and removed using FDG.

The same hierarchy of adhesive strength has endured the increase to 1000 mg/L NaClO, although the 5 and 10 day biofilms have been weakened more substantially. The 14-day biofilms show the relative lack of impact of the extra disinfectant indicated in Figure 119. It shows the limitations of chemical disinfection, in that additional increases do not necessarily produce better results, and also indicates that the effect of aging in biofilms can be even more significant when chemicals are introduced, particularly considering the aim of reducing chemical use.

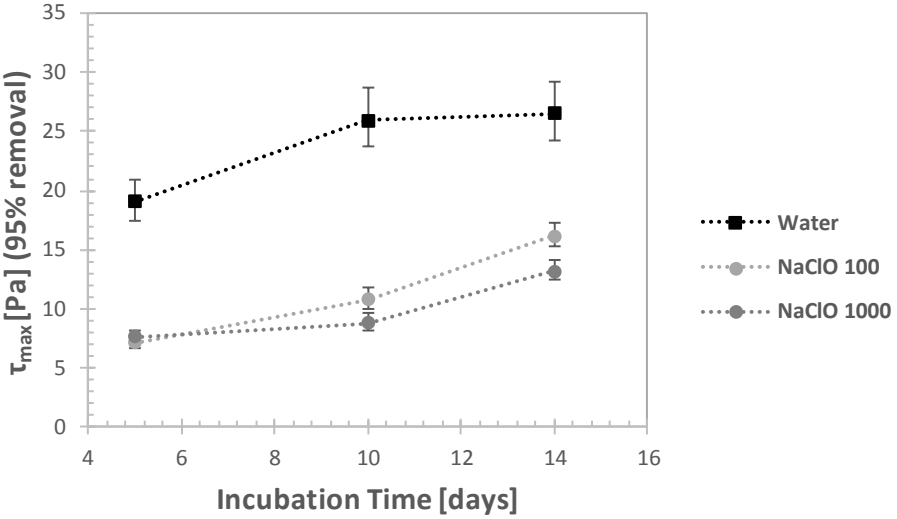

Figure 121: The shear stress required to remove 95% surface coverage of mixed species biofilms grown under drip flow on stainless steel, comparing the effect of exposure to sodium hypochlorite on adhesive strength.

Sodium hypochlorite appears to be effective at weakening the attachment of the biofilms to the surface. The introduction of 100 mg/L NaClO substantially reduced the shear stress required for removal, to below half of that necessary when using just water at the 5 and 10 day stages. There is evidence of an enduring resistance after 14 days, but the reduction in strength from 25 to 15 Pa is still considerable. Increasing the NaClO input to 1000 mg/L, conversely, had little additional effect and given the problems associated with a high chlorine content this would not be advisable.

Peracetic Acid

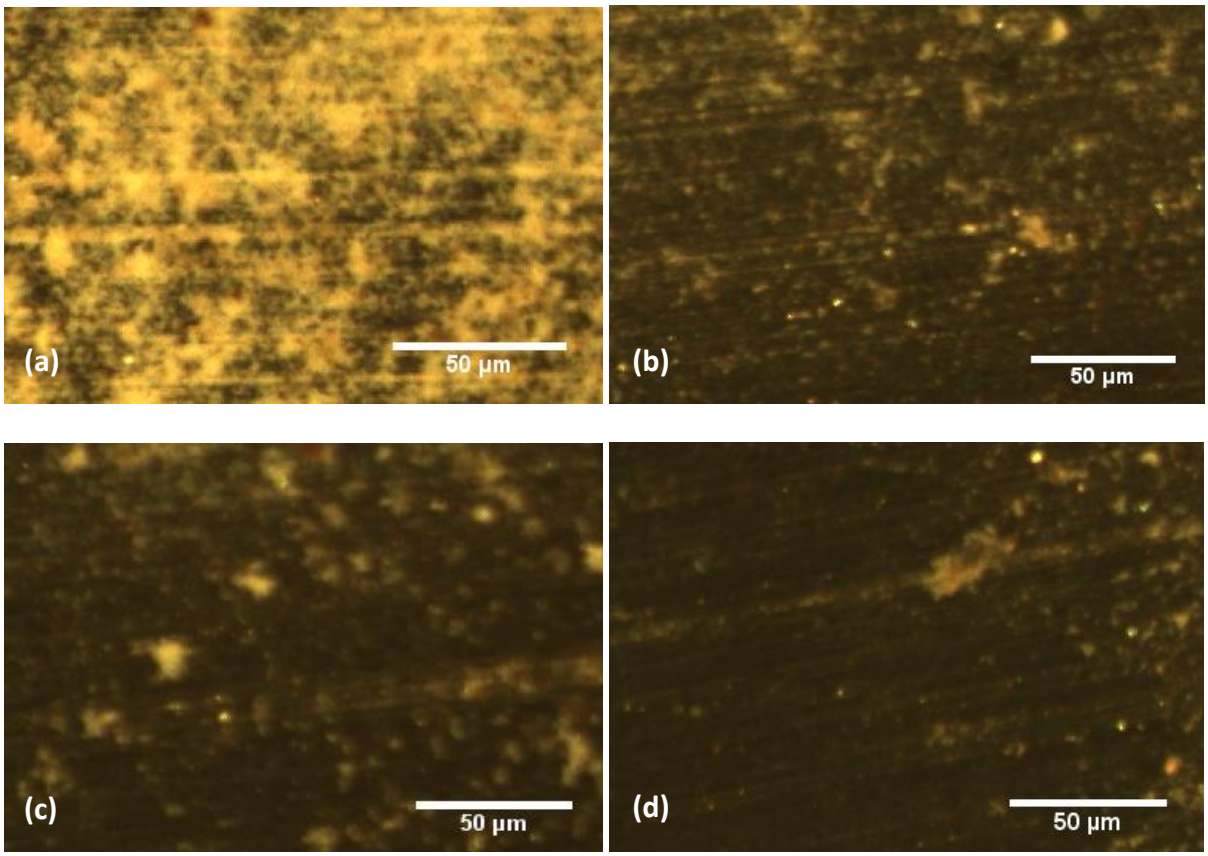

Figure 122: Optical microscope images of mixed species biofilms grown under flow on stainless steel for 14 days and exposed to 100 mg/L peracetic acid: tested under FDG at (a) $h/d_t = 0.25$, $\tau_w = 4 \pm 0.2$ Pa (b) $h/d_t = 0.18$, $\tau_w = 10 \pm 0.4$ Pa (c) $h/d_t = 0.11$, $\tau_w = 17 \pm 0.3$ Pa (d) $h/d_t = 0.06$, $\tau_w = 23 \pm 0.2$ Pa. The percentages of biofilm removed at each stage were: (a) 28%; (b) 73%; (c) 86%; (d) 94%.

The addition of 100 mg/L of peracetic acid to the removal process appears to have little impact on the ease of removal from the surface. In image d), 23 Pa was unable to clean the surface completely, and is similar to the shear stress required without the peracetic acid addition. The biofilm has become weaker than the hydrodynamic force example, although not significant enough to draw any real conclusions.

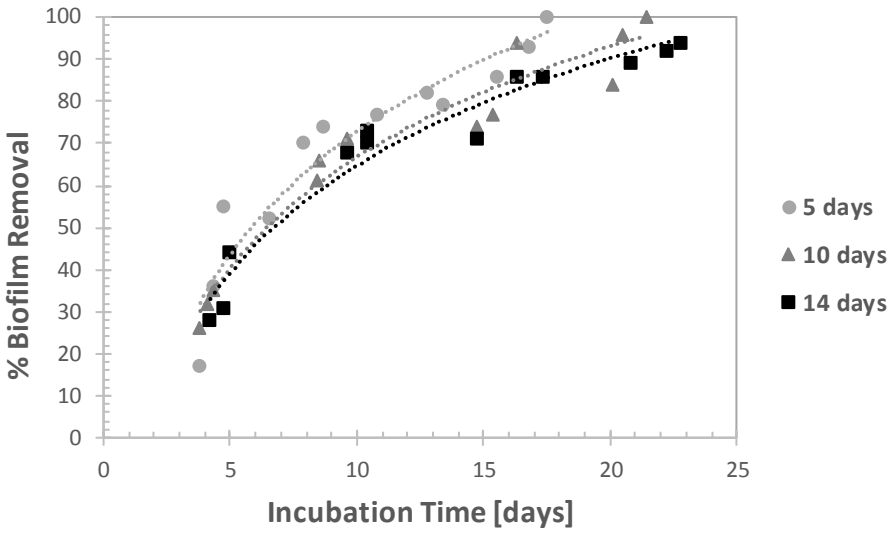

Figure 123: The complete set of strength test results for mixed species biofilms grown on stainless steel using the drip flow reactor, after being exposed to a 100 mg/L peracetic acid solution for 15 minutes and removed using FDG.

Figure 123 suggests that the input of 100 mg/L peracetic acid prior to the FDG process is able to weaken the adhesion to the surface, albeit only by small margins. This impact does not change much depending on the ages of the biofilms. Following this, the concentration of peracetic acid was increased to 1000 mg/L for the next stage.

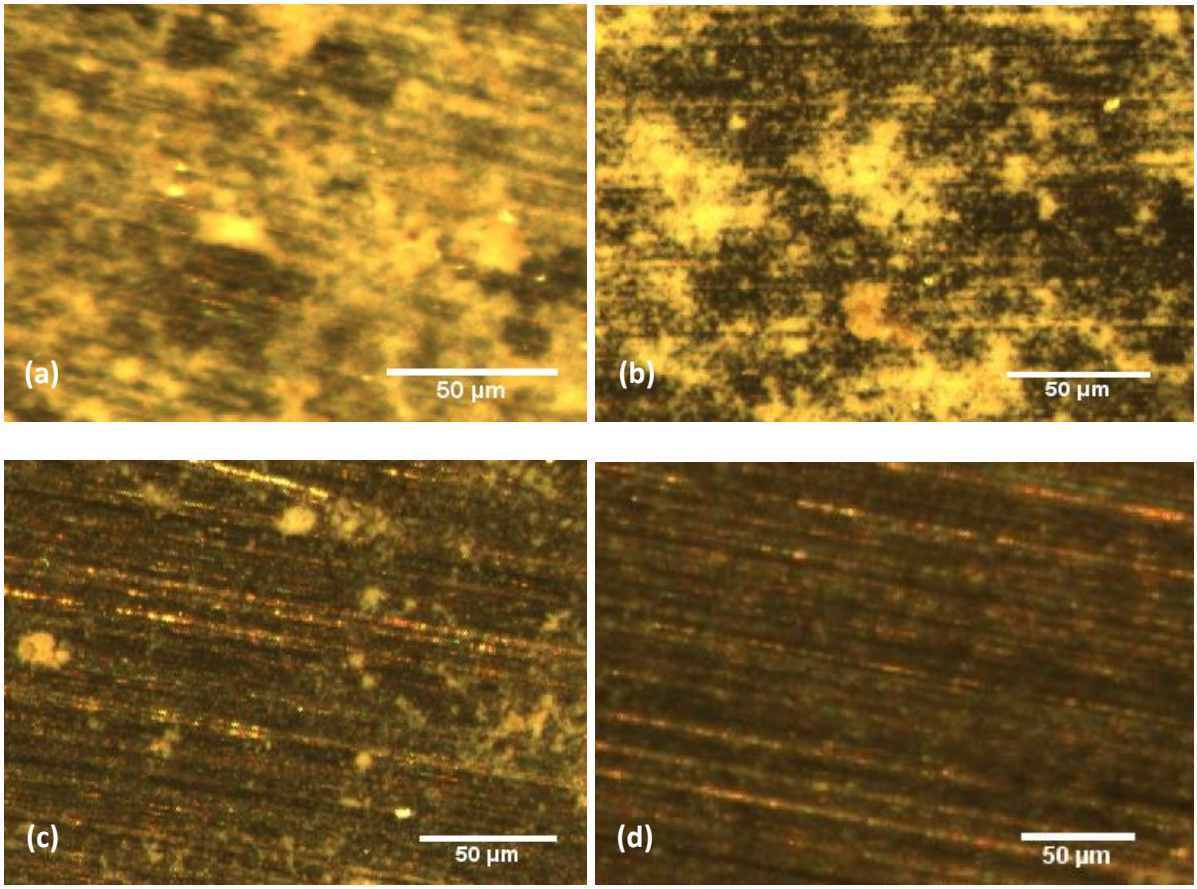

Figure 124: Optical microscope images of mixed species biofilms grown under flow on stainless steel for 14 days and exposed to 1000 mg/L peracetic acid: tested under FDG at (a) $h/d_t = 0.25$, $\tau_w = 4 \pm 0.2$ Pa (b) $h/d_t = 0.18$, $\tau_w = 10 \pm 0.1$ Pa (c) $h/d_t = 0.12$, $\tau_w = 16 \pm 0.4$ Pa (d) $h/d_t = 0.06$, $\tau_w = 23 \pm 0.1$ Pa. The percentages of biofilm removed at each stage were: (a) 24%; (b) 63%; (c) 86%; (d) 99%.

The result in Figure 124 is a continuation of the effect noted for 100 mg/L peracetic acid. There is evidence of a slight reduction in strength of attachment, with the surface almost entirely cleaned using a shear stress of 23 Pa (which resulted in a 94% surface reduction for 100 mg/L). At the same time however, 10 Pa was able to remove 63% here and as much as 73% in the previous example, indicating that the impact of the increase in concentration may have produced no discernible effect.

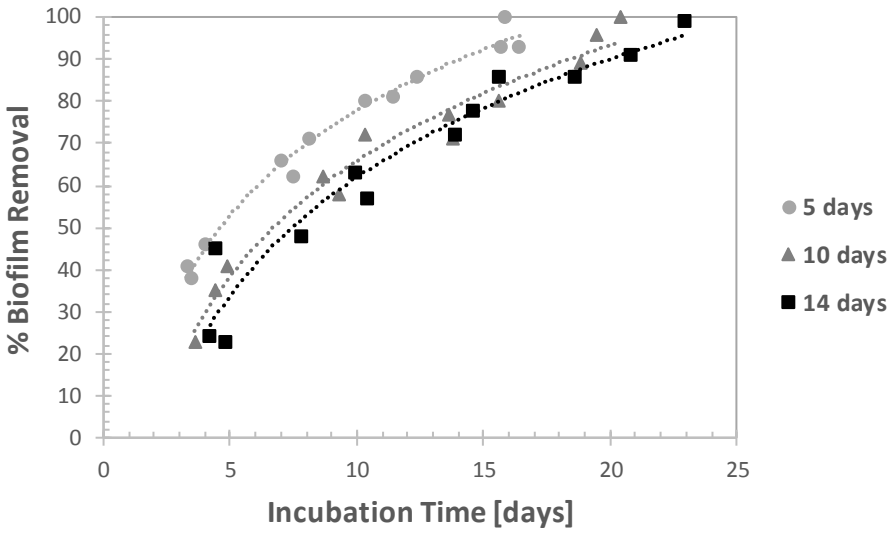

Figure 125: The complete set of strength test results for mixed species biofilms grown on stainless steel using the drip flow reactor, after being exposed to a 1000 mg/L peracetic acid solution for 15 minutes and removed using FDG.

The graph in Figure 125 indicates a lack of impact due to the increase of peracetic acid levels. In combination with Figure 123 for 100 mg/L, this suggests that peracetic acid has negligible effect on biofilm adhesion and would not be worth supplementing the hydrodynamic methods with.

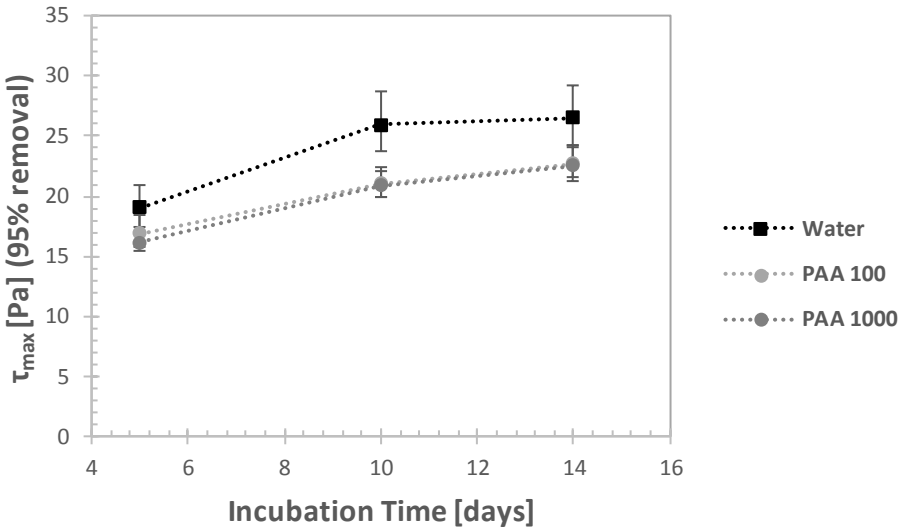

Figure 126: The shear stress required to remove 95% surface coverage of mixed species biofilms grown under drip flow on stainless steel, comparing the effect of exposure to peracetic acid on adhesive strength.

From Figure 126, it can be seen that peracetic acid is able to have some impact on the ease of removal of biofilms from the steel surface, but the level of success is minimal particularly when compared to

the effect of sodium hypochlorite on the same biofilms. This is especially true for the younger biofilms – those grown for 5 or 10 days had their adhesive strength reduced to less than half of its original level by 100 mg/L NaClO, yet the addition of peracetic acid only reduced the shear stress requirement by 2-3 Pa after 5 days' growth. The higher concentration had no additional effect (similar to NaClO). There would therefore be little to be gained in terms of surface removal by adding peracetic acid, and not enough of a benefit to compensate for the chemical addition, even taking into account the safe decomposition and minimal toxicity.

7.6.2 Thickness Tests

In this section are the results concerning the reduction of biofilm thickness after exposure to sodium hypochlorite and peracetic acid solutions. Shown first in Figure 127 is a graph showing an example of the loss of biofilm with increasing shear stress, including the effect of 1000 mg/L NaClO.

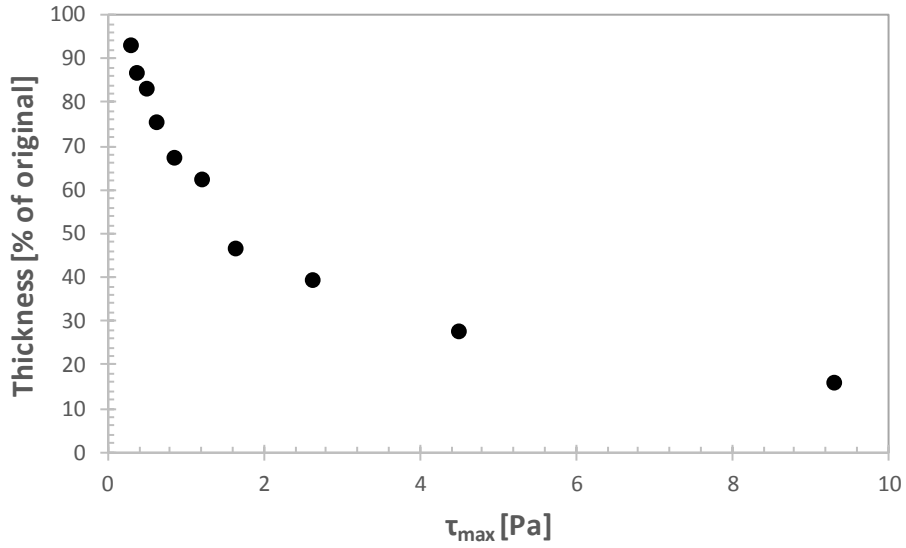

Figure 127: The percentage of biofilm thickness reduction in terms of the estimated wall shear stress deduced from the mass flow rate at the respective nozzle clearance (h/d_t), for a mixed species biofilm grown for 14 days under drip flow on a stainless steel surface. The biofilm was initially exposed to 1000 mg/L sodium hypochlorite for 15 minutes.

The obvious point of interest in Figure 127 is how rapidly the external regions of biofilm are shed using low shear stresses after sodium hypochlorite has been introduced. Less than 2 Pa was able to remove the outer 50% of biofilm, which is approximately half the shear stress required for just the hydrodynamic removal in Section 7.5.1. There is evidence of some weakening of the areas closer to the surface as well – 15.3 Pa removed 95% of the equivalent biofilms without chemical influence, and in this case 9.3 Pa has removed 84% thickness. The previous section showed a 95% reduction in surface coverage using 13.2 Pa with NaClO, so the cohesive strength is clearly reduced on the basis of this figure.

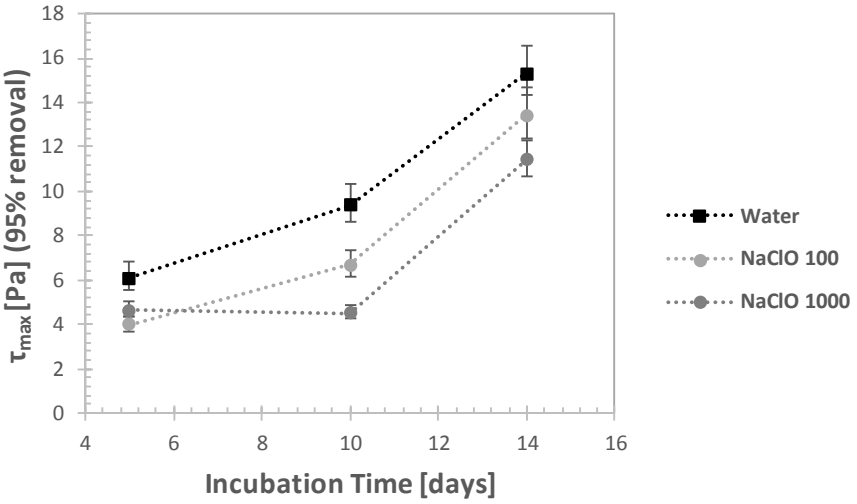

Figure 128: The shear stress required to remove 95% thickness of mixed species biofilms grown under drip flow on stainless steel, comparing the effect of exposure to sodium hypochlorite on cohesive strength.

Figure 128 indicates that the addition of sodium hypochlorite results in a general reduction in the cohesive strength of biofilms, with equivalent reductions in strength for the two different concentrations after 10 and 14 days' growth. The impact is not as pronounced as the reduction witnessed for adhesive strength in the previous section, and the exposure to NaClO has the effect of bringing the results for 95% surface removal and thickness reduction much closer together than previously, suggesting the comprehensive removal of regions of biofilm rather than a gradual reduction of layers. An example for peracetic acid is now shown.

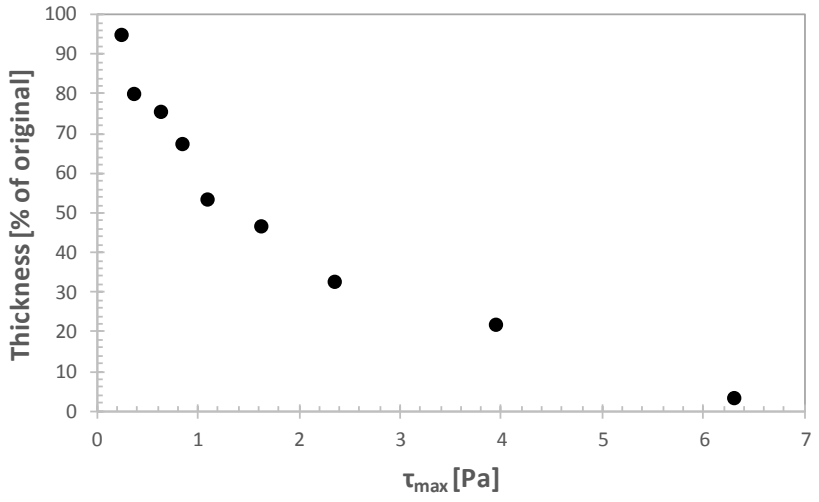

Figure 129: The percentage of biofilm thickness reduction in terms of the estimated wall shear stress deduced from the mass flow rate at the respective nozzle clearance (h/d_t), for a mixed species biofilm grown for 14 days under drip flow on stainless steel. The biofilm was initially exposed to 1000 mg/L peracetic acid for 15 minutes.

Peracetic acid had a far greater impact on biofilm cohesive strength than sodium hypochlorite. The reduction of the shear stress requirement from 15 Pa to between 6 and 7 Pa is a substantial one, and is more suggestive of biocidal effect than the adhesive strength test in Section 7.6.1 which showed little difference due to the addition of peracetic acid. The effect on the removal behaviour of the outer layers is similar to NaClO, with approximately 50% being removed by the application of under 2 Pa. The difference is in the removal of the remaining biofilm, which progresses much more rapidly in this case.

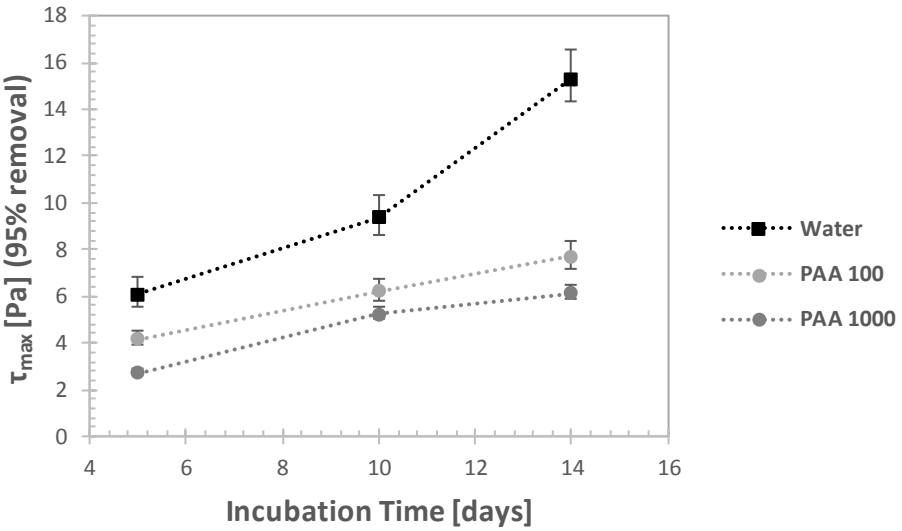

Figure 130: The shear stress required to remove 95% thickness of mixed species biofilms grown under drip flow on stainless steel, comparing the effect of exposure to peracetic acid on cohesive strength.

Figure 130 shows again that peracetic acid is able to have a significant impact on the cohesive strength of the biofilms, despite having been shown to be largely ineffective at removing the surface-attached cells. The graph also indicates that 100 mg/L would be sufficient to have the desired impact in most circumstances, with little difference made by the increase in concentration. The age of the biofilm also has considerably less effect on cohesive strength after treatment with peracetic acid.

7.6.3 Optimisation of Chemical Biocide Usage

The results in this sub-section highlight the importance of monitoring biocide concentrations to prevent excessive use. Figures 121 and 126, in particular, show that the ability of both sodium hypochlorite and peracetic acid to remove surface-attached cells was not noticeably improved by increasing the dose from 100 to 1000 mg/L. It follows that the must be a point at which the increase in chemical input outwheighs the savings in water used, and therefore the concentration should be kept below this amount. This is not a simple process, given that the energy required to pump water and biocides is also important. Additionally, a decision would have to be made regarding whether water

and chemical use should be assigned equal significance or if a weighting system should be applied. It is possible to make some estimates, however, which should give a reasonable indication of a suitable range of concentrations to use.

Given that removal from the surface is the most important function for biofouling removal due to re-growth, Figure 121 can be used as a basis for optimisation. If the surface is being cleaned after 14 days, the following shear stresses are required for 95% removal using a) just water, b) 100 mg/L NaClO, and c) 1000 mg/L NaClO: a) 26.5 Pa, b) 15.8 Pa, and c) 12.6 Pa. In order to analyse the amount of water required to achieve this, these must be converted into the equivalent pipe flow velocities, which are: a) 3.26 m/s, b) 2.51 m/s, and c) 2.24 m/s. If equal significance is given to water and chemical usage, the maximum NaClO concentration (1000 mg/L) becomes equal to the maximum water velocity (3.26 ms^{-1}) on the y-axis when plotting the total contribution of resources.

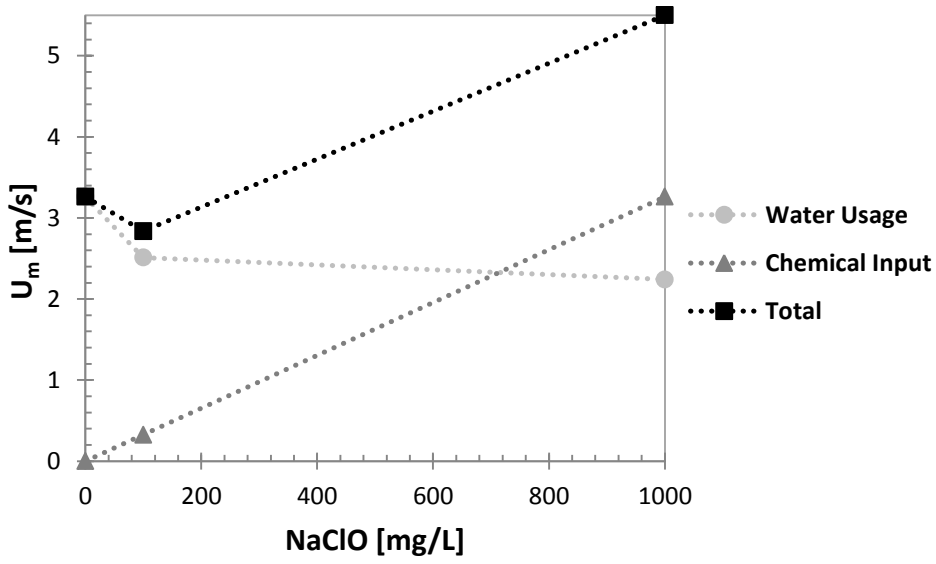

Figure 131: An estimate of the total required contribution of water and sodium hydroxide to remove 95% surface coverage of mixed species biofilms from stainless steel, as the concentration of NaClO is increased from zero to 1000 mg/L. Equal weighting is given to the two components when producing the Total curve.

With all the approximations stated before Figure 131 taken into account, it can be seen that the addition of some sodium hydroxide is, on balance, beneficial for a green cleaning approach. Determining a precise concentration would require more data points, but the approximations made mean that a high level of accuracy would be very hard to achieve anyway. The small change in water required between 100 and 1000 mg/L NaClO suggests that the optimum point may be lower than 100 mg/L, however.

Similarly, for peracetic acid in the same scenario, the shear stresses are required for 95% removal using a) just water, b) 100 mg/L PAA, and c) 1000 mg/L PAA are: a) 26.5 Pa, b) 21.9 Pa, and c) 21.8

Pa. In order to analyse the amount of water required to achieve this, these must be converted into the equivalent pipe flow velocities, which are: a) 3.26 m/s, b) 2.96 m/s, and c) 2.95 m/s. With the same method used as for sodium hypochlorite, the following result is seen:

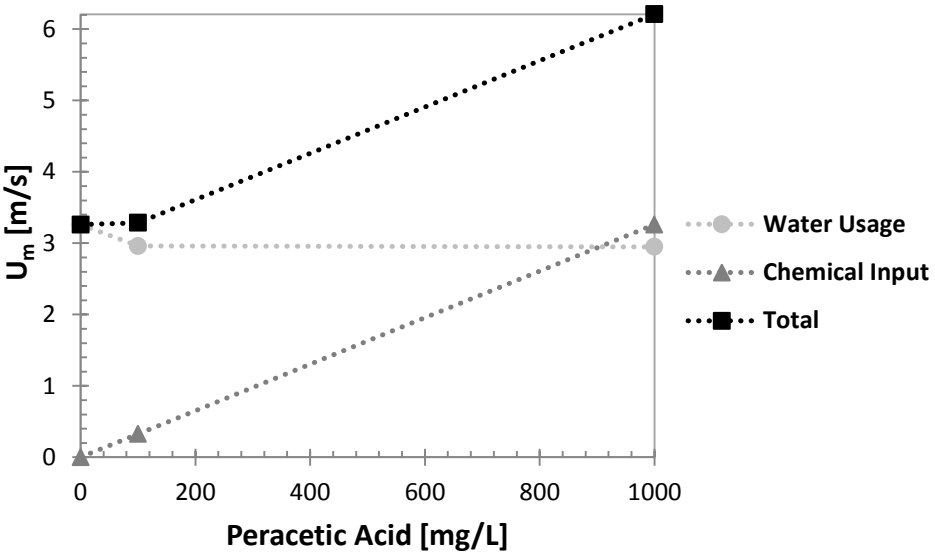

Figure 132: An estimate of the total required contribution of water and peracetic acid to remove 95% surface coverage of mixed species biofilms from stainless steel, as the concentration of PAA is increased from zero to 1000 mg/L. Equal weighting is given to the two components when producing the Total curve.

Figure 132 suggests that, as suspected, adding peracetic acid has an insuffient impact on ease of biofilm removal (in terms of surface coverage) to justify its inclusion. Any gains in surface removal due to PAA would be outweighed by the continued need for substantial amount of water for hydrodynamic removal. As suggested by Figure 130, though, it can have value in its ability to enable the removal of the outer layers of biofilm with relative ease which could be important to some applications where process efficiency takes precedence over the contamination risk (e.g. on ship hulls or in the production of non-consumable goods).

7.6.4 Summary

In the simplest terms, the results for this section show that sodium hypochlorite is more effective at improving the removal of biofilm from the surface, yet peracetic acid is more efficient in eliminating the rest of the bulk of biomass. For NaClO, the removal of most of the thickness of the biofilm is followed swiftly (in terms of shear stress) by removal from the surface, suggesting a comprehensive removal of chunks of cells. In terms of removal of 95% surface coverage, the introduction of NaClO reduced the required shear stress by approximately a half. The optimum amount of NaClO to balance with water use is difficult to determine with these results, but Figure 131 indicates that it could be found with further experimentation. A combined approach is almost certainly preferable to either

hydrodynamic or chemical methods alone. Gomes *et al.*, (2016) studied removal of *Acinetobacter calcoaceticus* and *Stenotrophomonas maltophila* from PVC, and showed that 0.5 mg/L of NaClO produced virtually no effect, but that the minimal bactericidal concentrations (M.I.C.s) (125 and 175mg/L respectively) did reduce the amount of biofilm remaining by a modest amount (in terms of cells per cm^2), in a fashion similar to that observed here, although they did observe a complete loss of colony forming units (CFUs) under M.I.C. levels. Vázquez-Sánchez *et al.*, (2014) assessed the minimal bactericidal concentrations of various *Staphylococcus aureus* strains during biofilm establishment, and reported that, depending on the strain, between 600 and 950 mg/L of NaClO was necessary to prevent biofilms from being formed. This indicates a higher level of resistance than reported here, although it concerned a different species and was instead related to the prevention of biofilm establishment. Mathieu *et al.*, (2014) studied the effect of a 60-minute chlorination (at 3.7 mg/L) on the cohesive strength of 2-month old drinking water biofilms, and reported a reduction from 15.4 to 13.1 kPa required to detach biofilm clusters. This study indicates again the efficacy of chlorine derivatives in biocidal functions, although the dangers of excessive chlorination are indicated here with little extra effect resulting from the extra increase in concentration. The effect of chlorine is well established, but issues regarding toxicity and acquired resistance still remain.

Peracetic acid, on the other hand, showed good potential in weakening the cohesive bonds within the biofilm structure, yet was almost ineffective in removing the cells attached to the surface. It has been suggested that peracetic acid has the potential to 'fix' biofilms to glass - a study by Loukili *et al.*, (2006) on the effects of peracetic acid on *E. coli* biofilms grown on glass showed a total failure of a 1100 mg/L solution to produce any detergent activity (although the addition of a non-ionic surfactant did result in some activity) - and this suggests that this may also be the case for stainless steel. The study by Vázquez-Sánchez *et al.*, (2014) mentioned previously also studied the MICs of peracetic acid required to prevent biofilm growth, and reported that concentrations of between 300 and 450 mg/L were necessary, lower than that for NaClO. It is believed to be adept at diffusing through the biofilm matrix due to its small size, which may account for its ability to reduce biofilm cohesion. Its strength in this area may make peracetic acid useful as a pre-treatment to reduce biomass prior to a secondary cleaning stage, but as a comprehensive solution to biofouling it appears to be ineffective, and when considering resource use relative to surface removal, using water alone would be a better option. The increased dose in particular showed little alteration in the resulting removal behaviour.

8. CONCLUSIONS

Main Findings

The adhesive and cohesive strengths of the biofilms tested peaked at the 14-day stage for the static case, with a minority of instances reaching their peak after 10 days (based on 95% removal of surface coverage). Biofilms proved to be much easier to remove after 5 days, and when grown for 21 or 28 days. The decline in strength at later stages was shown repeatedly for biofilms grown under static conditions – for flow, the maximum growth period was 14 days, however there are reasons to suggest that a similar trend will be observed. In some cases, peak strength was reached after 10 days, and for others the rate of strength increase was reduced suggesting a low likelihood of prolonged continuation.

It was consistently shown that the *Escherichia coli* strain formed stronger biofilms than either *Burkholderia cepacia* or the biofilms containing both species. This is useful because most biofilms in industrial situations contain multiple species, and an awareness of the potential complications this can cause is essential. Additionally, the removal behaviours of *B. cepacia* and mixed species biofilms were similar, implying a dominance of *B. cepacia* within the mixed culture, or a tendency of *E. coli* to colonise the nutrient-rich outer layers leaving *B. cepacia* attachment to govern the adhesive strength of the biofilms.

The thicknesses recorded for all of the biofilms also reached maximum levels at around 14 days, although differed from the strengths in that the thickness did not decline as biofilm age was increased further. Instead, little change in thickness was observed between 14 and 28 days, suggesting that an equilibrium was typically reached between natural detachment (sloughing) and continued growth. However, as already noted, the biofilms' cohesive strength was impacted by age, so even though cells continue to grow throughout this period the matrix structure would appear not to have remained fully intact.

Removing 95% biofilm thickness was shown to be considerably easier than reducing surface coverage by the same amount. Regularly, only half the shear stress required for surface removal was able to remove the bulk biomass. This is not especially surprising, but gives an indication of the extent to which biofilms can remain in place under high stress whilst the majority of biomass has been eliminated, something which can be easily neglected by more superficial cleaning processes which focus on killing cells rather than comprehensive cleaning.

The introduction of drip flow conditions improved the strength of adhesion of younger biofilms. Both *E. coli* and mixed species biofilms showed a greater adhesive strength after 5 days compared to the equivalent static biofilms, likely due to the steady supply of fresh media. The same effect was not observed at peak strength, but it does suggest that biofilms can establish themselves more rapidly in flow conditions. They were also substantially thicker at this stage as well, supporting that theory. On

the other hand, the biofilms grown under flow exhibited a lower cohesive strength than the static ones, particularly in the case of the top 50% of the layer. This fits in accordance with the theory behind the drip flow, in which low shear growth is recognised to produce thick, porous biofilms (Gerlach and Cunningham 2010).

In terms of the biofilm and surface characterisation methods used within the study, surface roughness is unlikely to be a significant factor in explaining strength trends, given the relative similarity of crevice sizes and frequency. The hydrophobicity of polyethylene could be viewed as a driving force behind the often-observed stronger biofilms on its surface in the earlier stages. However this could be contested because, as discussed in Section 2.5.2, it has been suggested that hydrophobicity may be more important for cell retention rather than adhesion, and other research has questioned the link altogether (with cell hydrophobicity a conflicting factor). The analysis with the significant promise related to the strength results was the protein levels recorded using the cation exchange method. The trends of increase and decline in strength were matched by similar changes in protein over the time period. The polysaccharide levels displayed a similar pattern, although the relationship was weaker due to a sharp peak after 10 days followed by decline. The loss of both components beyond 14 days is interesting because it contrasts with the result showing that biofilm thickness is maintained. The confocal microscopy results also indicated that the coverage of EPS did not markedly change at this point, nor were there a particularly higher proportion of dead cells within the older biofilms. This implies that degradation of vital components could be the best explanation for loss of biofilm strength over time.

The effect of chemical biocides was shown in the final section, with sodium hypochlorite substantially weakening the adhesion of biofilms to the surface and peracetic acid being adept at reducing cohesive strength. Both allowed the outer layers of the biofilms to be removed with great ease. In addition to this, neither showed an enhanced effect when the respective concentration was increased from 100 to 1000 mg/L, an indication of the importance of not adding excessive chemicals beyond the point at which they are useful. It was shown that removal of biofilms from a surface could be optimised using a combined approach of hydrodynamic and chemical methods, and that with the method of short-term chlorination used here, the ideal sodium hypochlorite input would be in the region of 100 mg/L.

Implications

There has previously been little study in the strength of biofilms over longer periods of time. Certain studies have, however, observed that adhesive strength can continue to increase beyond the 28 days tested in this study when grown under flow. Ohashi *et al.*, (1999) grew biofilms for up to 32 days using an open channel reactor, and observed that biofilm strength increased consistently up to this point in time. Chen *et al.*, (1998) suggested that adhesive strength increased with the flow velocity under which they were grown, and it is possible that the static biofilms grown in this study

experienced a loss of strength between 14 and 28 days as a result of their growth conditions (not strictly static due to the shaking plate – the maximum orbital shear stress was calculated as 0.086 Pa). If decay within the surface interfacial region of the biofilm can occur as a result of ageing, the lack of a prevailing flow rate may be responsible for inducing starvation of surface-attached cells due to a lack of fresh media supply, and the introduction of flow would at least have the potential to prevent this from occurring. Within this research, biofilms were only grown under flow conditions for 14 days so any conclusions beyond this point can only be speculative. It was suggested that the rate of strength increase was slowing down, but it is possible that this was temporary or that strength would remain relatively consistent over longer periods of time. The drip flow reactor is a low shear method, which in accordance with the effect of a relatively slow flow velocity, could be a reason for the lack of strength development through to 14 days, especially in terms of cohesion. Cohesive strength in the drip flow biofilms was consistently lower than the static biofilms, especially in the outer 50%.

The findings regarding biofilm thickness can also be important with regards to cleaning. Thicker biofilms cause substantial process issues concerning enhanced pressure drop and reduced heat transfer, as well as experiencing regular detachment of clusters of cells in to the flow for re-colonisation elsewhere or for contamination of products. It was found that the biofilms grown in static conditions reached a peak level at approximately 14 days, and retained the majority of that thickness thereafter. The drip flow biofilms continued to grow up to the 14-day point. This is in general agreement with other research into thickness development. Ohashi *et al.*, (1999) grew biofilms in an open channel reactor and recorded a peak thickness which occurred after 25 days and sustained beyond that period. Ahimou *et al.*, (2007) grew biofilms from up to 12 days in a membrane aerated bioreactor, and observed increases in thickness over the period. The thicker the biofilm, the greater the distance both nutrients and biocides must penetrate in order to affect the surface layer. It follows that the effect of biocides is likely to be diminished beyond 14 days of growth – in fact sodium hypochlorite, which was shown to be effective in reducing adhesive strength, can be seen to have been less effective against 14-day biofilms in Figure 120. This again raises the risk of excessive chemicals being used in cleaning if existing concentrations are seen to be ineffective, and it was consistently shown in this study that high increases in concentration have a negligible effect. The ability of peracetic acid to attack and weaken the external layers of biofilm would be useful in attacking thicker biofilms, and it was shown to be unaffected by the increase in thickness and strength displayed after 14 days. Overall, though, it appears that the risks of allowing biofilms to develop greatly in thickness are too great and outweigh the benefits of chemical input. In most cases regular cleaning would still be beneficial.

The observation that the mixed species biofilms were easier to remove than the *E. coli* monocultures is contrary to the majority of research which suggests that coaggregating species are typically harder to remove, but it is by no means an original feature. The ways in which different species interact in

combination vary greatly. Often, one species will colonise the surface first, and Cavalcanti *et al.*, (2014) showed that the level of colonisation by the first species can be important for the coaggregative effect. Another feature, recognised by Zhang *et al.,* (2013), is that the dominant strain can exert its superiority by occupying the outer layers in order to access more nutrients, leaving the other starved near the surface. What it does serve to highlight is the unique nature of each biofilm, particularly in pipelines or similar situations where the species present are likely to be unidentified. The ability of pathogens to attach themselves to existing structures is well known, and the unpredictability of biofilm formation and development should focus the minds of those who wish to remove them. It makes any temptation to neglect them and wait for natural detachment or death highly unwise.

The results for EPS composition showed the most promise as a possible explanation for the trends in removal behaviour. Differences between the surfaces used had relatively a very small impact on biofilm attachment – the ageing trends were the same and in terms of cleaning they behaved in much the same way in response to fluid shear irrespective of material. This distinction could be significant for biofouling prevention if a reliable method of EPS degradation could be found – surface coatings and modifications are the focus of much study, but EPS control could be a better strategy, particularly long-term (where coatings will need re-applying). Whilst EPS coverage was shown by confocal microscopy not to have altered significantly during the weakening phase, its composition showed changes which can be connected to the ease of removal. Both proteins and polysaccharides were lost in the later stages of growth, despite biofilm thickness being maintained and most EPS still being present. It has been recognised that EPS components can degrade, and this can be investigated using CLSM and Raman spectroscopy (Wagner *et al.,* 2009), although research into this has been limited. Whilst polysaccharide is believed to be the main source of structural strength, there was a stronger correlation between protein and strength in these results (adhesive strength in particular). Proteins are able to act as enzymes for the digestion of exogenous molecules in order to produce nutrients (Wingender *et al.*, 1999), and so this may account for the connection to strength, particularly with relevance to the already nutrient-starved surface-attached cells. With regards to polysaccharides, Chen *et al.,* (2005) noted an increase in adhesion when glucose levels were increased from 15 to 30 mg/L, but a decrease when it was increase further up to 45 mg/L. The highest amount recorded in this case was 12 mg/L, so it is possible that polysaccharide levels were not sufficient for this effect to be observed fully.

Both biocides used in this study displayed a clear weakening effect on biofilms, enabling removal with lower shear stresses. Removal of the top 50% of biofilm thickness was made distinctly easier by both sodium hypochlorite (NaClO) and peracetic acid. NaClO was able to make a considerable impact on surface removal, with little more shear stress required than was necessary to remove the outer layers. The most illuminating point was the ineffectuality of the step up from 100 to 1000 mg/L,

indicating that the demand of the biofilms must have been in the region of 100 mg/L, and the overuse of chemicals is the key point being examined by this research. An approximate optimum concentration could be found with a greater range of test levels. If cells can be killed by a low concentration of biocide, this can enable the easier removal of biofilms by hydrodynamic forces.

The levels of wall shear stress required for effective biofilm removal is comparable to those employed in cleaning-in-place (CIP) systems, which operate under turbulent flow, despite the FDG process utilising laminar flow for removal. The shear stress levels required for biofilm removal indicate the necessity for turbulent flow in a larger scale system, and the corresponding fluid velocities are unjustifiably high in accordance with green cleaning principles. Therefore, it is clear that the input of disinfectants will be required, and the addition of smaller concentrations of chemicals has been shown to be adept at removing the external layers of biofilm, so this may be the way forward.

Conclusions

The main purpose of the study was to seek to suggest methods of implementing reductions in chemical, water and energy use in industrial biofilm removal without sacrificing efficacy. Eliminating the risk of biofouling is effectively impossible, so proportionate and timely management of the problem is essential. The technique of fluid dynamic gauging was employed in order to measure their strength and explain their removal behaviour. Chemicals are adept at killing cells, yet whilst the biofilm matrix structure remains in place, cells will re-attach and the biofilm will return. The entire structure must therefore be removed, but there is little in the way of consensus on a solution.

Having observed that the adhesive and cohesive strengths of biofilms increases steadily as far as 14 days of age, and combined with the evidence from previous research that this strength will most likely be sustained over longer periods under flow conditions, it would be highly preferable to conduct regular cleaning (no later than every 5 days) to prevent further fouling build-up and the development of stronger adhesive and cohesive bonds. This is especially true for hydrodynamic methods, for which both the water used and the associated pumping power must be considered. The risk of pathogens developing the longer the biofilm is left in place is another motivation for regular cleaning. The development of a greater and sustained thickness over time can also pose problems with heat transfer and enhanced pressure drop. Both sodium hypochlorite and peracetic acid can be used effectively to remove the outer layers with a lower shear stress, although surface layer removal is more important for the restriction of biofilm re-growth. Sodium hypochlorite was shown to be effective for weakening surface adhesion – for the 15-minute exposure used here, a concentration in the region of 100mg/L is optimum when combined with the shear stress applied by water. There are more risks associated with chlorine-based disinfectants than peracetic acid, although low concentrations would be sufficient and finding a more optimised level would be relatively simple using more iterations this method, as long as the criteria for the management of water and chemical inputs is pre-defined. As always,

preventative methods are an appealing alternative, and the apparent correlation between protein concentration in the EPS matrix and ease of removal is worth further exploration. If a method could be found to reliably induce protein degradation with a relatively minimal chemical input, this could be a important way of weakening biofilms and reducing resource use. This must be done safely i.e. without creating harmful by-products or contributing significantly more to the chemical demand for cleaning. Alternative removal methods may prove useful for this, such as ultrasound, UV irradiation or enzyme action.

For further research, using a higher media flow rate would encourage more stable biofilms, as long as fresh media could be produced regularly enough. *In situ* gauging would reduce the risk of disturbing biofilms during the testing stage, although adhesive strength could not be quantified in the same way. Taking a multispecies inoculation sample from a process flow would be advisable to have a more realistic approximation of industrial biofilms. Surface coatings aimed at biofilm prevention are the focus of large amounts of current research, and could be an alternative to reactive methods, although recoating can lead to process downtime.

In summary, there is no simple answer to the problem, which is further complicated by the unpredictability of the species would be present in industrial biofouling. The best way of minimising the risk of spoiling and contamination would be to clean surfaces regularly, which would also serve to minimise the resources used by preventing biofilms from becoming too strongly attached or too thick. The chemical input would need to be determined by testing for the optimum concentration necessary for a suitable effect (eliminating excess use), and discovering the correct balance to avoid use of excess water and energy in the process.

9. FUTURE RECOMMENDATIONS

Operating Conditions

The most obvious way of continuing this research would be to study the growth of drip flow biofilms beyond 14 days, given that previous work suggests that their strength would not decline with further ageing, in contrast with the static biofilms. Time and the inability to run parallel experiments hampered the prospects of doing this within this research, and a specific focus on studying older biofilms would be necessary to test that theory. However, this may be unnecessary, given that the results shown here suggest that regular cleaning prior to widespread establishment is the best method for biofilm removal and management of associated risks. Viewed from this perspective the behaviour of biofilms older than 14 days is irrelevant, at least from a practical viewpoint regarding cleaning.

Another focus would perhaps be to increase the flow rate of media during growth. The change from static to drip flow resulted in an increase in difficulty in removing 50% of surface coverage, indicating a more widespread strong adhesion under flow. Growth under high shear is believed to promote greater stability – i.e. they detach under an accordingly higher shear stress. If this could be shown to be true using the techniques outlined here, then it could raise doubts as to the efficacy of cleaning in the early stages of development, if the biofilms were not sufficiently weaker. The volume of media required for a greater flow rate during growth would have proved impossible to produce quickly enough in this study, and would have required replacement in the feed tank far too regularly – about every hour or two which is unmanageable over the course of several days.

Apparatus Design

Previous research conducted using FDG has involved *in situ* gauging, incorporating the nozzle into the design of the flow cell. This was demonstrated by Tuladhar *et al.*, (2003), who monitored fouling development in a square duct using an FDG nozzle situated within the flow. Later, computational fluid dynamics was used by Gu *et al.*, (2007) to simulate this system, showing a strong agreement with the results shown by Tuladhar *et al.*, (2003). It can be advantageous to study bacterial deposits in this fashion, because as previously discussed (Section 2.8.6), biofilms are prone to slumping outside of their growth environment and can be deformed easily by physical contact. However, the downside to this approach is that it would not be possible to analyse surface coverage before gauging, so the adhesive strength would not be quantified. That said, as a follow-up to this study, knowledge of the cohesive strength could be taken from *in situ* studies with these results used as a reference point.

A recent study by Lemos *et al.*, (2016) looked at the possibility of a similar system in which a cylindrical duct was used. The gauging mechanism was verified using CFD, and some tests were conducted on biofilms on polyethylene and stainless steel surfaces. Perhaps unsurprisingly due to the geometry, the biofilms varied considerably in thickness, but the closer similarity with industrial pipe networks makes it an interesting and vital focus for further research. The same difficulties regarding

measuring adhesive strength would have to be overcome, however. This study suggested video microscopy as a potential option for studying surface removal.

Coatings

A promising alternative to cleaning to remove biofilms is to instead utilise preventative measures, typically in the form of coatings. For example, Demling *et al.,* (2010) demonstrated that polytetrafluoroethylene (PTFE) coating could reduce biofilm formation on orthodontic brackets to a minimum, and Liu and Zhao (2011) incorporated PTFE into existing Ni-P coatings and showed strong anti-bacterial performance compared to the existing steel surface. This could theoretically negate the need for chemical inputs, if biofilm formation was reduced to level which could be removed by hydrodynamic forces only. The need to clean still remains, and therefore the strength of bacterial adhesion would still be an important feature to be aware of. Surfaces also require periodical re-coating as layers can deplete over time and due to exposure to chemicals in the flow.

Multi-Species Biofilms

Typically, most biofilms found in industrial settings contain a wide range of species, as opposed to the two strains used in this study. The more species present, the more complex the interactions governing the biofilm's function can be. The importance of interactions between different species has been recognised in biofilm bacteria found in process systems, water distribution networks and natural environments (Burmølle *et al.,* 2014). A typical inoculation method is to obtain a sample of contaminated fluid from a process system (Pechaud *et al.,* 2012). This has the advantage of creating a good representation of the biofouling experienced in industry, although its impreciseness makes its repeatability difficult to assess and patterns hard to discern. However, this is the nature of industrial biofouling – each case is different from the last.

Further Characterisation

Better understanding of the processes surrounding protein and polysaccharide degradation would also be beneficial. If they (protein in particular) play a significant role in the adhesion of biofilms and the difficulty of their removal, then any method of triggering degradation may help to enable easier removal. They have previously been shown to be highly effective in the removal of surface layers, and it is possible that protein degradation may be a factor in this.

Identifying the chemical demand of the biofilms tested would be another useful next step. It was observed that there was negligible difference in impact between 100 and 1000 mg/L of either sodium hypochlorite or peracetic acid, despite the influences of each being clearly noticeable. It follows that in order to minimise the negative effects of chemicals in cleaning (especially chlorine), locating the optimum point of removal efficacy without unnecessary further increases is an essential component of developing a green cleaning strategy given that hydrodynamic methods alone are unlikely to be suitable in most cases.

REFERENCES

Aantrekker, Esther D. den, Wouter W. Vernooij, Martine W. Reij, Marcel H. Zwietering, Rijkelt R. Beumer, Mick van Schothorst, and Remko M. Boom. "A Biofilm Model for Flowing Systems in the Food Industry." *Journal of Food Protection* 66, no. 8 (August 2003): 1432–38.

Abdul Azis, P. K., Ibrahim Al-Tisan, and N. Sasikumar. "Biofouling Potential and Environmental Factors of Seawater at a Desalination Plant Intake." *Desalination* 135, no. 1 (April 20, 2001): 69–82. doi:10.1016/S0011-9164(01)00140-0.

Abe, Yumiko, Salaheddine Skali-Lami, Jean-Claude Block, and Grégory Francius. "Cohesiveness and Hydrodynamic Properties of Young Drinking Water Biofilms." *Water Research* 46, no. 4 (March 15, 2012): 1155–66. doi:10.1016/j.watres.2011.12.013.

Adamson, A. W., and A. P. Gast. *Physical Chemistry of Surfaces*. 6th ed. New York: John Wiley & Sons, Inc., 1997.

Adetunji, V. O., and T. O. Isola. "Crystal Violet Binding Assay for Assessment of Biofilm Formation by Listeria Monocytogenes and Listeria Spp on Wood, Steel and Glass Surfaces." *Global Veterinaria* 6, no. 1 (2011): 6–10.

Ahimou, Francois, Michael J. Semmens, Greg Haugstad, and Paige J. Novak. "Effect of Protein, Polysaccharide, and Oxygen Concentration Profiles on Biofilm Cohesiveness." *Applied and Environmental Microbiology* 73, no. 9 (May 1, 2007): 2905–10. doi:10.1128/AEM.02420-06.

Ahimou, Francois, Michael J. Semmens, Paige J. Novak, and Greg Haugstad. "Biofilm Cohesiveness Measurement Using a Novel Atomic Force Microscopy Methodology." *Applied and Environmental Microbiology* 73, no. 9 (May 1, 2007): 2897–2904. doi:10.1128/AEM.02388-06.

Al-Ahmad, A., M. Wiedmann-Al-Ahmad, A. Fackler, M. Follo, E. Hellwig, M. Bächle, C. Hannig, J.-S. Han, M. Wolkewitz, and R. Kohal. "In Vivo Study of the Initial Bacterial Adhesion on Different Implant Materials." *Archives of Oral Biology* 58, no. 9 (September 2013): 1139–47. doi:10.1016/j.archoralbio.2013.04.011.

Al-Bakeri, Faisal, and Hassan El Hares. "Experimental Optimization of Sponge Ball Cleaning System Operation in Umm AI Nar MSF Desalination Plants." *Desalination* 94, no. 2 (December 1993): 133–50. doi:10.1016/0011-9164(93)EO126-I.

Albrich, Werner C., Dominique L. Monnet, and Stephan Harbarth. "Antibiotic Selection Pressure and Resistance in Streptococcus Pneumoniae and Streptococcus Pyogenes." *Emerging Infectious Diseases* 10, no. 3 (March 2004): 514–17. doi:10.3201/eid1003.030252.

Al-Darbi, M. M., Z. M. Muntasser, M. Tango, and M. R. Islam. "Control of Microbial Corrosion Using Coatings and Natural Additives." *Energy Sources* 24, no. 11 (November 1, 2002): 1009–18. doi:10.1080/00908310290086941.

Aldén, L., F. Demoling, and E. Bååth. "Rapid Method of Determining Factors Limiting Bacterial Growth in Soil." *Applied and Environmental Microbiology* 67, no. 4 (April 1, 2001): 1830–38. doi:10.1128/AEM.67.4.1830-1838.2001.

Alhede, Morten, Klaus Qvortrup, Ramon Liebrechts, Niels Høiby, Michael Givskov, and Thomas Bjarnsholt. "Combination of Microscopic Techniques Reveals a Comprehensive Visual Impression of Biofilm Structure and Composition." *FEMS Immunology & Medical Microbiology* 65, no. 2 (July 1, 2012): 335–42. doi:10.1111/j.1574-695X.2012.00956.x.

Ali, A., G. J. Chapman, Y. M. J. Chew, T. Gu, W. R. Paterson, and D. I. Wilson. "A Fluid Dynamic Gauging Device for Measuring Fouling Deposit Thickness in Opaque Liquids at Elevated Temperature and Pressure." *Experimental Thermal and Fluid Science* 48 (July 2013): 19–28. doi:10.1016/j.expthermflusci.2013.02.004.

Ali, Akin, Dominic de'Ath, Douglas Gibson, Jennifer Parkin, Zayeed Alam, Glenn Ward, and D. Ian Wilson. "Development of a 'millimanipulation' Device to Study the Removal of Soft Solid Fouling Layers from Solid Substrates and Its Application to Cooked Lard Deposits."

Food and Bioproducts Processing 93 (January 2015): 256–68. doi:10.1016/j.fbp.2014.09.001.
Al-Juboori, Raed A., and Talal Yusaf. "Biofouling in RO System: Mechanisms, Monitoring and Controlling." *Desalination* 302 (September 17, 2012): 1–23. doi:10.1016/j.desal.2012.06.016.
Allison, D. G., B. Ruiz, C. SanJose, A. Jaspe, and P. Gilbert. "Extracellular Products as Mediators of the Formation and Detachment of Pseudomonas Fluorescens Biofilms." *FEMS Microbiology Letters* 167, no. 2 (October 15, 1998): 179–84.
Almatroudi, A., I. B. Gosbell, H. Hu, S. O. Jensen, B. A. Espedido, S. Tahir, T. O. Glasbey, et al., "Staphylococcus Aureus Dry-Surface Biofilms Are Not Killed by Sodium Hypochlorite: Implications for Infection Control." *The Journal of Hospital Infection* 93, no. 3 (July 2016): 263–70. doi:10.1016/j.jhin.2016.03.020.
Alsteens, David, Etienne Dague, Paul G. Rouxhet, Alain R. Baulard, and Yves F. Dufrêne. "Direct Measurement of Hydrophobic Forces on Cell Surfaces Using AFM." *Langmuir: The ACS Journal of Surfaces and Colloids* 23, no. 24 (November 20, 2007): 11977–79. doi:10.1021/la702765c.
Altekruse, S. F., M. L. Cohen, and D. L. Swerdlow. "Emerging Foodborne Diseases." *Emerging Infectious Diseases* 3, no. 3 (1997): 285–93. doi:10.3201/eid0303.970304.
Altmann, Justus, and Siegfried Ripperger. "Particle Deposition and Layer Formation at the Crossflow Microfiltration." *Journal of Membrane Science* 124, no. 1 (February 1, 1997): 119–28. doi:10.1016/S0376-7388(96)00235-9.
Applegate, David H., and James D. Bryers. "Effects of Carbon and Oxygen Limitations and Calcium Concentrations on Biofilm Removal Processes." *Biotechnology and Bioengineering* 37, no. 1 (January 5, 1991): 17–25. doi:10.1002/bit.260370105.
Ascon-Cabrera, M. A., D. Thomas, and J. M. Lebeault. "Activity of Synchronized Cells of a Steady-State Biofilm Recirculated Reactor during Xenobiotic Biodegradation." *Applied and Environmental Microbiology* 61, no. 3 (March 1995): 920–25.
Auerbach, Ilene D., Cody Sorensen, Helen G. Hansma, and Patricia A. Holden. "Physical Morphology and Surface Properties of Unsaturated Pseudomonas Putida Biofilms." *Journal of Bacteriology* 182, no. 13 (July 1, 2000): 3809–15. doi:10.1128/JB.182.13.3809-3815.2000.
Azeredo, J., and R. Oliveira. "The Role of Exopolymers in the Attachment of Sphingomonas Paucimobilis." *Biofouling* 16, no. 1 (October 1, 2000): 59–67. doi:10.1080/08927010009378430.
Baier, R. E. "Substrate Influences on Adhesion of Microorganisms and Their Resultant New Surface Properties." In *Adsorption of Microorganisms to Surfaces*, 59–104. New York: Wiley - Interscience, 1980.
Bakke, R. "Biofilm Detachment." PhD, Montana State University, 1986.
Bakke, R., R. Kommedal, and S. Kalvenes. "Quantification of Biofilm Accumulation by an Optical Approach." *Journal of Microbiological Methods* 44, no. 1 (February 1, 2001): 13–26.
Bakke, R., and P. Q. Olsson. "Biofilm Thickness Measurements by Light Microscopy." *Journal of Microbiological Methods* 5, no. 2 (July 1, 1986): 93–98. doi:10.1016/0167-7012(86)90005-9.
Baribeau, H., N. L. Pozos, L. Boulos, G. F. Crozes, G. A. Gagnon, S. Rutledge, D. Skinner, et al., "Impact of Distribution System Water Quality on Disinfection Efficacy." Denver, CO: Awwa Research Foundation, 2005.
Barraud, Nicolas, Daniel J. Hassett, Sung-Hei Hwang, Scott A. Rice, Staffan Kjelleberg, and Jeremy S. Webb. "Involvement of Nitric Oxide in Biofilm Dispersal of Pseudomonas Aeruginosa." *Journal of Bacteriology* 188, no. 21 (November 2006): 7344–53. doi:10.1128/JB.00779-06.
Barua, Subit, Paramita Basu, and IrvinN Hirshfield. "Overview of Biofilms and Some Key Methods for Their Study." In *Practical Handbook of Microbiology, Second Edition*, 675–88. CRC Press, 2008. http://www.crcnetbase.com/doi/abs/10.1201/9781420009330.ch42.

Basu, Srijoni, Chandra Bose, Nupur Ojha, Nabajit Das, Jagaree Das, Mrinmoy Pal, and Sukant Khurana. “Evolution of Bacterial and Fungal Growth Media.” *Bioinformation* 11, no. 4 (April 30, 2015): 182–84. doi:10.6026/97320630011182.

Bayer, A. S., F. Eftekhar, J. Tu, C. C. Nast, and D. P. Speert. “Oxygen-Dependent up-Regulation of Mucoid Exopolysaccharide (Alginate) Production in Pseudomonas Aeruginosa.” *Infection and Immunity* 58, no. 5 (May 1990): 1344–49.

Beech, Iwona B., C. W. Sunny Cheung, D. Barrie Johnson, and James R. Smith. “Comparative Studies of Bacterial Biofilms on Steel Surfaces Using Atomic Force Microscopy and Environmental Scanning Electron Microscopy.” *Biofouling* 10, no. 1–3 (September 1, 1996): 65–77. doi:10.1080/08927019609386271.

Beech, Iwona B, James R Smith, Andrew A Steele, Ian Penegar, and Sheelagh A Campbell. “The Use of Atomic Force Microscopy for Studying Interactions of Bacterial Biofilms with Surfaces.” *Colloids and Surfaces B: Biointerfaces* 23, no. 2–3 (February 2002): 231–47. doi:10.1016/S0927-7765(01)00233-8.

Berg, D. van den, G. W. Robijn, A. C. Janssen, M. Giuseppin, R. Vreeker, J. P. Kamerling, J. Vliegenthart, A. M. Ledeboer, and C. T. Verrips. “Production of a Novel Extracellular Polysaccharide by Lactobacillus Sake 0-1 and Characterization of the Polysaccharide.” *Applied and Environmental Microbiology* 61, no. 8 (August 1995): 2840–44.

Berry, J. A., J. F. Biedlingmaier, and P. J. Whelan. “In Vitro Resistance to Bacterial Biofilm Formation on Coated Fluoroplastic Tympanostomy Tubes.” *Otolaryngology--Head and Neck Surgery: Official Journal of American Academy of Otolaryngology-Head and Neck Surgery* 123, no. 3 (September 2000): 246–51. doi:10.1067/mhn.2000.107458.

Bigelow, Timothy A., Trevor Northagen, Thomas M. Hill, and Frances C. Sailer. “The Destruction of Escherichia Coli Biofilms Using High-Intensity Focused Ultrasound.” *Ultrasound in Medicine & Biology* 35, no. 6 (June 2009): 1026–31. doi:10.1016/j.ultrasmedbio.2008.12.001.

Black, J. G. *Microbiology: Principles and Explorations*. 8th ed. Hoboken, NJ: John Wiley & Sons, Inc., 2012.

Blake II, Robert C., and Megan N. Griff. “In Situ Spectroscopy on Intact Leptospirillum Ferrooxidans Reveals That Reduced Cytochrome 579 Is an Obligatory Intermediate in the Aerobic Iron Respiratory Chain.” *Frontiers in Microbiology* 3 (2012): 136. doi:10.3389/fmicb.2012.00136.

Blanchard, Alex P., Michael R. Bird, and S. John L. Wright. “Peroxygen Disinfection of Pseudomonas Aeruginosa Biofilms on Stainless Steel Discs.” *Biofouling* 13, no. 3 (December 1, 1998): 233–53. doi:10.1080/08927019809378383.

Blankemeier, A., D. E. Huber, H. L. Fraser, W. Goodson, R. E. A. Williams, and H. O. Colijn. “Characterization of Pseudomonas Fluorescens Bacteria on Polyurethane Using DB-FIB, SEM and STEM.” *Microscopy and Microanalysis* 16, no. S2 (July 2010): 234–35. doi:10.1017/S1431927610062045.

Bloetscher, Frederick, Daniel E. Meeroff, John V. Pisani, and Sharon C. Long. “Resolving Problematic Biofilms in Buildings and Compounds.” *Environmental Engineering Science* 27, no. 9 (September 1, 2010): 767–76. doi:10.1089/ees.2009.0422.

Bloss, R., and G. Kampf. “Test Models to Determine Cleaning Efficacy with Different Types of Bioburden and Its Clinical Correlation.” *The Journal of Hospital Infection* 56 Suppl 2 (April 2004): S44-48. doi:10.1016/j.jhin.2003.12.029.

Boleij, Annemarie, Carla M. J. Muytjens, Sarah I. Bukhari, Nadège Cayet, Philippe Glaser, Peter W. M. Hermans, Dorine W. Swinkels, Albert Bolhuis, and Harold Tjalsma. “Novel Clues on the Specific Association of Streptococcus Gallolyticus Subsp Gallolyticus With Colorectal Cancer.” *Journal of Infectious Diseases* 203, no. 8 (April 15, 2011): 1101–9. doi:10.1093/infdis/jiq169.

Bollen, Curd M. L., William Papaioanno, Johan Van Eldere, Evert Schepers, Marc Quirynen, and Daniel Van Steenberghe. “The Influence of Abutment Surface Roughness on Plaque Accumulation and Peri-Implant Mucositis.” *Clinical Oral Implants Research* 7, no. 3 (September 1, 1996): 201–11. doi:10.1034/j.1600-0501.1996.070302.x.

Borriello, Giorgia, Erin Werner, Frank Roe, Aana M. Kim, Garth D. Ehrlich, and Philip S. Stewart. “Oxygen Limitation Contributes to Antibiotic Tolerance of Pseudomonas Aeruginosa in Biofilms.” *Antimicrobial Agents and Chemotherapy* 48, no. 7 (July 2004): 2659–64. doi:10.1128/AAC.48.7.2659-2664.2004.

Bos, R., H. C. van der Mei, J. Gold, and H. J. Busscher. “Retention of Bacteria on a Substratum Surface with Micro-Patterned Hydrophobicity.” *FEMS Microbiology Letters* 189, no. 2 (August 15, 2000): 311–15.

Bos, Rolf, Henny C. van der Mei, and Henk J. Busscher. “Physico-Chemistry of Initial Microbial Adhesive Interactions – Its Mechanisms and Methods for Study.” *FEMS Microbiology Reviews* 23, no. 2 (April 1, 1999): 179–230. doi:10.1111/j.1574-6976.1999.tb00396.x.

Bott, T. R. *Fouling of Heat Exchangers*. Elsevier, 1995.

———. “General Fouling Problems.” In *Fouling Science and Technology*, edited by L. F. Melo, T. R. Bott, and C. A. Bernardo, 3–14. NATO ASI Series 145. Springer Netherlands, 1988. http://link.springer.com/chapter/10.1007/978-94-009-2813-8_1.

Bott, T. R. “Techniques for Reducing the Amount of Biocide Necessary to Counteract the Effects of Biofilm Growth in Cooling Water Systems.” *Applied Thermal Engineering* 18, no. 11 (November 1998): 1059–66. doi:10.1016/S1359-4311(98)00017-9.

Bott, T. R., and P. C. Miller. “Mechanisms of Biofilm Formation on Aluminium Tubes.” *Journal of Chemical Technology and Biotechnology. Biotechnology* 33, no. 3 (March 1, 1983): 177–84. doi:10.1002/jctb.280330307.

Bott, T. R., and M. M. V. P. S. Pinheiro. “Biological Fouling — Velocity and Temperature Effects.” *The Canadian Journal of Chemical Engineering* 55, no. 4 (August 1, 1977): 473–74. doi:10.1002/cjce.5450550420.

Bott, T. R., and R. J. Taylor. “The Effects of Velocity on Biocide Use for Biofilm in Flowing Systems.” *AlChemE Symposium Series* 314 (1997): 322–25.

Boulêtreau, Stéphanie, Jean-Yves Charcosset, Jean Gamby, Emilie Lyautey, Sylvain Mastrorillo, Frédéric Azémar, Frédéric Moulin, Bernard Tribollet, and Frédéric Garabetian. “Rotating Disk Electrodes to Assess River Biofilm Thickness and Elasticity.” *Water Research* 45, no. 3 (January 2011): 1347–57. doi:10.1016/j.watres.2010.10.016.

Bradford, Marion M. “A Rapid and Sensitive Method for the Quantitation of Microgram Quantities of Protein Utilizing the Principle of Protein-Dye Binding.” *Analytical Biochemistry* 72, no. 1 (May 7, 1976): 248–54. doi:10.1016/0003-2697(76)90527-3.

Bradshaw, D. J., and P. D. Marsh. “Effect of Sugar Alcohols on the Composition and Metabolism of a Mixed Culture of Oral Bacteria Grown in a Chemostat.” *Caries Research* 28, no. 4 (1994): 251–56.

Bragonzi, Alessandra, Ilaria Farulla, Moira Paroni, Kate B. Twomey, Luisa Pirone, Nicola Ivan Lorè, Irene Bianconi, Claudia Dalmastri, Robert P. Ryan, and Annamaria Bevivino. “Modelling Co-Infection of the Cystic Fibrosis Lung by Pseudomonas Aeruginosa and Burkholderia Cenocepacia Reveals Influences on Biofilm Formation and Host Response.” *PloS One* 7, no. 12 (2012): e52330. doi:10.1371/journal.pone.0052330.

Branda, Steven S., Frances Chu, Daniel B. Kearns, Richard Losick, and Roberto Kolter. “A Major Protein Component of the Bacillus Subtilis Biofilm Matrix.” *Molecular Microbiology* 59, no. 4 (February 2006): 1229–38. doi:10.1111/j.1365-2958.2005.05020.x.

Brant, Jonathan A., and Amy E. Childress. “Membrane–Colloid Interactions: Comparison of Extended DLVO Predictions with AFM Force Measurements.” *Environmental Engineering Science* 19, no. 6 (November 1, 2002): 413–27. doi:10.1089/109287502320963409.

Breidenstein, Elena B. M., César de la Fuente-Núñez, and Robert E. W. Hancock. “Pseudomonas Aeruginosa: All Roads Lead to Resistance.” *Trends in Microbiology* 19, no. 8 (August 2011): 419–26. doi:10.1016/j.tim.2011.04.005.

Bremer, Philip J., Suzanne Fillery, and A. James McQuillan. “Laboratory Scale Clean-In-Place (CIP) Studies on the Effectiveness of Different Caustic and Acid Wash Steps on the Removal of Dairy Biofilms.” *International Journal of Food Microbiology* 106, no. 3 (February 15, 2006): 254–62. doi:10.1016/j.ijfoodmicro.2005.07.004.

Bridge, S. P., P. T. Robbins, W. R. Paterson, and D. I. Wilson. “A Pneumatic Gauging Sensor for Measuring the Thickness of Soft Films.” *Proceedings of the Institution of Mechanical Engineers, Part E: Journal of Process Mechanical Engineering* 215, no. 1 (February 1, 2001): 19–27. doi:10.1243/0954408011530262.

Bridier, A., R. Briandet, V. Thomas, and F. Dubois-Brissonnet. “Comparative Biocidal Activity of Peracetic Acid, Benzalkonium Chloride and Ortho-Phthalaldehyde on 77 Bacterial Strains.” *The Journal of Hospital Infection* 78, no. 3 (July 2011): 208–13. doi:10.1016/j.jhin.2011.03.014.

Bridier, A., F. Dubois-Brissonnet, G. Greub, V. Thomas, and R. Briandet. “Dynamics of the Action of Biocides in Pseudomonas Aeruginosa Biofilms.” *Antimicrobial Agents and Chemotherapy* 55, no. 6 (June 2011): 2648–54. doi:10.1128/AAC.01760-10.

Bridier, A., T. Meylheuc, and R. Briandet. “Realistic Representation of Bacillus Subtilis Biofilms Architecture Using Combined Microscopy (CLSM, ESEM and FESEM).” *Micron (Oxford, England: 1993)* 48 (May 2013): 65–69. doi:10.1016/j.micron.2013.02.013.

Brown, Michael R. W., and Peter Gilbert, eds. *Microbiological Quality Assurance: A Guide towards Relevance and Reproducibility of Inocula*. Boca Raton, Fl: CRC Press, 1995.

Brown, M.r.w., and P. Gilbert. “Sensitivity of Biofilms to Antimicrobial Agents.” *Journal of Applied Bacteriology* 74 (June 1, 1993): 87S–97S. doi:10.1111/j.1365-2672.1993.tb04345.x.

Brugnoni, Lorena Inés, Jorge Enrique Lozano, and María Amelia Cubitto. “Efficacy of Sodium Hypochlorite and Quaternary Ammonium Compounds on Yeasts Isolated from Apple Juice.” *Journal of Food Process Engineering* 35, no. 1 (February 1, 2012): 104–19. doi:10.1111/j.1745-4530.2009.00574.x.

Bryers, James D., and William G. Characklis. “Biofilm Laboratory Methods: The Use of Flow Reactors.” In *Biofilms — Science and Technology*, edited by L. F. Melo, T. R. Bott, M. Fletcher, and B. Capdeville, 615–29. NATO ASI Series 223. Springer Netherlands, 1992. http://link.springer.com/chapter/10.1007/978-94-011-1824-8_55.

Buckingham, E. “On Physically Similar Systems: Illustrations of the Use of Dimensional Equations.” *Physical Review* 4 (1914): 345–76.

Buckingham-Meyer, Kelli, Darla M. Goeres, and Martin A. Hamilton. “Comparative Evaluation of Biofilm Disinfectant Efficacy Tests.” *Journal of Microbiological Methods* 70, no. 2 (August 2007): 236–44. doi:10.1016/j.mimet.2007.04.010.

Buckley, Donald H. *Surface Effects in Adhesion, Friction, Wear, and Lubrication*. Elsevier, 1981.

Burfoot, Dean, and Karen Middleton. “Effects of Operating Conditions of High Pressure Washing on the Removal of Biofilms from Stainless Steel Surfaces.” *Journal of Food Engineering* 90, no. 3 (February 1, 2009): 350–57. doi:10.1016/j.jfoodeng.2008.07.006.

Burmølle, Mette, Dawei Ren, Thomas Bjarnsholt, and Søren J. Sørensen. “Interactions in Multispecies Biofilms: Do They Actually Matter?” *Trends in Microbiology* 22, no. 2 (February 1, 2014): 84–91. doi:10.1016/j.tim.2013.12.004.

Burton, Zachary F., and Jon Masato Kaguni. *Experiments in Molecular Biology: Biochemical Applications*. Academic Press, 1997.

Busscher, H. J., R. Bos, and H. C. van der Mei. “Initial Microbial Adhesion Is a Determinant for the Strength of Biofilm Adhesion.” *FEMS Microbiology Letters* 128, no. 3 (May 15, 1995): 229–34.

Buswell, C.m., Y.m. Herlihy, P.d. Marsh, C.w. Keevil, and S.a. Leach. “Coaggregation amongst Aquatic Biofilm Bacteria.” *Journal of Applied Microbiology* 83, no. 4 (September 1, 1997): 477–84. doi:10.1046/j.1365-2672.1997.00260.x.

CAC. “Recommended International Code of Practice — General Principles of Hygiene, Including Annex on Hazard Analysis and Critical Control Point (HACCP)system and Guidelines for Its Application.” Codex Alimentarus, 2003.

Calazans, S. H., L. V. Fernandes, and F. C. Fernandes. “Outros Compostos.” In *Moluscos Limnicos Invasores No Brasil: Biologia, Prevencao E Controle*, 311–15. Porto Alegre-RS, Brasil: Redes Editora, 2012.

Carlén, A., K. Nikdel, A. Wennerberg, K. Holmberg, and J. Olsson. “Surface Characteristics and in Vitro Biofilm Formation on Glass Ionomer and Composite Resin.” *Biomaterials* 22, no. 5 (March 2001): 481–87.

Carpentier, Brigitte, and Danielle Chassaing. “Interactions in Biofilms between Listeria Monocytogenes and Resident Microorganisms from Food Industry Premises.” *International Journal of Food Microbiology* 97, no. 2 (December 15, 2004): 111–22. doi:10.1016/j.ijfoodmicro.2004.03.031.

Castegnier, Françoise, Nathalie Ross, Robert P. Chapuis, Louise Deschênes, and Réjean Samson. “Long-Term Persistence of a Nutrient-Starved Biofilm in a Limestone Fracture.” *Water Research* 40, no. 5 (March 2006): 925–34. doi:10.1016/j.watres.2005.12.038.

Cavalcanti, Yuri Wanderley, Martinna Mendonça Bertolini, Wander José da Silva, Altair Antoninha Del-Bel-Cury, Livia Maria Andaló Tenuta, and Jaime Aparecido Cury. “A Three-Species Biofilm Model for the Evaluation of Enamel and Dentin Demineralization.” *Biofouling* 30, no. 5 (2014): 579–88. doi:10.1080/08927014.2014.905547.

Cerf, O., B. Carpentier, and P. Sanders. “Tests for Determining in-Use Concentrations of Antibiotics and Disinfectants Are Based on Entirely Different Concepts: ‘resistance’ has Different Meanings.” *International Journal of Food Microbiology* 136, no. 3 (January 1, 2010): 247–54. doi:10.1016/j.ijfoodmicro.2009.10.002.

Ceri, H., M. E. Olson, C. Stremick, R. R. Read, D. Morck, and A. Buret. “The Calgary Biofilm Device: New Technology for Rapid Determination of Antibiotic Susceptibilities of Bacterial Biofilms.” *Journal of Clinical Microbiology* 37, no. 6 (June 1, 1999): 1771–76.

Chandraprabha, M. N., P. Somasundaran, and K. A. Natarajan. “Modeling and Analysis of Nanoscale Interaction Forces between Acidithiobacillus Ferrooxidans and AFM Tip.” *Colloids and Surfaces. B, Biointerfaces* 75, no. 1 (January 1, 2010): 310–18. doi:10.1016/j.colsurfb.2009.09.002.

Characklis, W. G. “Bioengineering Report: Fouling Biofilm Development: A Process Analysis.” *Biotechnology and Bioengineering* 23, no. 9 (September 1, 1981): 1923–60. doi:10.1002/bit.260230902.

———. “Microbial Biofouling.” In *Biofilms*, edited by W. G. Characklis and K. C. Marshall, 523–84. New York: Wiley, 1990.

Characklis, W. G., and K. E. Cooksey. “Biofilms and Microbial Fouling.” In *Advances in Applied Microbiology*, edited by Allen I. Laskin, 29:93–138. Academic Press, 1983. http://www.sciencedirect.com/science/article/pii/S0065216408703551.

Characklis, W. G., G. A. McFeeters, and K. C. Marshall. “Physiological Ecology in Biofilm Systems.” In *Biofilms*, 341–94. New York: Wiley and Sons, 1990.

Characklis, William G., and Kevin C. Marshall. *Biofilms*. Vol. 1. Wiley, 1990.

Chaturongkasumrit, Yuphakhun, Hajime Takahashi, Suwimon Keeratipibul, Takashi Kuda, and Bon Kimura. “The Effect of Polyesterurethane Belt Surface Roughness on Listeria Monocytogenes Biofilm Formation and Its Cleaning Efficiency.” *Food Control* 22, no. 12 (December 2011): 1893–99. doi:10.1016/j.foodcont.2011.04.032.

Chen, C.-Y., and S.-D. Chen. “Biofilm Characteristics in Biological Denitrification Biofilm Reactors.” *Water Science and Technology* 41, no. 4–5 (February 1, 2000): 147–54.

Chen, M. J., Z. Zhang, and T. R. Bott. “Direct Measurement of the Adhesive Strength of Biofilms in Pipes by Micromanipulation.” *Biotechnology Techniques* 12, no. 12 (December 1, 1998): 875–80. doi:10.1023/A:1008805326385.

———. “Effects of Operating Conditions on the Adhesive Strength of Pseudomonas Fluorescens Biofilms in Tubes.” *Colloids and Surfaces. B, Biointerfaces* 43, no. 2 (June 25, 2005): 61–71. doi:10.1016/j.colsurfb.2005.04.004.

Chen, X., and P. S. Stewart. “Role of Electrostatic Interactions in Cohesion of Bacterial Biofilms.” *Applied Microbiology and Biotechnology* 59, no. 6 (September 2002): 718–20. doi:10.1007/s00253-002-1044-2.

Chen, Xiao Dong, Dolly X. Y. Li, Sean X. Q. Lin, and Necati Özkan. “On-Line Fouling/cleaning Detection by Measuring Electric Resistance—equipment Development and Application to Milk Fouling Detection and Chemical Cleaning Monitoring.” *Journal of Food Engineering* 61, no. 2 (February 2004): 181–89. doi:10.1016/S0260-8774(03)00085-2.

Chen, Xiao, and Philip S. Stewart. “Chlorine Penetration into Artificial Biofilm Is Limited by a Reaction−Diffusion Interaction.” *Environmental Science & Technology* 30, no. 6 (May 1, 1996): 2078–83. doi:10.1021/es9509184.

Chenoweth, James M. “General Design of Heat Exchangers for Fouling Conditions.” In *Fouling Science and Technology*, edited by L. F. Melo, T. R. Bott, and C. A. Bernardo, 477–94. NATO ASI Series 145. Springer Netherlands, 1988. http://link.springer.com/chapter/10.1007/978-94-009-2813-8_32.

Chew, J. Y. M., S. S. S. Cardoso, W. R. Paterson, and D. I. Wilson. “CFD Studies of Dynamic Gauging.” *Chemical Engineering Science* 59, no. 16 (August 1, 2004): 3381–98. doi:10.1016/j.ces.2004.03.042.

Chew, J. Y. M., W. R. Paterson, and D. I. Wilson. “Fluid Dynamic Gauging for Measuring the Strength of Soft Deposits.” *Journal of Food Engineering* 65, no. 2 (November 2004): 175–87. doi:10.1016/j.jfoodeng.2004.01.013.

Chisti, Y. “Modern Systems of Plant Cleaning.” In *Encyclopedia of Food Microbiology*, 1086–1815. London: Academic Press, 1999.

Choi, Y. C., and E. Morgenroth. “Monitoring Biofilm Detachment under Dynamic Changes in Shear Stress Using Laser-Based Particle Size Analysis and Mass Fractionation.” *Water Science and Technology: A Journal of the International Association on Water Pollution Research* 47, no. 5 (2003): 69–76.

Christensen, G. D., W. A. Simpson, A. L. Bisno, and E. H. Beachey. “Adherence of Slime-Producing Strains of Staphylococcus Epidermidis to Smooth Surfaces.” *Infection and Immunity* 37, no. 1 (July 1982): 318–26.

Christensen, G D, W A Simpson, J J Younger, L M Baddour, F F Barrett, D M Melton, and E H Beachey. “Adherence of Coagulase-Negative Staphylococci to Plastic Tissue Culture Plates: A Quantitative Model for the Adherence of Staphylococci to Medical Devices.” *Journal of Clinical Microbiology* 22, no. 6 (December 1985): 996–1006.

Ciofu, O., T. J. Beveridge, J. Kadurugamuwa, J. Walther-Rasmussen, and N. Høiby. “Chromosomal Beta-Lactamase Is Packaged into Membrane Vesicles and Secreted from Pseudomonas Aeruginosa.” *The Journal of Antimicrobial Chemotherapy* 45, no. 1 (January 2000): 9–13.

Cloete, Eugene, and Hans-Curt Flemming. “Environmental Impact of Cooling Water Treatment for Biofouling and Biocorrosion Control.” In *Operational and Environmental Consequences of Large Industrial Cooling Water Systems*, edited by Sanjeevi Rajagopal, Henk A. Jenner, and Vayalam P. Venugopalan, 303–14. Springer US, 2012. http://link.springer.com/chapter/10.1007/978-1-4614-1698-2_13.

Cloete, T. E. “Biofouling Control in Industrial Water Systems: What We Know and What We Need to Know.” *Materials and Corrosion* 54, no. 7 (July 1, 2003): 520–26. doi:10.1002/maco.200390115.

Cogan, N. G. “Concepts in Disinfection of Bacterial Populations.” *Mathematical Biosciences* 245, no. 2 (October 2013): 111–25. doi:10.1016/j.mbs.2013.07.007.

Collins, D. S., and R. J. Huey. *Gracey’s Meat Hygiene*. 11th ed. Chichester: John Wiley & Sons, 2015.

Colwell, Rita R. “Viable but Not Cultivable Bacteria.” In *Uncultivated Microorganisms*, edited by Slava S. Epstein, 121–29. Microbiology Monographs 10. Springer Berlin Heidelberg, 2009. http://link.springer.com/chapter/10.1007/978-3-540-85465-4_1.

Conrad, Arnaud, Merja Kontro, Minna M. Keinänen, Aurore Cadoret, Pierre Faure, Laurence Mansuy-Huault, and Jean-Claude Block. “Fatty Acids of Lipid Fractions in Extracellular Polymeric Substances of Activated Sludge Flocs.” *Lipids* 38, no. 10 (October 1, 2003): 1093–1105. doi:10.1007/s11745-006-1165-y.

Coombe, R. A., A. Tatevossian, and J. W. P. Wimpenny. “Factors Affecting the Growth of Thin Bacterial Films in Vitro.” In *Bacterial Adhesion and Preventive Dentistry*, 193–205. Oxford: IRL Press Ltd., 1984.

Cope, Emily K., Natalia Goldstein-Daruech, Jennifer M. Kofonow, Lanette Christensen, Bridget McDermott, Fernando Monroy, James N. Palmer, et al., “Regulation of Virulence Gene Expression Resulting from Streptococcus Pneumoniae and Nontypeable Haemophilus Influenzae Interactions in Chronic Disease.” *PloS One* 6, no. 12 (2011): e28523. doi:10.1371/journal.pone.0028523.

Cordell, J. L. “Pigging Research.” Houston, 1991.

Cornelissen, E. R., J. S. Vrouwenvelder, S. G. J. Heijman, X. D. Viallefont, D. Van Der Kooij, and L. P. Wessels. “Periodic Air/water Cleaning for Control of Biofouling in Spiral Wound Membrane Elements.” *Journal of Membrane Science* 287, no. 1 (January 5, 2007): 94–101. doi:10.1016/j.memsci.2006.10.023.

Costerton, J. W., K. J. Cheng, G. G. Geesey, T. I. Ladd, J. C. Nickel, M. Dasgupta, and T. J. Marrie. “Bacterial Biofilms in Nature and Disease.” *Annual Review of Microbiology* 41, no. 1 (1987): 435–64. doi:10.1146/annurev.mi.41.100187.002251.

Costerton, J. W., Z. Lewandowski, D. E. Caldwell, D. R. Korber, and H. M. Lappin-Scott. “Microbial Biofilms.” *Annual Review of Microbiology* 49 (1995): 711–45. doi:10.1146/annurev.mi.49.100195.003431.

Costerton, J W, Z Lewandowski, D DeBeer, D Caldwell, D Korber, and G James. “Biofilms, the Customized Microniche.” *Journal of Bacteriology* 176, no. 8 (April 1994): 2137–42.

Costerton, J. W., P. S. Stewart, and E. P. Greenberg. “Bacterial Biofilms: A Common Cause of Persistent Infections.” *Science (New York, N.Y.)* 284, no. 5418 (May 21, 1999): 1318–22.

Costerton, William, Richard Veeh, Mark Shirtliff, Mark Pasmore, Christopher Post, and Garth Ehrlich. “The Application of Biofilm Science to the Study and Control of Chronic Bacterial Infections.” *Journal of Clinical Investigation* 112, no. 10 (November 15, 2003): 1466–77. doi:10.1172/JCI200320365.

Coufort, C., N. Derlon, J. Ochoa-Chaves, A. Liné, and E. Paul. “Cohesion and Detachment in Biofilm Systems for Different Electron Acceptor and Donors.” *Water Science and Technology: A Journal of the International Association on Water Pollution Research* 55, no. 8–9 (2007): 421–28.

Crispim, Cézar Augusto, Christine C. Gaylarde, and Peter M. Gaylarde. “Biofilms on Church Walls in Porto Alegre, RS, Brazil, with Special Attention to Cyanobacteria.” *International Biodeterioration & Biodegradation*, 12th International Biodeterioration and Biodegradation Symposium (Biosorption and Bioremediation III), 54, no. 2–3 (September 2004): 121–24. doi:10.1016/j.ibiod.2004.03.001.

Curtis, M. A., J. Aduse-Opoku, and M. Rangarajan. “Cysteine Proteases of Porphyromonas Gingivalis.” *Critical Reviews in Oral Biology and Medicine: An Official Publication of the American Association of Oral Biologists* 12, no. 3 (2001): 192–216.

Daniels, D., and T. Selby. “Biofouling Control Options for Cooling Systems.” Electric Power, 2007. http://www.powermag.com/biofouling-control-options-for-cooling-systems/.

Darrag, Abeer M. “Antimicrobial Efficacy of Endodontic Irrigation Solutions against Planktonic Microorganisms and Dual-Species Biofilm.” *Tanta Dental Journal* 10, no. 3 (December 2013): 129–37. doi:10.1016/j.tdj.2013.11.005.

Das, J. R., M. Bhakoo, M. V. Jones, and P. Gilbert. “Changes in the Biocide Susceptibility of Staphylococcus Epidermidis and Escherichia Coli Cells Associated with Rapid Attachment to Plastic Surfaces.” *Journal of Applied Microbiology* 84, no. 5 (June 1, 1998): 852–58. doi:10.1046/j.1365-2672.1998.00422.x.

Das, R., and P. D. Blanc. “Chlorine Gas Exposure and the Lung: A Review.” *Toxicology and Industrial Health* 9, no. 3 (June 1993): 439–55.

Datta, C., and P. S. Basu. “Production of Extracellular Polysaccharides by a Rhizobium Species from Root Nodules of Cajanus Cajan.” *Acta Biotechnologica* 19, no. 1 (January 1, 1999): 59–68. doi:10.1002/abio.370190110.

Daughton, C. G., and T. A. Ternes. “Pharmaceuticals and Personal Care Products in the Environment: Agents of Subtle Change?” *Environmental Health Perspectives* 107 Suppl 6 (December 1999): 907–38.

Davies, D. G., M. R. Parsek, J. P. Pearson, B. H. Iglewski, J. W. Costerton, and E. P. Greenberg. “The Involvement of Cell-to-Cell Signals in the Development of a Bacterial Biofilm.” *Science (New York, N.Y.)* 280, no. 5361 (April 10, 1998): 295–98.

Davies, David. “Understanding Biofilm Resistance to Antibacterial Agents.” *Nature Reviews Drug Discovery* 2, no. 2 (February 2003): 114–22. doi:10.1038/nrd1008.

Davies, David G. “Regulation of Matrix Polymer in Biofilm Formation and Dispersion.” In *Microbial Extracellular Polymeric Substances*, edited by Dr Jost Wingender, Dr Thomas R. Neu, and Prof Dr Hans-Curt Flemming, 93–117. Springer Berlin Heidelberg, 1999. http://link.springer.com/chapter/10.1007/978-3-642-60147-7_5.

Davies, J. E. “Origins, Acquisition and Dissemination of Antibiotic Resistance Determinants.” *Ciba Foundation Symposium* 207 (1997): 15-27-35.

Davies, T. J., S. C. Henstridge, C. R. Gillham, and D. I. Wilson. “Investigation of Whey Protein Deposit Properties Using Heat Flux Sensors.” *Food and Bioproducts Processing* 75, no. 2 (June 1, 1997): 106–10. doi:10.1205/096030897531414.

Davy, V. “Optimization of Cleaning-In-Place (CIP) Process for Bottled Water Industry.” Oviedo, 2010.

De Kievit, Teresa R., Richard Gillis, Steve Marx, Chris Brown, and Barbara H. Iglewski. “Quorum-Sensing Genes in Pseudomonas Aeruginosa Biofilms: Their Role and Expression Patterns.” *Applied and Environmental Microbiology* 67, no. 4 (April 1, 2001): 1865–73. doi:10.1128/AEM.67.4.1865-1873.2001.

Declerck, Priscilla. “Biofilms: The Environmental Playground of Legionella Pneumophila.” *Environmental Microbiology* 12, no. 3 (March 2010): 557–66. doi:10.1111/j.1462-2920.2009.02025.x.

Delcour, Anne H. “Outer Membrane Permeability and Antibiotic Resistance.” *Biochimica et Biophysica Acta* 1794, no. 5 (May 2009): 808–16. doi:10.1016/j.bbapap.2008.11.005.

Delplace, F., and J. C. Leuliet. “Generalized Reynolds Number for the Flow of Power Law Fluids in Cylindrical Ducts of Arbitrary Cross-Section.” *The Chemical Engineering Journal and the Biochemical Engineering Journal* 56, no. 2 (January 1, 1995): 33–37. doi:10.1016/0923-0467(94)02849-6.

Demling, A., C. Elter, T. Heidenblut, Fr-W. Bach, A. Hahn, R. Schwestka-Polly, M. Stiesch, and W. Heuer. “Reduction of Biofilm on Orthodontic Brackets with the Use of a Polytetrafluoroethylene Coating.” *European Journal of Orthodontics* 32, no. 4 (August 2010): 414–18. doi:10.1093/ejo/cjp142.

Denkhaus, Evelin, Stefan Meisen, Ursula Telgheder, and Jost Wingender. “Chemical and Physical Methods for Characterisation of Biofilms.” *Microchimica Acta* 158, no. 1 (April 1, 2007): 1–27. doi:10.1007/s00604-006-0688-5.

Derlon, Nicolas, Anthony Massé, Renaud Escudié, Nicolas Bernet, and Etienne Paul. “Stratification in the Cohesion of Biofilms Grown under Various Environmental Conditions.” *Water Research* 42, no. 8–9 (April 2008): 2102–10. doi:10.1016/j.watres.2007.11.016.

Deshpande, Mohan D., and Ramesh N. Vaishnav. “Submerged Laminar Jet Impingement on a Plane.” *Journal of Fluid Dynamics* 114, no. JAN (January 1, 1982): 213–36. doi:10.1017/S0022112082000111.

Desrousseaux, C., V. Sautou, S. Descamps, and O. Traoré. “Modification of the Surfaces of Medical Devices to Prevent Microbial Adhesion and Biofilm Formation.” *The Journal of Hospital Infection* 85, no. 2 (October 2013): 87–93. doi:10.1016/j.jhin.2013.06.015.

Dewanti, R., and A. C. Wong. “Influence of Culture Conditions on Biofilm Formation by Escherichia Coli O157:H7.” *International Journal of Food Microbiology* 26, no. 2 (July 1995): 147–64.

Dhanasekaran, D., K. Vinothini, S. Latha, N. Thajuddin, and A. Panneerselvam. “Human Dental Biofilm: Screening, Characterization, in Vitro Biofilm Formation and Antifungal Resistance of Candida Spp.” *The Saudi Journal for Dental Research* 5, no. 1 (January 2014): 55–70. doi:10.1016/j.ksujds.2013.10.001.

Dheilly, Alexandra, Emmanuelle Soum-Soutéra, Géraldine L. Klein, Alexis Bazire, Chantal Compère, Dominique Haras, and Alain Dufour. “Antibiofilm Activity of the Marine Bacterium Pseudoalteromonas Sp. Strain 3J6.” *Applied and Environmental Microbiology* 76, no. 11 (June 2010): 3452–61. doi:10.1128/AEM.02632-09.

Dibdin, George, and Julian Wimpenny. “[23] Steady-State Biofilm: Practical and Theoretical Models.” edited by BT - Methods in Enzymology, 310:296–322. Biofilms. Academic Press, 1999. http://www.sciencedirect.com/science/article/pii/S0076687999100259.

Dickson, J S, and M Koohmaraie. “Cell Surface Charge Characteristics and Their Relationship to Bacterial Attachment to Meat Surfaces.” *Applied and Environmental Microbiology* 55, no. 4 (April 1989): 832–36.

Dignac, M. -F., V. Urbain, D. Rybacki, A. Bruchet, D. Snidaro, and P. Scribe. “Chemical Description of Extracellular Polymers: Implication on Activated Sludge Floc Structure.” *Water Science and Technology*, Water Quality International ’98 Part 7. Wastewater: Biological Processes, 38, no. 8 (January 1, 1998): 45–53. doi:10.1016/S0273-1223(98)00676-3.

Dodds, Walter K., Barry J. F. Biggs, and Rex L. Lowe. “Photosynthesis-Irradiance Patterns in Benthic Microalgae: Variations as a Function of Assemblage Thickness and Community Structure.” *Journal of Phycology* 35, no. 1 (February 1, 1999): 42–53. doi:10.1046/j.1529-8817.1999.3510042.x.

Doiron, Kim, Isabelle Linossier, Fabienne Fay, Julius Yong, Effendy Abd Wahid, Dimitre Hadjiev, and Nathalie Bourgougnon. “Dynamic Approaches of Mixed Species Biofilm Formation Using Modern Technologies.” *Marine Environmental Research* 78 (July 2012): 40–47. doi:10.1016/j.marenvres.2012.04.001.

Donlan, R. M. “Role of Biofilms in Antimicrobial Resistance.” *ASAIO Journal (American Society for Artificial Internal Organs: 1992)* 46, no. 6 (December 2000): S47-52.

Donlan, Rodney M. “Biofilms: Microbial Life on Surfaces.” *Emerging Infectious Diseases* 8, no. 9 (September 2002): 881–90. doi:10.3201/eid0809.020063.

Donlan, Rodney M., and J. William Costerton. “Biofilms: Survival Mechanisms of Clinically Relevant Microorganisms.” *Clinical Microbiology Reviews* 15, no. 2 (April 2002): 167–93.

Dreszer, C., Johannes S. Vrouwenvelder, Astrid H. Paulitsch-Fuchs, Arie Zwijnenburg, Joop C. Kruithof, and Hans Curt Flemming. “Hydraulic Resistance of Biofilms.” *Journal of Membrane Science*, February 1, 2013. doi:10.1016/j.memsci.2012.11.030.

Dreszer, C., A. D. Wexler, S. Drusová, T. Overdijk, A. Zwijnenburg, H.-C. Flemming, J. C. Kruithof, and J. S. Vrouwenvelder. “In-Situ Biofilm Characterization in Membrane Systems Using Optical Coherence Tomography: Formation, Structure, Detachment and Impact of Flux Change.” *Water Research* 67 (December 15, 2014): 243–54. doi:10.1016/j.watres.2014.09.006.

DuBois, Michel., K. A. Gilles, J. K. Hamilton, P. A. Rebers, and Fred. Smith. “Colorimetric Method for Determination of Sugars and Related Substances.” *Analytical Chemistry* 28, no. 3 (March 1, 1956): 350–56. doi:10.1021/ac60111a017.

Dufrêne, Yves F. “Atomic Force Microscopy, a Powerful Tool in Microbiology.” *Journal of Bacteriology* 184, no. 19 (October 1, 2002): 5205–13. doi:10.1128/JB.184.19.5205-5213.2002.

Durkee, John B. “The Future of Metal Finishing.” *Metal Finishing* 104, no. 9 (September 1, 2006): 60–62. doi:10.1016/S0026-0576(06)80306-5.

Dychdala, G. R. “Chlorine and Chlorine Compounds.” In *Disinfection, Sterilization and Preservation*, 5th ed., 135–57. Philadelphia: Lippincott, Williams & Wilkins, 2001.

Dynes, James J., John R. Lawrence, Darren R. Korber, George D. W. Swerhone, Gary G. Leppard, and Adam P. Hitchcock. “Morphological and Biochemical Changes in Pseudomonas Fluorescens Biofilms Induced by Sub-Inhibitory Exposure to Antimicrobial Agents.” *Canadian Journal of Microbiology* 55, no. 2 (February 2009): 163–78. doi:10.1139/w08-109.

Eberl, H. J, C Picioreanu, J. J Heijnen, and M. C. M van Loosdrecht. “A Three-Dimensional Numerical Study on the Correlation of Spatial Structure, Hydrodynamic Conditions, and Mass Transfer and Conversion in Biofilms.” *Chemical Engineering Science* 55, no. 24 (December 2000): 6209–22. doi:10.1016/S0009-2509(00)00169-X.

Elexson, N., L. Afsah-Hejri, Y. Rukayadi, P. Soopna, H. Y. Lee, T. C. Tuan Zainazor, M. Nor Ainy, Y. Nakaguchi, N. Mitsuaki, and R. Son. “Effect of Detergents as Antibacterial Agents on Biofilm of Antibiotics-Resistant Vibrio Parahaemolyticus Isolates.” *Food Control* 35, no. 1 (January 2014): 378–85. doi:10.1016/j.foodcont.2013.07.020.

Elvers, K. T., K. Leeming, and H. M. Lappin-Scott. “Binary and Mixed Population Biofilms: Time-Lapse Image Analysis and Disinfection with Biocides.” *Journal of Industrial Microbiology & Biotechnology* 29, no. 6 (December 2002): 331–38. doi:10.1038/sj.jim.7000318.

Entis, Phyllis. *Food Microbiology: The Laboratory*. Washington DC: Food Processors Institute, 2002.

Erriu, Matteo, Cornelio Blus, Serge Szmukler-Moncler, Silvano Buogo, Raffaello Levi, Giulio Barbato, Daniele Madonnaripa, Gloria Denotti, Vincenzo Piras, and Germano Orrù. “Microbial Biofilm Modulation by Ultrasound: Current Concepts and Controversies.” *Ultrasonics Sonochemistry* 21, no. 1 (January 2014): 15–22. doi:10.1016/j.ultsonch.2013.05.011.

Fagerlind, Magnus G., Jeremy S. Webb, Nicolas Barraud, Diane McDougald, Andreas Jansson, Patric Nilsson, Mikael Harlén, Staffan Kjelleberg, and Scott A. Rice. “Dynamic Modelling of Cell Death during Biofilm Development.” *Journal of Theoretical Biology* 295 (February 21, 2012): 23–36. doi:10.1016/j.jtbi.2011.10.007.

Fakhru’l-Razi, Ahmadun, Alireza Pendashteh, Luqman Chuah Abdullah, Dayang Radiah Awang Biak, Sayed Siavash Madaeni, and Zurina Zainal Abidin. “Review of Technologies for Oil

and Gas Produced Water Treatment." *Journal of Hazardous Materials* 170, no. 2–3 (October 30, 2009): 530–51. doi:10.1016/j.jhazmat.2009.05.044.

Fang, Ying, Zhe Shen, Lan Li, Yong Cao, Li-Ying Gu, Qing Gu, Xiao-Qi Zhong, Chao-Hui Yu, and You-Ming Li. "A Study of the Efficacy of Bacterial Biofilm Cleanout for Gastrointestinal Endoscopes." *World Journal of Gastroenterology : WJG* 16, no. 8 (February 28, 2010): 1019–24. doi:10.3748/wjg.v16.i8.1019.

Fattom, Ali, and Moshe Shilo. "Hydrophobicity as an Adhesion Mechanism of Benthic Cyanobacteria." *Applied and Environmental Microbiology* 47, no. 1 (January 1984): 135–43.

Feazel, Leah M., Laura K. Baumgartner, Kristen L. Peterson, Daniel N. Frank, J. Kirk Harris, and Norman R. Pace. "Opportunistic Pathogens Enriched in Showerhead Biofilms." *Proceedings of the National Academy of Sciences* 106, no. 38 (September 22, 2009): 16393–99. doi:10.1073/pnas.0908446106.

Finlay, John A., Maureen E. Callow, Linnea K. Ista, Gabriel P. Lopez, and James A. Callow. "The Influence of Surface Wettability on the Adhesion Strength of Settled Spores of the Green Alga Enteromorpha and the Diatom Amphora." *Integrative and Comparative Biology* 42, no. 6 (December 2002): 1116–22. doi:10.1093/icb/42.6.1116.

Fitridge, Isla, Tim Dempster, Jana Guenther, and Rocky de Nys. "The Impact and Control of Biofouling in Marine Aquaculture: A Review." *Biofouling* 28, no. 7 (August 1, 2012): 649–69. doi:10.1080/08927014.2012.700478.

Flemming, Hans-Curt. "Microbial Biofouling: Unsolved Problems, Insufficient Approaches, and Possible Solutions." In *Biofilm Highlights*, edited by Hans-Curt Flemming, Jost Wingender, and Ulrich Szewzyk, 81–109. Springer Series on Biofilms 5. Springer Berlin Heidelberg, 2011. http://link.springer.com/chapter/10.1007/978-3-642-19940-0_5.

———. "The Perfect Slime." *Colloids and Surfaces. B, Biointerfaces* 86, no. 2 (September 1, 2011): 251–59. doi:10.1016/j.colsurfb.2011.04.025.

Flemming, Hans-Curt, Thomas Griebe, and Gabriela Schaule. "Antifouling Strategies in Technical Systems – a Short Review." *Water Science and Technology* 34, no. 5–6 (September 1, 1996): 517–24.

Flemming, Hans-Curt, P. Sriyutha Murthy, R. Venkatesan, and Keith E. Cooksey. *Marine and Industrial Biofouling*. Springer Science & Business Media, 2008.

Fletcher, Madilyn. "The Effects of Culture Concentration and Age, Time, and Temperature on Bacterial Attachment to Polystyrene." *Canadian Journal of Microbiology* 23, no. 1 (January 1, 1977): 1–6. doi:10.1139/m77-001.

———. "The Measurement of Bacterial Attachment to Surfaces in Static Systems." In *Biofilms — Science and Technology*, edited by L. F. Melo, T. R. Bott, M. Fletcher, and B. Capdeville, 603–14. NATO ASI Series 223. Springer Netherlands, 1992. http://link.springer.com/chapter/10.1007/978-94-011-1824-8_54.

Fletcher, Madilyn, and James Howard Pringle. "The Effect of Surface Free Energy and Medium Surface Tension on Bacterial Attachment to Solid Surfaces." *Journal of Colloid and Interface Science* 104, no. 1 (March 1, 1985): 5–14. doi:10.1016/0021-9797(85)90004-9.

Fowler, H. W., and A. J. McKay. "The Measurement of Microbial Adhesion." In *Microbial Adhesion to Surfaces*, 143–61. Chichester: Ellis Horwood Ltd, 1980.

Frølund, Bo, Rikke Palmgren, Kristian Keiding, and Per Halkjær Nielsen. "Extraction of Extracellular Polymers from Activated Sludge Using a Cation Exchange Resin." *Water Research* 30, no. 8 (August 1, 1996): 1749–58. doi:10.1016/0043-1354(95)00323-1.

Frota, M. N., E. M. Ticona, A. V. Neves, R. P. Marques, S. L. Braga, and G. Valente. "On-Line Cleaning Technique for Mitigation of Biofouling in Heat Exchangers: A Case Study of a Hydroelectric Power Plant in Brazil." *Experimental Thermal and Fluid Science* 53 (February 2014): 197–206. doi:10.1016/j.expthermflusci.2013.12.006.

Fryer, P. J., N. K. Slater, and J. E. Duddridge. “Suggestions for the Operation of Radial Flow Cells in Cell Adhesion and Biofouling Studies.” *Biotechnology and Bioengineering* 27, no. 4 (April 1985): 434–38. doi:10.1002/bit.260270407.

Fryer, P. J., and N. K. H. Slater. “A Novel Fouling Monitor.” *Chemical Engineering Communications* 57, no. 1–6 (July 1, 1987): 139–52. doi:10.1080/00986448708960481.

Fuente-Núñez, César de la, Fany Reffuveille, Lucía Fernández, and Robert E. W. Hancock. “Bacterial Biofilm Development as a Multicellular Adaptation: Antibiotic Resistance and New Therapeutic Strategies.” *Current Opinion in Microbiology* 16, no. 5 (October 2013): 580–89. doi:10.1016/j.mib.2013.06.013.

Fukuzaki, Satoshi. “Mechanisms of Actions of Sodium Hypochlorite in Cleaning and Disinfection Processes.” *Biocontrol Science* 11, no. 4 (2006): 147–57. doi:10.4265/bio.11.147.

Furukawa, Soichi, Yuko Akiyoshi, Mei Komoriya, Hirokazu Ogihara, and Yasushi Morinaga. “Removing Staphylococcus Aureus and Escherichia Coli Biofilms on Stainless Steel by Cleaning-in-Place (CIP) Cleaning Agents.” *Food Control* 21, no. 5 (May 2010): 669–72. doi:10.1016/j.foodcont.2009.10.005.

Fux, C. A., S. Wilson, and P. Stoodley. “Detachment Characteristics and Oxacillin Resistance of Staphyloccocus Aureus Biofilm Emboli in an in Vitro Catheter Infection Model.” *Journal of Bacteriology* 186, no. 14 (July 2004): 4486–91. doi:10.1128/JB.186.14.4486-4491.2004.

Galajda, Peter, Juan Keymer, Paul Chaikin, and Robert Austin. “A Wall of Funnels Concentrates Swimming Bacteria.” *Journal of Bacteriology* 189, no. 23 (December 1, 2007): 8704–7. doi:10.1128/JB.01033-07.

Garnett, James A., and Steve Matthews. “Interactions in Bacterial Biofilm Development: A Structural Perspective.” *Current Protein and Peptide Science* 13, no. 8 (December 10, 2012). doi:10.2174/138920312804871166.

Garrett, Trevor Roger, Manmohan Bhakoo, and Zhibing Zhang. “Bacterial Adhesion and Biofilms on Surfaces.” *Progress in Natural Science* 18, no. 9 (September 10, 2008): 1049–56. doi:10.1016/j.pnsc.2008.04.001.

Gauri, Samiran Sona, Santi M. Mandal, Keshab C. Mondal, Satyahari Dey, and Bikas R. Pati. “Enhanced Production and Partial Characterization of an Extracellular Polysaccharide from Newly Isolated Azotobacter Sp. SSB81.” *Bioresource Technology* 100, no. 18 (May 1, 2009): 4240–43. doi:10.1016/j.biortech.2009.03.064.

Geesey, G. G. “Microbial Exopolymers: Ecological and Economic Considerations.” *ASM News* 48 (1982): 9–14.

Geisse, Nicholas A. “AFM and Combined Optical Techniques.” *Materials Today* 12, no. 7–8 (July 2009): 40–45. doi:10.1016/S1369-7021(09)70201-9.

Geoghegan, Mark, Johanna S. Andrews, Catherine A. Biggs, Kevin E. Eboigbodin, David R. Elliott, Stephen Rolfe, Julie Scholes, et al., “The Polymer Physics and Chemistry of Microbial Cell Attachment and Adhesion.” *Faraday DIscussions* 139 (August 18, 2008): 85–103. doi:10.1039/B717046G.

Gerlach, Robin, and AlfredB Cunningham. “Influence of Biofilms on Porous Media Hydrodynamics.” In *Porous Media*, 173–230. CRC Press, 2010. http://www.crcnetbase.com/doi/abs/10.1201/9781420065428-6.

Gerstel, Ulrich, and Ute Römling. “The csgD Promoter, a Control Unit for Biofilm Formation in Salmonella Typhimurium.” *Research in Microbiology* 154, no. 10 (December 1, 2003): 659–67. doi:10.1016/j.resmic.2003.08.005.

Giaouris, Efstathios, Nikos Chorianopoulos, Agapi Doulgeraki, and George-John Nychas. “Co-Culture with Listeria Monocytogenes within a Dual-Species Biofilm Community Strongly Increases Resistance of Pseudomonas Putida to Benzalkonium Chloride.” *PLOS ONE* 8, no. 10 (October 10, 2013): e77276. doi:10.1371/journal.pone.0077276.

Gilbert, EricS., and JayD. Keasling. “Bench Scale Flow Cell for Nondestructive Imaging of Biofilms.” In *Environmental Microbiology*, edited by JohnM. Walker, JohnF.T. Spencer, and AliciaL. Ragout de Spencer, 109–18. Methods in Biotechnology 16. Humana Press, 2004. http://dx.doi.org/10.1385/1-59259-765-3%3A109.

Gilbert, Peter, and Andrew J. McBain. “Potential Impact of Increased Use of Biocides in Consumer Products on Prevalence of Antibiotic Resistance.” *Clinical Microbiology Reviews* 16, no. 2 (April 2003): 189–208.

Gillespie, I. A., S. J. O’Brien, G. K. Adak, L. R. Ward, and H. R. Smith. “Foodborne General Outbreaks of Salmonella Enteritidis Phage Type 4 Infection, England and Wales, 1992-2002: Where Are the Risks?” *Epidemiology and Infection* 133, no. 5 (October 2005): 795–801. doi:10.1017/S0950268805004474.

Goeres, Darla M., Martin A. Hamilton, Nicholas A. Beck, Kelli Buckingham-Meyer, Jackie D. Hilyard, Linda R. Loetterle, Lindsey A. Lorenz, Diane K. Walker, and Philip S. Stewart. “A Method for Growing a Biofilm under Low Shear at the Air-Liquid Interface Using the Drip Flow Biofilm Reactor.” *Nature Protocols* 4, no. 5 (2009): 783–88. doi:10.1038/nprot.2009.59.

Goeres, Darla M., Linda R. Loetterle, Martin A. Hamilton, Ricardo Murga, Douglas W. Kirby, and Rodney M. Donlan. “Statistical Assessment of a Laboratory Method for Growing Biofilms.” *Microbiology (Reading, England)* 151, no. Pt 3 (March 2005): 757–62. doi:10.1099/mic.0.27709-0.

Gomes, I. B., M. Simões, and Lúcia C. Simões. “The Effects of Sodium Hypochlorite against Selected Drinking Water-Isolated Bacteria in Planktonic and Sessile States.” *Science of the Total Environment* 565 (September 15, 2016): 40–48. doi:10.1016/j.scitotenv.2016.04.136.

Goode, Kylee Rebecca. “Characterising the Cleaning Behaviour of Brewery Foulants - to Minimise the Cost of Cleaning in Place Operations.” D_en, University of Birmingham, 2012. http://etheses.bham.ac.uk/3908/.

Gordon, Andrew S., and Frank J. Millero. “Electrolyte Effects on Attachment of an Estuarine Bacterium.” *Applied and Environmental Microbiology* 47, no. 3 (March 1984): 495–99.

Gordon, Patrick W., Anju D. M. Brooker, Y. M. John Chew, Nathalie Letzelter, David W. York, and D. Ian Wilson. “Elucidating Enzyme-Based Cleaning of Protein Soils (Gelatine and Egg Yolk) Using a Scanning Fluid Dynamic Gauge.” *Chemical Engineering Research and Design* 90, no. 1 (January 1, 2012): 162–71. doi:10.1016/j.cherd.2011.07.007.

Gordon, Patrick W., Anju D. M. Brooker, Y. M. John Chew, D. Ian Wilson, and David W. York. “Studies into the Swelling of Gelatine Films Using a Scanning Fluid Dynamic Gauge.” *Food and Bioproducts Processing* 88, no. 4 (December 1, 2010): 357–64. doi:10.1016/j.fbp.2010.08.012.

Gordon, Patrick W., Martin Schöler, Henning Föste, Manuel Helbig, Wolfgang Augustin, Y. M. John Chew, Stephan Scholl, Jens-Peter Majschak, and D. Ian Wilson. “A Comparison of Local Phosphorescence Detection and Fluid Dynamic Gauging Methods for Studying the Removal of Cohesive Fouling Layers: Effect of Layer Roughness.” *Food and Bioproducts Processing*, January 2014. doi:http://dx.doi.org/10.1016/j.fbp.2013.07.010.

Graf von der Schulenburg, D. A., J. S. Vrouwenvelder, S. A. Creber, M. C. M. van Loosdrecht, and M. L. Johns. “Nuclear Magnetic Resonance Microscopy Studies of Membrane Biofouling.” *Journal of Membrane Science* 323, no. 1 (October 1, 2008): 37–44. doi:10.1016/j.memsci.2008.06.012.

Gross, M. J., and B. E. Logan. “Influence of Different Chemical Treatments on Transport of Alcaligenes Paradoxus in Porous Media.” *Applied and Environmental Microbiology* 61, no. 5 (1995): 1750–56.

Gu, T., F. Albert, W. Augustin, Y. M. J. Chew, M. Mayer, W. R. Paterson, S. Scholl, I. Sheikh, K. Wang, and D. I. Wilson. “Application of Fluid Dynamic Gauging to Annular Test

Apparatuses for Studying Fouling and Cleaning." *Experimental Thermal and Fluid Science* 35, no. 3 (April 2011): 509–20. doi:10.1016/j.expthermflusci.2010.12.002.
Gu, T., Y. M. J. Chew, W. R. Paterson, and D. I. Wilson. "Experimental and CFD Studies of Fluid Dynamic Gauging in Annular Flows." *AIChE Journal* 55, no. 8 (August 1, 2009): 1937–47. doi:10.1002/aic.11789.
———. "Experimental and CFD Studies of Fluid Dynamic Gauging in Duct Flows." *Chemical Engineering Science* 64, no. 2 (January 2009): 219–27. doi:10.1016/j.ces.2008.09.032.
———. "Fluid Dynamic Gauging in Duct Flows - Experiments and CFD Simulations." In *ECI Symposium Series, Volume RP5*. Tomar, Portugal, 2007.
Gubner, R., and I. B. Beech. "The Effect of Extracellular Polymeric Substances on the Attachment of Pseudomonas NCIMB 2021 to AISI 304 and 316 Stainless Steel." *Biofouling* 15, no. 1–3 (2000): 25–36. doi:10.1080/08927010009386295.
Guérin, Romuald, Gilles Ronse, Laurent Bouvier, Pascal Debreyne, and Guillaume Delaplace. "Structure and Rate of Growth of Whey Protein Deposit from in Situ Electrical Conductivity during Fouling in a Plate Heat Exchanger." *Chemical Engineering Science* 62, no. 7 (April 2007): 1948–57. doi:10.1016/j.ces.2006.12.038.
Hadjiev, D., D. Dimitrov, M. Martinov, and Olivier Sire. "Enhancement of the Biofilm Formation on Polymeric Supports by Surface Conditioning." *Enzyme and Microbial Technology* 40, no. 4 (March 1, 2007): 840–48. doi:10.1016/j.enzmictec.2006.06.022.
Haisch, C., and R. Niessner. "Visualisation of Transient Processes in Biofilms by Optical Coherence Tomography." *Water Research* 41, no. 11 (June 2007): 2467–72. doi:10.1016/j.watres.2007.03.017.
Hallab, N. J., K. J. Bundy, K. O'Connor, R. L. Moses, and J. J. Jacobs. "Evaluation of Metallic and Polymeric Biomaterial Surface Energy and Surface Roughness Characteristics for Directed Cell Adhesion." *Tissue Engineering* 7, no. 1 (February 2001): 55–71. doi:10.1089/107632700300003297.
Hall-Stoodley, Luanne, and Paul Stoodley. "Biofilm Formation and Dispersal and the Transmission of Human Pathogens." *Trends in Microbiology* 13, no. 1 (January 2005): 7–10. doi:10.1016/j.tim.2004.11.004.
Hamanaka, Daisuke, Mami Onishi, Takuma Genkawa, Fumihiko Tanaka, and Toshitaka Uchino. "Effects of Temperature and Nutrient Concentration on the Structural Characteristics and Removal of Vegetable-Associated Pseudomonas Biofilm." *Food Control* 24, no. 1–2 (March 2012): 165–70. doi:10.1016/j.foodcont.2011.09.021.
Hamilton, Shea, Roy J. M. Bongaerts, Francis Mulholland, Brett Cochrane, Jonathan Porter, Sacha Lucchini, Hilary M. Lappin-Scott, and Jay C. D. Hinton. "The Transcriptional Programme of Salmonella Enterica Serovar Typhimurium Reveals a Key Role for Tryptophan Metabolism in Biofilms." *BMC Genomics* 10 (December 11, 2009): 599. doi:10.1186/1471-2164-10-599.
Hansen, Susse Kirkelund, Janus A. J. Haagensen, Morten Gjermansen, Thomas Martini Jørgensen, Tim Tolker-Nielsen, and Søren Molin. "Characterization of a Pseudomonas Putida Rough Variant Evolved in a Mixed-Species Biofilm with Acinetobacter Sp. Strain C6." *Journal of Bacteriology* 189, no. 13 (July 1, 2007): 4932–43. doi:10.1128/JB.00041-07.
Hayes, K. C. "Taurine Requirement in Primates." *Nutrition Reviews* 43, no. 3 (March 1985): 65–70.
Haysom, Iain, and Kay Sharp. "Cross- contamination from Raw Chicken during Meal Preparation." *British Food Journal* 106, no. 1 (January 1, 2004): 38–50. doi:10.1108/00070700410515190.
Heidrich, D. D., S. Steckelbroeck, and D. Klingmuller. "Inhibition of Human Cytochrome P450 Aromatase Activity by Butyltins." *Steroids* 66, no. 10 (October 2001): 763–69.
Hemmen, J. J. van. "Biocides Steering Group on Human Exposure Assessment: A Preliminary Report." *Toxicology Letters* 107, no. 1–3 (June 30, 1999): 95–102.

Henderson, Peter. “Fouling and Antifouling in Other Industries – Power Stations, Desalination Plants – Drinking Water Supplies and Sensors.” In *Biofouling*, edited by Simone Dürr and Jeremy C. Thomason, 288–305. Wiley-Blackwell, 2009. http://onlinelibrary.wiley.com/doi/10.1002/9781444315462.ch20/summary.

Herbert, S., D. Worlitzsch, B. Dassy, A. Boutonnier, J. M. Fournier, G. Bellon, A. Dalhoff, and G. Döring. “Regulation of Staphylococcus Aureus Capsular Polysaccharide Type 5: In Vitro and in Vivo Inhibition by CO2.” *Pneumologie (Stuttgart, Germany)* 51, no. 11 (November 1997): 1043–50.

Herbert-Guillou, D, B Tribollet, D Festy, and L Kiéné. “In Situ Detection and Characterization of Biofilm in Waters by Electrochemical Methods.” *Electrochimica Acta* 45, no. 7 (December 31, 1999): 1067–75. doi:10.1016/S0013-4686(99)00310-2.

Heritage, J., E. G. V. Evans, and R. A. Killington. *Introductory Microbiology*. Cambridge University Press, 1996.

Hernández-Jiménez, Enrique, Rosa Del Campo, Victor Toledano, Maria Teresa Vallejo-Cremades, Aurora Muñoz, Carlota Largo, Francisco Arnalich, Francisco García-Rio, Carolina Cubillos-Zapata, and Eduardo López-Collazo. “Biofilm vs. Planktonic Bacterial Mode of Growth: Which Do Human Macrophages Prefer?” *Biochemical and Biophysical Research Communications* 441, no. 4 (November 29, 2013): 947–52. doi:10.1016/j.bbrc.2013.11.012.

Heydorn, A., A. T. Nielsen, M. Hentzer, C. Sternberg, M. Givskov, B. K. Ersbøll, and S. Molin. “Quantification of Biofilm Structures by the Novel Computer Program COMSTAT.” *Microbiology (Reading, England)* 146 (Pt 10) (October 2000): 2395–2407. doi:10.1099/00221287-146-10-2395.

Hočevar, M., Monika Jenko, Matjaz Godec, and Damjana Drobne. “An Overview of the Influence of Stainless-Steel Surface Properties on Bacterial Adhesion.” *Materiali in Technologije* 48, no. 5 (September 1, 2014): 609–17.

Hoehn, R. C., and A. D. Ray. “Effects of Thickness on Bacterial Film.” *Journal - Water Pollution Control Federation* 45, no. 11 (November 1973): 2302–20.

Høiby, Niels, Oana Ciofu, Helle Krogh Johansen, Zhi-jun Song, Claus Moser, Peter Østrup Jensen, Søren Molin, Michael Givskov, Tim Tolker-Nielsen, and Thomas Bjarnsholt. “The Clinical Impact of Bacterial Biofilms.” *International Journal of Oral Science* 3, no. 2 (April 2011): 55–65. doi:10.4248/IJOS11026.

Holah, J. T., R. P. Betts, and R. H. Thorpe. “The Use of Epifluorescence Microscopy to Determine Surface Hygiene.” *International Biodeterioration*, Special Issue: Biodeterioration 7, 25, no. 1 (January 1, 1989): 147–53. doi:10.1016/0265-3036(89)90040-7.

Holden, Patricia A., James R. Hunt, and Mary K. Firestone. “Toluene Diffusion and Reaction in Unsaturated Pseudomonas Putida Biofilms.” *Biotechnology and Bioengineering* 56, no. 6 (December 20, 1997): 656–70. doi:10.1002/(SICI)1097-0290(19971220)56:6<656::AID-BIT9>3.0.CO;2-M.

Hope, C. K., D. Clements, and M. Wilson. “Determining the Spatial Distribution of Viable and Nonviable Bacteria in Hydrated Microcosm Dental Plaques by Viability Profiling.” *Journal of Applied Microbiology* 93, no. 3 (2002): 448–55.

Hope, C. K., and M. Wilson. “Analysis of the Effects of Chlorhexidine on Oral Biofilm Vitality and Structure Based on Viability Profiling and an Indicator of Membrane Integrity.” *Antimicrobial Agents and Chemotherapy* 48, no. 5 (May 2004): 1461–68. doi:10.1128/AAC.48.5.1461-1468.2004.

Hori, Katsutoshi, and Shinya Matsumoto. “Bacterial Adhesion: From Mechanism to Control.” *Biochemical Engineering Journal*, Invited Review Issue 2010, 48, no. 3 (February 15, 2010): 424–34. doi:10.1016/j.bej.2009.11.014.

Hu, Xiao-bing, Ke Xu, Zhao Wang, Li-li Ding, and Hong-qiang Ren. “Characteristics of Biofilm Attaching to Carriers in Moving Bed Biofilm Reactor Used to Treat Vitamin C Wastewater.” *Scanning* 35, no. 5 (September 1, 2013): 283–91. doi:10.1002/sca.21064.

Huang, Chi-Yu, Shou-Pin Hsieh, Pei-An Kuo, Wann-Neng Jane, Jenn Tu, Ya-Nan Wang, and Chun-Han Ko. “Impact of Disinfectant and Nutrient Concentration on Growth and Biofilm Formation for a Pseudomonas Strain and the Mixed Cultures from a Fine Papermachine System.” *International Biodeterioration & Biodegradation* 63, no. 8 (December 2009): 998–1007. doi:10.1016/j.ibiod.2009.07.004.

Huang, Chunming, Sanfeng Wu, Ana M. Sanchez, Jonathan J. P. Peters, Richard Beanland, Jason S. Ross, Pasqual Rivera, Wang Yao, David H. Cobden, and Xiaodong Xu. “Lateral Heterojunctions within Monolayer MoSe2–WSe2 Semiconductors.” *Nature Materials* 13, no. 12 (December 2014): 1096–1101. doi:10.1038/nmat4064.

Hunt, Stephen M., Erin M. Werner, Baochuan Huang, Martin A. Hamilton, and Philip S. Stewart. “Hypothesis for the Role of Nutrient Starvation in Biofilm Detachment.” *Applied and Environmental Microbiology* 70, no. 12 (December 2004): 7418–25. doi:10.1128/AEM.70.12.7418-7425.2004.

Hyde, F. W., M. Alberg, and K. Smith. “Comparison of Fluorinated Polymers against Stainless Steel, Glass and Polypropylene in Microbial Biofilm Adherence and Removal.” *Journal of Industrial Microbiology & Biotechnology* 19, no. 2 (August 1997): 142–49.

Irving, Tyler, and D. Grant Allen. “Microalgal Biofilm Reactor: Investigation of Microalgal Attachment to Surfaces.” *Proceedings of the Water Environment Federation* 2010, no. 7 (January 1, 2010): 114–29. doi:10.2175/193864710798208764.

Irving, Tyler E., and D. Grant Allen. “Species and Material Considerations in the Formation and Development of Microalgal Biofilms.” *Applied Microbiology and Biotechnology* 92, no. 2 (October 1, 2011): 283–94. doi:10.1007/s00253-011-3341-0.

Jacquet, Ch., J. Rocourt, and A. Reynaud. “Study of Listeria Monocytogenes Contamination in a Dairy Plant and Characterization of the Strains Isolated.” *International Journal of Food Microbiology* 20, no. 1 (October 1, 1993): 13–22. doi:10.1016/0168-1605(93)90056-M.

Jahn, A., T. Griebe, and P. H. Nielsen. “Composition of Pseudomonas Putida Biofilms: Accumulation of Protein in the Biofilm Matrix.” *Biofouling* 14, no. 1 (June 1, 1999): 49–57. doi:10.1080/08927019909378396.

Janknecht, Peter, and Luis F. Melo. “Online Biofilm Monitoring.” *Reviews in Environmental Science and Biotechnology* 2, no. 2–4 (June 1, 2003): 269–83. doi:10.1023/B:RESB.0000040461.69339.04.

Jass, J., J. W. Costerton, and H. M. Lappin-Scott. “Assessment of a Chemostat-Coupled Modified Robbins Device to Study Biofilms.” *Journal of Industrial Microbiology* 15, no. 4 (October 1, 1995): 283–89. doi:10.1007/BF01569981.

Jefferson, Kimberly K. “What Drives Bacteria to Produce a Biofilm?” *FEMS Microbiology Letters* 236, no. 2 (July 1, 2004): 163–73. doi:10.1111/j.1574-6968.2004.tb09643.x.

Jensen, Bo B.b., and Alan Friis. “Predicting the Cleanability of Mix-Proof Valves by Use of Wall Shear Stress.” *Journal of Food Process Engineering* 28, no. 2 (April 1, 2005): 89–106. doi:10.1111/j.1745-4530.2005.00370.x.

Jhass, Aneka K., David Annandale Johnston, Aakshay Gulati, Rajiv Anand, Paul Stoodley, and Sanjay Sharma. “A Scanning Electron Microscope Characterisation of Biofilm on Failed Craniofacial Osteosynthesis Miniplates.” *Journal of Cranio-Maxillofacial Surgery*, no. 10.1016/j.jcms.2014.03.021 (2014). doi:Jhass, Aneka K., Johnston, David Annandale, Gulati, Aakshay, Anand, Rajiv, Stoodley, Paul and Sharma, Sanjay (2014) A scanning electron microscope characterisation of biofilm on failed craniofacial osteosynthesis miniplates. Journal of Cranio-Maxillofacial Surgery (doi:10.1016/j.jcms.2014.03.021 <http://dx.doi.org/10.1016/j.jcms.2014.03.021>).

Johnsson, M., M. J. Levine, and G. H. Nancollas. “Hydroxyapatite Binding Domains in Salivary Proteins.” *Critical Reviews in Oral Biology and Medicine: An Official Publication of the American Association of Oral Biologists* 4, no. 3–4 (1993): 371–78.
Jones, Rhonda D. “Bacterial Resistance and Topical Antimicrobial Wash Products.” *American Journal of Infection Control* 27, no. 4 (August 1999): 351–63. doi:10.1016/S0196-6553(99)70056-8.
Jones, Warren L., Michael P. Sutton, Ladean McKittrick, and Philip S. Stewart. “Chemical and Antimicrobial Treatments Change the Viscoelastic Properties of Bacterial Biofilms.” *Biofouling* 27, no. 2 (February 2011): 207–15. doi:10.1080/08927014.2011.554977.
Joyce, E., S. S. Phull, J. P. Lorimer, and T. J. Mason. “The Development and Evaluation of Ultrasound for the Treatment of Bacterial Suspensions. A Study of Frequency, Power and Sonication Time on Cultured Bacillus Species.” *Ultrasonics Sonochemistry* 10, no. 6 (October 2003): 315–18. doi:10.1016/S1350-4177(03)00101-9.
Jung, Jin-Ho, Na-Young Choi, and Sun-Young Lee. “Biofilm Formation and Exopolysaccharide (EPS) Production by Cronobacter Sakazakii Depending on Environmental Conditions.” *Food Microbiology* 34, no. 1 (May 2013): 70–80. doi:10.1016/j.fm.2012.11.008.
Kampf, G., R. Bloss, and H. Martiny. “Surface Fixation of Dried Blood by Glutaraldehyde and Peracetic Acid.” *The Journal of Hospital Infection* 57, no. 2 (June 2004): 139–43. doi:10.1016/j.jhin.2004.02.004.
Kaplan, Jeffrey B., Chandran Ragunath, Kabilan Velliyagounder, Daniel H. Fine, and Narayanan Ramasubbu. “Enzymatic Detachment of Staphylococcus Epidermidis Biofilms.” *Antimicrobial Agents and Chemotherapy* 48, no. 7 (July 1, 2004): 2633–36. doi:10.1128/AAC.48.7.2633-2636.2004.
Karl, D M. “Cellular Nucleotide Measurements and Applications in Microbial Ecology.” *Microbiological Reviews* 44, no. 4 (December 1980): 739–96.
Karunakaran, Esther, Joy Mukherjee, Bharathi Ramalingam, and Catherine A. Biggs. “‘Biofilmology’: A Multidisciplinary Review of the Study of Microbial Biofilms.” *Applied Microbiology and Biotechnology* 90, no. 6 (June 2011): 1869–81. doi:10.1007/s00253-011-3293-4.
Kavita, Kumari, Avinash Mishra, and Bhavanath Jha. “Extracellular Polymeric Substances from Two Biofilm Forming Vibrio Species: Characterization and Applications.” *Carbohydrate Polymers* 94, no. 2 (May 15, 2013): 882–88. doi:10.1016/j.carbpol.2013.02.010.
Kays, W. M., and A. L. London. *Compact Heat Exchangers*. 2nd ed. New York: McGraw-Hill, 1964.
Keevil, C. W. “The Physico-Chemistry of Biofilm-Mediated Pitting Corrosion of Copper Pipe Supplying Potable Water.” *Water Science and Technology* 49, no. 2 (January 1, 2004): 91–98.
Keren, Iris, Niilo Kaldalu, Amy Spoering, Yipeng Wang, and Kim Lewis. “Persister Cells and Tolerance to Antimicrobials.” *FEMS Microbiology Letters* 230, no. 1 (January 15, 2004): 13–18.
Kerr, C. J., K. S. Osborn, G. D. Robson, and P. S. Handley. “The Relationship between Pipe Material and Biofilm Formation in a Laboratory Model System.” *Journal of Applied Microbiology* 85 Suppl 1 (December 1998): 29S–38S. doi:10.1111/j.1365-2672.1998.tb05280.x.
Kim, B. R., J. E. Anderson, S. A. Mueller, W. A. Gaines, and A. M. Kendall. “Literature Review—efficacy of Various Disinfectants against Legionella in Water Systems.” *Water Research* 36, no. 18 (November 2002): 4433–44. doi:10.1016/S0043-1354(02)00188-4.
Kinsella, K. J., T. A. Rowe, I. S. Blair, D. A. McDowell, and J. J. Sheridan. “The Influence of Attachment to Beef Surfaces on the Survival of Cells of Salmonella Enterica Serovar

Typhimurium DT104, at Different A(w) Values and at Low Storage Temperatures." *Food Microbiology* 24, no. 7–8 (December 2007): 786–93. doi:10.1016/j.fm.2006.12.004.
Kirzhner, F., Y. Zimmels, A. Malkovskaja, and J. Starosvetsky. "Removal of Microbial Biofilm on Water Hyacinth Plants Roots by Ultrasonic Treatment." *Ultrasonics* 49, no. 2 (February 2009): 153–58. doi:10.1016/j.ultras.2008.09.004.
Kives, Juliana, Belén Orgaz, and Carmen Sanjosé. "Polysaccharide Differences between Planktonic and Biofilm-Associated EPS from Pseudomonas Fluorescens B52." *Colloids and Surfaces. B, Biointerfaces* 52, no. 2 (October 1, 2006): 123–27. doi:10.1016/j.colsurfb.2006.04.018.
Klayman, Benjamin J., Paul A. Volden, Philip S. Stewart, and Anne K. Camper. "Escherichia Coli O157:H7 Requires Colonizing Partner to Adhere and Persist in a Capillary Flow Cell." *Environmental Science & Technology* 43, no. 6 (March 15, 2009): 2105–11. doi:10.1021/es802218q.
Klingeren, B. van, and W. Pullen. "Glutaraldehyde Resistant Mycobacteria from Endoscope Washers." *The Journal of Hospital Infection* 25, no. 2 (October 1993): 147–49.
Klotz, S A. "Adherence of Candida Albicans to Endothelial Cells Is Inhibited by Prostaglandin I2." *Infection and Immunity* 62, no. 4 (April 1994): 1497–1500.
Ko, Chun-Han, Chi-Yu Huang, Shou-Pin Hsieh, and Pei-An Kuo. "Characterization of Two Quaternary Ammonium Chloride-Resistant Bacteria Isolated from Papermaking Processing Water and the Biocidal Effect on Their Biofilm Formation." *International Biodeterioration & Biodegradation* 60, no. 4 (2007): 250–57. doi:10.1016/j.ibiod.2007.04.003.
Koneman, Elmer W. *Koneman's Color Atlas and Textbook of Diagnostic Microbiology*. 6th ed. Philadelphia: Lippincott Williams & Wilkins, 2006.
Koop, H. M., M. Valentijn-Benz, A. V. Nieuw Amerongen, P. A. Roukema, and J. De Graaff. "Aggregation of 27 Oral Bacteria by Human Whole Saliva. Influence of Culture Medium, Calcium, and Bacterial Cell Concentration, and Interference by Autoaggregation." *Antonie Van Leeuwenhoek* 55, no. 3 (March 1989): 277–90.
Korber, D. R., J. R. Lawrence, H. M. Lappin-Scott, and J. W. Costerton. "Growth of Microorganisms on Surfaces." In *Microbial Biofilms, Plant and Microbial Biotechnology Research*, 15–45. 5. Cambridge: University Press, 1995.
Kornreich, B. G., M. Craven, S. P. McDonough, D. V. Nydam, V. Scorza, S. Assarasakorn, M. Lappin, and K. W. Simpson. "Fluorescence in-Situ Hybridization for the Identification of Bacterial Species in Archival Heart Valve Sections of Canine Bacterial Endocarditis." *Journal of Comparative Pathology* 146, no. 4 (May 2012): 298–307. doi:10.1016/j.jcpa.2011.07.006.
Kovaleva, J., J. E. Degener, and H. C. van der Mei. "Mimicking Disinfection and Drying of Biofilms in Contaminated Endoscopes." *The Journal of Hospital Infection* 76, no. 4 (December 2010): 345–50. doi:10.1016/j.jhin.2010.07.008.
Krishnamurthy, Ajay, and Jennelle Kyd. "The Roles of Epithelial Cell Contact, Respiratory Bacterial Interactions and Phosphorylcholine in Promoting Biofilm Formation by Streptococcus Pneumoniae and Nontypeable Haemophilus Influenzae." *Microbes and Infection* 16, no. 8 (August 2014): 640–47. doi:10.1016/j.micinf.2014.06.008.
Kroukamp, Otini, Romeo G. Dumitrache, and Gideon M. Wolfaardt. "Pronounced Effect of the Nature of the Inoculum on Biofilm Development in Flow Systems." *Applied and Environmental Microbiology* 76, no. 18 (September 2010): 6025–31. doi:10.1128/AEM.00070-10.
Kujundzic, Elmira, A. Cristina Fonseca, Emily A. Evans, Michael Peterson, Alan R. Greenberg, and Mark Hernandez. "Ultrasonic Monitoring of Early-Stage Biofilm Growth on Polymeric Surfaces." *Journal of Microbiological Methods* 68, no. 3 (March 2007): 458–67. doi:10.1016/j.mimet.2006.10.005.

Kumar, Amit, and Yen-Peng Ting. “Effect of Sub-Inhibitory Antibacterial Stress on Bacterial Surface Properties and Biofilm Formation.” *Colloids and Surfaces. B, Biointerfaces* 111 (November 1, 2013): 747–54. doi:10.1016/j.colsurfb.2013.07.011.

Kumari, Sarita, and Prabir K. Sarkar. “In Vitro Model Study for Biofilm Formation by Bacillus Cereus in Dairy Chilling Tanks and Optimization of Clean-in-Place (CIP) Regimes Using Response Surface Methodology.” *Food Control* 36, no. 1 (February 2014): 153–58. doi:10.1016/j.foodcont.2013.08.014.

Kurzbaum, Eyal, Felix Kirzhner, Shlomo Sela, Yoram Zimmels, and Robert Armon. “Efficiency of Phenol Biodegradation by Planktonic Pseudomonas Pseudoalcaligenes (a Constructed Wetland Isolate) vs. Root and Gravel Biofilm.” *Water Research* 44, no. 17 (September 2010): 5021–31. doi:10.1016/j.watres.2010.07.020.

Kusumaningrum, H. D., G. Riboldi, W. C. Hazeleger, and R. R. Beumer. “Survival of Foodborne Pathogens on Stainless Steel Surfaces and Cross-Contamination to Foods.” *International Journal of Food Microbiology* 85, no. 3 (August 25, 2003): 227–36.

Kwon, Kideok D., Virginia Vadillo-Rodriguez, Bruce E. Logan, and James D. Kubicki. “Interactions of Biopolymers with Silica Surfaces: Force Measurements and Electronic Structure Calculation Studies.” *Geochimica et Cosmochimica Acta* 70, no. 15 (August 1, 2006): 3803–19. doi:10.1016/j.gca.2006.05.016.

Kyllönen, H. M., P. Pirkonen, and M. Nyström. “Membrane Filtration Enhanced by Ultrasound: A Review.” *Desalination* 181, no. 1 (September 5, 2005): 319–35. doi:10.1016/j.desal.2005.06.003.

Lackner, Susanne, Maria Holmberg, Akihiko Terada, Peter Kingshott, and Barth F. Smets. “Enhancing the Formation and Shear Resistance of Nitrifying Biofilms on Membranes by Surface Modification.” *Water Research* 43, no. 14 (August 2009): 3469–78. doi:10.1016/j.watres.2009.05.011.

Lamminen, Mikko O, Harold W Walker, and Linda K Weavers. “Mechanisms and Factors Influencing the Ultrasonic Cleaning of Particle-Fouled Ceramic Membranes.” *Journal of Membrane Science* 237, no. 1–2 (July 1, 2004): 213–23. doi:10.1016/j.memsci.2004.02.031.

Laspidou, Chrysi S., and Bruce E. Rittmann. “A Unified Theory for Extracellular Polymeric Substances, Soluble Microbial Products, and Active and Inert Biomass.” *Water Research* 36, no. 11 (June 2002): 2711–20.

Lauchnor, Ellen G., and Lewis Semprini. “Inhibition of Phenol on the Rates of Ammonia Oxidation by Nitrosomonas Europaea Grown under Batch, Continuous Fed, and Biofilm Conditions.” *Water Research* 47, no. 13 (September 1, 2013): 4692–4700. doi:10.1016/j.watres.2013.04.052.

Lazarova, Valentina, Danièle Bellahcen, Jacques Manem, David A. Stahl, and Bruce E. Rittmann. “Influence of Operating Conditions on Population Dynamics in Nitrifying Biofilms.” *Water Science and Technology* 39, no. 7 (April 1, 1999): 5–11.

LeChevallier, M W, T M Babcock, and R G Lee. “Examination and Characterization of Distribution System Biofilms.” *Applied and Environmental Microbiology* 53, no. 12 (December 1987): 2714–24.

Lee, Jin-Hyung, Joo-Hyeon Park, Jung-Ae Kim, Ganesh Prasad Neupane, Moo Hwan Cho, Chang-Soo Lee, and Jintae Lee. “Low Concentrations of Honey Reduce Biofilm Formation, Quorum Sensing, and Virulence in Escherichia Coli O157:H7.” *Biofouling* 27, no. 10 (November 2011): 1095–1104. doi:10.1080/08927014.2011.633704.

Lee, Kai Wei Kelvin, Saravanan Periasamy, Manisha Mukherjee, Chao Xie, Staffan Kjelleberg, and Scott A. Rice. “Biofilm Development and Enhanced Stress Resistance of a Model, Mixed-Species Community Biofilm.” *The ISME Journal* 8, no. 4 (April 2014): 894–907. doi:10.1038/ismej.2013.194.

Lehtola, Markku J., Ilkka T. Miettinen, Terttu Vartiainen, Panu Rantakokko, Arja Hirvonen, and Pertti J. Martikainen. “Impact of UV Disinfection on Microbially Available Phosphorus, Organic Carbon, and Microbial Growth in Drinking Water.” *Water Research* 37, no. 5 (March 2003): 1064–70.

Lemos, M., S. Wang, A. Ali, M. Simões, and D. I. Wilson. “A Fluid Dynamic Gauging Device for Measuring Biofilm Thickness on Cylindrical Surfaces.” *Biochemical Engineering Journal* 106 (February 15, 2016): 48–60. doi:10.1016/j.bej.2015.11.006.

Lens, P., V. O’Flaherty, A. P. Moran, P. Stoodley, and T. Mahony. *Biofilms in Medicine, Industry and Environmental Biotechnology*. IWA Publishing, 2003. http://www.iwapublishing.com/books/9781843390190/biofilms-medicine-industry-and-environmental-biotechnology.

Leriche, V., P. Sibille, and B. Carpentier. “Use of an Enzyme-Linked Lectinsorbent Assay to Monitor the Shift in Polysaccharide Composition in Bacterial Biofilms.” *Applied and Environmental Microbiology* 66, no. 5 (May 2000): 1851–56.

Lewandowski, Zbigniew, and H. Beyenal. *Fundamentals of Biofilm Research, Second Edition. CRC Press, 2014. Z. Lewandowski and H. Beyenal (Authors).*, 2013. https://www.researchgate.net/publication/265336195_Fundamentals_of_Biofilm_Research_Second_Edition_CRC_Press_2014_Z_Lewandowski_and_H_Beyenal_Authors.

Lewis, K. “Riddle of Biofilm Resistance.” *Antimicrobial Agents and Chemotherapy* 45, no. 4 (April 2001): 999–1007. doi:10.1128/AAC.45.4.999-1007.2001.

Lewis, William J. T., Y. M. John Chew, and Michael R. Bird. “The Application of Fluid Dynamic Gauging in Characterising Cake Deposition during the Cross-Flow Microfiltration of a Yeast Suspension.” *Journal of Membrane Science* 405–406 (July 1, 2012): 113–22. doi:10.1016/j.memsci.2012.02.065.

Li, Tinggang, Renbi Bai, and Junxin Liu. “Distribution and Composition of Extracellular Polymeric Substances in Membrane-Aerated Biofilm.” *Journal of Biotechnology* 135, no. 1 (May 20, 2008): 52–57. doi:10.1016/j.jbiotec.2008.02.011.

Lin, Jing, Soon-Hwan Oh, Rhian Jones, James A. Garnett, Paula S. Salgado, Sophia Rusnakova, Steve J. Matthews, Lois L. Hoyer, and Ernesto Cota. “The Peptide-Binding Cavity Is Essential for Als3-Mediated Adhesion of Candida Albicans to Human Cells.” *The Journal of Biological Chemistry* 289, no. 26 (June 27, 2014): 18401–12. doi:10.1074/jbc.M114.547877.

Lin, Justin Chun-Te, Duu-Jong Lee, and Chihpin Huang. “Membrane Fouling Mitigation: Membrane Cleaning.” *Separation Science and Technology* 45, no. 7 (April 28, 2010): 858–72. doi:10.1080/01496391003666940.

Lindh, Liselott. “On the Adsorption Behaviour of Saliva and Purified Salivary Proteins at Solid/liquid Interfaces.” *Swedish Dental Journal. Supplement*, no. 152 (2002): 1–57.

Lindsay, D., and A. von Holy. “Bacterial Biofilms within the Clinical Setting: What Healthcare Professionals Should Know.” *The Journal of Hospital Infection* 64, no. 4 (December 2006): 313–25. doi:10.1016/j.jhin.2006.06.028.

Lisle, J. T., S. C. Broadaway, A. M. Prescott, B. H. Pyle, C. Fricker, and G. A. McFeters. “Effects of Starvation on Physiological Activity and Chlorine Disinfection Resistance in Escherichia Coli O157:H7.” *Applied and Environmental Microbiology* 64, no. 12 (December 1998): 4658–62.

Lister, Vincent Y., Claire Lucas, Patrick W. Gordon, Y. M. John Chew, and D. Ian Wilson. “Pressure Mode Fluid Dynamic Gauging for Studying Cake Build-up in Cross-Flow Microfiltration.” *Journal of Membrane Science* 366, no. 1–2 (January 1, 2011): 304–13. doi:10.1016/j.memsci.2010.10.017.

Little, Brenda, Patricia Wagner, Richard Ray, Robert Pope, and Raymond Scheetz. “Biofilms: An ESEM Evaluation of Artifacts Introduced during SEM Preparation.” *Journal of Industrial Microbiology* 8, no. 4 (November 1, 1991): 213–21. doi:10.1007/BF01576058.

Liu, Chen, and Qi Zhao. “Influence of Surface-Energy Components of Ni-P-TiO2-PTFE Nanocomposite Coatings on Bacterial Adhesion.” *Langmuir: The ACS Journal of Surfaces and Colloids* 27, no. 15 (August 2, 2011): 9512–19. doi:10.1021/la200910f.

Liu, Jun, Xudong Pan, Guanglin Wang, and Aoyu Chen. “Design and Accuracy Analysis of Pneumatic Gauging for Form Error of Spool Valve Inner Hole.” *Flow Measurement and Instrumentation* 23, no. 1 (March 2012): 26–32. doi:10.1016/j.flowmeasinst.2011.12.007.

Liu, W., G. K. Christian, Z. Zhang, and P. J. Fryer. “Development and Use of a Micromanipulation Technique for Measuring the Force Required to Disrupt and Remove Fouling Deposits.” *Food and Bioproducts Processing* 80, no. 4 (December 1, 2002): 286–91. doi:10.1205/096030802321154790.

Liu, W., P. J. Fryer, Z. Zhang, Q. Zhao, and Y. Liu. “Identification of Cohesive and Adhesive Effects in the Cleaning of Food Fouling Deposits.” *Innovative Food Science & Emerging Technologies* 7, no. 4 (December 2006): 263–69. doi:10.1016/j.ifset.2006.02.006.

Lodish, Harvey, Arnold Berk, S. Lawrence Zipursky, Paul Matsudaira, David Baltimore, and James Darnell. “Structure of Nucleic Acids.” In *Molecular Cell Biology*, 4th ed. New York: WH Freeman, 2000. https://www.ncbi.nlm.nih.gov/books/NBK21514/.

Long, Guoyu, Pingting Zhu, Yun Shen, and Meiping Tong. “Influence of Extracellular Polymeric Substances (EPS) on Deposition Kinetics of Bacteria.” *Environmental Science & Technology* 43, no. 7 (April 1, 2009): 2308–14. doi:10.1021/es802464v.

Loosdrecht, M. C. M. van, J. J. Heijnen, H. Eberl, J. Kreft, and C. Picioreanu. “Mathematical Modelling of Biofilm Structures.” *Antonie Van Leeuwenhoek* 81, no. 1–4 (August 2002): 245–56.

Lorite, Gabriela S., Carolina M. Rodrigues, Alessandra A. de Souza, Christine Kranz, Boris Mizaikoff, and Mônica A. Cotta. “The Role of Conditioning Film Formation and Surface Chemical Changes on Xylella Fastidiosa Adhesion and Biofilm Evolution.” *Journal of Colloid and Interface Science* 359, no. 1 (July 1, 2011): 289–95. doi:10.1016/j.jcis.2011.03.066.

Loukili, N. H., H. Becker, J. Harno, M. Bientz, and O. Meunier. “Effect of Peracetic Acid and Aldehyde Disinfectants on Biofilm.” *The Journal of Hospital Infection* 58, no. 2 (October 2004): 151–54. doi:10.1016/j.jhin.2004.06.022.

Loukili, N. Henoun, B. Granbastien, K. Faure, B. Guery, and G. Beaucaire. “Effect of Different Stabilized Preparations of Peracetic Acid on Biofilm.” *Journal of Hospital Infection* 63, no. 1 (May 1, 2006): 70–72. doi:10.1016/j.jhin.2005.11.015.

Lowry, O. H., N. J. Rosebrough, A. L. Farr, and R. J. Randall. “Protein Measurement with the Folin Phenol Reagent.” *The Journal of Biological Chemistry* 193, no. 1 (November 1951): 265–75.

Lu, Wen, Laurent Kiéné, and Yves Lévi. “Chlorine Demand of Biofilms in Water Distribution Systems.” *Water Research* 33, no. 3 (February 1999): 827–35. doi:10.1016/S0043-1354(98)00229-2.

Lüdecke, Claudia, Klaus D. Jandt, Daniel Siegismund, Marian J. Kujau, Emerson Zang, Markus Rettenmayr, Jörg Bossert, and Martin Roth. “Reproducible Biofilm Cultivation of Chemostat-Grown Escherichia Coli and Investigation of Bacterial Adhesion on Biomaterials Using a Non-Constant-Depth Film Fermenter.” *PloS One* 9, no. 1 (2014): e84837. doi:10.1371/journal.pone.0084837.

Lund, Vidar, and Kari Ormerod. “The Influence of Disinfection Processes on Biofilm Formation in Water Distribution Systems.” *Water Research* 29, no. 4 (April 1, 1995): 1013–21. doi:10.1016/0043-1354(94)00280-K.

Luppens, Suzanne B. I., Martine W. Reij, Rob W. L. van der Heijden, Frank M. Rombouts, and Tjakko Abee. “Development of a Standard Test To Assess the Resistance of Staphylococcus

Aureus Biofilm Cells to Disinfectants." *Applied and Environmental Microbiology* 68, no. 9 (September 1, 2002): 4194–4200. doi:10.1128/AEM.68.9.4194-4200.2002.
Madigan, M. T., J. M. Martinko, D. Stahl, and D. P. Clark. *Brock Biology of Microorganisms*. 13th ed. San Francisco: Pearson Benjamin-Cummings, 2010.
Madigan, Michael T., and John M. Martinko. *Brock Biology of Microorganisms*. Pearson Prentice Hall, 2006.
Mairal, Anurag P, Alan R Greenberg, William B Krantz, and Leonard J Bond. "Real-Time Measurement of Inorganic Fouling of RO Desalination Membranes Using Ultrasonic Time-Domain Reflectometry." *Journal of Membrane Science* 159, no. 1–2 (July 1, 1999): 185–96. doi:10.1016/S0376-7388(99)00058-7.
Marcato-Romain, C. E., Y. Pechaud, E. Paul, E. Girbal-Neuhauser, and V. Dossat-Létisse. "Removal of Microbial Multi-Species Biofilms from the Paper Industry by Enzymatic Treatments." *Biofouling* 28, no. 3 (2012): 305–14. doi:10.1080/08927014.2012.673122.
Marsh, P. D. "Dental Plaque as a Microbial Biofilm." *Caries Research* 38, no. 3 (June 2004): 204–11. doi:10.1159/000077756.
Marsh, Philip D. "Dental Plaque as a Biofilm and a Microbial Community – Implications for Health and Disease." *BMC Oral Health* 6, no. Suppl 1 (June 15, 2006): S14. doi:10.1186/1472-6831-6-S1-S14.
Martin, D. J. H., S. P. Denyer, G. McDonnell, and J.-Y. Maillard. "Resistance and Cross-Resistance to Oxidising Agents of Bacterial Isolates from Endoscope Washer Disinfectors." *The Journal of Hospital Infection* 69, no. 4 (August 2008): 377–83. doi:10.1016/j.jhin.2008.04.010.
Mascotti, K., J. McCullough, and S.r. Burger. "HPC Viability Measurement: Trypan Blue versus Acridine Orange and Propidium Iodide." *Transfusion* 40, no. 6 (June 1, 2000): 693–96. doi:10.1046/j.1537-2995.2000.40060693.x.
Masuko, Tatsuya, Akio Minami, Norimasa Iwasaki, Tokifumi Majima, Shin-Ichiro Nishimura, and Yuan C. Lee. "Carbohydrate Analysis by a Phenol-Sulfuric Acid Method in Microplate Format." *Analytical Biochemistry* 339, no. 1 (April 1, 2005): 69–72. doi:10.1016/j.ab.2004.12.001.
Mather, J. P., and P. E. Roberts. *Introduction to Cell and Tissue Culture - Theory and Technique*. Springer, 1998. http://www.springer.com/gb/book/9780306458590.
Mathieu, L., I. Bertrand, Y. Abe, E. Angel, J. C. Block, S. Skali-Lami, and G. Francius. "Drinking Water Biofilm Cohesiveness Changes under Chlorination or Hydrodynamic Stress." *Water Research* 55 (May 15, 2014): 175–84. doi:10.1016/j.watres.2014.01.054.
Matin, Asif, Z. Khan, S. M. J. Zaidi, and M. C. Boyce. "Biofouling in Reverse Osmosis Membranes for Seawater Desalination: Phenomena and Prevention." *Desalination* 281 (October 17, 2011): 1–16. doi:10.1016/j.desal.2011.06.063.
Mattila, Pirjo, Vieno Piironen, Riitta Haapala, Timo Hirvi, and Esko Uusi-Rauva. "Possible Factors Responsible for the High Variation in the Cholecalciferol Contents of Fish." *Journal of Agricultural and Food Chemistry* 45, no. 10 (October 1, 1997): 3891–96. doi:10.1021/jf970243j.
McCall, E., J. E. Stout, V. Yu, and R. Vidic. "Efficacy of Biocides against Biofilm-Associated Legionella in a Model System." In *Proceedings of the 60th Annual Meeting*. Pittsburgh, PA, 1999.
McCarty, Rachael, and S. Nima Mahmoodi. "Dynamic Mulitmode Analysis of Non-Linear Piezoelectric Microcantilever Probe in Bistable Region of Tapping Mode Atomic Force Microscopy." *International Journal of Non-Linear Mechanics* Complete, no. 74 (2015): 25–37. doi:10.1016/j.ijnonlinmec.2015.03.010.

McCoy, W. F., and J. W. Costerton. “Fouling Biofilm Development in Tubular Flow Systems.” *Developments in Industrial Microbiology (USA)*, 1982. http://agris.fao.org/agris-search/search.do?recordID=US8251805.
McCoy, William F., and John W. Wireman. “Efficacy of Bromochlorodimethylhydantoin againstLegionella Pneumophila in Industrial Cooling Water.” *Journal of Industrial Microbiology* 4, no. 6 (November 1, 1989): 403–8. doi:10.1007/BF01569635.
McDonogh, Richard, Gabriela Schaule, and Hans-Curt Flemming. “The Permeability of Biofouling Layers on Membranes.” *Journal of Membrane Science* 87, no. 1 (February 23, 1994): 199–217. doi:10.1016/0376-7388(93)E0149-E.
McGuire, Joseph, and Kenneth R. Swartzel. “On the Use of Water in the Measurement of Solid Surface Tension.” *Surface and Interface Analysis* 10, no. 8 (October 1, 1987): 430–33. doi:10.1002/sia.740100809.
McKee, C. J. “The Interaction between Turbulent Bursts and Fouled Surfaces.” PhD, University of Birmingham, 1991.
Medilanski, Edi, Karin Kaufmann, Lukas Y. Wick, Oskar Wanner, and Hauke Harms. “Influence of the Surface Topography of Stainless Steel on Bacterial Adhesion.” *Biofouling* 18, no. 3 (January 1, 2002): 193–203. doi:10.1080/08927010290011370.
Mei, Henny C. van der, Minie Rustema-Abbing, Joop de Vries, and Henk J. Busscher. “Bond Strengthening in Oral Bacterial Adhesion to Salivary Conditioning Films.” *Applied and Environmental Microbiology* 74, no. 17 (September 1, 2008): 5511–15. doi:10.1128/AEM.01119-08.
Mei, Li, Henk J. Busscher, Henny C. van der Mei, and Yijin Ren. “Influence of Surface Roughness on Streptococcal Adhesion Forces to Composite Resins.” *Dental Materials: Official Publication of the Academy of Dental Materials* 27, no. 8 (August 2011): 770–78. doi:10.1016/j.dental.2011.03.017.
Melián-Martel, N., J. J. Sadhwani, S. Malamis, and M. Ochsenkühn-Petropoulou. “Structural and Chemical Characterization of Long-Term Reverse Osmosis Membrane Fouling in a Full Scale Desalination Plant.” *Desalination* 305 (November 1, 2012): 44–53. doi:10.1016/j.desal.2012.08.011.
Melo, L. F., and T. R. Bott. “Biofouling in Water Systems.” *Experimental Thermal and Fluid Science* 14, no. 4 (May 1, 1997): 375–81. doi:10.1016/S0894-1777(96)00139-2.
Meng, Fangang, Hanmin Zhang, Fenglin Yang, Shoutong Zhang, Yansong Li, and Xingwen Zhang. “Identification of Activated Sludge Properties Affecting Membrane Fouling in Submerged Membrane Bioreactors.” *Separation and Purification Technology* 51, no. 1 (August 2006): 95–103. doi:10.1016/j.seppur.2006.01.002.
MERUS. “MERUS - Newsletter No. 1.” *MERUS Online*, 2011. http://www.merusonline.com/merusnewsletter1.
Michels, Corinne A. “Techniques in Cell and Molecular Biology.” In *Genetic Techniques for Biological Research*, 23–42. John Wiley & Sons, Ltd, 2002. http://onlinelibrary.wiley.com/doi/10.1002/0470846623.ch2/summary.
Miqueleto, A. P., C. C. Dolosic, E. Pozzi, E. Foresti, and M. Zaiat. “Influence of Carbon Sources and C/N Ratio on EPS Production in Anaerobic Sequencing Batch Biofilm Reactors for Wastewater Treatment.” *Bioresource Technology* 101, no. 4 (February 2010): 1324–30. doi:10.1016/j.biortech.2009.09.026.
Möhle, Roland B., Timo Langemann, Marian Haesner, Wolfgang Augustin, Stephan Scholl, Thomas R. Neu, Dietmar C. Hempel, and Harald Horn. “Structure and Shear Strength of Microbial Biofilms as Determined with Confocal Laser Scanning Microscopy and Fluid Dynamic Gauging Using a Novel Rotating Disc Biofilm Reactor.” *Biotechnology and Bioengineering* 98, no. 4 (November 1, 2007): 747–55. doi:10.1002/bit.21448.

Momba, Maggy NB, and N. Makala. “Comparing the Effect of Various Pipe Materials on Biofilm Formation in Chlorinated and Combined Chlorine-Chloraminated Water Systems.” *Water SA* 30, no. 2 (January 1, 2004): 175–82. doi:10.4314/wsa.v30i2.5061.

Momba, M. N. B., R. Kfir, S. N. Venter, and T. E. CLeote. “An Overview of Biofilm Formation in Distribution Systems and Its Impact on the Deterioration of Water Quality.” *Water SA* 26, no. 1 (2000).

Monod, J. “The Growth of Bacterial Cultures.” *Annual Review of Microbiology* 3, no. 1 (1949): 371–94. doi:10.1146/annurev.mi.03.100149.002103.

Monroe, Don. “Looking for Chinks in the Armor of Bacterial Biofilms.” *PLOS Biology* 5, no. 11 (November 13, 2007): e307. doi:10.1371/journal.pbio.0050307.

Moreira, Leandro Marcio, Agda Paula Facincani, Cristiano Barbalho Ferreira, Rafael Marine Ferreira, Maria Inês Tiraboshi Ferro, Fabio Cesar Gozzo, Julio Cezar Franco de Oliveira, Jesus Aparecido Ferro, and Márcia Regina Soares. “Chemotactic Signal Transduction and Phosphate Metabolism as Adaptive Strategies during Citrus Canker Induction by Xanthomonas Citri.” *Functional & Integrative Genomics* 15, no. 2 (March 2015): 197–210. doi:10.1007/s10142-014-0414-z.

Møretrø, T., and M.a. Daeschel. “Wine Is Bactericidal to Foodborne Pathogens.” *Journal of Food Science* 69, no. 9 (December 1, 2004): M251–57. doi:10.1111/j.1365-2621.2004.tb09938.x.

Møretrø, Trond, Even Heir, Live L. Nesse, Lene K. Vestby, and Solveig Langsrud. “Control of Salmonella in Food Related Environments by Chemical Disinfection.” *Food Research International*, Salmonella in Foods: Evolution, Strategies and Challenges, 45, no. 2 (March 2012): 532–44. doi:10.1016/j.foodres.2011.02.002.

Mott, I. E. C., and T. R. Bott. “The Adhesion of Biofilms to Selected Materials of Construction for Heat Exchangers.” In *Proceedings of the 9th International Heat Transfer Conference*, 5:21–26. Jerusalem, 1991.

Mozes, N., F. Marchal, M. P. Hermesse, J. L. Van Haecht, L. Reuliaux, A. J. Leonard, and P. G. Rouxhet. “Immobilization of Microorganisms by Adhesion: Interplay of Electrostatic and Nonelectrostatic Interactions.” *Biotechnology and Bioengineering* 30, no. 3 (August 20, 1987): 439–50. doi:10.1002/bit.260300315.

Mukherjee, A., K. V. Mohan Rao, and U. S. Ramesh. “Predicted Concentrations of Biocides from Antifouling Paints in Visakhapatnam Harbour.” *Journal of Environmental Management* 90 Suppl 1 (February 2009): S51-59. doi:10.1016/j.jenvman.2008.07.018.

Müller-Steinhagen, Hans. *Heat Exchanger Fouling: Mitigation and Cleaning Techniques*. IChemE, 2000.

Murthy, Dr P. Sriyutha, and Dr R. Venkatesan. “Industrial Biofilms and Their Control.” In *Marine and Industrial Biofouling*, edited by Prof Dr Hans-Curt Flemming, Dr P. Sriyutha Murthy, Dr R. Venkatesan, and Prof Dr Keith Cooksey, 65–101. Springer Series on Biofilms 4. Springer Berlin Heidelberg, 2009. http://link.springer.com/chapter/10.1007/978-3-540-69796-1_4.

Nannipieri, P., J. Ascher, M. T. Ceccherini, L. Landi, G. Pietramellara, and G. Renella. “Microbial Diversity and Soil Functions.” *European Journal of Soil Science* 54, no. 4 (December 1, 2003): 655–70. doi:10.1046/j.1351-0754.2003.0556.x.

Navarro, Lionel, Rajendra Bari, Patrick Achard, Purificación Lisón, Adnane Nemri, Nicholas P. Harberd, and Jonathan D. G. Jones. “DELLAs Control Plant Immune Responses by Modulating the Balance of Jasmonic Acid and Salicylic Acid Signaling.” *Current Biology: CB* 18, no. 9 (May 6, 2008): 650–55. doi:10.1016/j.cub.2008.03.060.

Nejadnik, M. Reza, Henny C. van der Mei, Henk J. Busscher, and Willem Norde. “Determination of the Shear Force at the Balance between Bacterial Attachment and Detachment in Weak-Adherence Systems, Using a Flow Displacement Chamber.” *Applied and Environmental Microbiology* 74, no. 3 (February 1, 2008): 916–19. doi:10.1128/AEM.01557-07.

Ngene, Ikenna S., Rob G. H. Lammertink, Antoine J. B. Kemperman, Wilhelmus J. C. van de Ven, L. Peter Wessels, Matthias Wessling, and Walter G. J. Van der Meer. "CO2 Nucleation in Membrane Spacer Channels Remove Biofilms and Fouling Deposits." *Industrial & Engineering Chemistry Research* 49, no. 20 (October 20, 2010): 10034–39. doi:10.1021/ie1011245.

Nguyen, T., B. Pellegrin, C. Bernard, S. Rabb, P. Stuztman, J. M. Gorham, X. Gu, L. L. Yu, and J. W. Chin. "Characterization of Surface Accumulation and Release of Nanosilica during Irradiation of Polymer Nanocomposites by Ultraviolet Light." *Journal of Nanoscience and Nanotechnology* 12, no. 8 (August 2012): 6202–15.

Nguyen, Thang, Felicity A. Roddick, and Linhua Fan. "Biofouling of Water Treatment Membranes: A Review of the Underlying Causes, Monitoring Techniques and Control Measures." *Membranes* 2, no. 4 (November 21, 2012): 804–40. doi:10.3390/membranes2040804.

Nickel, J. C., I. Ruseska, J. B. Wright, and J. W. Costerton. "Tobramycin Resistance of Pseudomonas Aeruginosa Cells Growing as a Biofilm on Urinary Catheter Material." *Antimicrobial Agents and Chemotherapy* 27, no. 4 (April 1985): 619–24.

Nigaud, Yohan, Pascal Cosette, Anthony Collet, Philippe Chan Tchi Song, David Vaudry, Hubert Vaudry, Guy-Alain Junter, and Thierry Jouenne. "Biofilm-Induced Modifications in the Proteome of Pseudomonas Aeruginosa Planktonic Cells." *Biochimica et Biophysica Acta (BBA) - Proteins and Proteomics* 1804, no. 4 (April 2010): 957–66. doi:10.1016/j.bbapap.2010.01.008.

Nishijima, Wataru, Tetsuji Okuda, Satoshi Nakai, and Mitsumasa Okada. "A Green Procedure Using Ozone for Cleaning-in-Place in the Beverage Industry." *Chemosphere* 105 (June 2014): 106–11. doi:10.1016/j.chemosphere.2014.01.019.

Niyonsaba, Francois, Isao Nagaoka, and Hideoki Ogawa. "Human Defensins and Cathelicidins in the Skin: Beyond Direct Antimicrobial Properties." *Critical Reviews in Immunology* 26, no. 6 (2006): 545–76.

Núñez, Megan E., Mark O. Martin, Phyllis H. Chan, and Eileen M. Spain. "Predation, Death, and Survival in a Biofilm: Bdellovibrio Investigated by Atomic Force Microscopy." *Colloids and Surfaces. B, Biointerfaces* 42, no. 3–4 (May 25, 2005): 263–71. doi:10.1016/j.colsurfb.2005.03.003.

Nutan, M. T. H., and I. K. Reddy. "General Principles of Suspensions." In *Pharmaceutical Suspensions: From Formulation Development to Manufacturing*, 39–66. Springer, 2009.

Nyvad, B. "Microbial Colonization of Human Tooth Surfaces." *APMIS. Supplementum* 32 (1993): 1–45.

Nyvad, B., and O. Fejerskov. "Scanning Electron Microscopy of Early Microbial Colonization of Human Enamel and Root Surfaces in Vivo." *Scandinavian Journal of Dental Research* 95, no. 4 (August 1987): 287–96.

O'Donoghue, A. "Why Pigs Get Stuck and How to Avoid It." Glasgow, UK: Pipeline Research Limited, 2003. http://www.apachepipe.com/assets/why-pigs-get-stuck.pdf.

Oh, Y. J., N. R. Lee, W. Jo, W. K. Jung, and J. S. Lim. "Effects of Substrates on Biofilm Formation Observed by Atomic Force Microscopy." *Ultramicroscopy*, Proceedings of the 10th International Scanning Probe Microscopy Conference, 109, no. 8 (July 2009): 874–80. doi:10.1016/j.ultramic.2009.03.042.

Ohashi, Akiyoshi, Takashi Koyama, Kazuaki Syutsubo, and Hideki Harada. "A Novel Method for Evaluation of Biofilm Tensile Strength Resisting Erosion." *Water Science and Technology* 39, no. 7 (April 1, 1999): 261–68.

Okada, Ayako, Toru Nikaido, Masaomi Ikeda, Koichi Okada, Junichi Yamauchi, Richard M. Foxton, Hideo Sawada, Junji Tagami, and Khairul Matin. "Inhibition of Biofilm Formation

Using Newly Developed Coating Materials with Self-Cleaning Properties." *Dental Materials Journal* 27, no. 4 (July 2008): 565–72.
Oliveira, R., J. Azeredo, P. Teixeira, and A. P. Fonseca. "The Role of Hydrophobicity in Bacterial Adhesion." In *Biofilm Community Interactions: Chance or Necessity?*, 11–22. Cardiff, UK: Bioline, 2001.
Olsson, Adam L. J., Narasimhan Arun, Johannes S. Kanger, Henk Busscher, Ivan E. Ivanov, Terri A. Camesano, Yun Chen, et al., "The Influence of Ionic Strength on the Adhesive Bond Stiffness of Oral Streptococci Possessing Different Surface Appendages as Probed Using AFM and QCM-D." *Soft Matter* 8, no. 38 (2012): 9870–76. doi:10.1039/c2sm26025e.
Omoike, Anselm, and Jon Chorover. "Spectroscopic Study of Extracellular Polymeric Substances from Bacillus Subtilis: Aqueous Chemistry and Adsorption Effects." *Biomacromolecules* 5, no. 4 (August 2004): 1219–30. doi:10.1021/bm034461z.
Orgaz, B., R. J. Neufeld, and C. SanJose. "Single-Step Biofilm Removal with Delayed Release Encapsulated Pronase Mixed with Soluble Enzymes." *Enzyme and Microbial Technology* 40, no. 5 (April 3, 2007): 1045–51. doi:10.1016/j.enzmictec.2006.08.003.
Oss, C. J. van. "Acid—base Interfacial Interactions in Aqueous Media." *Colloids and Surfaces A: Physicochemical and Engineering Aspects* 78 (October 15, 1993): 1–49. doi:10.1016/0927-7757(93)80308-2.
———. "Hydrophobicity of Biosurfaces — Origin, Quantitative Determination and Interaction Energies." *Colloids and Surfaces B: Biointerfaces*, Hydrophobicity, 5, no. 3 (November 10, 1995): 91–110. doi:10.1016/0927-7765(95)01217-7.
O'Toole, G. A., and R. Kolter. "Initiation of Biofilm Formation in Pseudomonas Fluorescens WCS365 Proceeds via Multiple, Convergent Signalling Pathways: A Genetic Analysis." *Molecular Microbiology* 28, no. 3 (May 1998): 449–61.
O'Toole, George, Heidi B. Kaplan, and Roberto Kolter. "Biofilm Formation as Microbial Development." *Annual Review of Microbiology* 54, no. 1 (2000): 49–79. doi:10.1146/annurev.micro.54.1.49.
Otto, Karen. "Biophysical Approaches to Study the Dynamic Process of Bacterial Adhesion." *Research in Microbiology* 159, no. 6 (July 2008): 415–22. doi:10.1016/j.resmic.2008.04.007.
Oulahal-Lagsir, Nadia, Adele Martial-Gros, Marc Bonneau, and Loic J. Blum. "'Escherichia Coli-Milk' biofilm Removal from Stainless Steel Surfaces: Synergism between Ultrasonic Waves and Enzymes." *Biofouling* 19, no. 3 (June 2003): 159–68. doi:10.1080/08927014.2003.10382978.
Ozok, Ahmet Rifat, Min-Kai Wu, Suzanne Bernardina Ida Luppens, and Paul Rudolf Wesselink. "Comparison of Growth and Susceptibility to Sodium Hypochlorite of Mono- and Dual-Species Biofilms of Fusobacterium Nucleatum and Peptostreptococcus (Micromonas) Micros." *Journal of Endodontics* 33, no. 7 (July 2007): 819–22. doi:10.1016/j.joen.2007.03.008.
Packman, R., B. Knudsen, and I. Hansen. "Perspectives in Tank Cleaning: Hygiene Requirements, Device Selection, Risk Evaluation and Management Respoinsibility." In *Cleaning-in-Place: Dairy, Food and Beverage Operations*, 108–45. England: Blackwell Publishing Limited, 2008.
Paramonova, E. "Compressive Strength of Fungal and Oral Bacterial Biofilms: Biological and Environmental Influences." PhD, Rijksuniversiteit Groningen, 2009.
Park, Chul, and John T. Novak. "Characterization of Activated Sludge Exocellular Polymers Using Several Cation-Associated Extraction Methods." *Water Research* 41, no. 8 (April 2007): 1679–88. doi:10.1016/j.watres.2007.01.031.
Parker, A. E., D. K. Walker, D. M. Goeres, N. Allan, M. E. Olson, and A. Omar. "Ruggedness and Reproducibility of the MBEC Biofilm Disinfectant Efficacy Test." *Journal of Microbiological Methods* 102 (July 2014): 55–64. doi:10.1016/j.mimet.2014.04.013.

Parrotta, M. J., and F. Bekdash. “UV Disinfection of Small Groundwater Supplies.” *American Water Works Association Journal* 90, no. 2 (1998).
Passos, Maria Laura, and Claudio P. Ribeiro. *Innovation in Food Engineering: New Techniques and Products*. CRC Press, 2016.
Patel, Jitendra, and Manan Sharma. “Differences in Attachment of Salmonella Enterica Serovars to Cabbage and Lettuce Leaves.” *International Journal of Food Microbiology* 139, no. 1–2 (April 30, 2010): 41–47. doi:10.1016/j.ijfoodmicro.2010.02.005.
Pechaud, Y., C. E. Marcato-Romain, E. Girbal-Neuhauser, I. Queinnec, Y. Bessiere, and E. Paul. “Combining Hydrodynamic and Enzymatic Treatments to Improve Multi-Species Thick Biofilm Removal.” *Chemical Engineering Science* 80 (October 1, 2012): 109–18. doi:10.1016/j.ces.2012.06.014.
Pedersen, K. “Method for Studying Microbial Biofilms in Flowing-Water Systems.” *Applied and Environmental Microbiology* 43, no. 1 (January 1982): 6–13.
Percival, R. S., S. J. Challacombe, and P. D. Marsh. “Age-Related Microbiological Changes in the Salivary and Plaque Microflora of Healthy Adults.” *Journal of Medical Microbiology* 35, no. 1 (1991): 5–11. doi:10.1099/00222615-35-1-5.
Percival, Steven, and James T. Walker. “Methods Used to Assess Biofouling of Material Used in Distribution and Domestic Water Systems.” In *Methods in Enzymology*, edited by Ron J. Doyle, 337:187–200. Microbial Growth in Biofilms - Part B: Special Environments and Physicochemical Aspects. Academic Press, 2001. http://www.sciencedirect.com/science/article/pii/S0076687901370143.
Pereni, C. I., Q. Zhao, Y. Liu, and E. Abel. “Surface Free Energy Effect on Bacterial Retention.” *Colloids and Surfaces B: Biointerfaces* 48, no. 2 (March 15, 2006): 143–47. doi:10.1016/j.colsurfb.2006.02.004.
Perni, Stefano, Timothy G. Aldsworth, Suzanne J. Jordan, Isabel Fernandes, Manuela Barbosa, Manuela Sol, Rogério P. Tenreiro, et al., “The Resistance to Detachment of Dairy Strains of Listeria Monocytogenes from Stainless Steel by Shear Stress Is Related to the Fluid Dynamic Characteristics of the Location of Isolation.” *International Journal of Food Microbiology* 116, no. 3 (May 30, 2007): 384–90. doi:10.1016/j.ijfoodmicro.2007.03.002.
Perrozzi, Francesco, Salvatore Croce, Emanuele Treossi, Vincenzo Palermo, Sandro Santucci, Guilia Fioravanti, Luca Ottaviano. "Reduction dependent wetting properties of graphene oxide". *Carbon* 77, Supplement C (October 1, 2014); 473-480. 10.1016/j.carbon.2014.05.052
Perry, J. L., and S. G. Kandlikar. “Fouling and Its Mitigation in Silicon Microchannels Used for IC Chip Cooling.” *Microfluidics and Nanofluidics* 5 (2008): 357–71.
Petrova, Olga E., and Karin Sauer. “Dispersion by Pseudomonas Aeruginosa Requires an Unusual Posttranslational Modification of BdlA.” *Proceedings of the National Academy of Sciences of the United States of America* 109, no. 41 (October 9, 2012): 16690–95. doi:10.1073/pnas.1207832109.
Peyton, Brent M. “Effects of Shear Stress and Substrate Loading Rate on Pseudomonas Aeruginosa Biofilm Thickness and Density.” *Water Research* 30, no. 1 (January 1, 1996): 29–36. doi:10.1016/0043-1354(95)00110-7.
Picioreanu, C., M. C. van Loosdrecht, and J. J. Heijnen. “Two-Dimensional Model of Biofilm Detachment Caused by Internal Stress from Liquid Flow.” *Biotechnology and Bioengineering* 72, no. 2 (January 20, 2001): 205–18.
Picologlou, Basil F., William G. Characklis, and Nicholas Zelver. “Biofilm Growth and Hydraulic Performance.” *Journal of the Hydraulics Division* 106, no. 5 (1980): 733–46.
Pinheiro, M. M., L. F. Melo, T. R. Bott, J. D. Pinheiro, and L. Leitão. “Surface Phenomena and Hydrodynamic Effects on the Deposition of Pseudomonas Fluorescens.” *The Canadian*

Journal of Chemical Engineering 66, no. 1 (February 1, 1988): 63–67. doi:10.1002/cjce.5450660109.
Pommerville, Jeffrey C. *Alcamo's Laboratory Fundamentals of Microbiology*. Jones & Bartlett Publishers, 2010.
Pontié, Maxime, Sophie Rapenne, Anju Thekkedath, Jean Duchesne, Valérie Jacquemet, Jérôme Leparc, and Hervé Suty. "Tools for Membrane Autopsies and Antifouling Strategies in Seawater Feeds: A Review." *Desalination* 181, no. 1 (September 5, 2005): 75–90. doi:10.1016/j.desal.2005.01.013.
Poole, Keith. "Efflux-Mediated Antimicrobial Resistance." *The Journal of Antimicrobial Chemotherapy* 56, no. 1 (July 2005): 20–51. doi:10.1093/jac/dki171.
Pope, D. H., and D. M. Dziewulski. "Efficacy of Biocides in Controlling Microbial Populations, Including Legionella, in Cooling Systems." *Ashrae Transactions* 98, no. 2 (1992).
Prakash, Sangeeta, Nivedita Datta, and Hilton C. Deeth. "Methods of Detecting Fouling Caused by Heating of Milk." *Food Reviews International* 21, no. 3 (July 1, 2005): 267–93. doi:10.1080/FRI-200061609.
Pratt, L. A., and R. Kolter. "Genetic Analysis of Escherichia Coli Biofilm Formation: Roles of Flagella, Motility, Chemotaxis and Type I Pili." *Molecular Microbiology* 30, no. 2 (October 1998): 285–93.
Pu, Hui, Guo-liang Ding, Xiao-kui Ma, Hai-tao Hu, and Yi-feng Gao. "Effects of Biofouling on Air-Side Heat Transfer and Pressure Drop for Finned Tube Heat Exchangers." *International Journal of Refrigeration* 32, no. 5 (August 2009): 1032–40. doi:10.1016/j.ijrefrig.2008.10.007.
Quarini, Joe. "Ice-Pigging to Reduce and Remove Fouling and to Achieve Clean-in-Place." *Applied Thermal Engineering* 22, no. 7 (May 2002): 747–53. doi:10.1016/S1359-4311(02)00019-4.
Quelas, Juan Ignacio, Silvina L. López-García, Adriana Casabuono, M. Julia Althabegoiti, Elías J. Mongiardini, Julieta Pérez-Giménez, Alicia Couto, and Aníbal R. Lodeiro. "Effects of N-Starvation and C-Source on Bradyrhizobium Japonicum Exopolysaccharide Production and Composition, and Bacterial Infectivity to Soybean Roots." *Archives of Microbiology* 186, no. 2 (August 2006): 119–28. doi:10.1007/s00203-006-0127-3.
Quirynen, M., and C. M. Bollen. "The Influence of Surface Roughness and Surface-Free Energy on Supra- and Subgingival Plaque Formation in Man. A Review of the Literature." *Journal of Clinical Periodontology* 22, no. 1 (January 1995): 1–14.
Quirynen, M., M. Marechal, H. J. Busscher, A. H. Weerkamp, P. L. Darius, and D. van Steenberghe. "The Influence of Surface Free Energy and Surface Roughness on Early Plaque Formation." *Journal of Clinical Periodontology* 17, no. 3 (March 1, 1990): 138–44. doi:10.1111/j.1600-051X.1990.tb01077.x.
Radu, A. I., J. S. Vrouwenvelder, M. C. M. van Loosdrecht, and C. Picioreanu. "Effect of Flow Velocity, Substrate Concentration and Hydraulic Cleaning on Biofouling of Reverse Osmosis Feed Channels." *Chemical Engineering Journal* 188 (April 15, 2012): 30–39. doi:10.1016/j.cej.2012.01.133.
Rajagopal, Sanjeevi, and Henk A. Jenner. "Biofouling in Cooling Water Intake Systems: Ecological Aspects." In *Operational and Environmental Consequences of Large Industrial Cooling Water Systems*, edited by Sanjeevi Rajagopal, Henk A. Jenner, and Vayalam P. Venugopalan, 13–32. Springer US, 2012. http://link.springer.com/chapter/10.1007/978-1-4614-1698-2_2.
Raut, Jayant, Vimal Rathod, and S. Mohan Karuppayil. "Cell Surface Hydrophobicity and Adhesion: A Study on Fifty Clinical Isolates of Candida Albicans." *Nihon Ishinkin Gakkai Zasshi = Japanese Journal of Medical Mycology* 51, no. 3 (2010): 131–36.

Rehm, B. H., and S. Valla. “Bacterial Alginates: Biosynthesis and Applications.” *Applied Microbiology and Biotechnology* 48, no. 3 (September 1997): 281–88.

Reid, Gregor, Hanna Bialkowska-Hobrzanska, Henny C. van der Mei, and Henk J. Busscher. “Correlation between Genetic, Physico-Chemical Surface Characteristics and Adhesion of Four Strains ofLactobacillus.” *Colloids and Surfaces B Biointerfaces* 13, no. 2 (January 1, 1999). doi:10.1016/s0927-7765(98)00107-6.

Reyes-Romero, D. F., O. Behrmann, G. Dame, and G. A. Urban. “Dynamic Thermal Sensor for Biofilm Monitoring.” *Sensors and Actuators A: Physical* 213 (July 1, 2014): 43–51. doi:10.1016/j.sna.2014.03.032.

Ridgway, H. F., and H.-C. Flemming. “Membrane Biofouling.” In *Water Treatment: Membrane Processes*, 6.1-6.62. New York: McGraw-Hill, 1996.

Rimondini, L., S. Farè, E. Brambilla, A. Felloni, C. Consonni, F. Brossa, and A. Carrassi. “The Effect of Surface Roughness on Early in Vivo Plaque Colonization on Titanium.” *Journal of Periodontology* 68, no. 6 (June 1997): 556–62. doi:10.1902/jop.1997.68.6.556.

Rittschof, D. “Research on Practical Environmentally Benign Antifouling Coatings.” In *Biofouling*, edited by S. Durr and J. Thomason, 1st ed., 396–409. Chichester, UK: Blackwell Publishing Limited, 2010.

Rochex, A., and J.-M. Lebeault. “Effects of Nutrients on Biofilm Formation and Detachment of a Pseudomonas Putida Strain Isolated from a Paper Machine.” *Water Research* 41, no. 13 (July 2007): 2885–92. doi:10.1016/j.watres.2007.03.041.

Rogers, K., and R. J. Kadner. “Growth of Bacterial Populations.” *Encyclopedia Britannica*, 2007. https://www.britannica.com/science/bacteria/Growth-of-bacterial-populations.

Romney, A. J. D. *CIP: Cleaning in Place*. Society of Dairy Technology, 1990.

Rose, Helen, Adam Baldwin, Christopher G. Dowson, and Eshwar Mahenthiralingam. “Biocide Susceptibility of the Burkholderia Cepacia Complex.” *The Journal of Antimicrobial Chemotherapy* 63, no. 3 (March 2009): 502–10. doi:10.1093/jac/dkn540.

Ruardy, T. G., J. M. Schakenraad, H. C. van der Mei, and H. J. Busscher. “Preparation and Characterization of Chemical Gradient Surfaces and Their Application for the Study of Cellular Interaction Phenomena.” *Surface Science Reports* 29, no. 1 (January 1, 1997): 3–30. doi:10.1016/S0167-5729(97)00008-3.

Ruseska, I., J. Robbins, J. W. Costerton, and E. S. Lashen. “Biocide Testing against Corrosion-Causing Oil-Field Bacteria Helps Control Plugging.” *Oil and Gas Journal* 80 (1982): 253–58.

Russell, A. D. “Plasmids and Bacterial Resistance to Biocides.” *Journal of Applied Microbiology* 83, no. 2 (July 1, 1997): 155–65. doi:10.1046/j.1365-2672.1997.00198.x.

Russell, A. D., and I. Chopra. “Understanding Antibacterial Action and Resistance.” *Journal of Hospital Infection* 34, no. 3 (November 1, 1996): 241–42. doi:10.1016/S0195-6701(96)90077-8.

Ryu, Jee-Hoon, Hoikyung Kim, and Larry R. Beuchat. “Attachment and Biofilm Formation by Escherichia Coli O157:H7 on Stainless Steel as Influenced by Exopolysaccharide Production, Nutrient Availability, and Temperature.” *Journal of Food Protection* 67, no. 10 (October 2004): 2123–31.

Saad, M. A. “Biofouling Prevention in RO Polymeric Membrane Systems.” In *Desalination, Proceedings of the NWSIA 1992 Biennial Conference*, 2:85–105. Newport Beach, CA, 1992.

Sahoo, Pradeepta K., Y.M. John Chew, Ruben Mercadé-Prieto, D. Ian Wilson, and Xiao W. Dai. “Fluid Dynamic Gauging Studies of Swelling Behaviour of Whey Protein Gels in NaOH/NaCl Solutions.” *International Journal of Food Science & Technology* 43, no. 10 (October 1, 2008): 1901–7. doi:10.1111/j.1365-2621.2007.01689.x.

Saikhwan, Phanida, John Y. M. Chew, William R. Paterson, and D. Ian Wilson. “Swelling and Its Suppression in the Cleaning of Polymer Fouling Layers.” *Industrial & Engineering Chemistry Research* 46, no. 14 (July 1, 2007): 4846–55. doi:10.1021/ie0615943.

Salinas Rodriguez, S. G. “Particulate and Organic Matter Fouling of Seawater Reverse Osmosis Systems: Characterization, Modelling and Applications.” PhD, TU Delft, 2011. http://repository.tudelft.nl/islandora/object/uuid%3A2f5aeaac-01ed-49fe-9dbb-60f74cfaf044?collection=research.

Salley, B., P. W. Gordon, A. J. McCormick, A. C. Fisher, and D. I. Wilson. “Characterising the Structure of Photosynthetic Biofilms Using Fluid Dynamic Gauging.” *Biofouling* 28, no. 2 (2012): 159–73. doi:10.1080/08927014.2012.661047.

Samrakandi, M. M., C. Roques, and G. Michel. “Influence of Trophic Conditions on Exopolysaccharide Production: Bacterial Biofilm Susceptibility to Chlorine and Monochloramine.” *Canadian Journal of Microbiology* 43, no. 8 (August 1997): 751–58.

Sanderson, R., Jianxin Li, L. J. Koen, and L. Lorenzen. “Ultrasonic Time-Domain Reflectometry as a Non-Destructive Instrumental Visualization Technique to Monitor Inorganic Fouling and Cleaning on Reverse Osmosis Membranes.” *Journal of Membrane Science* 207, no. 1 (September 1, 2002): 105–17. doi:10.1016/S0376-7388(02)00122-9.

Santiago, Lizzie Y., Richard W. Nowak, J. Peter Rubin, and Kacey G. Marra. “Peptide-Surface Modification of Poly(caprolactone) with Laminin-Derived Sequences for Adipose-Derived Stem Cell Applications.” *Biomaterials* 27, no. 15 (May 2006): 2962–69. doi:10.1016/j.biomaterials.2006.01.011.

Schinteie, R., K. A. Campbell, and P. R. L. Browne. “Microfacies of Stromatolitic Sinter from Acid-Sulphate-Chloride Springs at Parariki Stream, Rotokawa Geothermal Field, New Zealand.” *Palaeo Electronica* 10, no. 1 (2007).

Schleheck, David, Nicolas Barraud, Janosch Klebensberger, Jeremy S. Webb, Diane McDougald, Scott A. Rice, and Staffan Kjelleberg. “Pseudomonas Aeruginosa PAO1 Preferentially Grows as Aggregates in Liquid Batch Cultures and Disperses upon Starvation.” *PLOS ONE* 4, no. 5 (May 13, 2009): e5513. doi:10.1371/journal.pone.0005513.

Schmidt, Ingo, Peter J. M. Steenbakkers, Huub J. M. op den Camp, Katrin Schmidt, and Mike S. M. Jetten. “Physiologic and Proteomic Evidence for a Role of Nitric Oxide in Biofilm Formation by Nitrosomonas Europaea and Other Ammonia Oxidizers.” *Journal of Bacteriology* 186, no. 9 (May 2004): 2781–88.

Schrader, M. E. “On Adhesion of Biological Substances to Low Energy Solid Surfaces.” *Journal of Colloid and Interface Science* 88, no. 1 (1982): 296–97.

Schulte, Simone, Jost Wingender, and Hans-Curt Flemming. “Efficacy of Biocides against Biofilms.” In *Directory of Microbicides for the Protection of Materials*, edited by Wilfried Paulus, 93–120. Springer Netherlands, 2004. http://link.springer.com/referenceworkentry/10.1007/1-4020-2818-0_7.

Seiler, Ralph L. "Mobilization of lead and other trace elements following shock chlorination of wells". *Science of the Total Environment* 367, no. 2 (August 31, 2006); 757-768. 10.1016/j.scitotenv.2006.01.020

Shafahi, Maryam, and Kambiz Vafai. “Synthesis of Biofilm Resistance Characteristics against Antibiotics.” *International Journal of Heat and Mass Transfer* 53, no. 15–16 (July 2010): 2943–50. doi:10.1016/j.ijheatmasstransfer.2010.04.004.

Shen, Yun, Guillermo L. Monroy, Nicolas Derlon, Dao Janjaroen, Conghui Huang, Eberhard Morgenroth, Stephen A. Boppart, Nicholas J. Ashbolt, Wen-Tso Liu, and Thanh H. Nguyen. “Role of Biofilm Roughness and Hydrodynamic Conditions in Legionella Pneumophila Adhesion to and Detachment from Simulated Drinking Water Biofilms.” *Environmental Science & Technology* 49, no. 7 (April 7, 2015): 4274–82. doi:10.1021/es505842v.

Sheng, Guo-Ping, Han-Qing Yu, and Xiao-Yan Li. “Extracellular Polymeric Substances (EPS) of Microbial Aggregates in Biological Wastewater Treatment Systems: Review.” *Biotechnology Advances* 28, no. 6 (November 1, 2010): 882–94. doi:10.1016/j.biotechadv.2010.08.001.

Sheng, Xiaoxia, Yen Peng Ting, and Simo Olavi Pehkonen. “The Influence of Ionic Strength, Nutrients and pH on Bacterial Adhesion to Metals.” *Journal of Colloid and Interface Science* 321, no. 2 (May 15, 2008): 256–64. doi:10.1016/j.jcis.2008.02.038.

Shumi, Wahhida, So Hyun Kim, Jeesun Lim, Kyung-Suk Cho, Hwataik Han, and Sungsu Park. “Shear Stress Tolerance of Streptococcus Mutans Aggregates Determined by Microfluidic Funnel Device (μFFD).” *Journal of Microbiological Methods* 93, no. 2 (May 2013): 85–89. doi:10.1016/j.mimet.2013.02.004.

Siebel, E., Y. Wang, T. Egli, and F. Hammes. “Correlations between Total Cell Concentration, Total Adenosine Tri-Phosphate Concentration and Heterotrophic Plate Counts during Microbial Monitoring of Drinking Water.” *Drinking Water Engineering and Science* 1, no. 1 (June 2, 2008): 1–6. doi:10.5194/dwes-1-1-2008.

Silva, Léa Assed Bezerra da, Paulo Nelson-Filho, Gisele Faria, Maria Cristina Monteiro de Souza-Gugelmin, and Izabel Yoko Ito. “Bacterial Profile in Primary Teeth with Necrotic Pulp and Periapical Lesions.” *Brazilian Dental Journal* 17, no. 2 (2006): 144–48.

Simões, Lúcia Chaves, Manuel Simões, and Maria João Vieira. “Biofilm Interactions between Distinct Bacterial Genera Isolated from Drinking Water.” *Applied and Environmental Microbiology* 73, no. 19 (October 2007): 6192–6200. doi:10.1128/AEM.00837-07.

Simões, Manuel, Maria Olivia Pereira, and Maria João Vieira. “Action of a Cationic Surfactant on the Activity and Removal of Bacterial Biofilms Formed under Different Flow Regimes.” *Water Research* 39, no. 2–3 (February 2005): 478–86. doi:10.1016/j.watres.2004.09.018.

———. “Effect of Mechanical Stress on Biofilms Challenged by Different Chemicals.” *Water Research* 39, no. 20 (December 2005): 5142–52. doi:10.1016/j.watres.2005.09.028.

Simões, Manuel, Lúcia C. Simões, and Maria J. Vieira. “A Review of Current and Emergent Biofilm Control Strategies.” *LWT - Food Science and Technology* 43, no. 4 (May 2010): 573–83. doi:10.1016/j.lwt.2009.12.008.

———. “Species Association Increases Biofilm Resistance to Chemical and Mechanical Treatments.” *Water Research* 43, no. 1 (January 2009): 229–37. doi:10.1016/j.watres.2008.10.010.

Singh, Harjinder. “The Milk Fat Globule membrane—A Biophysical System for Food Applications.” *Current Opinion in Colloid & Interface Science* 11, no. 2–3 (June 2006): 154–63. doi:10.1016/j.cocis.2005.11.002.

Skillman, L. C., I. W. Sutherland, and M. V. Jones. “The Role of Exopolysaccharides in Dual Species Biofilm Development.” *Journal of Applied Microbiology* 85 Suppl 1 (December 1998): 13S–18S. doi:10.1111/j.1365-2672.1998.tb05278.x.

Smith, P. K., R. I. Krohn, G. T. Hermanson, A. K. Mallia, F. H. Gartner, M. D. Provenzano, E. K. Fujimoto, N. M. Goeke, B. J. Olson, and D. C. Klenk. “Measurement of Protein Using Bicinchoninic Acid.” *Analytical Biochemistry* 150, no. 1 (October 1985): 76–85.

Sondossi, M., H. W. Rossmoore, and J. W. Wireman. “The Effect of Fifteen Biocides on Formaldehyde-Resistant Strains ofPseudomonas Aeruginosa.” *Journal of Industrial Microbiology* 1, no. 2 (June 1, 1986): 87–96. doi:10.1007/BF01569316.

Srey, Sokunrotanak, Iqbal Kabir Jahid, and Sang-Do Ha. “Biofilm Formation in Food Industries: A Food Safety Concern.” *Food Control* 31, no. 2 (June 2013): 572–85. doi:10.1016/j.foodcont.2012.12.001.

Staal, M., S. M. Borisov, L. F. Rickelt, I. Klimant, and M. Kühl. “Ultrabright Planar Optodes for Luminescence Life-Time Based Microscopic Imaging of O_2 Dynamics in Biofilms.” *Journal of Microbiological Methods* 85, no. 1 (April 2011): 67–74. doi:10.1016/j.mimet.2011.01.021.

Stanczak, M. “Biofouling: It’s Not Just Barnacles Anymore.” ProQuest, 2004. http://www.csa.com/discoveryguides/biofoul/overview.php.
Stewart, P. S. “A Review of Experimental Measurements of Effective Diffusive Permeabilities and Effective Diffusion Coefficients in Biofilms.” *Biotechnology and Bioengineering* 59, no. 3 (August 5, 1998): 261–72.
Stewart, P. S., M. A. Hamilton, B. R. Goldstein, and B. T. Schneider. “Modeling Biocide Action against Biofilms.” *Biotechnology and Bioengineering* 49, no. 4 (February 20, 1996): 445–55. doi:10.1002/(SICI)1097-0290(19960220)49:4<445::AID-BIT12>3.0.CO;2-9.
Stewart, P. S., B. M. Peyton, W. J. Drury, and R. Murga. “Quantitative Observations of Heterogeneities in Pseudomonas Aeruginosa Biofilms.” *Applied and Environmental Microbiology* 59, no. 1 (January 1993): 327–29.
Stewart, P. S., J. Rayner, F. Roe, and W. M. Rees. “Biofilm Penetration and Disinfection Efficacy of Alkaline Hypochlorite and Chlorosulfamates.” *Journal of Applied Microbiology* 91, no. 3 (September 2001): 525–32.
Stoodley, P., R. Cargo, C. J. Rupp, S. Wilson, and I. Klapper. “Biofilm Material Properties as Related to Shear-Induced Deformation and Detachment Phenomena.” *Journal of Industrial Microbiology and Biotechnology* 29, no. 6 (December 1, 2002): 361–67. doi:10.1038/sj.jim.7000282.
Stoodley, P., Z. Lewandowski, J. D. Boyle, and H. M. Lappin-Scott. “Oscillation Characteristics of Biofilm Streamers in Turbulent Flowing Water as Related to Drag and Pressure Drop.” *Biotechnology and Bioengineering* 57, no. 5 (March 5, 1998): 536–44.
Stoodley, P., K. Sauer, D. G. Davies, and J. W. Costerton. “Biofilms as Complex Differentiated Communities.” *Annual Review of Microbiology* 56, no. 1 (2002): 187–209. doi:10.1146/annurev.micro.56.012302.160705.
Stoodley, Paul, John D. Boyle, Dirk DeBeer, and Hilary M. Lappin- Scott. “Evolving Perspectives of Biofilm Structure.” *Biofouling* 14, no. 1 (June 1, 1999): 75–90. doi:10.1080/08927019909378398.
Stoodley, Paul, John D. Boyle, Ian Dodds, and Hilary M. Lappin-Scott. “Consensus Model of Biofilm Structure.” In *Biofilms: Community Interactions and Control: 3rd Meeting of the Biofilm Club*, edited by J. W. T. Wimpenny, P. S. Handley, P. Gilbert, H. M. Lappin-Scott, and M. Jones, 1–9, 1997. http://eprints.soton.ac.uk/157629/.
Stoodley, Paul, Dirk deBeer, and Zbigniew Lewandowski. “Liquid Flow in Biofilm Systems.” *Applied and Environmental Microbiology* 60, no. 8 (August 1994): 2711–16.
Straw, Jessica, and Dan Rittschof. “Responses of Mud Snails from Low and High Imposex Sites to Sex Pheromones.” *Marine Pollution Bulletin* 48, no. 11–12 (June 2004): 1048–54. doi:10.1016/j.marpolbul.2003.12.010.
Strelkauskas, A., J. Strelkauskas, and D. Moszyk-Strelkauskas. *Microbiology: A Clinical Approach*. New York: Garland Science, 2010.
Su, Xinying, Yu Tian, Hui Li, and Cuina Wang. “New Insights into Membrane Fouling Based on Characterization of Cake Sludge and Bulk Sludge: An Especial Attention to Sludge Aggregation.” *Bioresource Technology* 128 (January 2013): 586–92. doi:10.1016/j.biortech.2012.11.005.
Sutherland, Ian W. “Biofilm Exopolysaccharides.” In *Microbial Extracellular Polymeric Substances*, edited by Dr Jost Wingender, Dr Thomas R. Neu, and Prof Dr Hans-Curt Flemming, 73–92. Springer Berlin Heidelberg, 1999. http://link.springer.com/chapter/10.1007/978-3-642-60147-7_4.
Sutherland, I. W. “The Biofilm Matrix--an Immobilized but Dynamic Microbial Environment.” *Trends in Microbiology* 9, no. 5 (May 2001): 222–27.
Tachikawa, Mariko, Kenzo Yamanaka, and Katsuhiko Nakamuro. “Studies on the Disinfection and Removal of Biofilms by Ozone Water Using an Artificial Microbial Biofilm System.”

Ozone: Science & Engineering 31, no. 1 (January 23, 2009): 3–9. doi:10.1080/01919510802586566.
Tadmor, Rafael. "Line Energy and the Relation between Advancing, Receding, and Young Contact Angles." *Langmuir* 20, no. 18 (August 1, 2004): 7659–64. doi:10.1021/la049410h.
Teixeira, P., S. Silva, F. Araújo, J. Azeredo, and R. Oliveira. "Bacterial Adhesion to Food Contacting Surfaces." *Communicating Current Research and Educational Topics and Trends in Applied Microbiology*, 2007.
Telgmann, Ursula, Harald Horn, and Eberhard Morgenroth. "Influence of Growth History on Sloughing and Erosion from Biofilms." *Water Research* 38, no. 17 (October 2004): 3671–84. doi:10.1016/j.watres.2004.05.020.
TenEyck, M. "Great Ships Initiative Bench-Scale Test Findings: Technical Report - Public (NaOH)." Washington DC: Northeast-Midwest Institute, 2009.
Tezel, Ulas, and Spyros G. Pavlostathis. "Role of Quaternary Ammonium Compounds on Antimicrobial Resistance in the Environment." In *Antimicrobial Resistance in the Environment*, edited by Patricia L. Keen and rk H. M. M. Montforts, 349–87. John Wiley & Sons, Inc., 2011. http://onlinelibrary.wiley.com/doi/10.1002/9781118156247.ch20/summary.
Thackery, P. A. "The Cost of Fouling in Heat Exchanger Plant." *Effluent and Water Treatment* 20 (1980): 112–15.
Thomas, Laura. "The Molecular Basis for Preservative Resistance in Burkholderia Cepacia Complex Bacteria." Phd, Cardiff University, 2011. http://orca.cf.ac.uk/14475/.
Thomas, W. M., J. Eccles, and C. Fricker. "Laboratory Observations of Biocide Efficiency against Legionella in Model Cooling Tower Systems." Built Environment Group, West Midlands (GB), July 1, 1999. https://www.osti.gov/scitech/biblio/20085649-laboratory-observations-biocide-efficiency-against-legionella-model-cooling-tower-systems.
Thormann, Esben, Torbjörn Pettersson, John Kettle, and Per M. Claesson. "Probing Material Properties of Polymeric Surface Layers with Tapping Mode AFM: Which Cantilever Spring Constant, Tapping Amplitude and Amplitude Set Point Gives Good Image Contrast and Minimal Surface Damage?" *Ultramicroscopy* 110, no. 4 (March 2010): 313–19. doi:10.1016/j.ultramic.2010.01.002.
Thormann, Kai M., Renée M. Saville, Soni Shukla, and Alfred M. Spormann. "Induction of Rapid Detachment in Shewanella Oneidensis MR-1 Biofilms." *Journal of Bacteriology* 187, no. 3 (February 2005): 1014–21. doi:10.1128/JB.187.3.1014-1021.2005.
Thulukkanam, K. *Heat Exchanger Design Handbook*. 2nd ed. CRC Press, 2013.
Tian, Jia-yu, Zhong-lin Chen, Yan-ling Yang, Heng Liang, Jun Nan, and Gui-bai Li. "Consecutive Chemical Cleaning of Fouled PVC Membrane Using NaOH and Ethanol during Ultrafiltration of River Water." *Water Research* 44, no. 1 (January 2010): 59–68. doi:10.1016/j.watres.2009.08.053.
Timmis, Kenneth N. "Pseudomonas Putida: A Cosmopolitan Opportunist Par Excellence." *Environmental Microbiology* 4, no. 12 (December 1, 2002): 779–81. doi:10.1046/j.1462-2920.2002.00365.x.
Tomás, I., M. C. Cousido, L. García-Caballero, S. Rubido, J. Limeres, and P. Diz. "Substantivity of a Single Chlorhexidine Mouthwash on Salivary Flora: Influence of Intrinsic and Extrinsic Factors." *Journal of Dentistry* 38, no. 7 (July 2010): 541–46. doi:10.1016/j.jdent.2010.03.012.
Torres, Sebastian, Ashok Pandey, and Guillermo R. Castro. "Organic Solvent Adaptation of Gram Positive Bacteria: Applications and Biotechnological Potentials." *Biotechnology Advances* 29, no. 4 (August 2011): 442–52. doi:10.1016/j.biotechadv.2011.04.002.
Trevors, J. T. "Viable but Non-Culturable (VBNC) Bacteria: Gene Expression in Planktonic and Biofilm Cells." *Journal of Microbiological Methods* 86, no. 2 (August 2011): 266–73. doi:10.1016/j.mimet.2011.04.018.

Trivedi, Palak A., Preeti R. Parmar, and Parimal A. Parikh. “Spent FCC Catalyst: Potential Anti-Corrosive and Anti-Biofouling Material.” *Journal of Industrial and Engineering Chemistry* 20, no. 4 (July 25, 2014): 1388–96. doi:10.1016/j.jiec.2013.07.023.

Tsibouklis, J., M. Stone, A. A. Thorpe, P. Graham, V. Peters, R. Heerlien, J. R. Smith, K. L. Green, and T. G. Nevell. “Preventing Bacterial Adhesion onto Surfaces: The Low-Surface-Energy Approach.” *Biomaterials* 20, no. 13 (July 1999): 1229–35.

Tuladhar, T. R., W. R. Paterson, N. Macleod, and D. I. Wilson. “Development of a Novel Non-Contact Proximity Gauge for Thickness Measurement of Soft Deposits and Its Application in Fouling Studies.” *The Canadian Journal of Chemical Engineering* 78, no. 5 (October 1, 2000): 935–47. doi:10.1002/cjce.5450780511.

Tuladhar, T. R., W. R. Paterson, and D. I. Wilson. “Investigation of Alkaline Cleaning-in-Place of Whey Protein Deposits Using Dynamic Gauging.” *Food and Bioproducts Processing* 80, no. 3 (September 1, 2002): 199–214. doi:10.1205/096030802760309223.

Tuladhar, Tri R., William R. Paterson, and D Ian Wilson. “Dynamic Gauging in Duct Flows.” *The Canadian Journal of Chemical Engineering* 81, no. 2 (April 1, 2003): 279–84. doi:10.1002/cjce.5450810214.

Turner, A. M. P., N. Dowell, S. W. P. Turner, L. Kam, M. Isaacson, J. N. Turner, H. G. Craighead, and W. Shain. “Attachment of Astroglial Cells to Microfabricated Pillar Arrays of Different Geometries.” *Journal of Biomedical Materials Research* 51, no. 3 (September 5, 2000): 430–41. doi:10.1002/1097-4636(20000905)51:3<430::AID-JBM18>3.0.CO;2-C.

Väisänen, O. M., E.-L. Nurmiaho-Lassila, S. A. Marmo, and M. S. Salkinoja-Salonen. “Structure and Composition of Biological Slimes on Paper and Board Machines.” *Applied and Environmental Microbiology* 60, no. 2 (February 1, 1994): 641–53.

Van Houdt, Rob, and Chris W. Michiels. “Role of Bacterial Cell Surface Structures in Escherichia Coli Biofilm Formation.” *Research in Microbiology* 156, no. 5–6 (July 2005): 626–33. doi:10.1016/j.resmic.2005.02.005.

Vanysacker, Louise, Bart Boerjan, Priscilla Declerck, and Ivo F. J. Vankelecom. “Biofouling Ecology as a Means to Better Understand Membrane Biofouling.” *Applied Microbiology and Biotechnology*, August 16, 2014. doi:10.1007/s00253-014-5921-2.

Vargas, Ignacio T., Marco A. Alsina, Juan P. Pavissich, Gustavo A. Jeria, Pablo A. Pastén, Magdalena Walczak, and Gonzalo E. Pizarro. “Multi-Technique Approach to Assess the Effects of Microbial Biofilms Involved in Copper Plumbing Corrosion.” *Bioelectrochemistry (Amsterdam, Netherlands)* 97 (June 2014): 15–22. doi:10.1016/j.bioelechem.2013.11.005.

Vázquez-Sánchez, Daniel, Marta López Cabo, Paula Saá Ibusquiza, and Juan José Rodríguez-Herrera. “Biofilm-Forming Ability and Resistance to Industrial Disinfectants of Staphylococcus Aureus Isolated from Fishery Products.” *Food Control* 39 (May 2014): 8–16. doi:10.1016/j.foodcont.2013.09.029.

Veen, Stijn van der, and Tjakko Abee. “Mixed Species Biofilms of Listeria Monocytogenes and Lactobacillus Plantarum Show Enhanced Resistance to Benzalkonium Chloride and Peracetic Acid.” *International Journal of Food Microbiology* 144, no. 3 (January 5, 2011): 421–31. doi:10.1016/j.ijfoodmicro.2010.10.029.

Verran, Joanna, and M. V. Jones. “Problems of Biofilms in the Food and Beverage Industry.” In *Industrial Biofouling*. Wiley, 2000. https://e-space.mmu.ac.uk/71595/.

Videla, Héctor A., and Liz K. Herrera. “Microbiologically Influenced Corrosion: Looking to the Future.” *International Microbiology: The Official Journal of the Spanish Society for Microbiology* 8, no. 3 (September 2005): 169–80.

Vladkova, T. “Surface Engineering for Non-Toxic Biofouling Control.” *Journal of Chemical Technology and Metallurgy* 43 (2007): 239–56.

Volle, C. B., M. A. Ferguson, K. E. Aidala, E. M. Spain, and M. E. Núñez. “Spring Constants and Adhesive Properties of Native Bacterial Biofilm Cells Measured by Atomic Force

Microscopy." *Colloids and Surfaces. B, Biointerfaces* 67, no. 1 (November 15, 2008): 32–40. doi:10.1016/j.colsurfb.2008.07.021.
Vornhagen, Jay, Michael Stevens, David W. McCormick, Scot E. Dowd, Joseph N. S. Eisenberg, Blaise R. Boles, and Alexander H. Rickard. "Coaggregation Occurs amongst Bacteria within and between Biofilms in Domestic Showerheads." *Biofouling* 29, no. 1 (2013): 53–68. doi:10.1080/08927014.2012.744395.
Vrouwenvelder, J. S., C. Hinrichs, W. G. J. Van der Meer, M. C. M. Van Loosdrecht, and J. C. Kruithof. "Pressure Drop Increase by Biofilm Accumulation in Spiral Wound RO and NF Membrane Systems: Role of Substrate Concentration, Flow Velocity, Substrate Load and Flow Direction." *Biofouling* 25, no. 6 (2009): 543–55. doi:10.1080/08927010902972225.
Vrouwenvelder, J. S., C. Picioreanu, J. C. Kruithof, and M. C. M. van Loosdrecht. "Biofouling in Spiral Wound Membrane Systems: Three-Dimensional CFD Model Based Evaluation of Experimental Data." *Journal of Membrane Science* 346, no. 1 (January 1, 2010): 71–85. doi:10.1016/j.memsci.2009.09.025.
Wagner, Michael, Natalia P. Ivleva, Christoph Haisch, Reinhard Niessner, and Harald Horn. "Combined Use of Confocal Laser Scanning Microscopy (CLSM) and Raman Microscopy (RM): Investigations on EPS – Matrix." *Water Research* 43, no. 1 (January 2009): 63–76. doi:10.1016/j.watres.2008.10.034.
Waines, Paul L., Roy Moate, A. John Moody, Mike Allen, and Graham Bradley. "The Effect of Material Choice on Biofilm Formation in a Model Warm Water Distribution System." *Biofouling* 27, no. 10 (November 2011): 1161–74. doi:10.1080/08927014.2011.636807.
Walboomers, X. F., W. Monaghan, A. S. G. Curtis, and J. A. Jansen. "Attachment of Fibroblasts on Smooth and Microgrooved Polystyrene." *Journal of Biomedical Materials Research* 46, no. 2 (August 1, 1999): 212–20. doi:10.1002/(SICI)1097-4636(199908)46:2<212::AID-JBM10>3.0.CO;2-Y.
Walker, Sharon L. "The Role of Nutrient Presence on the Adhesion Kinetics of Burkholderia Cepacia G4g and ENV435g." *Colloids and Surfaces. B, Biointerfaces* 45, no. 3–4 (November 10, 2005): 181–88. doi:10.1016/j.colsurfb.2005.08.007.
Wallhäußer, E., M. A. Hussein, and T. Becker. "Detection Methods of Fouling in Heat Exchangers in the Food Industry." *Food Control* 27, no. 1 (September 2012): 1–10. doi:10.1016/j.foodcont.2012.02.033.
Walter, Maik, Ashkan Safari, Alojz Ivankovic, and Eoin Casey. "Detachment Characteristics of a Mixed Culture Biofilm Using Particle Size Analysis." *Chemical Engineering Journal* 228 (July 15, 2013): 1140–47. doi:10.1016/j.cej.2013.05.071.
Wang, Hsin-Neng, Andrew M. Fales, Aimee K. Zaas, Christopher W. Woods, Thomas Burke, Geoffrey S. Ginsburg, and Tuan Vo-Dinh. "Surface-Enhanced Raman Scattering Molecular Sentinel Nanoprobes for Viral Infection Diagnostics." *Analytica Chimica Acta* 786 (July 5, 2013): 153–58. doi:10.1016/j.aca.2013.05.017.
Wang, Huhu, Shijie Ding, Guangyu Wang, Xinglian Xu, and Guanghong Zhou. "In Situ Characterization and Analysis of Salmonella Biofilm Formation under Meat Processing Environments Using a Combined Microscopic and Spectroscopic Approach." *International Journal of Food Microbiology* 167, no. 3 (November 1, 2013): 293–302. doi:10.1016/j.ijfoodmicro.2013.10.005.
Wang, Sung-Ning, Michael D. Graham, Friedemann J. Hahn, and Li Xi. "Time-Series and Extended Karhunen–Loève Analysis of Turbulent Drag Reduction in Polymer Solutions." *AIChE Journal* 60, no. 4 (April 1, 2014): 1460–75. doi:10.1002/aic.14328.
Wäsche, Stefan, Harald Horn, and Dietmar C Hempel. "Influence of Growth Conditions on Biofilm Development and Mass Transfer at the Bulk/biofilm Interface." *Water Research* 36, no. 19 (November 2002): 4775–84. doi:10.1016/S0043-1354(02)00215-4.

Webb, Jeremy S., Michael Givskov, and Staffan Kjelleberg. “Bacterial Biofilms: Prokaryotic Adventures in Multicellularity.” *Current Opinion in Microbiology* 6, no. 6 (December 2003): 578–85.

Webb, Jeremy S., Lyndal S. Thompson, Sally James, Tim Charlton, Tim Tolker-Nielsen, Birgit Koch, Michael Givskov, and Staffan Kjelleberg. “Cell Death in Pseudomonas Aeruginosa Biofilm Development.” *Journal of Bacteriology* 185, no. 15 (August 2003): 4585–92.

Westgate, S. J., S. L. Percival, D. C. Knottenbelt, P. D. Clegg, and C. A. Cochrane. “Microbiology of Equine Wounds and Evidence of Bacterial Biofilms.” *Veterinary Microbiology* 150, no. 1–2 (May 12, 2011): 152–59. doi:10.1016/j.vetmic.2011.01.003.

White, David G, and Patrick F McDermott. “Biocides, Drug Resistance and Microbial Evolution.” *Current Opinion in Microbiology* 4, no. 3 (June 1, 2001): 313–17. doi:10.1016/S1369-5274(00)00209-5.

Whitehead, K. A., and J. Verran. “The Effect of Surface Topography on the Retention of Microorganisms.” *Food and Bioproducts Processing* 84, no. 4 (December 1, 2006): 253–59. doi:10.1205/fbp06035.

Wijman, Janneke G. E., Patrick P. L. A. de Leeuw, Roy Moezelaar, Marcel H. Zwietering, and Tjakko Abee. “Air-Liquid Interface Biofilms of Bacillus Cereus: Formation, Sporulation, and Dispersion.” *Applied and Environmental Microbiology* 73, no. 5 (March 2007): 1481–88. doi:10.1128/AEM.01781-06.

Wilkinson, M. H. F., and F. Schut. *Digital Image Analysis of Microbes: Imaging, Morphometry, Fluorometry and Motility Techniques and Applications*. John Wiley & Sons, 1998.

Williams, Margaret M., Jorge W. Santo Domingo, and Mark C. Meckes. “Population Diversity in Model Potable Water Biofilms Receiving Chlorine or Chloramine Residual.” *Biofouling* 21, no. 5–6 (January 1, 2005): 279–88. doi:10.1080/08927010500452695.

Wilson, D. I. “Challenges in Cleaning: Recent Developments and Future Prospects.” *Heat Transfer Engineering* 26, no. 1 (January 1, 2005): 51–59. doi:10.1080/01457630590890175.

Wingender, Jost, and Hans-Curt Flemming. “Biofilms in Drinking Water and Their Role as Reservoir for Pathogens.” *International Journal of Hygiene and Environmental Health* 214, no. 6 (November 2011): 417–23. doi:10.1016/j.ijheh.2011.05.009.

Wingender, Jost, Thomas R. Neu, and Hans-Curt Flemming. “What Are Bacterial Extracellular Polymeric Substances?” In *Microbial Extracellular Polymeric Substances*, edited by Dr Jost Wingender, Dr Thomas R. Neu, and Prof Dr Hans-Curt Flemming, 1–19. Springer Berlin Heidelberg, 1999. http://link.springer.com/chapter/10.1007/978-3-642-60147-7_1.

Withers, Peter M. “Ultrasonic, Acoustic and Optical Techniques for the Non-Invasive Detection of Fouling in Food Processing Equipment.” *Trends in Food Science & Technology* 7, no. 9 (September 1, 1996): 293–98. doi:10.1016/0924-2244(96)10031-5.

Wong, H. S., K. M. Townsend, S. G. Fenwick, R. D. Trengove, and R. M. O’Handley. “Comparative Susceptibility of Planktonic and 3-Day-Old Salmonella Typhimurium Biofilms to Disinfectants.” *Journal of Applied Microbiology* 108, no. 6 (June 2010): 2222–28. doi:10.1111/j.1365-2672.2009.04630.x.

Wood, S. R., J. Kirkham, P. D. Marsh, R. C. Shore, B. Nattress, and C. Robinson. “Architecture of Intact Natural Human Plaque Biofilms Studied by Confocal Laser Scanning Microscopy.” *Journal of Dental Research* 79, no. 1 (January 2000): 21–27.

Wu, Wei, Sébastien Wieckowski, Giorgia Pastorin, Monica Benincasa, Cédric Klumpp, Jean-Paul Briand, Renato Gennaro, Maurizio Prato, and Alberto Bianco. “Targeted Delivery of Amphotericin B to Cells by Using Functionalized Carbon Nanotubes.” *Angewandte Chemie (International Ed. in English)* 44, no. 39 (October 7, 2005): 6358–62. doi:10.1002/anie.200501613.

Wu, Yong, Joseph P. Zitelli, Kevor S. TenHuisen, Xiaojun Yu, and Matthew R. Libera. “Differential Response of Staphylococci and Osteoblasts to Varying Titanium Surface

Roughness." *Biomaterials* 32, no. 4 (February 2011): 951–60. doi:10.1016/j.biomaterials.2010.10.001.
Wu, Yonghong, Jiangzhou He, and Linzhang Yang. "Evaluating Adsorption and Biodegradation Mechanisms during the Removal of Microcystin-RR by Periphyton." *Environmental Science & Technology* 44, no. 16 (August 15, 2010): 6319–24. doi:10.1021/es903761y.
Xavier, Joao B., Cristian Picioreanu, Suriani Abdul Rani, Mark C. M. van Loosdrecht, and Philip S. Stewart. "Biofilm-Control Strategies Based on Enzymic Disruption of the Extracellular Polymeric Substance Matrix--a Modelling Study." *Microbiology (Reading, England)* 151, no. Pt 12 (December 2005): 3817–32. doi:10.1099/mic.0.28165-0.
Xu, Li-Chong, and Christopher A. Siedlecki. "Submicron-Textured Biomaterial Surface Reduces Staphylococcal Bacterial Adhesion and Biofilm Formation." *Acta Biomaterialia* 8, no. 1 (January 2012): 72–81. doi:10.1016/j.actbio.2011.08.009.
Xue, Runmiao, Honglan Shi, Yinfa Ma, John Yang, Bin Hua, Enos C. Inniss, Craig D. Adams, Todd Eichholz. "Evaluation of thirteen haloacetic acids and ten trihalomethanes formation by peracetic acid and chlorine drinking water disinfection". *Chemosphere*. (2017). 10.1016/j.chemosphere.2017.09.059
Xue, Zheng, Varun Raj Sendamangalam, Cyndee L. Gruden, and Youngwoo Seo. "Multiple Roles of Extracellular Polymeric Substances on Resistance of Biofilm and Detached Clusters." *Environmental Science & Technology* 46, no. 24 (December 18, 2012): 13212–19. doi:10.1021/es3031165.
Yabune, Toshiaki, Satoshi Imazato, and Shigeyuki Ebisu. "Inhibitory Effect of PVDF Tubes on Biofilm Formation in Dental Unit Waterlines." *Dental Materials: Official Publication of the Academy of Dental Materials* 21, no. 8 (August 2005): 780–86. doi:10.1016/j.dental.2005.01.016.
Yang, Li-Hua, Guang-Guo Ying, Hao-Chang Su, Jennifer L. Stauber, Merrin S. Adams, and Monique T. Binet. "Growth-Inhibiting Effects of 12 Antibacterial Agents and Their Mixtures on the Freshwater Microalga Pseudokirchneriella Subcapitata." *Environmental Toxicology and Chemistry* 27, no. 5 (May 2008): 1201–8. doi:10.1897/07-471.1.
Yang, Qianpeng, Akin Ali, Lin Shi, and D. Ian Wilson. "Zero Discharge Fluid Dynamic Gauging for Studying the Thickness of Soft Solid Layers." *Journal of Food Engineering* 127 (April 2014): 24–33. doi:10.1016/j.jfoodeng.2013.11.024.
Ye, Fenxia, Yangfang Ye, and Ying Li. "Effect of C/N Ratio on Extracellular Polymeric Substances (EPS) and Physicochemical Properties of Activated Sludge Flocs." *Journal of Hazardous Materials* 188, no. 1–3 (April 15, 2011): 37–43. doi:10.1016/j.jhazmat.2011.01.043.
Yebra, Diego Meseguer, Søren Kiil, Claus E. Weinell, and Kim Dam-Johansen. "Presence and Effects of Marine Microbial Biofilms on Biocide-Based Antifouling Paints." *Biofouling* 22, no. 1–2 (2006): 33–41. doi:10.1080/08927010500519097.
Ying, Guang-Guo, and Rai S. Kookana. "Triclosan in Wastewaters and Biosolids from Australian Wastewater Treatment Plants." *Environment International* 33, no. 2 (February 2007): 199–205. doi:10.1016/j.envint.2006.09.008.
Yung, Lin-Yue L., Robert W. Colman, and Stuart L. Cooper. "Neutrophil Adhesion on Polyurethanes Preadsorbed With High Molecular Weight Kininogen." *Blood* 94, no. 8 (October 15, 1999): 2716–24.
Zameer, Farhan, Shubha Gopal, Georg Krohne, and Jürgen Kreft. "Development of a Biofilm Model for Listeria Monocytogenes EGD-E." *World Journal of Microbiology and Biotechnology* 26, no. 6 (June 1, 2010): 1143–47. doi:10.1007/s11274-009-0271-4.
Záray, Gyula, Krisztina Kröpfl, Katalin Szabó, Györgyi Taba, Éva Ács, Balázs Berlinger, Mehmet Dogan, Bekir Salih, and Aydin Akbulut. "Comparison of Freshwater Biofilms Grown on Polycarbonate Substrata in Lake Velence (Hungary) and Lake Mogan (Turkey)."

Microchemical Journal, XI Italian Hungarian Symposium on Spectrochemistry, 79, no. 1–2 (January 2005): 145–48. doi:10.1016/j.microc.2004.08.012.
Zelver, N. "Biofilm Development and Associated Energy Losses in Water Conduits." M.S., Rice University, 1979.
Zhang, Peng, Fang Fang, You-Peng Chen, Yu Shen, Wei Zhang, Ji-Xiang Yang, Chun Li, et al., "Composition of EPS Fractions from Suspended Sludge and Biofilm and Their Roles in Microbial Cell Aggregation." *Chemosphere* 117 (December 2014): 59–65. doi:10.1016/j.chemosphere.2014.05.070.
Zhang, Ruiyong, Sören Bellenberg, Laura Castro, Thomas R. Neu, Wolfgang Sand, and Mario Vera. "Colonization and Biofilm Formation of the Extremely Acidophilic Archaeon Ferroplasma Acidiphilum." *Hydrometallurgy* 150 (July 1, 2014). doi:10.1016/j.hydromet.2014.07.001.
Zhang, T. C., and P. L. Bishop. "Experimental Determination of the Dissolved Oxygen Boundary Layer and Mass Transfer Resistance near the Fluid-Biofilm Interface." *Water Science and Technology* 30, no. 11 (1994): 47–58.
Zhang, Tian C., and Paul L. Bishop. "Density, Porosity, and Pore Structure of Biofilms." *Water Research* 28, no. 11 (November 1, 1994): 2267–77. doi:10.1016/0043-1354(94)90042-6.
Zhang, Wei, Tadas Sileika, and Aaron I. Packman. "Effects of Fluid Flow Conditions on Interactions between Species in Biofilms." *FEMS Microbiology Ecology* 84, no. 2 (May 2013): 344–54. doi:10.1111/1574-6941.12066.
Zhao, Q., Y. Liu, C. Wang, S. Wang, and H. Müller-Steinhagen. "Effect of Surface Free Energy on the Adhesion of Biofouling and Crystalline Fouling." *Chemical Engineering Science* 60, no. 17 (September 2005): 4858–65. doi:10.1016/j.ces.2005.04.006.
Zisman, W. A. "Relation of the Equilibrium Contact Angle to Liquid and Solid Constitution." In *Contact Angle, Wettability, and Adhesion*, 43:1–51. Advances in Chemistry 43. American Chemical Society, 1964. http://dx.doi.org/10.1021/ba-1964-0043.ch001.
Zobell, Claude E. "The Effect of Solid Surfaces upon Bacterial Activity." *Journal of Bacteriology* 46, no. 1 (July 1943): 39–56.
Zwietering, M. H., I. Jongenburger, F. M. Rombouts, and K. van 't Riet. "Modeling of the Bacterial Growth Curve." *Applied and Environmental Microbiology* 56, no. 6 (June 1990): 1875–81.

APPENDIX

1. Ionic Strength

The ionic strength, *I*, is calculated via the following equation:

$$I = \frac{1}{2}\sum_i c_i z_i^2 \quad (26)$$

where *i* is each chemical species in series, and *c* and *z* are the concentration and charge of the species respectively. Casein hydrolysate and glucose are non-ionic and so do not need to be considered. As an example, for $Na_2HPO_4.7H_2O$, the ions present are $2Na^+$ and HPO_4^{2-} with a molarity of 47.7mM. Equation 26 is completed thus:

$I = 0.5*[(2*0.047*1^2) + (0.047*2^2)] = 0.5*[0.094+0.188] = 0.5*0.282 = 0.141M$

Table 12: The components present in the M9 media used to grow biofilms throughout this research, and the ionic strengths of each component.

Media Component	**Ions Present**	**Ionic Strength**
47.7 mM $Na_2HPO_4.7H_2O$	$2Na^+$ HPO_4^{2-}	0.141
21.7 mM KH_2PO_4	K^+ $H_2PO_4^-$	0.0217
8.6 mM NaCl	Na^+ Cl^-	0.0086
18.7 mM NH_4Cl	NH_4^+ Cl^-	0.0187
1 mM $MgSO_4$	Mg^{2+} SO_4^{2-}	0.004

This adds up to a total ionic strength of 0.194M. If an equivalent solution of sodium chloride is to made up for the gauging experiments, this is then multiplied by the combined molar mass of Na and Cl (equal to 58.44) to give a concentration of 11.34 gL^{-1}.

2. Siphon Tube Effective Length

As described in Section 2.9.1, the pressure drop along the siphon tube (ΔP_{34}) can be calculated using the Hagen-Poiseulle equation (27) if the value of L_{eff}, the effective length of the tube, is known. This value converts the presence of bends in a pipe into an equivalent extension of the straight tube resulting in the same pressure drop. The effective length was determined experimentally by removing the nozzle to reduce ΔP_{13} to a negligible value. After set-up, the tube-surface clearance (h) was set and the hydrostatic head (H) was altered in steps by changing the height of the output tap. This ensures that the effective length is the remaining unknown variable impacting upon the flow rate. The upright tube section above the nozzle has a known length (0.4 m), so the pressure drop in this section can be calculated normally. The remaining loss in pressure can be attributed to the attached pipe, the length of which must be determined by this experimental method.

$$\Delta P_{13} = \rho g H - \frac{128 \mu_f . m . L_{eff}}{\rho_f \pi d_{tube}^4} \quad (27)$$

The point of outlet was the operational variable, which has the effect of altering the hydrostatic head (H). With ΔP_{13} effectively negligible, the pressure drop is simply equal to ΔP_{34}. The loss due to the known section of tubing can be subtracted from ρgH (the total pressure drop) to give the values plotted below in Figure 131 against the recorded mass flow rate.

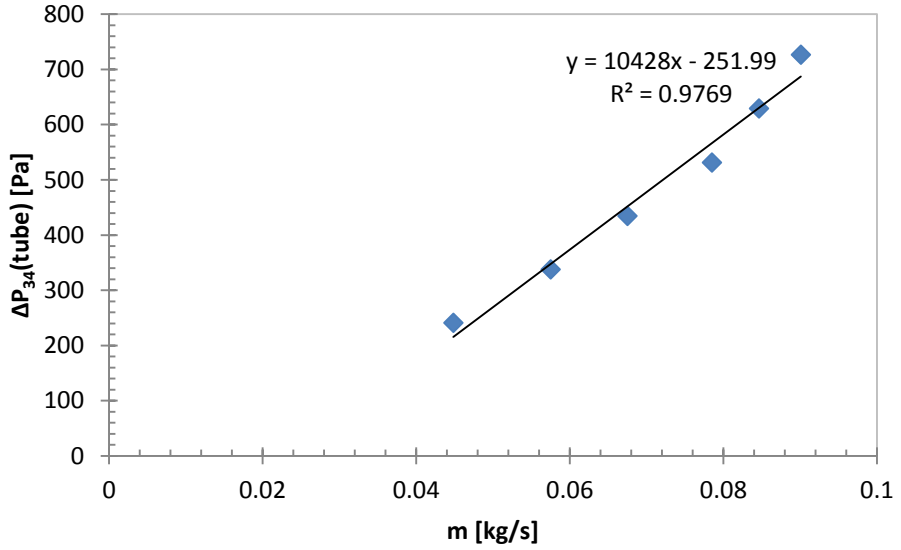

Figure 133: The result from the experiment undertaken to determine the effective length of the curved siphon tube. The mass flow rate is controlled via the hydrostatic head, and the pressure drop displayed is that for the unknown section of tubing. The equation of the trend line is included to show the gradient of the line.

The important value to be taken from Figure 131 is the gradient of the trend line. The Hagen-Poiseulle equation can be re-arranged into the following form by dividing both terms by *m*:

$$\frac{\Delta P_{34}}{m} = \frac{128 \mu_f . L_{eff}}{\rho_f \pi d_{tube}^4} \quad (28)$$

Substituting the gradient of 10428 into the equation for the left hand term and inputting the remaining constants leaves L_{eff} as the only unresolved variable. The effective length was therefore calculated to be 5.3m. This result was used to calculate the C_d values in the subsequent calibration plots.

3. Biofilm Assay: Strain Comparison – Absorbance Values

Table 13: The full set of absorbances, including control values, taken from the biofilm assay conducted in order to compare the species *Escherichia coli* Nissle1917, *Pseudomonas aeruginosa* NCTC and *P. aeruginosa* PA01

	Test Values					Control-Adjusted		
	E.coli	PA NCTC	PA01	Control		E.coli	PA NCTC	PA01
	0.4527	0.2111	0.1541	0.1209		0.3289	0.0873	0.0303
	0.5246	0.2019	0.1623	0.1215		0.4008	0.0781	0.0385
	0.5282	0.1776	0.1886	0.129		0.4044	0.0538	0.0648
	0.5685	0.226	0.1786			0.4447	0.1022	0.0548
Mean	0.519	0.204	0.171	0.124		**0.395**	**0.080**	**0.047**
S.D.	0.048	0.020	0.016	0.005		**0.048**	**0.020**	**0.016**

4. Surface Energy

Polyethylene

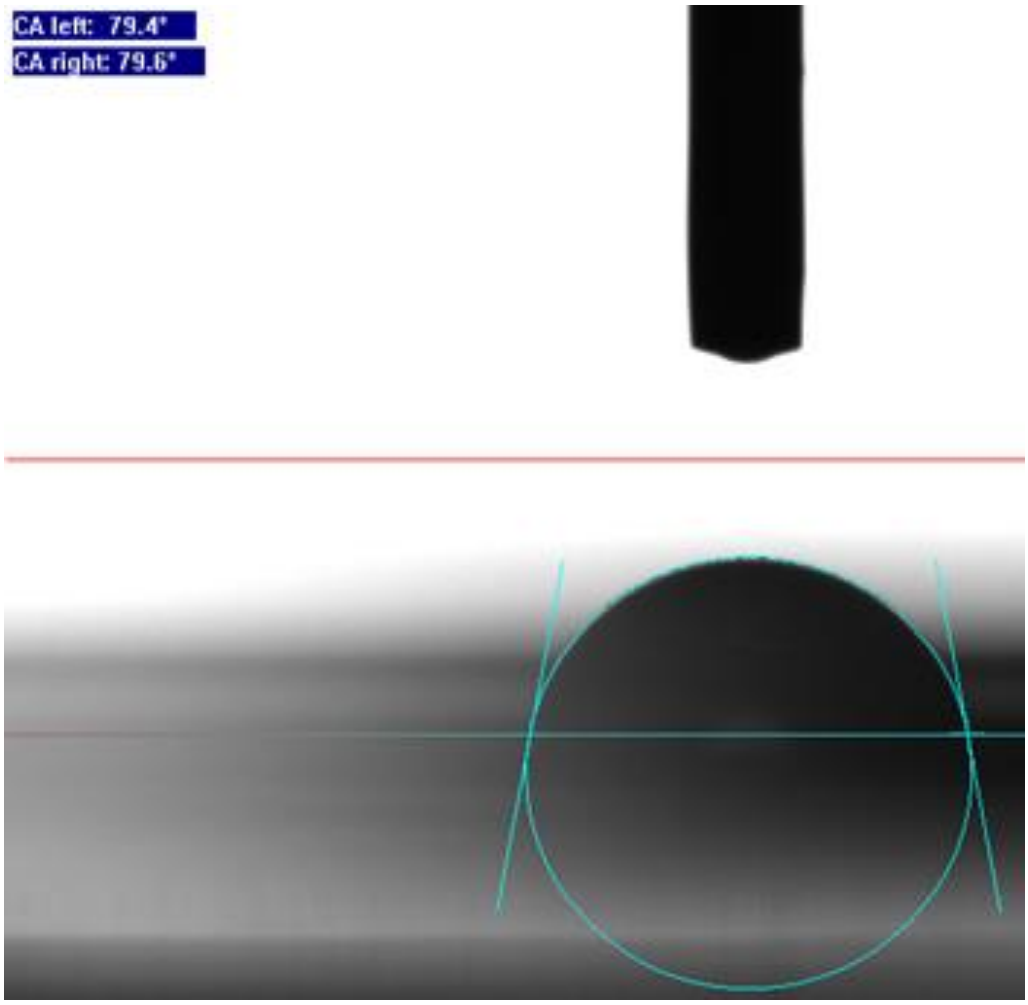

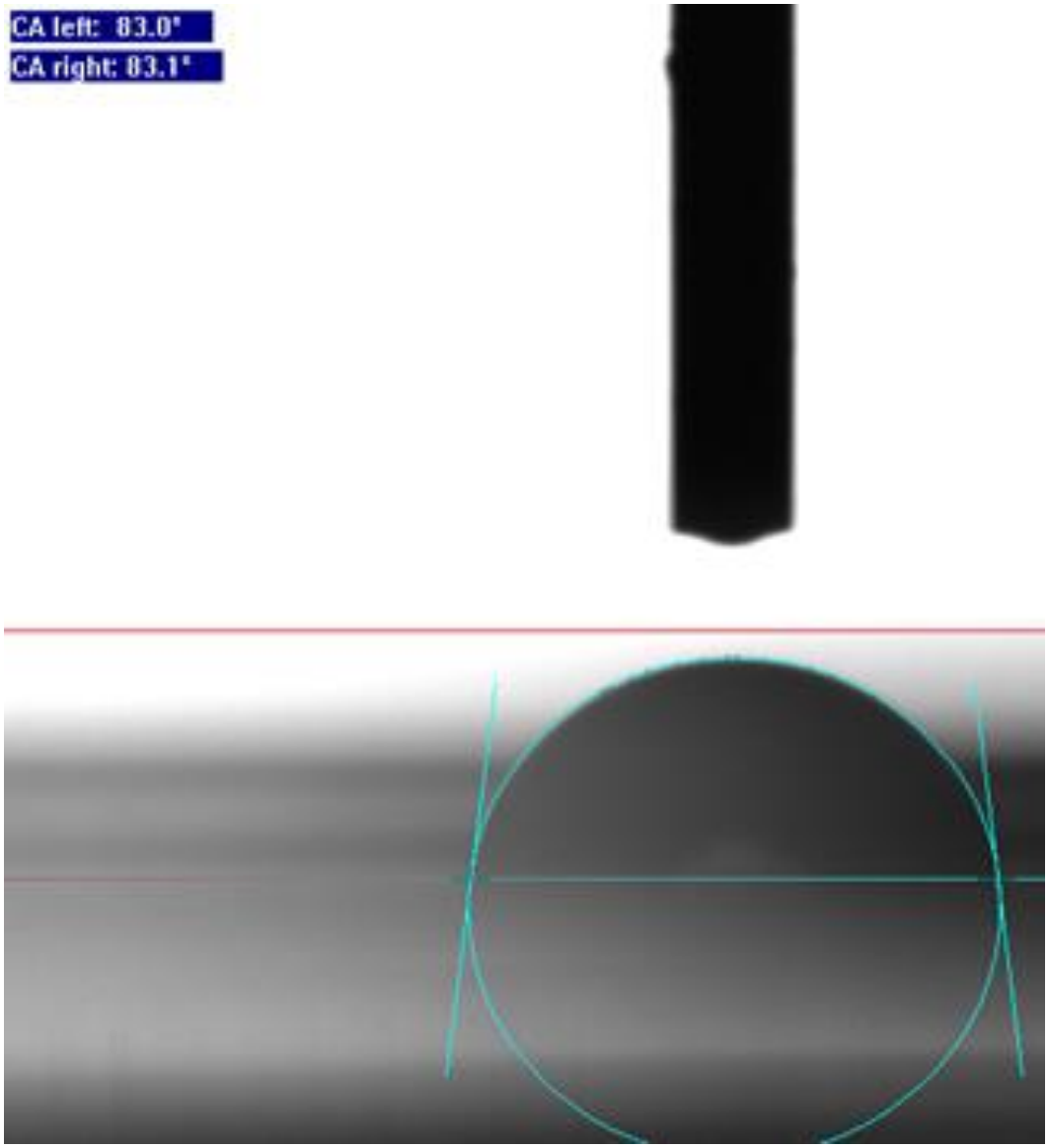
CA left: 83.0°
CA right: 83.1°

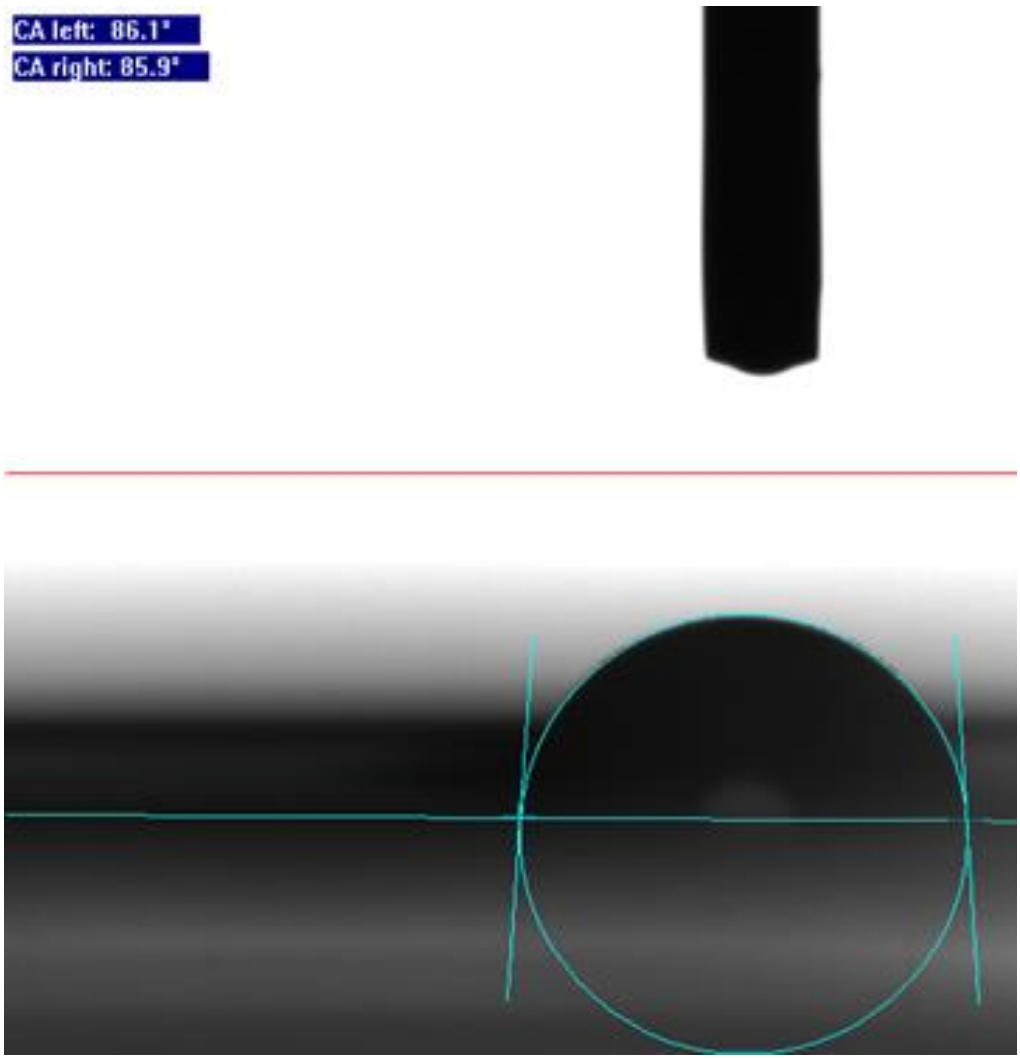
CA left: 86.1°
CA right: 85.9°

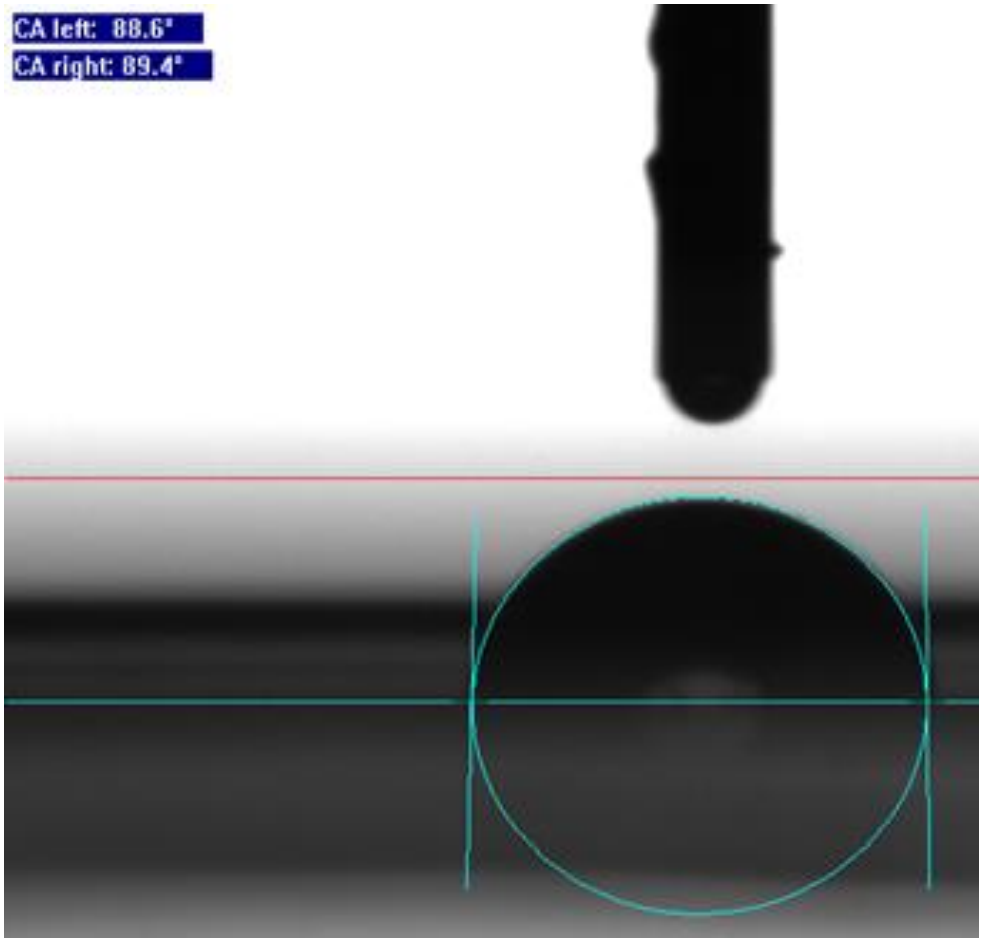

Figure 134: The full set of contact angle measurements on polyethylene in order to determine the critical surface energy. From top to bottom: water, 5%, 10% and 15% sodium chloride

Stainless Steel Disc

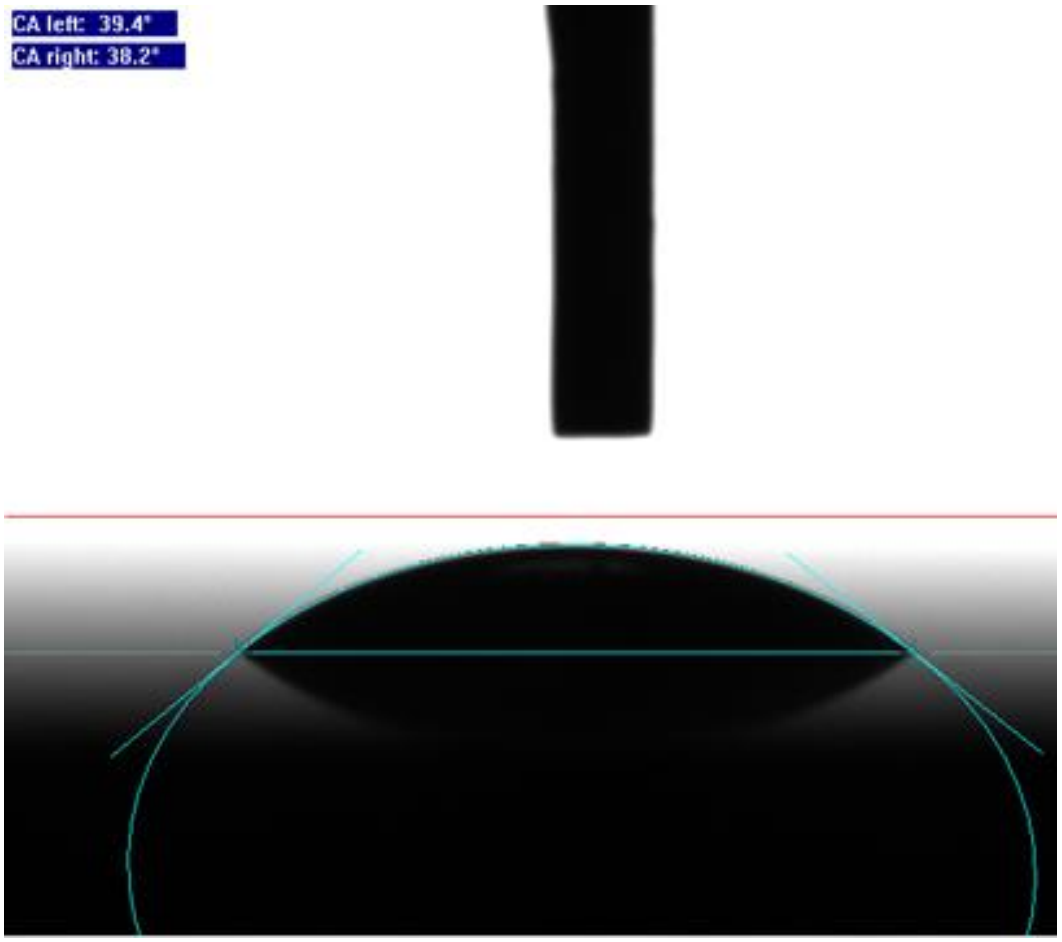

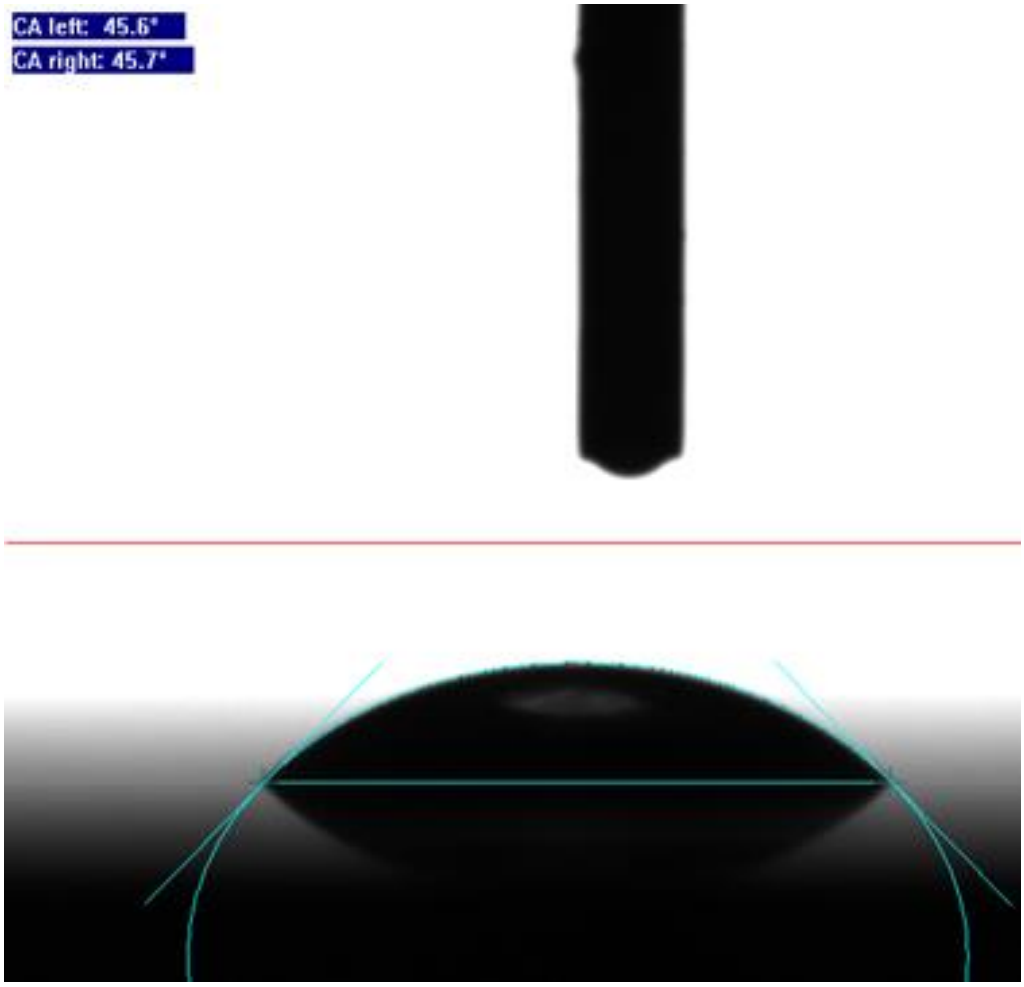
CA left: 45.6°
CA right: 45.7°

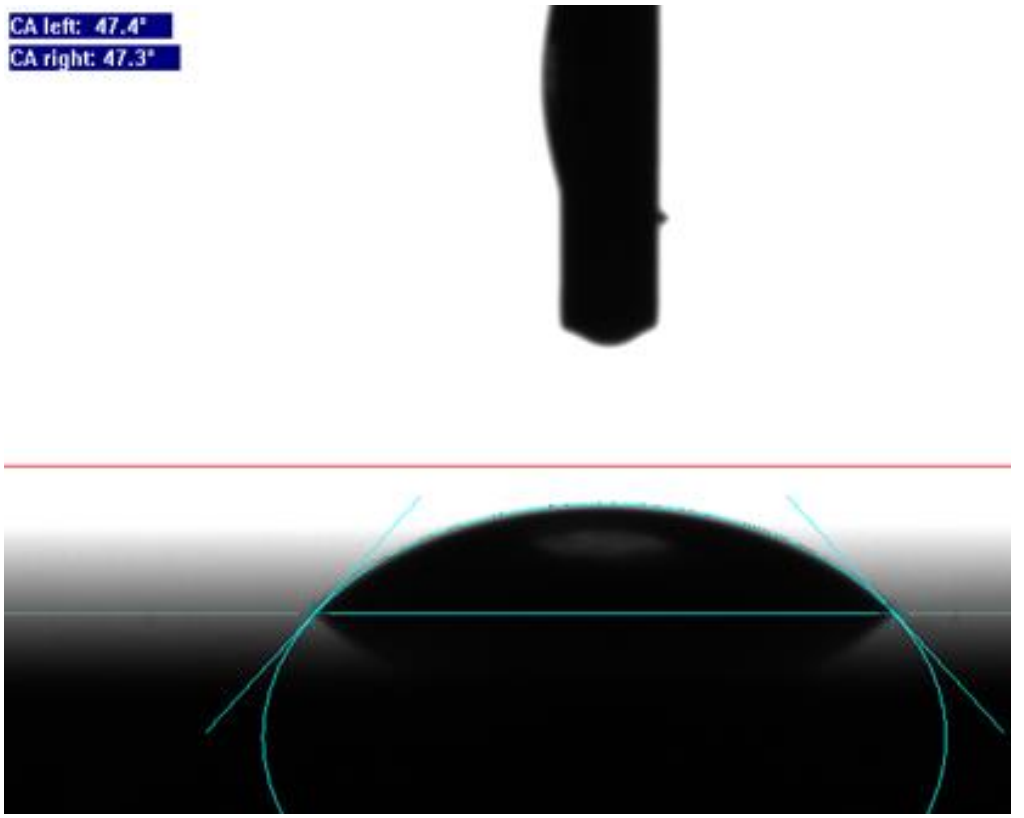
CA left: 47.4°
CA right: 47.3°

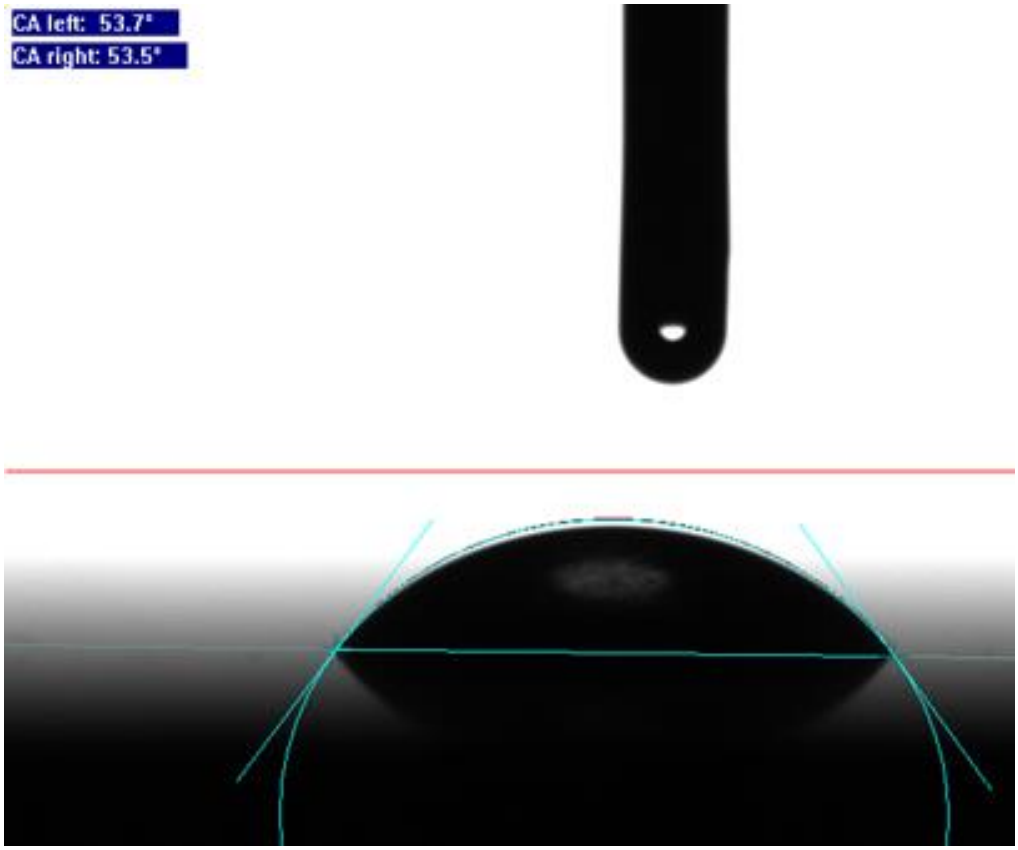

Figure 135: The full set of contact angle measurements on the stainless steel disc in order to determine the critical surface energy. From top to bottom: water, 5%, 10% and 15% sodium chloride

Stainless Steel Plate

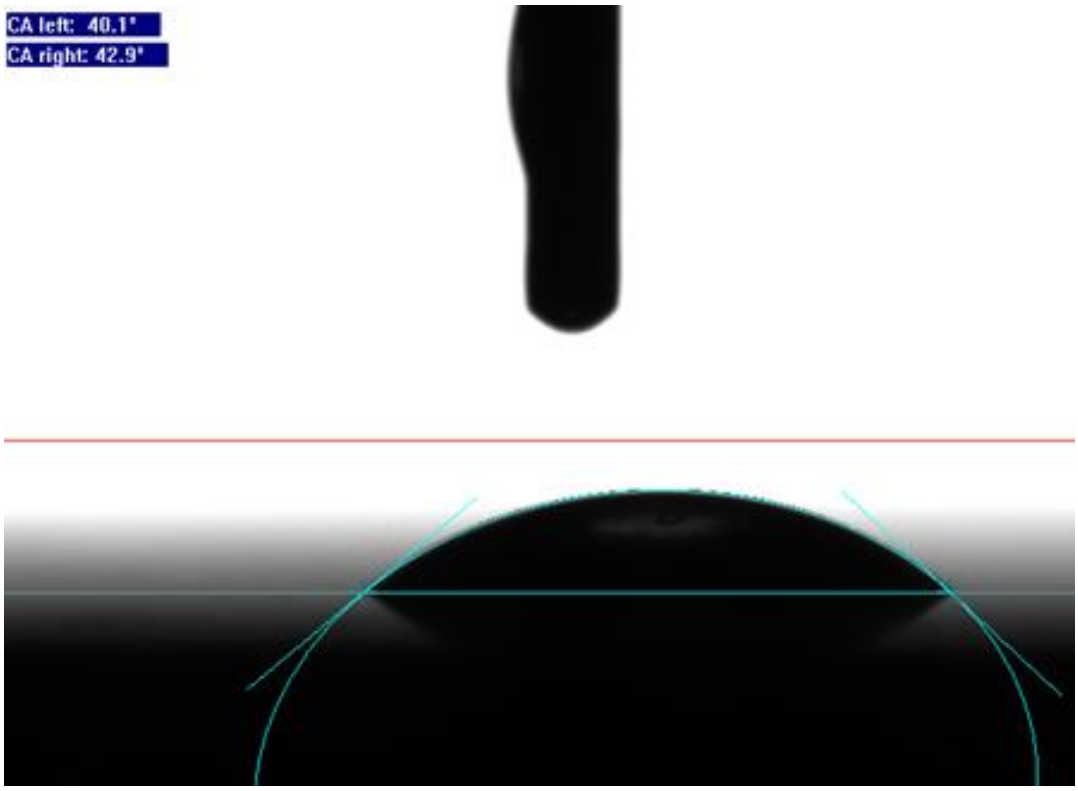

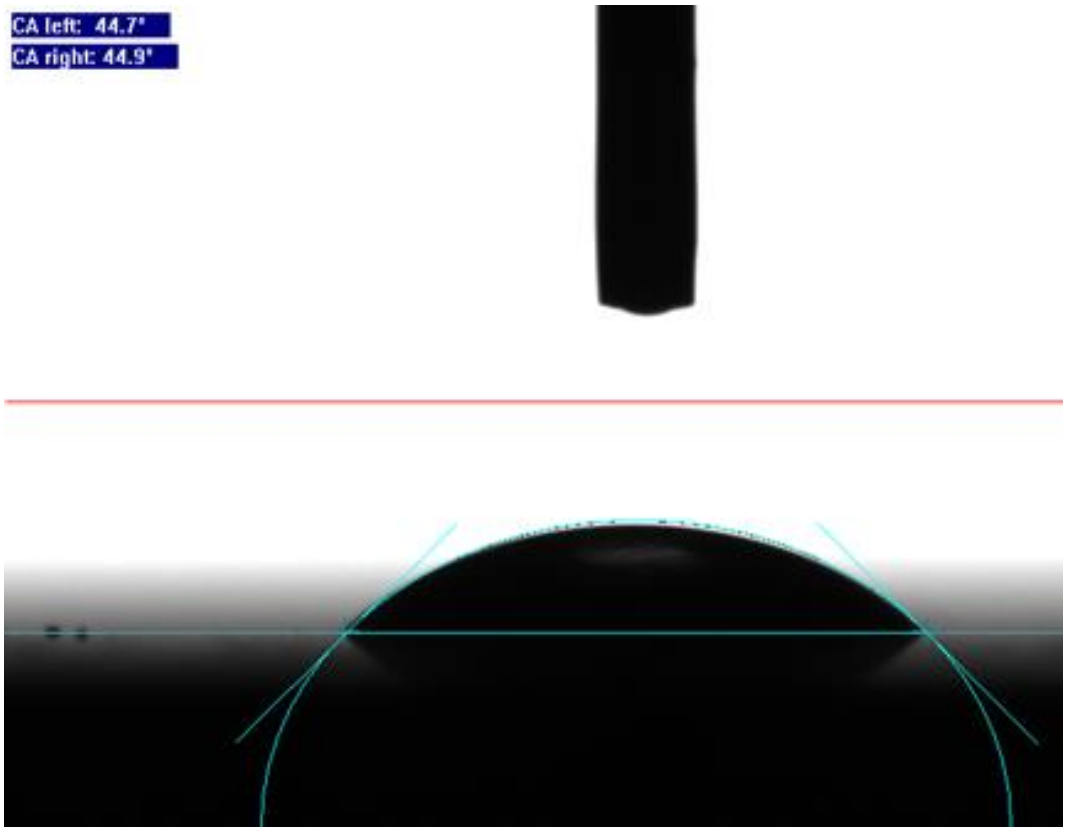

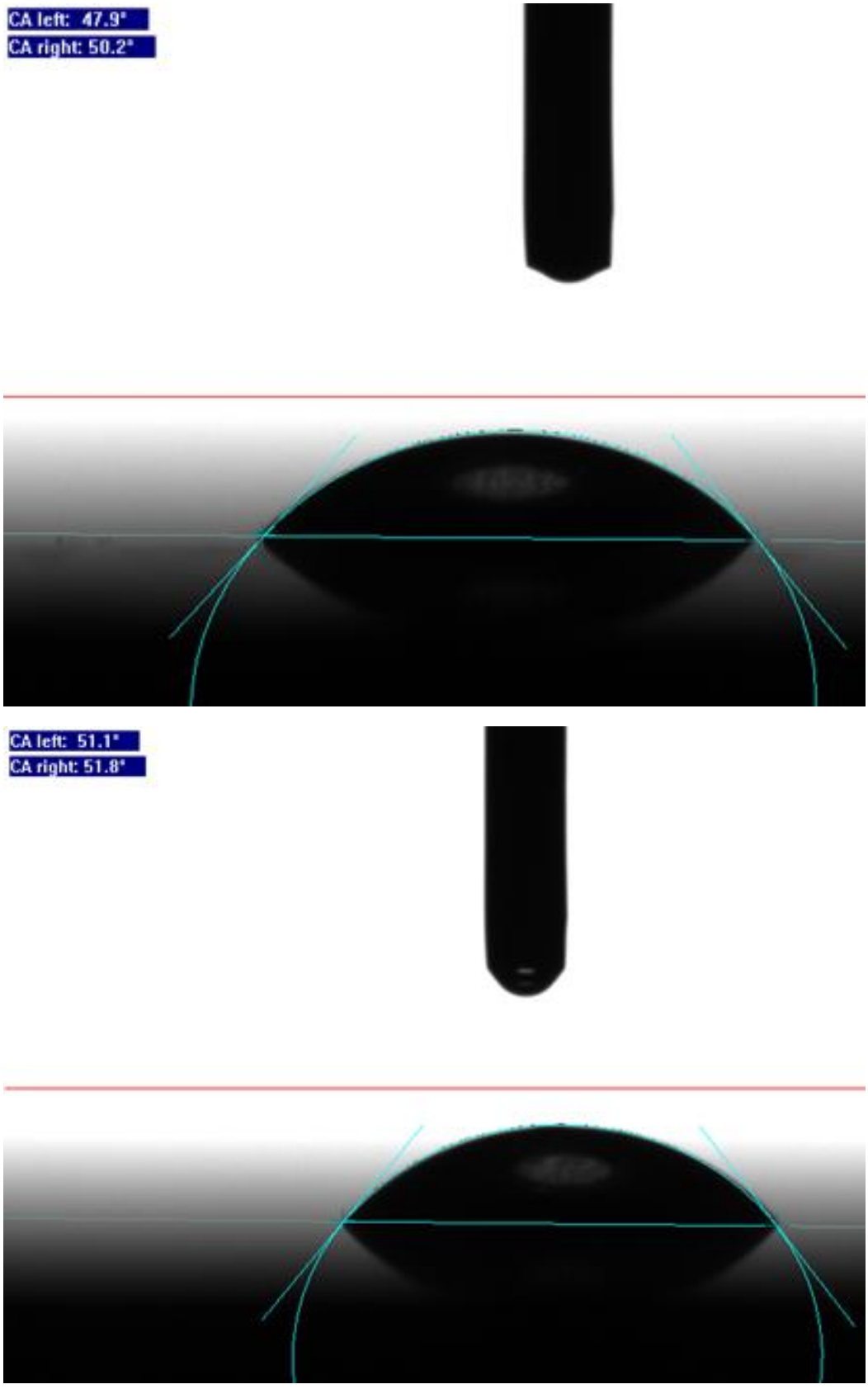

Figure 136: The full set of contact angle measurements on the stainless steel plate in order to determine the critical surface energy. From top to bottom: water, 5%, 10% and 15% sodium chloride

Glass Petri Dish

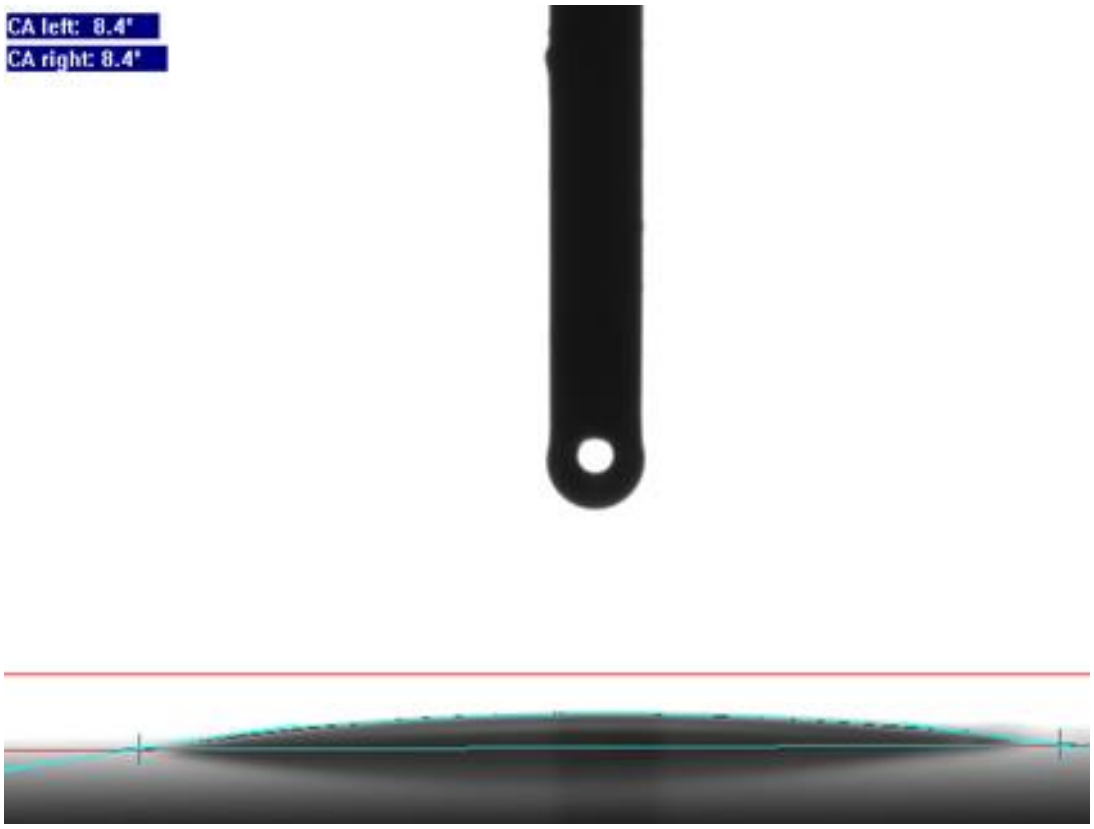

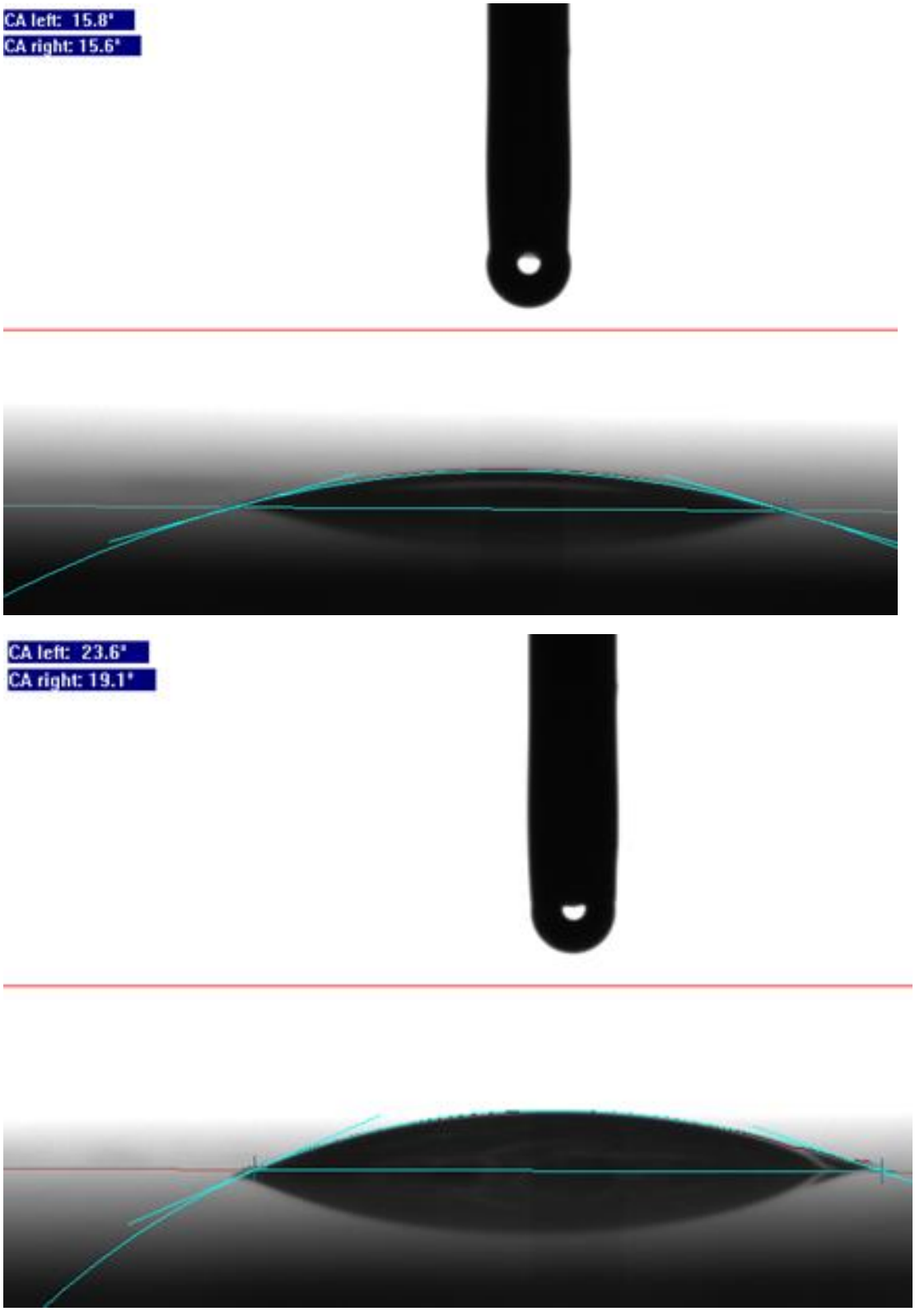

Figure 137: The full set of contact angle measurements on the glass petri dish in order to determine the critical surface energy. From top to bottom: water, 5%, 10% and 15% sodium chloride

Glass Coverslip

CA left: 33.5°
CA right: 33.9°

CA left: 34.1°
CA right: 39.1°

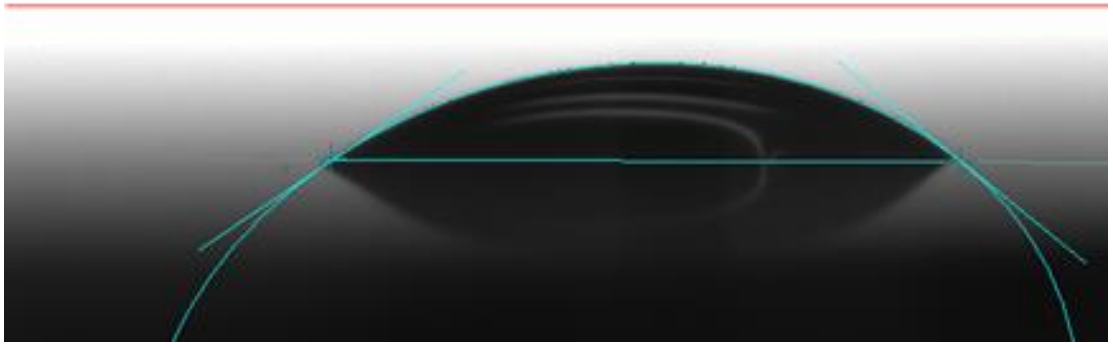

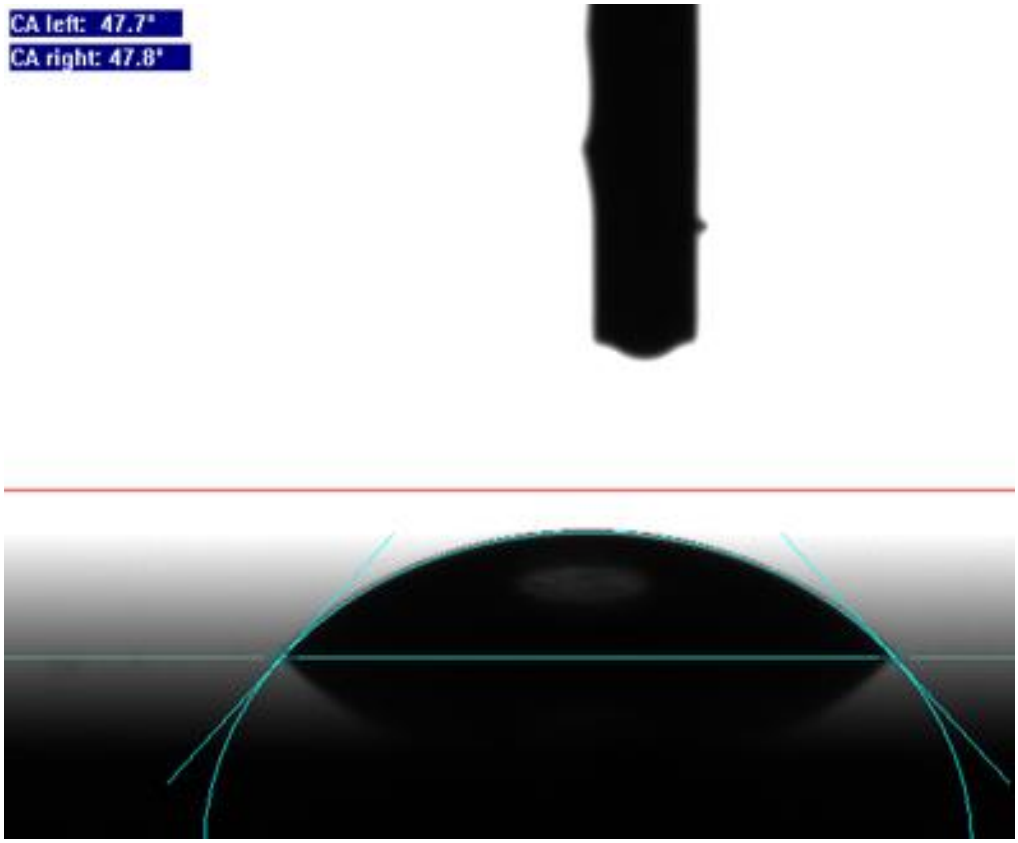
CA left: 47.7°
CA right: 47.8°

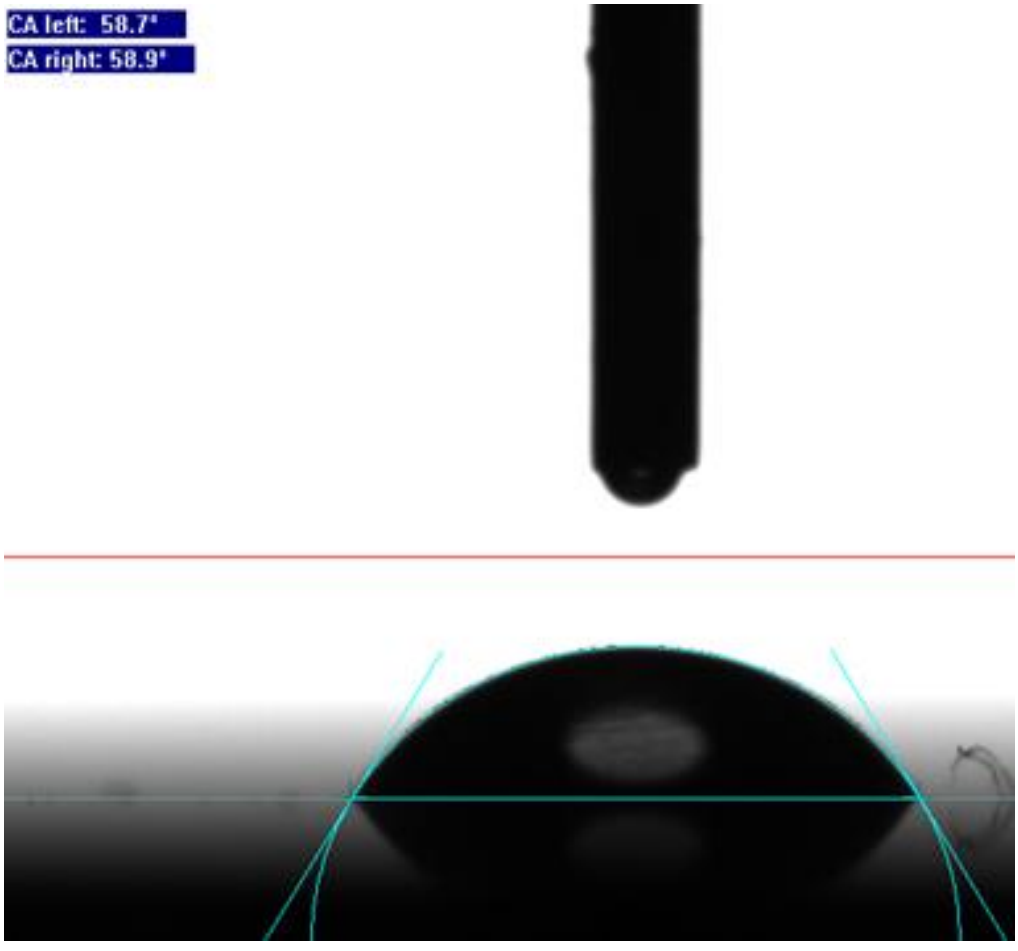
CA left: 58.7°
CA right: 58.9°

Figure 138: The full set of contact angle measurements on the glass coverslip in order to determine the critical surface energy. From top to bottom: water, 5%, 10% and 15% sodium chloride

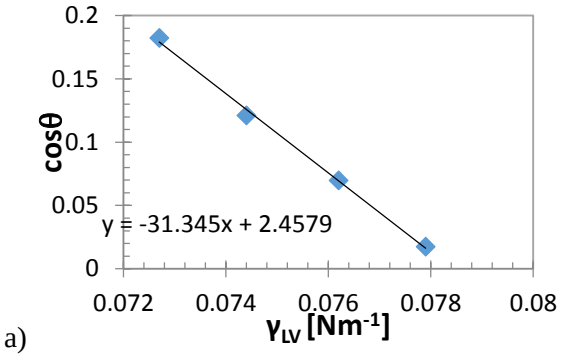

a)

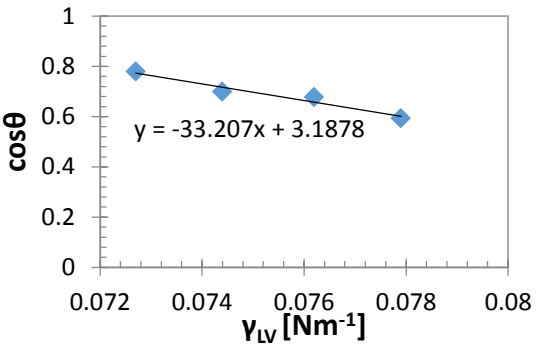

b)

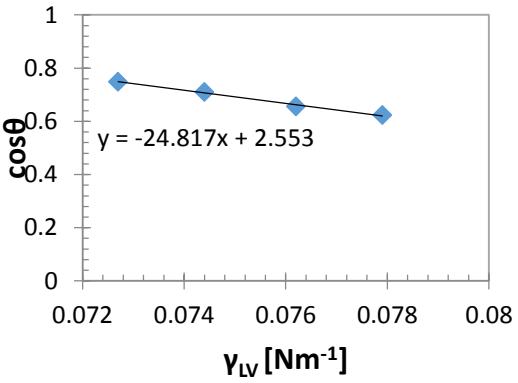

c)

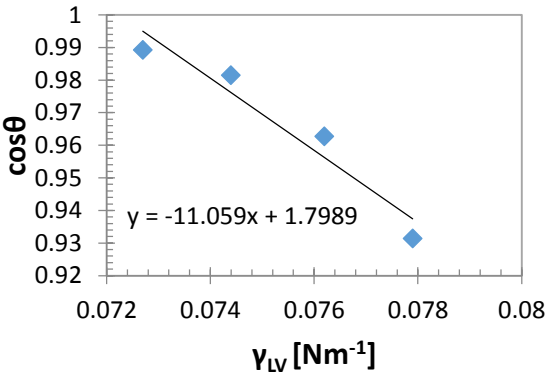

d)

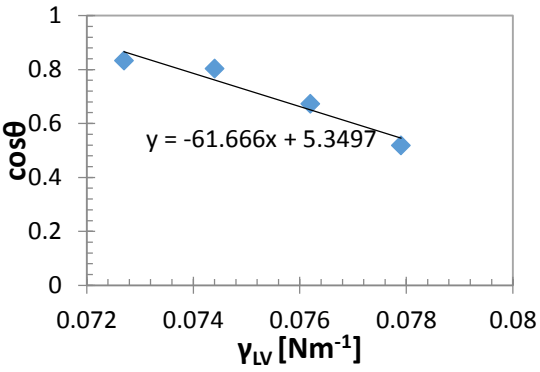

e)

Figure 139: Zisman plots shown for the five surfaces examined for contact angles using water and 5, 10 and 15 % sodium chloride solutions: a) polyethylene; b) steel disc; c) steel plate; d) glass dish, and e) glass coverslip. The equations of the trendlines are shown as these indicate the means of calculating the critical surface areas.

5. Thickness Tests – C_d Plots

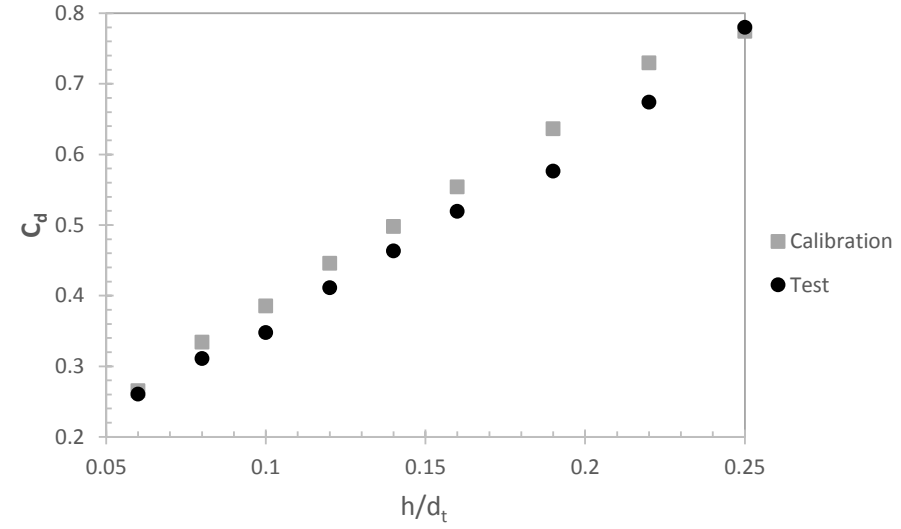

Figure 140: A graph showing how the discharge coefficient (C_d) relative to the dimensionless nozzle clearance distance (h/d_t) differs compared to a calibration plot due to the presence of a biofilm. This particular biofilm was of *E. coli* grown for 14 days on a polyethylene surface.

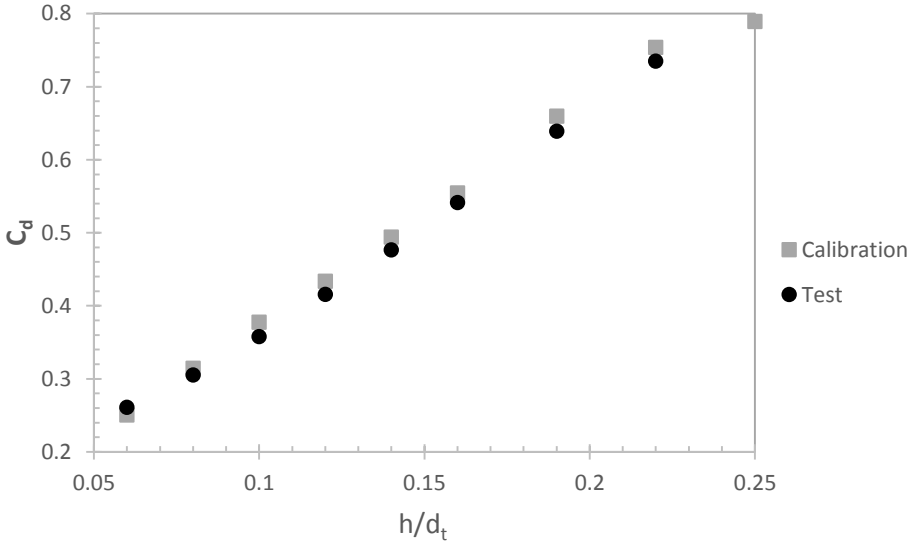

Figure 141: A graph showing how the discharge coefficient (C_d) relative to the dimensionless nozzle clearance distance (h/d_t) differs compared to a calibration plot due to the presence of a mixed species biofilm grown for 14 days on a glass surface.